frontiers | Research Topics

Trends in biomarkers for neurodegenerative diseases: Current research and future perspectives

Edited by
Suman Dutta, Miriam Sklerov, Charlotte Elisabeth Teunissen and Gal Bitan

Published in
Frontiers in Aging Neuroscience
Frontiers in Neuroscience
Frontiers in Cellular Neuroscience

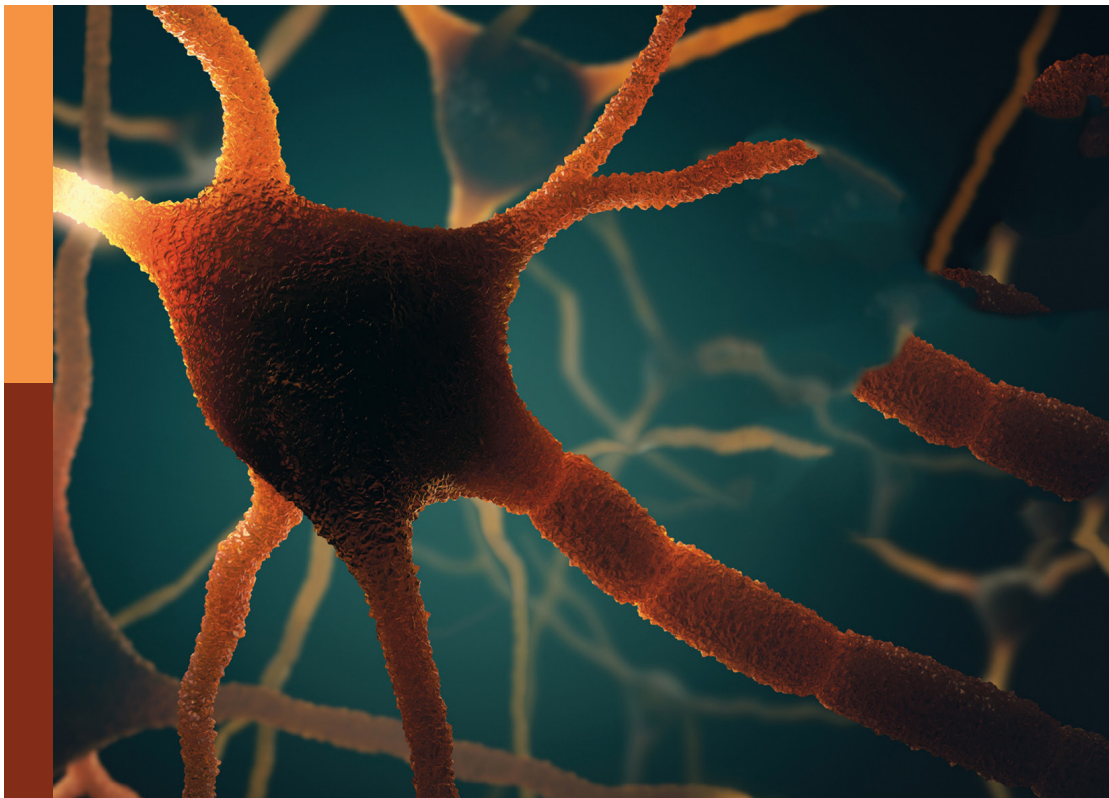

ISSN 1664-8714
ISBN 978-2-83251-800-7
DOI 10.3389/978-2-83251-800-7

About Frontiers

Frontiers is more than just an open access publisher of scholarly articles: it is a pioneering approach to the world of academia, radically improving the way scholarly research is managed. The grand vision of Frontiers is a world where all people have an equal opportunity to seek, share and generate knowledge. Frontiers provides immediate and permanent online open access to all its publications, but this alone is not enough to realize our grand goals.

Frontiers journal series

The Frontiers journal series is a multi-tier and interdisciplinary set of open-access, online journals, promising a paradigm shift from the current review, selection and dissemination processes in academic publishing. All Frontiers journals are driven by researchers for researchers; therefore, they constitute a service to the scholarly community. At the same time, the *Frontiers journal series* operates on a revolutionary invention, the tiered publishing system, initially addressing specific communities of scholars, and gradually climbing up to broader public understanding, thus serving the interests of the lay society, too.

Dedication to quality

Each Frontiers article is a landmark of the highest quality, thanks to genuinely collaborative interactions between authors and review editors, who include some of the world's best academicians. Research must be certified by peers before entering a stream of knowledge that may eventually reach the public - and shape society; therefore, Frontiers only applies the most rigorous and unbiased reviews. Frontiers revolutionizes research publishing by freely delivering the most outstanding research, evaluated with no bias from both the academic and social point of view. By applying the most advanced information technologies, Frontiers is catapulting scholarly publishing into a new generation.

What are Frontiers Research Topics?

Frontiers Research Topics are very popular trademarks of the *Frontiers journals series*: they are collections of at least ten articles, all centered on a particular subject. With their unique mix of varied contributions from Original Research to Review Articles, Frontiers Research Topics unify the most influential researchers, the latest key findings and historical advances in a hot research area.

Find out more on how to host your own Frontiers Research Topic or contribute to one as an author by contacting the Frontiers editorial office: frontiersin.org/about/contact

Trends in biomarkers for neurodegenerative diseases: Current research and future perspectives

Topic editors

Suman Dutta — International Institute of Innovation and Technology, India
Miriam Sklerov — University of North Carolina at Chapel Hill, United States
Charlotte Elisabeth Teunissen — VU Amsterdam, Netherlands
Gal Bitan — University of California, Los Angeles, United States

Citation

Dutta, S., Sklerov, M., Teunissen, C. E., Bitan, G., eds. (2023). *Trends in biomarkers for neurodegenerative diseases: Current research and future perspectives*. Lausanne: Frontiers Media SA. doi: 10.3389/978-2-83251-800-7

Table of contents

frontiers | Frontiers in Aging Neuroscience

TYPE Editorial
PUBLISHED 16 February 2023
DOI 10.3389/fnagi.2023.1153932

OPEN ACCESS

EDITED AND REVIEWED BY
Jorge Busciglio,
University of California, Irvine, United States

*CORRESPONDENCE
Suman Dutta
✉ sduttaucla@gmail.com

SPECIALTY SECTION
This article was submitted to Cellular and Molecular Mechanisms of Brain-aging, a section of the journal Frontiers in Aging Neuroscience

RECEIVED 30 January 2023
ACCEPTED 02 February 2023
PUBLISHED 16 February 2023

CITATION
Dutta S, Sklerov M, Teunissen CE and Bitan G (2023) Editorial: Trends in biomarkers for neurodegenerative diseases: Current research and future perspectives.
Front. Aging Neurosci. 15:1153932.
doi: 10.3389/fnagi.2023.1153932

Editorial: Trends in biomarkers for neurodegenerative diseases: Current research and future perspectives

Suman Dutta[1]*, Miriam Sklerov[2], Charlotte E. Teunissen[3] and Gal Bitan[4]

[1]International Institute of Innovation and Technology, Kolkata, India, [2]Department of Neurology, University of North Carolina School of Medicine, Chapel Hill, NC, United States, [3]Department of Clinical Chemistry, Vrije Universiteit Amsterdam, Amsterdam UMC, Amsterdam, Netherlands, [4]Department of Neurology, David Geffen School of Medicine, Brain Research Institute, Molecular Biology Institute, University of California, Los Angeles, Los Angeles, CA, United States

KEYWORDS

Parkinson's disease, Alzheimer's disease, cerebrospinal fluid (CSF), brain imaging (CT and MRI), Huntington's disease, amyotrophic lateral sclerosis (ALS), microRNA (miRNA), central nervous system (CNS)

Editorial on the Research Topic
Trends in biomarkers for neurodegenerative diseases: Current research and future perspectives

Neurodegenerative diseases are characterized by a progressive decline in brain function and are a growing global threat (Jellinger, 2010). Early and accurate diagnosis of these conditions is vital for the development of therapeutic interventions to prevent disease progression and improve patient outcomes. However, many currently available biomarkers for these conditions have limited sensitivity and specificity, and are not clinically applicable during early disease stages (Hornung et al., 2020; Hansson, 2021).

A challenge for the diagnosis and treatment of neurodegenerative diseases is the difficulty accessing the brain of living individuals. For most of these diseases, analysis of brain tissue postmortem is required for accurate diagnosis. Major advancements have been made in the development of cerebrospinal fluid (CSF), imaging, and blood-based biomarkers for several neurodegenerative diseases (Ashton et al., 2020; Kaipainen et al., 2020; Dutta et al., 2021; Taha et al., 2022), which are proof of concept for the possibilities of early diagnosis. Moreover, advances in proteomics, transcriptomics, and metabolomics have provided valuable insights into the mechanisms of these conditions and have opened the door to the development of novel diagnostic and therapeutic approaches (Peplow and Martinez, 2021).

Collaborative efforts across the globe have helped elucidate the underlying mechanistic pathways of neurodegenerative diseases, yet many remain poorly understood (Figure 1). This Research Topic is a collection of research articles and reviews from diverse groups around the globe discussing recent developments and insights in the field of biomarkers for neurodegenerative diseases, their utility and limitations, and future directions toward implementation of advanced biomarkers in regular clinical practice.

Zhang, Ghose, et al. at Oxford University used deep-learning neural networks to identify blood proteins that could predict the now commonly used biomarker paradigm of amyloid, tau, and neurodegeneration (AT[N]) pathologies in AD. The researchers determined the AT[N] status in the brain and compared it to the corresponding blood biomarkers. The study found enrichment of proteins in five AD-associated clusters that could serve as surrogate blood biomarkers for AD. Along similar lines, to study the relationship between blood-based biomarkers of AD and cognition in motoric cognitive risk (MCR) syndrome, Chen et al. at MacKay Memorial Hospital, Taiwan, determined the levels of plasma Aβ42 and total tau. They found that plasma tau levels were significantly higher in the MCR and AD groups compared to the normal cognition group. These findings suggest that MCR and AD may share underlying pathology and cognitive function may be related to tau levels in MCR. A study by Parvizi et al. at the Medical University of Vienna, Austria, examined the potential of blood neurofilament light chain (NfL) and glial fibrillary acidic protein (GFAP), in detecting early neuropathological changes in AD. A panel combining plasma NfL and GFAP with known AD risk factors had a promising discriminatory power in distinguishing AD from healthy controls and predicting amyloid positivity.

A retrospective, case-selective clinical study by Li et al. at Tianjin Huanhu Hospital, China, aimed to differentiate AD from frontotemporal lobar degeneration (FTLD) using clinical, neuropsychological, and neuroimaging features. AD patients had a higher prevalence of vascular disease-associated factors and a higher percentage of Apolipoprotein E4 carriers. The findings suggest that dynamic evaluation of cognitive function, behavioral symptoms, and multimodal neuroimaging may help differentiate between AD and FTLD.

In a systematic review of preclinical *in vitro* and *in vivo* studies, Fathi et al. at Shahid Beheshti University of Medical Sciences, Iran, evaluated genes and mechanisms of neuroinflammation in Parkinson's disease (PD). The review identified several neuroinflammatory factors and molecular mechanisms contributing to the initiation and progression of PD, and potential therapeutic approaches against them. A systematic review focusing on different aspects by Asadi et al. at Tabriz University of Medical Sciences, Iran, attempted to identify validated competing endogenous RNA (ceRNA) loops in PD. The reviewed studies indicate that ceRNA axes have a significant impact on PD development and may be useful for the diagnosis and treatment of PD. Bioinformatic analysis of genes targeted in ceRNA axes showed that they were involved in processes such as the cellular response to metal ions, oxidative stress, and regulation of macromolecule metabolism. Heng et al. at the Second Affiliated Hospital of Soochow University, China, explored the association between osteoarthritis and PD through genetic characterization and functional enrichment. Using bioinformatics methods and datasets from the Gene Expression Omnibus database, they identified 71 common genes affecting both diseases, which were enriched in antigen processing and presentation, mitochondrial translation, the mRNA surveillance pathway, and nucleocytoplasmic transport. The study suggested that the gene WDR43 may be useful for the diagnosis of osteoarthritis and PD and that several immune cell types may be associated with the pathogenesis of both diseases. Zheng et al. at Beijing Tiantan Hospital, China, investigated whether abnormal α-synuclein (α-syn) deposition occurs in the oral mucosa of patients with multiple system atrophy (MSA) and whether α-syn and pathological forms thereof in the oral mucosa could be potential biomarkers for MSA.

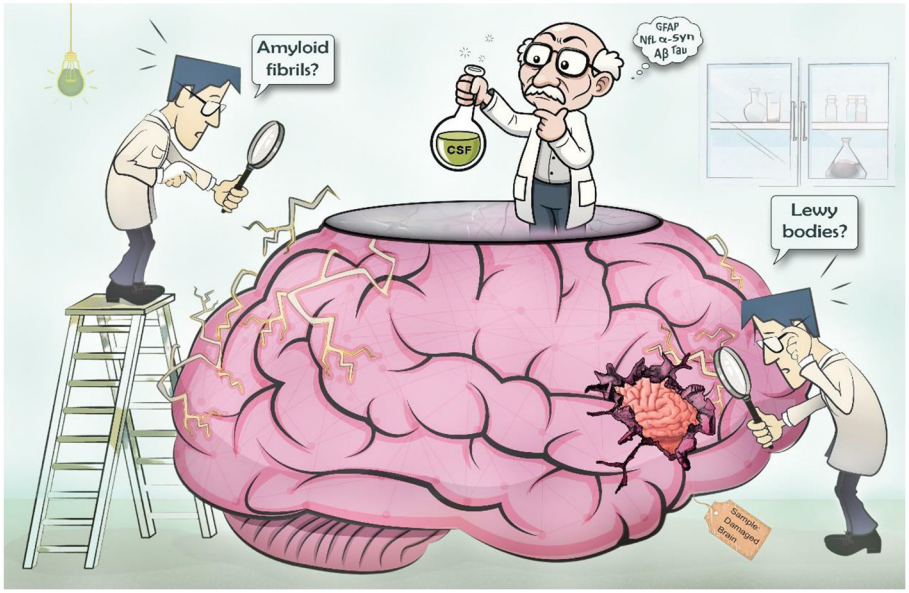

FIGURE 1
Challenges in identifying biomarkers for neurodegenerative diseases. Identifying biomarkers for neurodegenerative diseases is challenging because of the inaccessibility of the brain. As a result, there is a lack of detailed understanding of the underlying pathology. Additional challenges are variability in clinical presentation and overlapping symptoms, and the long latent period of many of these diseases making it difficult to pinpoint specific biomarkers for diagnosis and prediction of disease course.

They found elevated levels of all tested α-syn species in patients with MSA compared to controls. Interestingly, the α-syn levels correlated negatively with disease duration, suggesting that they will be most useful at early disease stages.

The ongoing COVID-19 pandemic has been linked to a range of neurological complications, including cognitive impairment and neurodegenerative changes (Li C. et al., 2022). A review article by Silva et al. at Benemérita Universidad Autónoma de Puebla, Mexico, discusses the possibility of SARS-CoV-2 entering the central nervous system (CNS) through various neuroinvasive pathways, including the transcribrial route, the ocular surface, and the hematogenous system leading to the development of neurodegenerative diseases. The authors highlighted that the virus may also cause cytokine storms, neuroinflammation, and oxidative stress, which may increase the risk of developing diseases, such as AD and PD. Alvarez et al. at Marshall University, West Virginia, reviewed the diverse neurodegenerative changes associated with COVID-19 and highlighted the importance of major circulating biomarkers, associated with disease progression and severity. Their literature survey indicates that important CNS proteins, such as GFAP, NfL, and pT181-tau, and various inflammatory cytokines are altered significantly in COVID-19 patients. The review summarizes the current understanding of the neuropathological changes associated with COVID-19 and the potential use of biomarkers in identifying patients at risk for developing severe forms of the disease.

Huntington's disease (HD) is a genetic neurodegenerative disorder that is influenced by epigenetic changes, such as non-coding RNA expression and accelerated DNA methylation age (Bassi et al., 2017). Ghafouri-Fard et al. at Shahid Beheshti University of Medical Sciences, Iran, review the potential interactions among these different layers of the epigenome in relation to HD onset and progression. The authors discuss recent findings of micro RNA (miRNA) and long noncoding RNA dysregulation, as well as methylation changes and epigenetic age in HD.

In a study focusing on amyotrophic lateral sclerosis (ALS), Behler et al. at Ulm University, Germany, investigated the use of diffusion tensor imaging (DTI) as a progression biomarker. The study used Monte Carlo simulations to estimate the statistical power and sample size needed for DTI studies in ALS considering factors such as the number of scans per session, time intervals between measurements, and measurement uncertainties. The results showed that multiple scans per session can increase the statistical power of DTI studies in ALS, particularly in cases of high measurement uncertainty and small sample sizes. Addressing the question of developing biomarkers for the spectrum of diseases caused by tauopathy or TPD-43 proteinopathy, Wong et al. at the University of Toronto, Canada, used spectral-domain optical coherence tomography (SD-OCT) to examine the peripapillary retinal nerve fiber layer (pRNFL) thickness and macular retinal thickness in the eyes of participants with ALS, progressive supranuclear palsy (a tauopathy), and the semantic variant of primary progressive aphasia presumed to be caused by TDP-43 proteinopathy. Their data indicated that the TDP-43 group had a significantly thinner pRNFL in the temporal sector compared to the tauopathy group. miRNAs, a class of small non-coding RNAs, often are altered in neurodegenerative diseases and have the potential to be used as biomarkers (Li S. et al., 2022). Alvia et al. at Boston University School of Medicine compared the levels of 47 miRNAs in the prefrontal cortex of brain donors with chronic traumatic encephalopathy (CTE), ALS, both CTE and ALS, and control subjects. They found that 60% of the studied miRNAs were significantly different between the pathology groups, of which 75% were upregulated in both CTE and ALS. The identified miRNAs were involved in pathways related to inflammation, apoptosis, and cell growth/differentiation. Importantly, the largest change was in miR-10b, which was increased in ALS but not in CTE or CTE + ALS, suggesting that it could be used as a diagnostic biomarker.

Zhang, Chen, et al. at the Second Hospital of Hebei Medical University, China, studied the role of endothelin-1 (ET-1) in ALS and found that ET-1 and its receptors were expressed in the spinal cord of a transgenic mouse model of ALS and their expression changed as the disease progressed. In addition, ET-1 had a toxic effect on motor neurons in a cell model of ALS, which was rescued by selective ET-A or ET-B receptor antagonists. They also found that Cdkn1b (P27) and Eif4ebp1 could be used as biomarkers for understanding and identifying the pathogenesis of ALS responding to ET-1 intervention.

NfLs are proteins found in neurons and their levels have been shown to be useful in the diagnosis, prognosis, and monitoring of treatment response for a variety of neurological conditions (Gaetani et al., 2019). In a review article, Delaby et al. at Université de Montpellier, France, discussed the potential value of NfL assays in the diagnosis and management of patients with ALS, PD, frontotemporal dementia, and other neurologic diseases. The authors also described the added value of NfL compared to other biomarkers and proposed specific indications where NfL may be helpful in diagnostic and prognostic clinical decision-making. The authors pointed out the importance of establishing reference ranges for NfL levels in different biological samples, depending on factors such as age, body mass index, and the specific medical indication considered.

A study by Fernandez-Alvarez et al. at Pablo de Olavide University, Spain, examined the relationship between plasma markers of amyloid and neurodegeneration, intracortical myelin content, and resting-state functional connectivity in cognitively normal older adults. The researchers found that lower plasma Aβ42 and higher plasma NfL were associated with lower myelin content in certain brain regions. They also found that higher NfL levels were associated with altered functional connectivity between the insula and medial orbitofrontal cortex. The findings suggest potential links among plasma Aβ42 and NfL, intracortical myelin content, and functional connectivity in brain regions vulnerable to aging and neurodegeneration.

Overall, this Research Topic highlights recent development and innovation in the field of biomarkers for neurodegenerative diseases, including AD, PD, HD, ALS, and others. The Research Topic covers a range of biomarkers, including those that can be measured in the periphery, such as blood and spinal fluid. The Research Topic also covers the potential

use of these biomarkers in clinical practice, including their potential to aid in the diagnosis, prognosis, and monitoring of disease progression and treatment response. Our goal as editors was to provide a comprehensive overview of the current state of the field and identify future directions for research and development in this important area and we hope the readers will find interest in the included articles and reviews.

Author contributions

SD wrote the article. GB, MS, and CT reviewed the article and provided critical feedback. All authors contributed to the article and approved the submitted version.

Conflict of interest

The authors declare that the research was conducted in the absence of any commercial or financial relationships that could be construed as a potential conflict of interest.

Publisher's note

References

Ashton, N. J., Hye, A., Rajkumar, A. P., Leuzy, A., Snowden, S., Suárez-Calvet, M., et al. (2020). An update on blood-based biomarkers for non-Alzheimer neurodegenerative disorders. *Nat. Rev. Neurol.* 16, 265–284. doi: 10.1038/s41582-020-0348-0

Bassi, S., Tripathi, T., Monziani, A., Di Leva, F., and Biagioli, M. (2017). "Epigenetics of Huntington's disease," in *Neuroepigenomics in Aging and Disease. Advances in Experimental Medicine and Biology, Vol. 978*, ed Delgado-Morales (Cham: Springer).

Dutta, S., Hornung, S., Kruayatidee, A., Maina, K. N., Del Rosario, I., Paul, K. C., et al. (2021). α-Synuclein in blood exosomes immunoprecipitated using neuronal and oligodendroglial markers distinguishes Parkinson's disease from multiple system atrophy. *Acta Neuropathol.* 142, 495–511. doi: 10.1007/s00401-021-02332-0

Gaetani, L., Blennow, K., Calabresi, P., Di Filippo, M., Parnetti, L., Zetterberg, H., et al. (2019). Neurofilament light chain as a biomarker in neurological disorders. *J. Neurol Neurosurg. Psychiatry* 90, 870–881. doi: 10.1136/jnnp-2018-320106

Hansson, O. (2021). Biomarkers for neurodegenerative diseases. *Nat. Med.* 27, 954–963. doi: 10.1038/s41591-021-01382-x

Hornung, S., Dutta, S., and Bitan, G. (2020). CNS-derived blood exosomes as a promising source of biomarkers: opportunities and challenges. *Front. Mol. Neurosci.* 13, 38. doi: 10.3389/fnmol.2020.00038

Jellinger, K. A. (2010). Basic mechanisms of neurodegeneration: a critical update. *J. Cell Mol. Med.* 14, 457–487. doi: 10.1111/j.1582-4934.2010.01010.x

Kaipainen, A., Jääskeläinen, O., Liu, Y., Haapalinna, F., Nykänen, N., Vanninen, R., et al. (2020). Cerebrospinal fluid and MRI biomarkers in neurodegenerative diseases: a retrospective memory clinic-based study. *J. Alzheimers Dis.* 75, 751–765. doi: 10.3233/JAD-200175

Li, C., Liu, J., Lin, J., and Shang, H. (2022). COVID-19 and risk of neurodegenerative disorders: a mendelian randomization study. *Transl. Psychiatry* 12, 283. doi: 10.1038/s41398-022-02052-3

Li, S., Lei, Z., and Sun, T. (2022). The role of microRNAs in neurodegenerative diseases: a review. *Cell. Biol. Toxicol.* 20, 1–31. doi: 10.1007/s10565-022-09761-x

Peplow, P. V., and Martinez, B. (Eds.). (2021). *Neurodegenerative Diseases Biomarkers: Towards Translating Research to Clinical Practice.* New York, NY: Springer Nature.

Taha, H. B., Hornung, S., Dutta, D., Fenwick, L., Lahgui, O., Howe, K., et al. (2022). Toward a biomarker panel measured in CNS-originating extracellular vesicles for improved differential diagnosis of parkinson's disease and multiple system atrophy. doi: 10.21203/rs.3.rs-2375640/v1

frontiers | Frontiers in Neuroscience

REVIEW
published: 03 May 2022
doi: 10.3389/fnins.2022.867825

Neuropathological Aspects of SARS-CoV-2 Infection: Significance for Both Alzheimer's and Parkinson's Disease

Jaime Silva[1†], Felipe Patricio[1†], Aleidy Patricio-Martínez[1,2], Gerardo Santos-López[3], Lilia Cedillo[4], Yousef Tizabi[5] and Ilhuicamina Daniel Limón[1]*

[1] Laboratorio de Neurofarmacología, Facultad de Ciencias Químicas, Benemérita Universidad Autónoma de Puebla, Puebla, Mexico, [2] Facultad de Ciencias Biológicas, Benemérita Universidad Autónoma de Puebla, Puebla, Mexico, [3] Laboratorio de Biología Molecular y Virología, Centro de Investigación Biomédica de Oriente, Instituto Mexicano del Seguro Social, Atlixco, Mexico, [4] Centro de Detección Biomolecular, Benemérita Universidad Autónoma de Puebla, Puebla, Mexico, [5] Department of Pharmacology, Howard University College of Medicine, Washington, DC, United States

Evidence suggests that SARS-CoV-2 entry into the central nervous system can result in neurological and/or neurodegenerative diseases. In this review, routes of SARS-Cov-2 entry into the brain *via* neuroinvasive pathways such as transcribrial, ocular surface or hematogenous system are discussed. It is argued that SARS-Cov-2-induced cytokine storm, neuroinflammation and oxidative stress increase the risk of developing neurodegenerative diseases such as Alzheimer's disease and Parkinson's disease. Further studies on the effects of SARS-CoV-2 and its variants on protein aggregation, glia or microglia activation, and blood-brain barrier are warranted.

Keywords: SARS-CoV-2, Alzheimer's disease, Parkinson's disease, neuroinvasive pathways, blood-brain barrier

OPEN ACCESS

Edited by:
Natalia P. Rocha, University of Texas Health Science Center at Houston, United States

Reviewed by:
Ulises Gomez-Pinedo, Health Research Institute of the Hospital Clínico San Carlos, Spain
Ravi Kant Narayan, Dr. B. C. Roy Multispeciality Medical Research Center (Under IIT Kharagpur), India
Nicolas Alejandro Bravo-Vasquez, University of Texas Health Science Center at Houston, United States

***Correspondence:**
Ilhuicamina Daniel Limón
ilhlimon@yahoo.com.mx; daniel.limon@correo.buap.mx

[†]These authors have contributed equally to this work and share first authorship

Specialty section:
This article was submitted to Neurodegeneration, a section of the journal Frontiers in Neuroscience

Received: *01 February 2022*
Accepted: *14 April 2022*
Published: *03 May 2022*

Citation:
Silva J, Patricio F, Patricio-Martínez A, Santos-López G, Cedillo L, Tizabi Y and Limón ID (2022) Neuropathological Aspects of SARS-CoV-2 Infection: Significance for Both Alzheimer's and Parkinson's Disease. Front. Neurosci. 16:867825. doi: 10.3389/fnins.2022.867825

INTRODUCTION

On December 12, 2019, in Wuhan City, Hubei Province, China, the first cases of an unexplained pneumonia failing to respond to the standard treatment regimen led to an exhaustive search for a new virus. The clinical symptoms of the condition were fever, dry cough, sore throat, pneumonia, severe dyspnea, and myalgia (Huang C. et al., 2020; Zhu N. et al., 2020). Subsequently, on February 11, 2020, the new coronavirus was identified and was termed severe acute respiratory syndrome coronavirus 2 (SARS-CoV-2). Coincidentally, a day earlier, the first draft genome of the virus was made publicly available. This enabled research groups to develop different molecular diagnostics such as RT-PCR and immunological assays. Later, CRISPR-based assays, nucleic acid microarray assays, and next generation sequencing were added (Habibzadeh et al., 2021).

The World Health Organization (WHO) is responsible for declaring a pandemic. WHO monitors disease activity on a global scale through a network of centers located in countries worldwide and has a pandemic preparedness plan that consists of six phases of pandemic alert. Phase 1 represents the lowest level of alert and usually indicates that a newly emerged or previously existing virus is circulating among animals, with low risk of transmission to humans. Phase 6, the pandemic phase, is declared when an outbreak is characterized by globally widespread and

sustained disease transmission among humans (Rogers, 2022). Since by the end of February 2020, COVID-19 had already registered 83,652 cases globally (Wassie et al., 2020; Carvalho et al., 2021). On March 11, 2020, WHO declared COVID-19 a pandemic.

Patients who have concomitant comorbidities and patients admitted to the intensive care unit are significantly more likely to develop complications from COVID-19 (Sanyaolu et al., 2020). Elderly and seriously ill patients with a clinical history of cardiovascular, liver, and/or kidney disease carry the highest risk of mortality. Obesity is also a risk factor for all ages (Huang Y. et al., 2020), and age, sex, ethnicity, socioeconomic group, and geographical location may also influence the outcome (Harwood et al., 2022).

The SARS-CoV-2 belongs to the *Coronaviridae* family of the genus *betacoronavirus* (βCoV) and was identified as the etiological agent of COVID-19. SARS-CoV-2, like other known coronaviruses, is an enveloped virus with single-stranded positive sense RNA and a genome approximately 29.9 kb in size (Masters, 2006; Rastogi et al., 2020). Genetically, SARS-CoV-2 and severe acute respiratory syndrome coronavirus (SARS-CoV) both have characteristically high homologous sequence, unlike the Middle East Syndrome (MERS)-CoV virus (Yu et al., 2020). The SARS-CoV-2 envelope is associated with four structural proteins: membrane protein (M); spike protein (S); envelope protein (E); and nucleocapsid protein (N) (Lu R. et al., 2020; **Figure 1**). Details on the structure and molecular biology of the SARS-CoV-2 virus have been recently reviewed by several groups (Arya et al., 2021; Hu et al., 2021; Peng et al., 2021; Rahimi et al., 2021).

Analysis of mutations in the coding and non-coding regions, genetic diversity, and pathogenicity of SARS-CoV-2 has also been carried out and based on the results it was suggested that a minimal variation in the genome sequence of SARS-CoV-2 may be responsible for a drastic change in the structures of target proteins, making available drugs ineffective (Naqvi et al., 2020). Clinical data show that the main structures of the body that are affected by COVID-19 are the respiratory and cardiovascular systems (Kapoor, 2020; Lazzeri et al., 2020; Yi et al., 2021). However, SARS-CoV-2 is able to infect other systems, such as the digestive, urogenital and nervous systems (Zhang Y. et al., 2020; Spudich and Nath, 2022). In this review, we discuss the recent reports on the infectivity of SARS-CoV-2 in the central nervous system (CNS) and the probable impact of COVID-19 on neurodegenerative diseases.

Neurological Consequences of COVID-19

There are reports of COVID-19 exerting neurological effects, the most common being hypogeusia (diminished sense of taste) and anosmia (loss of sense of smell) (Gilani et al., 2020; Spudich and Nath, 2022), and cerebrovascular damage (Beyrouti et al., 2020; Meegada et al., 2020; Gilpin et al., 2021). However, encephalopathies (Helms et al., 2020), demyelination (Domingues et al., 2020; Zanin et al., 2020), edema and symptom presentations similar to multiple sclerosis and Guillain-Barré have also been observed with COVID-19 (Toscano et al., 2020; Spudich and Nath, 2022). Other neurological/neuropsychiatric symptoms such as alterations in consciousness and hallucinations in COVID-19 have been attributed to SARS-CoV-2's effect on the frontal lobe cortex, an area intimately involved in perception (Ellul et al., 2020; Ferrando et al., 2020; Paniz-Mondolfi et al., 2020).

Because COVID-19 is a relatively recent disease, its full pathogenic mechanisms and possible sequelae in the nervous system remain unclear. Fortunately, novel molecular biology techniques, such as RT-PCR, RT-qPCR, CRISPR-based assays, and nucleic acid microarray assays have made it possible to elucidate some general aspects of the disease (Habibzadeh et al., 2021) and relate them to other public health emergencies caused by other coronaviruses, such as SARS in 2002–2003 and MERS in 2012 (Zhu Z. et al., 2020). Researchers have been able to ascertain complications associated with pre-existing conditions and the key role played by the immune system in resolution or further complication of the disease (de Wit et al., 2016; Abdelrahman et al., 2020; Ansariniya et al., 2021). In addition, SARS-CoV-2-induced acute and long-term neurological effects are a subject of intense investigation and a main focus of this article.

NEUROINVASIVE MECHANISMS OF SEVERE ACUTE RESPIRATORY SYNDROME CORONAVIRUS 2

Human coronaviruses not only cause common colds but can also infect neural cells as evidenced by neurotropism and neuroinvasion (Arbour et al., 2000). Studies carried out on brain samples taken from patients with SARS disease detected the presence of the SARS-CoV virus in nervous tissue (Ding et al., 2004; Xu et al., 2005). Moreover, SARS-CoV-2 has been detected in the brain and cerebrospinal fluid of COVID-19 patients using RT-qPCR and immunohistochemistry techniques (Domingues et al., 2020; Huang Y. H. et al., 2020; Moriguchi et al., 2020; Liu J. M. et al., 2021; Serrano et al., 2021; Song et al., 2021). Although the exact mechanism of neurological complications in COVID-19 patients is unknown, it has been shown that infection with SARS-CoV-2 damages the choroid plexus epithelium, leading to leakage across the blood brain barrier (Pellegrini et al., 2020). Nonetheless, potential mechanism (s) of SARS-CoV-2 entry into the CNS are a subject of intense relevance and interest (Hu et al., 2020).

It is known that both SARS-CoV and SARS-CoV-2 occupy the primary receptor angiotensin-converting enzyme 2 (ACE2) (Li et al., 2003; Lu R. et al., 2020) and can form a complex with other cofactors such as transmembrane serine protease 2 (TMPRSS2) (Hoffmann et al., 2020) and neuropilin-1 (Cantuti-Castelvetri et al., 2020; Daly et al., 2020). This interaction between SARS-CoV-2 and ACE2 is essential for the complex to be internalized into the cells (**Figure 1**). TMPRSS2 is vital for SARS-CoV-2 infection, although it has a low expression in the brain. However, SARS-CoV-2 can also infect cells *via* neuropilin-1 and furin protease which have a higher and broader expression in the brain compared to TMPRSS2 or ACE2 (Davies et al., 2020). Moreover, SARS-CoV-2 is likely to infect glutamatergic neurons due to higher expression of ACE2, neuropilin-1 and furin protease than GABAergic neurons (Dobrindt et al., 2021). Thus, other proteins

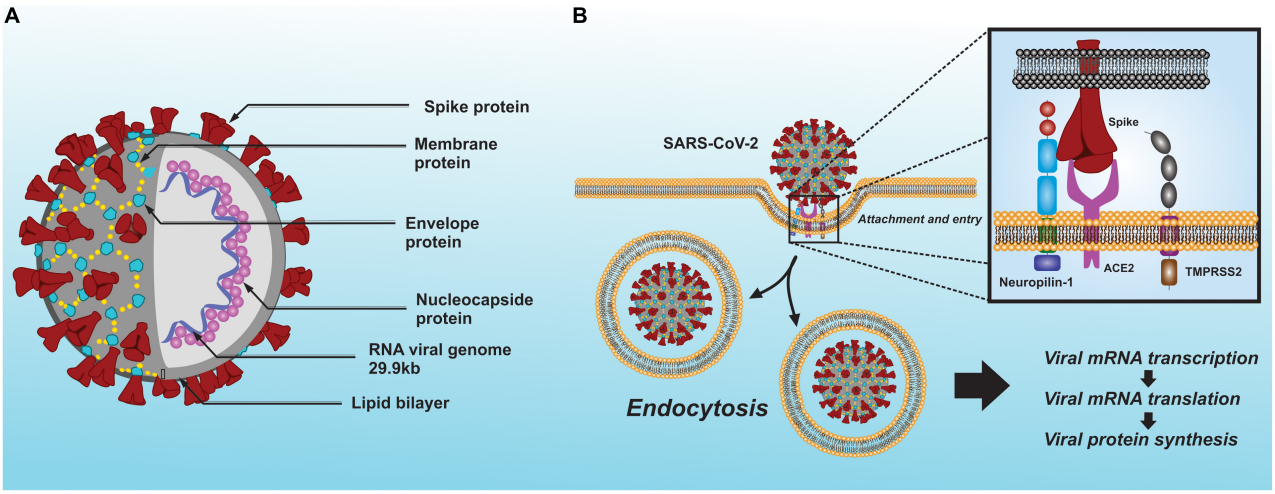

FIGURE 1 | Schematic model of the SARS-CoV-2 whit its structural proteins. **(A)** The virus envelope is associated with four structural proteins: membrane protein (M); spike protein (S); envelope protein (E); and nucleocapsid protein (N). Moreover, it has a single-stranded positive sense RNA and a genome approximately 29.9 kb in size. **(B)** To enter a host cell, the SARS-CoV-2 spike protein interacts with the ACE2 and neuropilin-1, while TMPRSS2 to activate its membrane-fusion capacity and subsequent endocytosis.

could be involved in SARS-CoV-2 entry into the brain. Indeed, a recent study suggests that SARS-CoV-2 may interact with metabotropic glutamate receptor 2 (mGluR2), which may play a role in internalization and perhaps in SARS-CoV-2 neurotropism (Wang J. et al., 2021).

ACE2 is highly expressed in adipose tissue and organs such as the kidney, small intestine, heart, and testicles, and to a lesser extent in the lung, liver, colon, spleen, muscle, blood, and brain (Li et al., 2020). Moreover, a low but constant expression of ACE2 has been revealed *via* the use of transcriptomic techniques on various brain structures, such as the brainstem, cortex, striatum, hypothalamus, choroid plexuses, and the paraventricular nuclei of the hypothalamus (Xia and Lazartigues, 2008; Chen R. et al., 2020). Given the evidence for the distribution of ACE2 in the brain, it can be inferred that multiple regions may be affected during SARS-CoV-2 infection. Furthermore, SARS-CoV-2 has a higher affinity for ACE2 than SARS-CoV and therefore, could have a major detrimental effect on the brain (Natoli et al., 2020).

The clinical severity of COVID-19 has been correlated with the frequency of neurological complications, while meningitis and encephalitis have been associated with paranasal sinusitis and could, in severe cases of SARS-CoV-2 infection, be an indicator of an aggravated viral infection due to an obstruction in the paranasal lymphatic vessels (Bridwell et al., 2020; Moriguchi et al., 2020). On the other hand, the glymphatic system, a glia-dependent elimination pathway for soluble wastes and metabolic products in the brain, is believed to play an important role in paranasal sinusitis. Serving as the brain's "front end," the glymphatic system is interconnected with the lymphatic network of the dura, cranial nerves, and veins of the skull (Benveniste et al., 2019). This interconnection could be used by SARS-CoV-2 to gain access to the brain in order to be internalized by the neurons. A compromised blood-brain barrier (BBB) and the perforation of the ethmoid bone are other suggested routes *via* which the virus enters the brain (Zubair et al., 2020; Pacheco-Herrero et al., 2021). Overall, three main routes for viral entry to the CNS have been proposed: (1) the transcribrial neuroinvasive route; (2) the neuroinvasive route *via* the ocular surface; and (3) the hematogenous neuroinvasive route (**Figure 2**). These proposed routes are discussed in the following sections.

Evidence of Neuroinvasive Routes *via* Retrograde Axonal Transport

It has been proposed that one of the main neuroinvasive pathways into the CNS by SARS-CoV-2, as well as other viruses is *via* tropism, where a virus can infect a distinct group of cells by binding to the virus receptors on the surface of the host cell (Bauer et al., 2022a). In fact, chronic viral infections can be a risk factor for neurodegenerative diseases. In this regard, potential involvement of Japanese encephalitic virus, the influenza virus, herpes simplex virus type-1 (HSV-1) and the human immunodeficiency virus (HIV) in etiology of Parkinson's disease and for Alzheimer's disease have been suggested (De Chiara et al., 2012; Limphaibool et al., 2019; Sait et al., 2021). It is worth noting that HSV-1 infections are common, and that the virus can persist in a latent form within the neurons of its human host. Therefore, viruses may cause damage in vulnerable brain areas leading to neurodegenerative disease (Lotz et al., 2021; Sait et al., 2021).

Transcribrial Neuroinvasive Route of Severe Acute Respiratory Syndrome Coronavirus 2

It is suggested that SARS-CoV-2 reaches the olfactory bulb *via* infection of the peripheral nerve terminals of the olfactory sensory neurons (Mori, 2015; Desforges et al., 2019; Paniz-Mondolfi et al., 2020; Kumar et al., 2021). This proposed transcribrial route is supported by reports of SARS-CoV-2 patients presenting symptoms of anosmia and dysgeusia

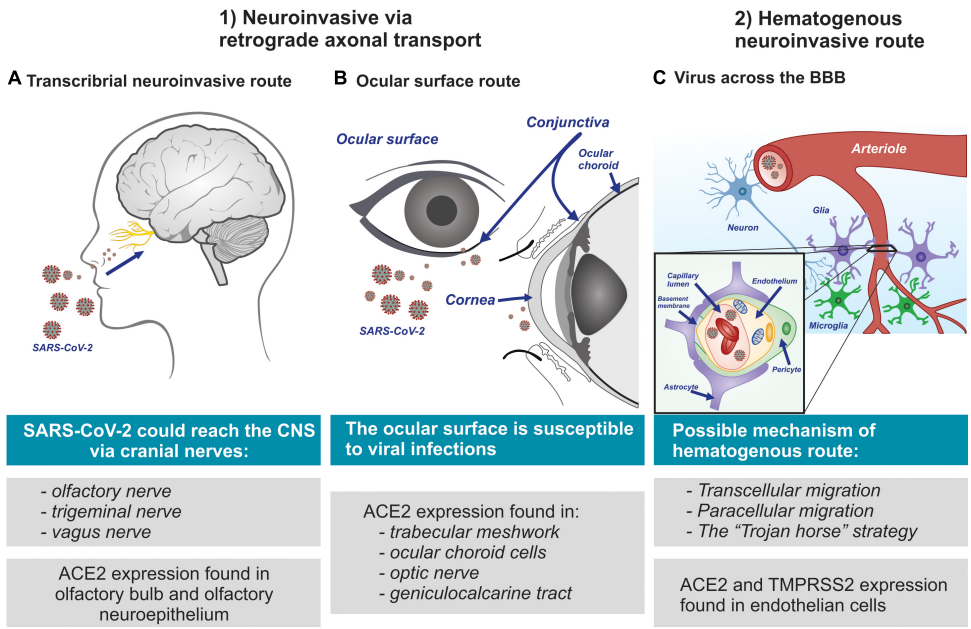

FIGURE 2 | Mechanisms suggested through which SARS-CoV-2 invades the nervous system. **(A)** Transcribrial neuroinvasive route; SARS-CoV-2 may invade the brain through the olfactory nerve, and *via* cranial nerves. **(B)** Route ocular surface; multiple cell types of the visual system are suggested provide as potential entry points for SARS-CoV-2 invasion to the brain. **(C)** Hematogenous neuroinvasive route; SARS-CoV-2 possibly infects vascular endothelial cells *via* the ACE2 and TMPRSS2 receptors. Viral particles can reach the brain through the BBB by infecting and replicating inside brain microvascular endothelial cells. Moreover, SARS-CoV-2 infection can cause excessive peripheral immune responses to result in BBB dysfunction *via* cytokine storm.

(Klopfenstein et al., 2020; Levinson et al., 2020; Mutiawati et al., 2021). It is noteworthy that ACE2 protein is highly expressed in the olfactory bulb (Brann et al., 2020) and the olfactory neuroepithelium (Sungnak et al., 2020; Ziegler et al., 2020). Thus, it is postulated that SARS-CoV-2 forms complexes with TMPRSS2 and neuropilin-1 *via* interaction with olfactory neuroepithelial ACE2, allowing it to enter into the brain retrogradely *via* the cranial nerves (Reza-Zaldívar et al., 2020; Messlinger et al., 2021). Indeed, there are reports that when some viruses infect the nociceptive neurons of the nasal cavity, they are able to reach the CNS through the trigeminal nerve (Deatly et al., 1990; Lochhead and Thorne, 2012) and other sensory terminals of the vagus nerve (Driessen et al., 2016). Hence, SARS-CoV-2 could follow the cranial nerves (Bulfamante et al., 2021; Messlinger et al., 2021) from their origin in the nasal cavity to the olfactory nerve, and then to the olfactory bulb, and finally arriving at the brain stem (Bougakov et al., 2021; **Figure 2A**). This pathway is also followed by the OC43 coronavirus strain (Dubé et al., 2018).

Neuroinvasive Route of Severe Acute Respiratory Syndrome Coronavirus 2 *via* the Ocular Surface

Recent studies conducted on both humans (Zhou et al., 2020; Collin et al., 2021) and mice (Ma et al., 2020) have demonstrated the expression of ACE2 and TMPRSS2 receptors in ocular surface cells, a region comprising the epithelial cells of the cornea and conjunctiva. Furthermore, a remarkable level of ubiquity of ACE2 receptor expression was recently found in the trabecular meshwork and ocular choroid cells of the outer eye, the optic nerve, and optic radiation or geniculocalcarine tract to the occipital cortex, which suggests that multiple cell types of the visual system provide potential entry points for SARS-CoV-2 invasion (Hill et al., 2021). However, as ACE2 expression has been observed more in the conjunctiva than in the cornea, SARS-CoV-2 has greater neuroinvasive potential *via* the conjunctiva (Leonardi et al., 2020; Ma et al., 2020). For the ocular surface to be considered a SARS-CoV-2 infection route, TMPRSS2 must be co-expressed along with ACE2, as TMPRSS2 acts as a cofactor in internalization of the complex (de Freitas Santoro et al., 2021). It should be noted that TMPRSS2 expression has been observed in both the cornea and the conjunctiva (Leonardi et al., 2020; Collin et al., 2021). However, the likelihood of the ocular surface being an infection gateway is low despite the potential of SARS-CoV-2 causing conjunctivitis and other ocular discomfort (Chen X. et al., 2021). However, the actual conjunctival transmission of SARS-CoV-2 is yet to be confirmed (de Freitas Santoro et al., 2021).

The ocular surface is susceptible to viral infections by means of aerosols or direct contact with fomites resulting from exposure to external contaminants and is vulnerable to a higher level of exposure than the oral cavity or the nostrils (Coroneo, 2021; **Figure 2B**). In addition, clinical cases where conjunctivitis was the initial symptomatic manifestation in COVID-19 positive patients have been reported and confirmed *via* both nasopharyngeal swab samples and PCR test which detected the presence of SARS-CoV-2 RNA in tears (Zhang X. et al., 2020; Hassan et al., 2021). Nonetheless, confirmation of the conjunctival transmission of SARS-CoV-2 into the CNS requires further investigation.

Evidence of a Hematogenous Neuroinvasive Route of Entry for Severe Acute Respiratory Syndrome Coronavirus 2 to the Brain

The BBB tightly regulates the movement of molecules, ions, and cells between blood and the CNS and prevents the neurotoxic components of plasma, blood cells, and pathogens from entering the brain (Montagne et al., 2017). This regulatory characteristic is attributed to the arteries, arterioles, and capillaries that supply blood to the brain and that act in response to neuronal stimuli that trigger an increased rate of neurovascular coupling, a mechanism generated by the cerebral blood flow and the supply of oxygen. The neurovascular unit is made up of the following structural components: vascular cells (endothelium and wall cells, pericytes, and smooth muscle cells); glia (astrocytes and microglia); and neurons (Kisler et al., 2017; Sweeney et al., 2019; Sanchez-Cano et al., 2021). The regulation conducted by the BBB provides strict control over the cellular permeability of neuronal tissues, which is essential for proper neuronal function and which, furthermore, requires precise ionic concentrations in the surrounding environment (Daneman, 2012; Daneman and Prat, 2015). Therefore, the loss of homeostatic regulation and deterioration in the restrictive capacity of the BBB play important roles in the progression of neurological conditions such as brain trauma, and infectious and neurodegenerative diseases (Sanchez-Cano et al., 2021).

It is of particular interest to note that the ACE2 and TMPRSS2 receptors are expressed in the endothelial cells of the BBB (Chen R. et al., 2020; Qiao et al., 2020; Torices et al., 2021). Due to these findings and the interaction of the virus with the protein complex discussed earlier in this paper, it has been suggested that SARS-CoV-2 could reach the brain *via* systemic circulation by crossing the BBB and damage the choroid plexus (Baig, 2020; Pellegrini et al., 2020). The actual hematogenous mechanism by which SARS-CoV-2 gains entry to brain is not known. However, several mechanisms have been suggested (Achar and Ghosh, 2020; Pellegrini et al., 2020). These include: (a) transcellular migration, where the virus invades the host's endothelial cells and is able to cross the BBB; (b) paracellular migration, where the virus invades the choroid plexus of the fenestrated endothelial cells and gets into the brain; and (c) the "Trojan horse" strategy, where the virus is internalized by phagocytic immune cells such as neutrophils and macrophages, and is subsequently replicated in the brain (Dahm et al., 2016; **Figure 2C**). Moreover, is likely that SARS-CoV-2 invades the brain by damaging the integral architecture of the BBB (Varghese et al., 2020). Thus, SARS-CoV-2 can get access into the brain by one or a combination of the above mechanisms.

Evidence of Neuroinvasive Mechanisms of Severe Acute Respiratory Syndrome Coronavirus 2 in Animal Models

Both the symptoms presented by infected patients and the findings of clinical pathology provide evidence of possible infection of the CNS by SARS-CoV-2. However, to further explore the viral pathogenesis in the host and characterize the mechanisms of viral access and dissemination in the CNS, a translational neuroscience approach (Johansen et al., 2020; Sanclemente-Alaman et al., 2020), similar to that employed in the early research conducted on SARS and MERS is necessary (Callaway, 2020; Natoli et al., 2020).

Because SARS-CoV-2 has a higher affinity for the human ACE2 receptor (hACE2) than animal ACE2, few studies have been carried out in animal models to determine the neuroinvasive pathways of the virus (Wan et al., 2020). In addition, hACE2 is structurally different from that in animal species. Hence, a significantly lower level of tropism is noted in animal vs. human tissue, particularly in relation to CNS (Natoli et al., 2020). Indeed, Brann et al. (2020) demonstrated that the olfactory sensory neurons of the whole olfactory mucosa of mice, unlike olfactory epithelial support cells, stem cells, and the cells of the nasal respiratory epithelium, do not express ACE2 and TMPRSS2 genes. Thus, it is argued that based off of animal studies, anosmia or other forms of olfactory dysfunction may not support olfactory bulb as an entry route for SARS-CoVs into the CNS (Brann et al., 2020; Natoli et al., 2020).

To overcome the discrepancy between animal and human studies, several animal models with closer resemblance to that of humans have been suggested. One suggestion is to develop humanized mouse models that express the hACE2 receptor (Sun et al., 2020), as the murine is the most widely used animal model for this purpose (Muñoz-Fontela et al., 2020). Another suggestion is to modify the SARS-CoV-2 spike to effectively bind with murine-ACE2 (Dinnon et al., 2020), however, this strategy is risky, since modifying the viruses can create a natural reservoir for a virus that might be completely different from the wild-type version. A third suggestion is to induce mice to be susceptible to SARS-CoV-2 infection by sensitizing the respiratory tract to the virus. The latter may be achieved *via* transduction with adenovirus or associated viruses that express hACE2 (Ad5-hACE2 or AAV-hACE2, respectively) (Israelow et al., 2020; Rathnasinghe et al., 2020). In all these suggestions, however, as mentioned earlier, it must be borne in mind that the co-expression of the ACE2 and TMPRSS2 receptors is necessary for the virus to be internalized.

It was recently demonstrated that neuroinvasion by SARS-CoV-2 could be achieved in an animal model where hACE2 was overexpressed by means of an adeno-associated virus infection (Song et al., 2021). Moreover, the neuronal infection could be prevented by blocking ACE2 with neutralizing antibodies or administering cerebrospinal fluid obtained from a COVID-19 patient, where presumably antibodies were present (Song et al., 2021). A recent study reported differences in the neuroinvasiveness and neurovirulence among the most relevant SARS-CoV-2 variants, D614G, Delta (B.1.617.2), and Omicron (B.1.1.529) 5 days post inoculation in a hamster model. The results showed that D614G variant had a high neuroinvasion *via* the olfactory nerve compared to the Delta and Omicron variants (Bauer et al., 2022b). While the results obtained provide evidence for the neuroinvasive capacity of SARS-CoV-2 in an animal model, the sequence of infection in different CNS cell types has

not yet been determined. Therefore, more studies on detailed mechanism (s) of SARS-CoV-2 infection of the CNS are needed.

NEUROPATHOLOGICAL FEATURES OF SEVERE ACUTE RESPIRATORY SYNDROME CORONAVIRUS 2

SARS-CoV-2 has been reported to manifest neurological symptoms that range from mild to fatal, while it can also occur asymptomatically in patients. Clinical studies conducted on patients hospitalized with COVID-19 report a level of neurological manifestation ranging from 15.2% (Flores-Silva et al., 2021), or 36.4% (Mao et al., 2020) to 54.7% (Romero-Sánchez et al., 2020), and up to 88% (García-Moncó et al., 2021). It should be noted that the frequency of neurological alterations observed in patients with COVID-19 depends on whether they have been evaluated by a neurologist and/or inclusion of patients with a history of neurological complication.

The most common early neurological manifestations in patients with COVID-19 are headache, dizziness, nausea, vomiting, myalgia, and neuralgia (Guan et al., 2020; Mao et al., 2020; Wang et al., 2020; Song et al., 2021). Anosmia and dysgeusia develop in the early stages of infection and are more frequent in less severe cases (Mao et al., 2020; Flores-Silva et al., 2021; García-Moncó et al., 2021). Late-infection neurological manifestations include acute cerebrovascular disease, meningoencephalitis, impaired consciousness, and skeletal muscle injury (Al Saiegh et al., 2020; Guan et al., 2020; Guidon and Amato, 2020; Parikh et al., 2020). Less-frequently reported symptoms include dysautonomia, seizures, movement disorders, Guillain Barré syndrome, Miller Fisher syndrome, and optic neuritis (Gutiérrez-Ortiz et al., 2020; Hwang et al., 2020; Manji et al., 2020). In addition, the University College London Queen Square Institute of Neurology has reported five categories of clinical presentations at a neurological level: (1) encephalopathy with delirium/psychosis and no magnetic resonance imaging or cerebrospinal fluid abnormalities; (2) inflammatory CNS syndromes including encephalitis and acute disseminated encephalomyelitis; (3) ischemic strokes; (4) peripheral neurological disorders including Guillain–Barré syndrome and brachial plexopathy; and (5) miscellaneous central nervous disorders (Paterson et al., 2020; Gasmi et al., 2021). Thus, neurological manifestations are variable and not uncommon in COVID-19 patients. Moreover, both morphological and biochemical pathological changes may be manifested as detailed below.

Morphological Changes

Research on the clinical and imaging aspects of COVID-19 infection as well as molecular biology studies conducted on both *in vitro* and *in vivo* models have provided valuable information in understanding the etiological mechanisms of SARS-CoV-2. However, despite the large amount of information available on the disease, there is little work conducted to characterize its pathological manifestations in the tissues of different systems of the body (Al Nemer, 2020; Skok et al., 2021; **Table 1**). Studies carried out on the anatomical brain pathology during autopsy reveal morphological alterations in the frontal and occipital lobes, olfactory bulb, cingulate gyrus, corpus callosum, hippocampus, basal ganglia, thalamus, cerebellum, midbrain, middle pons, medulla, brainstem, and the lateral ventricles (Barone et al., 2021; Caramaschi et al., 2021; Generoso et al., 2021). The most common gross findings are edema (Reichard et al., 2020), hemorrhagic lesions (Paniz-Mondolfi et al., 2020; Reichard et al., 2020), hydrocephalus (Lacy et al., 2020), atrophy and low brain mass (Lax et al., 2020; Wichmann et al., 2020), olfactory bulb asymmetry (Coolen et al., 2020), and infarcts (Solomon et al., 2020). SARS-CoV-2 has also been found to cause lesions and alterations in neuronal structures, while neuronal infection can cause encephalitis and the generation of lethal microthrombi (Bradley et al., 2020; von Weyhern et al., 2020). In addition, severe COVID-19 infection accompanied by multisystem inflammatory syndrome may cause fibrotic lesions and generate cerebral thrombosis (Turski et al., 2020).

Various studies have been carried out to ascertain the structural modifications in the brains of COVID-19 patients. Magnetic resonance techniques have shown a bilateral obliteration of the olfactory cleft in 50% of SARS-CoV-2-positive patients as well as a sudden loss of smell and subtle olfactory bulb asymmetry in 25% of the sampled patients (Niesen et al., 2021). Another study demonstrated microstructural changes using diffusion tensor imaging (DTI) and 3D high-resolution T1WI sequences in COVID-19 patients, where greater volume of bilateral gray matter (reported as gray matter volume) was observed in the hippocampus, olfactory cortices, insula, left rolandic operculum, left Heschl gyrus, and right cingulate gyrus (Lu Y. et al., 2020). These findings demonstrate possible alterations in the structural and functional integrity of brain microstructures in susceptible patients, and also suggest potential long-term consequences of SARS-CoV-2 infection, which may lead to or accelerate a variety of neurodegenerative diseases (ElBini Dhouib, 2021), discussed further below.

Molecular and Biochemical Changes

Given that most cases of SARS-CoV-2 infection present mild or moderate symptoms and that a group with severe infections develops multiple systemic dysfunctions as a consequence of imbalances in the immune and the oxidation-reduction systems, it is not surprising that inflammatory states and oxidative stress are commonly indicated in pathogenesis of COVID-19 (Mrityunjaya et al., 2020; Forcados et al., 2021). In addition, hyperactivation of the immune system leading to an exaggerated release of pro-inflammatory cytokines referred to as "cytokine storm" is not only associated with severe complications, but also poorer outcome (Chen G. et al., 2020; Noroozi et al., 2020; Tan et al., 2021; Yang et al., 2021).

Both the innate and adaptive immune systems have been widely described as working together, with the innate response representing the host's first line of defense and the adaptive response becoming prominent several days after infection, when T and B cells have undergone clonal expansion (Strbo et al., 2014). Furthermore, the components of the innate system contribute to the activation of antigen-specific cells, which amplify their

TABLE 1 | CNS damage by SARS-CoV-2 suggesting susceptibility to Parkinson's and Alzheimer's disease.

Characteristics	Alzheimer's disease	Parkinson's disease	References
Affected brain regions (Autopsy findings)	Hippocampus, cortex (Frontal, occipital, and cingulate), insula.	Midbrain, basal ganglia, thalamus.	Solomon et al., 2020; von Weyhern et al., 2020; Generoso et al., 2021
Brain morphological and macroscopic changes	Edema, hemorrhagic lesions, hydrocephalus, atrophy and low brain mass, infarcts.		Paniz-Mondolfi et al., 2020; Reichard et al., 2020; Wichmann et al., 2020
Brain regions expressing ACE2 and TMPRSS2	Prefrontal cortex, hippocampus.	Striatum (Human brain), SNpr, SNpc (mouse brain)	Chen R. et al., 2020; Qiao et al., 2020
Intracellular SARS-CoV-2	Frontal cortex	No findings report	Paniz-Mondolfi et al., 2020; Liu J. M. et al., 2021
Biochemical markers	Glia and microglia response, cytokine storm (increased interleukins IL-1β, IL-6, IL-8, IL-12, IL-17, IL-18). Oxidative stress in various brain regions such as BBB and neurons susceptible to cell death.		Chaudhry et al., 2020; Almutairi et al., 2021;Chiricosta et al., 2021; Frank et al., 2022

SNpr, substantia nigra pars reticulate; SNpc, substantia nigra pars compacta; IL, interleukin.

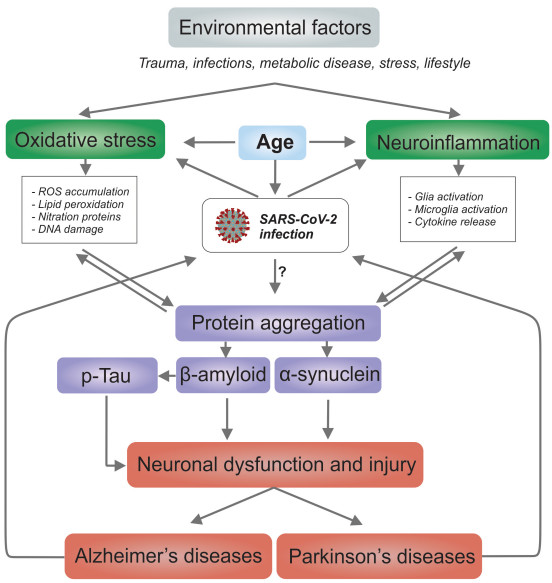

FIGURE 3 | SARS-CoV-2 infection and possible links for both Alzheimer's and Parkinson's disease. The common risk factors between COVID-19 and neurodegenerative diseases is the age; the oxidative stress; and, neuroinflammation. It's possible that COVID-19 patients are more susceptible to developing neurodegenerative diseases and that patients with neurodegenerative diseases are more susceptible to contracting COVID-19.

responses in order to achieve complete control over the pathogen by recruiting innate effector mechanisms. Therefore, the innate and adaptive responses are fundamentally different, although the synergy between them is essential for an effective immune response (Chaplin, 2010). Patients with severe SARS-CoV-2 infection manifest an increased innate immune response and a suppressed adaptive immunity, which is why a delayed elimination of the virus from the organism is observed (Pan Y. et al., 2021). This scenario aggravates the immune status of the patient as it increases the levels of various inflammatory factors and increases both the number and activation of immune cells at the site of the inflammation, a process from which cytokine storm originates (Catanzaro et al., 2020; Chen R. et al., 2021).

Neurons infected by SARS-CoV-2 release inflammatory mediators that are capable of activating adjacent cells such as glia, microglia, mast cells and endothelial cells, conditions which constitute the beginning of neuroinflammation (Almutairi et al., 2021; Frank et al., 2022). Elevated immunological mediators during SARS-CoV-2 infection include: tumor necrosis factor α (TNF-α); interferon gamma (INFγ); a series of chemokines such as CCL-2, CCL-5, and CXCL-10; a series of interleukins such as IL-1β, IL-6, IL-8, IL-12, IL-17, IL-18, and IL-33; and granulocyte macrophage colony stimulating factor (GM-CSF) (Kempuraj et al., 2020; Mehta and Fajgenbaum, 2021; Tripathy et al., 2021). SARS-CoV-2 infection induces the down-regulation of ACE2, disrupting the physiological balance between ACE/ACE2 and angiotensin II (Ang-II)/angiotensin and leading to severe multiple organ injury (Mehrabadi et al., 2021). In fact, it has been suggested that ACE2 downregulation may contribute to the pathogenesis of lung injury in COVID-19 (Ni et al., 2020). Angiotensin II stimulates gene expression of multiple inflammatory cytokines such as TNF-α and IL-6. TNF-α, in particular, induces macrophage differentiation of a pro-inflammatory phenotype, which exerts an antimicrobial effect. However, such differentiated macrophages are also responsible for recruiting more cell types *via* cytokine secretion, thus exacerbating the inflammatory response. Similarity, IL-6, essential for T cell differentiation, when elevated, signals a poorer SARS-CoV-2 prognosis (Banu et al., 2020; Patra et al., 2020; Ben Moftah and Eswayah, 2022).

Additionally, the pro-inflammatory factors discussed above are able to cross the BBB, increase vascular permeability, and trigger further release of pro-inflammatory cytokines from the microglia (da Fonseca et al., 2014; Zhang et al., 2021). This cascade results in increased apoptotic activity, increased levels of reactive oxygen species (ROS), mitochondrial dysfunction and eventual neurodegeneration (Chaudhry et al., 2020; Chiricosta et al., 2021; Kumar et al., 2021). Moreover, the high concentration of pro-inflammatory cytokines can lead to the activation of the coagulation cascade, suppression of anticoagulant factors, and hence increase the chance of thrombosis (Al Saiegh et al., 2020; Levi et al., 2020). An opposite scenario may also manifest itself where an increase in fibrinolytic activity leading to an increase in the level of fibrin degradation and hemorrhagic conditions

including aneurysms may be observed in certain patients infected with SARS-CoV-2 (Al Saiegh et al., 2020).

SEVERE ACUTE RESPIRATORY SYNDROME CORONAVIRUS 2 AND NEURODEGENERATIVE DISEASE

The link between systemic and central inflammation, as well as between neurological and neuropsychiatric diseases, is well known (Hurley and Tizabi, 2013; Schwartz and Deczkowska, 2016; Skaper et al., 2018). In nervous tissue, the increased levels of inflammatory mediators and glial cell activity caused by SARS-CoV-2 infection may pose an increased risk of neurodegenerative disease such as Alzheimer's disease (AD), Parkinson's disease (PD) as well as multiple sclerosis (MS), stroke and neurological trauma (Mohammadi et al., 2020; Li et al., 2021; Tekiela and Majersik, 2021). SARS-CoV-2 infection in people with senility is likely to increase the neuropathological intensity and contribute to the worsening of motor and cognitive deficits (Wang Y. et al., 2021; Yu et al., 2021). Indeed, one of the main risk factors for both COVID-19 and neurodegenerative disease is age (Ferini-Strambi and Salsone, 2021; **Figure 3**). Older people comprise the section of the population most prone to developing neurodegenerative diseases (Hou et al., 2019) and present with more severe clinical reaction to COVID-19 (Lebrasseur et al., 2021). In addition, lifestyle and preexisting conditions such as trauma, infection, metabolic disease, and stress can accelerate the onset and progression of neurodegenerative diseases (Graham and Sharp, 2019; Madore et al., 2020; Lotz et al., 2021).

It is important to note that protein aggregation in the brain is considered as one of the main reasons behind neurodegeneration. Protein aggregation has been observed for tau protein and Aβ peptide in AD; and α-synuclein for PD. The aggregation process spreads from one cell to another, and the aggregates and deposits formed impair brain function. It is unclear whether viral infections directly or indirectly cause neurodegeneration (Liu S. et al., 2021). However, it has been suggested that viruses can initiate pathological protein aggregation *via* a direct mechanism in Aβ peptide aggregation *in vitro* and in animal models infected with HSV-1 and respiratory syncytial virus (Ezzat et al., 2019). A recent study has shown direct interactions between the N-protein of SARS-CoV-2 and α-synuclein as the molecular basis for the observed correlation between SARS-CoV-2 infections and parkinsonism (Semerdzhiev et al., 2022). Given that cell-surface glycans function as initial, usually low-affinity attachment factors, these receptors play key roles in SARS-CoV-2 infection (Koehler et al., 2020; Prasad et al., 2021). Moreover, the ability of S1 protein of SARS-CoV-2 to interact with heparin receptor can lead to many misfolded brain proteins including amyloid complex and ultimately lead to neurodegeneration (Tavassoly et al., 2020; Idrees and Kumar, 2021).

Alzheimer's Disease

One of the main causes of disability among older people around the world is dementia, with AD as the most common form (Alzheimer's-Association, 2020). The mechanisms involved in the pathogenesis of AD are complex and not fully understood. However, the most accepted hypothesis involves molecular changes such as extracellular deposition of the β-amyloid protein and intracellular phosphorylation of the tau protein, causing the formation of amyloid plaques and neurofibrillary tangles, respectively (Liu et al., 2019). In addition, intense neuroinflammation, oxidative stress, mitochondrial dysfunction, and protein misfolding have also been implicated (Gandhi et al., 2019; Perez Ortiz and Swerdlow, 2019; Leng and Edison, 2021; **Figure 3**). Patients with AD are more susceptible to contracting COVID-19 (Finelli, 2021; Pan A. P. et al., 2021; Wang Q. et al., 2021), and COVID-19 patients are more susceptible to developing AD (Brown et al., 2020; Chiricosta et al., 2021; Villa et al., 2022). This might not be surprising due to the presence of common risk factors such as age, cardiovascular disease, metabolic, and psychological disorders between the two diseases (Brown et al., 2020; Finelli, 2021). Generally, inflammation increases with age, wherein higher levels of pro-inflammatory cytokines have been quantified in older people (Niraula et al., 2017; Rea et al., 2018). Furthermore, given that infection with a wide variety of pathogens is suspected to be a risk factor for the onset of AD (Seaks and Wilcock, 2020; Vigasova et al., 2021), an increased risk of developing AD and cognitive impairment in susceptible populations after SARS-CoV-2 infection would also be expected. Moreover, these patients often face social stigma and mental stress, which can further aggravate neuroinflammatory processes and result in psychiatric disorders (Justice, 2018; Milligan Armstrong et al., 2021). The presence of pathogens and other factors such as age, alcohol and tobacco consumption, cerebral hypoxia, metabolic diseases, pollution, sedentary lifestyle, or sleep disorders may cause BBB malfunction (Noe et al., 2020; Hussain et al., 2021), and hence lead to the infiltration of neurotoxic proteins such as the β-amyloid peptide (Wang D. et al., 2021). SARS-CoV-2 infection accompanied by a local immune response incorporating astrocytes and microglia could generate a state of neuroinflammation in susceptible patients that can manifest for a long term (Kumar et al., 2021; Villa et al., 2022). Such a scenario would be expected to exacerbate the current pathology in AD patients.

Genetically, apolipoprotein E ε4 allele (APOE4) has been determined the strongest risk factor for AD (Serrano-Pozo et al., 2021). Furthermore, APOE4 has been associate with increased susceptibility to SARS-CoV-2 infection and COVID-19 (Kurki et al., 2021). Cerebral microvasculature complications may be the basis of neurological issues in hospitalized COVID-19 patients (Miners et al., 2020; Lee et al., 2021). Interestingly APOE4 is also involved in BBB dysfunction and cerebrovascular diseases (Montagne et al., 2021). However, further research is needed to determine the exact role of APOE4 in COVID-19-induced AD.

Parkinson's Disease

Similar to AD, PD is related to COVID-19, sharing risk factors such as advanced age, cardiovascular and metabolic diseases (Park et al., 2020; Fearon and Fasano, 2021; Sharifi et al., 2021). Moreover, patients with PD may be immunosuppressed, which makes them more susceptible to infections of any type including

SARS-CoV-2 (Tansey and Romero-Ramos, 2019; Prasad et al., 2020).

Histologically, PD is characterized by the loss of dopaminergic neurons in the *substantia nigra pars compacta* (SNpc) and cytoplasmic inclusions, mainly composed of α-synuclein aggregates called Lewy bodies (Henderson et al., 2019; **Figure 3**). Although the precise etiology of PD is not well known, some hypotheses for its pathogenesis and development point to oxidative stress, neuroinflammation, mitochondrial dysfunction, synaptic pathogenesis, and also as a result of infection (Hurley and Tizabi, 2013; Meng et al., 2019). As patients in an advanced stage of PD have difficulties in chewing and swallowing, they commonly experience salivary accumulation and aspiration (Kwon and Lee, 2019). In addition, the stiffness of the chest wall common in PD inhibits the cough reflex, forming a favorable environment for SARS-CoV-2 infection. In the most severe cases, SARS-CoV-2 infection progresses to pneumonia, which is one of the leading causes of death in PD patients (Bhidayasiri et al., 2020). It is already well known that various viral infections can accentuate the pathological sequelae of PD (Jang et al., 2009).

Recently, a study demonstrated the ability of the H1N1 influenza virus to block protein degradation pathways and promoting the formation of α-synuclein aggregates in dopaminergic neurons *in vitro* (Marreiros et al., 2020), and a more recent study provided similar results in an *in vivo* model (Bantle et al., 2021). Furthermore, increased amounts of phosphorylated α-synuclein, activation of microglia and astrocytes, and selective loss of dopaminergic neurons in the SNpc with behavioral and motor consequences have been observed as secondary consequences of infection with the western equine encephalitis virus (WEEV) (Bantle et al., 2019). Thus, it is not unreasonable to expect similar consequences with SARS-CoV-2 infection (Chaná-Cuevas et al., 2020). Moreover, COVID-19 pandemic causing at least partial confinement and social distancing may not only limit the mobility but may also aggravate depression, mental stress, and loneliness in PD patients. It is noteworthy that there exists a substantial co-morbid condition of PD and depression (Tizabi et al., 2019, 2021).

IMMEDIATE PROSPECTS

In this article, we have reviewed the possible routes by means of which SARS-Cov-2 may enter the CNS, including transcribrial or the ocular surface, and the hematogenous neuroinvasive pathways. The increased occurrence of neuroinflammation, oxidative stress, and cytokine storm caused by the virus also increases the level of cellular damage in the CNS, thus increasing the risk of developing neurodegenerative diseases such as AD and PD. Further studies on effects of SARS-CoV-2 and its variants on protein aggregation, glia or microglia activation, BBB damage, oxidative stress, and neuroinflammation is warranted.

AUTHOR CONTRIBUTIONS

JS, FP, AP-M, and IL designed the sections and contents of the review article. IL and FP oversaw the organization to distribute the writing tasks among the authors and participated in article writing. FP made all the figures. JS, FP, AP-M, GS-L, LC, YT, and IL performed literature search and participated in the article writing. All authors critically reviewed and approved the final version of the article.

FUNDING

This study was supported by grants from the BUAP *Vicerrectoría de Investigación y Estudios de Posgrado* (Vice-rectory for Research and Postgraduate Study) 2021–2022, awarded to IL, while the support provided *via* CONACYT-Mexico grant (732793) was awarded to FP.

REFERENCES

Abdelrahman, Z., Li, M., and Wang, X. (2020). Comparative review of SARS-CoV-2. SARS-CoV, MERS-CoV, and influenza a respiratory viruses. *Front. Immunol.* 11:552909. doi: 10.3389/fimmu.2020.552909

Achar, A., and Ghosh, C. (2020). COVID-19-associated neurological disorders: the potential route of CNS invasion and blood-brain relevance. *Cells* 9:2360. doi: 10.3390/cells9112360

Al Nemer, A. (2020). Histopathologic and autopsy findings in patients diagnosed with coronavirus disease 2019 (COVID-19): what we know so far based on correlation with clinical, morphologic and pathobiological aspects. *Adv. Anat. Pathol.* 27, 363–370. doi: 10.1097/PAP.0000000000000276

Al Saiegh, F., Ghosh, R., Leibold, A., Avery, M. B., Schmidt, R. F., Theofanis, T., et al. (2020). Status of SARS-CoV-2 in cerebrospinal fluid of patients with COVID-19 and stroke. *J. Neurol. Neurosurg. Psychiatry* 91, 846–848. doi: 10.1136/jnnp-2020-323522

Almutairi, M. M., Sivandzade, F., Albekairi, T. H., Alqahtani, F., and Cucullo, L. (2021). Neuroinflammation and its impact on the pathogenesis of COVID-19. *Front. Med.* 8:745789. doi: 10.3389/fmed.2021.745789

Alzheimer's-Association (2020). 2020 Alzheimer's disease facts and figures. *Alzheimers Dement* 16, 391–460. doi: 10.1002/alz.12068

Ansariniya, H., Seifati, S. M., Zaker, E., and Zare, F. (2021). Comparison of immune response between SARS, MERS, and COVID-19 infection, perspective on vaccine design and development. *Biomed. Res. Int.* 2021:8870425. doi: 10.1155/2021/8870425

Arbour, N., Day, R., Newcombe, J., and Talbot, P. J. (2000). Neuroinvasion by human respiratory coronaviruses. *J. Virol.* 74, 8913–8921. doi: 10.1128/jvi.74.19.8913-8921.2000

Arya, R., Kumari, S., Pandey, B., Mistry, H., Bihani, S. C., Das, A., et al. (2021). Structural insights into SARS-CoV-2 proteins. *J. Mol. Biol.* 433:166725. doi: 10.1016/j.jmb.2020.11.024

Baig, A. M. (2020). Neurological manifestations in COVID-19 caused by SARS-CoV-2. *CNS Neurosci. Ther.* 26, 499–501. doi: 10.1111/cns.13372

Bantle, C. M., French, C. T., Cummings, J. E., Sadasivan, S., Tran, K., Slayden, R. A., et al. (2021). Manganese exposure in juvenile C57BL/6 mice increases glial inflammatory responses in the substantia nigra following infection with H1N1 influenza virus. *PLoS One* 16:e0245171. doi: 10.1371/journal.pone.0245171

Bantle, C. M., Phillips, A. T., Smeyne, R. J., Rocha, S. M., Olson, K. E., and Tjalkens, R. B. (2019). Infection with mosquito-borne alphavirus induces selective loss of dopaminergic neurons, neuroinflammation and widespread protein aggregation. *NPJ Parkinsons Dis.* 5:20. doi: 10.1038/s41531-019-0090-8

Banu, N., Panikar, S. S., Leal, L. R., and Leal, A. R. (2020). Protective role of ACE2 and its downregulation in SARS-CoV-2 infection leading to macrophage

activation syndrome: therapeutic implications. *Life Sci.* 256:117905. doi: 10.1016/j.lfs.2020.117905

Barone, R., Marino Gammazza, A., Paladino, L., Pitruzzella, A., Spinoso, G., Salerno, M., et al. (2021). Morphological alterations and stress protein variations in lung biopsies obtained from autopsies of COVID-19 subjects. *Cells* 10:3136. doi: 10.3390/cells10113136

Bauer, L., Laksono, B. M., de Vrij, F. M. S., Kushner, S. A., Harschnitz, O., and van Riel, D. (2022a). The neuroinvasiveness, neurotropism, and neurovirulence of SARS-CoV-2. *Trends Neurosci.* 45:6.doi: 10.1016/j.tins.2022.02.006

Bauer, L., Rissmann, M., Benavides, F. F. W., Lonneke, L., Leijten, L., Begeman, L., et al. (2022b). Differences in neuroinflammation in the olfactory bulb between D614G, Delta and Omicron BA.1 SARS-CoV-2 variants in the hamster model. *biorxiv [Preprint]*. doi: 10.1101/2022.03.24.485596

Ben Moftah, M., and Eswayah, A. (2022). Intricate relationship between SARS-CoV-2-induced shedding and cytokine storm generation: a signaling inflammatory pathway augmenting COVID-19. *Health Sci. Rev.* 2:100011. doi: 10.1016/j.hsr.2021.100011

Benveniste, H., Liu, X., Koundal, S., Sanggaard, S., Lee, H., and Wardlaw, J. (2019). The glymphatic system and waste clearance with brain aging: a review. *Gerontology* 65, 106–119. doi: 10.1159/000490349

Beyrouti, R., Adams, M. E., Benjamin, L., Cohen, H., Farmer, S. F., Goh, Y. Y., et al. (2020). Characteristics of ischaemic stroke associated with COVID-19. *J. Neurol. Neurosurg. Psychiatry* 91, 889–891. doi: 10.1136/jnnp-2020-323586

Bhidayasiri, R., Virameteekul, S., Kim, J. M., Pal, P. K., and Chung, S. J. (2020). COVID-19: an early review of its global impact and considerations for parkinson's disease patient care. *J. Mov. Disord.* 13, 105–114. doi: 10.14802/jmd.20042

Bougakov, D., Podell, K., and Goldberg, E. (2021). Multiple neuroinvasive pathways in COVID-19. *Mol. Neurobiol.* 58, 564–575. doi: 10.1007/s12035-020-02152-5

Bradley, B. T., Maioli, H., Johnston, R., Chaudhry, I., Fink, S. L., Xu, H., et al. (2020). Histopathology and ultrastructural findings of fatal COVID-19 infections in Washington State: a case series. *Lancet* 396, 320–332. doi: 10.1016/S0140-6736(20)31305-2

Brann, D. H., Tsukahara, T., Weinreb, C., Lipovsek, M., Van den Berge, K., Gong, B., et al. (2020). Non-neuronal expression of SARS-CoV-2 entry genes in the olfactory system suggests mechanisms underlying COVID-19-associated anosmia. *Sci. Adv.* 6:eabc5801. doi: 10.1126/sciadv.abc5801

Bridwell, R., Long, B., and Gottlieb, M. (2020). Neurologic complications of COVID-19. *Am. J. Emerg. Med.* 38, e1549e3–e1549e7. doi: 10.1016/j.ajem.2020.05.024

Brown, E. E., Kumar, S., Rajji, T. K., Pollock, B. G., and Mulsant, B. H. (2020). Anticipating and mitigating the impact of the COVID-19 pandemic on alzheimer's disease and related dementias. *Am. J. Geriatr. Psychiatry* 28, 712–721. doi: 10.1016/j.jagp.2020.04.010

Bulfamante, G., Bocci, T., Falleni, M., Campiglio, L., Coppola, S., Tosi, D., et al. (2021). Brainstem neuropathology in two cases of COVID-19: SARS-CoV-2 trafficking between brain and lung. *J. Neurol.* 268, 4486–4491. doi: 10.1007/s00415-021-10604-8

Callaway, E. (2020). Labs rush to study coronavirus in transgenic animals - some are in short supply. *Nature* 579:183. doi: 10.1038/d41586-020-00698-x

Cantuti-Castelvetri, L., Ojha, R., Pedro, L. D., Djannatian, M., Franz, J., Kuivanen, S., et al. (2020). Neuropilin-1 facilitates SARS-CoV-2 cell entry and infectivity. *Science* 370, 856–860. doi: 10.1126/science.abd2985

Caramaschi, S., Kapp, M. E., Miller, S. E., Eisenberg, R., Johnson, J., Epperly, G., et al. (2021). Histopathological findings and clinicopathologic correlation in COVID-19: a systematic review. *Mod. Pathol.* 34, 1614–1633. doi: 10.1038/s41379-021-00814-w

Carvalho, T., Krammer, F., and Iwasaki, A. (2021). The first 12 months of COVID-19: a timeline of immunological insights. *Nat. Rev. Immunol.* 21, 245–256. doi: 10.1038/s41577-021-00522-1

Catanzaro, M., Fagiani, F., Racchi, M., Corsini, E., Govoni, S., and Lanni, C. (2020). Immune response in COVID-19: addressing a pharmacological challenge by targeting pathways triggered by SARS-CoV-2. *Signal Transduct. Target. Ther.* 5:84. doi: 10.1038/s41392-020-0191-1

Chaná-Cuevas, P., Salles-Gándara, P., Rojas-Fernandez, A., Salinas-Rebolledo, C., and Milán-Solé, A. (2020). The potential role of SARS-COV-2 in the pathogenesis of parkinson's disease. *Front. Neurol.* 11:1044. doi: 10.3389/fneur.2020.01044

Chaplin, D. D. (2010). Overview of the immune response. *J. Allergy Clin. Immunol.* 125(2 Suppl. 2), S3–S23. doi: 10.1016/j.jaci.2009.12.980

Chaudhry, Z. L., Klenja, D., Janjua, N., Cami-Kobeci, G., and Ahmed, B. Y. (2020). COVID-19 and parkinson's disease: shared inflammatory pathways under oxidative stress. *Brain Sci.* 10:807. doi: 10.3390/brainsci10110807

Chen, G., Wu, D., Guo, W., Cao, Y., Huang, D., Wang, H., et al. (2020). Clinical and immunological features of severe and moderate coronavirus disease 2019. *J. Clin. Invest.* 130, 2620–2629. doi: 10.1172/JCI137244

Chen, R., Lan, Z., Ye, J., Pang, L., Liu, Y., Wu, W., et al. (2021). Cytokine storm: the primary determinant for the pathophysiological evolution of COVID-19 deterioration. *Front. Immunol.* 12:589095. doi: 10.3389/fimmu.2021.589095

Chen, R., Wang, K., Yu, J., Howard, D., French, L., Chen, Z., et al. (2020). The spatial and cell-type distribution of SARS-CoV-2 receptor ACE2 in the human and mouse brains. *Front. Neurol.* 11:573095. doi: 10.3389/fneur.2020.573095

Chen, X., Yu, H., Mei, T., Chen, B., Chen, L., Li, S., et al. (2021). SARS-CoV-2 on the ocular surface: is it truly a novel transmission route? *Br. J. Ophthalmol.* 105, 1190–1195. doi: 10.1136/bjophthalmol-2020-316263

Chiricosta, L., Gugliandolo, A., and Mazzon, E. (2021). SARS-CoV-2 exacerbates beta-amyloid neurotoxicity, inflammation and oxidative stress in alzheimer's disease patients. *Int. J. Mol. Sci.* 22:13603. doi: 10.3390/ijms222413603

Collin, J., Queen, R., Zerti, D., Dorgau, B., Georgiou, M., Djidrovski, I., et al. (2021). Co-expression of SARS-CoV-2 entry genes in the superficial adult human conjunctival, limbal and corneal epithelium suggests an additional route of entry via the ocular surface. *Ocul. Surf.* 19, 190–200. doi: 10.1016/j.jtos.2020.05.013

Coolen, T., Lolli, V., Sadeghi, N., Rovai, A., Trotta, N., Taccone, F. S., et al. (2020). Early postmortem brain MRI findings in COVID-19 non-survivors. *Neurology* 95, e2016–e2027. doi: 10.1212/WNL.0000000000010116

Coroneo, M. T. (2021). The eye as the discrete but defensible portal of coronavirus infection. *Ocul. Surf.* 19, 176–182. doi: 10.1016/j.jtos.2020.05.011

da Fonseca, A. C., Matias, D., Garcia, C., Amaral, R., Geraldo, L. H., Freitas, C., et al. (2014). The impact of microglial activation on blood-brain barrier in brain diseases. *Front. Cell Neurosci.* 8:362. doi: 10.3389/fncel.2014.00362

Dahm, T., Rudolph, H., Schwerk, C., Schroten, H., and Tenenbaum, T. (2016). Neuroinvasion and inflammation in viral central nervous system infections. *Mediators Inflamm.* 2016:8562805. doi: 10.1155/2016/8562805

Daly, J. L., Simonetti, B., Klein, K., Chen, K. E., Williamson, M. K., Antón-Plágaro, C., et al. (2020). Neuropilin-1 is a host factor for SARS-CoV-2 infection. *Science* 370, 861–865. doi: 10.1126/science.abd3072

Daneman, R. (2012). The blood-brain barrier in health and disease. *Ann. Neurol.* 72, 648–672. doi: 10.1002/ana.23648

Daneman, R., and Prat, A. (2015). The blood-brain barrier. *Cold Spring Harb. Perspect. Biol.* 7:a020412. doi: 10.1101/cshperspect.a020412

Davies, J., Randeva, H. S., Chatha, K., Hall, M., Spandidos, D. A., Karteris, E., et al. (2020). Neuropilin−1 as a new potential SARS−CoV−2 infection mediator implicated in the neurologic features and central nervous system involvement of COVID−19. *Mol. Med. Rep.* 22, 4221–4226. doi: 10.3892/mmr.2020.11510

De Chiara, G., Marcocci, M. E., Sgarbanti, R., Civitelli, L., Ripoli, C., Piacentini, R., et al. (2012). Infectious agents and neurodegeneration. *Mol. Neurobiol.* 46, 614–638. doi: 10.1007/s12035-012-8320-7

de Freitas Santoro, D., de Sousa, L. B., Câmara, N. O. S., de Freitas, D., and de Oliveira, L. A. (2021). SARS-COV-2 and ocular surface: from physiology to pathology, a route to understand transmission and disease. *Front. Physiol.* 12:612319. doi: 10.3389/fphys.2021.612319

de Wit, E., van Doremalen, N., Falzarano, D., and Munster, V. J. (2016). SARS and MERS: recent insights into emerging coronaviruses. *Nat. Rev. Microbiol.* 14, 523–534. doi: 10.1038/nrmicro.2016.81

Deatly, A. M., Haase, A. T., Fewster, P. H., Lewis, E., and Ball, M. J. (1990). Human herpes virus infections and Alzheimer's disease. *Neuropathol. Appl. Neurobiol.* 16, 213–223. doi: 10.1111/j.1365-2990.1990.tb01158.x

Desforges, M., Le Coupanec, A., Dubeau, P., Bourgouin, A., Lajoie, L., Dubé, M., et al. (2019). Human coronaviruses and other respiratory viruses: underestimated opportunistic pathogens of the central nervous system? *Viruses* 12:14. doi: 10.3390/v12010014

Ding, Y., He, L., Zhang, Q., Huang, Z., Che, X., Hou, J., et al. (2004). Organ distribution of severe acute respiratory syndrome (SARS) associated

coronavirus (SARS-CoV) in SARS patients: implications for pathogenesis and virus transmission pathways. *J. Pathol.* 203, 622–630. doi: 10.1002/path.1560

Dinnon, K. H., Leist, S. R., Schäfer, A., Edwards, C. E., Martinez, D. R., Montgomery, S. A., et al. (2020). A mouse-adapted model of SARS-CoV-2 to test COVID-19 countermeasures. *Nature* 586, 560–566. doi: 10.1038/s41586-020-2708-8

Dobrindt, K., Hoagland, D. A., Seah, C., Kassim, B., O'Shea, C. P., Murphy, A., et al. (2021). Common genetic variation in humans impacts in vitro susceptibility to SARS-CoV-2 infection. *Stem Cell Rep.* 16, 505–518. doi: 10.1016/j.stemcr.2021.02.010

Domingues, R. B., Mendes-Correa, M. C., de Moura Leite, F. B. V., Sabino, E. C., Salarini, D. Z., Claro, I., et al. (2020). First case of SARS-COV-2 sequencing in cerebrospinal fluid of a patient with suspected demyelinating disease. *J. Neurol.* 267, 3154–3156. doi: 10.1007/s00415-020-09996-w

Driessen, A. K., Farrell, M. J., Mazzone, S. B., and McGovern, A. E. (2016). Multiple neural circuits mediating airway sensations: recent advances in the neurobiology of the urge-to-cough. *Respir. Physiol. Neurobiol.* 226, 115–120. doi: 10.1016/j.resp.2015.09.017

Dubé, M., Le Coupanec, A., Wong, A. H. M., Rini, J. M., Desforges, M., and Talbot, P. J. (2018). Axonal transport enables neuron-to-neuron propagation of human coronavirus OC43. *J. Virol.* 92, e00404–e00418. doi: 10.1128/JVI.00404-18

ElBini Dhouib, I. (2021). Does coronaviruses induce neurodegenerative diseases? A systematic review on the neurotropism and neuroinvasion of SARS-CoV-2. *Drug Discov. Ther.* 14, 262–272. doi: 10.5582/ddt.2020.03106

Ellul, M. A., Benjamin, L., Singh, B., Lant, S., Michael, B. D., Easton, A., et al. (2020). Neurological associations of COVID-19. *Lancet Neurol.* 19, 767–783. doi: 10.1016/S1474-4422(20)30221-0

Ezzat, K., Pernemalm, M., Pålsson, S., Roberts, T. C., Järver, P., Dondalska, A., et al. (2019). The viral protein corona directs viral pathogenesis and amyloid aggregation. *Nat. Commun.* 10:2331. doi: 10.1038/s41467-019-10192-2

Fearon, C., and Fasano, A. (2021). Parkinson's Disease and the COVID-19 Pandemic. *J. Parkinsons Dis.* 11, 431–444. doi: 10.3233/JPD-202320

Ferini-Strambi, L., and Salsone, M. (2021). COVID-19 and neurological disorders: are neurodegenerative or neuroimmunological diseases more vulnerable? *J. Neurol.* 268, 409–419. doi: 10.1007/s00415-020-10070-8

Ferrando, S. J., Klepacz, L., Lynch, S., Tavakkoli, M., Dornbush, R., Baharani, R., et al. (2020). COVID-19 psychosis: a potential new neuropsychiatric condition triggered by novel coronavirus infection and the inflammatory response? *Psychosomatics* 61, 551–555. doi: 10.1016/j.psym.2020.05.012

Finelli, C. (2021). Metabolic syndrome, alzheimer's disease, and Covid 19: a possible correlation. *Curr. Alzheimer Res.* 18, 915–924. doi: 10.2174/1567205018666211209095652

Flores-Silva, F. D., García-Grimshaw, M., Valdés-Ferrer, S. I., Vigueras-Hernández, A. P., Domínguez-Moreno, R., Tristán-Samaniego, D. P., et al. (2021). Neurologic manifestations in hospitalized patients with COVID-19 in Mexico City. *PLoS One* 16:e0247433. doi: 10.1371/journal.pone.0247433

Forcados, G. E., Muhammad, A., Oladipo, O. O., Makama, S., and Meseko, C. A. (2021). Metabolic implications of oxidative stress and inflammatory process in SARS-CoV-2 pathogenesis: therapeutic potential of natural antioxidants. *Front. Cell Infect. Microbiol.* 11:654813. doi: 10.3389/fcimb.2021.654813

Frank, M. G., Nguyen, K. H., Ball, J. B., Hopkins, S., Kelley, T., Baratta, M. V., et al. (2022). SARS-CoV-2 spike S1 subunit induces neuroinflammatory, microglial and behavioral sickness responses: evidence of PAMP-like properties. *Brain Behav. Immun.* 100, 267–277. doi: 10.1016/j.bbi.2021.12.007

Gandhi, J., Antonelli, A. C., Afridi, A., Vatsia, S., Joshi, G., Romanov, V., et al. (2019). Protein misfolding and aggregation in neurodegenerative diseases: a review of pathogeneses, novel detection strategies, and potential therapeutics. *Rev. Neurosci.* 30, 339–358. doi: 10.1515/revneuro-2016-0035

García-Moncó, J. C., Cabrera Muras, A., Erburu Iriarte, M., Rodrigo Armenteros, P., Collía Fernández, A., Arranz-Martínez, J., et al. (2021). Neurologic manifestations in a prospective unselected series of hospitalized patients with COVID-19. *Neurol. Clin. Pract.* 11, e64–e72. doi: 10.1212/CPJ.0000000000000913

Gasmi, A., Tippairote, T., Mujawdiya, P. K., Gasmi Benahmed, A., Menzel, A., Dadar, M., et al. (2021). Neurological involvements of SARS-CoV2 infection. *Mol. Neurobiol.* 58, 944–949. doi: 10.1007/s12035-020-02070-6

Generoso, J. S., Barichello de Quevedo, J. L., Cattani, M., Lodetti, B. F., Sousa, L., Collodel, A., et al. (2021). Neurobiology of COVID-19: how can the virus affect the brain? *Braz. J. Psychiatry* 43, 650–664. doi: 10.1590/1516-4446-2020-1488

Gilani, S., Roditi, R., and Naraghi, M. (2020). COVID-19 and anosmia in Tehran, Iran. *Med. Hypotheses* 141:109757. doi: 10.1016/j.mehy.2020.109757

Gilpin, S., Byers, M., Byrd, A., Cull, J., Peterson, D., Thomas, B., et al. (2021). Rhabdomyolysis as the initial presentation of SARS-CoV-2 in an adolescent. *Pediatrics* 147:e2020019273. doi: 10.1542/peds.2020-019273

Graham, N. S., and Sharp, D. J. (2019). Understanding neurodegeneration after traumatic brain injury: from mechanisms to clinical trials in dementia. *J. Neurol. Neurosurg. Psychiatry* 90, 1221–1233. doi: 10.1136/jnnp-2017-317557

Guan, W. J., Ni, Z. Y., Hu, Y., Liang, W. H., Ou, C. Q., He, J. X., et al. (2020). Clinical characteristics of coronavirus disease 2019 in China. *N. Engl. J. Med.* 382, 1708–1720. doi: 10.1056/NEJMoa2002032

Guidon, A. C., and Amato, A. A. (2020). COVID-19 and neuromuscular disorders. *Neurology* 94, 959–969. doi: 10.1212/WNL.0000000000009566

Gutiérrez-Ortiz, C., Méndez-Guerrero, A., Rodrigo-Rey, S., San Pedro-Murillo, E., Bermejo-Guerrero, L., Gordo-Mañas, R., et al. (2020). Miller Fisher syndrome and polyneuritis cranialis in COVID-19. *Neurology* 95, e601–e605. doi: 10.1212/WNL.0000000000009619

Habibzadeh, P., Mofatteh, M., Silawi, M., Ghavami, S., and Faghihi, M. A. (2021). Molecular diagnostic assays for COVID-19: an overview. *Crit. Rev. Clin. Lab. Sci.* 58, 385–398. doi: 10.1080/10408363.2021.1884640

Harwood, R., Yan, H., Talawila Da Camara, N., Smith, C., Ward, J., Tudur-Smith, C., et al. (2022). Which children and young people are at higher risk of severe disease and death after hospitalisation with SARS-CoV-2 infection in children and young people: a systematic review and individual patient meta-analysis. *EClinical Med.* 44:101287. doi: 10.1016/j.eclinm.2022.101287

Hassan, M., Mustafa, F., Syed, F., Mustafa, A., Mushtaq, H. F., Khan, N. U., et al. (2021). Ocular surface: a route for SARS CoV-2 transmission- a case report. *Brain Hemorrhages* 2, 139–140. doi: 10.1016/j.hest.2021.09.003

Helms, J., Kremer, S., Merdji, H., Clere-Jehl, R., Schenck, M., Kummerlen, C., et al. (2020). Neurologic features in severe SARS-CoV-2 infection. *N. Engl. J. Med.* 382, 2268–2270. doi: 10.1056/NEJMc2008597

Henderson, M. X., Trojanowski, J. Q., and Lee, V. M. (2019). α-Synuclein pathology in Parkinson's disease and related α-synucleinopathies. *Neurosci. Lett.* 709:134316. doi: 10.1016/j.neulet.2019.134316

Hill, J. M., Clement, C., Arceneaux, L., and Lukiw, W. J. (2021). Angiotensin converting enzyme 2 (ACE2) expression in the aged brain and visual system. *J. Aging Sci.* 9(Suppl.):7.

Hoffmann, M., Kleine-Weber, H., Schroeder, S., Krüger, N., Herrler, T., Erichsen, S., et al. (2020). SARS-CoV-2 cell entry depends on ACE2 and TMPRSS2 and is blocked by a clinically proven protease inhibitor. *Cell* 181, 271.e–280.e. doi: 10.1016/j.cell.2020.02.052

Hou, Y., Dan, X., Babbar, M., Wei, Y., Hasselbalch, S. G., Croteau, D. L., et al. (2019). Ageing as a risk factor for neurodegenerative disease. *Nat. Rev. Neurol.* 15, 565–581. doi: 10.1038/s41582-019-0244-7

Hu, B., Guo, H., Zhou, P., and Shi, Z. L. (2021). Characteristics of SARS-CoV-2 and COVID-19. *Nat. Rev. Microbiol.* 19, 141–154. doi: 10.1038/s41579-020-00459-7

Hu, J., Jolkkonen, J., and Zhao, C. (2020). Neurotropism of SARS-CoV-2 and its neuropathological alterations: similarities with other coronaviruses. *Neurosci. Biobehav. Rev.* 119, 184–193. doi: 10.1016/j.neubiorev.2020.10.012

Huang, C., Wang, Y., Li, X., Ren, L., Zhao, J., Hu, Y., et al. (2020). Clinical features of patients infected with 2019 novel coronavirus in Wuhan, China. *Lancet* 395, 497–506. doi: 10.1016/S0140-6736(20)30183-5

Huang, Y. H., Jiang, D., and Huang, J. T. (2020). SARS-CoV-2 detected in cerebrospinal fluid by pcr in a case of COVID-19 encephalitis. *Brain Behav. Immun.* 87:149. doi: 10.1016/j.bbi.2020.05.012

Huang, Y., Lu, Y., Huang, Y. M., Wang, M., Ling, W., Sui, Y., et al. (2020). Obesity in patients with COVID-19: a systematic review and meta-analysis. *Metabolism* 113:154378. doi: 10.1016/j.metabol.2020.154378

Hurley, L. L., and Tizabi, Y. (2013). Neuroinflammation, neurodegeneration, and depression. *Neurotox Res.* 23, 131–144. doi: 10.1007/s12640-012-9348-1

Hussain, B., Fang, C., and Chang, J. (2021). Blood-brain barrier breakdown: an emerging biomarker of cognitive impairment in normal aging and dementia. *Front. Neurosci.* 15:688090. doi: 10.3389/fnins.2021.688090

Hwang, S. T., Ballout, A. A., Mirza, U., Sonti, A. N., Husain, A., Kirsch, C., et al. (2020). Acute seizures occurring in association with SARS-CoV-2. *Front. Neurol.* 11:576329. doi: 10.3389/fneur.2020.576329

Idrees, D., and Kumar, V. (2021). SARS-CoV-2 spike protein interactions with amyloidogenic proteins: potential clues to neurodegeneration. *Biochem. Biophys. Res. Commun.* 554, 94–98. doi: 10.1016/j.bbrc.2021.03.100

Israelow, B., Song, E., Mao, T., Lu, P., Meir, A., Liu, F., et al. (2020). Mouse model of SARS-CoV-2 reveals inflammatory role of type I interferon signaling. *J. Exp. Med.* 217:e20201241. doi: 10.1084/jem.20201241

Jang, H., Boltz, D. A., Webster, R. G., and Smeyne, R. J. (2009). Viral parkinsonism. *Biochim. Biophys. Acta* 1792, 714–721. doi: 10.1016/j.bbadis.2008.08.001

Johansen, M. D., Irving, A., Montagutelli, X., Tate, M. D., Rudloff, I., Nold, M. F., et al. (2020). Animal and translational models of SARS-CoV-2 infection and COVID-19. *Mucosal Immunol.* 13, 877–891. doi: 10.1038/s41385-020-00340-z

Justice, N. J. (2018). The relationship between stress and Alzheimer's disease. *Neurobiol. Stress* 8, 127–133. doi: 10.1016/j.ynstr.2018.04.002

Kapoor, M. C. (2020). Respiratory and cardiovascular effects of COVID-19 infection and their management. *J. Anaesthesiol. Clin. Pharmacol.* 36(Suppl. 1), S21–S28. doi: 10.4103/joacp.JOACP_242_20

Kempuraj, D., Selvakumar, G. P., Ahmed, M. E., Raikwar, S. P., Thangavel, R., Khan, A., et al. (2020). COVID-19, mast cells, cytokine storm, psychological stress, and neuroinflammation. *Neuroscientist* 26, 402–414. doi: 10.1177/1073858420941476

Kisler, K., Nelson, A. R., Rege, S. V., Ramanathan, A., Wang, Y., Ahuja, A., et al. (2017). Pericyte degeneration leads to neurovascular uncoupling and limits oxygen supply to brain. *Nat. Neurosci.* 20, 406–416. doi: 10.1038/nn.4489

Klopfenstein, T., Kadiane-Oussou, N. J., Toko, L., Royer, P. Y., Lepiller, Q., Gendrin, V., et al. (2020). Features of anosmia in COVID-19. *Med. Mal. Infect.* 50, 436–439. doi: 10.1016/j.medmal.2020.04.006

Koehler, M., Delguste, M., Sieben, C., Gillet, L., and Alsteens, D. (2020). Initial step of virus entry: virion binding to cell-surface glycans. *Ann. Rev. Virol.* 7, 143–165. doi: 10.1146/annurev-virology-122019-070025

Kumar, D., Jahan, S., Khan, A., Siddiqui, A. J., Redhu, N. S., Khan, J., et al. (2021). Neurological manifestation of SARS-CoV-2 induced inflammation and possible therapeutic strategies against COVID-19. *Mol. Neurobiol.* 58, 3417–3434. doi: 10.1007/s12035-021-02318-9

Kurki, S. N., Kantonen, J., Kaivola, K., Hokkanen, L., Mäyränpää, M. I., Puttonen, H., et al. (2021). APOE ε4 associates with increased risk of severe COVID-19, cerebral microhaemorrhages and post-COVID mental fatigue: a finnish biobank, autopsy and clinical study. *Acta Neuropathol. Commun.* 9:199. doi: 10.1186/s40478-021-01302-7

Kwon, M., and Lee, J. H. (2019). Oro-pharyngeal dysphagia in parkinson's disease and related movement disorders. *J. Mov. Disord.* 12, 152–160. doi: 10.14802/jmd.19048

Lacy, J. M., Brooks, E. G., Akers, J., Armstrong, D., Decker, L., Gonzalez, A., et al. (2020). COVID-19: postmortem diagnostic and biosafety considerations. *Am. J. For. Med. Pathol.* 41, 143–151. doi: 10.1097/PAF.0000000000000567

Lax, S. F., Skok, K., Zechner, P., Kessler, H. H., Kaufmann, N., Koelblinger, C., et al. (2020). Pulmonary arterial thrombosis in COVID-19 with fatal outcome : results from a prospective. single-center, clinicopathologic case series. *Ann. Intern. Med.* 173, 350–361. doi: 10.7326/M20-2566

Lazzeri, C., Bonizzoli, M., Batacchi, S., Cianchi, G., Franci, A., Fulceri, G. E., et al. (2020). Cardiac involvment in COVID-19-related acute respiratory distress syndrome. *Am. J. Cardiol.* 132, 147–149. doi: 10.1016/j.amjcard.2020.07.010

Lebrasseur, A., Fortin-Bédard, N., Lettre, J., Raymond, E., Bussières, E. L., Lapierre, N., et al. (2021). Impact of the COVID-19 pandemic on older adults: rapid review. *JMIR Aging* 4:e26474. doi: 10.2196/26474

Lee, M. H., Perl, D. P., Nair, G., Li, W., Maric, D., Murray, H., et al. (2021). Microvascular injury in the brains of patients with Covid-19. *N. Engl. J. Med.* 384, 481–483. doi: 10.1056/NEJMc2033369

Leng, F., and Edison, P. (2021). Neuroinflammation and microglial activation in Alzheimer disease: where do we go from here? *Nat. Rev. Neurol.* 17, 157–172. doi: 10.1038/s41582-020-00435-y

Leonardi, A., Rosani, U., and Brun, P. (2020). Ocular surface expression of SARS-CoV-2 receptors. *Ocul. Immunol. Inflamm.* 28, 735–738. doi: 10.1080/09273948.2020.1772314

Levi, M., Thachil, J., Iba, T., and Levy, J. H. (2020). Coagulation abnormalities and thrombosis in patients with COVID-19. *Lancet Haematol.* 7, e438–e440. doi: 10.1016/S2352-3026(20)30145-9

Levinson, R., Elbaz, M., Ben-Ami, R., Shasha, D., Levinson, T., Choshen, G., et al. (2020). Time course of anosmia and dysgeusia in patients with mild SARS-CoV-2 infection. *Infect. Dis.* 52, 600–602. doi: 10.1080/23744235.2020.1772992

Li, L., Acioglu, C., Heary, R. F., and Elkabes, S. (2021). Role of astroglial toll-like receptors (TLRs) in central nervous system infections, injury and neurodegenerative diseases. *Brain Behav. Immun.* 91, 740–755. doi: 10.1016/j.bbi.2020.10.007

Li, M. Y., Li, L., Zhang, Y., and Wang, X. S. (2020). Expression of the SARS-CoV-2 cell receptor gene ACE2 in a wide variety of human tissues. *Infect. Dis. Poverty* 9:45. doi: 10.1186/s40249-020-00662-x

Li, W., Moore, M. J., Vasilieva, N., Sui, J., Wong, S. K., Berne, M. A., et al. (2003). Angiotensin-converting enzyme 2 is a functional receptor for the SARS coronavirus. *Nature* 426, 450–454. doi: 10.1038/nature02145

Limphaibool, N., Iwanowski, P., Holstad, M. J. V., Kobylarek, D., and Kozubski, W. (2019). Infectious etiologies of parkinsonism: pathomechanisms and clinical implications. *Front. Neurol.* 10:652. doi: 10.3389/fneur.2019.00652

Liu, J. M., Tan, B. H., Wu, S., Gui, Y., Suo, J. L., and Li, Y. C. (2021). Evidence of central nervous system infection and neuroinvasive routes, as well as neurological involvement, in the lethality of SARS-CoV-2 infection. *J. Med. Virol.* 93, 1304–1313. doi: 10.1002/jmv.26570

Liu, P. P., Xie, Y., Meng, X. Y., and Kang, J. S. (2019). History and progress of hypotheses and clinical trials for Alzheimer's disease. *Signal Transduct. Target. Ther.* 4:29. doi: 10.1038/s41392-019-0063-8

Liu, S., Hossinger, A., Heumüller, S. E., Hornberger, A., Buravlova, O., Konstantoulea, K., et al. (2021). Highly efficient intercellular spreading of protein misfolding mediated by viral ligand-receptor interactions. *Nat. Commun.* 12:5739. doi: 10.1038/s41467-021-25855-2

Lochhead, J. J., and Thorne, R. G. (2012). Intranasal delivery of biologics to the central nervous system. *Adv. Drug. Deliv. Rev.* 64, 614–628. doi: 10.1016/j.addr.2011.11.002

Lotz, S. K., Blackhurst, B. M., Reagin, K. L., and Funk, K. E. (2021). Microbial infections are a risk factor for neurodegenerative diseases. *Front. Cell Neurosci.* 15:691136. doi: 10.3389/fncel.2021.691136

Lu, R., Zhao, X., Li, J., Niu, P., Yang, B., Wu, H., et al. (2020). Genomic characterisation and epidemiology of 2019 novel coronavirus: implications for virus origins and receptor binding. *Lancet* 395, 565–574. doi: 10.1016/S0140-6736(20)30251-8

Lu, Y., Li, X., Geng, D., Mei, N., Wu, P. Y., Huang, C. C., et al. (2020). Cerebral micro-structural changes in COVID-19 patients - an MRI-based 3-month follow-up study. *EClinicalMedicine* 25:100484. doi: 10.1016/j.eclinm.2020.100484

Ma, D., Chen, C. B., Jhanji, V., Xu, C., Yuan, X. L., Liang, J. J., et al. (2020). Expression of SARS-CoV-2 receptor ACE2 and TMPRSS2 in human primary conjunctival and pterygium cell lines and in mouse cornea. *Eye* 34, 1212–1219. doi: 10.1038/s41433-020-0939-4

Madore, C., Yin, Z., Leibowitz, J., and Butovsky, O. (2020). Microglia, lifestyle stress, and neurodegeneration. *Immunity* 52, 222–240. doi: 10.1016/j.immuni.2019.12.003

Manji, H. K., George, U., Mkopi, N. P., and Manji, K. P. (2020). Guillain-Barré syndrome associated with COVID-19 infection. *Pan. Afr. Med. J.* 35(Suppl. 2):118. doi: 10.11604/pamj.supp.2020.35.2.25003

Mao, L., Jin, H., Wang, M., Hu, Y., Chen, S., He, Q., et al. (2020). Neurologic manifestations of hospitalized patients with coronavirus disease 2019 in Wuhan, China. *JAMA Neurol.* 77, 683–690. doi: 10.1001/jamaneurol.2020.1127

Marreiros, R., Müller-Schiffmann, A., Trossbach, S. V., Prikulis, I., Hänsch, S., Weidtkamp-Peters, S., et al. (2020). Disruption of cellular proteostasis by H1N1 influenza A virus causes α-synuclein aggregation. *Proc. Natl. Acad. Sci. U.S.A.* 117, 6741–6751. doi: 10.1073/pnas.1906466117

Masters, P. S. (2006). The molecular biology of coronaviruses. *Adv. Virus Res.* 66, 193–292. doi: 10.1016/S0065-3527(06)66005-3

Meegada, S., Muppidi, V., Wilkinson, D. C., Siddamreddy, S., and Katta, S. K. (2020). Coronavirus disease 2019-induced rhabdomyolysis. *Cureus* 12:e10123. doi: 10.7759/cureus.10123

Mehrabadi, M. E., Hemmati, R., Tashakor, A., Homaei, A., Yousefzadeh, M., Hemati, K., et al. (2021). Induced dysregulation of ACE2 by SARS-CoV-2 plays a key role in COVID-19 severity. *Biomed. Pharmacother.* 137:111363. doi: 10.1016/j.biopha.2021.111363

Mehta, P., and Fajgenbaum, D. C. (2021). Is severe COVID-19 a cytokine storm syndrome: a hyperinflammatory debate. *Curr. Opin. Rheumatol.* 33, 419–430. doi: 10.1097/BOR.0000000000000822

Meng, L., Shen, L., and Ji, H. F. (2019). Impact of infection on risk of Parkinson's disease: a quantitative assessment of case-control and cohort studies. *J. Neurovirol.* 25, 221–228. doi: 10.1007/s13365-018-0707-4

Messlinger, K., Neuhuber, W., and May, A. (2021). Activation of the trigeminal system as a likely target of SARS-CoV-2 may contribute to anosmia in COVID-19. *Cephalalgia* 42, 176–180. doi: 10.1177/03331024211036665

Milligan Armstrong, A., Porter, T., Quek, H., White, A., Haynes, J., Jackaman, C., et al. (2021). Chronic stress and Alzheimer's disease: the?interplay between the hypothalamic-pituitary-adrenal axis, genetics and microglia. *Biol. Rev. Camb. Philos. Soc.* 96, 2209–2228. doi: 10.1111/brv.12750

Miners, S., Kehoe, P. G., and Love, S. (2020). Cognitive impact of COVID-19: looking beyond the short term. *Alzheimers Res. Ther.* 12:170. doi: 10.1186/s13195-020-00744-w

Mohammadi, S., Moosaie, F., and Aarabi, M. H. (2020). Understanding the immunologic characteristics of neurologic manifestations of SARS-CoV-2 and potential immunological mechanisms. *Mol. Neurobiol.* 57, 5263–5275. doi: 10.1007/s12035-020-02094-y

Montagne, A., Nikolakopoulou, A. M., Huuskonen, M. T., Sagare, A. P., Lawson, E. J., Lazic, D., et al. (2021). Accelerates advanced-stage vascular and neurodegenerative disorder in old Alzheimer's mice via cyclophilin A independently of amyloid-β. *Nat. Aging* 1, 506–520. doi: 10.1038/s43587-021-00073-z

Montagne, A., Zhao, Z., and Zlokovic, B. V. (2017). Alzheimer's disease: a matter of blood-brain barrier dysfunction? *J. Exp. Med.* 214, 3151–3169. doi: 10.1084/jem.20171406

Mori, I. (2015). Transolfactory neuroinvasion by viruses threatens the human brain. *Acta Virol.* 59, 338–349. doi: 10.4149/av_2015_04_338

Moriguchi, T., Harii, N., Goto, J., Harada, D., Sugawara, H., Takamino, J., et al. (2020). A first case of meningitis/encephalitis associated with SARS-Coronavirus-2. *Int. J. Infect. Dis.* 94, 55–58. doi: 10.1016/j.ijid.2020.03.062

Mrityunjaya, M., Pavithra, V., Neelam, R., Janhavi, P., Halami, P. M., and Ravindra, P. V. (2020). Immune-boosting, antioxidant and anti-inflammatory food supplements targeting pathogenesis of COVID-19. *Front. Immunol.* 11:570122. doi: 10.3389/fimmu.2020.570122

Muñoz-Fontela, C., Dowling, W. E., Funnell, S. G. P., Gsell, P. S., Riveros-Balta, A. X., Albrecht, R. A., et al. (2020). Animal models for COVID-19. *Nature* 586, 509–515. doi: 10.1038/s41586-020-2787-6

Mutiawati, E., Fahriani, M., Mamada, S. S., Fajar, J. K., Frediansyah, A., Maliga, H. A., et al. (2021). Anosmia and dysgeusia in SARS-CoV-2 infection: incidence and effects on COVID-19 severity and mortality, and the possible pathobiology mechanisms - a systematic review and meta-analysis. *F1000Res* 10:40. doi: 10.12688/f1000research.28393.1

Naqvi, A. A. T., Fatima, K., Mohammad, T., Fatima, U., Singh, I. K., Singh, A., et al. (2020). Insights into SARS-CoV-2 genome, structure, evolution, pathogenesis and therapies: structural genomics approach. *Biochim. Biophys. Acta Mol. Basis Dis.* 1866:165878. doi: 10.1016/j.bbadis.2020.165878

Natoli, S., Oliveira, V., Calabresi, P., Maia, L. F., and Pisani, A. (2020). Does SARS-Cov-2 invade the brain? Translational lessons from animal models. *Eur. J. Neurol.* 27, 1764–1773. doi: 10.1111/ene.14277

Ni, W., Yang, X., Yang, D., Bao, J., Li, R., Xiao, Y., et al. (2020). Role of angiotensin-converting enzyme 2 (ACE2) in COVID-19. *Crit. Care* 24:422. doi: 10.1186/s13054-020-03120-0

Niesen, M., Trotta, N., Noel, A., Coolen, T., Fayad, G., Leurkin-Sterk, G., et al. (2021). Structural and metabolic brain abnormalities in COVID-19 patients with sudden loss of smell. *Eur. J. Nucl. Med. Mol. Imaging* 48, 1890–1901. doi: 10.1007/s00259-020-05154-6

Niraula, A., Sheridan, J. F., and Godbout, J. P. (2017). Microglia priming with aging and stress. *Neuropsychopharmacology* 42, 318–333. doi: 10.1038/npp.2016.185

Noe, C. R., Noe-Letschnig, M., Handschuh, P., Noe, C. A., and Lanzenberger, R. (2020). Dysfunction of the blood-brain barrier-a key step in neurodegeneration and dementia. *Front. Aging Neurosci.* 12:185. doi: 10.3389/fnagi.2020.00185

Noroozi, R., Branicki, W., Pyrc, K., Łabaj, P. P., Pospiech, E., Taheri, M., et al. (2020). Altered cytokine levels and immune responses in patients with SARS-CoV-2 infection and related conditions. *Cytokine* 133:155143. doi: 10.1016/j.cyto.2020.155143

Pacheco-Herrero, M., Soto-Rojas, L. O., Harrington, C. R., Flores-Martinez, Y. M., Villegas-Rojas, M. M., León-Aguilar, A. M., et al. (2021). Elucidating the neuropathologic mechanisms of SARS-CoV-2 infection. *Front. Neurol.* 12:660087. doi: 10.3389/fneur.2021.660087

Pan, A. P., Meeks, J., Potter, T., Masdeu, J. C., Seshadri, S., Smith, M. L., et al. (2021). SARS-CoV-2 susceptibility and COVID-19 mortality among older adults with cognitive impairment: cross-sectional analysis from hospital records in a diverse us metropolitan area. *Front. Neurol.* 12:692662. doi: 10.3389/fneur.2021.692662

Pan, Y., Jiang, X., Yang, L., Chen, L., Zeng, X., Liu, G., et al. (2021). SARS-CoV-2-specific immune response in COVID-19 convalescent individuals. *Signal Transduct. Target. Ther.* 6:256. doi: 10.1038/s41392-021-00686-1

Paniz-Mondolfi, A., Bryce, C., Grimes, Z., Gordon, R. E., Reidy, J., Lednicky, J., et al. (2020). Central nervous system involvement by severe acute respiratory syndrome coronavirus-2 (SARS-CoV-2). *J. Med. Virol.* 92, 699–702. doi: 10.1002/jmv.25915

Parikh, N. S., Merkler, A. E., and Iadecola, C. (2020). Inflammation, autoimmunity, infection, and stroke: epidemiology and lessons from therapeutic intervention. *Stroke* 51, 711–718. doi: 10.1161/STROKEAHA.119.024157

Park, J. H., Kim, D. H., Park, Y. G., Kwon, D. Y., Choi, M., Jung, J. H., et al. (2020). Association of parkinson disease with risk of cardiovascular disease and all-cause mortality: a nationwide. Population-Based Cohort Study. *Circulation* 141, 1205–1207. doi: 10.1161/CIRCULATIONAHA.119.044948

Paterson, R. W., Brown, R. L., Benjamin, L., Nortley, R., Wiethoff, S., Bharucha, T., et al. (2020). The emerging spectrum of COVID-19 neurology: clinical, radiological and laboratory findings. *Brain* 143, 3104–3120. doi: 10.1093/brain/awaa240

Patra, T., Meyer, K., Geerling, L., Isbell, T. S., Hoft, D. F., Brien, J., et al. (2020). SARS-CoV-2 spike protein promotes IL-6 trans-signaling by activation of angiotensin II receptor signaling in epithelial cells. *PLoS Pathog.* 16:e1009128. doi: 10.1371/journal.ppat.1009128

Pellegrini, L., Albecka, A., Mallery, D. L., Kellner, M. J., Paul, D., Carter, A. P., et al. (2020). SARS-CoV-2 infects the brain choroid plexus and disrupts the blood-CSF barrier in human brain organoids. *Cell Stem Cell* 27, 951.e–961.e. doi: 10.1016/j.stem.2020.10.001

Peng, R., Wu, L. A., Wang, Q., Qi, J., and Gao, G. F. (2021). Cell entry by SARS-CoV-2. *Trends Biochem. Sci.* 46, 848–860. doi: 10.1016/j.tibs.2021.06.001

Perez Ortiz, J. M., and Swerdlow, R. H. (2019). Mitochondrial dysfunction in Alzheimer's disease: role in pathogenesis and novel therapeutic opportunities. *Br. J. Pharmacol.* 176, 3489–3507. doi: 10.1111/bph.14585

Prasad, K., AlOmar, S. Y., Alqahtani, S. A. M., Malik, M. Z., and Kumar, V. (2021). Brain disease network analysis to elucidate the neurological manifestations of COVID-19. *Mol. Neurobiol.* 58, 1875–1893. doi: 10.1007/s12035-020-02266-w

Prasad, S., Holla, V. V., Neeraja, K., Surisetti, B. K., Kamble, N., Yadav, R., et al. (2020). Parkinson's disease and COVID-19: perceptions and implications in patients and caregivers. *Mov. Disord.* 35, 912–914. doi: 10.1002/mds.28088

Qiao, J., Li, W., Bao, J., Peng, Q., Wen, D., Wang, J., et al. (2020). The expression of SARS-CoV-2 receptor ACE2 and CD147, and protease TMPRSS2 in human and mouse brain cells and mouse brain tissues. *Biochem. Biophys. Res. Commun.* 533, 867–871. doi: 10.1016/j.bbrc.2020.09.042

Rahimi, A., Mirzazadeh, A., and Tavakolpour, S. (2021). Genetics and genomics of SARS-CoV-2: a review of the literature with the special focus on genetic diversity and SARS-CoV-2 genome detection. *Genomics* 113(1 Pt 2), 1221–1232. doi: 10.1016/j.ygeno.2020.09.059

Rastogi, M., Pandey, N., Shukla, A., and Singh, S. K. (2020). SARS coronavirus 2: from genome to infectome. *Respir. Res.* 21:318. doi: 10.1186/s12931-020-01581-z

Rathnasinghe, R., Strohmeier, S., Amanat, F., Gillespie, V. L., Krammer, F., García-Sastre, A., et al. (2020). Comparison of transgenic and adenovirus hACE2 mouse models for SARS-CoV-2 infection. *Emerg. Microbes Infect.* 9, 2433–2445. doi: 10.1080/22221751.2020.1838955

Rea, I. M., Gibson, D. S., McGilligan, V., McNerlan, S. E., Alexander, H. D., and Ross, O. A. (2018). Age and age-related diseases: role of inflammation triggers and cytokines. *Front. Immunol.* 9:586. doi: 10.3389/fimmu.2018.00586

Reichard, R. R., Kashani, K. B., Boire, N. A., Constantopoulos, E., Guo, Y., and Lucchinetti, C. F. (2020). Neuropathology of COVID-19: a spectrum of vascular and acute disseminated encephalomyelitis (ADEM)-like pathology. *Acta Neuropathol.* 140, 1–6. doi: 10.1007/s00401-020-02166-2

Reza-Zaldívar, E. E., Hernández-Sapiéns, M. A., Minjarez, B., Gómez-Pinedo, U., Márquez-Aguirre, A. L., Mateos-Díaz, J. C., et al. (2020). Infection mechanism of SARS-COV-2 and its implication on the nervous system. *Front. Immunol.* 11:621735. doi: 10.3389/fimmu.2020.621735

Rogers, K. (2022). *Who Can Declare a Pandemic and What Criteria Are Required for an Outbreak to Be Called a Pandemic?*. Available online at: https://www.britannica.com/story/who-can-declare-a-pandemic-and-what-criteria-are-required-for-an-outbreak-to-be-called-a-pandemic. (accessed April 7, 2022).

Romero-Sánchez, C. M., Díaz-Maroto, I., Fernández-Díaz, E., Sánchez-Larsen, Á, Layos-Romero, A., and García-García, J. (2020). Neurologic manifestations in hospitalized patients with COVID-19: the ALBACOVID registry. *Neurology* 95, e1060–e1070. doi: 10.1212/WNL.0000000000009937

Sait, A., Angeli, C., Doig, A. J., and Day, P. J. R. (2021). Viral involvement in alzheimer's disease. *ACS Chem. Neurosci.* 12, 1049–1060. doi: 10.1021/acschemneuro.0c00719

Sanchez-Cano, F., Hernández-Kelly, L. C., and Ortega, A. (2021). The blood-brain barrier: much more than a selective access to the brain. *Neurotox. Res.* 39, 2154–2174. doi: 10.1007/s12640-021-00431-0

Sanclemente-Alaman, I., Moreno-Jiménez, L., Benito-Martín, M. S., Canales-Aguirre, A., Matías-Guiu, J. A., Matías-Guiu, J., et al. (2020). Experimental models for the study of central nervous system infection by SARS-CoV-2. *Front. Immunol.* 11:2163. doi: 10.3389/fimmu.2020.02163

Sanyaolu, A., Okorie, C., Marinkovic, A., Patidar, R., Younis, K., Desai, P., et al. (2020). Comorbidity and its impact on patients with COVID-19. *SN Compr. Clin. Med.* 2, 1069–1076. doi: 10.1007/s42399-020-00363-4

Schwartz, M., and Deczkowska, A. (2016). Neurological disease as a failure of brain-immune crosstalk: the multiple faces of neuroinflammation. *Trends Immunol.* 37, 668–679. doi: 10.1016/j.it.2016.08.001

Seaks, C. E., and Wilcock, D. M. (2020). Infectious hypothesis of Alzheimer disease. *PLoS Pathog.* 16:e1008596. doi: 10.1371/journal.ppat.1008596

Semerdzhiev, S. A., Fakhree, M. A. A., Segers-Nolten, I., Blum, C., and Claessens, M. M. A. E. (2022). Interactions between SARS-CoV-2 N-protein and α-synuclein accelerate amyloid formation. *ACS Chem. Neurosci.* 13, 143–150. doi: 10.1021/acschemneuro.1c00666

Serrano, G. E., Walker, J. E., Arce, R., Glass, M. J., Vargas, D., Sue, L. I., et al. (2021). Mapping of SARS-CoV-2 brain invasion and histopathology in COVID-19 disease. *medRxiv [Preprint]*. doi: 10.1101/2021.02.15.21251511

Serrano-Pozo, A., Das, S., and Hyman, B. T. (2021). APOE and Alzheimer's disease: advances in genetics, pathophysiology, and therapeutic approaches. *Lancet Neurol.* 20, 68–80. doi: 10.1016/S1474-4422(20)30412-9

Sharifi, Y., Payab, M., Mohammadi-Vajari, E., Aghili, S. M. M., Sharifi, F., Mehrdad, N., et al. (2021). Association between cardiometabolic risk factors and COVID-19 susceptibility, severity and mortality: a review. *J. Diabetes Metab. Disord.* 20, 1743–1765. doi: 10.1007/s40200-021-00822-2

Skaper, S. D., Facci, L., Zusso, M., and Giusti, P. (2018). An inflammation-centric view of neurological disease: beyond the neuron. *Front. Cell Neurosci.* 12:72. doi: 10.3389/fncel.2018.00072

Skok, K., Vander, K., Setaffy, L., Kessler, H. H., Aberle, S., Bargfrieder, U., et al. (2021). COVID-19 autopsies: procedure, technical aspects and cause of fatal course. Experiences from a single-center. *Pathol. Res. Pract.* 217:153305. doi: 10.1016/j.prp.2020.153305

Solomon, I. H., Normandin, E., Bhattacharyya, S., Mukerji, S. S., Keller, K., Ali, A. S., et al. (2020). Neuropathological features of Covid-19. *N. Engl. J. Med.* 383, 989–992. doi: 10.1056/NEJMc2019373

Song, E., Zhang, C., Israelow, B., Lu-Culligan, A., Prado, A. V., Skriabine, S., et al. (2021). Neuroinvasion of SARS-CoV-2 in human and mouse brain. *J. Exp. Med.* 218:e20202135. doi: 10.1084/jem.20202135

Spudich, S., and Nath, A. (2022). Nervous system consequences of COVID-19. *Science* 375, 267–269. doi: 10.1126/science.abm2052

Strbo, N., Yin, N., and Stojadinovic, O. (2014). Innate and adaptive immune responses in wound epithelialization. *Adv. Wound Care* 3, 492–501. doi: 10.1089/wound.2012.0435

Sun, S. H., Chen, Q., Gu, H. J., Yang, G., Wang, Y. X., Huang, X. Y., et al. (2020). A mouse model of SARS-CoV-2 infection and pathogenesis. *Cell Host Microbe* 28, 124.e–133.e. doi: 10.1016/j.chom.2020.05.020

Sungnak, W., Huang, N., Bécavin, C., Berg, M., Queen, R., Litvinukova, M., et al. (2020). SARS-CoV-2 entry factors are highly expressed in nasal epithelial cells together with innate immune genes. *Nat. Med.* 26, 681–687. doi: 10.1038/s41591-020-0868-6

Sweeney, M. D., Zhao, Z., Montagne, A., Nelson, A. R., and Zlokovic, B. V. (2019). Blood-brain barrier: from physiology to disease and back. *Physiol. Rev.* 99, 21–78. doi: 10.1152/physrev.00050.2017

Tan, L. Y., Komarasamy, T. V., and Rmt Balasubramaniam, V. (2021). Hyperinflammatory immune response and COVID-19: a double edged sword. *Front. Immunol.* 12:742941. doi: 10.3389/fimmu.2021.742941

Tansey, M. G., and Romero-Ramos, M. (2019). Immune system responses in Parkinson's disease: early and dynamic. *Eur. J. Neurosci.* 49, 364–383. doi: 10.1111/ejn.14290

Tavassoly, O., Safavi, F., and Tavassoly, I. (2020). Seeding brain protein aggregation by SARS-CoV-2 as a possible long-term complication of COVID-19 infection. *ACS Chem. Neurosci.* 11, 3704–3706. doi: 10.1021/acschemneuro.0c00676

Tekiela, P., and Majersik, J. J. (2021). The impact of COVID-19 on developing neurologic disorders. *Neurology* 96, e647–e649. doi: 10.1212/WNL.0000000000011348

Tizabi, Y., Getachew, B., and Aschner, M. (2021). Novel pharmacotherapies in parkinson's disease. *Neurotox. Res.* 39, 1381–1390. doi: 10.1007/s12640-021-00375-5

Tizabi, Y., Getachew, B., Csoka, A. B., Manaye, K. F., and Copeland, R. L. (2019). Novel targets for parkinsonism-depression comorbidity. *Prog. Mol. Biol. Transl. Sci.* 167, 1–24. doi: 10.1016/bs.pmbts.2019.06.004

Torices, S., Cabrera, R., Stangis, M., Naranjo, O., Fattakhov, N., Teglas, T., et al. (2021). Expression of SARS-CoV-2-related receptors in cells of the neurovascular unit: implications for HIV-1 infection. *J. Neuroinflammation* 18:167. doi: 10.1186/s12974-021-02210-2

Toscano, G., Palmerini, F., Ravaglia, S., Ruiz, L., Invernizzi, P., Cuzzoni, M. G., et al. (2020). Guillain-barré syndrome associated with SARS-CoV-2. *N. Engl. J. Med.* 382, 2574–2576. doi: 10.1056/NEJMc2009191

Tripathy, A. S., Vishwakarma, S., Trimbake, D., Gurav, Y. K., Potdar, V. A., Mokashi, N. D., et al. (2021). Pro-inflammatory CXCL-10, TNF-α, IL-1β, and IL-6: biomarkers of SARS-CoV-2 infection. *Arch. Virol.* 166, 3301–3310. doi: 10.1007/s00705-021-05247-z

Turski, W. A., Wnorowski, A., Turski, G. N., Turski, C. A., and Turski, L. (2020). AhR and IDO1 in pathogenesis of Covid-19 and the "Systemic AhR Activation Syndrome:" a translational review and therapeutic perspectives. *Restor. Neurol. Neurosci.* 38, 343–354. doi: 10.3233/RNN-201042

Varghese, P. M., Tsolaki, A. G., Yasmin, H., Shastri, A., Ferluga, J., Vatish, M., et al. (2020). Host-pathogen interaction in COVID-19: pathogenesis, potential therapeutics and vaccination strategies. *Immunobiology* 225:152008. doi: 10.1016/j.imbio.2020.152008

Vigasova, D., Nemergut, M., Liskova, B., and Damborsky, J. (2021). Multi-pathogen infections and Alzheimer's disease. *Microb. Cell Fact.* 20:25. doi: 10.1186/s12934-021-01520-7

Villa, C., Rivellini, E., Lavitrano, M., and Combi, R. (2022). Can SARS-CoV-2 infection exacerbate alzheimer's disease? An overview of shared risk factors and pathogenetic mechanisms. *J. Pers. Med.* 12:29. doi: 10.3390/jpm12010029

von Weyhern, C. H., Kaufmann, I., Neff, F., and Kremer, M. (2020). Early evidence of pronounced brain involvement in fatal COVID-19 outcomes. *Lancet* 395:e109. doi: 10.1016/S0140-6736(20)31282-4

Wan, Y., Shang, J., Graham, R., Baric, R. S., and Li, F. (2020). Receptor recognition by the novel coronavirus from wuhan: an analysis based on decade-long structural studies of SARS coronavirus. *J. Virol.* 94, e00127–e00220. doi: 10.1128/JVI.00127-20

Wang, D., Chen, F., Han, Z., Yin, Z., Ge, X., and Lei, P. (2021). Relationship between amyloid-β deposition and blood-brain barrier dysfunction in alzheimer's disease. *Front. Cell Neurosci.* 15:695479. doi: 10.3389/fncel.2021.695479

Wang, D., Hu, B., Hu, C., Zhu, F., Liu, X., Zhang, J., et al. (2020). Clinical characteristics of 138 hospitalized patients with 2019 novel coronavirus-infected pneumonia in Wuhan, China. *JAMA* 323, 1061–1069. doi: 10.1001/jama.2020.1585

Wang, J., Yang, G., Wang, X., Wen, Z., Shuai, L., Luo, J., et al. (2021). SARS-CoV-2 uses metabotropic glutamate receptor subtype 2 as an internalization factor to infect cells. *Cell Discov.* 7:119. doi: 10.1038/s41421-021-00357-z

Wang, Q., Davis, P. B., Gurney, M. E., and Xu, R. (2021). COVID-19 and dementia: analyses of risk, disparity, and outcomes from electronic health records in the US. *Alzheimers Dement* 17, 1297–1306. doi: 10.1002/alz.12296

Wang, Y., Yang, Y., Ren, L., Shao, Y., Tao, W., and Dai, X. J. (2021). Preexisting mental disorders increase the risk of COVID-19 infection and associated mortality. *Front. Public Health* 9:684112. doi: 10.3389/fpubh.2021.684112

Wassie, G. T., Azene, A. G., Bantie, G. M., Dessie, G., and Aragaw, A. M. (2020). Incubation period of severe acute respiratory syndrome novel coronavirus 2 that causes coronavirus disease 2019: a systematic review and meta-analysis. *Curr. Ther. Res. Clin. Exp.* 93:100607. doi: 10.1016/j.curtheres.2020.100607

Wichmann, D., Sperhake, J. P., Lütgehetmann, M., Steurer, S., Edler, C., Heinemann, A., et al. (2020). Autopsy findings and venous thromboembolism in patients with COVID-19: a prospective cohort study. *Ann. Intern. Med.* 173, 268–277. doi: 10.7326/M20-2003

Xia, H., and Lazartigues, E. (2008). Angiotensin-converting enzyme 2 in the brain: properties and future directions. *J. Neurochem.* 107, 1482–1494. doi: 10.1111/j.1471-4159.2008.05723.x

Xu, J., Zhong, S., Liu, J., Li, L., Li, Y., Wu, X., et al. (2005). Detection of severe acute respiratory syndrome coronavirus in the brain: potential role of the chemokine mig in pathogenesis. *Clin. Infect. Dis.* 41, 1089–1096. doi: 10.1086/444461

Yang, L., Xie, X., Tu, Z., Fu, J., Xu, D., and Zhou, Y. (2021). The signal pathways and treatment of cytokine storm in COVID-19. *Signal Transduct. Target. Ther.* 6:255. doi: 10.1038/s41392-021-00679-0

Yi, Y., Xu, Y., Jiang, H., and Wang, J. (2021). Cardiovascular disease and COVID-19: insight from cases with heart failure. *Front. Cardiovasc. Med.* 8:629958. doi: 10.3389/fcvm.2021.629958

Yu, F., Du, L., Ojcius, D. M., Pan, C., and Jiang, S. (2020). Measures for diagnosing and treating infections by a novel coronavirus responsible for a pneumonia outbreak originating in Wuhan, China. *Microbes Infect.* 22, 74–79. doi: 10.1016/j.micinf.2020.01.003

Yu, Y., Travaglio, M., Popovic, R., Leal, N. S., and Martins, L. M. (2021). Alzheimer's and parkinson's diseases predict different COVID-19 outcomes: a uk biobank study. *Geriatrics* 6:10. doi: 10.3390/geriatrics6010010

Zanin, L., Saraceno, G., Panciani, P. P., Renisi, G., Signorini, L., Migliorati, K., et al. (2020). SARS-CoV-2 can induce brain and spine demyelinating lesions. *Acta Neurochir.* 162, 1491–1494. doi: 10.1007/s00701-020-04374-x

Zhang, L., Zhou, L., Bao, L., Liu, J., Zhu, H., Lv, Q., et al. (2021). SARS-CoV-2 crosses the blood-brain barrier accompanied with basement membrane disruption without tight junctions alteration. *Signal Transduct. Target Ther.* 6:337. doi: 10.1038/s41392-021-00719-9

Zhang, X., Chen, X., Chen, L., Deng, C., Zou, X., Liu, W., et al. (2020). The evidence of SARS-CoV-2 infection on ocular surface. *Ocul. Surf.* 18, 360–362. doi: 10.1016/j.jtos.2020.03.010

Zhang, Y., Geng, X., Tan, Y., Li, Q., Xu, C., Xu, J., et al. (2020). New understanding of the damage of SARS-CoV-2 infection outside the respiratory system. *Biomed. Pharmacother.* 127:110195. doi: 10.1016/j.biopha.2020.110195

Zhou, L., Xu, Z., Castiglione, G. M., Soiberman, U. S., Eberhart, C. G., and Duh, E. J. (2020). ACE2 and TMPRSS2 are expressed on the human ocular surface, suggesting susceptibility to SARS-CoV-2 infection. *Ocul. Surf.* 18, 537–544. doi: 10.1016/j.jtos.2020.06.007

Zhu, N., Zhang, D., Wang, W., Li, X., Yang, B., Song, J., et al. (2020). A novel coronavirus from patients with pneumonia in china, 2019. *N. Engl. J. Med.* 382, 727–733. doi: 10.1056/NEJMoa2001017

Zhu, Z., Lian, X., Su, X., Wu, W., Marraro, G. A., and Zeng, Y. (2020). From SARS and MERS to COVID-19: a brief summary and comparison of severe acute respiratory infections caused by three highly pathogenic human coronaviruses. *Respir. Res.* 21:224. doi: 10.1186/s12931-020-01479-w

Ziegler, C. G. K., Allon, S. J., Nyquist, S. K., Mbano, I. M., Miao, V. N., Tzouanas, C. N., et al. (2020). SARS-CoV-2 receptor ACE2 is an interferon-stimulated gene in human airway epithelial cells and is detected in specific cell subsets across tissues. *Cell* 181, 1016.e–1035.e. doi: 10.1016/j.cell.2020.04.035

Zubair, A. S., McAlpine, L. S., Gardin, T., Farhadian, S., Kuruvilla, D. E., and Spudich, S. (2020). Neuropathogenesis and neurologic manifestations of the coronaviruses in the age of coronavirus disease 2019: a review. *JAMA Neurol.* 77, 1018–1027. doi: 10.1001/jamaneurol.2020.2065

Conflict of Interest: The authors declare that the research was conducted in the absence of any commercial or financial relationships that could be construed as a potential conflict of interest.

frontiers | Frontiers in Neuroscience

ORIGINAL RESEARCH
published: 19 May 2022
doi: 10.3389/fnins.2022.855096

MicroRNA Alterations in Chronic Traumatic Encephalopathy and Amyotrophic Lateral Sclerosis

*Marcela Alvia[1], Nurgul Aytan[1,2], Keith R. Spencer[3], Zachariah W. Foster[3], Nazifa Abdul Rauf[3], Latease Guilderson[3], Ian Robey[4], James G. Averill[4], Sean E. Walker[4], Victor E. Alvarez[1,2,3,5], Bertrand R. Huber[1,2,3], Rebecca Mathais[1], Kerry A. Cormier[1,3,5], Raymond Nicks[1], Morgan Pothast[1], Adam Labadorf[2,3], Filisia Agus[2], Michael L. Alosco[1,2], Jesse Mez[1,2], Neil W. Kowall[1,2,3], Ann C. McKee[1,2,3,5,6], Christopher B. Brady[2,3,5] and Thor D. Stein[1,3,5,6]**

[1] Boston University Alzheimer's Disease Research Center, Boston University CTE Center, Boston University School of Medicine, Boston, MA, United States, [2] Department of Neurology, Boston University School of Medicine, Boston, MA, United States, [3] VA Boston Healthcare System, Boston, MA, United States, [4] Southern Arizona VA Healthcare System, Tucson, AZ, United States, [5] Department of Veterans Affairs Medical Center, Bedford, MA, United States, [6] Department of Pathology and Laboratory Medicine, Boston University School of Medicine, Boston, MA, United States

OPEN ACCESS

Edited by:
Wang-Xia Wang,
University of Kentucky, United States

Reviewed by:
Hsiuying Wang,
National Yang Ming Chiao Tung University, Taiwan
Savina Apolloni,
University of Rome Tor Vergata, Italy

***Correspondence:**
Thor D. Stein
tdstein@bu.edu

Specialty section:
This article was submitted to Neurodegeneration, a section of the journal Frontiers in Neuroscience

Received: *14 January 2022*
Accepted: *09 March 2022*
Published: *19 May 2022*

Citation:
Alvia M, Aytan N, Spencer KR, Foster ZW, Rauf NA, Guilderson L, Robey I, Averill JG, Walker SE, Alvarez VE, Huber BR, Mathais R, Cormier KA, Nicks R, Pothast M, Labadorf A, Agus F, Alosco ML, Mez J, Kowall NW, McKee AC, Brady CB and Stein TD (2022) MicroRNA Alterations in Chronic Traumatic Encephalopathy and Amyotrophic Lateral Sclerosis. Front. Neurosci. 16:855096. doi: 10.3389/fnins.2022.855096

Repetitive head impacts (RHI) and traumatic brain injuries are risk factors for the neurodegenerative diseases chronic traumatic encephalopathy (CTE) and amyotrophic lateral sclerosis (ALS). ALS and CTE are distinct disorders, yet in some instances, share pathology, affect similar brain regions, and occur together. The pathways involved and biomarkers for diagnosis of both diseases are largely unknown. MicroRNAs (miRNAs) involved in gene regulation may be altered in neurodegeneration and be useful as stable biomarkers. Thus, we set out to determine associations between miRNA levels and disease state within the prefrontal cortex in a group of brain donors with CTE, ALS, CTE + ALS and controls. Of 47 miRNAs previously implicated in neurological disease and tested here, 28 (60%) were significantly different between pathology groups. Of these, 21 (75%) were upregulated in both ALS and CTE, including miRNAs involved in inflammatory, apoptotic, and cell growth/differentiation pathways. The most significant change occurred in miR-10b, which was significantly increased in ALS, but not CTE or CTE + ALS. Overall, we found patterns of miRNA expression that are common and unique to CTE and ALS and that suggest shared and distinct mechanisms of pathogenesis.

Keywords: chronic traumatic encephalopathy, amyotrophic lateral sclerosis, microRNA, contact sports, p-tau, TDP-43, prefrontal cortex

INTRODUCTION

Chronic traumatic encephalopathy (CTE) is a neurodegenerative disease associated with years exposure to repetitive head impacts (RHI). Chronic traumatic encephalopathy has been reported in a wide variety of RHI exposures, including contact sports such as American football, boxing, hockey, and rugby as well as from military blast injuries. Clinical symptoms may involve multiple

domains, including mood, behavior, and cognitive functions (Katz et al., 2021). In some cases, motor symptoms can emerge in the form of parkinsonism (Adams et al., 2018) or motor neuron disease/amyotrophic lateral sclerosis (ALS) (McKee et al., 2009). Amyotrophic lateral sclerosis is four times more frequent in National Football League players (Lehman et al., 2012; Daneshvar et al., 2021) and is found within ∼6% of contact sports athletes with CTE (Mez et al., 2017). Microscopically, the hallmark of CTE involves phosphorylated tau (p-tau) neurofibrillary tangles (NFTs) that accumulate within neurons and neuronal processes in the cerebral cortex, preferentially at sulcal depths and around blood vessels. TDP-43 is present in approximately half of low stage (stage I and II) CTE and first appears within the CTE p-tau lesions at the sulcal depths of the frontal cortex (Danielsen et al., 2017). In high stage (stage III and IV) CTE, TDP-43 pathology is more frequent and involves additional brain regions (McKee et al., 2013).

Amyotrophic lateral sclerosis (ALS) is characterized by progressive degeneration of motor neurons within the motor cortex of the brain (upper motor neurons) and spinal cord (lower motor neurons). Symptoms typically manifest in one region of the body and progress to paralysis, respiratory failure, and eventual death. In most sporadic cases, pTDP-43 inclusions are present within motor neurons and variably in other regions of the brain. The disease course tends to be rapid with death occurring in 2 to 5 years. Both genetic and environmental factors are linked to the etiology of ALS (Saez-Atienzar et al., 2021). A 2007 study found that a diagnosis of ALS was 11-fold higher in those with multiple head injuries within 10 years than in those with no head injuries (H. Chen et al., 2007; Schmidt et al., 2010).

Chronic traumatic encephalopathy (CTE) with TDP-43 proteinopathy and ALS was first reported in contact sport athletes, including 2 former NFL athletes and one professional boxer (McKee et al., 2010) as well as a young soccer player (McKee et al., 2014). In a study done on the military cohort of the Department of Veterans Affairs Biorepository Brain Bank 5.8% of those with ALS were also comorbid with CTE. These comorbid subjects were more likely to have a history of traumatic brain injury (TBI). Clinically, they were more likely to have a bulbar onset and mood and behavioral alterations (Moszczynski et al., 2018; Walt et al., 2018).

MicroRNAs (miRNAs) are small non-coding strands of RNA of approximately 22 base pairs that are involved in regulating translation of messenger RNA. They target mRNA at the 3′ UTR and may either silence their translation or degrade them (O'Brien et al., 2018). MiRNAs are fairly new in the biomarker field and several studies have been performed that describe that their fluctuations in relation to diseases such as ALS and Alzheimer's disease (Cheng et al., 2015; Mez et al., 2017; Miya Shaik et al., 2018; Ricci et al., 2018; Dewan and Traynor, 2021; Magen et al., 2021). Their putative involvement in CTE is thus far unknown.

The overlap in CTE and ALS pathologies and risk factors suggests they may share common disease mechanisms, yet the pathways of neurodegeneration might be sufficiently divergent to allow biomarker distinctions and diagnosis during life. Here we set out to determine whether miRNA levels were altered in the prefrontal cortex of participants with CTE, ALS, and comorbid CTE + ALS compared to controls. We hypothesized that individual miRNAs would be differentially regulated in each disease and that some miRNAs would be shared by CTE and ALS.

MATERIALS AND METHODS

Participants and Pathological Groups

Brain donors were selected from the Department of Veterans Affairs Biorepository Brain Bank (Brady et al., 2013) and the Understanding Neurology Injury and Traumatic Encephalopathy (UNITE) study brain bank (Mez et al., 2015, 2017). All consents for research participation and brain donation were provided by next of kin. Institutional Review Boards of the Boston and Bedford VA Healthcare Systems and Boston University Medical Center approved the relevant study protocols.

All brains were examined by neuropathologists (TS, AM, BH, VA) with no knowledge of the clinical data. Diagnoses were made using previously reported protocols and well-established criteria (Mez et al., 2015). The diagnosis of ALS required degeneration of upper and lower motor neurons with degeneration of lateral and ventral corticospinal tracts of the spinal cord and loss of anterior horn cells from cervical, thoracic and lumbar spinal cord with gliosis (Mackenzie et al., 2010). Chronic traumatic encephalopathy was diagnosed using established National Institute of Neurological Disorders and Stroke, NIBIB consensus criteria (McKee et al., 2016; Bieniek et al., 2021) and the McKee staging system (McKee et al., 2013; Alosco et al., 2020).

Brain donors were age and sex (all men) matched, had no other neurodegenerative disease co-morbidities and CTE cases were selected to include all 4 stages. The groups included 16 participants with CTE, 12 with CTE and ALS (CTE + ALS), and 2 controls from the UNITE brain bank (Mez et al., 2015). Fourteen participants with ALS, 9 with CTE + ALS, and 5 controls were selected based on matching diagnosis, age, and sex from the Department of VABBB (Brady et al., 2013). An additional 13 controls were included from the VA National Post-Traumatic Stress Disorder brain bank (Friedman et al., 2017). Controls were without a clinical neurodegenerative disease at post mortem examination. Overall, there were 71 participants, 16 in the CTE group, 21 in the CTE + ALS group, 14 in the ALS group, and 20 participants in the control group (**Table 1**). There was no significant difference in the age at death or RIN values between the groups.

MiRNA Selection

A custom miRNA plate (*Applied BioSystems, Waltham MA*) was designed to include 47 targets previously implicated in human neurodegenerative diseases including Alzheimer disease, ALS, Multiple Sclerosis and Huntington's disease as determined by PubMed search in May 2019 (**Supplementary Tables 1**, **2**). This study is the first to examine miRNA levels in CTE. MiRNA pathways were determined via Pubmed searches conducted in December 2019 using terms including each miRNA name, Alzheimer Disease, ALS, Huntington's disease, TBI, multiple sclerosis, Parkinson's disease, inflammatory, cell death, apoptosis,

TABLE 1 | Variation in pathological group demographics.

	Control *n* = 20	**ALS *n* = 14**	**CTE *n* = 16**	**CTE+ALS *n* = 21**
Age (years)	53.6 (2.5)	59.1 (1.4)	64.9 (3.2)	59.1 (3.4)
Age range (years)	39–70	48–64	34–89	29–87
CTE stage	N/A	N/A	2.56 (0.26)	2.62 (0.2)
RIN	6.8 (0.26)	6.93 (1.4)	6.56 (0.32)	7.48 (0.29)

Data are expressed as mean (SEM). Amyotrophic lateral sclerosis (ALS), chronic traumatic encephalopathy (CTE).

TABLE 2 | Changes in miRNA expression between pathological groups.

MicroRNA	**Control**	**CTE**		**ALS**		**CTE+ALS**	
	Δ CT	**Δ CT**	**P-value**	**Δ CT**	**P-value**	**Δ CT**	**P-value**
miR-107	−0.07	**−1.48**	**0.0100**	**−1.31**	**0.0337**	**−1.18**	**0.0342**
miR-181c-5p	−2.23	**−3.40**	**0.0489**	−2.89	0.4215	−2.99	0.2298
miR-34c-5p	6.60	**5.18**	**0.0292**	5.35	0.0765	**5.31**	**0.0331**
let-7b-5p	0.02	**−1.43**	**0.0128**	−1.18	0.0591	**−1.23**	**0.0226**
miR-9-5p	−4.78	**−6.06**	**0.0148**	−5.76	0.0971	**−5.94**	**0.0179**
miR-125b-5p	−5.17	**−6.62**	**0.0098**	−6.23	0.0948	**−6.29**	**0.0387**
miR-210-3p	3.54	2.45	0.0747	2.42	0.0789	**2.45**	**0.0491**
miR-124-3p	−6.43	**−7.49**	**0.0493**	−7.01	0.4540	−7.22	0.1439
let-7d-5p	−1.07	−2.03	0.1351	−2.12	0.1112	−1.68	0.4122
miR-146b-5p	1.47	**0.32**	**0.0181**	**0.29**	**0.0184**	0.89	0.3034
miR-197-3p	−6.97	**−8.02**	**0.0444**	−7.89	0.1066	−7.78	0.1181
miR-148a-3p	1.59	**0.52**	**0.0403**	**0.40**	**0.0262**	0.64	0.0533
miR-26b-5p	−3.99	**−5.46**	**0.0069**	−4.99	0.1147	**−5.27**	**0.0129**
miR-26a-5p	−3.81	**−5.36**	**0.0029**	−4.72	0.1395	**−5.04**	**0.0125**
miR-128-3p	−4.35	**−5.79**	**0.0099**	−5.41	0.0952	**−5.45**	**0.0428**
miR-23a-3p	−2.89	−3.90	0.0849	−3.73	0.2038	−3.69	0.1693
miR-34a-5p	−1.50	−5.51	0.0992	**−2.73**	**0.0418**	−2.56	0.0552
miR-100-5p	0.68	**−0.66**	**0.0271**	−0.24	0.2071	−0.26	0.1260
miR-16-5p	−1.34	**−2.72**	**0.0138**	−2.40	0.0920	−2.29	0.0934
miR-19b-3p	0.039	**−1.17**	**0.0333**	−0.92	0.1358	**−1.11**	**0.0289**
miR-30d-5p	−1.09	**−2.13**	**0.0495**	−1.93	0.1535	**−2.25**	**0.0142**
miR-30e-5p	−4.30	−5.35	0.0881	**−5.57**	**0.0380**	**−5.78**	**0.0044**
let-7i-5p	−4.38	**−5.80**	**0.0173**	−5.48	0.1035	**−5.69**	**0.0199**
miR-15a-5p	−2.02	**−3.31**	**0.0161**	**−3.36**	**0.0161**	**−3.08**	**0.0399**
miR-146a-5p	0.44	**−0.69**	**0.0450**	**−0.93**	**0.0153**	**−0.68**	**0.0300**
miR-30c-5p	−4.78	−5.78	0.0553	−5.81	0.0581	**−5.75**	**0.0434**
miR-196a-5p	2.14	0.95	0.0866	**0.68**	**0.0265**	**0.67**	**0.0171**
miR-186	2.40	**0.96**	**0.0112**	1.44	0.1522	**1.30**	**0.0475**
miR-30a-5p	−4.40	−4.81	0.8045	−5.62	0.2241	−5.47	0.0991
miR-132-3p	−0.62	−1.37	0.2381	−1.29	0.3511	−0.91	0.8370
miR-221-3p	−2.68	**−3.94**	**0.0316**	**−3.96**	**0.0370**	**−3.99**	**0.0150**
miR-10b	2.14	1.65	0.6900	**0.195**	**0.0013***	1.10	0.0949
miR-212-3p	−0.48	−1.06	0.3908	−1.30	0.1647	−1.26	0.1364
miR-153-3p	−1.32	−2.25	0.0742	−1.80	0.5561	−1.99	0.2126
miR-101-5p	−1.66	−2.78	0.2891	−2.79	0.2913	−2.58	0.3736
miR-422a	−0.72	−1.25	0.6501	−1.41	0.4741	−1.83	0.0803
miR-23b-3p	−4.35	−4.71	0.8332	−5.01	0.4834	−5.33	0.1175
miR-133b	7.29	6.08	0.0686	6.32	0.2049	6.19	0.0772

ΔCTs of the 38 successfully amplified miRNAs are shown. P-values are from ANOVA with post-hoc Dunnett multiple comparison test between the disease and control groups. All bolded values are significant with α = 0.05. Asterisks (*) indicate p-values that are below Bonferroni correction value of 0.0013.

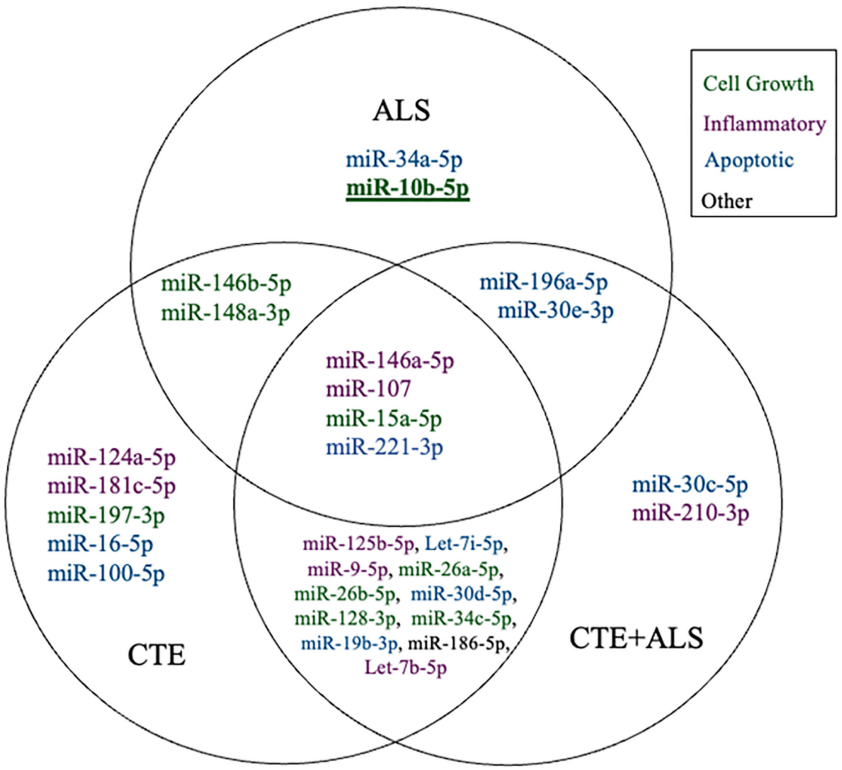

FIGURE 1 | Venn Diagram showing distinct and overlapping significantly altered miRNA within CTE, ALS, and CTE + ALS compared to controls. Bold and underline indicates a p-value at or below the Bonferroni number of 0.0013. Purple indicates miRNAs involved in inflammatory pathways; green indicates cell growth; blue indicates apoptotic; and black indicates miRNA that did not fit in any group.

cell growth, cell proliferation, development, human brain. Each individual miRNA may be involved in multiple different processes, and there is likely overlap between involved pathways.

Samples and MiRNA Extraction

Whole brain and spinal cord were half frozen and half fixed for complete neuropathological workup as described previously (Brady et al., 2013; Mez et al., 2015). miRNAs were measured within frozen dorsolateral prefrontal cortex gray matter. This region was chosen because it is affected in both diseases and has been utilized in previous studies of gene expression in neurodegenerative diseases (Labadorf et al., 2018).

Approximately 30 mg of frozen prefrontal cortex was homogenized over wet ice by hand using thioglyecrol provided by the *Maxwell RSC miRNA kit (*Promega, Madison WI*).* From this same kit the homogenized tissue was then processed with lysis buffer, DNase and proteinase K solutions. The solution was then inserted into a ready-made cartridge from the kit with all the reagents needed for extraction. MiRNA was extracted and eluted using the *Maxwell 16 Instrument* (Promega).

Quantitative Real Time Polymerase Chain Reaction

Samples were diluted to 5ng/μl and transcribed into cDNA using a *Taqman Advanced MiRNA cDNA Synthesis Kit from Applied BioSciences*. The cDNA underwent an additional amplification step to increase yields of unstable miRNAs (*MiR-Amp*). Samples were diluted 1:10 and loaded onto qPCR plates with *Taqman Fast Advanced Master Mix*. Each sample received 2 qPCR runs using the *StepOnePlus Real Time polymerase chain reaction (PCR) System* (Applied Biosystems, Foster City, CA), including one to evaluate for U6 a small non-coding spliceosome RNA that is a common endogenous control (Campos-Melo et al., 2013). The next qPCR run was with the custom miRNA plates with primers for selected targets. Samples were tested in duplicate.

Statistical Analysis

Targets that were successfully amplified had their ΔCT calculated using U6 endogenous control values. All statistics and graphs were generated using GraphPad Prism. Outliers were excluded using the ROUT method set to 0.1%, which resulted in the exclusion of miR-15a-5p from one CTE + ALS sample. Significant changes in each miRNA ΔCT were determined between experimental groups and controls using ANOVA with Dunnett's multiple comparison testing. In order to further account for the multiple miRNAs tested, a Bonferroni correction of α-value (0.05) divided by the number of successfully amplified miRNA (38) was applied to give a cut-off p-value of 0.00132. For the purposes of graphing the relative change was calculated using the $2^{-\Delta\Delta CT}$ method (Livak and Schmittgen, 2001).

TABLE 3 | Upregulated miRNAs between control and pathology groups.

MicroRNA	CTE	ALS	CTE+ALS
miR-107	✓	✓	✓
miR-181c-5p	✓		
miR-34c-5p	✓		✓
let-7b-5p	✓		✓
miR-9-5p	✓		✓
miR-125b-5p	✓		✓
miR-210-3p			✓
miR-124-3p	✓		
let-7d-5p			
miR-146b-5p	✓	✓	
miR-197-3p	✓		
miR-148a-3p	✓	✓	
miR-26b-5p	✓		✓
miR-26a-5p	✓		✓
miR-128-3p	✓		✓
miR-23a-3p			
miR-34a-5p		✓	
miR-100-5p	✓		
miR-16-5p	✓		
miR-19b-3p	✓		✓
miR-30d-5p	✓		✓
miR-30e-5p		✓	✓
let-7i-5p	✓		✓
miR-15a-5p	✓	✓	✓
miR-146a-5p	✓	✓	✓
miR-30c-5p			✓
miR-196a-5p		✓	✓
miR-186	✓		✓
miR-30a-5p			
miR-132-3p			
miR-221-3p	✓	✓	✓
miR-10b		✓	
miR-212-3p			
miR-153-3p			
miR-101-5p			
miR-422a			
miR-23b-3p			
miR-133b			

✓ denotes if a miRNA ΔCT was upregulated in its pathological group in relation to the control group. Statistical analysis was done via ANOVA and Dunnett's multiple comparison testing.

RESULTS

A total of 38 of the 47 targets were successfully amplified, indicating reliable expression in the human prefrontal cortex. Of those 38 miRNAs, 28 showed a significant difference in ΔCT values across pathology groups using ANOVA (**Table 2**). **Figure 1** shows the distribution and overlap of upregulated miRNA across pathology groups.

MiRNAs significantly upregulated across pathology groups are summarized in **Table 3**. Those altered in only one disease group included two (7%) miRNAs (miR-34a-5p and miR-10b-5p) upregulated in ALS; five miRNAs (18%; miR-124-3p, miR-181c-5p, miR-197-3p, miR-16-5p, and miR-100-5p) were significantly altered in CTE; and two (7%; miR-30c-5p and miR-210-3p) were unique to CTE + ALS. Of the miRNAs that were significantly altered in two disease groups, two miRNAs (7%; miR-146b-5p and miR-148a-3p) were upregulated in ALS and CTE; two (7%; miR-196a-5p and miR-30e-5p) were upregulated in both ALS and in the CTE + ALS; eleven (39%; miR-125b-5p, miR-9-5p, let-7i-5p, miR-26a-5p, miR-26b-5p, miR-30d-5p, miR-128-3p, miR-34c-5p, miR-19b-3p, miR-186 and let-7b-5p) were upregulated in CTE and CTE + ALS. Finally, four miRNAs (14%; miR-146a-5p, miR-107, miR-15a-5p and miR-221-3p) had significant upregulation in all 3 pathological groups (**Figure 1**). Only miR-10b had a p-value less than 0.00132 (Bonferroni corrected for multiple comparisons).

Based on previous studies, miRNAs were categorized according to their role in physiological processes. The majority of miRNAs altered in ALS, CTE, or CTE + ALS have roles in inflammation, apoptosis, or cell growth and differentiation (**Supplementary Tables 3–5**). Specifically, eight (29%) upregulated miRNAs are involved in inflammatory processes (**Figure 2**), nine (32%) are involved in cell growth and differentiation (**Figure 3**) and 10 (36%) play a role in apoptosis (**Figure 4**). There was one miRNA (3%) (miR-186) that was upregulated in CTE and CTE + ALS that has been shown to affect synaptic activity and inhibit BACE1 (Kim et al., 2016). The cell growth and differentiation miR-10b was increased in ALS, but not CTE or CTE + ALS (**Figure 3**). Apoptotic miRNAs were increased similarly across ALS, CTE, and CTE + ALS (**Figure 4**).

Within each disease, the percentage of miRNA pathways involved differed (**Figure 5**). In ALS, altered miRNAs were most frequently involved in cell growth (40%) and apoptosis (40%) and less frequently inflammation (20%). CTE also showed frequent alterations in cell growth (36%), but greater involvement in inflammatory pathways (32%) compared to ALS. Finally, when ALS and CTE were comorbid, apoptosis (37%) and inflammatory (32%) pathways were the most frequently involved.

DISCUSSION

Overall, we found that CTE and ALS were characterized by similar changes in miRNAs previously implicated in neurological disease. The majority of miRNAs (72%) were similarly involved in ALS and CTE, suggesting common pathogenetic pathways of inflammation, cell growth, and apoptosis. The most significantly changed miRNA was miR-10b-5p, which was increased in ALS.

Cell Growth and Differentiation Pathways

MiR-10b is involved in cell growth and differentiation pathways. Mir-10b-5p has been shown to interact with the HOX gene cluster in both Alzheimer's disease (AD) (Ruan et al., 2021) and Huntington's disease (Hoss et al., 2014). In Alzheimer disease Ruan and colleagues showed that HOX genes were decreased and inhibited by miR-10b-5p, leading to more severe disease. Hoss et al. showed that three miRNAs that

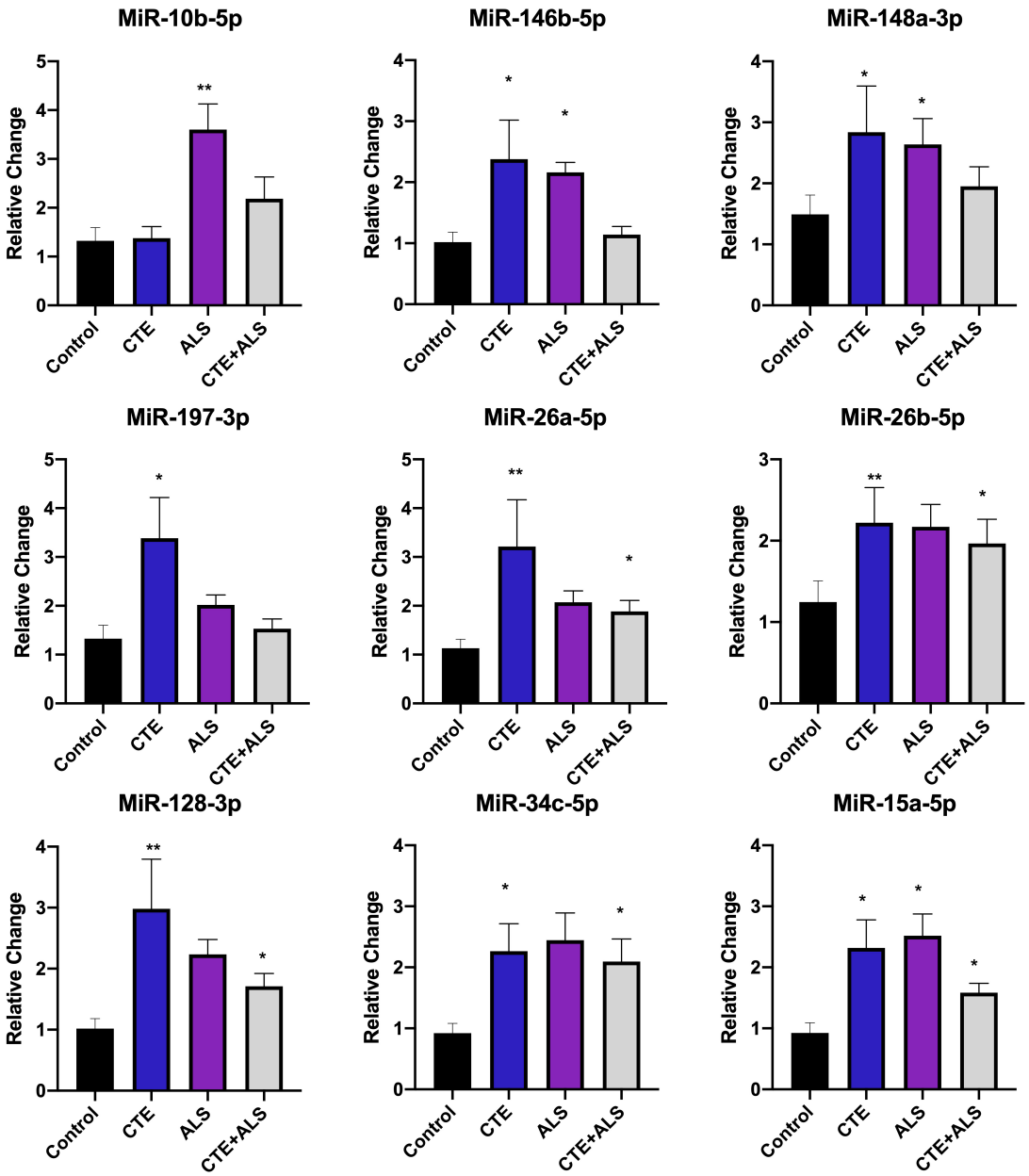

FIGURE 2 | Cell Growth and Differentiation miRNAs significantly altered in CTE, ALS, or CTE + ALS. MiR-10b was upregulated in ALS alone. MiR-146b-5p and miR-148a-3p were significantly upregulated in non-comorbid ALS and CTE. MiR-197-3p was upregulated in CTE. Four miRNAs, miR-26a-5p, miR-26b-5p, miR-128-3p, miR-34c-5p were upregulated in CTE and CTE + ALS. Finally, miR-15a-5p was upregulated in all 3 conditions. Error bars denote standard error of the mean. $^{*}p < 0.05$, $^{**}p < 0.01$ compared to control group. Refer to **Table 3** for statistical analyses between the pathologic groups and the control group.

originate at or near the HOX gene cluster, miR-10b-5p, miR-196a-5p and miR-148a-3p, are significantly upregulated in Huntington's disease, a neurodegeneration characterized by motor dysfunction, personality change, and cognitive decline. MiR-10b-5p has been studied in its relation to ALS though results have been mixed. Down regulation in ALS has been observed in muscle tissue (Si et al., 2018) and in plasma (Banack et al., 2020), but upregulation has been observed in whole blood (De Felice et al., 2018).

Another target of miR-10b-5p is brain derived neurotrophic growth factor (BDNF), which is a key regulator of cell growth and plasticity in the brain and has been shown to enhance cell survival. MiR-10b-5p has been shown to directly inhibit BDNF (L. Wang et al., 2020). The BDNF/TrkB pathway has been shown to be altered in ALS and BDNF was increased in skeletal muscle (Lanuza et al., 2019). Decreases in BDNF have also been reported after TBI (Korley et al., 2016), in AD, and in aging (Jiao et al., 2016). Other miRNAs that disrupt BDNF and may be involved

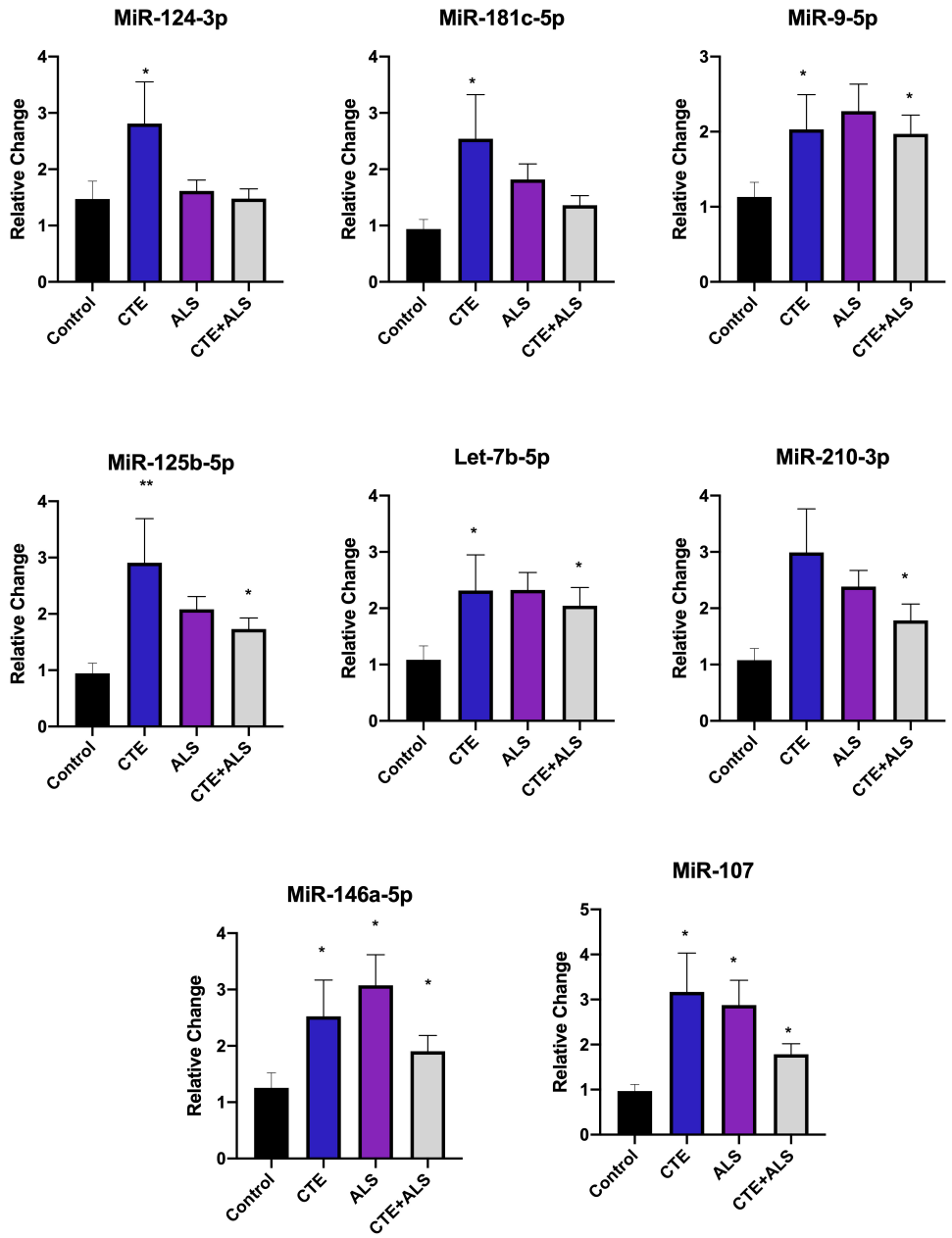

FIGURE 3 | Inflammatory miRNAs significantly altered in CTE, ALS, or CTE + ALS. MiR-124-3p, miR-181c-5p were significantly upregulated in CTE only. MiR-9-5p, let-7b-5p, miR-125-5p, let-7b-5p were significantly upregulated in both CTE and CTE + ALS. MiR-210-3p was significantly upregulated in comorbid CTE + ALS. Finally, miR-146a-5p and miR-107 were significantly upregulated in all three groups. Error bars denote standard error of the mean. $^{*}p < 0.05$, $^{**}p < 0.01$ compared to control group. Refer to **Table 3** for statistical analyses between the pathologic groups and the control group.

include miR-26a-5p, miR-26b-5p, and miR-15a-5p. These were also found to be altered in CTE and CTE + ALS.

Inflammatory Pathways

Altered inflammatory pathways are a feature of RHI and CTE (Cherry et al., 2016, 2021) and ALS (Spencer et al., 2020), and numerous miRNAs might regulate these processes (**Supplementary Table 3**). Of the miRNAs altered in CTE and CTE + ALS compared to ALS, many were inflammatory, which supports the roles of RHI and inflammation in CTE pathogenesis. On the other hand, some inflammatory miRNAs were upregulated similarly in all three disease groups (miR-146a-5p, miR-107). MiR-146a-5p and miR-107 along with miR-9-5p, miR-181c-5p and miR-125b-5p are involved in the NF-κB pathway. The NF-κB has been previously implicated in ALS (Parisi et al., 2016; Tahamtan et al., 2018; Slota and Booth, 2019; Källstig et al., 2021) and TBI (Jassam et al., 2017;

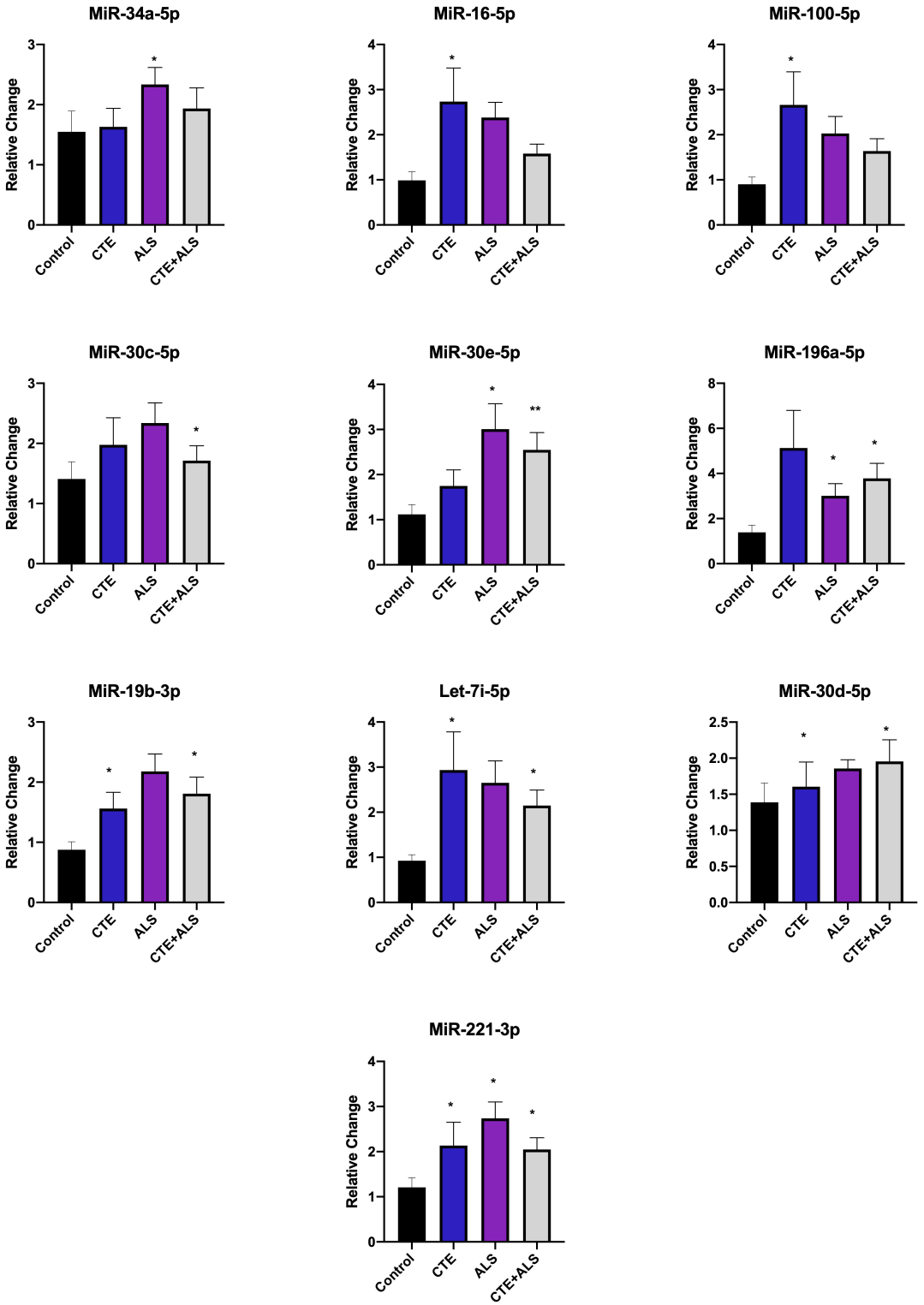

FIGURE 4 | Apoptotic miRNAs significantly altered in CTE, ALS, or CTE + ALS. MiR-34a-5p-5p was significantly upregulated in ALS alone. miR-16-5p and miR-100-5p were upregulated in CTE. MiR-30c-5p was upregulated in comorbid CTE + ALS. MiR-196a-5p and miR-30e-5p miRNAs were upregulated in both ALS and CTE + ALS. Let-7i-5p, miR-30d-5p, and miR-19-3p were upregulated in both CTE and CTE + ALS. Finally, miR-221-3p was upregulated in all three groups. Error bars denote standard error of the mean. $^{*}p < 0.05$, $^{**}p < 0.01$ compared to control group. Refer to **Table 3** for statistical analyses between the pathologic groups and the control group.

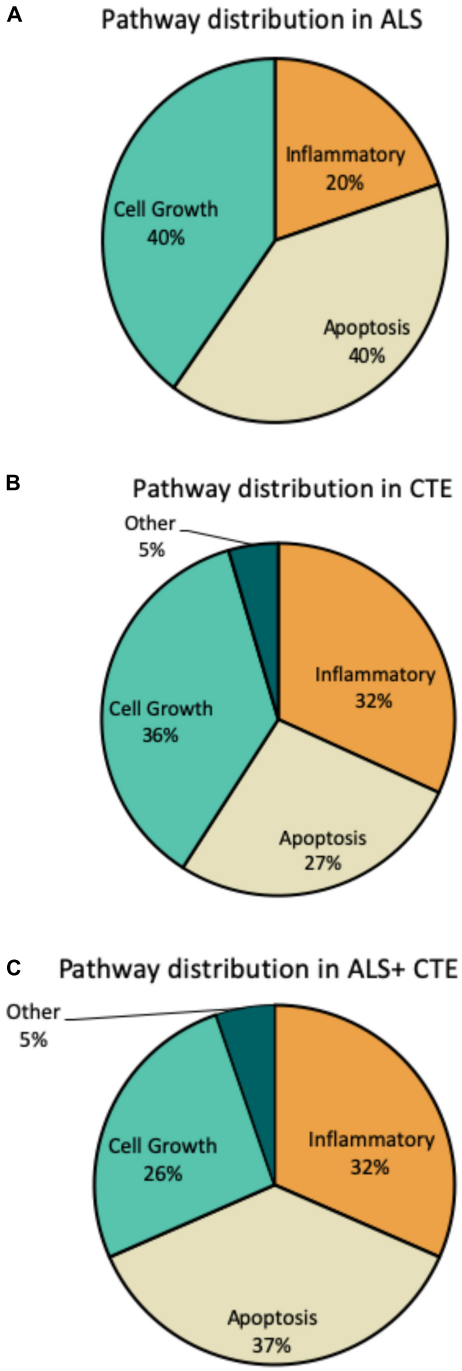

FIGURE 5 | Frequency of miRNA pathways in disease. MiRNAs were classified into inflammatory, cell growth, apoptotic, and other pathways and the frequency within each pathway is shown. **(A)**. Frequency of miRNA pathways in ALS. **(B)**. Frequency of miRNA pathways in CTE. **(C)**. Frequency of miRNA pathways in CTE + ALS.

Pierre et al., 2021). Outside of the NF-κB pathway, miR-125b-5p has been directly implicated in hyperphosphorylation of tau (Banzhaf-Strathmann et al., 2014) and might contribute to CTE pathogenesis.

Apoptotic Pathways

Several upregulated miRNAs have a role in apoptosis and autophagy in neurodegenerative diseases. Protein and damaged cell clearance are especially important in ALS and CTE in which abnormal p-TDP-43 and p-tau proteins accumulate. MiRNAs related to apoptosis and autophagy were the predominantly altered group in ALS and CTE + ALS (**Figure 5**). MiR-34a-5p upregulation was unique to ALS. It has been previously demonstrated an upregulation in the plasma of familial ALS research participants with the C9orf72 mutation (Kmetzsch et al., 2021). The autophagy pathway is primarily regulated by inhibition of mTOR (mammalian target of rapamycin). mTOR is directly inhibited by miR-100-5p which was also found to be upregulated in CTE and has previously been implicated in altered protein deposition in AD (Ye et al., 2015). PI3K/akt, an activator of mTOR which is inhibited by miR-16-5p (T. Li et al., 2019), also found to be upregulated in CTE. Another key player in both apoptosis and autophagy pathways is Beclin, which fosters removal of old proteins and damaged cells. MiR-30c-5p, miR-30d-5p, and miR-30e-5p were all upregulated in ALS and CTE and have been shown to inhibit Beclin (Millan, 2017; Zhao et al., 2017), a protein involved in apoptosis and autophagy.

Biomarker Development

MiRNAs have been proposed as potential biomarkers for disease (Ghosh et al., 2021). Currently, CTE can only be diagnosed at autopsy and ALS is typically diagnosed after motor functions have declined. It remains to be determined whether miRNAs, such as miR-10b-5p are altered in biofluids such as the cerebrospinal fluid or blood during life in individuals with ALS or CTE. There have been recent studies that have examined the utility of select miRNA biomarkers in blood. MiR-181 is widely expressed in neurons and may be a marker for neuronal density, and miR-181 levels in serum have recently been associated with increased risk of death in ALS (Magen et al., 2021). We did not see differences in ALS prefrontal cortex but found that miR-181c-5p was significantly upregulated in the CTE group. Other promising miRNA targets that may be used as blood biomarkers of ALS patients include miR-206 and miR-124-3p (Soliman et al., 2021; Vaz et al., 2021). Correlations with blood and brain miRNA levels require further study.

Limitations

There were several limitations to this study. Only select miRNAs previously implicated in neurological disease were tested. Future studies should include more cases and examine additional miRNA targets as well as correlation between miRNA expression and markers for inflammation, cell growth, and apoptosis. This study also focused on changes in miRNAs within postmortem tissue from prefrontal cortex. Whether these changes are specific to prefrontal cortex in CTE and ALS or characteristics of widespread brain areas remains to be determined. Postmortem human brain tissue was evaluated; however, miRNAs are generally stable to degradation, and RIN values, a measure of

tissue quality, were not significantly different between groups. Study participants were limited to primarily Caucasian men, limiting the generalizability of these findings.

CONCLUSION

Shared miRNA alterations in CTE and ALS suggest that inflammation, apoptosis, and cell growth are neurodegenerative pathways common to both disorders. Unique increases in miR-100-5p in brain donors with CTE, and unique increases in miR-10b-5p in brain donors with ALS suggest that miRNA analysis might prove useful in distinguishing these disorders but will require future studies of additional brain donors using broader regions of brain and spinal cord. Future studies in biofluids during life are warranted, including cerebrospinal fluid and serum, to determine the utility of miRNAs for potential biomarker development. Overall, these shared and distinct miRNA profiles suggest that miRNA analysis might prove useful in the future development of biomarkers for CTE and ALS.

DATA AVAILABILITY STATEMENT

The original contributions presented in the study are included in the article/**Supplementary Material**, further inquiries can be directed to the corresponding author.

AUTHOR CONTRIBUTIONS

MaA and TS: study design, conception, and drafting of the manuscript. MaA, TS, NA, KS, ZF, NR, LG, IR, JA, SW, VA, BH, RM, KC, RN, MP, AL, FA, JM, NK, AM, and CB: acquisition and analysis of data. All authors contributed to the article and approved the submitted version.

FUNDING

This work was supported by the United States (U.S.) Department of Veterans Affairs, Veterans Health Administration, Veterans Affairs Biorepository (BX002466), Clinical Sciences Research and Development Merit Award (I01-CX001038), BLRD Merit Award (I01-BX005161), National Institute of Neurological Disorders and Stroke (U54NS115266, U01NS086659, and K23NS102399), National Institute of Aging Boston University AD Research Center (P30AG072978) and the Concussion Legacy Foundation. This work was also supported by unrestricted gifts from the Andlinger Foundation and WWE.

ACKNOWLEDGMENTS

We wholeheartedly acknowledge the use of resources and facilities at the Edith Nourse Rogers Memorial Veterans Hospital (Bedford, MA), Jamacia Plain VA Medical Center as well as the donors and their families who make this research possible.

SUPPLEMENTARY MATERIAL

The Supplementary Material for this article can be found online at: https://www.frontiersin.org/articles/10.3389/fnins.2022.855096/full#supplementary-material

REFERENCES

Absalon, S., Kochanek, D. M., Raghavan, V., and Krichevsky, A. M. (2013). MiR-26b, upregulated in Alzheimer's disease, activates cell cycle entry, tau-phosphorylation, and apoptosis in postmitotic neurons. *J. Neurosci.* 33, 14645–14659. doi: 10.1523/JNEUROSCI.1327-13.2013

Adams, J. W., Alvarez, V. E., Mez, J., Huber, B. R., Tripodis, Y., Xia, W., et al. (2018). Lewy body pathology and chronic traumatic encephalopathy associated with contact sports. *J. Neuropathol. Exp. Neurol.* 77, 757–768. doi: 10.1093/jnen/nly065

Alosco, M. L., Cherry, J. D., Huber, B. R., Tripodis, Y., Baucom, Z., Kowall, N. W., et al. (2020). Characterizing tau deposition in chronic traumatic encephalopathy (CTE): utility of the McKee CTE staging scheme. *Acta Neuropathol.* 140, 495–512. doi: 10.1007/s00401-020-02197-9

Balakathiresan, N., Bhomia, M., Chandran, R., Chavko, M., McCarron, R. M., and Maheshwari, R. K. (2012). MicroRNA Let-7i Is a promising serum biomarker for blast-induced traumatic brain injury. *J. Neurotrauma* 29, 1379–1387. doi: 10.1089/neu.2011.2146

Banack, S. A., Dunlop, R. A., and Cox, P. A. (2020). An miRNA fingerprint using neural-enriched extracellular vesicles from blood plasma: towards a biomarker for amyotrophic lateral sclerosis/motor neuron disease. *Open Biol.* 10:200116. doi: 10.1098/rsob.200116

Banzhaf-Strathmann, J., Benito, E., May, S., Arzberger, T., Tahirovic, S., Kretzschmar, H., et al. (2014). Micro RNA -125b induces tau hyperphosphorylation and cognitive deficits in Alzheimer's disease. *EMBO J.* 33, 1667–1680. doi: 10.15252/embj.201387576

Basavaraju, M., and de Lencastre, A. (2016). Alzheimer's disease: presence and role of microRNAs. *Biomol. Concepts* 7, 241–252. doi: 10.1515/bmc-2016-0014

Bieniek, K. F., Cairns, N. J., Crary, J. F., Dickson, D. W., Folkerth, R. D., Keene, C. D., et al. (2021). The second NINDS/NIBIB consensus meeting to define neuropathological criteria for the diagnosis of chronic traumatic encephalopathy. *J. Neuropathol. Exp. Neurol.* 80, 210–219. doi: 10.1093/jnen/nlab001

Brady, C. B., Trevor, K. T., Stein, T. D., Deykin, E. Y., Perkins, S. D., Averill, J. G., et al. (2013). The department of veterans affairs biorepository brain bank: a national resource for amyotrophic lateral sclerosis research. *Amyotroph. Lateral Scler. Frontotemporal Degener.* 14, 591–597. doi: 10.3109/21678421.2013.822516

Brennan, S., Keon, M., Liu, B., Su, Z., and Saksena, N. K. (2019). Panoramic visualization of circulating MicroRNAs across neurodegenerative diseases in humans. *Mol. Neurobiol.* 56, 7380–7407. doi: 10.1007/s12035-019-1615-1

Caggiu, E., Paulus, K., Mameli, G., Arru, G., Sechi, G. P., and Sechi, L. A. (2018). Differential expression of miRNA 155 and miRNA 146a in Parkinson's disease patients. *eNeurologicalSci* 13, 1–4. doi: 10.1016/j.ensci.2018.09.002

Campos-Melo, D., Droppelmann, C. A., He, Z., Volkening, K., and Strong, M. J. (2013). Altered microRNA expression profile in amyotrophic lateral sclerosis: a role in the regulation of NFL mRNA levels. *Mol. Brain* 6:26. doi: 10.1186/1756-6606-6-26

Caputo, V., Sinibaldi, L., Fiorentino, A., Parisi, C., Catalanotto, C., Pasini, A., et al. (2011). Brain derived neurotrophic factor (BDNF) expression is regulated by MicroRNAs miR-26a and miR-26b allele-specific binding. *PLoS One* 6:e28656. doi: 10.1371/journal.pone.0028656

Chen, C., Zhang, Y., Zhang, L., Weakley, S. M., and Yao, Q. (2011). MicroRNA-196: critical roles and clinical applications in development and cancer. *J. Cell. Mol. Med.* 15, 14–23. doi: 10.1111/j.1582-4934.2010.01219.x

Chen, H., Richard, M., Sandler, D. P., Umbach, D. M., and Kamel, F. (2007). Head injury and amyotrophic lateral sclerosis. *Am. J. Epidemiol.* 166, 810–816. doi: 10.1093/aje/kwm153

Chen, L., Yang, J., Lü, J., Cao, S., Zhao, Q., and Yu, Z. (2018). Identification of aberrant circulating miRNAs in Parkinson's disease plasma samples. *Brain Behav.* 8:e00941. doi: 10.1002/brb3.941

Cheng, L., Doecke, J. D., Sharples, R. A., Villemagne, V. L., Fowler, C. J., Rembach, A., et al. (2015). Prognostic serum miRNA biomarkers associated with Alzheimer's disease shows concordance with neuropsychological and neuroimaging assessment. *Mol. Psychiatry* 20, 1188–1196. doi: 10.1038/mp.2014.127

Cherry, J. D., Agus, F., Dixon, E., Huber, B., Alvarez, V. E., Mez, J., et al. (2021). Differential gene expression in the cortical sulcus compared to the gyral crest within the early stages of chronic traumatic encephalopathy. *Free Neuropathol.* 2, 3453. doi: 10.17879/freeneuropathology-2021-3453

Cherry, J. D., Tripodis, Y., Alvarez, V. E., Huber, B., Kiernan, P. T., Daneshvar, D. H., et al. (2016). Microglial neuroinflammation contributes to tau accumulation in chronic traumatic encephalopathy. *Acta Neuropathol. Comm.* 4:112. doi: 10.1186/s40478-016-0382-8

Chitramuthu, B. P., Bennett, H. P. J., and Bateman, A. (2017). Progranulin: a new avenue towards the understanding and treatment of neurodegenerative disease. *Brain* 140, 3081–3104. doi: 10.1093/brain/awx198

Cui, J. G., Li, Y. Y., Zhao, Y., Bhattacharjee, S., and Lukiw, W. J. (2010). Differential regulation of interleukin-1 receptor-associated kinase-1 (IRAK-1) and IRAK-2 by MicroRNA-146a and NF-κB in Stressed human astroglial cells and in Alzheimer disease. *J. Biol. Chem.* 285, 38951–38960. doi: 10.1074/jbc.M110.178848

Daneshvar, D. H., Mez, J., Alosco, M. L., Baucom, Z. H., Mahar, I., Baugh, C. M., et al. (2021). Incidence of and mortality from amyotrophic lateral sclerosis in national football league athletes. *JAMA Netw. Open* 4:e2138801. doi: 10.1001/jamanetworkopen.2021.38801

Danielsen, T., Reichard, R., Shang, P., and White, C. (2017). "Utility of TDP-43 immunohistochemistry in differentiating chronic traumatic encephalopathy from other tauopathies of aging," in *Proceedings of the Abstracts of 93rd Annual Meeting June 8–11, 2017*, Vol. 76. (Garden Grove, CA: American Association of Neuropathologists, Inc.), 491–546. doi: 10.1093/jnen/nlx029

De Felice, B., Manfellotto, F., Fiorentino, G., Annunziata, A., Biffali, E., Pannone, R., et al. (2018). Wide-ranging analysis of MicroRNA profiles in sporadic amyotrophic lateral sclerosis using next-generation sequencing. *Front. Genet.* 9:310. doi: 10.3389/fgene.2018.00310

Dewan, R., and Traynor, B. J. (2021). Plasma microRNA signature as biomarker for disease progression in frontotemporal dementia and amyotrophic lateral sclerosis. *J. Neurol. Neurosurg. Psychiatry* 92:458. doi: 10.1136/jnnp-2020-325478

Femminella, G. D., Ferrara, N., and Rengo, G. (2015). The emerging role of microRNAs in Alzheimer's disease. *Front. Physiol.* 6:40. doi: 10.3389/fphys.2015.00040

Friedman, M. J., Huber, B. R., Brady, C. B., Ursano, R. J., Benedek, D. M., Kowall, N. W., et al. (2017). VA's national PTSD Brain bank: a national resource for research. *Curr. Psychiatry Rep.* 19:73. doi: 10.1007/s11920-017-0822-6

Gao, Y., Su, J., Guo, W., Polich, E. D., Magyar, D. P., Xing, Y., et al. (2015). Inhibition of miR-15a promotes BDNF expression and rescues dendritic maturation deficits in MeCP2-deficient neurons: MiR-15a regulation of BDNF and neuronal maturation. *Stem Cells* 33, 1618–1629. doi: 10.1002/stem.1950

Ghosh, S., Kumar, V., Mukherjee, H., Lahiri, D., and Roy, P. (2021). Nutraceutical regulation of miRNAs involved in neurodegenerative diseases and brain cancers. *Heliyon* 7:e07262. doi: 10.1016/j.heliyon.2021.e07262

Guessous, F., Zhang, Y., Kofman, A., Catania, A., Li, Y., Schiff, D., et al. (2010). MicroRNA-34a is tumor suppressive in brain tumors and glioma stem cells. *Cell Cycle* 9, 1031–1036. doi: 10.4161/cc.9.6.10987

Gui, Y., Liu, H., Zhang, L., Lv, W., and Hu, X. (2015). Altered microRNA profiles in cerebrospinal fluid exosome in Parkinson disease and Alzheimer disease. *Oncotarget* 6, 37043–37053. doi: 10.18632/oncotarget.6158

Heyn, J., Luchting, B., Hinske, L. C., Hübner, M., Azad, S. C., and Kreth, S. (2016). MiR-124a and miR-155 enhance differentiation of regulatory T cells in patients with neuropathic pain. *J. Neuroinflammation* 13:248. doi: 10.1186/s12974-016-0712-6

Hoss, A. G., Kartha, V. K., Dong, X., Latourelle, J. C., Dumitriu, A., Hadzi, T. C., et al. (2014). MicroRNAs located in the hox gene clusters are implicated in Huntington's disease pathogenesis. *PLoS Genet.* 10:e1004188. doi: 10.1371/journal.pgen.1004188

Jassam, Y. N., Izzy, S., Whalen, M., McGavern, D. B., and El Khoury, J. (2017). Neuroimmunology of traumatic brain injury: time for a paradigm shift. *Neuron* 95:1246. doi: 10.1016/j.neuron.2017.07.010

Jensen, L., Jørgensen, L. H., Bech, R. D., Frandsen, U., and Schrøder, H. D. (2016). Skeletal muscle remodelling as a function of disease progression in amyotrophic lateral sclerosis. *Biomed Res. Int.* 2016, 1–12. doi: 10.1155/2016/5930621

Jiao, S.-S., Shen, L.-L., Zhu, C., Bu, X.-L., Liu, Y.-H., Liu, C.-H., et al. (2016). Brain-derived neurotrophic factor protects against tau-related neurodegeneration of Alzheimer's disease. *Transl. Psychiatry* 6:e907. doi: 10.1038/tp.2016.186

Joilin, G., Leigh, P. N., Newbury, S. F., and Hafezparast, M. (2019). An overview of MicroRNAs as biomarkers of ALS. *Front. Neurol.* 10:186. doi: 10.3389/fneur.2019.00186

Källstig, E., McCabe, B. D., and Schneider, B. L. (2021). The links between ALS and NF-κB. *Int. J. Mol. Sci.* 22:3875. doi: 10.3390/ijms22083875

Kao, Y.-C., Wang, I.-F., and Tsai, K.-J. (2018). MiRNA-34c overexpression causes dendritic loss and memory decline. *Int. J. Mol. Sci.* 19:2323. doi: 10.3390/ijms19082323

Karnati, H. K., Panigrahi, M. K., Gutti, R. K., Greig, N. H., and Tamargo, I. A. (2015). miRNAs: key players in neurodegenerative disorders and epilepsy. *J. Alzheimers Dis.* 48, 563–580. doi: 10.3233/JAD-150395

Katz, D. I., Bernick, C., Dodick, D. W., Mez, J., Mariani, M. L., Adler, C. H., et al. (2021). National institute of neurological disorders and stroke consensus diagnostic criteria for traumatic encephalopathy syndrome. *Neurology* 96:848. doi: 10.1212/WNL.0000000000011850

Kim, J., Yoon, H., Chung, D., Brown, J. L., Belmonte, K. C., and Kim, J. (2016). MiR-186 is decreased in aged brain and suppresses BACE1 expression. *J. Neurochem.* 137, 436–445. doi: 10.1111/jnc.13507

Kmetzsch, V., Anquetil, V., Saracino, D., Rinaldi, D., Camuzat, A., Gareau, T., et al. (2021). Plasma microRNA signature in presymptomatic and symptomatic subjects with C9orf72-associated frontotemporal dementia and amyotrophic lateral sclerosis. *J. Neurol. Neurosurg. Psychiatry* 92, 485–493. doi: 10.1136/jnnp-2020-324647

Korley, F. K., Diaz-Arrastia, R., Wu, A. H. B., Yue, J. K., Manley, G. T., Sair, H. I., et al. (2016). Circulating brain-derived neurotrophic factor has diagnostic and prognostic value in traumatic brain injury. *J. Neurotrauma* 33, 215–225. doi: 10.1089/neu.2015.3949

Labadorf, A., Choi, S. H., and Myers, R. H. (2018). Evidence for a pan-neurodegenerative disease response in Huntington's and Parkinson's disease expression profiles. *Front. Mol. Neurosci.* 10:430. doi: 10.3389/fnmol.2017.00430

Lanuza, M. A., Just-Borràs, L., Hurtado, E., Cilleros-Mañé, V., Tomàs, M., Garcia, N., et al. (2019). The impact of kinases in amyotrophic lateral sclerosis at the neuromuscular synapse: insights into BDNF/TrkB and PKC signaling. *Cells* 8:1578. doi: 10.3390/cells8121578

Lehman, E. J., Hein, M. J., Baron, S. L., and Gersic, C. M. (2012). Neurodegenerative causes of death among retired National Football League players. *Neurology* 79:1970. doi: 10.1212/WNL.0b013e31826daf50

Li, B., Dasgupta, C., Huang, L., Meng, X., and Zhang, L. (2020). MiRNA-210 induces microglial activation and regulates microglia-mediated neuroinflammation in neonatal hypoxic-ischemic encephalopathy. *Cell. Mol. Immunol.* 17, 976–991. doi: 10.1038/s41423-019-0257-6

Li, T., Wan, Y., Sun, L., Tao, S., Chen, P., Liu, C., et al. (2019). Inhibition of MicroRNA-15a/16 expression alleviates neuropathic pain development through upregulation of G protein-coupled receptor Kinase 2. *Biomol. Ther.* 27, 414–422. doi: 10.4062/biomolther.2018.073

Liguori, M., Nuzziello, N., Introna, A., Consiglio, A., Licciulli, F., D'Errico, E., et al. (2018). Dysregulation of MicroRNAs and target genes networks in peripheral blood of patients with sporadic amyotrophic lateral sclerosis. *Front. Mol. Neurosci.* 11:288. doi: 10.3389/fnmol.2018.00288

Livak, K. J., and Schmittgen, T. D. (2001). Analysis of relative gene expression data using real-time quantitative PCR and the $2^{-\Delta\Delta CT}$ method. *Methods* 25, 402–408. doi: 10.1006/meth.2001.1262

Long, J. M., Ray, B., and Lahiri, D. K. (2012). MicroRNA-153 physiologically inhibits expression of amyloid-β precursor protein in cultured human fetal brain cells and is dysregulated in a subset of Alzheimer disease patients. *J. Biol. Chem.* 287, 31298–31310. doi: 10.1074/jbc.M112.366336

Lukiw, W. J., Andreeva, T. V., Grigorenko, A. P., and Rogaev, E. I. (2013). Studying micro RNA function and dysfunction in Alzheimer's disease. *Front. Genet.* 3:327. doi: 10.3389/fgene.2012.00327

Mackenzie, I. R., Rademakers, R., and Neumann, M. (2010). TDP-43 and FUS in amyotrophic lateral sclerosis and frontotemporal dementia. *Lancet Neurol.* 9, 995–1007. doi: 10.1016/S1474-4422(10)70195-2

Magen, I., Yacovzada, N. S., Yanowski, E., Coenen-Stass, A., Grosskreutz, J., Lu, C.-H., et al. (2021). Circulating miR-181 is a prognostic biomarker for amyotrophic lateral sclerosis. *Nat. Neurosci.* 24, 1534–1541. doi: 10.1038/s41593-021-00936-z

Marcuzzo, S., Bonanno, S., Kapetis, D., Barzago, C., Cavalcante, P., D'Alessandro, S., et al. (2015). Up-regulation of neural and cell cycle-related microRNAs in brain of amyotrophic lateral sclerosis mice at late disease stage. *Mol. Brain* 8:5. doi: 10.1186/s13041-015-0095-0

Martí, E., Pantano, L., Bañez-Coronel, M., Llorens, F., Miñones-Moyano, E., Porta, S., et al. (2010). A myriad of miRNA variants in control and Huntington's disease brain regions detected by massively parallel sequencing. *Nucleic Acids Res.* 38, 7219–7235. doi: 10.1093/nar/gkq575

McKee, A. C., Alosco, M. L., and Huber, B. R. (2016). Repetitive head impacts and chronic traumatic encephalopathy. *Neurosurg. Clin. North Am.* 27, 529–535. doi: 10.1016/j.nec.2016.05.009

McKee, A. C., Cantu, R. C., Nowinski, C. J., Hedley-Whyte, E. T., Gavett, B. E., Budson, A. E., et al. (2009). Chronic traumatic encephalopathy in athletes: progressive tauopathy after repetitive head injury. *J. Neuropathol. Exp. Neurol.* 68, 709–735. doi: 10.1097/NEN.0b013e3181a9d503

McKee, A. C., Daneshvar, D. H., Alvarez, V. E., and Stein, T. D. (2014). The neuropathology of sport. *Acta Neuropathol.* 127, 29–51. doi: 10.1007/s00401-013-1230-6

McKee, A. C., Gavett, B. E., Stern, R. A., Nowinski, C. J., Cantu, R. C., Kowall, N. W., et al. (2010). TDP-43 proteinopathy and motor neuron disease in chronic traumatic encephalopathy. *J. Neuropath. Exp. Neurol.* 69, 918–929. doi: 10.1097/NEN.0b013e3181ee7d85

McKee, A. C., Stein, T. D., Nowinski, C. J., Stern, R. A., Daneshvar, D. H., Alvarez, V. E., et al. (2013). The spectrum of disease in chronic traumatic encephalopathy. *Brain* 136, 43–64. doi: 10.1093/brain/aws307

Mez, J., Daneshvar, D. H., Kiernan, P. T., Abdolmohammadi, B., Alvarez, V. E., Huber, B. R., et al. (2017). Clinicopathological evaluation of chronic traumatic encephalopathy in players of American football. *JAMA* 318, 360–370. doi: 10.1001/jama.2017.8334

Mez, J., Solomon, T. M., Daneshvar, D. H., Murphy, L., Kiernan, P. T., Montenigro, P. H., et al. (2015). Assessing clinicopathological correlation in chronic traumatic encephalopathy: rationale and methods for the UNITE study. *Alzheimers Res. Ther.* 7:62. doi: 10.1186/s13195-015-0148-8

Millan, M. J. (2017). Linking deregulation of non-coding RNA to the core pathophysiology of Alzheimer's disease: an integrative review. *Prog. Neurobiol.* 156, 1–68. doi: 10.1016/j.pneurobio.2017.03.004

Miya Shaik, M., Tamargo, I., Abubakar, M., Kamal, M., Greig, N., and Gan, S. (2018). The role of microRNAs in Alzheimer's disease and their therapeutic potentials. *Genes* 9:174. doi: 10.3390/genes9040174

Moszczynski, A. J., Strong, W., Xu, K., McKee, A., Brown, A., and Strong, M. J. (2018). Pathologic Thr(175) tau phosphorylation in CTE and CTE with ALS. *Neurology* 90, e380–e387. doi: 10.1212/WNL.0000000000004899

O'Brien, J., Hayder, H., Zayed, Y., and Peng, C. (2018). Overview of MicroRNA biogenesis, mechanisms of actions, and circulation. *Front. Endocrinol.* 9:402. doi: 10.3389/fendo.2018.00402

Parisi, C., Napoli, G., Amadio, S., Spalloni, A., Apolloni, S., Longone, P., et al. (2016). MicroRNA-125b regulates microglia activation and motor neuron death in ALS. *Cell Death Differ.* 23, 531–541. doi: 10.1038/cdd.2015.153

Pegoraro, V., Merico, A., and Angelini, C. (2017). Micro-RNAs in ALS muscle: differences in gender, age at onset and disease duration. *J. Neurol. Sci.* 380, 58–63. doi: 10.1016/j.jns.2017.07.008

Peng, H., Yang, H., Xiang, X., and Li, S. (2020). MicroRNA-221 participates in cerebral ischemic stroke by modulating endothelial cell function by regulating the PTEN/PI3K/AKT pathway. *Exp. Ther. Med.* 19, 443–450. doi: 10.3892/etm.2019.8263

Pierre, K., Dyson, K., Dagra, A., Williams, E., Porche, K., and Lucke-Wold, B. (2021). Chronic traumatic encephalopathy: update on current clinical diagnosis and management. *Biomedicines* 9:415. doi: 10.3390/biomedicines9040415

Ricci, C., Marzocchi, C., and Battistini, S. (2018). MicroRNAs as biomarkers in amyotrophic lateral sclerosis. *Cells* 7:219. doi: 10.3390/cells7110219

Ruan, Z., Li, Y., He, R., and Li, X. (2021). Inhibition of microRNA-10b-5p up-regulates HOXD10 to attenuate Alzheimer's disease in rats via the Rho/ROCK signalling pathway. *J. Drug Target.* 29, 531–540. doi: 10.1080/1061186X.2020.1864739

Russell, A. P., Wada, S., Vergani, L., Hock, M. B., Lamon, S., Léger, B., et al. (2013). Disruption of skeletal muscle mitochondrial network genes and miRNAs in amyotrophic lateral sclerosis. *Neurobiol. Dis.* 49, 107–117. doi: 10.1016/j.nbd.2012.08.015

Saez-Atienzar, S., Bandres-Ciga, S., Langston, R. G., Kim, J. J., Choi, S. W., Reynolds, R. H., et al. (2021). Genetic analysis of amyotrophic lateral sclerosis identifies contributing pathways and cell types. *Sci. Adv.* 7:eabd9036. doi: 10.1126/sciadv.abd9036

Schmidt, S., Kwee, L. C., Allen, K. D., and Oddone, E. Z. (2010). Association of ALS with head injury, cigarette smoking and APOE genotypes. *J. Neurol. Sci.* 291, 22–29. doi: 10.1016/j.jns.2010.01.011

Sethi, P., and Lukiw, W. J. (2009). Micro-RNA abundance and stability in human brain: specific alterations in Alzheimer's disease temporal lobe neocortex. *Neurosci. Lett.* 459, 100–104. doi: 10.1016/j.neulet.2009.04.052

Si, Y., Cui, X., Crossman, D. K., Hao, J., Kazamel, M., Kwon, Y., et al. (2018). Muscle microRNA signatures as biomarkers of disease progression in amyotrophic lateral sclerosis. *Neurobiol. Dis.* 114, 85–94. doi: 10.1016/j.nbd.2018.02.009

Slota, J. A., and Booth, S. A. (2019). MicroRNAs in neuroinflammation: implications in disease pathogenesis, biomarker discovery and therapeutic applications. *Non Coding RNA* 5:35. doi: 10.3390/ncrna5020035

Soliman, R., Mousa, N. O., Rashed, H. R., Moustafa, R. R., Hamdi, N., Osman, A., et al. (2021). Assessment of diagnostic potential of some circulating microRNAs in amyotrophic lateral sclerosis patients, an Egyptian study. *Clin. Neurol. Neurosurg.* 208:106883. doi: 10.1016/j.clineuro.2021.106883

Spencer, K. R., Foster, Z. W., Rauf, N. A., Guilderson, L., Collins, D., Averill, J. G., et al. (2020). Neuropathological profile of long-duration amyotrophic lateral sclerosis in military Veterans. *Brain Pathol.* 30, 1028–1040. doi: 10.1111/bpa.12876

Su, Y., Deng, M.-F., Xiong, W., Xie, A.-J., Guo, J., Liang, Z.-H., et al. (2019). MicroRNA-26a/Death-associated protein kinase 1 signaling induces synucleinopathy and dopaminergic neuron degeneration in Parkinson's disease. *Biol. Psychiatry* 85, 769–781. doi: 10.1016/j.biopsych.2018.12.008

Sun, Y., Luo, Z.-M., Guo, X.-M., Su, D.-F., and Liu, X. (2015). An updated role of microRNA-124 in central nervous system disorders: a review. *Front. Cell. Neurosci.* 9:193. doi: 10.3389/fncel.2015.00193

Taguchi, Y., and Wang, H. (2018). Exploring MicroRNA biomarkers for Parkinson's disease from mRNA expression profiles. *Cells* 7:245. doi: 10.3390/cells7120245

Tahamtan, A., Teymoori-Rad, M., Nakstad, B., and Salimi, V. (2018). Anti-inflammatory MicroRNAs and their potential for inflammatory diseases treatment. *Front. Immunol.* 9:1377. doi: 10.3389/fimmu.2018.01377

Tatura, R., Kraus, T., Giese, A., Arzberger, T., Buchholz, M., Höglinger, G., et al. (2016). Parkinson's disease: SNCA-, PARK2-, and LRRK2- targeting microRNAs elevated in cingulate gyrus. *Parkinsonism Relat. Disord.* 33, 115–121. doi: 10.1016/j.parkreldis.2016.09.028

Toivonen, J. M., Manzano, R., Oliván, S., Zaragoza, P., García-Redondo, A., and Osta, R. (2014). MicroRNA-206: a potential circulating biomarker candidate for amyotrophic lateral sclerosis. *PLoS One* 9:e89065. doi: 10.1371/journal.pone.0089065

Vaz, A. R., Vizinha, D., Morais, H., Colaço, A. R., Loch-Neckel, G., Barbosa, M., et al. (2021). Overexpression of miR-124 in motor neurons plays a key role in ALS pathological processes. *Int. J. Mol. Sci.* 22:6128. doi: 10.3390/ijms22116128

Vrabec, K., Boštjančič, E., Koritnik, B., Leonardis, L., Dolenc Grošelj, L., Zidar, J., et al. (2018). Differential expression of several miRNAs and the host genes

AATK and DNM2 in leukocytes of sporadic ALS patients. *Front. Mol. Neurosci.* 11:106. doi: 10.3389/fnmol.2018.00106

Walt, G. S., Burris, H. M., Brady, C. B., Spencer, K. R., Alvarez, V. E., Huber, B. R., et al. (2018). Chronic traumatic encephalopathy within an amyotrophic lateral sclerosis brain bank Cohort. *J. Neuropathol. Exp. Neurol.* 77, 1091–1100. doi: 10.1093/jnen/nly092

Wang, H., Pan, J.-Q., Luo, L., Ning, X., Ye, Z.-P., Yu, Z., et al. (2015). NF-κB induces miR-148a to sustain TGF-β/Smad signaling activation in glioblastoma. *Mol. Cancer* 14:2. doi: 10.1186/1476-4598-14-2

Wang, L., Liu, W., Zhang, Y., Hu, Z., Guo, H., Lv, J., et al. (2020). Dexmedetomidine had neuroprotective effects on hippocampal neuronal cells via targeting lncRNA SHNG16 mediated microRNA-10b-5p/BDNF axis. *Mol. Cell. Biochem.* 469, 41–51. doi: 10.1007/s11010-020-03726-6

Wang, W.-X., Rajeev, B. W., Stromberg, A. J., Ren, N., Tang, G., Huang, Q., et al. (2008). The expression of MicroRNA miR-107 decreases early in Alzheimer's disease and may accelerate disease progression through regulation of -site amyloid precursor protein-cleaving enzyme 1. *J. Neurosci.* 28, 1213–1223. doi: 10.1523/JNEUROSCI.5065-07.2008

Wang, Y.-M., Zheng, Y.-F., Yang, S.-Y., Yang, Z.-M., Zhang, L.-N., He, Y.-Q., et al. (2019). MicroRNA-197 controls ADAM10 expression to mediate MeCP2's role in the differentiation of neuronal progenitors. *Cell Death Differ.* 26, 1863–1879. doi: 10.1038/s41418-018-0257-6

Wong, H.-K. A., Veremeyko, T., Patel, N., Lemere, C. A., Walsh, D. M., Esau, C., et al. (2013). De-repression of FOXO3a death axis by microRNA-132 and -212 causes neuronal apoptosis in Alzheimer's disease. *Hum. Mol. Genet.* 22, 3077–3092. doi: 10.1093/hmg/ddt164

Ye, X., Luo, H., Chen, Y., Wu, Q., Xiong, Y., Zhu, J., et al. (2015). MicroRNAs 99b-5p/100-5p regulated by endoplasmic reticulum stress are involved in abeta-induced pathologies. *Front. Aging Neurosci.* 7:210. doi: 10.3389/fnagi.2015.00210

Zhang, N., Lyu, Y., Pan, X., Xu, L., Xuan, A., He, X., et al. (2017). MiR-146b-5p promotes the neural conversion of pluripotent stem cells by targeting Smad4. *Int. J. Mol. Med.* 40, 814–824. doi: 10.3892/ijmm.2017.3064

Zhang, W., Kim, P. J., Chen, Z., Lokman, H., Qiu, L., Zhang, K., et al. (2016). MiRNA-128 regulates the proliferation and neurogenesis of neural precursors by targeting PCM1 in the developing cortex. *Elife* 5:e11324. doi: 10.7554/eLife.11324

Zhao, F., Qu, Y., Zhu, J., Zhang, L., Huang, L., Liu, H., et al. (2017). MiR-30d-5p plays an important role in autophagy and apoptosis in developing rat brains after hypoxic–ischemic injury. *J. Neuropathol. Exp. Neurol.* 76, 709–719. doi: 10.1093/jnen/nlx052

Conflict of Interest: The authors declare that the research was conducted in the absence of any commercial or financial relationships that could be construed as a potential conflict of interest.

Publisher's Note: All claims expressed in this article are solely those of the authors and do not necessarily represent those of their affiliated organizations, or those of the publisher, the editors and the reviewers. Any product that may be evaluated in this article, or claim that may be made by its manufacturer, is not guaranteed or endorsed by the publisher.

frontiers | Frontiers in Aging Neuroscience

ORIGINAL RESEARCH
published: 17 June 2022
doi: 10.3389/fnagi.2022.896848

Linking Plasma Amyloid Beta and Neurofilament Light Chain to Intracortical Myelin Content in Cognitively Normal Older Adults

*Marina Fernandez-Alvarez[1,2], Mercedes Atienza[1,2], Fatima Zallo[3], Carlos Matute[2,3], Estibaliz Capetillo-Zarate[2,3,4] and Jose L. Cantero[1,2]**

[1] Laboratory of Functional Neuroscience, Pablo de Olavide University, Seville, Spain, [2] Network Center for Biomedical Research in Neurodegenerative Diseases (CIBERNED), Madrid, Spain, [3] Departamento de Neurociencias, Achucarro Basque Center for Neuroscience, Universidad del País Vasco, Leioa, Spain, [4] Ikerbasque, Basque Foundation for Science, Bilbao, Spain

Evidence suggests that lightly myelinated cortical regions are vulnerable to aging and Alzheimer's disease (AD). However, it remains unknown whether plasma markers of amyloid and neurodegeneration are related to deficits in intracortical myelin content, and whether this relationship, in turn, is associated with altered patterns of resting-state functional connectivity (rs-FC). To shed light into these questions, plasma levels of amyloid-β fragment 1–42 ($A\beta_{1-42}$) and neurofilament light chain (NfL) were measured using ultra-sensitive single-molecule array (Simoa) assays, and the intracortical myelin content was estimated with the ratio T1-weigthed/T2-weighted (T1w/T2w) in 133 cognitively normal older adults. We assessed: (i) whether plasma $A\beta_{1-42}$ and/or NfL levels were associated with intracortical myelin content at different cortical depths and (ii) whether cortical regions showing myelin reductions also exhibited altered rs-FC patterns. Surface-based multiple regression analyses revealed that lower plasma $A\beta_{1-42}$ and higher plasma NfL were associated with lower myelin content in temporo-parietal-occipital regions and the insular cortex, respectively. Whereas the association with $A\beta_{1-42}$ decreased with depth, the NfL-myelin relationship was most evident in the innermost layer. Older individuals with higher plasma NfL levels also exhibited altered rs-FC between the insula and medial orbitofrontal cortex. Together, these findings establish a link between plasma markers of amyloid/neurodegeneration and intracortical myelin content in cognitively normal older adults, and support the role of plasma NfL in boosting aberrant FC patterns of the insular cortex, a central brain hub highly vulnerable to aging and neurodegeneration.

Keywords: aging, Alzheimer's disease, intracortical myelin, functional connectivity, blood biomarkers, amyloid-beta, neurofilament light

OPEN ACCESS

Edited by:
David Baglietto-Vargas, University of Málaga, Spain

Reviewed by:
Hakon Grydeland, University of Oslo, Norway
Alexis Moscoso, University of Gothenburg, Sweden

***Correspondence:**
Jose L. Cantero
jlcanlor@upo.es

Specialty section:
This article was submitted to Alzheimer's Disease and Related Dementias, a section of the journal Frontiers in Aging Neuroscience

Received: *15 March 2022*
Accepted: *23 May 2022*
Published: *17 June 2022*

Citation:
Fernandez-Alvarez M, Atienza M, Zallo F, Matute C, Capetillo-Zarate E and Cantero JL (2022) Linking Plasma Amyloid Beta and Neurofilament Light Chain to Intracortical Myelin Content in Cognitively Normal Older Adults. Front. Aging Neurosci. 14:896848. doi: 10.3389/fnagi.2022.896848

INTRODUCTION

Aging is the major risk factor for Alzheimer's disease (AD), but the reasons why aging increases susceptibility to AD are poorly understood. One contributing factor may be the perturbation of myelin-related genes (Mathys et al., 2019) that eventually leads to widespread degeneration of myelin sheaths. This phenomenon results in slowing of conduction velocity along nerve fibers, modifying the timing of network oscillations, and ultimately affecting

functional connections within neural circuits (Peters, 2002). The efficiency of remyelination also declines with age, likely due to the limited regenerative capacity of oligodendrocyte progenitor cells (Irvine and Blakemore, 2006). Consequently, lightly myelinated axons become more vulnerable to irreversible degeneration during aging, favoring cognitive decline (Wang et al., 2020) and the spread of AD pathology before the onset of symptoms (Mitew et al., 2010; Braak and Del Tredici, 2015; Couttas et al., 2016; Dean et al., 2017; Luo et al., 2019).

New ultrasensitive quantitative technologies allow the identification of proteins in blood at subfemtomolar concentrations (Rissin et al., 2010; Yang et al., 2017), opening new avenues for the development of blood biomarkers capable of detecting individuals at risk for cognitive decline and AD. Accumulated evidence suggests that lower levels of plasma amyloid-β fragment 1–42 ($A\beta_{1-42}$) are associated with accelerated aging and AD. Accordingly, low levels of plasma $A\beta_{1-42}$ at baseline have shown to increase the risk of cognitive decline (Seppälä et al., 2010), mild cognitive impairment (MCI) (Rembach et al., 2014) and AD (Rembach et al., 2014; Chouraki et al., 2015; Hilal et al., 2018; de Wolf et al., 2020). Moreover, higher plasma concentrations of neurofilament light chain (NfL), the main cytoskeletal structure of myelinated axons, have been associated with increased brain Aβ load in cognitively unimpaired older adults (Chatterjee et al., 2018; Benedet et al., 2020), and have shown to predict cortical thinning and subsequent cognitive impairment in the preclinical stage of both familial and sporadic AD (Preische et al., 2019; Lee et al., 2022). However, it remains largely unknown whether plasma markers of amyloid and neurodegeneration bear any relation to brain myelin content in cognitively normal older individuals, which may be relevant to establish surrogate markers of vulnerability to AD.

Although myelination is a prominent feature of the subcortical white matter (WM), the gray matter (GM) of the cerebral cortex also contains a substantial amount of myelinated axons unevenly distributed in layers (Nieuwenhuys, 2013). Thus, myelin density is higher in deeper than in superficial cortical layers and in sensorimotor than in association regions (Nave and Werner, 2014). This particular distribution of cortical myelin may partially account for the functional organization of the neocortex (Beul et al., 2017; Huntenburg et al., 2017). Moreover, evidence has shown that subtle changes in myelin have meaningful effects on neuronal network function (Waxman, 1980; Felts et al., 1997; Pajevic et al., 2014). Therefore, aging-related patterns of rs-FC may be driven by cortical regions showing myelin deficits, which, in turn, may be conditioned by plasma markers of amyloid and neurodegeneration.

Here, we specifically addressed these questions by investigating whether the T1w/T2w ratio, considered as a proxy of myelin content in the cortical GM (Glasser and Van Essen, 2011), is associated with plasma levels of $A\beta_{1-42}$ and NfL in cognitively normal older adults, and whether this relationship varies with cortical depth. Next, we assessed whether those cortical areas showing plasma measurements-related myelin deficits also exhibited alterations in their pattern of rs-FC, which in turn may account for the variability in cognitive functioning. Therefore, the present study sought to test three inter-related hypotheses. As amyloid pathology has been previously associated, either direct or indirectly, with myelin damage (Desai et al., 2010; Mitew et al., 2010; Schmued et al., 2013; Dean et al., 2017; Luo et al., 2019; Chen et al., 2021), we first hypothesized that lower levels of plasma $A\beta_{1-42}$ will be associated with lower intracortical myelin content in cognitively normal older adults. The relationship between aging-related axonal damage and myelin breakdown is likely strengthened by dysfunctional oligodendrocytes, which supply energy for axonal metabolism (Mot et al., 2018). Accordingly, our second prediction was that higher levels of plasma NfL will be accompanied by lower myelin content, and that this relationship will become more evident in inner cortical layers, where oligodendrogenesis is most impaired (Orthmann-Murphy et al., 2020; Xu et al., 2021). Finally, and given the critical role of myelin in neuronal communication and fine-tuning of neuronal circuits (Fields, 2015; Monje, 2018), we postulated that cortical regions showing lower myelin content related to plasma levels of $A\beta_{1-42}$ and/or NfL will also show altered patterns of rs-FC.

MATERIALS AND METHODS

Participants

One hundred thirty-three cognitively normal older adults participated in the study (65 ± 5.9 years; range: 54–76 years; 81 females). They were recruited from senior citizen's associations, health-screening programs, and hospital outpatient services. All of them underwent neurological and neuropsychological assessment to discard both the presence of dementia and objective cognitive impairment. Individuals with medical conditions that affect brain structure or function (e.g., cerebrovascular disease, epilepsy, head trauma, history of neurodevelopmental disease, alcohol abuse, hydrocephalus, and/or intracranial mass) were not included in the study. Participants met the following criteria: (i) normal global cognitive status in the Mini-Mental State Examination (scores $\geq$ 26); (ii) normal cognitive performance in the neuropsychological tests relative to appropriate reference values for age and education level; (iii) global score of 0 (no dementia) in the Clinical Dementia Rating; (iv) functional independence as assessed by the Spanish version of the Interview for Deterioration in Daily Living Activities (Böhm et al., 1998); (v) scores $\leq$5 (no depression) in the short form of the Geriatric Depression Scale (Sheikh and Yesavage, 1986); and (vi) not be taking medications that affected cognition, sleep, renal or hepatic function. All participants gave informed consent to the experimental protocol approved by the Ethical Committee for Clinical Research of the Junta de Andalucía according to the principles outlined in the Declaration of Helsinki. **Table 1** contains sample characteristics.

Neuropsychological Assessment

All participants received neuropsychological assessment. They were administered with the following tests: the Spanish version of the Memory Binding Test (MBT) (Gramunt et al., 2016); the short form of the Boston Naming Test (BNT); the semantic and phonological fluency tests based on the "Animal" and letter

TABLE 1 | Demographics, cognitive and biochemical variables.

Age	65 ± 5.9
Sex (F/M)	81/52
Education years	11.7 ± 4.5
ApoE4 (yes/no)	31/102
MMSE	28.6 ± 1.3
Memory Binding Test	
Total free recall	16.2 ± 4.6
Pairs in free recall	5.3 ± 2.6
Total paired recall	27.1 ± 4.9
Paired recall pairs	9.8 ± 4.1
Total delayed free recall	15.1 ± 5.0
Pairs in delayed free recall	5.8 ± 3.9
Total delayed paired recall	28.9 ± 5.4
Boston Naming Test	12.1 ± 2.1
Phonological fluency	15.7 ± 4.4
Semantic fluency	22.0 ± 17.0
Trail Making Test-A	47.0 ± 21.5
Trail Making Test-B	119.5 ± 67.7
Tower of London	319.3 ± 113.2
Plasma $A\beta_{1-42}$ (pg/ml)	12.1 ± 5.1 (2.4 – 24)
Plasma NfL (pg/ml)	12.9 ± 7.2 (2.3 – 39.6)

Results are expressed as mean ± SD, unless otherwise stated. F/M, females/males; MMSE, Mini Mental State Examination; NfL: neurofilament light.

"P" naming tasks; the two forms of the Trail Making Test (TMT-A and TMT-B); and the Tower of London (TL). All neuropsychological scores were z transformed. In the case of TMT-A and TMT-B, we used the inverse z-values, while in the case of the MBT and TL we first computed a composite measure by summing the z-scores of the different scores. We then applied principal component analysis to obtain the Spearman's "*g*" factor as an index of global cognitive function. This analysis was done with R Statistical Software v3.0.1 (R Foundation for Statistical Computing, Vienna, Austria) using the *prcomp* function. We only retained the first component (eigenvalue 3.4), which explained 53.7% of variance in the data, due to the contribution of MBT (24.2), BNT (24.2), phonological fluency (24.2), semantic fluency (3.2), TMT-A (8.6), TMT-B (9.5), and TL (6.0). The standardized residuals were used to obtain the latent variable *g* (factor loading MBT: 0.92; BNT: 0.92; phonological fluency: 0.92; semantic fluency: 0.33; TMT-A: 0.55; TMT-B: 0.57; TL: 0.46).

Measurements of Plasma $A\beta_{1-42}$ and NfL

Fasting blood samples were taken at 9:00-10:00 AM in all participants to control for potential circadian effects. Briefly, venous blood samples were collected in 10 ml dipotassium ethylene diamine tetraacetic acid (EDTA) coated tubes (BD Diagnostics), and immediately centrifuged (1,989 *g*) at 4°C for 5 min. Supernatant plasma was aliquoted into polypropylene tubes containing 300 μl of plasma mixed with 10 μl of a protease inhibitor cocktail (cOmplete Ultra Tablets mini, Roche), and stored at –80°C until analysis. Plasma samples used in the present study were not previously thawed.

Plasma $A\beta_{1-42}$ and NfL levels were measured on the ultra-sensitive single-molecule array (Simoa) HD-1 analyzer platform (Quanterix, MA, United States) following the manufacturer's instructions. The $A\beta_{1-42}$ Simoa 2.0 assay (Cat. No. 101664) and the NF-light Simoa assay advantage kits (Cat. No. 103186) were purchased from Quanterix. These assays measure $A\beta_{1-42}$ and NfL levels in human plasma with a detection limit of 0.044 and 0.038 pg/ml, respectively. Two quality control samples were run on each plate for each analyte. Plasma $A\beta_{1-42}$ and NfL determinations were run in duplicates, and the average of the two measurements (pg/ml) was used for statistical analysis. Samples with coefficients of variation higher than 20% were excluded.

Magnetic Resonance Imaging Acquisition

Structural and functional magnetic resonance imaging (MRI) scans were performed on a 3T Philips Ingenia MRI scanner, equipped with a 32-channel radio-frequency (RF) receive head coil and body RF transmit coil (Philips, Best, Netherlands). The following MRI sequences were acquired in the same session: (i) 3D T1-weighted (T1w) magnetization prepared rapid gradient echo (MPRAGE) in the sagittal plane: repetition time (TR)/echo time (TE) = 2,600 ms/4.7 ms, flip angle (FA) = 9°, acquisition matrix = 384 × 384, voxel resolution = 0.65 mm^3 isotropic, resulting in 282 slices without gap between adjacent slices; (ii) 3D T2w scan in the sagittal plane: TR/TE: 2,500 ms/251 ms, FA = 90°, acquisition matrix = 384 mm × 384 mm, voxel resolution = 0.65 mm^3 isotropic, resulting in 282 slices without gap between adjacent slices; and (iii) T2w Fast Field Echo images using a blood-oxygen-level-dependent (BOLD) sensitive single-shot echo-planar imaging (EPI) sequence in the axial plane: TR/TE: 2,000 ms/30 ms, FA = 80°, acquisition matrix = 80 mm × 80 mm, voxel resolution = 3 mm^3 isotropic, resulting in 35 slices with 1 mm of gap between adjacent slices. To allow for optimal B1 shimming, a B1 calibration scan was applied before starting the EPI sequence. We acquired 250 EPI scans preceded by four dummy volumes to allow time for equilibrium in the spin excitation. Before starting the acquisition of the EPI sequence, participants were asked to remain still and keep their eyes closed without falling sleep. Pulse and respiratory rates were recorded using the scanner's built-in pulse oximeter placed on the left-hand index finger and a pneumatic respiratory belt strapped around the upper abdomen, respectively. Brain images were visually examined after each MRI sequence; they were repeated if artifacts were clearly identified. All participants underwent the same MRI protocol at the MRI facility of Pablo de Olavide University.

Structural MRI Preprocessing and Generation of Cortical Myelin Maps

T1w scans were preprocessed using Freesurfer v6.0.[1] The Freesurfer's pipeline included brain extraction, intensity normalization, automated tissue segmentation, generation of white matter (WM) and pial surfaces, correction of surface topology and inflation, co-registration, and projection of cortical surfaces to a sphere for establishing a surface-based coordinate system (Fischl and Dale, 2000). Pial surface misplacements and erroneous WM segmentation were manually corrected on a slice-by-slice basis by one experienced technician. The T2w image was

[1] https://surfer.nmr.mgh.harvard.edu/

registered to the T1w image with *bbregister* employing a trilinear interpolation method. *bbregister* is a within-subject, cross-modal registration program that uses a boundary-based cost function constrained to 6 degrees of freedom (Greve and Fischl, 2009).

We have used the T1w/T2w ratio image to indirectly estimate the relative intracortical myelin content in individual cortical surfaces. Previous studies have shown that regional variations in the T1w/T2w ratio match the myelin content derived from histologically-defined cortical areas (Glasser and Van Essen, 2011) and they further correlate with cortical myelination patterns across the lifespan (Grydeland et al., 2019). This is partially due because myelin alters the signal intensity of T1w and T2w images in opposite directions and, consequently, the T1w/T2w ratio provides both enhanced tissue contrast and sensitivity to brain myelin content (Uddin et al., 2019). Furthermore, the T1w/T2w ratio cancels radiofrequency (RF) receive field (B1−) artifacts in the absence of head motion, and corrects reasonably well for RF transmit field (B1+) effects when the participants' head is precisely located at the isocenter of the magnetic field (Glasser et al., in press). In the present study, the latter requirements were strictly met to reduce transmit field biases and spurious results in cortical myelin maps.

The tissue fraction effect was corrected in individual T1w/T2w ratio images using PETsurfer (Greve et al., 2016), setting the point spread function estimate to zero. Next, three intermediate surfaces were generated within the cortical GM at fixed relative distances between the WM and pial surfaces (Polimeni et al., 2010). These surfaces were located at 90% (outer layer), 50% (medium layer) and 10% (inner layer) of the cortical thickness away from the WM surface. Finally, individual myelin maps obtained at different cortical depths were projected onto the average cortical surface, transformed to z-scores, and smoothed using non-linear spherical wavelet-based de-noising schemes (Bernal-Rusiel et al., 2008). All processing steps were visually checked for quality assurance. **Figure 1** illustrates the analysis pipeline for intracortical myelin mapping.

Functional MRI Preprocessing and Resting State-Functional Connectivity Analysis

Resting-state functional magnetic resonance imaging (rs-fMRI) data were preprocessed using AFNI functions,[2] version AFNI_20.3.01. For each participant, high-frequency spikes were eliminated (*3dDespike*), time-locked cardiac and respiratory motion artifacts on cerebral BOLD signals were minimized using RETROICOR (Glover et al., 2000), time differences in slice-acquisition were corrected (*3dTshift*), EPI scans were aligned using rigid body motion correction and selecting the first volume as reference (*3dVolreg*), and aligned EPI scans were co-registered to their corresponding T1w volumes (*3dAllineate;* cost function: lpc + ZZ).

Dynamics were removed provided that more than 5% of voxels exhibited signal intensities that deviated from the median absolute deviation of time series (*3dToutcount*); and/or when the Euclidean norm (*enorm*) threshold exceeded 0.3 mm in head motion. None of the participants showed more than 20% of artifactual dynamics after applying censoring. Simultaneous regression was further applied to minimize the impact of non-neuronal fluctuations on the rs-fMRI signal (*3dTproject*). Nuisance regressors included: (i) six head motion parameters (3 translational and 3 rotational) derived from the EPI scan alignment along with their first-order derivatives, (ii) time series of mean total WM/CSF signal intensity, and (iii) cardiac (measured by pulse oximeter) and respiratory fluctuations plus their derivatives to mitigate effects of extracerebral physiological artifacts on cerebral BOLD signals. No temporal band-pass filtering was applied.

Preprocessed rs-fMRI scans were projected onto the *fsaverage5* cortical surface space. Seeds for FC analyses were derived from cortical regions showing significant associations between plasma measurements (i.e., $A\beta_{1-42}$ and NfL levels) and intracortical myelin content. Surface-based rs-FC seed to whole cortex maps were obtained using the Fisher's z-transform of the corresponding Pearson's correlation coefficients.

Sample Size Estimation

To estimate the sample size, we performed power analysis with the G*Power software (v3.1.9.6).[3] Only two studies have previously assessed the relationship between $A\beta_{1-42}$ and intracortical myelin content, one in the AD continuum using both CSF $A\beta_{1-42}$ and amyloid PET (Luo et al., 2019) and other in cognitively normal older adults using amyloid PET (Yasuno et al., 2017). To our knowledge, research investigating associations between NfL levels and intracortical myelin content or addressing the potential moderating effect of plasma measurements (i.e., $A\beta_{1-42}$ or NfL) on the relationship between intracortical myelin content and cortical rs-FC patterns is lacking. Therefore, we computed an *a priori* (prospective) power analysis (fixed model, R^2 deviation from zero) to achieve statistical power of 80% given a 0.025 two-sided significance level and an overall Cohen's effect size (f^2) ranging from 0.05 to 0.2. **Supplementary Figure 1** shows the results of this analysis for additive models evaluating the relationship between one of the plasma measurements (either $A\beta_{1-42}$ or NfL) and intracortical myelin content (3 predictors), and for interactive models assessing the moderating effect of one of the aforementioned plasma measurements on the relationship between intracortical myelin and rs-FC (5 predictors). This analysis revealed that 263 and 308 participants are required to detect an overall effect size of 0.05 for additive and interactive models, respectively. As the study sample consisted of 133 participants, interpretation of significances is conditional on the existence of overall effect sizes equal to or greater than 0.10 and 0.12 for main and interaction effects, respectively.

Statistical Analysis

We first applied the frequentist approach to determine whether age was related to plasma measurements and intracortical myelin

[2]https://afni.nimh.nih.gov/afni

[3]https://www.psychologie.hhu.de/arbeitsgruppen/allgemeine-psychologie-und-arbeitspsychologie/gpower.html

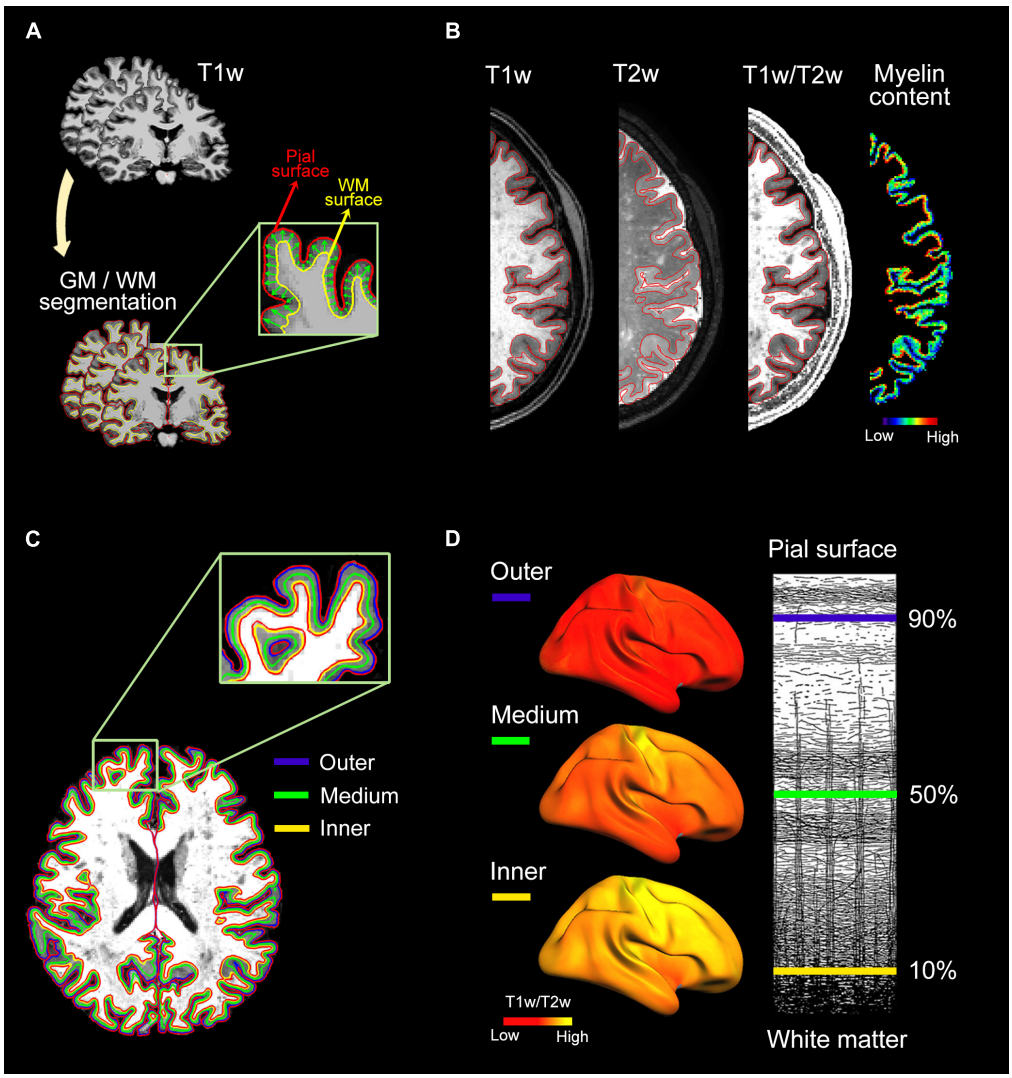

FIGURE 1 | Analysis pipeline for intracortical myelin mapping. **(A)** Individual T1w scans were skull-stripped. Next, pial and WM boundaries were established using semi-automatic segmentation procedures implemented in Freesurfer. **(B)** Intracortical myelin content was obtained by computing the voxel-wise ratio of T1w to T2w. Warm colors represent regions of high intracortical myelin while cold colors represent regions of low myelin content, as revealed by T1w/T2w ratio values. **(C)** Three uniformly spaced layers were delineated within the cortical ribbon of the T1w/T2w ratio image: 90% (outer layer), 50% (medium layer) and 10% (inner layer) of the cortical thickness away from the WM surface. (**D**, Left panel) Individual myelin maps obtained at different cortical depths were projected onto the average cortical surface. (Right panel) Illustrative representations of the three cortical depths superimposed on myeloarchitectonic organization of the human neocortex (Figure adapted from Vogt, 1903).

after adjusting for the effects of sex. Next, by applying the same approach, we performed vertex-wise multiple linear regression analyses to evaluate the relationship of plasma measurements (either $A\beta_{1-42}$ or NfL) with intracortical myelin content at different cortical depths (90, 50, and 10% away from the WM surface), including age and sex as covariates of no interest. To assess whether associations between plasma measurements and intracortical myelin content differed with cortical depth, we first computed the mean of the sum of all significant regions at the three cortical depths to extract the fitted values. These fitted values were entered into a mixed model with subjects as random effect to determine whether the strength of these associations varied significantly as a function of cortical depth. The effect of the moderator factor (i.e., cortical depth) was evaluated through an ANOVA that compared the null model only including the intercept with the experimental model including cortical depth as a fixed effect. If differences reached significance, *post hoc* comparisons were performed with the R package emmeans and multiple comparisons were adjusted using the Bonferroni correction.

Using the frequentist approach, we further evaluated whether cortical regions showing significant associations with plasma measurements also exhibited altered patterns of rs-FC. For this, we applied a vertex-wise multiple regression model that

included as regressor of interest the interaction between plasma measurements (either $A\beta_{1-42}$ or NfL) and the mean intracortical myelin of the region used as seed in the rs-FC analysis. These models were adjusted by age and sex.

Vertex-wise regression analyses for intracortical myelin and rs-FC were performed using the SurfStat package.[4] Results were corrected for multiple comparisons using a hierarchical statistical model that first controls the family-wise error rate at the level of clusters by applying random field theory over smoothed statistical maps ($p_{vertex} < 0.001$, $p_{cluster} < 0.05$), and next controls the false discovery rate at the level of vertex within each cluster ($p < 0.05$) over unsmoothed statistical maps (Bernal-Rusiel et al., 2010). The anatomical location of significant results was based on vertices showing the maximum statistic within each significant cluster (Desikan et al., 2006).

After inferential evidence of a main or an interaction effect, we computed the standardized measure of effect size (i.e., Cohen's f^2) to evaluate local effect size within the context of a multivariate regression model (Cohen, 1988). To establish the precision of standardized effect sizes, we computed 95% confidence intervals ($CI_{95\%}$) using the normal approximated interval with bootstrapped bias and standard error (N = 10,000 bootstrap samples) with the Matlab's *bootci* function.

Next, for each cortical vertex showing the maximum statistic within each significant cluster, we applied Bayesian linear regression analyses using JASP, version 0.12.2.[5] The Bayesian approach allowed us to quantify the evidence for the alternative hypothesis and to overcome the problem of multiple comparisons resulting from performing different models for two hemispheres and three cortical depths. Bayesian linear regression analyses were based on non-informative priors such as the Jeffreys-Zellner-Siow prior with an r scale of 0.354 (Liang et al. (2008). We compared the strength of the Bayes factor for the model including all covariates of no interest (null model) with the model including the predictor of interest (experimental model) (BF_{10}). The classification scheme proposed by Lee and Wagenmakers (2013) was employed to interpret the BF_{10}. We only reported those results that reached significance according to the frequentist approach as long as the evidence in favor of the alternative hypothesis was at least moderate ($BF_{10} \geq 3$).

Finally, we evaluated whether associations of intracortical myelin content with either plasma $A\beta_{1-42}$/NfL levels or rs-FC accounted for the variability in global cognitive function. For this purpose, we first applied the Yeo-Johnson transformation to the cognitive index (i.e., the latent variable g) to reduce the detrimental effects of skewedness and heteroscedasticity in the different models (Yeo and Johnson, 2000). Next, we built four models to assess main and interaction effects. The first model only included the covariates of no interest; the second model the main effects; the third model the two-way interactions between the different predictors of interest; and the fourth model the three-way interaction. We first calculated F-tests between the different sequential models, and then compared the relative strength of the Bayes factor between the models.

[4]https://www.math.mcgill.ca/keith/surfstat/

[5]https://jasp-stats.org/

RESULTS

Associations of Age With Intracortical Myelin and Plasma Levels of $A\beta_{1-42}$ and NfL

Age was positively related to plasma $A\beta_{1-42}$ ($F_{1,130} = 9.8$, $p = 0.002$) and NfL levels ($F_{1,130} = 28.8$, $p < 10^{-6}$). On the contrary, age was negatively associated with intracortical myelin content in postcentral regions of the left hemisphere ($F_{1,130} = 21.2$, $p < 10^{-5}$) and superior parietal lobe of the right hemisphere ($F_{1,130} = 21.3$, $p < 10^{-5}$). These results are illustrated in **Supplementary Figure 2**.

Relationship Between Intracortical Myelin and Plasma Levels of $A\beta_{1-42}$ and NfL

Figure 2 displays intracortical myelin maps projected onto the average cortical surface obtained at different depths (i.e., outer, medium and inner layers) before z-transformation. As expected, T1w/T2w ratio values increased with cortical depth (Nieuwenhuys, 2013; Nave and Werner, 2014). Our T1w/T2w ratio maps differ from those reported in Glasser and Van Essen (2011), especially in some regions of the occipital cortex, whose intracortical myelin content was associated with plasma levels of $A\beta_{1-42}$ (see **Figure 3**). These differences may be due to the distinct approaches used to obtain the intracortical myelin maps in the two studies. Thus, we used absolute values comprising the entire range of T1w/T2w ratio values instead of a percentile scaling between 3 and 96%, as in Glasser and Van Essen (2011). Neither we adjusted the color palette to identify the transitions between adjacent areas, since we were not interested in delineating spatial gradients or myeloarchitectural features of cortical regions (Glasser and Van Essen, 2011).

Plasma levels of $A\beta_{1-42}$ were positively associated with T1w/T2w ratio values in temporo-parietal-occipital regions of both hemispheres at the three cortical depths, as illustrated in **Figure 3** and reported in **Table 2**. The evidence in favor of the alternative hypothesis was extreme ($BF_{10} > 100$) for myelin content of inner and outer layers, and moderate in the medium layer (BF_{10} was reported in **Table 2**).

Regarding the association between $A\beta_{1-42}$ and intracortical myelin, mixed model ANOVAs revealed a significant main effect of cortical depth for the right hemisphere ($\chi^2 = 346.6$, $p < 10^{-15}$) that was not extended to the left hemisphere ($\chi^2 = 5.7$, $p = 0.06$). *Post hoc* analyses showed that the strength of positive associations in the right hemisphere decreased with cortical depth, being stronger for the outer than for the other two layers ($p < 0.0001$), and stronger for the medium than for the innermost layer ($p < 0.0001$). **Figures 4A,B** illustrate these results.

The regression analysis also revealed a negative association between plasma NfL levels and T1w/T2w ratio values of the right insular cortex (**Figure 5** and **Table 2**). This result was restricted to the inner layer, where the Bayesian linear regression analysis showed a BF_{10} of 3.4, indicating that the alternative hypothesis is

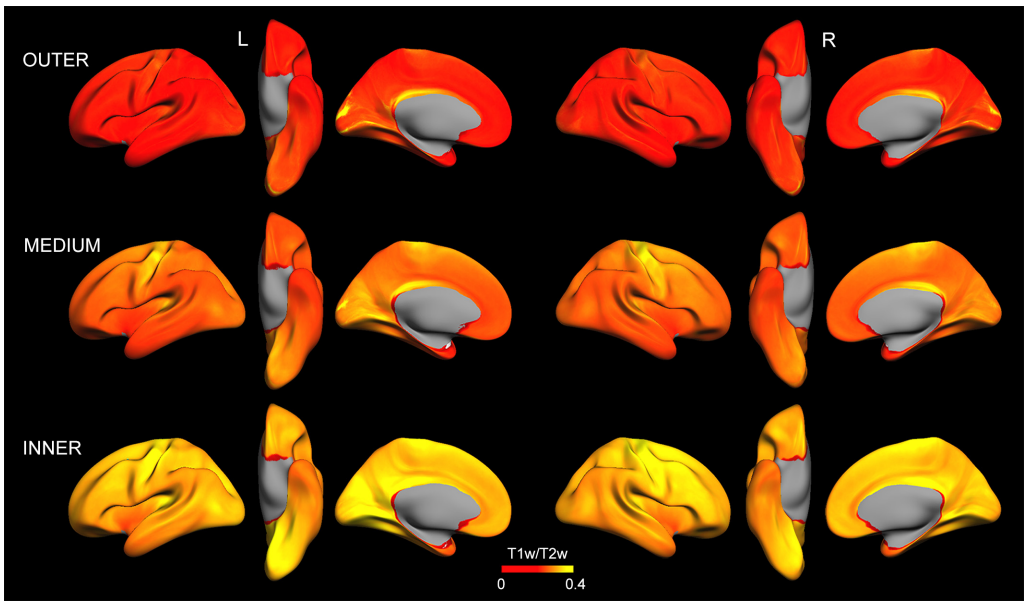

FIGURE 2 | Intracortical myelin maps projected onto the average cortical surface obtained at different depths (outer, medium, and inner layer) before z-transformation. Note that, in general, T1w/T2w ratio values increase with cortical depth. Left (L) and right (R).

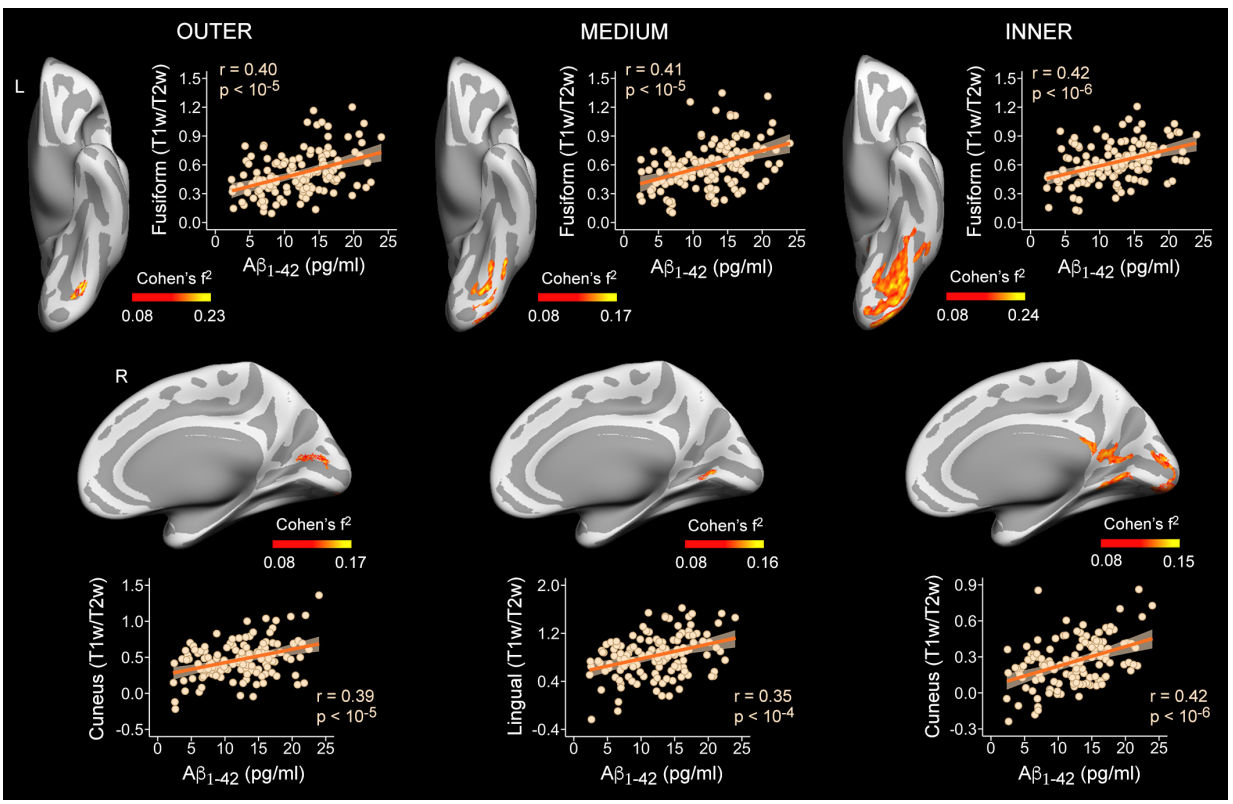

FIGURE 3 | Associations between plasma $A\beta_{1-42}$ levels and intracortical myelin content (T1w/T2w ratio values) on cortical surfaces obtained at 90% (outer layer), 50% (medium layer) and 10% (inner layer) of the cortical thickness away from the WM surface. Projected size effects on inflated cortical surfaces indicate positive associations of plasma $A\beta_{1-42}$ levels with intracortical myelin content, after adjusting for age and sex. The color bar indicates the range of overall size effects (Cohen's f^2). Left (L) and right (R). Scatter plots show partial correlations between plasma $A\beta_{1-42}$ levels and the mean myelin content of the most significant cluster for each cortical depth and hemisphere, adjusted by age and sex.

TABLE 2 | Significant associations of plasma Ab_{1-42} and NfL with T1w/T2w ratio intensity values.

Vertex location with maximum statistic	MNI	R^2	$F_{5,127}$	f^2_{local}	$CI_{95\%}$	BF_{10}
Positive associations with Aβ$_{1-42}$ (inner layer)						
L fusiform ($p_{cluster} = 10^{-6}$)	–40 –73 –14	0.18	27.3	0.50	0.47–0.54	220^{E}
L lateral occipital ($p_{cluster} = 10^{-5}$)	–30 –90 –15	0.19	34.7	0.53	0.50–0.56	1234^{E}
L inferior temporal ($p_{cluster} = 0.02$)	–42 –51 –11	0.12	16.4	0.28	0.25–0.32	87^{VS}
R lateral occipital ($p_{cluster} = 10^{-6}$)	19 –85 –8	0.11	18.3	0.35	0.32–0.38	2436^{E}
R precuneus ($p_{cluster} = 0.0004$)	13 –54 16	0.13	19.0	0.38	0.35–0.42	6145^{E}
R lingual ($p_{cluster} = 0.003$)	7 –60 2	0.13	19.4	0.35	0.32–0.38	2047^{E}
Positive associations with Aβ$_{1-42}$ (medium layer)						
L fusiform ($p_{cluster} = 0.0003$)	–30 –72 –16	0.14	13.2	0.31	0.28–0.34	3.9^{M}
R lingual ($p_{cluster} = 10^{-5}$)	4 –62 7	0.14	16.7	0.36	0.32–0.39	4.2^{M}
Positive associations with Aβ$_{1-42}$ (outer layer)						
L fusiform ($p_{cluster} = 10^{-5}$)	–40 –71 –18	0.19	13.2	0.34	0.31–0.37	1817^{E}
L superior parietal ($p_{cluster} = 0.0002$)	–23 –84 24	0.14	18.8	0.37	0.34–0.40	2643^{E}
R pericalcarine ($p_{cluster} = 10^{-5}$)	5 –78 12	0.12	5.5	0.34	0.31–0.37	7472^{E}
R lateral occipital ($p_{cluster} = 10^{-5}$)	20 –89 –8	0.15	21.3	0.36	0.33–0.39	3547^{E}
Negative associations with NfL (inner layer)						
R insula ($p_{cluster} = 0.04$)	41 0 4	0.16	25.4	0.46	0.42–0.49	3.4^{M}

MNI coordinates are in MNI152 space. f^2: measure of local effect size. $CI_{95\%}$: 95% confidence interval. BF_{10}: Bayes factor yielded by the Bayesian linear regression analysis. The superscript of the BF_{10} indicates the qualitative interpretation of the evidence for the alternative hypothesis: ^{M} moderate; ^{VS} very strong; ^{E} extreme. L: left; R: right.

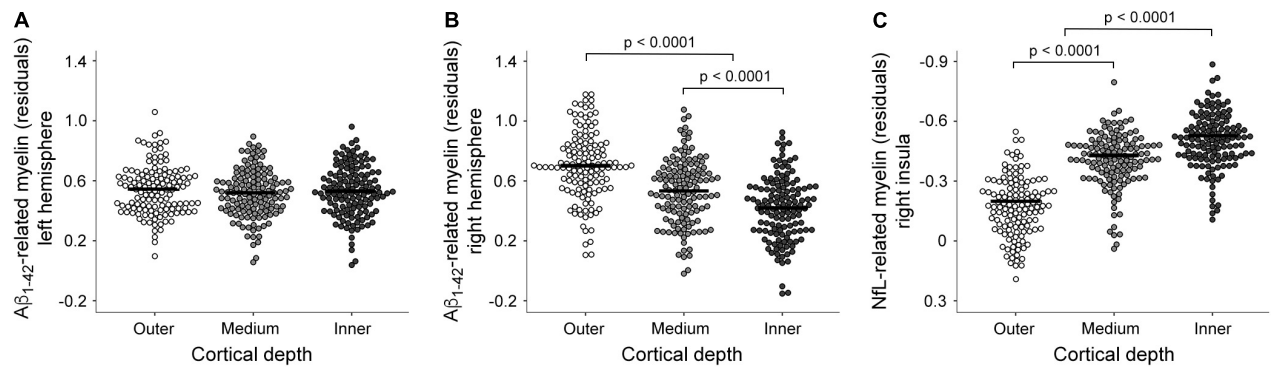

FIGURE 4 | Boxplots showing individual fitted mean intracortical myelin values for regions showing a significant association with plasma measurements at different cortical depths. Effect of cortical depth for the $A\beta_{1-42}$ associations with intracortical myelin in the left **(A)** and right hemisphere **(B)**. Note that positive associations between plasma $A\beta_{1-42}$ levels and intracortical myelin content (T1w/T2w ratio values) increased from inner to outer cortical layers only in the right hemisphere. **(C)** Effect of cortical depth for the NfL associations with intracortical myelin of the right insula. Note that the association between plasma NfL levels and intracortical myelin content (T1w/T2w ratio values) was more negative in the inner than in the medium and outer layers.

about three times more likely than the null, which is classified as moderate. The mixed model ANOVA addressing the effect of cortical depth on the strength of this association revealed a significant main effect in the right insular cortex ($\chi^2 = 354.9$, $p < 10^{-15}$). The association of NfL with intracortical myelin was more negative for the innermost layer than for the other two layers ($p < 0.0001$). **Figure 4C** illustrates these results.

Effect of the Relationship Between Plasma Measurements and Myelin Content on Rs-FC

We next performed rs-FC analysis using as seeds those regions derived from significant associations between plasma measurements ($A\beta_{1-42}$ and NfL) and myelin content (regions displayed in **Figures 3**, **5**). The interaction between plasma $A\beta_{1-42}$ and intracortical myelin did not predict rs-FC for none of the seeds evaluated. Conversely, the multiple regression analysis performed on the rs-FC map with the right insula as seed revealed a significant two-way interaction in the left medial orbitofrontal cortex ($R^2_{max} = 0.13$, $t_{max} = 4.36$, $p_{cluster} = 0.006$, *rho* = –2.22, $CI_{95\%}$[–2.81 to –1.63]). **Figure 6A** shows the spatial location of this result. *Post hoc* analyses shown in **Figure 6B** revealed a negative relationship between FC and myelin in individuals with higher plasma levels of NfL (i.e., the group with + 1SD) and a positive relationship in those with lower NfL levels (i.e., the group with –1SD). The Bayesian analysis yielded a BF_{10}

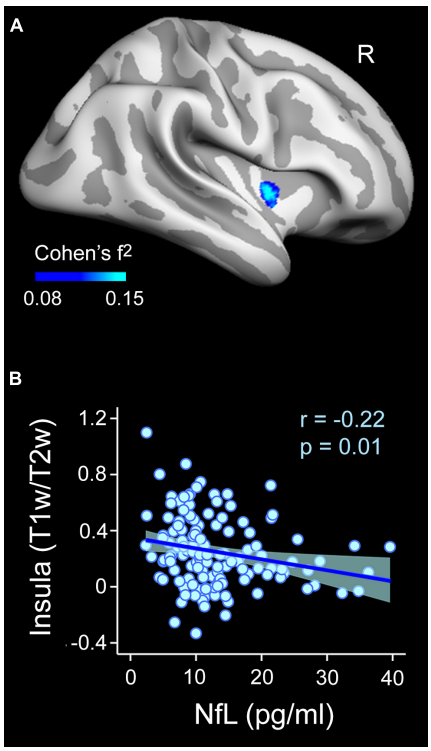

FIGURE 5 | Associations between plasma NfL levels and intracortical myelin content (T1w/T2w ratio values) on the cortical surface obtained at 10% of the cortical thickness away from the WM surface (inner layer). **(A)** Projected size effects on the inflated cortical surface indicate negative associations of plasma NfL levels with intracortical myelin content, adjusted by age and sex. The color bar indicates the range of overall size effects (Cohen's f^2). Right (R). **(B)** The scatter plot shows the partial correlation between plasma NfL levels and the mean myelin content of the significant cluster for the inner cortical layer located in the right insula, adjusted by age and sex.

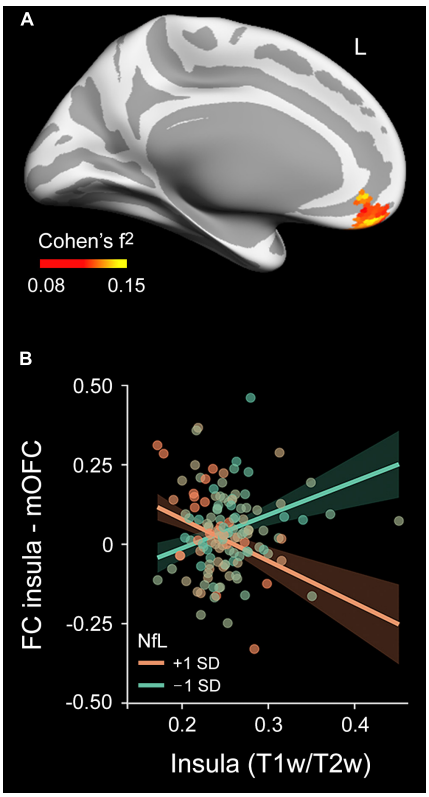

FIGURE 6 | Moderating effect of plasma NfL levels on the relationship between the mean myelin content and the rs-FC pattern of the right insula. **(A)** Projected size effects on the inflated cortical surface show the moderating role of plasma NfL levels in the association between the myelin content and rs-FC pattern of the right insula. The color bar indicates the overall range of size effects (Cohen's f^2). Left (L). **(B)** Scatter plot for the association of the mean myelin content of the right insula with rs-FC between the right insula and left medial orbitofrontal cortex (mOFC) at 1 SD below and above the mean of plasma NfL levels, adjusted by age and sex.

of 304, and therefore the evidence in favor of the alternative hypothesis is considered as extreme.

Associations of Plasma Measurements, Intracortical Myelin and Resting State-Functional Connectivity With Cognition

The ANOVAs performed to compare the sequential models revealed no significant main or interaction effects on cognition. BF_{10} ranged between 0.33 and 1. Accordingly, no evidence in favor of the null hypothesis was observed in either case.

DISCUSSION

We showed that plasma levels of Aβ1-42 and NfL were associated with intracortical myelin content, suggesting that they are able to track variations in myelin content in the aging neocortex. Interestingly, associations with plasma NfL were most evident in inner cortical layers, where fibers are more densely myelinated (Nave and Werner, 2014) and oligodendrogenesis is most impaired (Orthmann-Murphy et al., 2020; Xu et al., 2021). Furthermore, we found that higher concentrations of plasma NfL were associated with aberrant FC patterns of the insular cortex, a central brain hub highly vulnerable to neurodegeneration involved in affective and cognitive processes (Cauda et al., 2011). Considering that myelin undergoes significant alterations during aging and that aging is the major risk factor for AD, these results may be helpful in detecting myelin dysfunctions in aging and hypothetically serve to identify vulnerability to develop AD.

Plasma $A\beta_{1-42}$ Levels Are Positively Associated With Intracortical Myelin Content

Previous studies have shown that low plasma $A\beta_{1-42}$ concentrations appear in MCI/AD patients carrying the Apolipoprotein E ε4 allele (APOE4) (Kleinschmidt et al., 2016) and in cognitively normal individuals showing abnormal CSF-amyloid status and positive amyloid PET scans (Verberk et al., 2018). Moreover, plasma $A\beta_{1-42}$ levels have been

negatively associated with WM hyperintensities and positively with global cognition, memory performance, hippocampal volume and cortical thickness of the temporal lobe (Llado-Saz et al., 2015; Poljak et al., 2016; Hilal et al., 2018), as well as with a steeper rate of subsequent cognitive decline (Rembach et al., 2014; Poljak et al., 2016, Verberk et al., 2020) and increased risk of AD (Chouraki et al., 2015; Hilal et al., 2018; de Wolf et al., 2020).

Our results revealed a positive relationship between plasma $A\beta_{1-42}$ levels and intracortical myelin in cognitively normal older adults, linking plasma amyloid markers to cortical myelin integrity in normal aging. The association between cerebral amyloid aggregation and myelin deficits has been mainly supported by research in mouse models of AD (Desai et al., 2010; Mitew et al., 2010; Schmued et al., 2013; Chen et al., 2021). These studies showed that myelin pathology extends across regions with Aβ deposits (Mitew et al., 2010; Schmued et al., 2013), suggesting that the absence of oligodendrocytes in the plaque core may contribute to the destabilization of neuronal networks surrounding Aβ deposits (Palop and Mucke, 2010). This interpretation has been reinforced by research showing *in vivo* associations between myelin alterations and amyloid pathology in preclinical AD (Dean et al., 2017; Luo et al., 2019). In particular, lower CSF $A\beta_{1-42}$ levels were found to be associated with lower myelin water fraction (MWF) in the WM of late myelinating brain regions (Dean et al., 2017), which are affected by AD lesions from the earliest stage (Braak and Del Tredici, 2015). Further evidence indicates that preclinical AD patients exhibit the lowest T1w/T2w ratio in the inferior parietal lobe, which continues to decrease with disease progression (Luo et al., 2019). Our results complement these findings, providing evidence that positive associations of intracortical myelin with plasmatic $A\beta_{1-42}$ are restricted to posterior cortical regions in normal aging. Together, these results suggest that myelin breakdown in aging and preclinical AD occurs in the reverse direction in which myelination develops, from cortical association regions to subcortical WM projection tracts, and from posterior to anterior brain regions (Bartzokis, 2004).

An alternative interpretation is that the load of WM lesions, instead of Aβ deposition in plaques, could drive the relationship between plasma $A\beta_{1-42}$ and intracortical myelin content. In line with this hypothesis, it has been reported that associations between CSF $A\beta_{1-42}$ levels and cortical atrophy are noticeable in dementia patients but absent in cognitively normal older adults, whereas correlations between CSF $A\beta_{1-42}$ and WM lesions are present in normal elderly individuals but lacked in dementia patients (Skoog et al., 2018). Further, if associations between plasma $A\beta_{1-42}$ and intracortical myelin content were a reflection of the cerebral amyloid burden, this relationship should be stronger in deeper cortical layers, where the myelin content is higher (Hughes et al., 2018). This prediction is supported by evidence indicating that Aβ staining in 5×FAD transgenic mice is more intense in deeper than in superficial cortical layers. As a result, T1 and T2 values were more drastically reduced in deeper cortical regions in transgenic mice compared to wild-type mice (Spencer et al., 2013). Moreover, analysis of the laminar distribution of transmitter receptors in the human neocortex has shown that deeper layers of temporo-occipital regions concentrate a high density of kainate receptors (Palomero-Gallagher and Zilles, 2019). Given that oligodendrocytes contribute to the control of extracellular glutamate levels (Matute et al., 2001) and oligodendrogenesis is mostly impaired in the deeper cortical layers (Orthmann-Murphy et al., 2020; Xu et al., 2021), alterations in glutamate homeostasis may result in overactivation of kainate receptors and subsequent excitotoxic oligodendroglial death, especially in the innermost layers. However, our results showed that associations between plasma $A\beta_{1-42}$ and intracortical were stronger in the outer cortical layer (at least in the right hemisphere), suggesting that plasma $A\beta_{1-42}$-myelin associations are not likely driven by cerebral amyloid burden.

It is also worth noting that T1 relaxation rate correlates with iron concentration in the brain, showing much higher iron relaxivity values in the cortex than in other brain structures (Ogg and Steen, 1998). Accordingly, high-field MRI data from postmortem brain samples has revealed a layered organization of iron content in the cortical mantle suggestive of each region's myeloarchitecture (Fukunaga et al., 2010). Therefore, we cannot rule out that associations between plasma measurements and intracortical myelin content are partially due to iron accumulation. Future experiments should use more sophisticated *in vivo* approaches to separate iron and myelin content in the human cortex (Shin et al., 2021) in order to reliably determine their specific effects on aging and aging-related neurodegenerative conditions.

Plasma NfL Levels Are Negatively Associated With Intracortical Myelin Content and Abnormal Resting State-Functional Connectivity

Neurofilament light chain is one of the scaffolding proteins of the axonal cytoskeleton with important roles in axonal and dendritic branching (Yuan et al., 2017). NfL is particularly abundant in myelinated axons and is released to the periphery upon damage of the central nervous system (Gafson et al., 2020). Although plasma NfL is not a specific AD biomarker, it has been positively associated with higher risk of cognitive decline in cognitively normal older adults, MCI and AD patients (Mattsson et al., 2017; Aschenbrenner et al., 2020; Lee et al., 2022) and higher CSF NfL concentration in the early presymptomatic stages of familial AD (Preische et al., 2019) and in all stages of sporadic AD (Mattsson et al., 2017). At baseline, it has been positively related to neocortical Aβ and tau in cognitively unimpaired and impaired older adults, respectively (Chatterjee et al., 2018; Benedet et al., 2020) and negatively to hippocampal atrophy in all stages of AD (Mattsson et al., 2017; Hu et al., 2019) and to the mean cortical thickness of the whole-brain and specific brain regions in MCI and cognitively normal older adults (Lee et al., 2022). Over time, decreasing plasma NfL levels have also been related to progressive enlargement of the lateral ventricles and decreasing brain metabolism, hippocampal volume and cortical thickness especially in MCI and AD patients (Mattsson et al., 2017; Benedet et al., 2020). Consequently, plasma NfL is considered a promising

and cost-effective biomarker of axonal injury in AD and a variety of neurological conditions (Khalil et al., 2018).

High blood NfL levels may further reflect myelin breakdown, presumably due to dysfunctional oligodendrocytes, which provide trophic support to axons (Mot et al., 2018). Multiple lines of evidence indirectly support this hypothesis in humans. For instance, recent experiments have revealed associations between high serum NfL levels and MRI markers of myelin damage in multiple sclerosis (Yik et al., 2022), pediatric acquired demyelinating syndrome (Simone et al., 2021), and X-linked adrenoleukodystrophy (Weinhofer et al., 2021). Our results add further support to this hypothesis, showing a negative relationship between plasma NfL levels and intracortical myelin content of the right insular cortex, a lightly myelinated cortical region that has shown increased vulnerability in aging (Hu et al., 2014), preclinical (Cantero et al., 2020) and prodromal AD (Cantero et al., 2017).

We also showed that plasma NfL levels modulated patterns of FC between the insula and medial orbitofrontal cortex, two lightly myelinated cortical areas that appeared to be vulnerable to detrimental effects of aging (Bartzokis, 2011; Vidal-Piñeiro et al., 2016). Recent evidence has linked rs-FC patterns of insular cortex and orbitofrontal cortex to apathy (Jang et al., 2021), a multi-domain syndrome associated with poor outcomes and incident dementia in normal older adults (van Dalen et al., 2018), suggesting that impaired FC of these two regions may have unfavorable implications for aging. Tract tracing studies in primates have revealed that the anterior insula has prominent connections to the orbitofrontal cortex (Flynn et al., 1999), forming a functional unit that serves in the integration of complex autonomic, cognitive and emotional processes (Morel et al., 2013), all of them manifestly affected by aging (Salthouse, 2012). We speculate that as long as plasma NfL levels are elevated, reduced myelin content of the insular cortex may affect synchronized timing of neuronal impulses leading to abnormal functional connections with the medial orbitofrontal cortex.

Study Limitations

Results of the present study were cross-sectionally obtained, which has strengths and weaknesses that should be acknowledged. While cross-sectional studies are valuable for establishing preliminary evidence in planning advanced studies, they are not helpful for drawing predictive conclusions. As long as the study sample is representative of the overall population, cross-sectional studies are adequate for measuring the prevalence of health outcomes, understand determinants of health, and describe features of a population (Wang and Cheng, 2020). Therefore, our results cannot establish a true cause and effect relationship between T1w/T2w ratio values and plasma levels of $A\beta_{1-42}$ and NfL, nor can they determine a temporal relationship between outcomes and risk factors. However, they could be used to generate predictive hypothesis for longitudinal studies in which T1w/T2w ratio values are used as a predictive or dependent variable.

Linking our results to AD requires caution. Brain-specific proteins are present in much lower concentrations in blood than in CSF because the blood-brain barrier prevents free passage of molecules between the CNS and blood compartments (Zetterberg and Burnham, 2019). More importantly, Aβ species are expressed in non-brain tissues and bind to a variety of blood proteins (Marcello et al., 2009), which may not reflect brain Aβ turnover/metabolism and consequently reduce the potential for monitoring Aβ pathology in the blood. Moreover, the plasma $A\beta_{1-42}/A\beta_{1-40}$ ratio has shown better concordance with cerebral amyloid load than plasma $A\beta_{1-42}$ alone (Janelidze et al., 2016; Schindler et al., 2019), suggesting that the $A\beta_{1-42}/A\beta_{1-40}$ ratio has an added value as a pre-screening biomarker in AD.

CONCLUSION

The present study showed that lower plasma $A\beta_{1-42}$ and higher plasma NfL levels were associated with lower intracortical myelin content in temporo-parietal-occipital regions and the insula, respectively. Notably, the latter association was most evident in inner cortical layers, where axons are more heavily myelinated (Nave and Werner, 2014) and oligodendrogenesis is most impaired (Orthmann-Murphy et al., 2020; Xu et al., 2021). Plasma NfL levels further moderated the relationship between intracortical myelin content and rs-FC, likely revealing a complex inter-relationship between axonal damage, myelin breakdown and FC in aging. As myelin undergoes significant alterations in aging, the most important risk factor for AD, these results may be helpful in detecting aging-related myelin dysfunctions and potentially serve to identify vulnerability to develop AD.

DATA AVAILABILITY STATEMENT

The raw data supporting the conclusions of this article will be made available by the authors on reasonable request.

ETHICS STATEMENT

The studies involving human participants were reviewed and approved by Ethical Committee for Clinical Research of the Junta de Andalucía. The patients/participants provided their written informed consent to participate in this study.

AUTHOR CONTRIBUTIONS

JLC conceived the study and wrote the manuscript. MF-A, MA, and JLC contributed to data acquisition, data analysis, and preparation of figures and tables. FZ, CM, and EC-Z performed the plasma $A\beta_{1-42}$ and NfL determinations. All authors read and approved the final version of the manuscript.

FUNDING

This work was supported by the Spanish Ministry of Economy and Competitiveness (PID2020-119978RB-I00 to JLC and PID2020-118825GB-I00 to MA), CIBERNED (JLC, MA, CM, EC-Z, and FZ), Alzheimer's Association (AARG-NFT-22-924702 to

JLC), the Basque Government (IT1203-19; ELKARTEK KK-2020/00034 to EC-Z), the Research Program for a Long-Life Society of the Fundación General CSIC (0551_PSL_6_E to JLC), the Junta de Andalucía (PY20_00858 to JLC), and the Andalucía-FEDER Program (UPO-1380913 to JLC).

SUPPLEMENTARY MATERIAL

The Supplementary Material for this article can be found online at: https://www.frontiersin.org/articles/10.3389/fnagi.2022.896848/full#supplementary-material

REFERENCES

Aschenbrenner, A. J., Gordon, B. A., Fagan, A. M., Schindler, S. E., Balota, D. A., Morris, J. C., et al. (2020). Neurofilament light predicts decline in attention but not episodic memory in preclinical Alzheimer's disease. *J. Alzheimers Dis.* 74, 1119–1129. doi: 10.3233/JAD-200018

Bartzokis, G. (2004). Age-related myelin breakdown: a developmental model of cognitive decline and Alzheimer's disease. *Neurobiol. Aging* 25, 5–18. doi: 10.1016/j.neurobiolaging.2003.03.001

Bartzokis, G. (2011). Alzheimer's disease as homeostatic responses to age-related myelin breakdown. *Neurobiol. Aging* 32, 1341–1371. doi: 10.1016/j.neurobiolaging.2009.08.007

Benedet, A. L., Leuzy, A., Pascoal, T. A., Ashton, N. J., Mathotaarachchi, S., Savard, M., et al. (2020). Stage-specific links between plasma neurofilament light and imaging biomarkers of Alzheimer's disease. *Brain* 143, 3793–3804. doi: 10.1093/brain/awaa342

Bernal-Rusiel, J. L., Atienza, M., and Cantero, J. L. (2008). Detection of focal changes in human cortical thickness: spherical wavelets versus Gaussian smoothing. *Neuroimage* 41, 1278–1292. doi: 10.1016/j.neuroimage.2008.03.022

Bernal-Rusiel, J. L., Atienza, M., and Cantero, J. L. (2010). Determining the optimal level of smoothing in cortical thickness analysis: a hierarchical approach based on sequential statistical thresholding. *Neuroimage* 52, 158–171. doi: 10.1016/j.neuroimage.2010.03.074

Beul, S. F., Barbas, H., and Hilgetag, C. C. (2017). A predictive structural model of the primate connectome. *Sci. Rep.* 7:43176. doi: 10.1038/srep43176

Böhm, P., Peña-Casanova, J., Aguilar, M., Hernández, G., Sol, J. M., and Blesa, R. (1998). Clinical validity and utility of the interview for deterioration of daily living in dementia for Spanish-speaking communities NORMACODEM Group. *Int. Psychogeriatr.* 10, 261–270. doi: 10.1017/s1041610298005377

Braak, H., and Del Tredici, K. (2015). The preclinical phase of the pathological process underlying sporadic Alzheimer's disease. *Brain* 138, 2814–2833. doi: 10.1093/brain/awv236

Cantero, J. L., Atienza, M., Lage, C., Zaborszky, L., Vilaplana, E., Lopez-Garcia, S., et al. (2020). Atrophy of basal forebrain initiates with tau pathology in individuals at risk for Alzheimer's disease. *Cereb. Cortex* 30, 2083–2098. doi: 10.1093/cercor/bhz224

Cantero, J. L., Zaborszky, L., and Atienza, M. (2017). Volume loss of the nucleus basalis of meynert is associated with atrophy of innervated regions in mild cognitive impairment. *Cereb. Cortex* 27, 3881–3889. doi: 10.1093/cercor/bhw195

Cauda, F., D'Agata, F., Sacco, K., Duca, S., Geminiani, G., and Vercelli, A. (2011). Functional connectivity of the insula in the resting brain. *Neuroimage* 55, 8–23. doi: 10.1016/j.neuroimage.2010.11.049

Chatterjee, P., Goozee, K., Sohrabi, H. R., Shen, K., Shah, T., Asih, P. R., et al. (2018). Association of plasma neurofilament light chain with neocortical amyloid-β load and cognitive performance in cognitively normal elderly participants. *J. Alzheimers Dis.* 63, 479–487. doi: 10.3233/JAD-180025

Chen, J. F., Liu, K., Hu, B., Li, R. R., Xin, W., Chen, H., et al. (2021). Enhancing myelin renewal reverses cognitive dysfunction in a murine model of Alzheimer's disease. *Neuron* 109, 2292–2307. doi: 10.1016/j.neuron.2021.05.012

Chouraki, V., Beiser, A., Younkin, L., Preis, S. R., Weinstein, G., Hansson, O., et al. (2015). Plasma amyloid-β and risk of Alzheimer's disease in the Framingham Heart Study. *Alzheimers Dement.* 11, 249–257. doi: 10.1016/j.jalz.2014.07.001

Cohen, J. E. (1988). *Statistical Power Analysis for the Behavioral Sciences*. Hillsdale, NJ: Lawrence Erlbaum Associates, Inc.

Couttas, T. A., Kain, N., Suchowerska, A. K., Quek, L. E., Turner, N., Fath, T., et al. (2016). Loss of ceramide synthase 2 activity, necessary for myelin biosynthesis, precedes tau pathology in the cortical pathogenesis of Alzheimer's disease. *Neurobiol. Aging* 43, 89–100. doi: 10.1016/j.neurobiolaging.2016.03.027

de Wolf, F., Ghanbari, M., Licher, S., McRae-McKee, K., Gras, L., Weverling, G. J., et al. (2020). Plasma tau, neurofilament light chain and amyloid-β levels and risk of dementia; a population-based cohort study. *Brain* 143, 1220–1232. doi: 10.1093/brain/awaa054

Dean, D. C. III, Hurley, S. A., Kecskemeti, S. R., O'Grady, J. P., Canda, C., Davenport-Sis, N. J., et al. (2017). Association of amyloid pathology with myelin alteration in preclinical Alzheimer disease. *JAMA Neurol.* 74, 41–49. doi: 10.1001/jamaneurol.2016.3232

Desai, M. K., Mastrangelo, M. A., Ryan, D. A., Sudol, K. L., Narrow, W. C., and Bowers, W. J. (2010). Early oligodendrocyte/myelin pathology in Alzheimer's disease mice constitutes a novel therapeutic target. *Am. J. Pathol.* 177, 1422–1435. doi: 10.2353/ajpath.2010.100087

Desikan, R. S., Ségonne, F., Fischl, B., Quinn, B. T., Dickerson, B. C., Blacker, D., et al. (2006). An automated labeling system for subdividing the human cerebral cortex on MRI scans into gyral based regions of interest. *Neuroimage* 31, 968–980. doi: 10.1016/j.neuroimage.2006.01.021

Felts, P. A., Baker, T. A., and Smith, K. J. (1997). Conduction in segmentally demyelinated mammalian central axons. *J. Neurosci.* 17, 7267–7277. doi: 10.1523/JNEUROSCI.17-19-07267.1997

Fields, R. D. (2015). A new mechanism of nervous system plasticity: activity-dependent myelination. *Nat. Rev. Neurosci.* 16, 756–767. doi: 10.1038/nrn4023

Fischl, B., and Dale, A. M. (2000). Measuring the thickness of the human cerebral cortex from magnetic resonance images. *Proc. Natl. Acad. Sci. U. S. A.* 97, 11050–11055. doi: 10.1073/pnas.200033797

Flynn, F. G., Benson, F., and Ardila, A. (1999). Anatomy of the insula – Functional and clinical correlates. *Aphasiology* 13, 55–78. doi: 10.1080/026870399402325

Fukunaga, M., Li, T. Q., van Gelderen, P., de Zwart, J. A., Shmueli, K., Yao, B., et al. (2010). Layer-specific variation of iron content in cerebral cortex as a source of MRI contrast. *Proc. Natl. Acad. Sci. U. S. A.* 107, 3834–3839. doi: 10.1073/pnas.0911177107

Gafson, A. R., Barthélemy, N. R., Bomont, P., Carare, R. O., Durham, H. D., Julien, J. P., et al. (2020). Neurofilaments: neurobiological foundations for biomarker applications. *Brain* 143, 1975–1998. doi: 10.1093/brain/awaa098

Glasser, M. F., Coalson, T. S., Harms, M. P., Xu, J., Baum, G. L., Autio, J. A., et al. (in press). Empirical transmit field bias correction of T1w/T2w myelin maps. *bioRxiv* [Preprint]. doi: 10.1101/2021.08.08.455570

Glasser, M. F., and Van Essen, D. C. (2011). Mapping human cortical areas *in vivo* based on myelin content as revealed by T1- and T2-weighted MRI. *J. Neurosci.* 31, 11597–11616. doi: 10.1523/JNEUROSCI.2180-11.2011

Glover, G. H., Li, T. Q., and Ress, D. (2000). Image-based method for retrospective correction of physiological motion effects in fMRI: RETROICOR. *Magn. Reson. Med.* 44, 162–167. doi: 10.1002/1522-2594(200007)44:1<162::aid-mrm23>3.0.co;2-e

Gramunt, N., Sánchez-Benavides, G., Buschke, H., Diéguez-Vide, F., Peña-Casanova, J., Masramon, X., et al. (2016). The memory binding test: development of two alternate forms into Spanish and Catalan. *J. Alzheimers Dis.* 52, 283–293. doi: 10.3233/JAD-151175

Greve, D. N., and Fischl, B. (2009). Accurate and robust brain image alignment using boundary-based registration. *Neuroimage* 48, 63–72. doi: 10.1016/j.neuroimage.2009.06.060

Greve, D. N., Salat, D. H., Bowen, S. L., Izquierdo-Garcia, D., Schultz, A. P., Catana, C., et al. (2016). Different partial volume correction methods lead to different conclusions: an 18 F-FDG-PET study of aging. *Neuroimage* 132, 334–343. doi: 10.1016/j.neuroimage.2016.02.042

Grydeland, H., Vértes, P. E., Váša, F., Romero-Garcia, R., Whitaker, K., Alexander-Bloch, A. F., et al. (2019). Waves of maturation and senescence in micro-structural MRI markers of human cortical myelination over the lifespan. *Cereb. Cortex* 29, 1369–1381. doi: 10.1093/cercor/bhy330

Hilal, S., Woltersm, F. J., Verbeek, M. M., Vanderstichele, H., Ikram, M. K., Stoops, E., et al. (2018). Plasma amyloid-β levels, cerebral atrophy and risk of dementia: a population-based study. *Alzheimers Res. Ther.* 10:63. doi: 10.1186/s13195-018-0395-6

Hu, H., Chen, K. L., Ou, Y. N., Cao, X. P., Chen, S. D., Cui, M., et al. (2019). Neurofilament light chain plasma concentration predicts neurodegeneration and clinical progression in nondemented elderly adults. *Aging* 11, 6904–6914. doi: 10.18632/aging.102220

Hu, S., Chao, H. H., Zhang, S., Ide, J. S., and Li, C. S. (2014). Changes in cerebral morphometry and amplitude of low-frequency fluctuations of BOLD signals during healthy aging: correlation with inhibitory control. *Brain Struct. Funct.* 219, 983–994. doi: 10.1007/s00429-013-0548-0

Hughes, E. G., Orthmann-Murphy, J. L., Langseth, A. J., and Bergles, D. E. (2018). Myelin remodeling through experience-dependent oligodendrogenesis in the adult somatosensory cortex. *Nat. Neurosci.* 21, 696–706. doi: 10.1038/s41593-018-0121-5

Huntenburg, J. M., Bazin, P. L., Goulas, A., Tardif, C. L., Villringer, A., and Margulies, D. S. (2017). A systematic relationship between functional connectivity and intracortical myelin in the human cerebral cortex. *Cereb. Cortex* 27, 981–997. doi: 10.1093/cercor/bhx030

Irvine, K. A., and Blakemore, W. F. (2006). Age increases axon loss associated with primary demyelination in cuprizone-induced demyelination in C57BL/6 mice. *J. Neuroimmunol.* 175, 69–76. doi: 10.1016/j.jneuroim.2006.03.002

Janelidze, S., Zetterberg, H., Mattsson, N., Palmqvist, S., Vanderstichele, H., Lindberg, O., et al. (2016). CSF Aβ42/Aβ40 and Aβ42/Aβ38 ratios: better diagnostic markers of Alzheimer disease. *Ann. Clin. Transl. Neurol.* 3, 154–165. doi: 10.1002/acn3.274

Jang, J. Y., Han, S. D., Yew, B., Blanken, A. E., Dutt, S., Li, Y., et al. (2021). Resting-state functional connectivity signatures of apathy in community-living older adults. *Front. Aging Neurosci.* 13:691710. doi: 10.3389/fnagi.2021.691710

Khalil, M., Teunissen, C. E., Otto, M., Piehl, F., Sormani, M. P., Gattringer, T., et al. (2018). Neurofilaments as biomarkers in neurological disorders. *Nat. Rev. Neurol.* 14, 577–589. doi: 10.1038/s41582-018-0058-z

Kleinschmidt, M., Schoenfeld, R., Göttlich, C., Bittner, D., Metzner, J. E., Leplow, B., et al. (2016). Characterizing aging, mild cognitive impairment, and dementia with blood-based biomarkers and neuropsychology. *J. Alzheimers Dis.* 50, 111–126. doi: 10.3233/JAD-143189

Lee, E. H., Kwon, H. S., Koh, S. H., Choi, S. H., Jin, J. H., Jeong, J. H., et al. (2022). Serum neurofilament light chain level as a predictor of cognitive stage transition. *Alzheimers Res. Ther.* 14:6. doi: 10.1186/s13195-021-00953-x

Lee, M. D., and Wagenmakers, E. J. (2013). *Bayesian Cognitive Modeling: A Practical Course*. Cambridge: Cambridge University Press.

Liang, F., Paulo, R., Molina, G., Clyde, M. A., and Berger, J. O. (2008). Mixtures of g priors for Bayesian variable selection. *J. Am. Stat. Assoc.* 103, 410–423. doi: 10.1198/016214507000001337

Llado-Saz, S., Atienza, M., and Cantero, J. L. (2015). Increased levels of plasma amyloid-beta are related to cortical thinning and cognitive decline in cognitively normal elderly subjects. *Neurobiol. Aging* 36, 2791–2797. doi: 10.1016/j.neurobiolaging.2015.06.023

Luo, X., Li, K., Zeng, Q., Huang, P., Jiaerken, Y., Wang, S., et al. (2019). Application of T1-/T2-weighted ratio mapping to elucidate intracortical demyelination process in the Alzheimer's disease continuum. *Front. Neurosci.* 13:904. doi: 10.3389/fnins.2019.00904

Marcello, A., Wirthsm, O., Schneider-Axmann, T., Degerman-Gunnarsson, M., Lannfelt, L., and Bayer, T. A. (2009). Circulating immune complexes of Abeta and IgM in plasma of patients with Alzheimer's disease. *J. Neural Transm.* 116, 913–920. doi: 10.1007/s00702-009-0224-y

Mathys, H., Davila-Velderrain, J., Peng, Z., Gao, F., Mohammadi, S., Young, J. Z., et al. (2019). Single-cell transcriptomic analysis of Alzheimer's disease. *Nature* 570, 332–337. doi: 10.1038/s41586-019-1195-2

Mattsson, N., Andreasson, U., Zetterberg, H., Blennow, K., and Alzheimer's Disease Neuroimaging Initiative. (2017). Association of plasma neurofilament light with neurodegeneration in patients with Alzheimer Disease. *JAMA Neurol.* 74, 557–566. doi: 10.1001/jamaneurol.2016.6117

Matute, C., Alberdi, E., Domercq, M., Pérez-Cerdá, F., Pérez-Samartín, A., and Sánchez-Gómez, M. V. (2001). The link between excitotoxic oligodendroglial death and demyelinating diseases. *Trends Neurosci.* 24, 224–230. doi: 10.1016/s0166-2236(00)01746-x

Mitew, S., Kirkcaldie, M. T., Halliday, G. M., Shepherd, C. E., Vickers, J. C., and Dickson, T. C. (2010). Focal demyelination in Alzheimer's disease and transgenic mouse models. *Acta Neuropathol.* 119, 567–577. doi: 10.1007/s00401-010-0657-2

Monje, M. (2018). Myelin plasticity and nervous system function. *Annu. Rev. Neurosci.* 41, 61–76. doi: 10.1146/annurev-neuro-080317-061853

Morel, A., Gallay, M. N., Baechler, A., Wyss, M., and Gallay, D. S. (2013). The human insula: architectonic organization and postmortem MRI registration. *Neuroscience* 236, 117–135. doi: 10.1016/j.neuroscience.2012.12.076

Mot, A. I., Depp, C., and Nave, K. A. (2018). An emerging role of dysfunctional axon-oligodendrocyte coupling in neurodegenerative diseases. *Dialogues Clin. Neurosci.* 20, 283–292. doi: 10.31887/DCNS.2018.20.4/knave

Nave, K. A., and Werner, H. B. (2014). Myelination of the nervous system: mechanisms and functions. *Annu. Rev. Cell Dev. Biol.* 30, 503–533. doi: 10.1146/annurev-cellbio-100913-013101

Nieuwenhuys, R. (2013). The myeloarchitectonic studies on the human cerebral cortex of the Vogt-Vogt school, and their significance for the interpretation of functional neuroimaging data. *Brain Struct. Funct.* 218, 303–352. doi: 10.1007/s00429-012-0460-z

Ogg, R. J., and Steen, R. G. (1998). Age-related changes in brain T1 are correlated with iron concentration. *Magn. Reson. Med.* 40, 749–753. doi: 10.1002/mrm.1910400516

Orthmann-Murphy, J., Call, C. L., Molina-Castro, G. C., Hsieh, Y. C., Rasband, M. N., Calabresi, P. A., et al. (2020). Remyelination alters the pattern of myelin in the cerebral cortex. *Elife* 9:e56621. doi: 10.7554/eLife.56621

Pajevic, S., Basser, P. J., and Fields, R. D. (2014). Role of myelin plasticity in oscillations and synchrony of neuronal activity. *Neuroscience* 276, 135–147. doi: 10.1016/j.neuroscience.2013.11.007

Palomero-Gallagher, N., and Zilles, K. (2019). Cortical layers: cyto-, myelo-, receptor- and synaptic architecture in human cortical areas. *Neuroimage* 197, 716–741. doi: 10.1016/j.neuroimage.2017.08.035

Palop, J. J., and Mucke, L. (2010). Amyloid-beta-induced neuronal dysfunction in Alzheimer's disease: from synapses toward neural networks. *Nat. Neurosci.* 13, 812–818. doi: 10.1038/nn.2583

Peters, A. (2002). The effects of normal aging on myelin and nerve fibers: a review. *J. Neurocytol.* 31, 581–593. doi: 10.1023/a:1025731309829

Polimeni, J. R., Fischl, B., Greve, D. N., and Wald, L. L. (2010). Laminar analysis of 7T BOLD using an imposed spatial activation pattern in human V1. *Neuroimage* 52, 1334–1346. doi: 10.1016/j.neuroimage.2010.05.005

Poljak, A., Crawford, J. D., Smythe, G. A., Brodaty, H., Slavin, M. J., Kochan, N. A., et al. (2016). The relationship between plasma Aβ levels, cognitive function and brain volumetrics: sydney Memory and Ageing Study. *Curr. Alzheimer Res.* 13, 243–255. doi: 10.2174/1567205013666151218150202

Preische, O., Schultz, S. A., Apel, A., Kuhle, J., Kaeser, S. A., Barro, C., et al. (2019). Serum neurofilament dynamics predicts neurodegeneration and clinical progression in presymptomatic Alzheimer's disease. *Nat. Med.* 25, 277–283. doi: 10.1038/s41591-018-0304-3

Rembach, A., Watt, A. D., Wilson, W. J., Villemagne, V. L., Burnham, S. C., Ellis, K. A., et al. (2014). Plasma amyloid-β levels are significantly associated with a transition toward Alzheimer's disease as measured by cognitive decline and change in neocortical amyloid burden. *J. Alzheimers Dis.* 40, 95–104. doi: 10.3233/JAD-131802

Rissin, D. M., Kan, C. W., Campbell, T. G., Howes, S. C., Fournier, D. R., Song, L., et al. (2010). Single-molecule enzyme-linked immunosorbent assay detects serum proteins at subfemtomolar concentrations. *Nat. Biotechnol.* 28, 595–599. doi: 10.1038/nbt.1641

Salthouse, T. (2012). Consequences of age-related cognitive declines. *Annu. Rev. Psychol.* 63, 201–226. doi: 10.1146/annurev-psych-120710-100328

Schindler, S. E., Bollinger, J. G., Ovod, V., Mawuenyega, K. G., Li, Y., Gordon, B. A., et al. (2019). High-precision plasma β-amyloid 42/40 predicts current and future brain amyloidosis. *Neurology* 93, e1647–e1659. doi: 10.1212/WNL.0000000000008081

Schmued, L. C., Raymick, J., Paule, M. G., Dumas, M., and Sarkar, S. (2013). Characterization of myelin pathology in the hippocampal complex of a transgenic mouse model of Alzheimer's disease. *Curr. Alzheimer Res.* 10, 30–37. doi: 10.2174/1567205011310010005

Seppälä, T. T., Herukka, S. K., Hänninen, T., Tervo, S., Hallikainen, M., Soininen, H., et al. (2010). Plasma Abeta42 and Abeta40 as markers of cognitive change

in follow-up: a prospective, longitudinal, population-based cohort study. *J. Neurol. Neurosurg. Psychiatry* 81, 1123–1127. doi: 10.1136/jnnp.2010.205757

Sheikh, J. L., and Yesavage, J. A. (1986). Geriatric Depression Scale (GDS): recent evidence and development of a shorter version. *Clin. Gerontol.* 5, 165–173. doi: 10.1300/J018v05n01_09

Shin, H. G., Lee, J., Yun, Y. H., Yoo, S. H., Jang, J., Oh, S. H., et al. (2021). χ-separation: magnetic susceptibility source separation toward iron and myelin mapping in the brain. *Neuroimage* 240:118371. doi: 10.1016/j.neuroimage.2021.118371

Simone, M., Palazzo, C., Mastrapasqua, M., Bollo, L., Pompamea, F., Gabellone, A., et al. (2021). Serum neurofilament light chain levels and myelin oligodendrocyte glycoprotein antibodies in pediatric acquired demyelinating syndromes. *Front. Neurol.* 12:754518. doi: 10.3389/fneur.2021.754518

Skoog, I., Kern, S., Zetterberg, H., Östling, S., Börjesson-Hanson, A., Guo, X., et al. (2018). Low cerebrospinal fluid Aβ42 and Aβ40 are related to white matter lesions in cognitively normal elderly. *J. Alzheimers Dis.* 62, 1877–1886. doi: 10.3233/JAD-170950

Spencer, N. G., Bridges, L. R., Elderfield, K., Amir, K., Austen, B., and Howe, F. A. (2013). Quantitative evaluation of MRI and histological characteristics of the 5xFAD Alzheimer mouse brain. *Neuroimage* 76, 108–115. doi: 10.1016/j.neuroimage.2013.02.071

Uddin, M. N., Figley, T. D., Solar, K. G., Shatil, A. S., and Figley, C. R. (2019). Comparisons between multi-component myelin water fraction, T1w/T2w ratio, and diffusion tensor imaging measures in healthy human brain structures. *Sci. Rep.* 9:2500. doi: 10.1038/s41598-019-39199-x

van Dalen, J. W., Van Wanrooij, L. L., van Charante, E. P. M., Richard, E., and van Gool, W. A. (2018). Apathy is associated with incident dementia in community-dwelling older people. *Neurology* 90, e82–e89. doi: 10.1212/WNL.0000000000004767

Verberk, I. M. W., Hendriksen, H. M. A., van Harten, A. C., Wesselman, L. M. P., Verfaillie, S. C. J., van den Bosch, K. A., et al. (2020). Plasma amyloid is associated with the rate of cognitive decline in cognitively normal elderly: the SCIENCe project. *Neurobiol. Aging* 89, 99–107. doi: 10.1016/j.neurobiolaging.2020.01.007

Verberk, I. M. W., Slot, R. E., Verfaillie, S. C. J., Heijst, H., Prins, N. D., van Berckel, B. N. M., et al. (2018). Plasma amyloid as prescreener for the earliest Alzheimer pathological changes. *Ann. Neurol.* 84, 648–658. doi: 10.1002/ana.25334

Vidal-Piñeiro, D., Walhovd, K. B., Storsve, A. B., Grydeland, H., Rohani, D. A., and Fjell, A. M. (2016). Accelerated longitudinal gray/white matter contrast decline in aging in lightly myelinated cortical regions. *Hum. Brain Mapp.* 37, 3669–3684. doi: 10.1002/hbm.23267

Vogt, O. (1903). Zur anatomischen Gliederung des Cortex cerebri. *J. Psychol. Neurol.* 2, 160–180.

Wang, F., Ren, S. Y., Chen, J. F., Liu, K., Li, R. X., Li, Z. F., et al. (2020). Myelin degeneration and diminished myelin renewal contribute to age-related deficits in memory. *Nat. Neurosci.* 23, 481–486. doi: 10.1038/s41593-020-0588-8

Wang, X., and Cheng, Z. (2020). Cross-sectional studies: strengths, weaknesses, and recommendations. *Chest* 158, S65–S71. doi: 10.1016/j.chest.2020.03.012

Waxman, S. G. (1980). Determinants of conduction velocity in myelinated nerve fibers. *Muscle Nerve* 3, 141–150. doi: 10.1002/mus.880030207

Weinhofer, I., Rommer, P., Zierfuss, B., Altmann, P., Foiani, M., Heslegrave, A., et al. (2021). Neurofilament light chain as a potential biomarker for monitoring neurodegeneration in X-linked adrenoleukodystrophy. *Nat. Commun.* 12:1816. doi: 10.1038/s41467-021-22114-2

Xu, Y. K. T., Call, C. L., Sulam, J., and Bergles, D. E. (2021). Automated *in vivo* tracking of cortical oligodendrocytes. *Front. Cell. Neurosci.* 15:667595. doi: 10.3389/fncel.2021.667595

Yang, S. Y., Chiu, M. J., Chen, T. F., and Horng, H. E. (2017). Detection of plasma biomarkers using immunomagnetic reduction: a promising method for the early diagnosis of Alzheimer's disease. *Neurol. Ther.* 6, 37–56. doi: 10.1007/s40120-017-0075-7

Yasuno, F., Kazui, H., Morita, N., Kajimoto, K., Ihara, M., Taguchi, A., et al. (2017). Use of T1-weighted/T2-weighted magnetic resonance ratio to elucidate changes due to amyloid β accumulation in cognitively normal subjects. *Neuroimage Clin.* 13, 209–214. doi: 10.1016/j.nicl.2016.11.029

Yeo, I. K., and Johnson, R. A. (2000). A new family of power transformations to improve normality or symmetry. *Biometrika* 87, 954–959. doi: 10.1093/biomet/87.4.954

Yik, J. T., Becquart, P., Gill, J., Petkau, J., Traboulsee, A., Carruthers, R., et al. (2022). Serum neurofilament light chain correlates with myelin and axonal magnetic resonance imaging markers in multiple sclerosis. *Mult. Scler.* 57:103366. doi: 10.1016/j.msard.2021.103366

Yuan, A., Rao, M. V., Veeranna, and Nixon, R. A. (2017). Neurofilaments and neurofilament proteins in health and disease. *Cold Spring Harb. Perspect. Biol.* 9:a018309. doi: 10.1101/cshperspect.a018309

Zetterberg, H., and Burnham, S. C. (2019). Blood-based molecular biomarkers for Alzheimer's disease. *Mol. Brain* 12:26. doi: 10.1186/s13041-019-0448-1

Conflict of Interest: The authors declare that the research was conducted in the absence of any commercial or financial relationships that could be construed as a potential conflict of interest.

Publisher's Note: All claims expressed in this article are solely those of the authors and do not necessarily represent those of their affiliated organizations, or those of the publisher, the editors and the reviewers. Any product that may be evaluated in this article, or claim that may be made by its manufacturer, is not guaranteed or endorsed by the publisher.

frontiers | Frontiers in Aging Neuroscience

SYSTEMATIC REVIEW
published: 04 July 2022
doi: 10.3389/fnagi.2022.855776

Pre-clinical Studies Identifying Molecular Pathways of Neuroinflammation in Parkinson's Disease: A Systematic Review

Mobina Fathi[1†], Kimia Vakili[1†], Shirin Yaghoobpoor[1†], Mohammad Sadegh Qadirifard[2,3], Mohammadreza Kosari[4], Navid Naghsh[5], Afsaneh Asgari taei[6], Andis Klegeris[7], Mina Dehghani[8], Ashkan Bahrami[9], Hamed Taheri[10], Ashraf Mohamadkhani[11], Ramtin Hajibeygi[12], Mostafa Rezaei Tavirani[13] and Fatemeh Sayehmiri[1*†]*

[1] Student Research Committee, Faculty of Medicine, Shahid Beheshti University of Medical Sciences, Tehran, Iran, [2] Department of Nursing and Midwifery, Islamic Azad University, Tehran, Iran, [3] Department of Nursing, Garmsar Branch, Islamic Azad University, Garmsar, Iran, [4] The First Clinical College, Wuhan Union Hospital, Tongji Medical College, Huazhong University of Science and Technology, Wuhan, China, [5] Department of Pharmacy, Shahid Sadoughi University of Medical Sciences, Yazd, Iran, [6] Neuroscience Research Center, Shahid Beheshti University of Medical Sciences, Tehran, Iran, [7] Department of Biology, Faculty of Science, University of British Columbia Okanagan Campus, Kelowna, BC, Canada, [8] School of Medicine, Isfahan University of Medical Sciences, Isfahan, Iran, [9] Faculty of Medicine, Kashan University of Medical Science, Kashan, Iran, [10] Dental School, Kazan Federal University, Kazan, Russia, [11] Digestive Disease Research Center, Tehran University of Medical Sciences, Tehran, Iran, [12] Department of Cardiology, Faculty of Medicine, Tehran Medical Sciences, Islamic Azad University, Tehran, Iran, [13] Proteomics Research Center, Faculty of Paramedical Sciences, Shahid Beheshti University of Medical Sciences, Tehran, Iran

Parkinson's disease (PD), the second most common neurodegenerative disorder, is characterized by neuroinflammation, formation of Lewy bodies, and progressive loss of dopaminergic neurons in the substantia nigra of the brain. In this review, we summarize evidence obtained by animal studies demonstrating neuroinflammation as one of the central pathogenetic mechanisms of PD. We also focus on the protein factors that initiate the development of PD and other neurodegenerative diseases. Our targeted literature search identified 40 pre-clinical *in vivo* and *in vitro* studies written in English. Nuclear factor *kappa* B (NF-kB) pathway is demonstrated as a common mechanism engaged by neurotoxins such as 1-methyl-4-phenyl-1,2,3,6-tetrahydropyridine (MPTP) and 6-hydroxydopamine (6-OHDA), as well as the bacterial lipopolysaccharide (LPS). The α-synuclein protein, which plays a prominent role in PD neuropathology, may also contribute to neuroinflammation by activating mast cells. Meanwhile, 6-OHDA models of PD identify microsomal prostaglandin E synthase-1 (mPGES-1) as one of the contributors to neuroinflammatory processes in this model. Immune responses are used by the central nervous system to fight and remove pathogens; however, hyperactivated and prolonged immune responses can lead to a harmful neuroinflammatory state, which is one of the key mechanisms in the pathogenesis of PD.

Keywords: Parkinson's disease, nuclear factor *kappa* B (NF-κB), NLRP3 inflammasome, microglia, mast cells, neuroinflammation

OPEN ACCESS

Edited by:
Suman Dutta,
University of California, Los Angeles, United States

Reviewed by:
Surya Pratap Singh,
Banaras Hindu University, India
Eduard Bentea,
KU Leuven, Belgium
Yao Longping,
Doctor Peset University Hospital, Spain

***Correspondence:**
Mostafa Rezaei Tavirani
tavirany@yahoo.com
Fatemeh Sayehmiri
Fsayehmiri@yahoo.com

[†] These authors have contributed equally to this work

Specialty section:
This article was submitted to Cellular and Molecular Mechanisms of Brain-aging, a section of the journal Frontiers in Aging Neuroscience

Received: *15 January 2022*
Accepted: *23 May 2022*
Published: *04 July 2022*

Citation:
Fathi M, Vakili K, Yaghoobpoor S, Qadirifard MS, Kosari M, Naghsh N, Asgari taei A, Klegeris A, Dehghani M, Bahrami A, Taheri H, Mohamadkhani A, Hajibeygi R, Rezaei Tavirani M and Sayehmiri F (2022) Pre-clinical Studies Identifying Molecular Pathways of Neuroinflammation in Parkinson's Disease: A Systematic Review. Front. Aging Neurosci. 14:855776. doi: 10.3389/fnagi.2022.855776

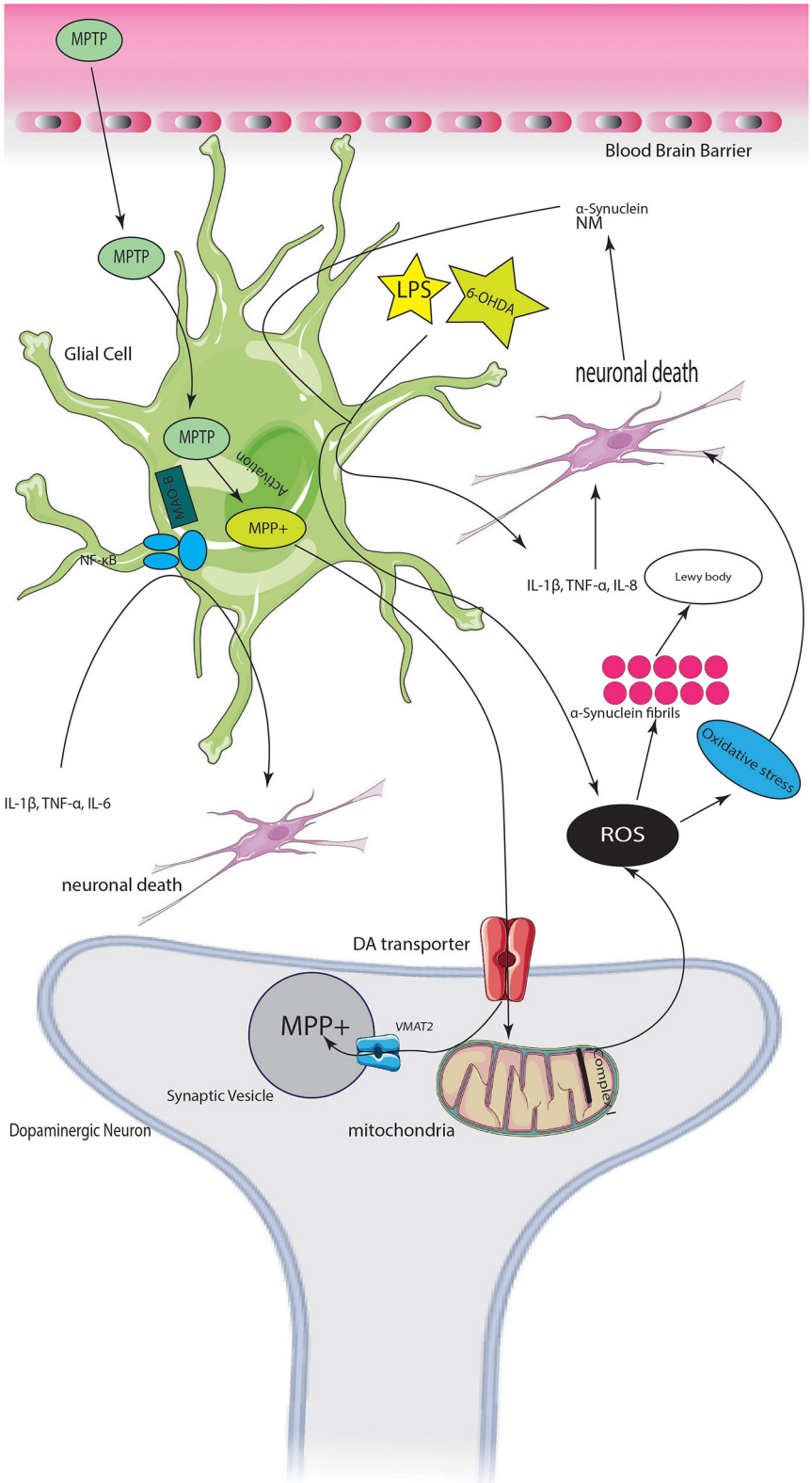

GRAPHICAL ABSTRACT | Servier (2022).

INTRODUCTION

Parkinson's disease (PD) is a neurodegenerative disorder defined by dopaminergic neuronal loss in the substantia nigra (SN) pars compacta, aggregation of misfolded α-synuclein (α-syn) as Lewy bodies, and motor dysfunction (Trudler et al., 2015). Degeneration of the nigrostriatal pathway leads to hallmark motor symptoms of this disease, including bradykinesia, rigidity, tremor at rest, and postural instability. Furthermore, most patients exhibit non-motor symptoms, such as sleep disorders, autonomic nervous system dysfunction, and cognitive impairment (Trudler et al., 2015; Kempuraj et al., 2016). Currently, pharmacological and surgical interventions are the main treatment options in PD which provide only symptomatic relief for patients. Among various disease-specific pathogenetic mechanisms, neuroinflammation plays a prominent role in the onset and progression of a broad range of neurodegenerative disorders, including PD, Alzheimer's disease (AD), and multiple sclerosis (MS). It has been demonstrated that the sterile neuroinflammation in neurodegenerative diseases embodies a cascade of events involving abnormal protein aggregates, upregulated inflammatory mediators, and activation of non-neuronal glial cells, which leads to neuronal damage. Neurodegeneration, in turn, induces further glial activation and neuroinflammation in the central nervous system (CNS). Out of the several different non-neuronal cell types of the CNS, microglia are the most prominent contributors to neuroimmune reactions. They express several different pattern recognition receptors (PRRs), such as toll-like receptor (TLR)2, TLR4, TLR9, and receptor for advanced glycation end products (RAGE), that recognize various pathogens and abnormal proteins. Microglial activation leads to the secretion of various pro-inflammatory mediators, including interleukin (IL) 1β, IL-6, and tumor necrosis factor α (TNF-α), to restore tissue hemostasis and also facilitate tissue repair (Ransohoff and Brown, 2012; Ransohoff, 2016; Molteni and Rossetti, 2017). Astrocytes represent another type of glial cells, which are critical for neuronal networks and maintenance of brain tissue homeostasis. Similar to microglia, astrocytes express PRRs and can contribute to neuroimmune responses by releasing a broad range of inflammatory mediators (Cunningham et al., 2019). Although acute inflammatory response can clear abnormal proteins, eliminate cell debris, and promote tissue repair, persistent inflammation is detrimental since it produces harmful inflammatory mediators and cytotoxins, as well as inhibits neural regeneration.

Neuroinflammation contributes to PD pathogenesis throughout the progression of this disease from early α-syn aggregation to causing dopaminergic cell loss and ultimately PD symptoms. For example, the accumulation of misfolded α-syn has been suggested to cause dysregulation of both innate and adaptive immune responses (Harms et al., 2021). Strong support to the neuroinflammatory hypothesis of PD is provided by genome-wide association studies linking sporadic PD to polymorphism in the human leukocyte antigen (HLA) region containing HLA-DR gene (Mohamadkhani et al., 2009; Simón-Sánchez et al., 2009; Hamza et al., 2010; Ahmed et al., 2012). The sustained inflammatory responses have been described in both PD patients and animal models of this disease, which through various mechanisms can cause neuronal dysfunction. In addition to reactive microglia and astrocytes releasing neurotoxic molecules, other mechanisms contributing to neuronal death and neurodegeneration in PD have been discovered; they include brain infiltration and activation of inflammatory mast cells and T lymphocytes, increased oxidative stress, and upregulation of inflammatory signaling molecules (Lyman et al., 2014; Jarrott and Williams, 2016; Kempuraj et al., 2016).

Activated glial cells and infiltrating peripheral immune cells are the main sources of the various pro-inflammatory mediators contributing to the onset and progression of PD. Activated glial cells release a broad range of both pro- and anti-inflammatory cytokines, such as TNF-α, IL-1β/IL-1α, IL-6, IL-8, and IL-10, as well as the brain inflammatory protein called glia maturation factor (GMF), which regulates functions of glial cells and can also induce neurodegeneration in the brain (Lim et al., 2004; Zaheer et al., 2008a,b; Tore and Tuncel, 2009; Kempuraj et al., 2013; Molteni and Rossetti, 2017; Mukai et al., 2018). Activated mast cells release potentially harmful mediators, such as proteases, utilizing the degranulation process (Tore and Tuncel, 2009; Taracanova et al., 2017; Mukai et al., 2018).

Dopaminergic neurotoxins such as 6-OHDA, 1-methyl-4-phenyl-1,2,3,6-tetrahydropyridine (MPTP), and its metabolite 1-methyl-4-phenylpyridinium (MPP^+) have been shown to adversely alter neuronal functions in both mature and developing nervous tissue. They have been used to induce PD in animal models where they, in addition to dopaminergic neuronal damage, cause glial activation, oxidative stress, mitochondrial damage, and the release of inflammatory cytokines (Członkowska et al., 1996; Stojkovska et al., 2015; Trudler et al., 2015; Pourasgari and Mohamadkhani, 2020). *In vivo* and *in vitro* studies show that the mechanism of action for dopaminergic neurotoxins could involve high-mobility group box 1 (HMGB1) (Huang et al., 2017), which is a nuclear DNA binding non-histone protein that facilitates the assembly of nucleoprotein complexes, but can also be released extracellularly and act as a damage-associated molecular pattern (DAMP) triggering neuroimmune responses (Sims et al., 2010).

The present systematic review aims to identify and evaluate the underlying genes and mechanisms of neuroinflammation in PD pre-clinical studies. Following this, a gene list-independent approach to compare different disease models is used.

METHOD

Search Strategy

Electronic databases PubMed, Scopus, Google Scholar, Web of Science, and EMBASE were searched using the medical subject headings (MeSH) aimed at identifying all research articles related to the topic "The association between neuroinflammation and Parkinson's disease." Two authors independently conducted the search using search strategies specific for each database and reviewed all relevant peer-reviewed articles published before April 2022. The following search terms were used "[(neuro-inflammation) AND Parkinson's disease],"

"[(neuro-inflammation) AND neurodegenerative disease]," "[((inflammation) AND Parkinson's disease) AND brain]," "(adaptive immunity) AND (Parkinson), (immunological biomarkers) AND (Parkinson), (hHumoral immunity) AND (Parkinson)," "[((inflammation) AND neurodegenerative disease) AND brain]," "[(inflammatory markers) AND Parkinson's disease]," and "[(inflammatory markers) AND neurodegenerative disease]," "[((inflammation) AND Parkinson's disease) AND animal]." A total of 40 articles were included.

Types of Studies (Selection Criteria)

This review article considered both quantitative and qualitative data on the association between neuroinflammation and PD, which were obtained by reviewing all available *in vivo* and *in vitro* pre-clinical studies relevant to this topic. Review articles and studies with human subjects were excluded. Only articles published in English were included. Duplicate data and low-quality studies, identified by the Systematic Review Center for Laboratory animal Experimentation (SYRCLES) quality assessment checklist (Hooijmans et al., 2014), were excluded. All eligible studied, both with positive and negative findings have been included in this systematic review. SYRCLES quality assessment checklist (Hooijmans et al., 2014) was used to assess selection bias, performance bias, detection bias, attrition bias, reporting bias, and other sources of bias (see **Supplementary Table 1**).

Data Extraction

The relevant studies were selected after the title, abstract, and full-text screening of the articles. In addition, the reference lists of selected studies were reviewed to identify any additional articles, should they have not been identified by the search process. The following information was extracted from each of the identified studies: cell culture and animal model used, the size of the PD model and control groups, inflammatory markers studied, and the key results obtained (see **Table 1**). This study was approved by the Iranian National Committee for Ethics in Biomedical Sciences (Code of Ethics: IR.SBMU.RETECH.REC.1399.992).

RESULTS

Study Selection

The current study has been run based on PRISMA checklist (Tore and Tuncel, 2009). At first, 2,499 papers were identified through the search on PubMed, and 7,560 were identified through searching other databases (Scopus, Google Scholar, Web of Science, and EMBASE). However, 4,823 of those 10,059 articles were excluded due to duplication in different databases. After screening the abstracts and titles of these obtained studies, 2,121 more papers were excluded due to unavailability of abstracts, or articles written in non-English, or being review articles. Moreover, 3,003 more papers were removed due to being irrelevant to the main subject or human studies. Finally, from the 112 remaining articles, 36 records excluded because of not relevant for the topic of the review. The full texts of the 76 remaining papers were fully assessed, and 36 more studies were excluded due to insufficient or unclear data ($n = 19$) and low quality ($n = 17$). Finally, 40 articles, published before April 2022, were chosen for systematic review (**Figure 1**).

Types of Studies Included at a Glance

The main results of all the papers included in this review are summarized first based on the neuroinflammatory pathways of PD. The method used to induce PD in animal models might be a key factor which affects the mechanism of neuroinflammation observed in a particular study; therefore, we reviewed the methods in both **Table 1** and a separate subsection of the results. The other subsections are introduced based on the most frequently appearing topics and mechanisms discussed in the reviewed articles.

A total of 40 articles are included in this review. Twenty-one out of 40 studies used only *in vivo models,* 11 were based on *in vitro experiments,* and 8 studies employed both *in vitro* and *in vivo* experiments. A variety of methods were used in different studies to induce PD: 11 studies used MPTP, 10 α-Syn injection, 6 LPS, 5 A53T α-Syn transgenic mice, and 2 paraquat. Two studies used both 6-OHDA and LPS, 1 used both MPTP and LPS, 1 6-OHDA, and 1 used prothrombin kringle 2.

Summary of Methods Used to Induce PD in Animal Models

Table 1 illustrates a variety of methods used by the reviewed studies to induce PD in animal models. Each method initiates its own pathway leading to PD-like pathology. Administration of MPTP to different animal species has been used extensively to model PD neuropathology. MPTP mimics the destruction of dopaminergic neurons of the substantia nigra pars compacta observed in PD. The mechanism by which MPTP causes damage to dopaminergic neurons involves a sequence of events including disturbance in the mitochondrial function, oxidative stress and respiratory failure. MPTP leads to inducible nitric oxide synthase (iNOS) overexpression. MPP+ is the active metabolite of MPTP which accumulates in dopaminergic (DA) neurons of the model after treatment with MPTP. MPP+ provokes the production of superoxide radicals which react with nitric oxide and generate peroxynitrite. This substance inhibits the function of many proteins including tyrosine hydroxylase. As a result, the production of dopamine is disturbed leading to damage of DA neurons (Przedborski et al., 2000; Burré et al., 2014, 2018).The loss of DA cells after MPTP administration has also been shown to activate microglia in the SN of rhesus monkeys (McGeer and McGeer, 2007). Therefore, *in vivo* and *in vitro* use of MPTP and its metabolite MPP+ can help elucidate the molecular mechanisms of the neuroinflammatory reactions in PD. Injection of lipopolysaccharide (LPS) and the following brain region-specific inflammation in mice provides *in vivo* models to investigate neurodegenerative diseases such as PD (Noh et al., 2014). LPS treatment in mice causes a decrease in the level of IL-4 and IL-10 but an elevation in the level of TNF-α, interleukin-1β, prostaglandin (PG) E_2, and nitric oxide. IL-10 has a neuroprotective effect against LPS intoxication (Tansey and Goldberg, 2010). As shown in **Table 1**, some studies have used this method to create a PD model. 6-hydroxydopamine (6-OHDA) is another neurotoxin used to

TABLE 1 | A rapid review of articles assessed.

References	Type of *in vitro/in vivo* models	Age and sex of animal models	Experimental design	Method used to induce PD	Type of immune cell	Inflammatory factors	Disease mechanism	New therapeutic targets
Zhang et al. (2022)	N9 microglial cells C57BL/6 mice	Age and sex not specified	*In vivo/In vitro*	LPS	Microglia	NLRP3, caspase-1, tumor necrosis factor-α (TNF-α), IL-1β and inducible nitric oxide synthase (iNOS)	AMS-17 inhibits NLRP3 pathways and microglial activation.	
Karikari et al. (2022)	Wildtype C57BL/6 or Recombination-activating gene 1 $(RAG1)^{-/-}$ mice		*In vivo* stereotactically injection of Adeno-associated Vector 1/2 serotype (AAV1/2) containing A53T α-syn to the SN	AAV-A53T-α-syn	B cells		B cells do not protect neurons from neurodegeneration	
Lai et al. (2021)	Young adult wild-type mice (C57BL/6N)	2.5-month-old Male	*In vivo* The unilateral intracranial injection	PFF α-syn–injected	Microglia	α-syn	Neuroinflammation may occur before α-syn pathologic aggregation	
La Vitola et al. (2021)	C57BL/6 naive mice and A53T α-synuclein transgenic PD mice	8-week-old C57BL/6 naive mice 8-months-old A53T mice Sex not specified	*In vivo*	LPS	Microglia and astrocytes	α-syn	Peripheral neuroinflammation induces PD by α-syn accumulation and causes motor deficits in A53T mice	
Mao et al. (2021)	PC12 cells	–	*In vitro*	LPS	Microglia	Lipoic acid	Lipoic acid inhibits p53/NF–κB pathway	
Zhang et al. (2021)	*In vitro*: BV2 murine microglial cells Human embryonic kidney (HEK) 293T cells Rat primary microglia extracted from the brains of Sprague-Dawley rats *In vitvo*: Sprague-Dawley rats	0 or 1-day-old Male	*In vitro/in vivo* stereotaxic injection of LPS	LPS	Microglia	α-syn metabotropic glutamate receptor 5 (mGluR5)	α-syn causes lysosome-dependent degradation of mGluR5 to occur faster. mGluR5 regulates neuroinflammation	

(Continued)

TABLE 1 | Continued

References	Type of *in vitro/in vivo* models	Age and sex of animal models	Experimental design	Method used to induce PD	Type of immune cell	Inflammatory factors	Disease mechanism	New therapeutic targets
Williams et al. (2021)	C57BL/6 (wild-type), *Tcrb*$^{-/-}$, *Cd4*$^{-/-}$, and *Cd8*$^{-/-}$ mice	Sex and age not specified	*In vivo* stereotaxic surgery	The α-synuclein overexpression mouse model, T cell deficiency	Myeloid cells CD4 and CD8 T cells	α-syn major histocompatibility complex II (MHCII) IFNγ	α-syn causes the major histocompatibility complex II (MHCII) protein on CNS myeloid cells to be upregulated and leads to recruitment of CD4 and CD8 T cells into the CNS. These cells produce IFNγ	
Trudler et al. (2021)	Human induced pluripotent stem cell (hiPSC)-derived microglia (hiMG) hiMG with αSyn in humanized mouse brain	Sex and age not specified	*In vitro/In vivo* stereotactically injection of hiMG	A53T α-syn secreted from hiPSC-derived A9-DA neurons	Microglia	α-syn antibody Caspase 1 TLR2	In vitro, NLRP3) inflammasome is activated by α-syn through TLR2 leading to interleukin-1β secretion. αSyn–antibody complexes had a positive effect on this inflammation process. In vivo, α-syn antibody worsened caspase-1 activation and neurotoxicity	
Huang et al. (2020)	SH-SY5Y cells	–	*In vitro* plated in 10 cm dishes with various doses of PQ added	Paraquat		HMGB1	Paraquat induces an increase of HMGB1 which results in cytokine release through RAGE-P38-NF-κB signaling pathway	Knockdown of HMGB1
Sarkar et al. (2020a)	C57/BL mice Primary microglial cells from postnatal mouse pups	Sex and age not specified	*In vitro/In vivo*	αSyn_{Agg} pre-formed fibrils	Microglia	αSyn_{Agg}	αSyn_{Agg} causes downregulation of progranulin (*Grn*) gene in microglia demonstrating immune roles of this gene in PD	
Subbarayan et al. (2020)	T cell deficient (athymic nude) and T cell competent (heterozygous) rats	Sex and age not specified	*In vivo* adeno-associated virus (AAV) α-syn	AAV9-α-syn	CD4+ and CD8+ T cells, micoglia		CD4+ and CD8+ T cells cause overexpression of MHCII in microglia and DA cell loss	
Iba et al. (2020)	α-syn transgenic (tg) mice (e.g., Thy1 promoter line 61)	10–11 months old Sex not specified	*In vivo*	α-syn	CD3+/CD4+ T cells		CD3+/CD4+ T cells recruited into the brain in synucleinopathies	
Morales-Garcia et al. (2020)	SH-SY5Y Cell Culture, Primary rat ventral mesencephalic neuron/glia cultures, male Wistar rats	Age not specified	*In vitro/In vivo* Injection of LPS into the right side of the SN.	6-OHDA LPS		PDE7	An elevated level of PDE7 happens due to oxidative stress caused by 6-OHDA or LPS.	

(Continued)

TABLE 1 | Continued

References	Type of *in vitro/in vivo* models	Age and sex of animal models	Experimental design	Method used to induce PD	Type of immune cell	Inflammatory factors	Disease mechanism	New therapeutic targets
Sarkar et al. (2020b)	Primary mouse microglia	–	*In vitro*	Aggregated αSyn stimulation	Microglia	Kv1.3: a voltage-gated potassium channel	Fyn kinase mediates Kv1.3 channels. Expression of Kv1.3 channels increases	
Javed et al. (2020)	GMF knockout ($GMF^{-/-}$) and C57BL/6 wild-type (WT) mice	Sex and age not specified	*In vivo*	MPTP: 1-methyl-4-phenyl-1,2,3,6-tetrahydropyridine		GMF IL-1β and IL-18	GMF causes NLRP3 inflammasome inhibition and decrease in the level of IL-1β and IL-18	
Li Y. et al. (2019)	A53T mice, Murine microglial cell line BV-2 and murine RAW 264.7 cell line, B Brain tissue from Neonatal and 3-month-old mice	Brain tissue from 3-months-old mice Sex not specified	*In vivo/in vitro* Stereotaxic surgery	α-syn	Microglia	α-syn CXCL12	α-syn induces CXCL12 upregulation and its release from microglia through TLR4/IκB-α/NF-κB pathway. Microglia migrate to the SN as a result	
Kempuraj et al. (2019)	Mouse bone marrow-derived mast cells (BMMCs), astrocytes of C57BL/6 fetal mice.	–	*In vitro*	MPTP	Astrocytes, Mast cells, Microglia	Interleukin-33 ERK1/2 MAPKs NF-κB GMF p38	Astrocytes and glia-neurons affected by mast cell proteases and mast cells affected by GMF and MPP+ are activated through ERK1/2 MAPKs and NF-κB pathways and release IL-33 MPTP-induced mast cells secrete CCL2 and express UDP4 which are both significant in the pathogenesis of PD	Abrogation of ERK1/2 MAPKs and NF-κB pathways in mast cells, glia-neurons, and astrocytes
Kempuraj et al. (2016)	Primary mouse bone marrow-derived mast cells (BMMCs), mouse primary astrocyte culture	–	*In vitro*	MPTP	Mast cells	CCL2 UCP4	MPTP-induced mast cells secrete CCL2 and express UDP4 which are both significant in the pathogenesis of PD	
Ikeda-Matsuo et al. (2019)	mPGES-1 knockout mice, Male and female wild-type mice primary mesencephalic culture generated from pregnant mPGES-1 KO and WT mice at E15	Male Age not specified Female Age not specified	*In vivo/In vitro* Administration of the neurotoxin locally and unilaterally	6-OHDA		mPGES-1 PGE2	6-OHDA induces PD in mice and causes expression of mPGES-1 which subsequently results in PGE2 production and neural cell loss in the SN	

(Continued)

TABLE 1 | Continued

References	Type of *in vitro/in vivo* models	Age and sex of animal models	Experimental design	Method used to induce PD	Type of immune cell	Inflammatory factors	Disease mechanism	New therapeutic targets
Cao et al. (2012)	Primary microglial cultures from wild-type mice	–	*In vitro*	α-syn	Microglia	Fcγ receptor α-SYN NF-κB p65	FcγRs play an important role in the α-SYN interaction with microglia.	Inhibition of FcγRs
Yao et al. (2019)	BV2 microglia cells, human DA cell line, SH-SY5Y cells	–	*In vitro*	LPS MPTP	Microglia	p38 p62	The level of p38 and p62 elevates. They cause pro-inflammatory cytokines secretion	MicroRNA-124 have an effect on p38 and p62 negatively and on autophagy positively
Panicker et al. (2019)	HEK-293T cells	–	*In vitro*	AAV-αSyn	Microglia	Fyn kinase αSyn NLRP3-inflammasome CD36	β-Syn uptake in microglia is regulated by Fyn and CD36 α-syn activates NLRP3 inflammasome	Inhibition of the NLRP3 inflammasome and Fyn
Jo et al. (2019)	C57BL/6N wild-type (WT) mice	Male Age not specified	*In vivo*	MPTP		Gintonin, a ginseng-derived glycolipoprotein	Gintonin reduces the level of α-syn aggregation induced by MPTP in the SN and striatum of the mouse model	
Earls et al. (2019)	C57BL/6J mice	8-week-old males and females	*In vivo* Intrastriatal injection	PFF α-syn–injected	Microglia, Astrocytes, B, CD4+ T, CD8+ T, and natural killer cells	PFF α-syn	Intrastriatal injection of PFF α-syn leads to the activation of Microglia, Astrocytes, B, CD4+ T, CD8+ T, and natural killer cells in not only CNS but also peripheral lymphoid organs	
Hong et al. (2018)	C57BL/6 mice	Male Age not specified	*In vivo*	MPTP	Mast cells	TG2	Mast cells release TG2 after activation of NF-κB pathway by MPP+	
Neal et al. (2018)	C57 BL/6J mice	Sex and age not specified	*In vivo* Intraperitoneal injection	MPTP	Astrocyte	GPNMB	GPNMB activates the CD44 receptor leading to an anti-inflammatory phenotype in astrocyte	
Zhu et al. (2018)	Mouse primary astrocytes	–	*In vitro*	MPTP		Drd2 NLRP3 inflammasome	Dopamine D2 receptor limits NLRP3 inflammasome in astrocytes	
Ambrosi et al. (2017)	Sprague–Dawley rats	Male Age not specified	*In vivo* Unilateral infusion to the SN	6-OHDA	CD4+ T regulatory (Treg) cells		CD4+ T regulatory (Treg) cells are decreased in the circulation	

(Continued)

TABLE 1 | Continued

References	Type of *in vitro/in vivo* models	Age and sex of animal models	Experimental design	Method used to induce PD	Type of immune cell	Inflammatory factors	Disease mechanism	New therapeutic targets
Kim B. W. et al. (2016)	C57BL/6 mice	8–12 weeks old Male	*In vivo* Intraperitoneal injections	MPTP	Microglia Astrocytes	LCN2	Expression of LCN2 increases in the nigrostriatal DA system as MPTP-induced PD in mice activates glia and astrocytes	Abrogation of LCN2 in the nigrostriatal DA system
Main et al. (2016)	C57Bl/6 wildtype mice and IFNAR1$^{-/-}$ mice	Sex and age not specified	*In vivo*	MPTP		Type-1 IFNs	Type-1 IFNs contribute to neurodegeneration in PD	
Zhu et al. (2015)	Cell culture from ventral mesencephalic tissues of embryonic Sprague Dawley rats	–	*In vitro*	LPS	Astrocytes	IL-10	LPS treatment results in neural cell loss and activates astrocytes to release IL-10	IL-10
Shin et al. (2015)	Sprague Dawley (SD) rats, C57BL/6 mice	Sex and age not specified	*In vivo* Intranigral injection of pKr-2	Prothrombin kringle-2	Microglia	TLR4	Prothrombin kringle-2 (pkr-2) administration in rat and mouse brains increases TLR4 expression	Inhibition of pkr-2 induced increase of TLR4
Paumier et al. (2015)	Sprague Dawley rats	Three-month-old Male	*In vivo* Intrastriatal injection	α-syn PFF injection		α-syn	α-syn PFF injection leads to α-syn accumulation and neurodegeneration	
Li et al. (2013)	A53T human alpha-synuclein transgenic mice	Sex and age not specified	*In vivo*	A53T α-syn			A53T α-syn causes mitochondrial damage	
Kim et al. (2013)	SH-SY5Y human neuroblastoma, primary cortical neurons, rat and mouse primary microglia, BV2 murine microglial cell lines, and COS-7 cells Sprague-Dawley rats and C57BL/6 mice	Sex and age not specified	*In vitro/In vivo* Stereotaxically injection of AAV-αSyn to the putamen. Transportation of AAV-αsyn retrogradely to the substantia nigra.	α-syn	Microglia	TLR2 α-synuclein	α-syn is a ligand of TLR2 on microglia and causes a release of cytokines from the activated microglia	Drugs that affect TLR2 or extracellular α-syn
Gu et al. (2010)	A53T human alpha-synuclein transgenic mice	Sex and age not specified	*In vivo*	A53T α-syn	Astrocytes	COX-1 IL-1β	A53T α-syn expressed in astrocytes causes microglia activation and release of proinflammatory cytokines	
Fernagut et al. (2007)	Thy1-aSyn mice	10–12 weeks old Sex not specified	*In vivo*	Paraquat		α-syn	α-syn aggregates in the *substantia nigra* and is resistant to proteinase K	

(Continued)

TABLE 1 | Continued

References	Type of *in vitro/in vivo* models	Age and sex of animal models	Experimental design	Method used to induce PD	Type of immune cell	Inflammatory factors	Disease mechanism	New therapeutic targets
Brochard et al. (2009)	C57BL/6J mice	Age not specified Male	*In vivo*	MPTP	CD4 + T cells		CD4 + T cell-dependent Fas/FasL cytotoxic pathway causes DA cell death	
Miklossy et al. (2006)	Rhesus monkeys (*Macaca mulatta*)	Sex and age not specified	*In vivo*	MPTP	Astrocyte	ICAM-1	ICAM-1 is upregulated in astrocytes which shows inflammation is significant in the pathogenesis of PD	Administration of anti-inflammatory agents
Giasson et al. (2002)	wild-type and A53T human alpha-synuclein expressing transgenic mice	Sex and age not specified	*In vivo*	A53T α-syn		α-syn	A53T α-syn causes neurodegeneration	

TLR2, Toll-like receptor 2; GMF, glial maturation factor; CCL2, chemokine (C-C motif) ligand 2; UCP4, Uncoupling protein 4; LCN2, Lipocalin-2; mPGES-1, microsomal prostaglandin E synthase-1; PGE2, prostaglandin E2; HMGB1, High-mobility group box 1; TG2, Transglutaminase 2; PDE7, Phosphodiesterase 7; Drd2, dopamine D2 receptor; ICAM-1, intercellular adhesion molecule-1; COX-1, cyclooxygenase 1; IFN, Interferon.

create PD models which affects nerve terminals as well as cell bodies and induces death of neurons through inhibition of the mitochondrial respiratory enzymes. In PD models 6-OHDA lesions are made in nigrostriatal dopaminergic pathways (Deumens et al., 2002). One of the studies used paraquat to induce PD *in vitro* (Trudler et al., 2021). Paraquat is a pesticide exposure to which is epidemiologically known to be a risk factor for PD (Berry et al., 2010). The rotenone-induced PD is another method, which is the best model to study mitochondrial complex I deficiency in PD (Greenamyre et al., 2003).

α-Synuclein-Induced Neuroinflammation *in vivo* and *in vitro*

α-Synuclein: A Key Regulator of Glial Immune Responses

Synucleins are proteins highly expressed in the brain. There are three members in this protein family: α-, β-, and γ-synuclein. α-Synuclein is a pre-synaptic protein mostly found in nerve terminals (Goedert, 2001). Under physiological conditions, α-Syn interacts with many neuronal proteins to play a variety of functional roles such as inhibiting phospholipase D, regulating microtubules, elevating the rate of tau phosphorylation, etc. It also interacts with soluble NSF attachment protein receptors (SNAREs), which play a role in neurotransmitter release through meditating fusion of vesicles. This indicates that α-Syn is a likely contributor to the release of neurotransmitters (Burré et al., 2010, 2014, 2018). Point mutations in the gene encoding α-Syn (SNCA) are linked to the familial form of PD. A variety of mutations are known to be linked to PD including A53T, A30P, E46K, G51D, and H50Q. We will discuss some of these mutations in transgenic PD models in the following section in more details. Lewy bodies, the hallmark neuronal inclusions observed in neurodegenerative diseases including idiopathic PD, mainly consist of insoluble fibrillar α-syn protein (Goedert, 2001; Marques and Outeiro, 2012; Bendor et al., 2013). In pathological situations, soluble monomeric α-syn generates β-sheet-like oligomers (protofibrils), which form into amyloid fibrils. Amyloid fibrils, then, accumulate in Lewy bodies (Burré et al., 2015). Neurons can also release α-syn, inducing inflammatory responses of microglia (Kim et al., 2013). The fibrillar α-syn, but not its monomeric or oligomeric forms, is the main trigger of neuroinflammation in PD. It interacts with microglial TLR2 as well as another innate immune sensor, the nucleotide oligomerization domain-like receptor family, pyrin domain containing 3 (NLRP3), resulting in activation of the nuclear factor κB (NF-κB) and assembly of NLRP3 inflammasomes. This sequence of events ultimately leads to the release of TNF-α and IL-1β by the microglia, two potent pro-inflammatory cytokines that are known to play a role in the pathogenesis of PD (Gustot et al., 2015; Zhou et al., 2016; Panicker et al., 2019; Trudler et al., 2021). AMS-17 is known to inhibit NLRP3 pathways and activation of microglia. Further investigations using PD model mice indicate that microglial endocytosis of α-syn, impairment of lysosomal functions, and the release of lysosomal protease cathepsin B into the cytoplasm are required for α-syn-induced assembly of

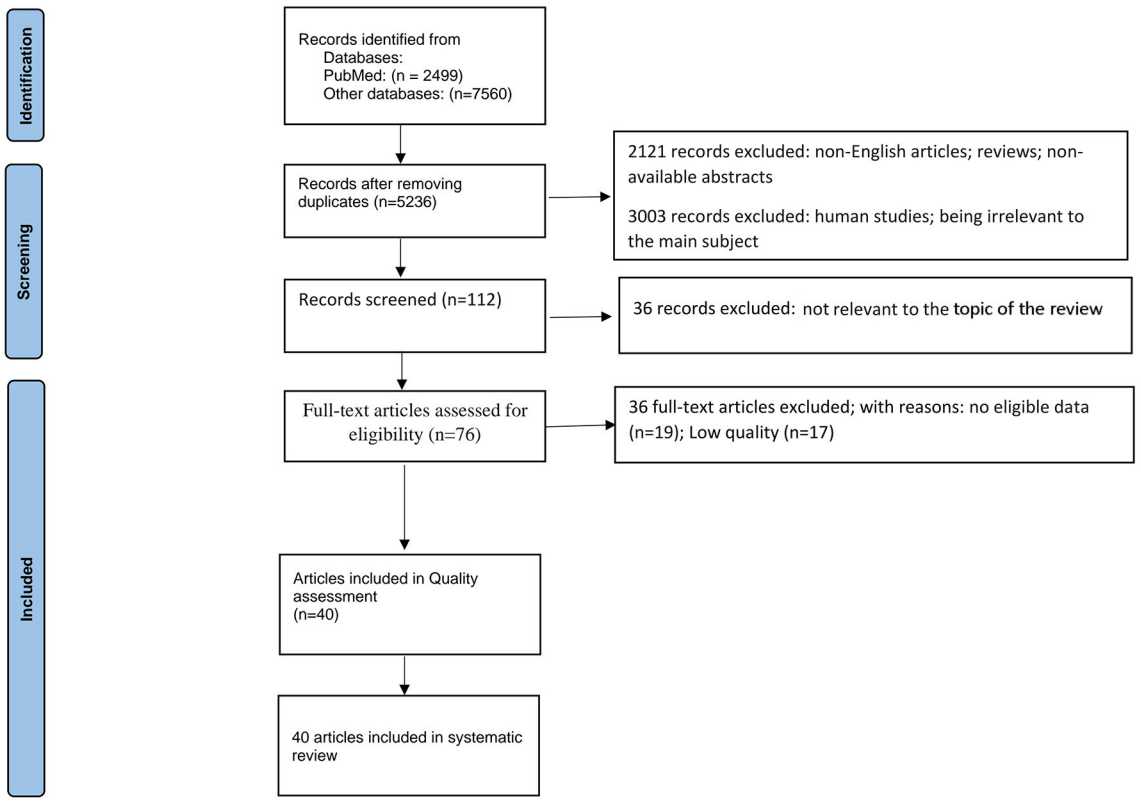

FIGURE 1 | PRISMA 2020 flow diagram for systematic reviews which included searches of databases.

the NLRP3 inflammasomes in microglia. α-Syn also negatively regulates the AMP-activated protein kinase (AMPK)-mediated autophagy, which leads to the intracellular accumulation of reactive oxygen species (ROS), followed by activation of the NLRP3 inflammasome (Zhou et al., 2016). Furthermore, α-syn binds to the microglial CD36 receptor, resulting in the activation of Fyn kinase and subsequently the activation of the NF-kB pathway. Fyn kinase also participates in the activation of NLRP3 since it is decreased in the $fyn^{-/-}$ mice injected with adeno-associated virus overexpressing α-syn (AAV-αSyn) compared to the wild-type animals (Panicker et al., 2019). In addition, Fcγ receptors (FcγR) located on the surface of microglia can mediate α-syn intracellular trafficking leading to pro-inflammatory activation of these cells (Cao et al., 2012). α-Syn can also promote neuroinflammation by interacting with astrocytes since it has been shown to upregulate secretion of interleukin IL-6 and expression of intercellular adhesion molecule-1 (ICAM-1) by human astrocytes. Notably, the PD-causing mutations of α-syn upregulate its potency as a pro-inflammatory stimulant of astrocytes (Klegeris et al., 2006; Jo et al., 2019). In addition to stimulating glial cells, α-syn facilitates aggregation of other inflammatory proteins. For example, co-localization and co-aggregation of α-syn with S100A9 protein have been observed in Lewy bodies and neuronal cells in the SN and frontal lobe areas of PD patients. S100A9 is a member of a family of structurally homologous calcium-binding S100 proteins, which are involved in many inflammatory and neurodegenerative diseases (Srikrishna, 2012; Markowitz and Carson, 2013; Horvath et al., 2018). Aggregated a-syn leads to downregulation of progranulin (GRN) gene in microglia which affects immune functions of these cells (Sarkar et al., 2020a). Another effect of α-syn is related to metabotropic glutamate receptor 5 (mGluR5). This receptor has a neuroprotective role, but its lysosome-dependent degradation occurs faster as a result of synucleinopathy (Zhang et al., 2021). Even though α-syn has been demonstrated to be an initiator in neuroinflammation processes, some studies indicated that inflammation can occur before synucleinopathy (Lai et al., 2021).

α-Syn and Transgenic PD Mouse Models

To further study the pathophysiology of α-syn, various transgenic mouse models of PD have been created including α-syn knockout models and models overexpressing wildtype or mutated human α-syn (Fernagut and Chesselet, 2004). α-Syn KO mice are used to identify the role of α-syn in PD pathogenesis. A study on α-syn KO mice demonstrated that these PD models are resistant to acute administration of MPTP, which highlights the key role of α-syn in increasing the vulnerability of DA neurons to neurodegeneration when exposed to environmental neurotoxins (Dauer et al., 2002). As previously mentioned, two missense

mutations of α-syn gene are linked to PD: A53T and A30P. Homozygous transgenic A30P*A53T α-syn mice manifest many features of PD phenotype and are useful models to study this disease (Kilpeläinen et al., 2019). Mutant α-syn in transgenic A53T mice does not form aggregates but is distributed in different parts of neurons abnormally leading to motor impairment in transgenic mice followed by further paralysis and death (Giasson et al., 2002; Gispert et al., 2003). In transgenic mice which overexpressed A53T α-syn selectively in astrocytes, microglia became reactive and produced proinflammatory cytokines, such as IL-1β, and upregulated cyclooxygenase (COX)-1 leading to neurodegeneration (Gu et al., 2010). Accumulation of A53T α-syn in transgenic mice leads to peripheral inflammation and motor deficits (La Vitola et al., 2021). A53T α-syn has a destructive effect on mitochondrial function in the DA neurons of transgenic mice. It causes damage to mitochondrial transport and respiratory mechanisms (Li et al., 2013). Some other transgenic mouse models are also created to investigate PD such as Thy1-aSyn and α-syn pre-formed fibril (PFF)-injected models. Intrastriatal injection of PFF α-syn leads to the activation of microglia, astrocytes, B, CD4+ T, CD8+ T, and natural killer cells in not only CNS but also peripheral lymphoid organs (Earls et al., 2019). Thy1-aSyn models overexpress human wildtype α-syn by the murine Thy-1 promoter. In this model, many manifestations of sporadic PD are seen including inflammation, biochemical and molecular changes resembling those observed in PD (Chesselet et al., 2012). To study pre-clinical stages of PD, Thy1-aSyn transgenic mice are helpful as in this model high levels of α-syn cause no DA neuronal death up to 8 months (Fleming et al., 2008).

Role of NF-κB Pathway in Neuroinflammation

As described above, the interaction of α-syn with microglia causes activation of NF-kB, which is central to a broad range of neuroinflammatory processes (Tobon-Velasco et al., 2014); therefore, inhibition of this signaling pathway could be a therapeutic target for PD. Panicker et al. treated $Fyn^{-/-}$ mice with LPS to evaluate the role of Fyn in NF-κB activation (Greenamyre et al., 2003). NF-kB signaling in microglia can be activated by the DAMPs released from damaged CNS cells, such as HMGB1, IL-33, ATP, cytochrome C, mitochondrial DNA, and several different heat shock proteins (HSP) (Klegeris, 2021). HMGB1 is a prototypical DAMP present in most nucleated cells, which can be actively secreted or passively released from stimulated and necrotic cells, respectively. a-Syn-induced upregulation of CXCL12 and its release from microglia through TLR4/IκB-α/NF-κB pathway results in microglia migration to the SN (Li Y. et al., 2019). GMF causes NLRP3 inflammasome inhibition and decreases levels of IL-1β and IL-18 (Javed et al., 2020). An *in vitro* study showed that knockdown of HMGB1 alleviated upregulation of NF-κB signaling and inflammatory responses; therefore, anti-HMGB1 monoclonal antibody therapy should be considered as a potential treatment strategy for PD (Nishibori et al., 2019; Huang et al., 2020). The pro-neuroinflammatory effects of DAMPs in the CNS can be counterbalanced by several different resolution-associated molecular patterns, including HSP10, αB-crystallin, prothymosin α, and binding immunoglobulin protein (BiP), also known as HSP70 (Wenzel et al., 2020). Thus, an *in vitro* model of PD was used to demonstrate that HSP70 inhibited the mRNA and protein expressions of NF-κB along with another key pro-inflammatory signaling molecule signal transducer and activator of transcription (STAT)-3 (Li et al., 2019). Notably, select miRNAs, such as miR-124 and miR-7, can also inhibit the progression of neuroinflammation in PD models by modulating NF-κB signaling pathways (Zhou et al., 2016; Yao et al., 2019). One study showed the Lipoic acid (LA) has an anti-inflammatory effect by inhibiting the p53/NF-κB pathway in an LPS-induced model of PD (Mao et al., 2021).

Contribution of Mast Cells to Neuroinflammation in PD Models

The essential role of mast cells in neuroinflammation is supported by several studies. Kempuraj et al. showed that exposure of murine and human mast cells to MPP+ induced release of chemokine c-c motif ligand 2 (CCL2), which in turn has been implicated in the pathogenesis of PD (Kempuraj et al., 2016). MMP+ treatment-induced secretion of IL-33 and a high level of ROS generation by murine mast cells. In addition, mouse mast cell protease (MMCP)-6 and MMCP-7 triggered the release of IL-33 from glia-neuron mixed cultures and primary mouse astrocytes. All these events involved the activation of the NF-kB pathway demonstrating its critical role in neuroinflammation associated with PD (Kempuraj et al., 2019). Furthermore, MPP+ activated NF-κB in mast cells leading to upregulation of transglutaminase 2 (TG2) and subsequent release of the pro-inflammatory TNF-α and IL-1β. This study also demonstrated that TG2-expressing mast cells recruited into SN tissues might contribute to neuroinflammation in PD (Hong et al., 2018).

Role of Adaptive Immunity in PD Models

Nigrostriatal damage correlates with complex alterations in both central and peripheral immunity (Ambrosi et al., 2017). Regarding *in vivo* studies, some immunological features change in MPTP-treated mice as a result of the damage to central dopaminergic cells (Bieganowska et al., 1993). In 6-OHDA-treated rats, a decrease in the percentage of circulating CD4+ T regulatory (Treg) cells was observed (Ambrosi et al., 2017). Upregulation of a-syn provokes adaptive immune system (Theodore et al., 2008). Upregulation of the major histocompatibility complex II (MHCII) protein in CNS myeloid cells and recruitment of CD4+ and CD8+ T cells into the CNS occur due to α-syn accumulation (Williams et al., 2021). One study demonstrated that CD3+/CD4+ T cells are recruited into the perivascular parenchyma of the neocortex, hippocampus, and striatum in α-syn transgenic mice. This study supports the role of adaptive immune cells in neuroinflammation in synucleinopathies (Iba et al., 2020). Degeneration of DA cells occurs through a CD4+ T cell-dependent Fas/FasL cytotoxic pathway (Brochard et al., 2009). CD4+ and CD8+ T cells, in an α-syn rat model of PD, cause an upregulation of MHCII

in microglia and significant loss of DA neurons (Subbarayan et al., 2020). One study on A53T α-syn mice indicated that T cells contribute to the neurodegeneration caused by α-syn, while B cells have no neuroprotective effect against this neurodegeneration (Karikari et al., 2022). Taken together, these studies indicate that the adaptive immune system is associated with neuroinflammation and neurodegeneration in PD.

Other Factors Contributing to Neuroinflammation in PD Models

TLR4 is a cell-surface protein that interacts with bacterial endotoxin and other pathogen-associated molecular patterns (PAMPs) as well as several different DAMPs (Leitner et al., 2019). This receptor is expressed by many different cell types including glial cells. TLR4 activation causes motor impairment in MPTP-treated mice. TLR4 signaling has been suggested to initiate neuroinflammation in PD since microglia express this receptor and α-syn activates it. A decrease in the inflammatory response to α-syn oligomers is observed in murine macrophages derived from bone marrow. In TLR4-deficient mice, the activation of microglia and astrocytes is inhibited by the suppression of NF-κB and the NLRP3 inflammasome signaling pathways (Campolo et al., 2019; Hughes et al., 2019; Shao et al., 2019). An elevated level of microglial TLR4 damages the nigrostriatal DA system. The increase in this receptor occurs after the administration of prothrombin kringle-2 (pKr-2) in rat and mouse brains, which indicates pKr-2 as a new potential TLR4-linked therapeutic target for PD (Shin et al., 2015). Lee et al. report that apoptosis signal-regulating kinase 1 (ASK1) is responsible for the MPTP-induced glial activation and neurotoxicity (Lee et al., 2012). PD model mice were also used to identify glial lipocalin-2 (Lcn-2) as a protein contributing to the disease pathogenesis since its levels were increased in the SN and striatum of the MPTP-treated animals (Kim B. W. et al., 2016).

A microsomal isoform of prostaglandin E synthase-1 (mPGES-1) plays a vital role in the inflammatory processes of peripheral tissues and the CNS by producing the inflammatory PGE2. It contributes to clinical manifestations of inflammation, such as pyrexia and pain, and has been shown to contribute to accelerated neuronal death in PD (Uematsu et al., 2002; Engblom et al., 2003; Kamei et al., 2004). Furthermore, mPGES-1 is upregulated in nigrostriatal DA neurons from postmortem PD brain specimens and the 6-hydroxydopamine (6-OHDA) model of PD. Elevated PGE2 produced by this enzyme is believed to contribute to the DA neuronal death in this model (Ikeda-Matsuo et al., 2019). The type 7 cyclic nucleotide phosphodiesterase 7 (PDE7) is another pro-inflammatory enzyme revealed by several pre-clinical models to contribute to PD pathogenesis. PDE7 inhibitors display anti-inflammatory and neuroprotective activities and can stimulate adult neurogenesis both *in vivo* and *in vitro* (Morales-Garcia et al., 2011, 2015, 2017). Recently, small non-coding RNAs, such as microRNAs (miRNAs), have been identified as biomarkers of neurodegenerative processes and shown to be involved in PD pathogenesis (Kim et al., 2016). Specific miRNAs bind to the three prime untranslated regions (3′-UTRs) of target mRNAs regulating gene expression in the post-transcriptional phase (Bartel, 2004). In the MPTP model of PD, type-I IFNs mediate neuroinflammation in its early stages and worsen PD pathology (Main et al., 2016).

Comparison Between Different Cell Lines Used to Model PD *in vitro*

As seen in **Table 1**, BV2 murine microglial cells (four articles) and and SH-SY5Y human neuroblastoma cell line (four articles) are the two most commonly-used cell lines to induce PD *in vitro* in the articles included in this review. Six *in vitro* studies used rat/mice primary neuron/glia to model PD rather the previously mentioned cell lines. Primary neuronal cultures are useful PD models obtained from the embryonic rodent brain which resemble the morphology and physiology of human neurons (Lopes et al., 2017a). Experimental variations and difficulty in maintenance are some disadvantages of this model (Slanzi et al., 2020). To study the role of microglial cells in PD pathology, the immortalized murine microglial cell line BV-2 has been widely used instead of primary microglial cells. LPS administration in this model leads to pathological pattern of PD similar to that observed in microglial cells *in vitro* and *in vivo* (Henn et al., 2009). SH-SY5Y human neuroblastoma cells is a widely-used PD model which mimics some aspects of DA neuron phenotype, such as the expression of tyrosine hydroxylase, dopamine-β-hydroxylase, and dopamine transporter (Hong-rong et al., 2010). SH-SY5Y neuroblastoma can be differentiated to cells that are similar to cholinergic, dopaminergic, or noradrenergic neurons (Slanzi et al., 2020). However, one disadvantage of this model is that there is no standard differentiation protocol and variation in the source of the cells and their culture maintenance techniques lead to different results. In order to provide a PD model, SH-SY5Y neuroblastoma lineage is manipulated both chemically and genetically. MPP+, 6-OHDA, and rotenone treatment as well as overexpression of mutated α-syn are some examples. SH-SY5Y cells cannot transform MPTP to its metabolite and must be treated by MPP+ itself (Xicoy et al., 2017). Some other cell lines are also mentioned in **Table 1**. For example, PC12 cells are derived from rat pheochromocytoma of the adrenal medulla. These cells produce and secrete catecholamines. However, due to their tumoral origin, they may manifest altered signaling pathways (Slanzi et al., 2020). HEK 293 cell line (or immortalized human embryonic kidney cells) has been used for large-scale experiments but their non-neuronal origin is the main disadvantage of this model (Falkenburger and Schulz, 2006). Animal models of PD are appropriate for studies on motor deficits in PD as the disease progresses. However, since PD is a human-specific neurodegenerative diseases, its pathology, such as damage to DA neurons, needs to be induced. No animal model has been able to recreate all the PD aspects so far. *In vitro* models provide a controlled environment to investigate the disease mechanisms. However, these models do not have the complexity of CNS. In addition, the source of cells used, their morphology, physiology, and maintenance under different culture conditions result in different outcomes (Lopes et al., 2017a).

DISCUSSION

The complex pathological features of PD include the death of dopaminergic neurons in SN as well as α-syn aggregation accompanied by neuroinflammation (Hirsch and Hunot, 2009; Tansey and Goldberg, 2010; Hirsch et al., 2012; Guo et al., 2017; Mohamadkhani, 2018). In the current systematic review, we considered 40 original *in vitro* and *in vivo* studies describing the molecular mechanism, signaling pathways, and other factors that potentially contribute to the PD pathophysiology in animal models. Our review highlights the following main findings: (1) the methods applied to create PD animal models include treatment of the animals with MPTP, LPS, 6-OHDA, paraquat, and rotenone, in addition to transgenic animal models (Giasson et al., 2002; Miklossy et al., 2006; Fernagut et al., 2007; Gu et al., 2010; Li et al., 2013; Paumier et al., 2015; Zhu et al., 2015, 2018; Kempuraj et al., 2016, 2019; Kim B. W. et al., 2016; Main et al., 2016; Hong et al., 2018; Neal et al., 2018; Earls et al., 2019; Ikeda-Matsuo et al., 2019; Jo et al., 2019; Li Y. et al., 2019; Panicker et al., 2019; Yao et al., 2019; Huang et al., 2020; Javed et al., 2020; Morales-Garcia et al., 2020; Sarkar et al., 2020a; Lai et al., 2021; La Vitola et al., 2021; Trudler et al., 2021; Williams et al., 2021; Zhang et al., 2021). (2) α-syn is an important regulator of glial immune responses, which can induce neuroinflammation and, thus, lead to PD development (Cao et al., 2012; Kim et al., 2013; Ikeda-Matsuo et al., 2019; Jo et al., 2019; Panicker et al., 2019); (3) the NF-κB pathway, induced by α-syn, contributes to the neuroinflammatory process during PD progression (Zhou et al., 2016; Li et al., 2019; Nishibori et al., 2019; Yao et al., 2019; Huang et al., 2020; Wenzel et al., 2020; Klegeris, 2021); (4) mast cells are important contributors to the disease pathogenesis in PD mouse models (Kempuraj et al., 2016, 2019; Hong et al., 2018); (5) adaptive immune system plays role in neuroinflammation and neurodegeneration in PD pathogenesis (Bieganowska et al., 1993; Brochard et al., 2009; Ambrosi et al., 2017; Iba et al., 2020). (6) additional factors contributing to PD neuroinflammation involve the pKr-2 protein, which can facilitate neuroinflammation and PD progression in rodent models by upregulating microglial TLR4 (Shin et al., 2015); mPGES-1, which is upregulated in the SN of 6-OHDA-induced PD models and could lead to neurotoxicity (Uematsu et al., 2002; Engblom et al., 2003; Kamei et al., 2004; Morales-Garcia et al., 2011, 2015, 2017; Kim et al., 2016; Ikeda-Matsuo et al., 2019); and type-I IFN, which aggravates PD by inducing neuroinflammation in the early stages of this disease (Main et al., 2016).

MPTP is one of the agents used to create animal Parkinson models (Miklossy et al., 2006; Kim B. W. et al., 2016; Main et al., 2016; Hong et al., 2018; Neal et al., 2018; Zhu et al., 2018; Kempuraj et al., 2019; Yao et al., 2019). For performing its toxicity, MPTP is initially transformed to MPP^+. In DA neurons, ASK1 conveys the MPP^+-induced signals leading to the generation of glial-activating molecules like COX-2. During the MPTP-induced toxicity in mice, ASK1 signaling plays a significant role as a connection between neuroinflammation and oxidative stress (Lee et al., 2012). A review by Guo et al. illustrates that ASK1 signaling is linked to the pathogenesis of several neurodegenerative diseases including PD (Guo et al., 2017). Therefore, ASK1 is important in the neurotoxicity caused by MPTP treatment. Furthermore, it is suggested that ASK1 may be a target for treating or preventing PD and other neurodegenerative diseases (Guo et al., 2017). Treatment of mice with MPTP also increases glial Lcn-2 levels, according to Kim B. W. et al. (2016). This is consistent with previously reported inflammatory functions of this protein potentially playing a role in various age-related CNS diseases. Lcn-2 has been shown to promote cell death and iron dysregulation, in addition to neuroinflammation, leading to cognitive impairments. Therefore, elevated Lcn-2 levels can be considered a risk factor for age-related CNS disorders (Dekens et al., 2021). Additionally, it is indicated that MPP+ causes superoxide radicals to form, which combine with nitric oxide to form peroxynitrite. Many proteins, including tyrosine hydroxylase, are inhibited by this chemical. As a result, dopamine synthesis is disrupted, leading to injury of DA neurons (Liberatore et al., 1999; Przedborski et al., 2000, 2004). McGeer et al. demonstrated that in the SN of rhesus monkeys, the loss of DA cells after MPTP treatment caused microglia activation, which contributes to neuroinflammation (McGeer and McGeer, 2007) (**Figure 2**).

An LPS-induced mouse model of neuroinflammation has been shown to be a useful tool for studying the pathogenic mechanisms behind neurodegeneration and testing possible therapeutic agents (Noh et al., 2014; Zhu et al., 2015; Panicker et al., 2019; Yao et al., 2019; Morales-Garcia et al., 2020; La Vitola et al., 2021; Zhang et al., 2021). The TLR4 and NF-κB signaling pathway is activated by LPS injections, which stimulates microglia. This causes release of IL-6, TNF-α, and insulin-like growth factor 1 (IGF-1), which can be beneficial or harmful to surrounding tissues depending on conditions (Wyss-Coray and Mucke, 2002; Block et al., 2007; Noh et al., 2014). In both the mouse and the rat, LPS injection causes the expression of pro-inflammatory markers such as TNF-α and IL-1b in the entire brain and plasma (Qin et al., 2007; Henry et al., 2009; Nikodemova and Watters, 2011; Oskvig et al., 2012; Molteni et al., 2013). LPS injections produce systemic inflammation and neuroinflammation, which lead to an increase in Aβ levels and neuronal cell death, resulting in cognitive impairment. Thus, systemic inflammation can play a role in the progression of cognitive impairments observed in Alzheimer's disease (AD) and PD (Zhao et al., 2019). According to the study by Morales-Garcia et al. (2020), PDE7 is involved in the progression of neuronal damage in neurodegenerative illnesses, in part due to its role in the regulation of neuroinflammation, suggesting that it could be a key factor in the advancement of PD. In fact, this study detected a strong rise of PDE7 expression, both *in vitro* and *in vivo,* primarily in microglial cells, implying that PDE7 expression is critical for the neuroinflammatory response triggered by these cells, which leads to an increase in DA neuron degeneration (Morales-Garcia et al., 2020).

Another agent used for creating PD animal models is 6-OHDA (Ikeda-Matsuo et al., 2019; Morales-Garcia et al., 2020). 6-OHDA was the first chemical agent shown to have selective neurotoxic effects on catecholaminergic pathways (Ungerstedt, 1968; Sachs and Jonsson, 1975). 6-OHDA

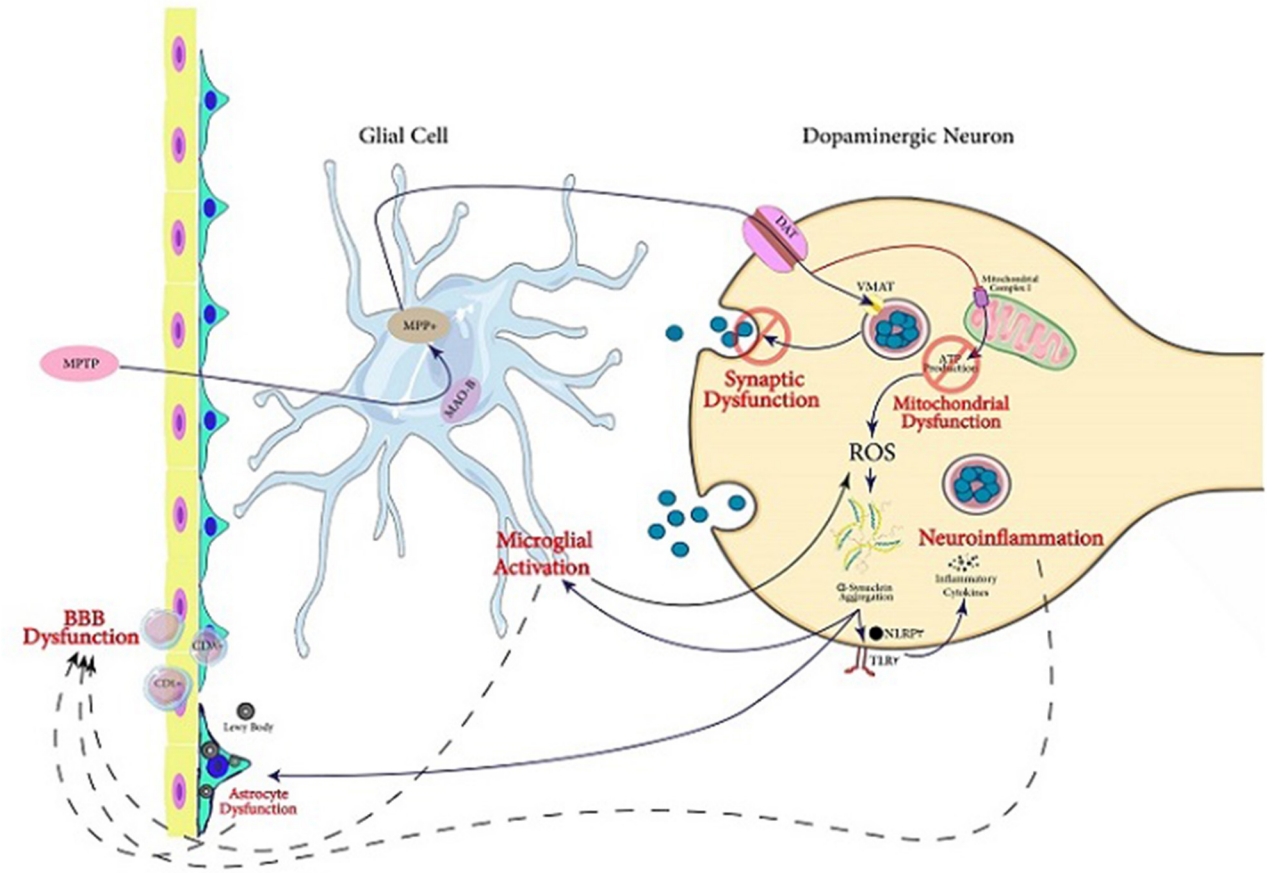

FIGURE 2 | Servier (2022) mechanisms involved in PD pathogenesis. In this figure, the mechanisms following MPTP exposure through which dopaminergic cell death occurs are illustrated. The active metabolite of MPTP, MPP^+, is produced in glial cells and transfers into dopaminergic neurons *via* DA transporter. In the neuron, this activated metabolite causes synaptic dysfunction as well as mitochondrial dysfunction which triggers aggregation of α-Syn. It also can lead to neuroinflammation and microglial activation. Acting together, the mentioned mechanisms can lead to dysfunction of BBB, which is one of the main pathological findings in PD, in addition to Lewy bodies and α-Syn aggregation.

causes catecholaminergic neuron degeneration by using the same catecholamine transport mechanism as dopamine and norepinephrine (**Figure 3**) in the substantia nigra, the nigrostriatal tract, or the striatum to specifically target the nigrostriatal DA system (Perese et al., 1989; Przedbroski et al., 1995). DA neurons start degenerating 24 h after 6-OHDA (Przedbroski et al., 1995; Schwarting and Huston, 1996) injections into the SN or the nigrostriatal tract, and striatal dopamine is reduced 2–3 days later (Faull and Laverty, 1969). There is substantial evidence that oxidative stress plays a role in the neurotoxic effects of 6-OHDA. In the presence of iron, 6-OHDA-induced degeneration has been linked to the production of hydrogen peroxide and hydroxyl radicals (Sachs and Jonsson, 1975). The fact that intranigral iron injection has similar neurotoxic effects to 6-OHDA suggests that iron may play a role in 6-OHDA-induced degeneration. Furthermore, investigations have shown that 6-OHDA causes a decrease in glutathione peroxidase (GSH) and superoxide dismutase (SOD) activity as well as an increase in malondialdehyde levels in the striatum (Perumal et al., 1992; Kumar et al., 1995). 6-OHDA is similarly harmful to mitochondrial complex I, resulting in the generation of superoxide free radicals (Hasegawa et al., 1990; Cleeter et al., 1992).

Paraquat, a well-studied neurotoxic agent, is commonly regarded as one of the environmental elements contributing to PD (Fernagut et al., 2007; Huang et al., 2020). Because of its structural similarities to MPP+, Paraquat has presented as a possible risk factor for PD. Paraquat can pass the blood-brain-barrier, but only to a limited degree. It induces a dose-dependent decrease in DA nigral neurons and striatal DA innervation, and subsequent reduced mobility, when administered systemically to mice (Boireau et al., 1995). Paraquat method of action is thought to entail oxidative stress, and its harmful effects could be mediated through the mitochondria because of its structural resemblance to MPP+ (Betarbet et al., 2002). Paraquat has been shown in several studies to cause neuroinflammation and

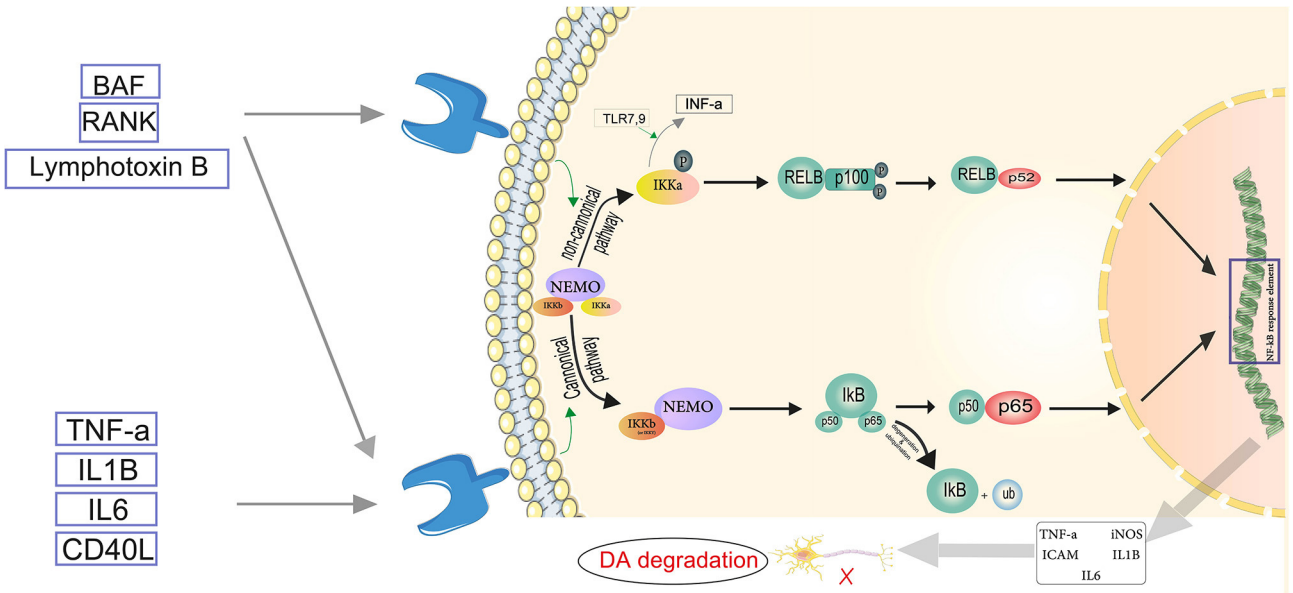

FIGURE 3 | Servier (2022) the neuroinflammatory cascade mediated by NF-κB. TNF-α, IL-1β, IL-6, and CD-40L are proinflammatory substances activating the canonical pathway. In the canonical pathway, an inhibitor of κβ kinase (IKK) β (or IKKγ) is required for NF-κB activation. IKKβ phosphorylates Iκβ. The regulatory subunit of the IKK complex is the NF-κB essential modulator (NEMO). In the cytosol, IκB is degraded by proteasomes, and the phosphorylated heterodimer of NF-κB (p50–p65) is transferred to the nucleus and binds to the NF-κB response element. Thus, pro-inflammatory mediators such as TNF-α, IL-1β, IL-6, iNOS, and ICAM become activated, which play role in the degradation of dopaminergic neurons (DA). In the non-canonical pathway, NEMO phosphorylates IKK-α and induces proteasomal destruction as well as proteasomal processing of p100, a subunit of the NF-B heterodimer, creating the p52-RELB active heterodimer. IKκ induces INF-α production, triggered by TLR7,9. The p52-RELB active heterodimer enters the nucleus and binds to the NF-κB response element, regulating the expression of pro-inflammatory factors. Eventually NF-κB mediated neuroinflammation plays role in Parkinson's disease through DA degradation.

microglial activation. Underlying inflammatory processes greatly increase the sensitivity of DA neurons to toxic damage (Purisai et al., 2007; Mitra et al., 2011). According to a study by Ishola et al. TNF-α levels in the midbrain were considerably elevated by Paraquat, indicating neuroinflammation (Ishola et al., 2018). TNF-α is a cytokine that makes up the acute phase reaction and is a cell signaling protein implicated in inflammatory cascades (Tweedie et al., 2007; Ishola et al., 2013). Xiao et al. reported that Paraquat could activate BV-2 microglia and cause neuroinflammation. This involves inhibition of Akt1 activation, mediated by the increased ROS. Also, Paraquat treatment was followed by a significant increase in the expression of M1 microglia markers including TNF-α, IL-1β, and IL-6. Therefore, Paraquat elevated the M1 phenotype of BV-2 microglia (Xiao et al., 2022). According to Mitra et al. Paraquat induced ROS production and differential α-syn expression, which promoted neuroinflammation. This was characterized by area-specific changes in microglial cell localization and appearance, as well as an increase in TNF-α expression patterns in the substantia nigra, frontal cortex, and hippocampus (Mitra et al., 2011). Paraquat may also act through HGMB1 (Huang et al., 2020). In SH-SY5Y cells, a well-established *in vitro* model for PD research, Paraquat exposure resulted in a significant increase in HMGB1, which was translocated to cytosol and then released into the extracellular milieu of SH-SY5Y cells in a concentration and time-dependent manner. The activation of the RAGE-P38-NF-kB signaling pathway and the generation of inflammatory cytokines such as TNF-α and IL-6 were both reduced when HMGB1 was knocked out. These findings suggest that HMGB1 plays role in Paraquat-induced cell death by increasing neuroinflammatory responses and activating RAGE signaling pathways (Huang et al., 2020).

Another agent used for inducing PD in animal models is rotenone. This agent is an inhibitor of mitochondrial complex I, which is neurotoxic to non-DA and DA neurons (Chen et al., 2006; Choi et al., 2015). This is to some extent because of its inhibitory impact on mitochondria and also causing elevation of oxidative stress. It is indicated in studies using primary cultured glia or microglia that rotenone triggers oxidative stress and neuroinflammation, leading to elevated secretion of pro-inflammatory cytokines (Ye et al., 2016). According to Main et al. type-I IFNs play critical role in mediating the neuroinflammation caused by rotenone in both primary cultured glia and neurons in *vitro*. They also observed a neuroprotective effect by attenuating type-I IFNs signaling. This confirms the important role of these cytokines in neuroinflammation, which leads to death of neurons in chronic neuropathologies (Main et al., 2017) as was shown in another study by Main et al. on MPTP-induced mice (Main et al., 2016).

According to this systematic review, α-syn has a potentially significant role in the pathogenesis of PD. α-Syn performs many functions through its interactions with different proteins (Burré et al., 2018). It can inhibit phospholipase D (PLD). Many experimental studies, clearly show that α-syn and PLD have a functional interaction. PLD2 overexpression in the

rat substantia nigra pars compacta, for example, induced dopaminergic neuron death due to increased lipase activity, while α-syn co-expression decreased PLD2 toxicity (Mendez-Gomez et al., 2018). Furthermore, PLD1 controls autophagic flux and clearance of α-syn aggregates (Bae et al., 2014), whereas overexpression of wild-type α-syn in human neuroblastoma cells reduces PLD1 expression (Conde et al., 2018). An important interaction of α-syn is with SNARE, which facilitates the formation of synaptic vesicles (Burré et al., 2010, 2014, 2018; Huang et al., 2019). SNARE complex assembly requires monomeric α-syn, and deficiencies in this protein can impair vesicle formation. Aggregated α-syn, on the other hand, prevents SNARE-mediated membrane fusion (Hawk et al., 2019). The findings explain a potential mechanism for SNARE-mediated neuronal dopamine release deficiencies leading to neurodegeneration due to a lack of monomeric α-syn and/or increased insoluble α-syn aggregation. However, since SNARE proteins are required for a variety of membrane fusion processes, changes in α-syn could affect vesicle production in a variety of cell types, particularly during fetal development when α-syn is most widely expressed (Baltic et al., 2004). Because vesicle formation is essential for microglia to phagocytose and transfer extracellular cargo to the lysosome for destruction, the deficiency of endogenous α-syn may have an impact on vesicle formation. During the beginning phase of autophagy, SNARE proteins are necessary for the synthesis of precursor vesicles that convert to the phagophore (Wang et al., 2020). This microglial process aids in the elimination of harmful proteins and protects against neuron-derived α-syn aggregation (Choi et al., 2016). Microglia's ability to remove misfolded α-syn could be harmed if vesicle production during autophagy is impaired and consequently contribute to aggregation of α-syn. The SNARE complex is also involved in vesicle exocytosis during microglia cytokine release (Murray et al., 2005). One probable reason for decreased cytokine release is α-syn interaction with SNAP23, a subunit of SNARE complex. Many microglial activities rely on vesicle production to protect against harmful protein buildup and to enhance inflammatory responses in the brain (Gardai et al., 2013).

α-sSyn induces neuroinflammation directly. This process is initiated by α-syn activating microglial TLR2 and NLRP3, which ultimately increases their secretion of IL-1β, TNF-α, and other pro-inflammatory cytokines (Panicker et al., 2019). For example, Bauernfeind et al. (2009) and Qiao et al. (2012) have demonstrated that α-syn is recognized by microglial TLR2, leading to activation of the NF-κB pathway and subsequent production of IL-1β (Bauernfeind et al., 2009; Qiao et al., 2012). Wang et al. (2019) highlight that NLRP3 inflammasome activation not only induces IL-1β secretion by microglia, but also causes a type of inflammatory cell death known as pyroptosis leading to rupture of microglial plasma membrane and further release of IL-1β (Wang et al., 2019). A meta-analysis by Qin et al. showed that peripheral levels of several inflammatory cytokines including TNF-α and IL-1β are higher in PD patients compared to healthy controls (Qin et al., 2016). IL-1β released from microglia has been suggested to participate in inflammatory responses that cause impairment of DA neurons (Block et al., 2007). Injection of IL-1β into the SN of rats induces the death of DA neurons, which is the pathological feature of PD (Ferrari et al., 2006; Block et al., 2007). This, in turn, increases the release of α-syn and creates a vicious circle that amplifies neuroinflammation and accelerates the pathogenesis of PD. Due to its critical role in neuroinflammation, inhibition of NLRP3 pathways is a recently suggested therapeutic strategy for PD (Wang et al., 2019). FcγR on the surface of microglia can mediate α-syn intracellular trafficking, causing microglia to become pro-inflammatory (Cao et al., 2012). According to a study by Javed et al. GMF inhibits the NLRP3 inflammasome and leads to a decrease in the levels of IL-1β and IL-18 (Javed et al., 2020). Miklossy et al. showed that ICAM-1 is upregulated in astrocytes of PD and MPTP-treated monkeys. Also, lymphocyte function-associated antigen 1 (LFA-1) was increased in the reactive microglia. Therefore, inflammation is a potential factor in PD pathogenesis (Miklossy et al., 2006).

The NF-κB pathway is found to be a significant mechanism driving neuroinflammatory reactions (Kempuraj et al., 2019). The two major routes involved in the activation of NF-κB are the canonical or classical pathway and the non-canonical or alternate pathway. The canonical pathway involves dimers of Rel proteins p50 and p65 forming complexes with inhibitory complex IκBα in the cytosol, where they are activated and regulate the production of pro-inflammatory cytokines (Lawrence, 2009). TNF, LPS, IL-1β, and T cell receptor or B cell receptor, as well as other cell, surfaces receptors such as TLRs, TNF receptor, and IL-1 receptor, activate NF-κB throughout the canonical pathway (Baeuerle and Baltimore, 1996). Members of the TNF receptor superfamily, such as B cell-activating factor (BAF), receptor activator of NF-κB (RANK), lymphotoxin B (LT) receptor, and CD40, activate the non-canonical NF-κB pathway in response to diverse stimuli. These receptors also activate the canonical pathway at the same time. Only IKKα homodimers, not IKKβ or IKKγ implicated in the canonical pathway for IκB phosphorylation, are responsible for non-canonical NF-κB pathway activation (Singh et al., 2020) (**Figure 3**). Inhibition or capture of HMBG1 can suppress this pathway and has been considered as a therapeutic approach. A review by Nishibori et al. illustrates that administration of anti-HMGB1 monoclonal antibodies inhibits Dneuronal loss in a 6-OHDA rat model of PD by suppressing ROS production and neuroinflammation (Nishibori et al., 2019). The protective effects of miR-124 and miR-7 against inflammation may make them protective in PD as already suggested by Titze-de-Almeida and Titze-de-Almeida, who describe the potential benefits of miR-7 replacement therapy in this disease (Titze-de-Almeida and Titze-de-Almeida, 2018). Microglia migration to the substantia nigra is triggered by α-syn-induced increase of CXCL12 and its release from microglia *via* the TLR4/IB/NF-κB pathway (Ahmed et al., 2012).α-Syn is also a CD36 agonist (Panicker et al., 2019). It has been shown that CD36 and Fyn kinase facilitate the uptake of α-syn by microglia and initiate the assembly of inflammasomes through a protein kinase Cδ-dependent nuclear translocation of NF-κB-p65. Furthermore, uptake of α-syn is reduced in Fyn-deficient microglia and bone marrow-derived macrophages (BMDM) that lack CD36. Therefore, Fyn plays an important role in promoting neuroinflammation in PD (Panicker et al., 2019). In addition, based on a genome-wide association

study (GWAS), the Fyn locus is linked to the increased risk of PD (Nalls et al., 2019). Sarkar et al. showed that in PD models, Kv1.3 is elevated. The downstream mediator of the NF-κB and p38 MAPK pathways, the Fyn/PKC signaling cascade, proximally controlled the Kv1.3 upregulation. They showed that Kv1.3 overexpression contributes significantly to neuroinflammation-mediated neurodegeneration in PD models. These findings also point to a possible Kv1.3-mediated signaling pathway which can modulate microglial inflammation in PD (Sarkar et al., 2020b). Sarkar et al. in another study discovered new molecular pathways for α-syn aggregation-induced neuroinflammation. α-Syn upregulated the expression of RNA binding proteins in mouse microglia, implying higher RNA processing and splicing as well as mitochondrial oxidative stress. They also found evidence for decreased microglial progranulin as a new disease mechanism in PD, suggesting that lysosomal dysfunction and autophagy are involved in the disease pathogenesis (Sarkar et al., 2020a). Zhang et al. proposed another novel mechanism. They discovered that mGluR5 was critical in preventing α-syn-induced neuroinflammation. This effect was dependent on the interaction between mGluR5 and α-syn, as well as mGluR5 degradation via the lysosomal pathway induced by α-syn. According to this study, the separation of the mGluR5—α-syn complex in microglia is induced by increased mGluR5 expression (Zhang et al., 2021).

A large number of αsyn transgenic mice models have been developed to replicate a spectrum of clinical and behavioral characteristics of PD and other synucleinopathies. The form of α-syn expressed (wild type vs. mutant) and its promoter-specific expression pattern are the key differences between the existing mouse lines (Kahle, 2008; Chesselet and Richter, 2011; Magen and Chesselet, 2011). A number of mouse lines with α-syn deficiency have also been employed to help researchers understand the roles of this protein in the brain cellular processes (Abeliovich et al., 2000; Specht and Schoepfer, 2004; Kokhan et al., 2012). Transgenic α-syn KO mice (Abeliovich et al., 2000) were initially reported to be unimpaired in spatial memory learning, as demonstrated by the Morris Water Maze (MWM) challenge (Chen et al., 2002). A further study indicated that there are actually cognitive abnormalities in this transgenic mouse model but at more advanced ages compared to the initial report (Kokhan et al., 2012). A likely confounding element in understanding the potential role of α-syn in cognitive dysfunction seems to be the compensatory function of gamma synuclein (γ-syn) in synaptic regulation during the absence of α-syn, resulting in the alleviation of cognitive abnormalities in α-syn-KO mice (Senior et al., 2008). Therefore, γ-syn could perform a compensatory function by restoring cognitive functions in α-syn-KO mice (Hatami and Chesselet, 2015).

A53T α-syn causes neurodegeneration (Giasson et al., 2002; Gu et al., 2010). Mice with A53T α-syn have significant motor impairments, which can lead to paralysis and death (Giasson et al., 2002). In a study by Gu et al. (2010), inflammation and microglial activation were promoted by the A53T α-syn, which caused astrogliosis, particularly in the midbrain, brainstem, and spinal cord. This study also discovered a significant DA neurons loss in the midbrain and motor neurons of the spinal cord in symptomatic mice, which could explain the paralysis characteristics of mutant mice. Furthermore, COX-1-mediated inflammatory pathways can play a role in neurodegeneration, as indicated by the COX-1 inhibitor's ability to lengthen the lifespan of A53T mice. The A53T α-syn mice also developed age-dependent α-syn inclusions, which mimic the pathology seen in people with PD. Overexpression of A53T α-syn inhibited complex I function in DA neurons of transgenic mice (Chinta et al., 2010), depolarized mitochondrial membrane potential, increased ROS in human neuroblastoma cells (Parihar et al., 2009), and induced mitochondrial autophagy in neurons bearing the A53T mutation (Chinta et al., 2010; Choubey et al., 2011). Furthermore, α-syn has been demonstrated to alter mitochondrial motility (Xie and Chung, 2012). One theory for the mechanism underlying the effect of A53T α-syn on mitochondria is that it raises Ca2+ signal in neurons, which has been demonstrated to limit mitochondrial mobility (Yi et al., 2004; Wang and Schwarz, 2009). Previous investigations have suggested that A53T α-syn can create Ca2+ permeable holes in the plasma membrane (Furukawa et al., 2006) and can control Ca2+ entry pathway (Hettiarachchi et al., 2009). Li et al. discovered that A53T α-syn decreased both overall mitochondrial mobility and the fraction of mobile mitochondria. In other words, in A53T α-syn neurons, the percentage of stationary mitochondria rose (Li et al., 2013); therefore, it is probable that A53T α-syn controls syntaphilin or myosin (Kang et al., 2008; Pathak et al., 2010) to improve anchoring of stationary mitochondria. Mice expressing A30P α-syn have failed to exhibit alterations in locomotor activity, and dopamine levels in spite of the buildup of α-syn in various brain regions (Kahle et al., 2001; Yavich et al., 2004; Freichel et al., 2007). Kilpeläinen et al. characterized homozygous double mutant A30P*A53T α-syn transgenic mice and reported that these animals did show early onset and age-dependent alterations in striatal dopaminergic function and locomotor activity, as well as formation of α-syn oligomers, suggesting that it could be a useful tool for modeling early onset PD associated with familial SNCA mutations (Kilpeläinen et al., 2019). Thy-1 promoter has been used for producing transgenic α-syn overexpressing mice. The α-syn transgene is widely expressed in these mice, and cytoplasmic and nuclear inclusions containing human α-syn appear in various brain areas, including the cortex, hippocampus, olfactory bulb, and to a lesser extent, the substantia nigra (Cenci and Björklund, 2020).

Our review also highlighted the roles of adaptive immune response in PD models. T lymphocyte infiltration and enhanced MHC II immunoreactivity were seen in MPTP-treated mice, but no B lymphocyte infiltration was reported (Kurkowska-Jastrzebska et al., 1999; Karikari et al., 2022). Furthermore, the injection of regulatory T cells reduced the neurotoxicity of MPTP (Reynolds et al., 2007). In contrast to T lymphocytes' obvious participation in human PD, there is no indication of B lymphocytes' presence in the brains of animal models of PD. It is worth mentioning that mice lacking both B and T lymphocytes were resistant to MPTP toxicity in a recent study employing the MPTP mouse model of PD (Benner et al., 2008). In the past, research on neuroinflammation in AD and PD has primarily focused on aberrant innate immune system activation

(Benner et al., 2008; Rodrigues et al., 2014; Caplan and Maguire-Zeiss, 2018; Labzin et al., 2018). Recent data suggests that changes in the adaptive immune response may also play a role in inflammation and neurodegeneration in Alzheimer's disease and age-related synucleinopathies (Kannarkat et al., 2013; Allen Reish and Standaert, 2015; Baird et al., 2019). α-Syn oligomers and fibrils increased the ratio of CD8+ to CD4+ T cells in the CNS and decreased the expression of STAT3, CD25, and CD127 in CD3+CD4+ T cells. CD4+ T cell infiltration into the CNS has also been linked to changes in the phenotype of brain microglia (Olesen et al., 2018). Thus, CD3+CD4+ T cells' homing and tolerance capabilities are affected by α-syn aggregates (Olesen et al., 2018). In acute neurotoxic models of PD, such as MPTP-injected mice, substantial T cell infiltration was detected in the substantia nigra at the first day following MPTP challenge, and gradually decreased and normalized by day 30 (Chandra et al., 2017). In addition to the potentially neurotoxic impacts of cytokines secreted by Th1 or Th17 cells (Park et al., 2017; Storelli et al., 2019), Th2 and Treg cells are considered to suppress innate immune activation in the CNS, indicating that an imbalance in T cell types may cause overactivation of glia and chronic inflammation (Gendelman and Appel, 2011; Olson and Gendelman, 2016; von Euler Chelpin and Vorup-Jensen, 2017). Previous research has revealed that α-syn aggregates are released into the extracellular space under pathological situations (Desplats et al., 2009; Lee et al., 2014; Emmanouilidou and Vekrellis, 2016; Steiner et al., 2018), in which they can potentially stimulate T cells. In the context of MHC class II, two types of antigen-presenting cells are reported to display epitopes originating from the α-syn Y39 region. IL-5 from CD4+ T cells and IFN from CD8+ T cells are the main triggers of this response (Sulzer et al., 2017). As a result, α-syn peptides can behave as antigenic epitopes, activating T cell responses, which could explain the link between PD and specific MHC alleles (Sulzer et al., 2017). Recent research has found that extracellular α-syn has a variety of impacts on CD4+ and CD8+ T cell populations in the peripheral and central nervous systems, implying that α-syn variations affect CD4+ T cell homing and tolerance capacity (Olesen et al., 2018). Another study used a combination of human α-syn PFF and AAV-human-α-syn injections into the rat substantia nigra and found both microglia activation and CD4+ and CD8+ T cell infiltration (Thakur et al., 2017). Furthermore, extracellular α-syn aggregates have been reported to inhibit CD25 expression, which could explain why recently activated T cells in PD have a lower survival potential (Olesen et al., 2018).

It is reported that Fas-deficient animals have less MPTP-induced DA neuron loss (Hayley et al., 2004). While the Fas/FasL pathway has been linked to the removal of activated macrophages and therefore to the resolution of inflammation in the setting of antigen presentation (Ashany et al., 1995), new evidence reveals that this pathway may alternatively generate proinflammatory cytokines in tissue macrophages (Park et al., 2003). As a result, CD4+ Th FasL-mediated activation of microglial cells may play a role in the inflammatory response and degeneration of DA neurons. FasL produced by T cells may potentially play a role in inflammatory responses in astrocytes, which are known to be highly resistant to Fas-mediated cell death and to produce proinflammatory cytokines and chemokines in response to Fas ligation (Choi and Benveniste, 2004). Fas expression has been found to be elevated on these glial cells in the MPTP model (Ferrer et al., 2000; Hayley et al., 2004). Alternatively, cell-to-cell interaction between infiltrating $CD4^+$ T cells and DA neurons may cause neuronal death (Giuliani et al., 2003).

Our review unveils the critical role of mast cells in the pathogenesis of PD. As stated above, MPP^+ treatment induces mast cell activation and a subsequent increase in levels of CCL2, IL-33, and ROS generation (Kempuraj et al., 2016, 2019). This is in line with a review by Sandhu and Kulka (2021) that reported MPP^+ is an active metabolite of MPTP that causes activation of mouse bone marrow-derived mast cells (BMMC) and increased release of CCL-2 and MMP-3. Thus, IL-33 secretion by mast cells is increased after MPP^+ treatment and plays its role through a heterodimeric receptor complex consisting of suppression of tumorigenicity 2 (ST2) and the accessory IL-1 receptor protein (IL-1RAP). The IL-33/ST2 pathway is involved in CNS homeostasis and its pathologies, including neurodegenerative diseases (Sun et al., 2021). Mast cells are a population of IL-33 targeting cells, recognizing it by IL-33 receptor, ST2 (Lunderius-Andersson et al., 2012). Mast cells activation is observed in PD brains and may play role in neuroinflammation in this disease (Kempuraj et al., 2015, 2019).

TG2 is expressed by mast cells in MPTP-treated mice, which can stimulate inflammatory cytokines and neuroinflammation (Hong et al., 2018). A review by Kim et al. (2013) confirms the roles of TG2 in PD and other neurodegenerative diseases. This gene has been reported to encode an enzyme with four different activities, including protein disulfide isomerase, transamidase, protein kinase, and GTPase. Its transamination function can cause a toxic and insoluble aggregation of amyloid and other proteins. In the Lewy bodies, large numbers of isopeptide bonds produced by TG2 were found. The SH-SY5Y neuroblastoma cell line was treated with MPP+, which greatly elevated TG2 activity (Beck et al., 2006; Verhaar et al., 2011). It is established that α-syn is one of TG2's substrates (Junn et al., 2003). TG2 catalyzes the cross-linking of α-synuclein, resulting in the formation of insoluble, high-molecular-weight aggregates. TG2 was recently discovered to be a substrate of PINK1, a PD-associated Ser/Thr protein kinase. PINK1 phosphorylates TG2 directly, increasing protein stability by preventing proteasomal breakdown (Min et al., 2015). As a result, PINK1 regulates TG2 activity, which may be linked to the production of aggresomes in neural cells (Min et al., 2015). According to recent studies, endoplasmic reticulum (ER) dysfunction is a key component of PD development. As a result, proper TG2 function is intimately linked to ER function. In MPP-treated SH-SY5Y cells, for example, biochemical contact and colocalization between TG2 and ER were detected (Verhaar et al., 2012). In a separate investigation, it was discovered that the localization of TG2 to the granular ER compartment in the PD brain is highly selective for stressed and melanized neurons (Wilhelmus et al., 2011). In this regard, TG2 inhibitors may be a promising therapy for alleviating the brain diseases which TG2 plays role in (Min and Chung, 2018). Additionally, inhibition of pKr-2 is identified as a potential therapeutic strategy in PD

since pKr-2 treatment of rats causes an increase in microglial TLR4, which is essential for their immune activation (Shin et al., 2015). Furthermore, TLR4 agonists can cause necroptosis, which leads to cell death and release of their intracellular contents triggering innate immune responses and neuroinflammation (Yu et al., 2021); therefore, TLR4 antagonists could have therapeutic potential in PD and other neuroinflammatory disorders as already summarized by Leitner et al. (2019). Suppression of PGE2 is another potential treatment strategy in PD, which is supported by observations that the DA toxin 6-OHDA upregulates mPGES-1 and triggers PGE2-dependent death of DA neurons (Ikeda-Matsuo et al., 2019). This therapeutic approach has been reviewed by Singh et al. (2021).

Aging is a physiological challenge that all organisms face throughout time, and it is also the leading risk factor for neurodegenerative illnesses. Therefore. effects of aging on the neuroinflammation within PD mice models should be considered. Zhao et al. showed that in aged mice, compared to young mice, behavioral performance decreased and DA neurons were depleted, which was followed by increased expression of pro-inflammatory factors (TLR2, p-NF-κB-p65, IL-1β, and TNF-α), as well as the pro-oxidative stress factor gp91phox. The inflammatory M1 microglia were increased by aging, and the equilibrium between oxidation and anti-oxidantswas disrupted. In LPS-treated, aged mice, poor behavioral performance and loss of DA neurons were observed, as well as upregulated TLR2, p-NF-κB-p65, IL-1β, TNF-α, iNOS, and gp91phox (Zhao et al., 2018). Also, Yao and Zhao demonstrated that in a MPTP-PD mouse model, aging enhanced M1 microglia activation while inhibiting M2 microglia activation in the substantia nigra, which was associated with an increase in proinflammatory cytokines TNF-α and IL-1β (Yao and Zhao, 2018).

We also reviewed cell models of PD used in the included studies. Rat/mice primary neuron/glia, BV2 murine microglial cells, and SH-SY5Y human neuroblastoma cell line were among the most common cell lines used for creating *in vitro* PD models. PD cell models have some advantages in comparison with animal models. First, PD-related genes can be efficiently overexpressed or knocked out in cultured cells. Second, in dopamine-producing cell lines, both MPP+ and 6-OHDA can be utilized to trigger cell death. Other benefits of these models include their unlimited proliferation which allows high-throughput experimentation with a wide range of experimental techniques and endpoints; homogeneity of cell populations which leads to high reproducibility; and the fact that some cell lines such as SH-SY5Y express important enzymes for dopamine metabolism and synapse formation (Han et al., 2003; Schildknecht et al., 2009; Lopes et al., 2010; Scholz et al., 2011; Thomas et al., 2013). Their main disadvantage is high proliferative capacity, which differs from neurons that do not divide. In comparison to primary neurons and organotypic cultures, immortalized cells are not only unable to replicate the appearance and physiology of a neuronal cell, but they also do not express many of the synaptic proteins. In addition, continuous proliferation induces a selection pressure that favors mutations that improve proliferation and survival, causing succeeding generations of cell lines to lose their DA phenotype in comparison to their parental lines. As a result, after repeated passaging, many cell lines become inappropriate for usage (Lopes et al., 2017a). Despite having important DA traits, SH-SY5Y cells lack neuronal characteristics. This cell line is in the early phases of neuronal development, with low numbers of neuronal markers. Furthermore, their oncogenic characteristics and persistent multiplication are incompatible with neurons (Gilany et al., 2008; Filograna et al., 2015; Lopes et al., 2017a). Both genetic and toxin-based techniques have been used to recreate PD pathology in this cell model, with 6-OHDA being the most widely used toxin. The majority of these investigations are concerned with achieving neuroprotection in cells exposed to 6-OHDA (Wei et al., 2015; Lin and Tsai, 2017). Undifferentiated SH-SY5Y cells have also been used to investigate the mechanisms of 6-OHDA toxicity (Soto-Otero et al., 2000; Izumi et al., 2005; Xicoy et al., 2017). 6-OHDA is taken up by DA neurons *via* DAT transporter and induces considerable oxidative stress. Undifferentiated cells do not mimic the 6-OHDA-induced cell death mechanisms that occur *in vivo* because they only express modest amounts of DAT (Lopes et al., 2017b).

CONCLUSION

In the current systematic review, we have collected data identifying the importance of several neuroinflammatory pathways and molecular mechanisms in the pathogenesis of PD. We conclude that neuroinflammation plays a role in both the initiation and progression of PD. We illustrate that neuroinflammatory reactions in PD models can be induced by various factors including MPTP, α-syn, 6-OHDA, and pKr-2, while other mechanisms, such as TLR2, NLRP3, IL-1β, TNF-α, NF-κB pathway, HMBG1, ROS production, CD36, Fyn, mast cells, ASK1, Lcn-2, TG2, CCL2, IL-33, TLR4, mPGES-1, and PGE2, contribute to the establishment and progression of the pathogenetic mechanisms in these models.

In addition, we identify several potential therapeutic approaches that may be effective in PD by alleviating neuroinflammation. They include miR-124 and miR-7 as well as inhibitors of NLRP3 inflammasomes, HMBG1, and TG2. We also acknowledge limitations to our work, which include very limited research on some of the mechanisms we review and a shortage of other comprehensive systematic reviews and meta-analyses that could be used to further validate our conclusions. Further research is needed to understand other neuroinflammatory mechanisms involved in the pathogenesis of PD and to develop new therapeutic approaches targeting them. By evaluating the relative impact of each factor and determining their collective contribution to neuroinflammation in PD, multitargeted therapeutic approaches could be developed that will hopefully solve the puzzle of PD, which currently lacks effective treatments.

DATA AVAILABILITY STATEMENT

Publicly available datasets were analyzed in this study. This data can be found at: https://pubmed.ncbi.nlm.nih.gov/.

AUTHOR CONTRIBUTIONS

MF, KV, and SY contributed to the conception and design of the study. MRT and FS contributed to the supervision of the manuscript. MD organized the database. AK edited the paper scientifically. All authors wrote the first draft of the manuscript, wrote sections of the manuscript, contributed to manuscript revision, read, and approved the submitted version.

FUNDING

This study was related to the Project (No. 1399/61320) from Student Research Committee, Shahid Beheshti University of Medical Sciences, Tehran, Iran.

ACKNOWLEDGMENTS

We also appreciate the Student Research Committee and Research & Technology Chancellor in Shahid Beheshti University of Medical Sciences as well as the Jack Brown and Family Alzheimer's Disease Research Foundation for their financial support of this study.

SUPPLEMENTARY MATERIAL

The Supplementary Material for this article can be found online at: https://www.frontiersin.org/articles/10.3389/fnagi.2022.855776/full#supplementary-material

REFERENCES

Abeliovich, A., Schmitz, Y., Fariñas, I., Choi-Lundberg, D., Ho, W.-H., Castillo, P. E., et al. (2000). Mice lacking α-synuclein display functional deficits in the nigrostriatal dopamine system. *Neuron* 25, 239–252. doi: 10.1016/S0896-6273(00)80886-7

Ahmed, I., Tamouza, R., Delord, M., Krishnamoorthy, R., Tzourio, C., Mulot, C., et al. (2012). Association between Parkinson's disease and the HLA-DRB1 locus. *Mov. Disord.* 27, 1104–1110. doi: 10.1002/mds.25035

Allen Reish, H. E., and Standaert, D. G. (2015). Role of α-synuclein in inducing innate and adaptive immunity in Parkinson disease. *J. Parkinsons Dis.* 5, 1–19. doi: 10.3233/JPD-140491

Ambrosi, G., Kustrimovic, N., Siani, F., Rasini, E., Cerri, S., Ghezzi, C., et al. (2017). Complex changes in the innate and adaptive immunity accompany progressive degeneration of the nigrostriatal pathway induced by intrastriatal injection of 6-hydroxydopamine in the rat. *Neurotox. Res.* 32, 71–81. doi: 10.1007/s12640-017-9712-2

Ashany, D., Song, X., Lacy, E., Nikolic-Zugic, J., Friedman, S. M., and Elkon, K. B. (1995). Th1 CD4+ lymphocytes delete activated macrophages through the Fas/APO-1 antigen pathway. *Proc. Natl. Acad. Sci. U.S.A.* 92, 11225–11229. doi: 10.1073/pnas.92.24.11225

Bae, E., Lee, H., Jang, Y., Michael, S., Masliah, E., Min, D., et al. (2014). Phospholipase D1 regulates autophagic flux and clearance of α-synuclein aggregates. *Cell Death Differ.* 21, 1132–1141. doi: 10.1038/cdd.2014.30

Baeuerle, P. A., and Baltimore, D. (1996). NF-kappa B: ten years after. *Cell* 87, 13–20. doi: 10.1016/S0092-8674(00)81318-5

Baird, J. K., Bourdette, D., Meshul, C. K., and Quinn, J. F. (2019). The key role of T cells in Parkinson's disease pathogenesis and therapy. *Parkinsonism Relat. Disord.* 60, 25–31. doi: 10.1016/j.parkreldis.2018.10.029

Baltic, S., Perovic, M., Mladenovic, A., Raicevic, N., Ruzdijic, S., Rakic, L., et al. (2004). α-Synuclein is expressed in different tissues during human fetal development. *J. Mol. Neurosci.* 22, 199–203. doi: 10.1385/JMN:22:3:199

Bartel, D. P. (2004). MicroRNAs: genomics, biogenesis, mechanism, and function. *Cell* 116, 281–297. doi: 10.1016/S0092-8674(04)00045-5

Bauernfeind, F. G., Horvath, G., Stutz, A., Alnemri, E. S., MacDonald, K., Speert, D., et al. (2009). Cutting edge: NF-κB activating pattern recognition and cytokine receptors license NLRP3 inflammasome activation by regulating NLRP3 expression. *J. Immunol.* 183, 787–791. doi: 10.4049/jimmunol.0901363

Beck, K. E., De Girolamo, L. A., Griffin, M., and Billett, E. E. (2006). The role of tissue transglutaminase in 1-methyl-4-phenylpyridinium (MPP+)-induced toxicity in differentiated human SH-SY5Y neuroblastoma cells. *Neurosci. Lett.* 405, 46–51. doi: 10.1016/j.neulet.2006.06.061

Bendor, J. T., Logan, T. P., and Edwards, R. H. (2013). The function of α-synuclein. *Neuron* 79, 1044–1066. doi: 10.1016/j.neuron.2013.09.004

Benner, E. J., Banerjee, R., Reynolds, A. D., Sherman, S., Pisarev, V. M., Tsiperson, V., et al. (2008). Nitrated alpha-synuclein immunity accelerates degeneration of nigral dopaminergic neurons. *PLoS ONE* 3, e1376. doi: 10.1371/journal.pone.0001376

Berry, C., La Vecchia, C., and Nicotera, P. (2010). Paraquat and Parkinson's disease. *Cell Death Differ.* 17, 1115–1125. doi: 10.1038/cdd.2009.217

Betarbet, R., Sherer, T. B., and Greenamyre, J. T. (2002). Animal models of Parkinson's disease. *Bioessays* 24, 308–318. doi: 10.1002/bies.10067

Bieganowska, K., Członkowska, A., Bidziński, A., Mierzewska, H., and Korlak, J. (1993). Immunological changes in the MPTP-induced Parkinson's disease mouse model. *J. Neuroimmunol.* 42, 33–37. doi: 10.1016/0165-5728(93)90209-H

Block, M. L., Zecca, L., and Hong, J.-S. (2007). Microglia-mediated neurotoxicity: uncovering the molecular mechanisms. *Nat. Rev. Neurosci.* 8, 57–69. doi: 10.1038/nrn2038

Boireau, A., Bordier, F., Dubédat, P., and Doble, A. (1995). Methamphetamine and dopamine neurotoxicity: differential effects of agents interfering with glutamatergic transmission. *Neurosci. Lett.* 195, 9–12. doi: 10.1016/0304-3940(95)11765-O

Brochard, V., Combadière, B., Prigent, A., Laouar, Y., Perrin, A., Beray-Berthat, V., et al. (2009). Infiltration of CD4+ lymphocytes into the brain contributes to neurodegeneration in a mouse model of Parkinson disease. *J. Clin. Invest.* 119, 182–192. doi: 10.1172/JCI36470

Burré, J., Sharma, M., and Südhof, T. C. (2014). α-Synuclein assembles into higher-order multimers upon membrane binding to promote SNARE complex formation. *Proc. Natl. Acad. Sci. U.S.A.* 111, E4274–E4283. doi: 10.1073/pnas.1416598111

Burré, J., Sharma, M., and Südhof, T. C. (2015). Definition of a molecular pathway mediating α-synuclein neurotoxicity. *J. Neurosci.* 35, 5221–5232. doi: 10.1523/JNEUROSCI.4650-14.2015

Burré, J., Sharma, M., and Südhof, T. C. (2018). Cell Biology and Pathophysiology of α-Synuclein. *Cold Spring Harb. Perspect. Med.* 8, ea024091. doi: 10.1101/cshperspect.a024091

Burré, J., Sharma, M., Tsetsenis, T., Buchman, V., Etherton, M. R., and Südhof, T. C. (2010). Alpha-synuclein promotes SNARE-complex assembly *in vivo* and *in vitro*. *Science* 329, 1663–1667. doi: 10.1126/science.1195227

Campolo, M., Paterniti, I., Siracusa, R., Filippone, A., Esposito, E., and Cuzzocrea, S. (2019). TLR4 absence reduces neuroinflammation and inflammasome activation in Parkinson's diseases *in vivo* model. *Brain Behav. Immun.* 76, 236–247. doi: 10.1016/j.bbi.2018.12.003

Cao, S., Standaert, D. G., and Harms, A. S. (2012). The gamma chain subunit of Fc receptors is required for alpha-synuclein-induced pro-inflammatory signaling in microglia. *J. Neuroinflammation* 9, 259. doi: 10.1186/1742-2094-9-259

Caplan, I. F., and Maguire-Zeiss, K. A. (2018). Toll-like receptor 2 signaling and current approaches for therapeutic modulation in synucleinopathies. *Front. Pharmacol.* 9, 417. doi: 10.3389/fphar.2018.00417

Cenci, M. A., and Björklund, A. (2020). Animal models for preclinical Parkinson's research: an update and critical appraisal. *Prog. Brain Res.* 252, 27–59. doi: 10.1016/bs.pbr.2020.02.003

Chandra, G., Roy, A., Rangasamy, S. B., and Pahan, K. (2017). Induction of adaptive immunity leads to nigrostriatal disease progression in

MPTP mouse model of Parkinson's disease. *J. Immunol.* 198, 4312–4326. doi: 10.4049/jimmunol.1700149

Chen, M. J., Yap, Y. W., Choy, M. S., Koh, C. H. V., Seet, S. J., Duan, W., et al. (2006). Early induction of calpains in rotenone-mediated neuronal apoptosis. *Neurosci. Lett.* 397, 69–73. doi: 10.1016/j.neulet.2005.12.011

Chen, P. E., Specht, C. G., Morris, R. G., and Schoepfer, R. (2002). Spatial learning is unimpaired in mice containing a deletion of the alpha-synuclein locus. *Euro. J. Neurosci.* 16, 154–158. doi: 10.1046/j.1460-9568.2002.02062.x

Chesselet, M.-F., and Richter, F. (2011). Modelling of Parkinson's disease in mice. *Lancet Neurol.* 10, 1108–1118. doi: 10.1016/S1474-4422(11)70227-7

Chesselet, M.-F., Richter, F., Zhu, C., Magen, I., Watson, M. B., and Subramaniam, S. R. (2012). A progressive mouse model of Parkinson's disease: the Thy1-aSyn ("Line 61") mice. *Neurotherapeutics* 9, 297–314. doi: 10.1007/s13311-012-0104-2

Chinta, S. J., Mallajosyula, J. K., Rane, A., and Andersen, J. K. (2010). Mitochondrial α-synuclein accumulation impairs complex I function in dopaminergic neurons and results in increased mitophagy *in vivo*. *Neurosci Lett.* 486, 235–239. doi: 10.1016/j.neulet.2010.09.061

Choi, C., and Benveniste, E. N. (2004). Fas ligand/Fas system in the brain: regulator of immune and apoptotic responses. *Brain Res. Rev.* 44, 65–81. doi: 10.1016/j.brainresrev.2003.08.007

Choi, I., Zhang, Y., Seegobin, S. P., Pruvost, M., Wang, Q., Purtell, K., et al. (2016). Microglia clear neuron-released α-synuclein via selective autophagy and prevent neurodegeneration. *Nat. Commun.* 11, 1386. doi: 10.1038/s41467-020-15119-w

Choi, W.-S., Kim, H.-W., and Xia, Z. (2015). JNK inhibition of VMAT2 contributes to rotenone-induced oxidative stress and dopamine neuron death. *Toxicology* 328, 75–81. doi: 10.1016/j.tox.2014.12.005

Choubey, V., Safiulina, D., Vaarmann, A., Cagalinec, M., Wareski, P., Kuum, M., et al. (2011). Mutant A53T alpha-synuclein induces neuronal death by increasing mitochondrial autophagy. *J. Biol. Chem.* 286, 10814–10824. doi: 10.1074/jbc.M110.132514

Cleeter, M., Cooper, J., and Schapira, A. (1992). Irreversible inhibition of mitochondrial complex I by 1-methyl-4-phenylpyridinium: evidence for free radical involvement. *J. Neurochem.* 58, 786–789. doi: 10.1111/j.1471-4159.1992.tb09789.x

Conde, M. A., Alza, N. P., González, P. A. I., Bilbao, P. G. S., Campos, S. S., Uranga, R. M., et al. (2018). Phospholipase D1 downregulation by α-synuclein: Implications for neurodegeneration in Parkinson's disease. *Biochim. Biophys. Acta* 1863, 639–650. doi: 10.1016/j.bbalip.2018.03.006

Cunningham, C., Dunne, A., and Lopez-Rodriguez, A. B. (2019). Astrocytes: heterogeneous and dynamic phenotypes in neurodegeneration and innate immunity. *Neuroscientist* 25, 455–474. doi: 10.1177/1073858418809941

Członkowska, A., Kohutnicka, M., Kurkowska-Jastrzebska, I., and Członkowski, A. (1996). Microglial reaction in MPTP (1-methyl-4-phenyl-1,2,3,6-tetrahydropyridine) induced Parkinson's disease mice model. *Neurodegeneration.* 5, 137–143. doi: 10.1006/neur.1996.0020

Dauer, W., Kholodilov, N., Vila, M., Trillat, A.-C., Goodchild, R., Larsen, K. E., et al. (2002). Resistance of alpha -synuclein null mice to the parkinsonian neurotoxin MPTP. *Proc. Natl. Acad. Sci. U.S.A.* 99, 14524–14529. doi: 10.1073/pnas.172514599

Dekens, D. W., Eisel, U. L. M., Gouweleeuw, L., Schoemaker, R. G., De Deyn, P. P., and Naud,é P. J. W. (2021). Lipocalin 2 as a link between ageing, risk factor conditions and age-related brain diseases. *Ageing Res. Rev.* 70, 101414. doi: 10.1016/j.arr.2021.101414

Desplats, P., Lee, H. J., Bae, E. J., Patrick, C., Rockenstein, E., Crews, L., et al. (2009). Inclusion formation and neuronal cell death through neuron-to-neuron transmission of alpha-synuclein. *Proc. Natl. Acad. Sci. U.S.A.* 106, 13010–13015. doi: 10.1073/pnas.0903691106

Deumens, R., Blokland, A., and Prickaerts, J. (2002). Modeling parkinson's disease in rats: an evaluation of 6-OHDA lesions of the nigrostriatal pathway. *Exp. Neurol.* 175, 303–317. doi: 10.1006/exnr.2002.7891

Earls, R. H., Menees, K. B., Chung, J., Barber, J., Gutekunst, C. A., Hazim, M. G., et al. (2019). Intrastriatal injection of preformed alpha-synuclein fibrils alters central and peripheral immune cell profiles in non-transgenic mice. *J. Neuroinflammation* 16, 250. doi: 10.1186/s12974-019-1636-8

Emmanouilidou, E., and Vekrellis, K. (2016). Exocytosis and spreading of normal and aberrant α-synuclein. *Brain Pathol.* 26, 398–403. doi: 10.1111/bpa.12373

Engblom, D., Saha, S., Engström, L., Westman, M., Audoly, L. P., Jakobsson, P. J., et al. (2003). Microsomal prostaglandin E synthase-1 is the central switch during immune-induced pyresis. *Nat. Neurosci.* 6, 1137–1138. doi: 10.1038/nn1137

Falkenburger, B., and Schulz, J. (2006). Limitations of cellular models in Parkinson's disease research. *Parkinsons Dis. Relat. Disord.* 261–268. doi: 10.1007/978-3-211-45295-0_40

Faull, R., and Laverty, R. (1969). Changes in dopamine levels in the corpus striatum following lesions in the substantia nigra. *Exp. Neurol.* 23, 332–340. doi: 10.1016/0014-4886(69)90081-8

Fernagut, P.-O., and Chesselet, M.-F. (2004). Alpha-synuclein and transgenic mouse models. *Neurobiol. Dis.* 17, 123–130. doi: 10.1016/j.nbd.2004.07.001

Fernagut, P. O., Hutson, C. B., Fleming, S. M., Tetreaut, N. A., Salcedo, J., Masliah, E., et al. (2007). Behavioral and histopathological consequences of paraquat intoxication in mice: effects of α-synuclein over-expression. *Synapse* 61, 991–1001. doi: 10.1002/syn.20456

Ferrari, C. C., Godoy, M. C. P., Tarelli, R., Chertoff, M., Depino, A. M., and Pitossi, F. J. (2006). Progressive neurodegeneration and motor disabilities induced by chronic expression of IL-1β in the substantia nigra. *Neurobiol. Dis.* 24, 183–193. doi: 10.1016/j.nbd.2006.06.013

Ferrer, I., Blanco, R., Cutillas, B., and Ambrosio, S. (2000). Fas and Fas-L expression in Huntington's disease and Parkinson's disease. *Neuropathol. Appl. Neurobiol.* 26, 424–433. doi: 10.1046/j.1365-2990.2000.00267.x

Filograna, R., Civiero, L., Ferrari, V., Codolo, G., Greggio, E., Bubacco, L., et al. (2015). Analysis of the catecholaminergic phenotype in human SH-SY5Y and BE (2)-M17 neuroblastoma cell lines upon differentiation. *PLoS ONE* 10, e0136769. doi: 10.1371/journal.pone.0136769

Fleming, S. M., Tetreault, N. A., Mulligan, C. K., Hutson, C. B., Masliah, E., and Chesselet, M. F. (2008). Olfactory deficits in mice overexpressing human wildtype alpha-synuclein. *Eur. J. Neurosci.* 28, 247–256. doi: 10.1111/j.1460-9568.2008.06346.x

Freichel, C., Neumann, M., Ballard, T., Müller, V., Woolley, M., Ozmen, L., et al. (2007). Age-dependent cognitive decline and amygdala pathology in α-synuclein transgenic mice. *Neurobiol. Aging* 28, 1421–1435. doi: 10.1016/j.neurobiolaging.2006.06.013

Furukawa, K., Matsuzaki-Kobayashi, M., Hasegawa, T., Kikuchi, A., Sugeno, N., Itoyama, Y., et al. (2006). Plasma membrane ion permeability induced by mutant alpha-synuclein contributes to the degeneration of neural cells. *J. Neurochem.* 97, 1071–1077. doi: 10.1111/j.1471-4159.2006.03803.x

Gardai, S. J., Mao, W., Schüle, B., Babcock, M., Schoebel, S., Lorenzana, C., et al. (2013). Elevated alpha-synuclein impairs innate immune cell function and provides a potential peripheral biomarker for Parkinson's disease. *PLoS ONE.* 8, e71634. doi: 10.1371/journal.pone.0071634

Gendelman, H. E., and Appel, S. H. (2011). Neuroprotective activities of regulatory T cells. *Trends Mol. Med.* 17, 687–688. doi: 10.1016/j.molmed.2011.08.005

Giasson, B. I., Duda, J. E., Quinn, S. M., Zhang, B., Trojanowski, J. Q., and Lee, V. M. (2002). Neuronal alpha-synucleinopathy with severe movement disorder in mice expressing A53T human alpha-synuclein. *Neuron* 34, 521–533. doi: 10.1016/S0896-6273(02)00682-7

Gilany, K., Van Elzen, R., Mous, K., Coen, E., Van Dongen, W., Vandamme, S., et al. (2008). The proteome of the human neuroblastoma cell line SH-SY5Y: an enlarged proteome. *Biochim. Biophys. Acta* 1784, 983–985. doi: 10.1016/j.bbapap.2008.03.003

Gispert, S., Turco, D. D., Garrett, L., Chen, A., Bernard, D. J., Hamm-Clement, J., et al. (2003). Transgenic mice expressing mutant A53T human alpha-synuclein show neuronal dysfunction in the absence of aggregate formation. *Mol. Cell. Neurosci.* 24, 419–429. doi: 10.1016/S1044-7431(03)00198-2

Giuliani, F., Goodyer, C. G., Antel, J. P., and Yong, V. W. (2003). Vulnerability of human neurons to T cell-mediated cytotoxicity. *J. Immunol.* 171, 368–379. doi: 10.4049/jimmunol.171.1.368

Goedert, M. (2001). Alpha-synuclein and neurodegenerative diseases. *Nat. Rev. Neurosci.* 2, 492–501. doi: 10.1038/35081564

Greenamyre, J. T., Betarbet, R., and Sherer, T. B. (2003). The rotenone model of Parkinson's disease: genes, environment and mitochondria. *Parkinsonism Relat. Disord.* 9, 59–64. doi: 10.1016/S1353-8020(03)00023-3

Gu, X. L., Long, C. X., Sun, L., Xie, C., Lin, X., and Cai, H. (2010). Astrocytic expression of Parkinson's disease-related A53T alpha-synuclein causes neurodegeneration in mice. *Mol. Brain* 3, 12. doi: 10.1186/1756-6606-3-12

Guo, X., Namekata, K., Kimura, A., Harada, C., and Harada, T. (2017). ASK1 in neurodegeneration. *Adv. Biol. Regul.* 66, 63–71. doi: 10.1016/j.jbior.2017.08.003

Gustot, A., Gallea, J. I., Sarroukh, R., Celej, M. S., Ruysschaert, J.-M., and Raussens, V. (2015). Amyloid fibrils are the molecular trigger of inflammation in Parkinson's disease. *Biochem. J.* 471, 323–333. doi: 10.1042/BJ20150617

Hamza, T. H., Zabetian, C. P., Tenesa, A., Laederach, A., Montimurro, J., Yearout, D., et al. (2010). Common genetic variation in the HLA region is associated with late-onset sporadic Parkinson's disease. *Nat. Genet.* 42, 781–785. doi: 10.1038/ng.642

Han, B. S., Hong, H.-S., Choi, W.-S., Markelonis, G. J., Oh, T. H., and Oh, Y. J. (2003). Caspase-dependent and-independent cell death pathways in primary cultures of mesencephalic dopaminergic neurons after neurotoxin treatment. *J. Neurosci.* 23, 5069–5078. doi: 10.1523/JNEUROSCI.23-12-05069.2003

Harms, A. S., Ferreira, S. A., and Romero-Ramos, M. (2021). Periphery and brain, innate and adaptive immunity in Parkinson's disease. *Acta Neuropathol.* 141, 527–545. doi: 10.1007/s00401-021-02268-5

Hasegawa, E., Takeshige, K., Oishi, T., Murai, Y., and Minakami, S. (1990). 1-Methyl-4-phenylpyridinium (MPP+) induces NADH-dependent superoxide formation and enhances NADH-dependent lipid peroxidation in bovine heart submitochondrial particles. *Biochem. Biophys. Res. Commun.* 170, 1049–1055. doi: 10.1016/0006-291X(90)90498-C

Hatami, A., and Chesselet, M. F. (2015). Transgenic rodent models to study alpha-synuclein pathogenesis, with a focus on cognitive deficits. *Curr. Top. Behav. Neurosci.* 22, 303–330. doi: 10.1007/7854_2014_355

Hawk, B. J., Khounlo, R., and Shin, Y.-K. (2019). Alpha-synuclein continues to enhance SNARE-dependent vesicle docking at exorbitant concentrations. *Front. Neurosci.* 13, 216. doi: 10.3389/fnins.2019.00216

Hayley, S., Crocker, S. J., Smith, P. D., Shree, T., Jackson-Lewis, V., Przedborski, S., et al. (2004). Regulation of dopaminergic loss by Fas in a 1-methyl-4-phenyl-1,2,3,6-tetrahydropyridine model of Parkinson's disease. *J. Neurosci.* 24, 2045–2053. doi: 10.1523/JNEUROSCI.4564-03.2004

Henn, A., Lund, S., Hedtjärn, M., Schrattenholz, A., Pörzgen, P., and Leist, M. (2009). The suitability of BV2 cells as alternative model system for primary microglia cultures or for animal experiments examining brain inflammation. *ALTEX* 26, 83–94. doi: 10.14573/altex.2009.2.83

Henry, C. J., Huang, Y., Wynne, A. M., and Godbout, J. P. (2009). Peripheral lipopolysaccharide (LPS) challenge promotes microglial hyperactivity in aged mice that is associated with exaggerated induction of both pro-inflammatory IL-1β and anti-inflammatory IL-10 cytokines. *Brain Behav. Immun.* 23, 309–317. doi: 10.1016/j.bbi.2008.09.002

Hettiarachchi, N. T., Parker, A., Dallas, M. L., Pennington, K., Hung, C. C., Pearson, H. A., et al. (2009). alpha-Synuclein modulation of Ca2+ signaling in human neuroblastoma (SH-SY5Y) cells. *J. Neurochem.* 111, 1192–1201. doi: 10.1111/j.1471-4159.2009.06411.x

Hirsch, E. C., and Hunot, S. (2009). Neuroinflammation in Parkinson's disease: a target for neuroprotection? *Lancet Neurol.* 8, 382–397. doi: 10.1016/S1474-4422(09)70062-6

Hirsch, E. C., Vyas, S., and Hunot, S. (2012). Neuroinflammation in Parkinson's disease. *Parkinsonism Relat. Disord.* 18, S210–S212. doi: 10.1016/S1353-8020(11)70065-7

Hong, G. U., Cho, J. W., Kim, S. Y., Shin, J. H., and Ro, J. Y. (2018). Inflammatory mediators resulting from transglutaminase 2 expressed in mast cells contribute to the development of Parkinson's disease in a mouse model. *Toxicol. Appl. Pharmacol.* 358, 10–22. doi: 10.1016/j.taap.2018.09.003

Hong-rong, X. I. E., Lin-sen, H. U., and Guo-yi, L. I. (2010). SH-SY5Y human neuroblastoma cell line: *in vitro* cell model of dopaminergic neurons in Parkinson's disease. *Chin. Med. J.* 123, 1086–1092. doi: 10.3760/cma.j.issn.0366-6999.2010.08.021

Hooijmans, C. R., Rovers, M. M., De Vries, R. B., Leenaars, M., Ritskes-Hoitinga, M., and Langendam, M. W. (2014). SYRCLE's risk of bias tool for animal studies. *BMC Med. Res. Methodol.* 14, 43. doi: 10.1186/1471-2288-14-43

Horvath, I., Iashchishyn, I. A., Moskalenko, R. A., Wang, C., Wärmländer, S., Wallin, C., et al. (2018). Co-aggregation of pro-inflammatory S100A9 with α-synuclein in Parkinson's disease: *ex vivo* and *in vitro* studies. *J. Neuroinflammation* 15, 172. doi: 10.1186/s12974-018-1210-9

Huang, J., Yang, J., Shen, Y., Jiang, H., Han, C., Zhang, G., et al. (2017). HMGB1 mediates autophagy dysfunction via perturbing beclin1-Vps34 complex in dopaminergic cell model. *Front. Mol. Neurosci.* 10, 13. doi: 10.3389/fnmol.2017.00013

Huang, M., Guo, M., Wang, K., Wu, K., Li, Y., Tian, T., et al. (2020). HMGB1 mediates paraquat-induced neuroinflammatory responses via activating RAGE signaling pathway. *Neurotox. Res.* 37, 913–925. doi: 10.1007/s12640-019-00148-1

Huang, M., Wang, B., Li, X., Fu, C., Wang, C., and Kang, X. (2019). α-synuclein: a multifunctional player in exocytosis, endocytosis, vesicle recycling. *Front. Neurosci.* 13, 28. doi: 10.3389/fnins.2019.00028

Hughes, C. D., Choi, M. L., Ryten, M., Hopkins, L., Drews, A., Botía, J. A., et al. (2019). Picomolar concentrations of oligomeric alpha-synuclein sensitizes TLR4 to play an initiating role in Parkinson's disease pathogenesis. *Acta Neuropathol.* 137, 103–120. doi: 10.1007/s00401-018-1907-y

Iba, M., Kim, C., Sallin, M., Kwon, S., Verma, A., Overk, C., et al. (2020). Neuroinflammation is associated with infiltration of T cells in Lewy body disease and α-synuclein transgenic models. *J. Neuroinflammation* 17, 214–214. doi: 10.1186/s12974-020-01888-0

Ikeda-Matsuo, Y., Miyata, H., Mizoguchi, T., Ohama, E., Naito, Y., Uematsu, S., et al. (2019). Microsomal prostaglandin E synthase-1 is a critical factor in dopaminergic neurodegeneration in Parkinson's disease. *Neurobiol. Dis.* 124, 81–92. doi: 10.1016/j.nbd.2018.11.004

Ishola, I., Chaturvedi, J., Rai, S., Rajasekar, N., Adeyemi, O., Shukla, R., et al. (2013). Evaluation of amentoflavone isolated from Cnestis ferruginea Vahl ex DC (*Connaraceae*) on production of inflammatory mediators in LPS stimulated rat astrocytoma cell line (C6) and THP-1 cells. *J. Ethnopharmacol.* 146, 440–448. doi: 10.1016/j.jep.2012.12.015

Ishola, I. O., Akinyede, A., Adeluwa, T., and Micah, C. (2018). Novel action of vinpocetine in the prevention of paraquat-induced parkinsonism in mice: involvement of oxidative stress and neuroinflammation. *Metab. Brain Dis.* 33, 1493–1500. doi: 10.1007/s11011-018-0256-9

Izumi, Y., Sawada, H., Sakka, N., Yamamoto, N., Kume, T., Katsuki, H., et al. (2005). p-Quinone mediates 6-hydroxydopamine-induced dopaminergic neuronal death and ferrous iron accelerates the conversion of p-quinone into melanin extracellularly. *J. Neurosci. Res.* 79, 849–860. doi: 10.1002/jnr.20382

Jarrott, B., and Williams, S. J. (2016). Chronic brain inflammation: the neurochemical basis for drugs to reduce inflammation. *Neurochem. Res.* 41, 523–533. doi: 10.1007/s11064-015-1661-7

Javed, H., Thangavel, R., Selvakumar, G. P., Dubova, I., Schwartz, N., Ahmed, M. E., et al. (2020). NLRP3 inflammasome and glia maturation factor coordinately regulate neuroinflammation and neuronal loss in MPTP mouse model of Parkinson's disease. *Int. Immunopharmacol.* 83, 106441. doi: 10.1016/j.intimp.2020.106441

Jo, M. G., Ikram, M., Jo, M. H., Yoo, L., Chung, K. C., Nah, S. Y., et al. (2019). Gintonin mitigates MPTP-induced loss of nigrostriatal dopaminergic neurons and accumulation of α-synuclein via the Nrf2/HO-1 pathway. *Mol. Neurobiol.* 56, 39–55. doi: 10.1007/s12035-018-1020-1

Junn, E., Ronchetti, R. D., Quezado, M. M., Kim, S. Y., and Mouradian, M. M. (2003). Tissue transglutaminase-induced aggregation of alpha-synuclein: Implications for lewy body formation in Parkinson's disease and dementia with lewy bodies. *Proc. Natl. Acad. Sci. U.S.A.* 100, 2047–2052. doi: 10.1073/pnas.0438021100

Kahle, P. J. (2008). α-Synucleinopathy models and human neuropathology: similarities and differences. *Acta Neuropathol.* 115, 87–95. doi: 10.1007/s00401-007-0302-x

Kahle, P. J., Neumann, M., Ozmen, L., Müller, V., Odoy, S., Okamoto, N., et al. (2001). Selective insolubility of α-synuclein in human lewy body diseases is recapitulated in a transgenic mouse model. *Am. J. Pathol.* 159, 2215–2225. doi: 10.1016/S0002-9440(10)63072-6

Kamei, D., Yamakawa, K., Takegoshi, Y., Mikami-Nakanishi, M., Nakatani, Y., Oh-Ishi, S., et al. (2004). Reduced pain hypersensitivity and inflammation in mice lacking microsomal prostaglandin e synthase-1. *J. Biol. Chem.* 279, 33684–33695. doi: 10.1074/jbc.M400199200

Kang, J. S., Tian, J. H., Pan, P. Y., Zald, P., Li, C., Deng, C., et al. (2008). Docking of axonal mitochondria by syntaphilin controls their mobility and affects short-term facilitation. *Cell* 132, 137–148. doi: 10.1016/j.cell.2007.11.024

Kannarkat, G. T., Boss, J. M., and Tansey, M. G. (2013). The role of innate and adaptive immunity in Parkinson's disease. *J. Parkinsons. Dis.* 3, 493–514. doi: 10.3233/JPD-130250

Karikari, A. A., McFleder, R. L., Ribechini, E., Blum, R., Bruttel, V., Knorr, S., et al. (2022). Neurodegeneration by α-synuclein-specific T cells in AAV-A53T-α-synuclein Parkinson's disease mice. *Brain Behav. Immun.* 101, 194–210. doi: 10.1016/j.bbi.2022.01.007

Kempuraj, D., Khan, M. M., Thangavel, R., Xiong, Z., Yang, E., and Zaheer, A. (2013). Glia maturation factor induces interleukin-33 release from astrocytes: implications for neurodegenerative diseases. *J. Neuroimmune Pharmacol.* 8, 643–650. doi: 10.1007/s11481-013-9439-7

Kempuraj, D., Thangavel, R., Fattal, R., Pattani, S., Yang, E., Zaheer, S., et al. (2016). Mast cells release chemokine CCL2 in response to parkinsonian toxin 1-methyl-4-phenyl-pyridinium (MPP(+)). *Neurochem. Res.* 41, 1042–1049. doi: 10.1007/s11064-015-1790-z

Kempuraj, D., Thangavel, R., Selvakumar, G. P., Ahmed, M. E., Zaheer, S., Raikwar, S. P., et al. (2019). Mast Cell proteases activate astrocytes and glia-neurons and release interleukin-33 by activating p38 and ERK1/2 MAPKs and NF-κB. *Mol. Neurobiol.* 56, 1681–1693. doi: 10.1007/s12035-018-1177-7

Kempuraj, D., Thangavel, R., Yang, E., Pattani, S., Zaheer, S., Santillan, D. A., et al. (2015). Dopaminergic toxin 1-methyl-4-phenylpyridinium, proteins α-synuclein and glia maturation factor activate mast cells and release inflammatory mediators. *PLoS ONE* 10, e0135776. doi: 10.1371/journal.pone.0135776

Kilpeläinen, T., Julku, U. H., Svarcbahs, R., and Myöhänen, T. T. (2019). Behavioural and dopaminergic changes in double mutated human A30P*A53T alpha-synuclein transgenic mouse model of Parkinson's disease. *Sci. Rep.* 9, 17382. doi: 10.1038/s41598-019-54034-z

Kim, B. W., Jeong, K. H., Kim, J. H., Jin, M., Kim, J. H., Lee, M. G., et al. (2016). Pathogenic upregulation of glial lipocalin-2 in the parkinsonian dopaminergic system. *J. Neurosci.* 36, 5608–5622. doi: 10.1523/JNEUROSCI.4261-15.2016

Kim, C., Ho, D. H., Suk, J. E., You, S., Michael, S., Kang, J., et al. (2013). Neuron-released oligomeric α-synuclein is an endogenous agonist of TLR2 for paracrine activation of microglia. *Nat. Commun.* 4, 1562. doi: 10.1038/ncomms2534

Kim, J., Fiesel, F. C., Belmonte, K. C., Hudec, R., Wang, W.-X., Kim, C., et al. (2016). miR-27a and miR-27b regulate autophagic clearance of damaged mitochondria by targeting PTEN-induced putative kinase 1 (PINK1). *Mol. Neurodegener.* 11, 55. doi: 10.1186/s13024-016-0121-4

Klegeris, A. (2021). Regulation of neuroimmune processes by damage- and resolution-associated molecular patterns. *Neural Regen. Res.* 16, 423–429. doi: 10.4103/1673-5374.293134

Klegeris, A., Giasson, B. I., Zhang, H., Maguire, J., Pelech, S., and McGeer, P. L. (2006). Alpha-synuclein and its disease-causing mutants induce ICAM-1 and IL-6 in human astrocytes and astrocytoma cells. *FASEB J.* 20, 2000–2008. doi: 10.1096/fj.06-6183com

Kokhan, V., Afanasyeva, M., and Van'Kin, G. (2012). α-Synuclein knockout mice have cognitive impairments. *Behav. Brain Res.* 231, 226–230. doi: 10.1016/j.bbr.2012.03.026

Kumar, R., Agarwal, A. K., and Seth, P. K. (1995). Free radical-generated neurotoxicity of 6-hydroxydopamine. *J. Neurochem.* 64, 1703–1707. doi: 10.1046/j.1471-4159.1995.64041703.x

Kurkowska-Jastrzebska, I., Wrońska, A., Kohutnicka, M., Członkowski, A., and Członkowska, A. (1999). MHC class II positive microglia and lymphocytic infiltration are present in the substantia nigra and striatum in mouse model of Parkinson's disease. *Acta Neurobiol. Exp.* 59, 1–8.

La Vitola, P., Balducci, C., Baroni, M., Artioli, L., Santamaria, G., Castiglioni, M., et al. (2021). Peripheral inflammation exacerbates α-synuclein toxicity and neuropathology in Parkinson's models. *Neuropathol. Appl. Neurobiol.* 47, 43–60. doi: 10.1111/nan.12644

Labzin, L. I., Heneka, M. T., and Latz, E. (2018). Innate immunity and neurodegeneration. *Annu. Rev. Med.* 69, 437–449. doi: 10.1146/annurev-med-050715-104343

Lai, T. T., Kim, Y. J., Nguyen, P. T., Koh, Y. H., Nguyen, T. T., Ma, H. I., et al. (2021). Temporal evolution of inflammation and neurodegeneration with alpha-synuclein propagation in Parkinson's disease mouse model. *Front. Integr. Neurosci.* 15, 715190. doi: 10.3389/fnint.2021.715190

Lawrence, T. (2009). The nuclear factor NF-kappaB pathway in inflammation. *Cold Spring Harb. Perspect. Biol.* 1, a001651. doi: 10.1101/cshperspect.a001651

Lee, H. J., Bae, E. J., and Lee, S. J. (2014). Extracellular α-synuclein-a novel and crucial factor in Lewy body diseases. *Nat. Rev. Neurol.* 10, 92–98. doi: 10.1038/nrneurol.2013.275

Lee, K. W., Zhao, X., Im, J. Y., Grosso, H., Jang, W. H., Chan, T. W., et al. (2012). Apoptosis signal-regulating kinase 1 mediates MPTP toxicity and regulates glial activation. *PLoS ONE* 7, e29935. doi: 10.1371/journal.pone.0029935

Leitner, G. R., Wenzel, T. J., Marshall, N., Gates, E. J., and Klegeris, A. (2019). Targeting toll-like receptor 4 to modulate neuroinflammation in central nervous system disorders. *Expert Opin. Ther. Targets* 23, 865–882. doi: 10.1080/14728222.2019.1676416

Li, H., Yang, J., Wang, Y., Liu, Q., Cheng, J., and Wang, F. (2019). Neuroprotective effects of increasing levels of HSP70 against neuroinflammation in Parkinson's disease model by inhibition of NF-κB and STAT3. *Life Sci.* 234, 116747. doi: 10.1016/j.lfs.2019.116747

Li, L., Nadanaciva, S., Berger, Z., Shen, W., Paumier, K., Schwartz, J., et al. (2013). Human A53T α-synuclein causes reversible deficits in mitochondrial function and dynamics in primary mouse cortical neurons. *PLoS ONE* 8, e85815. doi: 10.1371/journal.pone.0085815

Li, Y., Niu, M., Zhao, A., Kang, W., Chen, Z., Luo, N., et al. (2019). CXCL12 is involved in α-synuclein-triggered neuroinflammation of Parkinson's disease. *J. Neuroinflammation* 16, 263. doi: 10.1186/s12974-019-1646-6

Liberatore, G. T., Jackson-Lewis, V., Vukosavic, S., Mandir, A. S., Vila, M., McAuliffe, W. G., et al. (1999). Inducible nitric oxide synthase stimulates dopaminergic neurodegeneration in the MPTP model of Parkinson disease. *Nat. Med.* 5, 1403–1409. doi: 10.1038/70978

Lim, R., Zaheer, A., Khosravi, H., Freeman, J. H. Jr, Halverson, H. E., Wemmie, J. A., and Yang, B. (2004). Impaired motor performance and learning in glia maturation factor-knockout mice. *Brain Res.* 1024, 225–232. doi: 10.1016/j.brainres.2004.08.003

Lin, C.-Y., and Tsai, C.-W. (2017). Carnosic acid attenuates 6-hydroxydopamine-induced neurotoxicity in SH-SY5Y cells by inducing autophagy through an enhanced interaction of parkin and Beclin1. *Mol. Neurobiol.* 54, 2813–2822. doi: 10.1007/s12035-016-9873-7

Lopes, F. M., Bristot, I. J., da Motta, L. L., Parsons, R. B., and Klamt, F. (2017a). Mimicking Parkinson's disease in a dish: merits and pitfalls of the most commonly used dopaminergic *in vitro* models. *Neuromol. Med.* 19, 241–255. doi: 10.1007/s12017-017-8454-x

Lopes, F. M., da Motta, L. L., De Bastiani, M. A., Pfaffenseller, B., Aguiar, B. W., de Souza, L. F., et al. (2017b). RA differentiation enhances dopaminergic features, changes redox parameters, and increases dopamine transporter dependency in 6-hydroxydopamine-induced neurotoxicity in SH-SY5Y cells. *Neurotox. Res.* 31, 545–559. doi: 10.1007/s12640-016-9699-0

Lopes, F. M., Schröder, R., da Frota Júnior, M. L. C., Zanotto-Filho, A., Müller, C. B., Pires, A. S., et al. (2010). Comparison between proliferative and neuron-like SH-SY5Y cells as an *in vitro* model for Parkinson disease studies. *Brain Res.* 1337, 85–94. doi: 10.1016/j.brainres.2010.03.102

Lunderius-Andersson, C., Enoksson, M., and Nilsson, G. (2012). Mast cells respond to cell injury through the recognition of IL-33. *Front. Immunol.* 3, 82. doi: 10.3389/fimmu.2012.00082

Lyman, M., Lloyd, D. G., Ji, X., Vizcaychipi, M. P., and Ma, D. (2014). Neuroinflammation: the role and consequences. *Neurosci Res.* 79, 1–12. doi: 10.1016/j.neures.2013.10.004

Magen, I., and Chesselet, M.-F. (2011). Mouse models of cognitive deficits due to alpha-synuclein pathology. *J. Parkinsons Dis.* 1, 217–227. doi: 10.3233/JPD-2011-11043

Main, B. S., Zhang, M., Brody, K. M., Ayton, S., Frugier, T., Steer, D., et al. (2016). Type-1 interferons contribute to the neuroinflammatory response and disease progression of the MPTP mouse model of Parkinson's disease. *Glia.* 64, 1590–1604. doi: 10.1002/glia.23028

Main, B. S., Zhang, M., Brody, K. M., Kirby, F. J., Crack, P. J., and Taylor, J. M. (2017). Type-I interferons mediate the neuroinflammatory response and neurotoxicity induced by rotenone. *J. Neurochem.* 141, 75–85. doi: 10.1111/jnc.13940

Mao, J., Gao, H., Bai, W., Zeng, H., Ren, Y., Liu, Y., et al. (2021). Lipoic acid alleviates LPS-evoked PC12 cell damage by targeting p53 and inactivating the NF-κB pathway. *Acta Neurobiol. Exp.* 81, 375–385. doi: 10.21307/ane-2021-037

Markowitz, J., and Carson, W. E. (2013). Review of S100A9 biology and its role in cancer. *Biochim. Biophys. Acta.* 1835, 100–109. doi: 10.1016/j.bbcan.2012.10.003

Marques, O., and Outeiro, T. F. (2012). Alpha-synuclein: from secretion to dysfunction and death. *Cell Death Dis.* 3, e350–e350. doi: 10.1038/cddis.2012.94

McGeer, E. G., and McGeer, P. L. (2007). The role of anti-inflammatory agents in Parkinson's disease. *CNS Drugs* 21, 789–797. doi: 10.2165/00023210-200721100-00001

Mendez-Gomez, H. R., Singh, J., Meyers, C., Chen, W., Gorbatyuk, O. S., and Muzyczka, N. (2018). The lipase activity of phospholipase D2 is responsible for nigral neurodegeneration in a rat model of Parkinson's disease. *Neuroscience* 377, 174–183. doi: 10.1016/j.neuroscience.2018.02.047

Miklossy, J., Doudet, D. D., Schwab, C., Yu, S., McGeer, E. G., and McGeer, P. L. (2006). Role of ICAM-1 in persisting inflammation in Parkinson disease and MPTP monkeys. *Exp. Neurol.* 197, 275–283. doi: 10.1016/j.expneurol.2005.10.034

Min, B., and Chung, K. C. (2018). New insight into transglutaminase 2 and link to neurodegenerative diseases. *BMB Rep.* 51, 5–13. doi: 10.5483/BMBRep.2018.51.1.227

Min, B., Kwon, Y. C., Choe, K. M., and Chung, K. C. (2015). PINK1 phosphorylates transglutaminase 2 and blocks its proteasomal degradation. *J. Neurosci. Res.* 93, 722–735. doi: 10.1002/jnr.23535

Mitra, S., Chakrabarti, N., and Bhattacharyya, A. (2011). Differential regional expression patterns of α-synuclein, TNF-α, and IL-1β; and variable status of dopaminergic neurotoxicity in mouse brain after paraquat treatment. *J. Neuroinflammation* 8, 1–22. doi: 10.1186/1742-2094-8-163

Mohamadkhani, A. (2018). Gut microbiota and fecal metabolome perturbation in children with autism spectrum disorder. *Middle East J Dig Dis.* 10, 205–212. doi: 10.15171/mejdd.2018.112

Mohamadkhani, A., Sotoudeh, M., Bowden, S., Poustchi, H., Jazii, F. R., Sayehmiri, K., et al. (2009). Downregulation of HLA class II molecules by G1896A pre-core mutation in chronic hepatitis B virus infection. *Viral Immunol.* 22, 295–300. doi: 10.1089/vim.2009.0031

Molteni, M., and Rossetti, C. (2017). Neurodegenerative diseases: the immunological perspective. *J. Neuroimmunol.* 313, 109–115. doi: 10.1016/j.jneuroim.2017.11.002

Molteni, R., Macchi, F., Zecchillo, C., Dell'Agli, M., Colombo, E., Calabrese, F., et al. (2013). Modulation of the inflammatory response in rats chronically treated with the antidepressant agomelatine. *Euro. Neuropsychopharmacol.* 23, 1645–1655. doi: 10.1016/j.euroneuro.2013.03.008

Morales-Garcia, J. A., Alonso-Gil, S., Gil, C., Martinez, A., Santos, A., and Perez-Castillo, A. (2015). Phosphodiesterase 7 inhibition induces dopaminergic neurogenesis in hemiparkinsonian rats. *Stem Cells Transl. Med.* 4, 564–575. doi: 10.5966/sctm.2014-0277

Morales-Garcia, J. A., Alonso-Gil, S., Santos, Á., and Perez-Castillo, A. (2020). Phosphodiesterase 7 regulation in cellular and rodent models of Parkinson's disease. *Mol. Neurobiol.* 57, 806–822. doi: 10.1007/s12035-019-01745-z

Morales-Garcia, J. A., Echeverry-Alzate, V., Alonso-Gil, S., Sanz-SanCristobal, M., Lopez-Moreno, J. A., Gil, C., et al. (2017). Phosphodiesterase7 inhibition activates adult neurogenesis in hippocampus and subventricular zone *in vitro* and *in vivo*. *Stem Cells* 35, 458–472. doi: 10.1002/stem.2480

Morales-Garcia, J. A., Redondo, M., Alonso-Gil, S., Gil, C., Perez, C., Martinez, A., et al. (2011). Phosphodiesterase 7 inhibition preserves dopaminergic neurons in cellular and rodent models of Parkinson disease. *PLoS ONE* 6, e17240. doi: 10.1371/journal.pone.0017240

Mukai, K., Tsai, M., Saito, H., and Galli, S. J. (2018). Mast cells as sources of cytokines, chemokines growth factors. *Immunol. Rev.* 282, 121–150. doi: 10.1111/imr.12634

Murray, R. Z., Kay, J. G., Sangermani, D. G., and Stow, J. L. (2005). A role for the phagosome in cytokine secretion. *Science* 310, 1492–1495. doi: 10.1126/science.1120225

Nalls, M. A., Blauwendraat, C., Vallerga, C. L., Heilbron, K., Bandres-Ciga, S., Chang, D., et al. (2019). Identification of novel risk loci, causal insights, and heritable risk for Parkinson's disease: a meta-analysis of genome-wide association studies. *Lancet Neurol.* 18, 1091–1102. doi: 10.1016/S1474-4422(19)30320-5

Neal, M. L., Boyle, A. M., Budge, K. M., Safadi, F. F., and Richardson, J. R. (2018). The glycoprotein GPNMB attenuates astrocyte inflammatory responses through the CD44 receptor. *J. Neuroinflammation* 15, 73. doi: 10.1186/s12974-018-1100-1

Nikodemova, M., and Watters, J. J. (2011). Outbred ICR/CD1 mice display more severe neuroinflammation mediated by microglial TLR4/CD14 activation than inbred C57Bl/6 mice. *Neuroscience* 190, 67–74. doi: 10.1016/j.neuroscience.2011.06.006

Nishibori, M., Mori, S., and Takahashi, H. K. (2019). Anti-HMGB1 monoclonal antibody therapy for a wide range of CNS and PNS diseases. *J. Pharmacol. Sci.* 140, 94–101. doi: 10.1016/j.jphs.2019.04.006

Noh, H., Jeon, J., and Seo, H. (2014). Systemic injection of LPS induces region-specific neuroinflammation and mitochondrial dysfunction in normal mouse brain. *Neurochem. Int.* 69, 35–40. doi: 10.1016/j.neuint.2014.02.008

Olesen, M. N., Christiansen, J. R., Petersen, S. V., Jensen, P. H., Paslawski, W., Romero-Ramos, M., et al. (2018). CD4 T cells react to local increase of α-synuclein in a pathology-associated variant-dependent manner and modify brain microglia in absence of brain pathology. *Heliyon* 4, e00513. doi: 10.1016/j.heliyon.2018.e00513

Olson, K. E., and Gendelman, H. E. (2016). Immunomodulation as a neuroprotective and therapeutic strategy for Parkinson's disease. *Curr. Opin. Pharmacol.* 26, 87–95. doi: 10.1016/j.coph.2015.10.006

Oskvig, D. B., Elkahloun, A. G., Johnson, K. R., Phillips, T. M., and Herkenham, M. (2012). Maternal immune activation by LPS selectively alters specific gene expression profiles of interneuron migration and oxidative stress in the fetus without triggering a fetal immune response. *Brain Behav. Immun.* 26, 623–634. doi: 10.1016/j.bbi.2012.01.015

Panicker, N., Sarkar, S., Harischandra, D. S., Neal, M., Kam, T. I., Jin, H., et al. (2019). Fyn kinase regulates misfolded α-synuclein uptake and NLRP3 inflammasome activation in microglia. *J. Exp. Med.* 216, 1411–1430. doi: 10.1084/jem.20182191

Parihar, M. S., Parihar, A., Fujita, M., Hashimoto, M., and Ghafourifar, P. (2009). Alpha-synuclein overexpression and aggregation exacerbates impairment of mitochondrial functions by augmenting oxidative stress in human neuroblastoma cells. *Int. J. Biochem. Cell Biol.* 41, 2015–2024. doi: 10.1016/j.biocel.2009.05.008

Park, D. R., Thomsen, A. R., Frevert, C. W., Pham, U., Skerrett, S. J., Kiener, P. A., et al. (2003). Fas (CD95) induces proinflammatory cytokine responses by human monocytes and monocyte-derived macrophages. *J. Immunol.* 170, 6209–6216. doi: 10.4049/jimmunol.170.12.6209

Park, J., Lee, J. W., Cooper, S. C., Broxmeyer, H. E., Cannon, J. R., and Kim, C. H. (2017). Parkinson disease-associated LRRK2 G2019S transgene disrupts marrow myelopoiesis and peripheral Th17 response. *J. Leukoc. Biol.* 102, 1093–1102. doi: 10.1189/jlb.1A0417-147RR

Pathak, D., Sepp, K. J., and Hollenbeck, P. J. (2010). Evidence that myosin activity opposes microtubule-based axonal transport of mitochondria. *J. Neurosci.* 30, 8984–8992. doi: 10.1523/JNEUROSCI.1621-10.2010

Paumier, K. L., Luk, K. C., Manfredsson, F. P., Kanaan, N. M., Lipton, J. W., Collier, T. J., et al. (2015). Intrastriatal injection of pre-formed mouse α-synuclein fibrils into rats triggers α-synuclein pathology and bilateral nigrostriatal degeneration. *Neurobiol. Dis.* 82, 185–199. doi: 10.1016/j.nbd.2015.06.003

Perese, D., Ulman, J., Viola, J., Ewing, S., and Bankiewicz, K. (1989). A 6-hydroxydopamine-induced selective parkinsonian rat model. *Brain Res.* 494, 285–293. doi: 10.1016/0006-8993(89)90597-0

Perumal, A., Gopal, V., Tordzro, W., Cooper, T., and Cadet, J. (1992). Vitamin E attenuates the toxic effects of 6-hydroxydopamine on free radical scavenging systems in rat brain. *Brain Res. Bull.* 29, 699–701. doi: 10.1016/0361-9230(92)90142-K

Pourasgari, M., and Mohamadkhani, A. (2020). Heritability for stroke: essential for taking family history. *Caspian J. Intern. Med.* 11, 237–243. doi: 10.22088/cjim.11.3.237

Przedborski, S., Jackson-Lewis, V., Djaldetti, R., Liberatore, G., Vila, M., Vukosavic, S., et al. (2000). The parkinsonian toxin MPTP: action and mechanism. *Restor. Neurol. Neurosci.* 16, 135–142.

Przedborski, S., Tieu, K., Perier, C., and Vila, M. (2004). MPTP as a mitochondrial neurotoxic model of Parkinson's Disease. *J. Bioenerg. Biomembr*. 36, 375–379. doi: 10.1023/B:JOBB.0000041771.66775.d5

Przedbroski, S., Leviver, M., Jiang, H., Ferreira, M., Jackson-Lewis, V., Donaldson, D., et al. (1995). Dose-dependent lesions of the dopaminergic nigrostriatal pathway induced by instrastriatal injection of 6-hydroxydopamine. *Neuroscience* 67, 631–647. doi: 10.1016/0306-4522(95)00066-R

Purisai, M. G., McCormack, A. L., Cumine, S., Li, J., Isla, M. Z., and Di Monte, D. A. (2007). Microglial activation as a priming event leading to paraquat-induced dopaminergic cell degeneration. *Neurobiol. Dis*. 25, 392–400. doi: 10.1016/j.nbd.2006.10.008

Qiao, Y., Wang, P., Qi, J., Zhang, L., and Gao, C. (2012). TLR-induced NF-κB activation regulates NLRP3 expression in murine macrophages. *FEBS Lett*. 586, 1022–1026. doi: 10.1016/j.febslet.2012.02.045

Qin, L., Wu, X., Block, M. L., Liu, Y., Breese, G. R., Hong, J. S., et al. (2007). Systemic LPS causes chronic neuroinflammation and progressive neurodegeneration. *Glia* 55, 453–462. doi: 10.1002/glia.20467

Qin, X. Y., Zhang, S. P., Cao, C., Loh, Y. P., and Cheng, Y. (2016). Aberrations in peripheral inflammatory cytokine levels in Parkinson disease: a systematic review and meta-analysis. *JAMA Neurol*. 73, 1316–1324. doi: 10.1001/jamaneurol.2016.2742

Ransohoff, R. M. (2016). How neuroinflammation contributes to neurodegeneration. *Science* 353, 7777–83. doi: 10.1126/science.aag2590

Ransohoff, R. M., and Brown, M. A. (2012). Innate immunity in the central nervous system. *J. Clin. Invest*. 122, 1164–1171. doi: 10.1172/JCI58644

Reynolds, A. D., Banerjee, R., Liu, J., Gendelman, H. E., and Mosley, R. L. (2007). Neuroprotective activities of CD4+CD25+ regulatory T cells in an animal model of Parkinson's disease. *J. Leukoc. Biol*. 82, 1083–1094. doi: 10.1189/jlb.0507296

Rodrigues, M. C., Sanberg, P. R., Cruz, L. E., and Garbuzova-Davis, S. (2014). The innate and adaptive immunological aspects in neurodegenerative diseases. *J. Neuroimmunol*. 269, 1–8. doi: 10.1016/j.jneuroim.2013.09.020

Sachs, C., and Jonsson, G. (1975). Mechanisms of action of 6-hydroxydopamine. *Biochem. Pharmacol*. 24, 1–8. doi: 10.1016/0006-2952(75)90304-4

Sandhu, J. K., and Kulka, M. (2021). Decoding mast cell-microglia communication in neurodegenerative diseases. *Int. J. Mol. Sci*. 22, 1093. doi: 10.3390/ijms22031093

Sarkar, S., Dammer, E. B., Malovic, E., Olsen, A. L., Raza, S. A., Gao, T., et al. (2020a). Molecular signatures of neuroinflammation induced by αsynuclein aggregates in microglial cells. *Front. Immunol*. 11, 33. doi: 10.3389/fimmu.2020.00033

Sarkar, S., Nguyen, H. M., Malovic, E., Luo, J., Langley, M., Palanisamy, B. N., et al. (2020b). Kv1.3 modulates neuroinflammation and neurodegeneration in Parkinson's disease. *J. Clin. Invest*. 130, 4195–4212. doi: 10.1172/JCI136174

Schildknecht, S., Pöltl, D., Nagel, D. M., Matt, F., Scholz, D., Lotharius, J., et al. (2009). Requirement of a dopaminergic neuronal phenotype for toxicity of low concentrations of 1-methyl-4-phenylpyridinium to human cells. *Toxicol. Appl. Pharmacol*. 241, 23–35. doi: 10.1016/j.taap.2009.07.027

Scholz, D., Pöltl, D., Genewsky, A., Weng, M., Waldmann, T., Schildknecht, S., et al. (2011). Rapid, complete and large-scale generation of post-mitotic neurons from the human LUHMES cell line. *J. Neurochem*. 119, 957–971. doi: 10.1111/j.1471-4159.2011.07255.x

Schwarting, R., and Huston, J. (1996). Unilateral 6-hydroxydopamine lesions of meso-striatal dopamine neurons and their physiological sequelae. *Prog. Neurobiol*. 49, 215–266. doi: 10.1016/S0301-0082(96)00015-9

Senior, S. L., Ninkina, N., Deacon, R., Bannerman, D., Buchman, V. L., Cragg, S. J., et al. (2008). Increased striatal dopamine release and hyperdopaminergic-like behaviour in mice lacking both alpha-synuclein and gamma-synuclein. *Eur J Neurosci*. 27, 947–957. doi: 10.1111/j.1460-9568.2008.06055.x

Servier (2022). *Smart News*. Servier. Available online at: https://smart.servier.com/

Shao, Q.-H., Chen, Y., Li, F.-F, Wang, S., Zhang, X.-L., Yuan, Y.-H., et al. (2019). TLR4 deficiency has a protective effect in the MPTP/probenecid mouse model of Parkinson's disease. *Acta Pharmacol. Sin*. 40, 1503–1512. doi: 10.1038/s41401-019-0280-2

Shin, W. H., Jeon, M. T., Leem, E., Won, S. Y., Jeong, K. H., Park, S. J., et al. (2015). Induction of microglial toll-like receptor 4 by prothrombin kringle-2: a potential pathogenic mechanism in Parkinson's disease. *Sci. Rep*. 5, 14764. doi: 10.1038/srep14764

Simón-Sánchez, J., Schulte, C., Bras, J. M., Sharma, M., Gibbs, J. R., Berg, D., et al. (2009). Genome-wide association study reveals genetic risk underlying Parkinson's disease. *Nat. Genet*. 41, 1308–1312. doi: 10.1038/ng.487

Sims, G. P., Rowe, D. C., Rietdijk, S. T., Herbst, R., and Coyle, A. J. (2010). HMGB1 and RAGE in inflammation and cancer. *Annu. Rev. Immunol*. 28, 367–388. doi: 10.1146/annurev.immunol.021908.132603

Singh, A., Tripathi, P., and Singh, S. (2021). Neuroinflammatory responses in Parkinson's disease: relevance of ibuprofen in therapeutics. *Inflammopharmacology* 29, 5–14. doi: 10.1007/s10787-020-00764-w

Singh, S. S., Rai, S. N., Birla, H., Zahra, W., Rathore, A. S., and Singh, S. P. (2020). NF-κB-mediated neuroinflammation in Parkinson's disease and potential therapeutic effect of polyphenols. *Neurotox. Res*. 37, 491–507. doi: 10.1007/s12640-019-00147-2

Slanzi, A., Iannoto, G., Rossi, B., Zenaro, E., and Constantin, G. (2020). *In vitro* models of neurodegenerative diseases. *Front. Cell Dev. Biol*. 8, 328. doi: 10.3389/fcell.2020.00328

Soto-Otero, R., Méndez-Álvarez, E., Hermida-Ameijeiras, Á., Muñoz-Patiño, A. M., and Labandeira-Garcia, J. L. (2000). Autoxidation and neurotoxicity of 6-hydroxydopamine in the presence of some antioxidants: potential implication in relation to the pathogenesis of Parkinson's disease. *J. Neurochem*. 74, 1605–1612. doi: 10.1046/j.1471-4159.2000.0741605.x

Specht, C. G., and Schoepfer, R. (2004). Deletion of multimerin-1 in α-synuclein-deficient mice. *Genomics* 83, 1176–1178. doi: 10.1016/j.ygeno.2003.12.014

Srikrishna, G. (2012). S100A8 and S100A9: new insights into their roles in malignancy. *J. Innate Immun*. 4, 31–40. doi: 10.1159/000330095

Steiner, J. A., Quansah, E., and Brundin, P. (2018). The concept of alpha-synuclein as a prion-like protein: ten years after. *Cell Tissue Res*. 373, 161–173. doi: 10.1007/s00441-018-2814-1

Stojkovska, I., Wagner, B. M., and Morrison, B. E. (2015). Parkinson's disease and enhanced inflammatory response. *Exp. Biol. Med*. 240, 1387–1395. doi: 10.1177/1535370215576313

Storelli, E., Cassina, N., Rasini, E., Marino, F., and Cosentino, M. (2019). Do Th17 lymphocytes and IL-17 contribute to Parkinson's disease? A systematic review of available evidence. *Front. Neurol*. 10, 13. doi: 10.3389/fneur.2019.00013

Subbarayan, M. S., Hudson, C., Moss, L. D., Nash, K. R., and Bickford, P. C. (2020). T cell infiltration and upregulation of MHCII in microglia leads to accelerated neuronal loss in an α-synuclein rat model of Parkinson's disease. *J. Neuroinflammation* 17, 242. doi: 10.1186/s12974-020-01911-4

Sulzer, D., Alcalay, R. N., Garretti, F., Cote, L., Kanter, E., Agin-Liebes, J., et al. (2017). T cells from patients with Parkinson's disease recognize α-synuclein peptides. *Nature* 546, 656–661. doi: 10.1038/nature22815

Sun, Y., Wen, Y., Wang, L., Wen, L., You, W., Wei, S., et al. (2021). Therapeutic opportunities of interleukin-33 in the central nervous system. *Front. Immunol*. 12, 654626. doi: 10.3389/fimmu.2021.654626

Tansey, M. G., and Goldberg, M. S. (2010). Neuroinflammation in Parkinson's disease: its role in neuronal death and implications for therapeutic intervention. *Neurobiol. Dis*. 37, 510–518. doi: 10.1016/j.nbd.2009.11.004

Taracanova, A., Alevizos, M., Karagkouni, A., Weng, Z., Norwitz, E., Conti, P., et al. (2017). SP and IL-33 together markedly enhance TNF synthesis and secretion from human mast cells mediated by the interaction of their receptors. *Proc. Natl. Acad. Sci. U.S.A*. 114, E4002–e4009. doi: 10.1073/pnas.1524845114

Thakur, P., Breger, L. S., Lundblad, M., Wan, O. W., Mattsson, B., Luk, K. C., et al. (2017). Modeling Parkinson's disease pathology by combination of fibril seeds and α-synuclein overexpression in the rat brain. *Proc. Natl. Acad. Sci. U.S.A*. 114, E8284–e8293. doi: 10.1073/pnas.1710442114

Theodore, S., Cao, S., McLean, P. J., and Standaert, D. G. (2008). Targeted overexpression of human alpha-synuclein triggers microglial activation and an adaptive immune response in a mouse model of Parkinson disease. *J. Neuropathol. Exp. Neurol*. 67, 1149–1158. doi: 10.1097/NEN.0b013e31818e5e99

Thomas, M., Saldanha, M., Mistry, R., Dexter, D., Ramsden, D., and Parsons, R. (2013). Nicotinamide N-methyltransferase expression in SH-SY5Y neuroblastoma and N27 mesencephalic neurones induces changes in cell morphology via ephrin-B2 and Akt signalling. *Cell Death Dis*. 4, e669–e669. doi: 10.1038/cddis.2013.200

Titze-de-Almeida, R., and Titze-de-Almeida, S. S. (2018). miR-7 replacement therapy in Parkinson's Disease. *Curr. Gene Ther*. 18, 143–153. doi: 10.2174/1566523218666180430121323

Tobon-Velasco, C. J., Cuevas, E., and Torres-Ramos, M. A. (2014). Receptor for AGEs (RAGE) as mediator of NF-kB pathway activation in neuroinflammation and oxidative stress. *CNS Neurol. Disord. Drug Targ.* 13, 1615–1626. doi: 10.2174/1871527313666140806144831

Tore, F., and Tuncel, N. (2009). Mast cells: target and source of neuropeptides. *Curr. Pharm. Des.* 15, 3433–3445. doi: 10.2174/138161209789105036

Trudler, D., Nash, Y., and Frenkel, D. (2015). New insights on Parkinson's disease genes: the link between mitochondria impairment and neuroinflammation. *J. Neural Transm.* 122, 1409–1419. doi: 10.1007/s00702-015-1399-z

Trudler, D., Nazor, K. L., Eisele, Y. S., Grabauskas, T., Dolatabadi, N., Parker, J., et al. (2021). Soluble α-synuclein-antibody complexes activate the NLRP3 inflammasome in hiPSC-derived microglia. *Proc. Natl. Acad. Sci. U.S.A.* 118, e2025847118. doi: 10.1073/pnas.2025847118

Tweedie, D., Sambamurti, K., and Greig, N. H. (2007). TNF-α inhibition as a treatment strategy for neurodegenerative disorders: new drug candidates and targets. *Curr. Alzheimer Res.* 4, 378–385. doi: 10.2174/156720507781788873

Uematsu, S., Matsumoto, M., Takeda, K., and Akira, S. (2002). Lipopolysaccharide-dependent prostaglandin E(2) production is regulated by the glutathione-dependent prostaglandin E(2) synthase gene induced by the Toll-like receptor 4/MyD88/NF-IL6 pathway. *J. Immunol.* 168, 5811–5816. doi: 10.4049/jimmunol.168.11.5811

Ungerstedt, U. (1968). 6-Hydroxy-dopamine induced degeneration of central monoamine neurons. *Eur. J. Pharmacol.* 5, 107–110. doi: 10.1016/0014-2999(68)90164-7

Verhaar, R., Drukarch, B., Bol, J. G., Jongenelen, C. A., Musters, R. J., and Wilhelmus, M. M. (2012). Increase in endoplasmic reticulum-associated tissue transglutaminase and enzymatic activation in a cellular model of Parkinson's disease. *Neurobiol. Dis.* 45, 839–850. doi: 10.1016/j.nbd.2011.10.012

Verhaar, R., Jongenelen, C. A., Gerard, M., Baekelandt, V., Van Dam, A. M., Wilhelmus, M. M., et al. (2011). Blockade of enzyme activity inhibits tissue transglutaminase-mediated transamidation of α-synuclein in a cellular model of Parkinson's disease. *Neurochem. Int.* 58, 785–793. doi: 10.1016/j.neuint.2011.03.004

von Euler Chelpin, M., and Vorup-Jensen, T. (2017). Targets and mechanisms in prevention of Parkinson's disease through immunomodulatory treatments. *Scand. J. Immunol.* 85, 321–330. doi: 10.1111/sji.12542

Wang, S., Yuan, Y.-H., Chen, N.-H., and Wang, H.-B. (2019). The mechanisms of NLRP3 inflammasome/pyroptosis activation and their role in Parkinson's disease. *Int. Immunopharmacol.* 67, 458–464. doi: 10.1016/j.intimp.2018.12.019

Wang, X., and Schwarz, T. L. (2009). The mechanism of Ca2+ -dependent regulation of kinesin-mediated mitochondrial motility. *Cell* 136, 163–174. doi: 10.1016/j.cell.2008.11.046

Wang, Y., Li, L., Hou, C., Lai, Y., Long, J., Liu, J., et al. (2020). SNARE-mediated membrane fusion in autophagy. *Semi. Cell Dev. Biol.* 60, 97–104. doi: 10.1016/j.semcdb.2016.07.009

Wei, L., Ding, L., Mo, M.-,s, Lei, M., Zhang, L., Chen, K., and Xu, P. (2015). Wnt3a protects SH-SY5Y cells against 6-hydroxydopamine toxicity by restoration of mitochondria function. *Transl. Neurodegener.* 4, 1–8. doi: 10.1186/s40035-015-0033-1

Wenzel, T. J., Kwong, E., Bajwa, E., and Klegeris, A. (2020). Resolution-associated molecular patterns (RAMPs) as endogenous regulators of glia functions in neuroinflammatory disease. *CNS Neurol. Disord. Drug Targets.* 19, 483–494. doi: 10.2174/1871527319666200702143719

Wilhelmus, M. M., Verhaar, R., Andringa, G., Bol, J. G., Cras, P., Shan, L., et al. (2011). Presence of tissue transglutaminase in granular endoplasmic reticulum is characteristic of melanized neurons in Parkinson's disease brain. *Brain Pathol.* 21, 130–139. doi: 10.1111/j.1750-3639.2010.00429.x

Williams, G. P., Schonhoff, A. M., Jurkuvenaite, A., Gallups, N. J., Standaert, D. G., and Harms, A. S. (2021). CD4 T cells mediate brain inflammation and neurodegeneration in a mouse model of Parkinson's disease. *Brain* 144, 2047–2059. doi: 10.1093/brain/awab103

Wyss-Coray, T., and Mucke, L. (2002). Inflammation in neurodegenerative disease—a double-edged sword. *Neuron* 35, 419–432. doi: 10.1016/S0896-6273(02)00794-8

Xiao, H. X., Song, B., Li, Q., Shao, Y. M., Zhang, Y. B., Chang, X. L., et al. (2022). Paraquat mediates BV-2 microglia activation by raising intracellular ROS and inhibiting Akt1 phosphorylation. *Toxicol. Lett.* 355, 116–126. doi: 10.1016/j.toxlet.2021.11.017

Xicoy, H., Wieringa, B., and Martens, G. J. M. (2017). The SH-SY5Y cell line in Parkinson's disease research: a systematic review. *Mol. Neurodegener.* 12, 10. doi: 10.1186/s13024-017-0149-0

Xie, W., and Chung, K. K. (2012). Alpha-synuclein impairs normal dynamics of mitochondria in cell and animal models of Parkinson's disease. *J. Neurochem.* 122, 404–414. doi: 10.1111/j.1471-4159.2012.07769.x

Yao, K., and Zhao, Y. F. (2018). Aging modulates microglia phenotypes in neuroinflammation of MPTP-PD mice. *Exp. Gerontol.* 111, 86–93. doi: 10.1016/j.exger.2018.07.010

Yao, L., Zhu, Z., Wu, J., Zhang, Y., Zhang, H., Sun, X., et al. (2019). MicroRNA-124 regulates the expression of p62/p38 and promotes autophagy in the inflammatory pathogenesis of Parkinson's disease. *FASEB J.* 33, 8648–8665. doi: 10.1096/fj.201900363R

Yavich, L., Tanila, H., Vepsäläinen, S., and Jäkälä, P. (2004). Role of α-synuclein in presynaptic dopamine recruitment. *J. Neurosci.* 24, 11165–11170. doi: 10.1523/JNEUROSCI.2559-04.2004

Ye, J., Jiang, Z., Chen, X., Liu, M., Li, J., and Liu, N. (2016). Electron transport chain inhibitors induce microglia activation through enhancing mitochondrial reactive oxygen species production. *Exp. Cell Res.* 340, 315–326. doi: 10.1016/j.yexcr.2015.10.026

Yi, M., Weaver, D., and Hajnóczky, G. (2004). Control of mitochondrial motility and distribution by the calcium signal: a homeostatic circuit. *J. Cell Biol.* 167, 661–672. doi: 10.1083/jcb.200406038

Yu, Z., Jiang, N., Su, W., and Zhuo, Y. (2021). Necroptosis: a novel pathway in neuroinflammation. *Front. Pharmacol.* 12, 701564. doi: 10.3389/fphar.2021.701564

Zaheer, A., Knight, S., Zaheer, A., Ahrens, M., Sahu, S. K., and Yang, B. (2008a). Glia maturation factor overexpression in neuroblastoma cells activates glycogen synthase kinase-3beta and caspase-3. *Brain Res.* 1190, 206–214. doi: 10.1016/j.brainres.2007.11.011

Zaheer, A., Zaheer, S., Thangavel, R., Wu, Y., Sahu, S. K., and Yang, B. (2008b). Glia maturation factor modulates beta-amyloid-induced glial activation, inflammatory cytokine/chemokine production and neuronal damage. *Brain Res.* 1208, 192–203. doi: 10.1016/j.brainres.2008.02.093

Zhang, C., Sajith, A. M., Xu, X., Jiang, J., Phillip Bowen, J., Kulkarni, A., et al. (2022). Targeting NLRP3 signaling by a novel-designed sulfonylurea compound for inhibition of microglial inflammation. *Bioorg. Med. Chem.* 58, 116645. doi: 10.1016/j.bmc.2022.116645

Zhang, Y. N., Fan, J. K., Gu, L., Yang, H. M., Zhan, S. Q., and Zhang, H. (2021). Metabotropic glutamate receptor 5 inhibits α-synuclein-induced microglia inflammation to protect from neurotoxicity in Parkinson's disease. *J. Neuroinflammation* 18, 23. doi: 10.1186/s12974-021-02079-1

Zhao, J., Bi, W., Xiao, S., Lan, X., Cheng, X., Zhang, J., et al. (2019). Neuroinflammation induced by lipopolysaccharide causes cognitive impairment in mice. *Sci. Rep.* 9, 5790. doi: 10.1038/s41598-019-42286-8

Zhao, Y. F., Qiong, Z., Zhang, J. F., Lou, Z. Y., Zu, H. B., Wang, Z. G., et al. (2018). The synergy of aging and LPS exposure in a mouse model of Parkinson's disease. *Aging Dis.* 9, 785–797. doi: 10.14336/AD.2017.1028

Zhou, Y., Lu, M., Du, R. H., Qiao, C., Jiang, C. Y., Zhang, K. Z., et al. (2016). MicroRNA-7 targets Nod-like receptor protein 3 inflammasome to modulate neuroinflammation in the pathogenesis of Parkinson's disease. *Mol. Neurodegener.* 11, 28. doi: 10.1186/s13024-016-0094-3

Zhu, J., Hu, Z., Han, X., Wang, D., Jiang, Q., Ding, J., et al. (2018). Dopamine D2 receptor restricts astrocytic NLRP3 inflammasome activation via enhancing the interaction of β-arrestin2 and NLRP3. *Cell Death Differ.* 25, 2037–2049. doi: 10.1038/s41418-018-0127-2

Zhu, Y., Chen, X., Liu, Z., Peng, Y. P., and Qiu, Y. H. (2015). Interleukin-10 protection against lipopolysaccharide-induced

neuro-inflammation and neurotoxicity in ventral mesencephalic cultures. *Int. J. Mol. Sci.* 17, 25. doi: 10.3390/ijms17010025

Conflict of Interest: The authors declare that the research was conducted in the absence of any commercial or financial relationships that could be construed as a potential conflict of interest.

Publisher's Note: All claims expressed in this article are solely those of the authors and do not necessarily represent those of their affiliated organizations, or those of the publisher, the editors and the reviewers. Any product that may be evaluated in this article, or claim that may be made by its manufacturer, is not guaranteed or endorsed by the publisher.

frontiers | Frontiers in Neuroscience

TYPE Original Research
PUBLISHED 10 August 2022
DOI 10.3389/fnins.2022.929151

OPEN ACCESS

EDITED BY
Miriam Sklerov,
University of North Carolina at Chapel Hill, United States

REVIEWED BY
Ziliang Zhu,
University of North Carolina at Chapel Hill, United States
Matthew Sharrock,
University of North Carolina at Chapel Hill, United States

*CORRESPONDENCE
Hans-Peter Müller
hans-peter.mueller@uni-ulm.de

†These authors share senior authorship

SPECIALTY SECTION
This article was submitted to Neurodegeneration, a section of the journal Frontiers in Neuroscience

RECEIVED 26 April 2022
ACCEPTED 20 July 2022
PUBLISHED 10 August 2022

CITATION
Behler A, Lulé D, Ludolph AC, Kassubek J and Müller H-P (2022) Longitudinal monitoring of amyotrophic lateral sclerosis by diffusion tensor imaging: Power calculations for group studies. *Front. Neurosci.* 16:929151. doi: 10.3389/fnins.2022.929151

Longitudinal monitoring of amyotrophic lateral sclerosis by diffusion tensor imaging: Power calculations for group studies

Anna Behler[1], Dorothée Lulé[1], Albert C. Ludolph[1,2], Jan Kassubek[1,2†] and Hans-Peter Müller[1*†]

[1]Department of Neurology, University of Ulm, Ulm, Germany, [2]Deutsches Zentrum für Neurodegenerative Erkrankungen (DZNE), Ulm, Germany

Introduction: Diffusion tensor imaging (DTI) can be used to map disease progression in amyotrophic lateral sclerosis (ALS) and therefore is a promising candidate for a biomarker in ALS. To this end, longitudinal study protocols need to be optimized and validated regarding group sizes and time intervals between visits. The objective of this study was to assess the influences of sample size, the schedule of follow-up measurements, and measurement uncertainties on the statistical power to optimize longitudinal DTI study protocols in ALS.

Patients and methods: To estimate the measurement uncertainty of a tract-of–interest-based DTI approach, longitudinal test-retest measurements were applied first to a normal data set. Then, DTI data sets of 80 patients with ALS and 50 healthy participants were analyzed in the simulation of longitudinal trajectories, that is, longitudinal fractional anisotropy (FA) values for follow-up sessions were simulated for synthetic patient and control groups with different rates of FA decrease in the corticospinal tract. Monte Carlo simulations of synthetic longitudinal study groups were used to estimate the statistical power and thus the potentially needed sample sizes for a various number of scans at one visit, different time intervals between baseline and follow-up measurements, and measurement uncertainties.

Results: From the simulation for different longitudinal FA decrease rates, it was found that two scans per session increased the statistical power in the investigated settings unless sample sizes were sufficiently large and time intervals were appropriately long. The positive effect of a second scan per session on the statistical power was particularly pronounced for FA values with high measurement uncertainty, for which the third scan per session increased the statistical power even further.

Conclusion: With more than one scan per session, the statistical power of longitudinal DTI studies can be increased in patients with ALS. Consequently,

sufficient statistical power can be achieved even with limited sample sizes. An improved longitudinal DTI study protocol contributes to the detection of small changes in diffusion metrics and thereby supports DTI as an applicable and reliable non-invasive biomarker in ALS.

KEYWORDS

Amyotrophic Lateral Sclerosis, Diffusion Tensor Imaging, longitudinal design, statistical power, study optimization

Introduction

During the last decade, magnetic resonance imaging (MRI)-based parameters have gained increasing interest as a progression marker in neurodegenerative diseases (Agosta et al., 2015). Amyotrophic Lateral Sclerosis (ALS) is characterized by progressive motor neuron degeneration of both the upper motor neurons of the cerebral cortex and the lower motor neurons in the brainstem and spinal cord, leading to progressive immobility and breathing difficulties, and eventually died after an average of 3 years (van Es et al., 2017). In clinical trials, objective biomarkers, for example, based upon neuroimaging are needed to monitor the progression of the disease and thus improve the chances of identifying effective treatments for ALS (van den Berg et al., 2019). A promising and robust approach is the measurement of white matter (WM) degeneration by the use of diffusion tensor imaging (DTI) (Kassubek and Müller, 2020). In addition to the voxel-wise analysis of the whole brain (Müller et al., 2016), a tract-of-interest (TOI)-based approach can be used to analyze specific cerebral WM pathways that are involved in the progression of ALS (Kassubek et al., 2014). Longitudinally, the spread of pathology is reflected by tract-specific alterations in DTI metrics (Kassubek et al., 2018), which correlates with the clinical severity of the disease (Baldaranov et al., 2017).

Longitudinal MRI examinations of the brain are time-consuming, costly, and can be a burden for patients with ALS (especially in advanced disease stages). Thus, a careful design of such studies is mandatory. One of the most crucial variables in the conceptualization of a longitudinal study is the sample size as samples that are too small might lead to non-significant results of true effects (Blain et al., 2007, Alruwaili et al., 2019). Another essential aspect is the schedule of follow-up measurements, that is, the number of follow-ups and the time intervals between them. On one hand, it must be taken into consideration when the effect, that is, a change in diffusion metrics, can be measured at the earliest (Kalra et al., 2020), and on the other hand, the timing of follow-up measurements can be substantial for the validity of the results (Müller et al., 2021a). Confounding factors such as general and subject-specific noise cause diffusion metrics to be subject to measurement errors (Müller et al., 2013). A higher measurement error results in higher measurement uncertainty, that is, the measured value probably does not directly reflect the true value. Then, the measurement uncertainties affect the test-retest reliability of DTI metrics, that is, the ability to obtain similar values from different acquisitions of the same subject (Vollmar et al., 2010; Koller et al., 2021). The presence of high measurement errors can potentially bias the temporal association of variables in longitudinal studies (Saccenti et al., 2020). Especially in patients with burdening neurodegenerative diseases, more subject-specific measurement artifacts are to be expected compared to healthy subjects. All these aspects might be a reason why previously reported *post-hoc* effect sizes of longitudinal FA changes in patients with ALS were only limited (Kassubek et al., 2018). This indicates that DTI study protocols may be improved to increase the reliability of DTI metrics that might potentially serve as technical biomarkers in studies.

The objective of this study was to evaluate the effects of measurement uncertainty and scheduling of follow-up measurements on statistical power and sample size in a longitudinal study of patients with ALS. The approach is based on fractional anisotropy (FA) along the corticospinal tract (CST) which represents neuropathological ALS stage one (Kassubek et al., 2018) and is a robust and sensitive DTI-based parameter for disease progression (Kocar et al., 2021). This study aimed to establish a basis for the optimization of study protocols for longitudinal ALS imaging studies that are robust to different longitudinal FA decrease rates.

Methods

Participants

A total of 80 patients (58.5 ± 13.9 years, 48 male/32 female) with clinically definite or probable sporadic ALS according to the revised version of the El Escorial World Federation of Neurology criteria (Brooks et al., 2000) were included in the study. All patients underwent standardized clinical-neurological and routine laboratory examinations. None of the patients had any history of neurological or psychiatric disorders apart from ALS. The severity of disability as measured with the revised ALS

functional rating scale (ALS-FRS-R) (Cedarbaum et al., 1999) was 40 ± 5 (range 23–48). For analysis at the group level, 50 age- and sex-matched healthy controls (54.3 ± 9.8 years, 32 male/18 female) were analyzed. For test-retest measurements, 14 healthy subjects (age 36.3 ± 11.2 years, 6 male/8 female) participated. All healthy controls had no history of any medical condition and were medication-free.

All patients and healthy controls gave written consent for the MRI protocol according to the institutional guidelines. The study was approved by the Ethical Committee of the University of Ulm, Germany (reference # 19/12), and written consent was obtained from each participant.

Magnetic resonance imaging data acquisition and processing

Test-retest measurements of 14 healthy subjects were acquired on the same 1.5 T MRI scanner (Magnetom Symphony, Siemens Medical, Erlangen, Germany) with 151 ± 112 days in-between both scanning sessions. Since the reliability of diffusion metrics is affected by the number of GD (Teipel et al., 2011), each scanning session consisted of two DTI sequences with different protocols: Protocol A consisted of 52 gradient directions (GD) including four $b0$ directions (b = 1,000 s/mm^2, voxel size 2.0 mm × 2.0 mm × 2.8 mm, 128 × 128 × 64 matrix, TE = 95 ms, TR = 8,000 ms) and protocol B consisted of 62 GD including two $b0$ directions (b = 1,000 s/mm^2, voxel size 2.5 mm × 2.5 mm × 2.5 mm, 128 × 128 × 64 matrix, TE = 102 ms, TR = 8,700 ms). Between both sequences, the participants remained in the scanner. The ratio of the number of GD and $b0$ direction additionally influences the reliability of the diffusion metrics (Zhu et al., 2009). Optimization of the test-retest protocols was not performed in this respect, since the objective was not to minimize the error but to estimate the error from protocols commonly used in ALS studies (Kassubek et al., 2014; Müller et al., 2016; Behler et al., 2022; Münch et al., 2022).

The signal-to-noise ratio (SNR) may be lowered in patients with neurodegenerative diseases due to subject-related factors (Müller et al., 2013). Therefore, all 80 patients with ALS and a healthy control group (50 subjects) underwent protocol C at a 3.0 T MRI scanner (Allegra, Siemens Medical, Erlangen, Germany), as this has a higher SNR compared to a 1.5-T MRI scanner. Protocol C consisted of 49 GD including one $b0$ direction (b = 1,000 s/mm^2, voxel size 2.2 mm × 2.2 mm × 2.2 mm, 96 × 128 × 52 matrix, TE = 85 ms, TR = 7,600 ms).

Diffusion tensor imaging analysis

For DTI data post-processing, the software *Tensor Imaging and Fiber Tracking* (TIFT) (Müller et al., 2007) was used. First, all DTI data sets were checked for eddy current distortions, underwent quality control (Müller et al., 2011), and were resampled to an isotropic 1 mm grid. This was followed by a non-linear spatial normalization to the Montreal Neurological Institute (MNI) stereotaxic standard space (Brett et al., 2002) by using study-specific DTI templates as described previously in detail (Müller et al., 2012). Baseline and follow-up DTI data sets of the test-retest group were aligned using a halfway linear registration (Menke et al., 2014) before MNI normalization. FA maps were calculated from each data set and, finally, smoothed with a Gaussian filter with an 8 mm full width-at-half-maximum.

Fiber tracking

An averaged data set of MNI transformed controls' data was used for the identification of the CST by a seed-to-target TOI-based approach (Kassubek and Müller, 2020). A deterministic streamline fiber tracking approach (Müller et al., 2009) was used at which the FA threshold was set at 0.2 (Kunimatsu et al., 2004) and the Eigenvector scalar product threshold was set at 0.9. The seed regions had a radius of 5 mm and the target regions had a radius of 10 mm. In a final step, the technique of tract-wise fractional anisotropy statistics (TFAS) was applied to select FA values underlying the fiber tracks for arithmetic averaging. Bihemispheric mean FA values of fiber tracts were averaged and corrected for age (Behler et al., 2021). An age correction of the FA maps of the test-retest group was not performed since this group was only used to determine the measurement uncertainty which could be assumed to be independent of age and gender.

Simulation of longitudinal trajectories

For the single subject i, the FA value $FA_{t,i}$ of a follow-up measurement at time t after the baseline measurement (t = 0) can be calculated based on a linear relationship with a subject-specific rate of FA change β_i:

$$FA_{t,i} = FA_{0,i} + \beta_i \cdot t \quad (1)$$

However, FA values, like any other measured value, are not without measurement error. The measured FA value $\widehat{FA}_{t,i}$ is composed of the real value and a measurement error ε_t, which differs for each measurement:

$$\widehat{FA}_{t,i} = FA_{t,i} + \varepsilon_t \quad (2)$$

For the simulation of longitudinal FA values (**Figure 1A**), this results in:

$$\widehat{FA}_{t,i} = \widehat{FA}_{0,i} - \varepsilon_0 + \beta_i \cdot t + \varepsilon_t \quad (3)$$

The measurement errors, that is, the measurement uncertainties, ε_0 and ε_t, of the baseline and the follow-up measurement at time t originate from a normal distribution (**Table 1**).

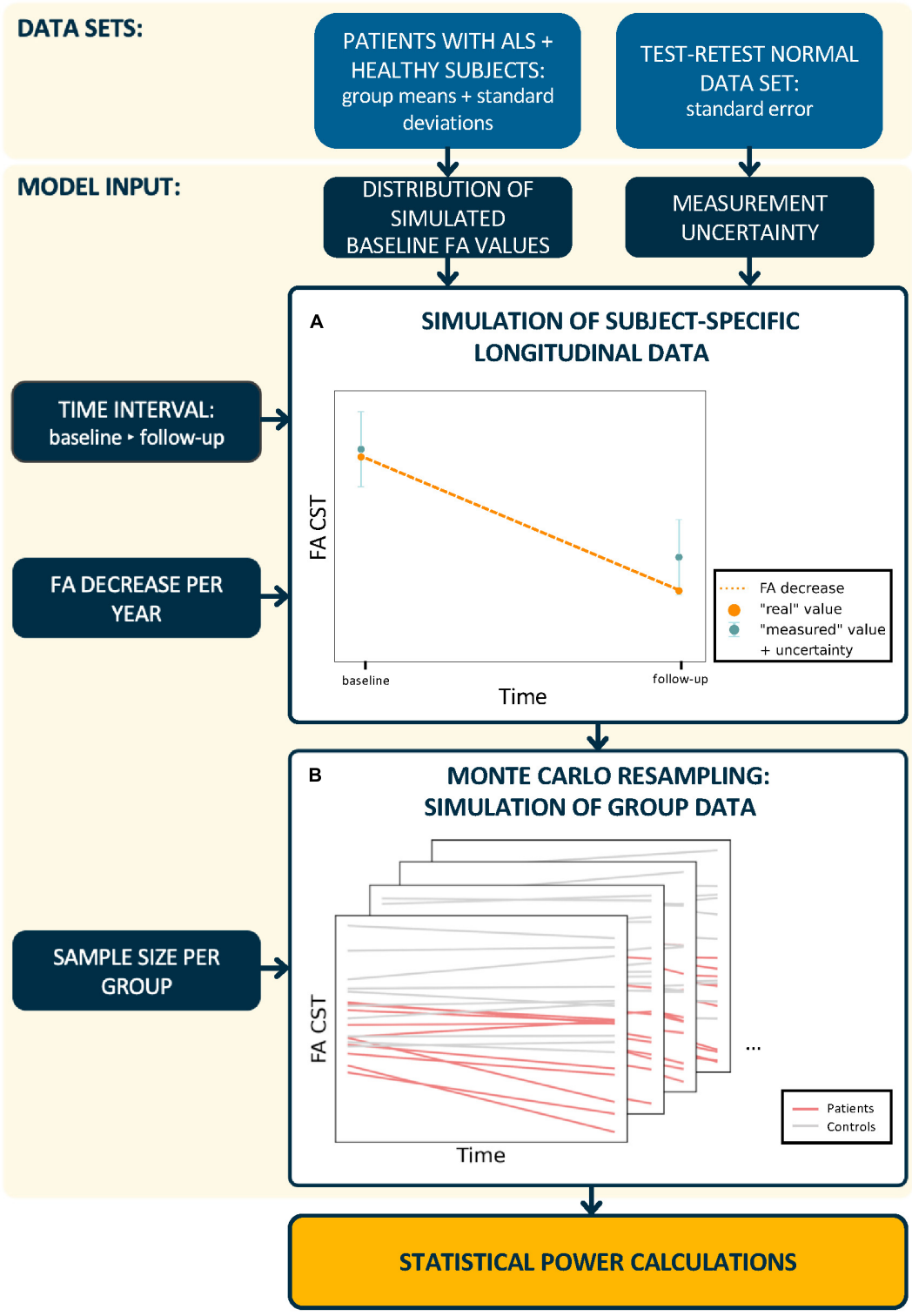

FIGURE 1
Schematic workflow of statistical power calculations. In a first step, **(A)** subject-specific longitudinal fractional anisotropy (FA) values in the corticospinal tract (CST) were simulated. Therefore, synthetic baseline values for patients and healthy controls were generated from real subject data distributions. The calculation of synthetic "measured" follow-up FA values incorporated a predefined FA decrease and measurement uncertainty. In a second step, **(B)** longitudinal trajectories were generated for *n* subjects per group and the statistical power was calculated from 2,000 Monte Carlo resampled data sets. This procedure was performed for different time intervals between baseline and follow-up sessions, measurement uncertainties, longitudinal FA decrease rates, and sample sizes.

TABLE 1 Description of the distributions used for longitudinal group data simulations.

Variables generated in simulation	Distribution	Basis for distribution parameters
"Measured" baseline FA values (group- and subject-specific)	$\widehat{FA}_{0,i} \sim \mathcal{N}(\mu_{patients}, \sigma_{patients})$	$\mu_{patients}$ and $\sigma_{patients}$ from 80 patients with ALS
	$\widehat{FA}_{0,i} \sim \mathcal{N}(\mu_{controls}, \sigma_{controls})$	$\mu_{controls}$ and $\sigma_{controls}$ from 50 healthy controls
Measurement uncertainty (measurement-specific)	$\varepsilon_i \sim \mathcal{N}(0, SEM)$	*SEM* from 14 test-retest normal data sets
Longitudinal FA decrease (subject-specific)	$\beta_i \sim \mathcal{N}(\mu_{\beta_i}, \sigma_{\beta_i})$	Specification of μ_{β_i} and σ_{β_i} based on previous studies (Cardenas-Blanco et al., 2016; Baldaranov et al., 2017; Kassubek et al., 2018; Kalra et al., 2020)

All random variables are normally distributed with mean μ and standard deviation σ.

To extend this approach to n subjects, a between-subject variability of the intercept $\widehat{FA}_{0,i}$ and slope β_i is considered, that is, these are subject-specific Gaussian random effects (**Table 1**).

Reliability analysis

To assess the measurement reliability of the FA values in the CST, the intraclass correlation coefficient (*ICC*) was calculated from the test-retest data sets of the healthy subjects with the following specifications: two-way mixed effect, single rater, that is, MRI scanner, and absolute agreement (Koo and Li, 2016). *ICC* values < 0.50 indicate poor reliability, values between 0.50–0.75 indicate moderate reliability, values between 0.75–0.90 indicate good reliability, and values > 0.90 indicate excellent reliability. The 95% confidence intervals (CI) were considered for this assessment.

The standard errors ε of a FA value (**Table 1**) were estimated using the standard error of the mean (*SEM)* from the *ICC* (Weir, 2005):

$$SEM = \frac{TSS}{(k-1)} \cdot \sqrt{ICC \cdot (1 - ICC)} \quad (4)$$

with *TSS* as the total "within-samples" sum of squares and k as the number of measurements.

Statistical power calculations

The statistical power was evaluated for the comparison of longitudinal FA decreases between a group of patients and a group of healthy controls using a Monte Carlo simulation approach (**Figure 1B**) for different study designs. The simulations of FA values at the follow-up session were based on subject-specific longitudinal FA decrease rates only in patients with ALS since the annual longitudinal FA decrease for healthy controls was set to null. The FA decrease group mean in patients with ALS was specified based on measurements in previous studies:

- to 0.05% representing a group with a slow longitudinal FA decrease (Baldaranov et al., 2017).
- to 2.00% representing a group of patients with intermediate longitudinal FA decrease rates (Kassubek et al., 2018; Kalra et al., 2020).
- to 3.50% representing a group with a fast longitudinal FA decrease (Cardenas-Blanco et al., 2016).

It has to be noted, in general, however, that the speed of deterioration of a technical measurement like MRI/DTI not necessarily has to be associated with the speed of progression at the clinical level, because, in complex diseases like ALS, many (individual) factors may influence the clinical disease course. Since the simulation was based on subject-specific trajectories, the coefficient of variation of those mean FA decrease rates was set to 67% in patients with ALS.

The algorithm to calculate the statistical power for a given sample size per group n and a given effect size, that is, mean longitudinal FA decrease rate in the patients with ALS, at a significance level of 0.05 is as follows:

Step 1: The time interval between the baseline and the follow-up session, the number of scans per session m, and the magnitude of the measurement uncertainty were specified. The time intervals chosen between baseline and follow-up sessions varied from 30 to 180 days, which are typical intervals in longitudinal studies (Baldaranov et al., 2017; Kassubek et al., 2018; Kalra et al., 2020).

Step 2: Based on cross-sectional data estimated from studies with real subjects (**Figure 1A**), synthetic "measured" baseline FA values $\widehat{FA}_{0,i}$ were generated for each subject from a normal distribution (**Table 1**) and m measurement repetitions were simulated by resampling using the normal distribution of the measurement uncertainty [equation (2)].

Step 3: A longitudinal FA decrease rate β_i was assigned to each subject (**Table 1**) and longitudinal FA values (m scans at one follow-up session t days after the baseline session) were calculated for each subject according to [equation (3)].

Step 4: The group comparison of longitudinal FA change was analyzed with a two-sided independent t-test and the p-value was calculated.

Step 5: Steps 2–4 were iterated 2,000 times and the number of significant iterations was obtained. Statistical power was

estimated as the proportion of iterations with statistically significant results out of all iterations (Figure 1B).

Results

Simulation input

The test-retest reliability of the FA of the CST was determined for two different DTI protocols (1.5 T scanner) and ranged from good to excellent with an *ICC* of 0.91 [CI: (0.74, 0.97)] for protocol A and an *ICC* of 0.97 [CI: (0.91, 0.99)] for protocol B. According to equation (4), the standard error ε of a FA value was calculated to be 0.00134 for protocol A and 0.00054 for protocol B, respectively. The analysis showed that DTI protocols on the same scanner could lead to different magnitudes of measurement uncertainty of FA values in the CST. In the following, the standard error ε of protocol A is referred to as "high measurement uncertainty" and that of protocol B as "low measurement uncertainty," since the latter provided more reliable values. As the magnitude of the measurement uncertainty directly affects the correlation structure of longitudinal data, the simulations and calculation of statistical power were performed for both measurement error magnitudes, that is, a low and high measurement uncertainty.

The tract-based group analysis of cross-sectional data showed a mean FA value of 0.326 (SEM, 0.002) with a standard deviation of 0.018 for the CST for patients with ALS and a mean FA value of 0.339 (SEM, 0.003) with a standard deviation of 0.023 for healthy controls.

Monte Carlo statistical power estimate

Overall, for both measurement uncertainties, it was shown that multiple repeated scans per session led to an increase of the statistical power in detecting longitudinal changes in the FA in the CST under otherwise identical conditions, that is, time interval and group size.

From the simulation of a 0.5% longitudinal FA decrease in the CST per year (slow longitudinal FA decrease), it was shown at the analyzed time intervals of 60, 120, and 180 days (Figure 2A) that a second scan per session resulted in increased statistical power across both measurement uncertainties and all time intervals. Due to the lower change per year, the third scan per session led to a further increase in the statistical power which was similar to the increase due to a second scan for high measurement uncertainty.

In the simulations with 2.0–3.5% longitudinal FA decrease, shorter time intervals were also analyzed, since effects should be observable after shorter time intervals with a more pronounced longitudinal decrease. In the simulation with an average annual FA decrease of 2.0% (Figure 2B), the statistical power of 0.8 could not be achieved with either low or high measurement uncertainty for a time interval of 30 days and one scan per session for less than 35 subjects per group. The second scan increased the statistical power so that a statistical power of 0.8 could be reached with 20 subjects per group (with a given low measurement uncertainty). A subsequent, third scan per session led to further improvement of the statistical power for both measurement uncertainties. For measurements with low measurement uncertainty, the third scan did not further increase the statistical power. This positive effect of the third scan per session was lower the higher the time intervals between the baseline and the follow-up session were. Thus, with a 90-day interval between baseline and follow-up, the third measurement did not provide any additional advantage over a two-time repeated scan. The analysis of the sample sizes per group which was needed to reach an effect size of 0.8 showed that, for FA values with high measurement uncertainty, the second scan per session resulted in a reduction of the required sample size per group by about 30–45% (Figure 3).

In the simulation with a longitudinal FA decrease of 3.5% per year in the CST ("fast FA progressors") (Figure 2C), it was shown that, with 90-days between baseline and follow-up measurement, a statistical power of more than 0.8 could already be achieved with 12 subjects per group, as well as for FA values with high measurement uncertainty. Repeated scans per session resulted in an increase of the statistical power in case of high measurement uncertainties and/or shorter time intervals (30 days). For a low measurement uncertainty, however, this improvement could not be demonstrated already at follow-up measurements 90-days after baseline. For measurements subject to high measurement uncertainty, the third scan brought no further advantage after 90-days, as compared to two scans per session.

Discussion

This study investigated how the potential of the DTI-based metric FA as a non-invasive progression marker may be further optimized to monitor longitudinal changes in the FA during the disease progression of ALS. The influences of sample size, scheduling of baseline and follow-up sessions, and measurement uncertainty on the statistical power were assessed for longitudinal FA studies in the CST. Follow-up FA values were simulated for patients with ALS and healthy controls based on real baseline data distributions. Based on these synthetic longitudinal FA values, it could be demonstrated that a second scan at each session substantially increased the statistical power of such studies, especially for uncertain measurements with a limited SNR, for example, due to subject-related factors (Müller et al., 2013). The application of these results will strengthen the reliability of the FA values, in line with SNR improvement by signal-averaging during individual scans (Farrell et al., 2007;

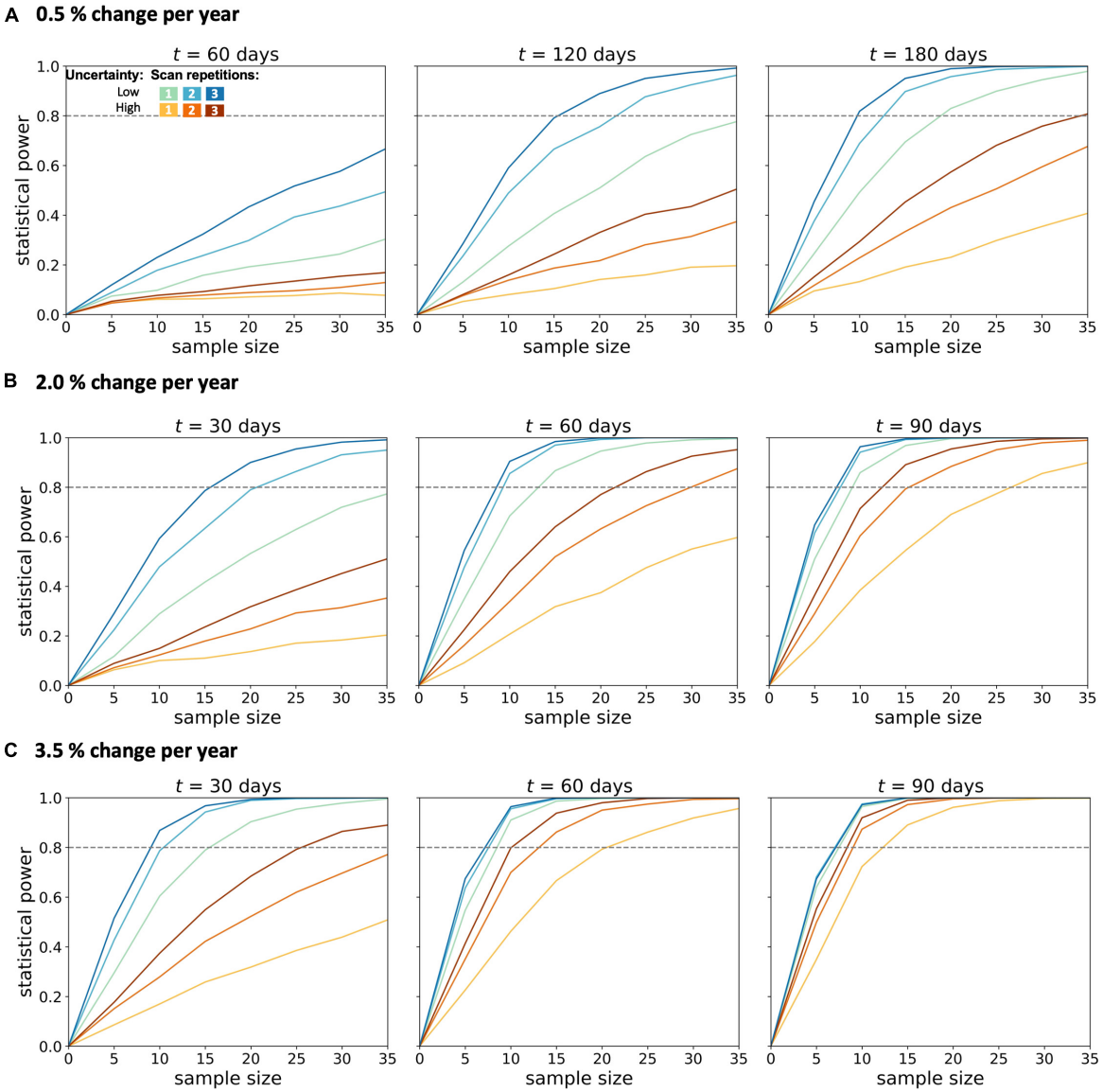

FIGURE 2
Statistical power for longitudinal diffusion tensor imaging studies in amyotrophic lateral sclerosis. Calculations were performed for **(A)** 0.5%, **(B)** 2.0%, and **(C)** 3.5% change per year of the fractional anisotropy in the corticospinal tract. Longitudinal simulations for a patient and a healthy control group were performed for different sample sizes per group, two magnitudes of measurement uncertainty, one to three scans per session, and time intervals *t* between baseline and the follow-up session.

Seo et al., 2019). Vice versa, the increased statistical power of a DTI protocol means that lower sample sizes suffice to measure small effects and/or effects after a short time, respectively. With repeated scans per session, longitudinal FA changes in the CST could be detected already after short time intervals. This can be useful to identify even small alterations in cerebral WM pathways (Bede and Hardiman, 2018; Müller et al., 2021b) or potentially even small treatment effects if studied in a given therapeutic intervention. From longitudinal simulations of MRI correlates of fast disease progression, it was shown that DTI can detect alterations in the CST with satisfactory statistical power even after a short time. This provides the opportunity to use DTI to differentiate between ALS variants with different progression rates (Baek et al., 2020; Kalra et al., 2020).

As additional scans are a burden for patients with neurodegenerative diseases, reliability analyses are often performed on healthy participants. Patients with ALS might present with reduced or restricted mobility, leading to suboptimal positioning within the scanner and/or discomfort. Breathing difficulties further interfere with lying supine in the MRI scanner. This may result in a decreased SNR and, therefore, decreased reliability of diffusion metrics. Therefore,

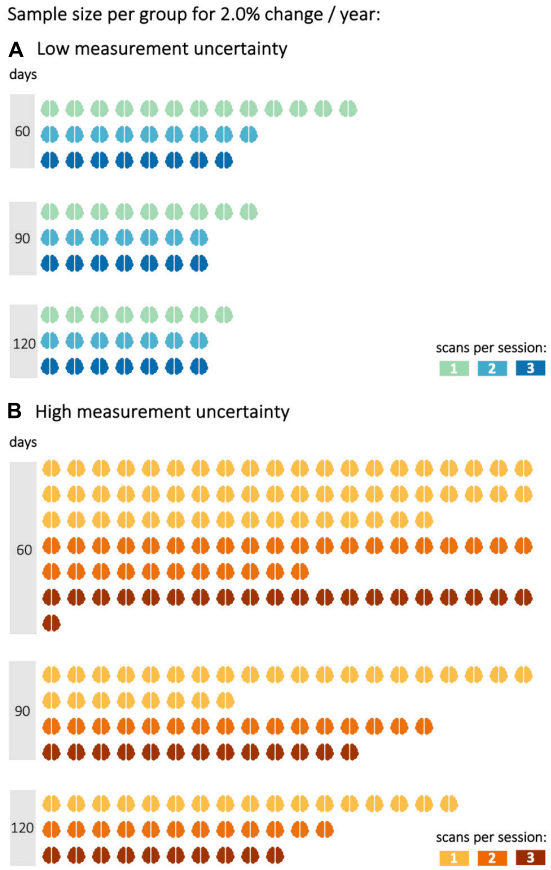

FIGURE 3
Sample size per group to reach a statistical power of 0.8 with different decrease rates in fractional anisotropy (FA). FA values were either subject to **(A)** low or **(B)** high measurement uncertainty. Statistical power calculations were performed for 60, 90, and 120 days between baseline and follow-up sessions and one to three scans per session.

measurement uncertainty of FA values determined for healthy subjects in this study might underestimate those in patients with ALS. Thus, it may be concluded that repeated scans at one visit are beneficial especially at an advanced disease stage to achieve sufficient statistical power even with small sample sizes. Of course, repeated scans per session can also be an additional burden, especially for patients in later disease stages, and it may be assumed that repeated scans per session are possible at baseline but might be declined by the patient at later follow-ups. However, even then the repeated scans at baseline have a high value for the longitudinal analysis, since the data may be automatically weighted. Therefore, time intervals between multiple follow-ups no longer bias the results (Müller et al., 2021a). Since several uncertainties of measurements might occur in a clinical study, depending on patient condition including disease progression, one possible improvement could be to scan subjects two times during one visit.

A separate analysis of data from 1.5 to 3.0 T MRI acquisition protocols showed that similar FA values could be obtained in patients with ALS at different field strengths (Kassubek et al., 2014). Therefore, measurement uncertainties acquired from 1.5 T scanner data could be used together with group data obtained at a 3.0 T scanner: 3.0 T data show a higher SNR compared to 1.5 T data, thus 1.5 T data were only used for uncertainty estimation in this study and simulations at the group level were performed on data recorded on a 3.0 T scanner. The reliability analysis of two different 1.5 T scanner protocols showed that the *ICC* of the FA in the CST, obtained by a tract-based approach, was in the same order of magnitude as reported for a 3.0 T scanner (Lewis et al., 2020). This finding is not surprising, since the reliability of diffusion metrics is not affected by the field strength alone (Vollmar et al., 2010) but also by the number of GD (Teipel et al., 2011), DTI data processing pipelines (Thieleking et al., 2021), and the MRI scanner itself (Palacios et al., 2017). Although field strength is only one of the several factors affecting test-retest reliability, scanners with different field strengths in multicenter studies lead to increased inter-site variability in diffusion metrics. This has an additional negative impact on the statistical power of longitudinal studies due to larger variability between subjects from different sites. Since multicenter studies are often required in rare diseases such as ALS, this limitation can be addressed with robust harmonization methods that reduce inter-site variability while preserving biological variability (Pinto et al., 2020). An approach using linear correction for scanner effects in multicenter longitudinal studies showed better estimates accounting for the within-subject variability (Venkatraman et al., 2015); an analysis approach for harmonizing multicenter DTI data have been reported previously (Müller et al., 2016; Kalra et al., 2020). Since the measurement uncertainty may differ between sites, it could be assumed that the acquisition of multiple scans per visit also might have a positive effect on the harmonization of multicenter studies and their evaluations.

This study is not without limitations. The sample size of the test-retest cohort was limited, and these DTI data sets were acquired on a different MRI scanner than those of the groups providing basic information for longitudinal simulation. To strengthen the power of such simulations, test-retest measurements on the scanner of the planned study would be ideal. This study focused on longitudinal alterations in FA in the CST because the CST alterations are to be robustly found early in the disease process of ALS (Menke et al., 2017; Bede and Hardiman, 2018; Kassubek et al., 2018; Baek et al., 2020). The reliability of other tract systems might be different from those of the CST (Marenco et al., 2006; Luque Laguna et al., 2020), leading to a limited transferability of results for optimal time intervals and sample sizes to other WM pathways. For the simulation, the same magnitude of time-independent measurement uncertainty was used for patients and healthy subjects, but this might not completely represent reality, since

it can be assumed that the quality of the patient data sets might be worse than that of the healthy subjects and thus, the measurement uncertainty would be higher for patients. Also, increasing disease severity during the course could further affect the quality and in that way the measurement uncertainty.

In summary, this study demonstrated that the statistical power of longitudinal DTI studies in ALS can be substantially increased by multiple scans of the same subject per session, especially in limited sample sizes. Such optimized study protocols can help to establish FA as an imaging biomarker in ALS, especially to monitor disease progression not only in the natural history but also under future disease-modifying therapeutic approaches.

Data availability statement

The raw data supporting the conclusions of this article will be made available by the authors, without undue reservation.

Ethics statement

The studies involving human participants were reviewed and approved by Ethical Committee of the University of Ulm, Germany. The patients/participants provided their written informed consent to participate in this study.

Author contributions

AB: study design, data analyis, simulations and interpretation of data, and drafting of the manuscript. DL and AL: interpretation of data and critical revision of the manuscript for intellectual content. H-PM and JK: study concept and design, interpretation of data, and critical revision of the manuscript for intellectual content. All authors contributed to the article and approved the submitted version.

Acknowledgments

Sonja Fuchs is thankfully acknowledged for her help in the acquisition of MRI data. We would like to thank the Ulm University Center for Translational Imaging MoMAN for its support.

Conflict of interest

The authors declare that the research was conducted in the absence of any commercial or financial relationships that could be construed as a potential conflict of interest.

Publisher's note

References

Agosta, F., Weiler, M., and Filippi, M. (2015). Propagation of pathology through brain networks in neurodegenerative diseases: from molecules to clinical phenotypes. *CNS Neurosci. Ther.* 21, 754–767. doi: 10.1111/cns.12410

Alruwaili, A. R., Pannek, K., Henderson, R. D., Gray, M., Kurniawan, N. D., and McCombe, P. A. (2019). Tract integrity in amyotrophic lateral sclerosis: 6–month evaluation using MR diffusion tensor imaging. *BMC Med. Imaging* 19:19. doi: 10.1186/s12880-019-0319-3

Baek, S.-H., Park, J., Kim, Y. H., Seok, H. Y., Oh, K.-W., Kim, H.-J., et al. (2020). Usefulness of diffusion tensor imaging findings as biomarkers for amyotrophic lateral sclerosis. *Sci. Rep.* 10:5199. doi: 10.1038/s41598-020-62049-0

Baldaranov, D., Khomenko, A., Kobor, I., Bogdahn, U., Gorges, M., Kassubek, J., et al. (2017). Longitudinal Diffusion Tensor Imaging-Based Assessment of Tract Alterations: An Application to Amyotrophic Lateral Sclerosis. *Front. Hum. Neurosci.* 11:567. doi: 10.3389/fnhum.2017.00567

Bede, P., and Hardiman, O. (2018). Longitudinal structural changes in ALS: a three time-point imaging study of white and gray matter degeneration. *Amyotroph. Lateral. Scler. Frontotemporal. Degener.* 19, 232–241. doi: 10.1080/21678421.2017.1407795

Behler, A., Kassubek, J., and Müller, H.-P. (2021). Age-Related Alterations in DTI Metrics in the Human Brain—Consequences for Age Correction. *Front. Aging Neurosci.* 13:682109. doi: 10.3389/fnagi.2021.682109

Behler, A., Müller, H., Del Tredici, K., Braak, H., Ludolph, A. C., Lulé, D., et al. (2022). Multimodal *in vivo* staging in amyotrophic lateral sclerosis using artificial intelligence. *Ann. Clin. Transl. Neurol.* 9, 1069–1079. doi: 10.1002/acn3.51601

Blain, C. R. V., Williams, V. C., Johnston, C., Stanton, B. R., Ganesalingam, J., Jarosz, J. M., et al. (2007). A longitudinal study of diffusion tensor MRI in ALS. *Amyotroph. Lateral. Scler.* 8, 348–355. doi: 10.1080/17482960701548139

Brett, M., Johnsrude, I. S., and Owen, A. M. (2002). The problem of functional localization in the human brain. *Nat. Rev. Neurosci.* 3, 243–249. doi: 10.1038/nrn756

Brooks, B. R., Miller, R. G., Swash, M., and Munsat, T. L. (2000). El Escorial revisited: Revised criteria for the diagnosis of amyotrophic lateral sclerosis. *Amyotroph. Lateral Scler. Other Motor Neuron Disord.* 1, 293–299. doi: 10.1080/146608200300079536

Cardenas-Blanco, A., Machts, J., Acosta-Cabronero, J., Kaufmann, J., Abdulla, S., Kollewe, K., et al. (2016). Structural and diffusion imaging versus clinical assessment to monitor amyotrophic lateral sclerosis. *Neuroimage Clin.* 11, 408–414. doi: 10.1016/j.nicl.2016.03.011

Cedarbaum, J. M., Stambler, N., Malta, E., Fuller, C., Hilt, D., Thurmond, B., et al. (1999). The ALSFRS-R: a revised ALS functional rating scale that incorporates assessments of respiratory function. *J. Neurol. Sci.* 169, 13–21. doi: 10.1016/S0022-510X(99)00210-5

Farrell, J. A. D., Landman, B. A., Jones, C. K., Smith, S. A., Prince, J. L., van Zijl, P. C. M., et al. (2007). Effects of signal-to-noise ratio on the accuracy and reproducibility of diffusion tensor imaging–derived fractional anisotropy, mean diffusivity, and principal eigenvector measurements at 1.5T. *J. Magn. Reson. Imaging* 26, 756–767. doi: 10.1002/jmri.21053

Kalra, S., Müller, H.-P., Ishaque, A., Zinman, L., Korngut, L., Genge, A., et al. (2020). A prospective harmonized multicenter DTI study of cerebral white matter degeneration in ALS. *Neurology* 95, e943–e952. doi: 10.1212/WNL.0000000000010235

Kassubek, J., and Müller, H.-P. (2020). Advanced neuroimaging approaches in amyotrophic lateral sclerosis: refining the clinical diagnosis. *Expert Rev. Neurother.* 20, 237–249. doi: 10.1080/14737175.2020.1715798

Kassubek, J., Müller, H.-P., Del Tredici, K., Brettschneider, J., Pinkhardt, E. H., Lule, D., et al. (2014). Diffusion tensor imaging analysis of sequential spreading of disease in amyotrophic lateral sclerosis confirms patterns of TDP-43 pathology. *Brain* 137, 1733–1740. doi: 10.1093/brain/awu090

Kassubek, J., Müller, H.-P., Del Tredici, K., Lulé, D., Gorges, M., Braak, H., et al. (2018). Imaging the pathoanatomy of amyotrophic lateral sclerosis in vivo: targeting a propagation-based biological marker. *J. Neurol. Neurosurg. Psychiatry* 89, 374–381. doi: 10.1136/jnnp-2017-316365

Kocar, T. D., Müller, H.-P., Ludolph, A. C., and Kassubek, J. (2021). Feature selection from magnetic resonance imaging data in ALS: a systematic review. *Ther. Adv. Chronic Dis.* 12:204062232110510. doi: 10.1177/20406223211051002

Koller, K., Rudrapatna, U., Chamberland, M., Raven, E. P., Parker, G. D., Tax, C. M. W., et al. (2021). MICRA: Microstructural image compilation with repeated acquisitions. *Neuroimage* 225:117406. doi: 10.1016/j.neuroimage.2020.117406

Koo, T. K., and Li, M. Y. (2016). A Guideline of Selecting and Reporting Intraclass Correlation Coefficients for Reliability Research. *J. Chiropr. Med.* 15, 155–163. doi: 10.1016/j.jcm.2016.02.012

Kunimatsu, A., Aoki, S., Masutani, Y., Abe, O., Hayashi, N., Mori, H., et al. (2004). The optimal trackability threshold of fractional anisotropy for diffusion tensor tractography of the corticospinal tract. *Magn. Reson. Med. Sci.* 3, 11–17. doi: 10.2463/mrms.3.11

Lewis, A. F., Myers, M., Heiser, J., Kolar, M., Baird, J. F., and Stewart, J. C. (2020). Test-retest reliability and minimal detectable change of corticospinal tract integrity in chronic stroke. *Hum. Brain Mapp.* 41, 2514–2526. doi: 10.1002/hbm.24961

Luque Laguna, P. A., Combes, A. J. E., Streffer, J., Einstein, S., Timmers, M., Williams, S. C. R., et al. (2020). Reproducibility, reliability and variability of FA and MD in the older healthy population: A test-retest multiparametric analysis. *Neuroimage Clin.* 26:102168. doi: 10.1016/j.nicl.2020.102168

Marenco, S., Rawlings, R., Rohde, G. K., Barnett, A. S., Honea, R. A., Pierpaoli, C., et al. (2006). Regional distribution of measurement error in diffusion tensor imaging. *Psychiatry Res. Neuroimaging* 147, 69–78. doi: 10.1016/j.pscychresns.2006.01.008

Menke, R. A. L., Agosta, F., Grosskreutz, J., Filippe, M., and Turner, M. R. (2017). Neuroimaging Endpoints in Amyotrophic Lateral Sclerosis. *Neurotherapeutics* 14, 11–23. doi: 10.1007/s13311-016-0484-9

Menke, R. A. L., Körner, S., Filippini, N., Douaud, G., Knight, S., Talbot, K., et al. (2014). Widespread grey matter pathology dominates the longitudinal cerebral MRI and clinical landscape of amyotrophic lateral sclerosis. *Brain* 137, 2546–2555. doi: 10.1093/brain/awu162

Müller, H.-P., Behler, A., Landwehrmeyer, G. B., Huppertz, H.-J., and Kassubek, J. (2021a). How to Arrange Follow-Up Time-Intervals for Longitudinal Brain MRI Studies in Neurodegenerative Diseases. *Front. Neurosci.* 15:682812. doi: 10.3389/fnins.2021.682812

Müller, H.-P., Lulé, D., Roselli, F., Behler, A., Ludolph, A. C., and Kassubek, J. (2021b). Segmental involvement of the corpus callosum in *C9orf72*-associated ALS: a tract of interest-based DTI study. *Ther. Adv. Chronic Dis.* 12:204062232110029. doi: 10.1177/20406223211002969

Müller, H.-P., Grön, G., Sprengelmeyer, R., Kassubek, J., Ludolph, A. C., Hobbs, N., et al. (2013). Evaluating multicenter DTI data in Huntington's disease on site specific effects: An ex post facto approach. *Neuroimage Clin.* 2, 161–167. doi: 10.1016/j.nicl.2012.12.005

Müller, H.-P., Süssmuth, S. D., Landwehrmeyer, G. B., Ludolph, A., Tabrizi, S. J., Kloppel, S., et al. (2011). Stability effects on results of diffusion tensor imaging analysis by reduction of the number of gradient directions due to motion artifacts: an application to presymptomatic Huntington's disease. *PLoS Curr.* 3:RRN1292. doi: 10.1371/currents.RRN1292

Müller, H.-P., Turner, M. R., Grosskreutz, J., Abrahams, S., Bede, P., Govind, V., et al. (2016). A large-scale multicentre cerebral diffusion tensor imaging study in amyotrophic lateral sclerosis. *J. Neurol. Neurosurg. Psychiatry* 87, 570–579. doi: 10.1136/jnnp-2015-311952

Müller, H.-P., Unrath, A., Huppertz, H.-J., Ludolph, A. C., and Kassubek, J. (2012). Neuroanatomical patterns of cerebral white matter involvement in different motor neuron diseases as studied by diffusion tensor imaging analysis. *Amyotroph. Lateral. Scler.* 13, 254–264. doi: 10.3109/17482968.2011.653571

Müller, H.-P., Unrath, A., Ludolph, A. C., and Kassubek, J. (2007). Preservation of diffusion tensor properties during spatial normalization by use of tensor imaging and fibre tracking on a normal brain database. *Phys. Med. Biol.* 52, N99–N109. doi: 10.1088/0031-9155/52/6/N01

Müller, H.-P., Unrath, A., Riecker, A., Pinkhardt, E. H., Ludolph, A. C., and Kassubek, J. (2009). Intersubject variability in the analysis of diffusion tensor images at the group level: fractional anisotropy mapping and fiber tracking techniques. *Magn. Reson. Imaging* 27, 324–334. doi: 10.1016/j.mri.2008.07.003

Münch, M., Müller, H.-P., Behler, A., Ludolph, A. C., and Kassubek, J. (2022). Segmental alterations of the corpus callosum in motor neuron disease: A DTI and texture analysis in 575 patients. *Neuroimage Clin.* 35:103061. doi: 10.1016/j.nicl.2022.103061

Palacios, E. M., Martin, A. J., Boss, M. A., Ezekiel, F., Chang, Y. S., Yuh, E. L., et al. (2017). Toward Precision and Reproducibility of Diffusion Tensor Imaging: A Multicenter Diffusion Phantom and Traveling Volunteer Study. *AJNR Am. J. Neuroradiol.* 38, 537–545. doi: 10.3174/ajnr.A5025

Pinto, M. S., Paolella, R., Billiet, T., Van Dyck, P., Guns, P.-J., Jeurissen, B., et al. (2020). Harmonization of Brain Diffusion MRI: Concepts and Methods. *Front. Neurosci.* 14:396. doi: 10.3389/fnins.2020.00396

Saccenti, E., Hendriks, M. H. W. B., and Smilde, A. K. (2020). Corruption of the Pearson correlation coefficient by measurement error and its estimation, bias, and correction under different error models. *Sci. Rep.* 10:438. doi: 10.1038/s41598-019-57247-4

Seo, Y., Rollins, N. K., and Wang, Z. J. (2019). Reduction of bias in the evaluation of fractional anisotropy and mean diffusivity in magnetic resonance diffusion tensor imaging using region-of-interest methodology. *Sci. Rep.* 9:13095. doi: 10.1038/s41598-019-49311-w

Teipel, S. J., Reuter, S., Stieltjes, B., Acosta-Cabronero, J., Ernemann, U., Fellgiebel, A., et al. (2011). Multicenter stability of diffusion tensor imaging measures: A European clinical and physical phantom study. *Psychiatry Res. Neuroimaging* 194, 363–371. doi: 10.1016/j.pscychresns.2011.05.012

Thieleking, R., Zhang, R., Paerisch, M., Wirkner, K., Anwander, A., Beyer, F., et al. (2021). Same Brain, Different Look? - The Impact of Scanner, Sequence and Preprocessing on Diffusion Imaging Outcome Parameters. *JCM* 10:4987. doi: 10.3390/jcm10214987

van den Berg, L. H., Sorenson, E., Gronseth, G., Macklin, E. A., Andrews, J., Baloh, R. H., et al. (2019). Revised Airlie House consensus guidelines for design and implementation of ALS clinical trials. *Neurology* 92, e1610–e1623. doi: 10.1212/WNL.0000000000007242

van Es, M. A., Hardiman, O., Chio, A., Al-Chalabi, A., Pasterkamp, R. J., Veldink, J. H., et al. (2017). Amyotrophic lateral sclerosis. *Lancet* 390, 2084–2098. doi: 10.1016/S0140-6736(17)31287-4

Venkatraman, V. K., Gonzalez, C. E., Landman, B., Goh, J., Reiter, D. A., An, Y., et al. (2015). Region of interest correction factors improve reliability of diffusion imaging measures within and across scanners and field strengths. *NeuroImage* 119, 406–416. doi: 10.1016/j.neuroimage.2015.06.078

Vollmar, C., O'Muircheartaigh, J., Barker, G. J., Symms, M. R., Thompson, P., Kumari, V., et al. (2010). Identical, but not the same: Intra-site and inter-site reproducibility of fractional anisotropy measures on two 3.0T scanners. *Neuroimage* 51, 1384–1394. doi: 10.1016/j.neuroimage.2010.03.046

Weir, J. P. (2005). Quantifying test-retest reliability using the intraclass correlation coefficient and the SEM. *J. Strength. Cond. Res.* 19, 231–240. doi: 10.1519/15184.1

Zhu, T., Liu, X., Gaugh, M. D., Connelly, P. R., Ni, H., Ekholm, S., et al. (2009). Evaluation of measurement uncertainties in human diffusion tensor imaging (DTI)-derived parameters and optimization of clinical DTI protocols with a wild bootstrap analysis. *J. Magn. Reson. Imaging* 29, 422–435. doi: 10.1002/jmri.21647

frontiers | Frontiers in Aging Neuroscience

TYPE Original Research
PUBLISHED 22 August 2022
DOI 10.3389/fnagi.2022.887498

OPEN ACCESS

EDITED BY
Parnetti Lucilla,
University of Perugia, Italy

REVIEWED BY
James C. Vickers,
University of Tasmania, Australia
Stefanie Flunkert,
QPS Austria (Austria), Austria
Samir Abu Rumeileh,
Martin Luther University of Halle-Wittenberg, Germany
Dag Aarsland,
King's College London, United Kingdom

*CORRESPONDENCE
Elisabeth Stögmann
elisabeth.stoegmann@meduniwien.ac.at

SPECIALTY SECTION
This article was submitted to Alzheimer's Disease and Related Dementias, a section of the journal Frontiers in Aging Neuroscience

RECEIVED 01 March 2022
ACCEPTED 04 July 2022
PUBLISHED 22 August 2022

CITATION
Parvizi T, König T, Wurm R, Silvaieh S, Altmann P, Klotz S, Rommer PS, Furtner J, Regelsberger G, Lehrner J, Traub-Weidinger T, Gelpi E and Stögmann E (2022) Real-world applicability of glial fibrillary acidic protein and neurofilament light chain in Alzheimer's disease. Front. Aging Neurosci. 14:887498. doi: 10.3389/fnagi.2022.887498

Real-world applicability of glial fibrillary acidic protein and neurofilament light chain in Alzheimer's disease

Tandis Parvizi[1], Theresa König[1], Raphael Wurm[1], Sara Silvaieh[1], Patrick Altmann[1], Sigrid Klotz[2], Paulus Stefan Rommer[1], Julia Furtner[3], Günther Regelsberger[2], Johann Lehrner[1], Tatjana Traub-Weidinger[4], Ellen Gelpi[2] and Elisabeth Stögmann[1]*

[1]Department of Neurology, Medical University of Vienna, Vienna, Austria, [2]Division of Neuropathology and Neurochemistry, Department of Neurology, Medical University of Vienna, Vienna, Austria, [3]Division of Neuroradiology and Musculoskeletal Radiology, Department of Biomedical Imaging and Image-Guided Therapy, Medical University of Vienna, Vienna, Austria, [4]Division of Nuclear Medicine, Department of Biomedical Imaging and Image-Guided Therapy, University of Vienna, Vienna, Austria

Background: Blood-based biomarkers may add a great benefit in detecting the earliest neuropathological changes in patients with Alzheimer's disease (AD). We examined the utility of neurofilament light chain (NfL) and glial fibrillary acidic protein (GFAP) regarding clinical diagnosis and differentiation between amyloid positive and negative patients. To evaluate the practical application of these biomarkers in a routine clinical setting, we conducted this study in a heterogeneous memory-clinic population.

Methods: We included 167 patients in this retrospective cross-sectional study, 123 patients with an objective cognitive decline [mild cognitive impairment (MCI) due to AD, *n* = 63, and AD-dementia, *n* = 60] and 44 age-matched

Abbreviations: Aβ, Amyloid-Beta; AD, Alzheimer's disease; ALS, Amyotrophic lateral sclerosis; APOE, Apolipoprotein E; AUC, Area under the curve; BDI-II, Beck Depression Inventory; CSF, Cerebrospinal fluid; CT, Computed tomography; CV, Coefficient of variation; DNA, Deoxyribonucleic acid; ELISA, Enzyme-linked immunosorbent; FLAIR, Fluid-attenuated inversion recovery; FTD, Frontotemporal dementia; GDS, Global Deterioration Scale; GFAP, Glial Fibrillary Acidic Protein; HC, Healthy controls; HIV, Human immunodeficiency virus; IATI, Innotest Amyloid Tau Index; IQR, Interquartile range; LBD, Lewy body dementia; MCI, Mild cognitive impairment; MMSE, Mini-Mental State Examination; MRI, Magnetic resonance imaging; MUV, Medical University of Vienna; NfL, Neurofilament light chain; NTBV, Neuropsychological Test Battery Vienna; NFT, Neurofibrillary tangles; NIA-AA, National Institute on Aging and Alzheimer's Association; PET, Positron emission tomography; PiB, Pittsburgh Compound B; pTau, Phosphorylated Tau; qPCR, Quantitative polymerase chain reaction; RDA, Research Documentation and Analysis; ROC, Receiver operating characteristic; SCD, Subjective cognitive decline; SIMOA, Single-molecule array; SNP, Single nucleotide polymorphisms; tTau, Total Tau; VVT-3.0, Vienna-Visuo-Constructional Test 3.0; WST, Wortschatztest.

healthy controls (HC). Cerebrospinal fluid (CSF) and plasma concentrations of NfL and GFAP were measured with single molecule array (SIMOA®) technology using the Neurology 2-Plex B kit from Quanterix. To assess the discriminatory potential of different biomarkers, age- and sex-adjusted receiver operating characteristic (ROC) curves were calculated and the area under the curve (AUC) of each model was compared.

Results: We constructed a panel combining plasma NfL and GFAP with known AD risk factors (Combination panel: age+sex+*APOE4*+GFAP+NfL). With an AUC of 91.6% (95%CI = 0.85–0.98) for HC vs. AD and 81.7% (95%CI = 0.73–0.90) for HC vs. MCI as well as an AUC of 87.5% (95%CI = 0.73–0.96) in terms of predicting amyloid positivity, this panel showed a promising discriminatory power to differentiate these populations.

Conclusion: The combination of plasma GFAP and NfL with well-established risk factors discerns amyloid positive from negative patients and could potentially be applied to identify patients who would benefit from a more invasive assessment of amyloid pathology. In the future, improved prediction of amyloid positivity with a noninvasive test may decrease the number and costs of a more invasive or expensive diagnostic approach.

KEYWORDS

Alzheimer's disease, dementia, biomarker, GFAP, NfL

Introduction

Alzheimer's disease (AD) represents a frequent neurodegenerative disorder, which leads to a progressive decline in cognitive functions (McKhann et al., 1984, 2011). Since the earliest neuropathological changes with the cerebral accumulation of amyloid-beta (Aβ) and neurofibrillary tangles (NFT) are expected to begin 10–20 years before clinical manifestation, the definition of AD shifted towards a rather biological construct with a better understanding of AD as a disease continuum (Sperling et al., 2011; Bateman et al., 2012; Jack et al., 2018). The diagnosis of early phases of AD is of particular interest concerning the inclusion in clinical trials and the development of disease-modifying therapies. Recent studies have been looking for a possibility to identify reliable blood-based biomarkers for an early AD diagnosis, as nowadays biomarker diagnosis is either performed with cost-intensive positron emission tomography (PET) imaging or invasive lumbar puncture.

The establishment of new and sensitive analytical methods may facilitate this approach. In comparison to the already established enzyme-linked immunosorbent assay (ELISA), the development of ultrasensitive single molecule arrays (SIMOA®) has improved the sensitivity of detecting proteins in the femtomolar range (Barro et al., 2020; Abdelhak et al., 2022).

Neurofilament light chain (NfL), a subunit of specific cytoskeletal proteins of neurons, represents a highly proposed biomarker for the detection of neuronal loss. Cerebrospinal fluid (CSF) and blood NfL levels are increased in the vast majority of neurological conditions with the highest concentrations in individuals with human immunodeficiency virus (HIV)-associated dementia, frontotemporal dementia (FTD), and amyotrophic lateral sclerosis (ALS; Bridel et al., 2019; Ashton et al., 2021). Furthermore, NfL is also elevated in AD and studies on autosomal dominant AD showed an elevation of NfL over a decade before the expected onset of clinical symptoms (Preische et al., 2019). Higher NfL levels are associated with cognitive decline, brain atrophy, and future disease progression in multiple neurological disorders (Mattsson et al., 2017; Lewczuk et al., 2018; Bridel et al., 2019). Additionally, several studies have indicated the use of NfL as a marker for treatment response (Olsson et al., 2019; Delcoigne et al., 2020).

Another promising biomarker for tracking neurodegenerative changes could be glial fibrillary acidic protein (GFAP), an intermediate filament protein of astrocytes. Neuropathological data have shown a close spatial relationship between reactive astrocytes and amyloid plaques in brain tissue of patients with AD (Verkhratsky et al., 2010; Kamphuis et al., 2014). Increased GFAP concentrations have been detected in CSF and blood of AD patients, with rising levels already at the preclinical phase of the disease, as well as an association between GFAP levels and cerebral amyloid pathology, brain atrophy, cognitive decline, and future conversion to dementia (Elahi et al., 2019; Oeckl et al., 2019; Asken et al., 2020;

Verberk et al., 2020; Benedet et al., 2021; Chatterjee et al., 2021; Cicognola et al., 2021). Furthermore, an elevation of GFAP has been observed in patients with traumatic brain injury, neuroinflammatory, and other neurodegenerative disorders including Lewy body dementia (LBD) and progranulin-associated FTD (Heller et al., 2020; Katisko et al., 2021; Zhu et al., 2021; Abdelhak et al., 2022; Chouliaras et al., 2022).

The aim of this study was to examine GFAP and NfL levels in CSF and plasma in various stages of the clinical AD continuum and to investigate the predictive value of these blood biomarkers in combination with well-established risk factors in relation to clinical diagnosis and amyloid positivity. Due to the fact, that most biomarker studies include a preselected population with stringent eligibility criteria, we aimed to evaluate the real-world application of these biomarkers in a relatively heterogenous population of memory-clinic outpatients.

Methods

Study population

One-hundred sixty-seven patients were enrolled in this retrospective study at the Memory Clinic of the Department of Neurology, Medical University of Vienna (MUV). As various patients with the main concern of subjective/objective cognitive decline are referred to our specialized memory clinic both by specialists and generalists, without a preselection, our patient cohort rather reflects a more heterogeneous study population and thus resembles more closely a real-world setting. Using two existing registries, the Dementia Registry RDA MUV (EK 1323/2018) and the BIOBANK MUV (EK 2195/2016), we identified 123 patients with a diagnosis along the clinical spectrum of cognitive decline, i.e., mild cognitive impairment (MCI, n = 63) due to AD and AD-dementia (n = 60). Additionally, 44 age-matched healthy controls (HC) were included. These participants were recruited from an unselected population of patients, that were administered to the Department of Neurology and received further neurological examination, including brain imaging and lumbar puncture, to rule out an underlying neurological disorder. The main diagnoses of these patient cohorts consisted of idiopathic cranial nerve palsies, headache syndromes, and somatic symptom disorders and showed no signs of a neurodegenerative disease or subjective/objective cognitive decline.

All 123 patients with an objective cognitive decline (MCI, AD) underwent a thorough standardized diagnostic examination including physical and neurological evaluation, neuropsychological testing, magnetic resonance imaging (MRI) of the brain, and basic laboratory testing. For a subset of patients, we extended our diagnosis with a biomarker-based approach. CSF analysis of established AD biomarkers [amyloid-beta 42 (Aβ42), total tau (tTau), and phosphorylated tau (pTau)] was available in 75 patients, amyloid-PET imaging was performed in 80 patients, and 60 patients underwent both diagnostic methods.

Diagnoses of MCI and dementia due to AD were based on the recommendation of the National Institute of Ageing and Alzheimer's Association (NIA-AA; Albert et al., 2011; McKhann et al., 2011). All 167 study participants were required to have a plasma EDTA sample stored in the Biobank MUV, for 103 study participants CSF samples were available as well.

The project was approved by the Ethics Committee of the Medical University of Vienna (EK 1965/2019) on November 28th, 2019.

Neuropsychological assessment

The Neuropsychological Test Battery Vienna (NTBV) was administered to assess cognitive function, including domains of attention, language, executive functioning, and episodic memory (Pusswald et al., 2013; Lehrner et al., 2015a). Adequate normative data from cognitively unimpaired individuals were available and z-scores for each variable were calculated and corrected for age, education, and sex. Screening of cognitive impairment consisted of Mini-Mental State Examination (MMSE), Global Deterioration Scale (GDS), and *Wortschatztest* (WST), a standardized vocabulary test providing an estimate of premorbid intelligence level (Schmidt and Metzler, 1992). Furthermore, the Vienna-Visuo-Constructional Test 3.0 (VVT-3.0) was applied to assess the visuo-constructive performance (Lehrner et al., 2015b). Depressive symptoms were measured *via* Beck Depression Inventory (BDI-II; Kühner et al., 2007).

APOE genotyping

Apolipoprotein E (*APOE*) genotyping was performed in 143 patients using quantitative polymerase chain reaction (qPCR) with TaqMan probes (Thermofisher) evaluating two single nucleotide polymorphisms (SNPs) in the *APOE* gene (rs429358 and rs7412). Each sample was tested for both SNPs in triplicates using 20 ng deoxyribonucleic acid (DNA). Allelic discrimination analysis was used to determine the *APOE* genotype of the study participants.

MR imaging

All patients underwent at least a T1-weighted MR sequence, a T2-weighted or a Fluid-attenuated inversion

recovery (FLAIR) MR sequence, and a diffusion-weighted MR sequence within the routine diagnostic setting for the evaluation of the extent and pattern of atrophy, the presence and degree of vascular lesions and to exclude other underlying pathologies causing cognitive decline and diffusion restricted areas.

Amyloid-PET imaging

Eighty patients underwent an amyloid-PET scan with [^{18}F] flutemetamol (n = 28) or [^{11}C] Pittsburgh compound-B (PiB, n = 52). Amyloid-PET imaging was performed on one of two possible PET scanner systems (Siemens Biograph 64 True Point, Erlangen, Germany or GE Advances PET, GE Healthcare Institute, Waukesha, Wisconsin, USA). All studies were performed under strictly controlled conditions. In short, either ∼400 MBq of [11C] PiB (in-house production according to previously published recommendations; Philippe et al., 2011) or 185 MBq of [18F] flutemetamol (Vizamyl®, GE Healthcare) were injected intravenously into a peripheral vein with starting image acquisition 40 min p.i. for [11C] PiB and 90 min p.i. for Vizamyl®, where the tracer accumulation in the brain is reaching the maximum. Subsequently, the image acquisition was performed for about 20 min following a computed tomography (CT) acquisition for attenuation correction using Siemens Biograph 64 True Point.

Scans were rated visually as positive or negative for the presence of amyloid pathology in the cortex by an experienced nuclear medicine physician according to the guidelines of the tracer manufacturers.

Fluid biomarkers

CSF was obtained by lumbar puncture between the L3/L4, L4/5, or L5/S1 intervertebral space, collected in polypropylene tubes and further stored at −20°C until biomarker analysis (as for Aβ42, pTau 181, and tTau), or immediately at −80°C for future research purposes (Teunissen et al., 2014; Duits et al., 2015). Levels of Aβ42, pTau 181, and tTau were measured with commercially available ELISA (Innotest hTAU-Ag, Innotest phosphoTAU 181p, Innotest beta-amyloid 1–42; Vanmechelen et al., 2000; Vanderstichele et al., 2009). The cut-off for these biomarkers were based on the manufacturer's recommendation (Aβ42 < 500 pg/ml, pTau 181 > 61 pg/ml, tTau > 300 pg/ml). From these measurements, Innotest Amyloid Tau Index (IATI) was calculated for each patient (measured as Aβ42/(240+1.18xtTau), reference values <1 pg/ml indicative of AD pathology, >1 pg/ml—normal; Hulstaert et al., 1999; Tabaraud et al., 2012).

EDTA plasma was collected through venepuncture and stored at −80°C in our local biobank. Concentrations of NfL and GFAP were quantified with an ultrasensitive single molecule array (SIMOA®) using the Neurology 2-Plex B kit from Quanterix in CSF and plasma. Detailed analyses are described elsewhere (Altmann et al., 2020). In short, equilibrated calibrators, samples, and controls were diluted (1:4 for plasma and 1:100 for CSF) and incubated with detector and paramagnetic reagents provided by the manufacturer. Streptavidin SS-galactosidase was added to each well before samples were transferred to the Quanterix SR-X analyzer for measurement of protein levels. All samples were analyzed as duplicates and all assay materials were obtained from the same kit lot. Intra-assay coefficient of variation (CV) was <12% for GFAP Plasma, <13% for GFAP CSF, <9% for NfL Plasma and <8% for NfL CSF. Inter-assay CV for two samples measured repeatedly on 10 plates was well acceptable (<12% for GFAP Plasma, <14% GFAP CSF, <8% NfL Plasma and <10% NfL CSF). Five patient samples were excluded from further analysis due to a high CV (>20%) and therefore not included in this study.

Amyloid positivity

Amyloid positivity was defined by CSF (IATI < 1) and/or amyloid-PET imaging. In cases where both examinations were available or discordant results were obtained, amyloid status was determined by PET.

Statistical analysis

Data are presented as n (percent) or median (interquartile range) as appropriate. Testing for differences between groups was performed using the chi-square test, the Mann-Whitney-U-test, or the Kruskal-Wallis-test. The correlation was assessed using Spearman's rank correlation coefficient. To evaluate the discriminatory performance of the biomarkers assessed herein, the cohort was split into pairs of two diagnoses (e.g., AD and HC) and the response variable was coded as existing for the more severe diagnosis (i.e., MCI when assessing MCI vs. HC). Next, a baseline model consisting of sex, age, and *APOE4* status was constructed using logistic regression. A receiver operating characteristic (ROC) curve was plotted and the area under the curve (AUC) was measured. Optimal cutoffs were calculated using Youden's J-Statistic (Youden, 1950). The baseline model was then supplemented by either level of plasma GFAP, plasma NfL, or both, and the AUC of each model was compared using DeLong's test for correlated AUC curves (DeLong et al., 1988). A p-value of <0.05 was interpreted as statistically significant. All calculations were performed in R (Version 4.0.4) and the pROC package was used for ROC calculations (Robin et al., 2011).

10.3389/fnagi.2022.887498

Results

Participant characteristics

Demographic and clinical characteristics are listed in Table 1.

We observed no significant difference in sex distribution between the groups, while HC were significantly younger than the two patient groups ($p < 0.01$ for HC vs. MCI and AD). MMSE decreased significantly with progressing disease with the lowest score in the AD group ($p < 0.001$). Data of *APOE4* carriership (carriers of at least one *APOE4* allele) was available for 143 patients, with the highest occurrence of *APOE4* alleles in AD patients (33 of 53 patients, 62.3%), compared to 22 out of 54 patients in the MCI group (40.7%). A chi-square test of independence was performed to examine the relationship between the *APOE4* status and the diagnosis. As can be seen by the frequencies cross-tabulated in Table 1, there was a significant relationship between *APOE4* status and diagnosis ($X^2_{(2,N=167)} = 8.5078$, $p < 0.05$.

For a subset of patients ($n = 75$) CSF analysis of established AD biomarkers was available (Aβ42, tTau, pTau). While CSF tTau and pTau levels increased significantly with progression from MCI to AD ($p < 0.001$ and $p < 0.05$, respectively), the difference in Aβ42 concentration between MCI and AD reached no statistical significance. Accordingly, the IATI value was significantly lower in the AD group than in the MCI group ($p < 0.001$).

Amyloid-PET imaging was performed in 39 of 63 patients with MCI (61.9%) and 41 of 60 patients with AD (68.3%). Positive amyloid-PET imaging was significantly higher in AD patients with a total of 39 (95.1%) positive subjects in AD, compared to 23 patients with MCI (59%, $p < 0.001$). Taken together, biomarker data (CSF analysis or PET imaging) was available for 95 patients (56.9%), which demonstrated signs of amyloid pathology in a total of 76 patients (80%), determined by CSF IATI and/or amyloid-PET imaging as outlined previously.

Concentration of GFAP and NfL in plasma and CSF

Plasma GFAP displayed a gradual increase along the three cohorts, with the highest concentration in patients with AD (median 181.9 pg/ml, IQR 129.6, 269.6, Table 1 and Figure 1A). While plasma levels were significantly higher in patients with MCI vs. HC and AD vs. HC ($p < 0.001$), we observed no significant difference of plasma GFAP levels between MCI vs. AD.

Plasma NfL performed similarly to GFAP regarding the difference in concentrations between MCI vs. HC and AD vs. HC ($p < 0.001$, Table 1 and Figure 1B). In contrast to plasma GFAP, NfL levels showed a significant discrimination between MCI vs. AD ($p < 0.05$).

For 103 patients, CSF samples in our local biobank were available. Levels of CSF NfL increased gradually, with the lowest concentration in the HC group (median 584.1 pg/ml, IQR 449.6, 832.8) and the highest concentration in the AD group (median 1,559 pg/ml, IQR 1,026.6, 2,513.9).

On the contrary, CSF GFAP presented the lowest concentration in the MCI group (median 8,946.2 pg/ml, IQR 7,028.8, 13,842.7), followed by HC (median 11,145.3 pg/ml, IQR 6,980.5, 14,373.8) and AD (median 13,663.5 pg/ml, IQR 9,945.4, 21,059.1).

Both CSF biomarker levels allowed a good distinction between AD vs. HC and MCI vs. AD (NfL $p < 0.001$ for both measurements, GFAP $p < 0.05$ and $p < 0.01$, respectively), while a significant differentiation between HC vs. MCI could not be demonstrated.

In a logistic regression model including GFAP or NfL as the dependent variable and age and diagnosis (with HC as the comparator) as predictors, age was significantly associated with GFAP ($B = 4.2$, $p < 0.001$) and NfL ($B = 0.4$, $p < 0.001$), while diagnosis remained significant in both models.

Using Spearman correlation coefficient, the correlation of NfL and GFAP in CSF and plasma were analyzed (Figures 2A,B). Correlation between NfL in CSF and plasma performed better ($R = 0.64$, $p < 0.001$, Figure 2A) than the correlation of GFAP in CSF and plasma ($R = 0.4$, $p < 0.001$, Figure 2B).

Diagnostic value of plasma GFAP and NfL in combination with known AD risk factors

To assess the clinical utility of GFAP and NfL in plasma, particularly in distinguishing healthy controls from patients with cognitive complaints (MCI and AD) and potentially predicting cerebral amyloid status, ROC analyses were performed and adjusted for sex and age. We constructed a diagnostic panel, consisting of well-established risk factors such as age, sex (defined as female > male), and *APOE4* carriership (defined as carrying at least one copy of the *APOE4* allele; i.e., age+sex+*APOE4* panel) and compared it with a panel of age, sex, *APOE4* carriership added by plasma NfL and plasma GFAP, called combination panel (i.e., age+sex+*APOE4*+GFAP+NfL panel, Figures 3A–D). Additionally, we analyzed each biomarker separately to evaluate the potential benefit of GFAP or NfL alone (i.e., age+sex+*APOE4*+GFAP panel and age+sex+*APOE4*+NfL panel).

When using the age+sex+*APOE4* panel alone, we calculated an AUC of 73.4% (95%CI = 0.63–0.84) for HC vs. AD (Figure 3A), AUC of 64.6% (95% CI = 0.53–0.76) for HC vs.

TABLE 1 Demographics and clinical characteristics.

	HC ($n = 44$)	MCI ($n = 63$)	AD ($n = 60$)	p value
Sex (f)	24 (54.5%)	29 (46%)	36 (60%)	$p = 0.294$
Age	61.2 (55.8, 69.5)	69.9 (59.3, 77.8)	69 (61.3, 75)	$p < 0.01$
MMSE	n.a.	27 (25, 28)	20 (14, 23)	$p < 0.001$
APOE4 carrier n/ total n (%)	12/36 (33.3%)	22/54 (40.7%)	33/53 (62.3%)	$p < 0.05$
CSF Aβ42 (pg/ml)*	n.a.	354 (248, 479.5)	332.5 (231.8, 454.8)	$p = 0.322$
CSF tTau (pg/ml)*	n.a.	310 (188, 504.5)	600.5 (404.3, 1106.8)	$p < 0.001$
CSF pTau (pg/ml)*	n.a.	53 (33.5, 79.5)	77.5 (51.3, 96.3)	$p < 0.05$
CSF IATI (pg/ml)*	n.a.	0.6 (0.3, 0.8)	0.3 (0.2, 0.5)	$p < 0.001$
Amyloid-PET positivity n/total n (%)	n.a.	23/39 (59%)	39/41 (95.1%)	$p < 0.001$
Amyloid positivity n/total n (%)**	n.a.	29/46 (63%)	47/49 (95.9%)	$p < 0.001$
Plasma NfL (pg/ml)	8.1 (5.9, 12.2)	12. 9 (8.5, 20.4)	15.5 (11.8, 23.2)	$p < 0.001$
Plasma GFAP (pg/ml)	79 (53.7, 120.6)	167.5 (93.8, 256.3)	181.9 (129.6, 269.6)	$p < 0.001$
CSF NfL (pg/ml)***	584.1 (449.6, 832.8)	807.7 (507.7, 1103.2)	1,559 (1026.6, 2513.9)	$p < 0.001$
CSF GFAP (pg/ml)***	11,145.3 (6980.5, 14373.8)	8,946.2 (7028.8, 13842.7)	13,663.5 (9945.4, 21059.1)	$p < 0.01$

Data are presented as the median and interquartile range (IQR, 25th–75th percentile) or n (%). Demographic and clinical differences were measured using the Kruskal-Wallis test or the chi-square tests as appropriate. *CSF AD biomarkers (Aβ42, tTau, pTau, IATI) were available for 75 patients (37 MCI, 38 AD). **Amyloid positivity was defined by CSF IATI <1 pg/ml and/or positive amyloid-PET imaging. ***CSF NfL and GFAP levels were analyzed in 103 patients (36 HC, 30 MCI, 37 AD). HC, healthy controls; *MCI*, mild cognitive impairment; *AD*, Alzheimer's disease; *f*, female; *MMSE*, mini-mental state examination; *CSF*, cerebrospinal fluid; *Aβ42*, amyloid-beta 42; *tTau*, total tau; *pTau*, phosphorylated tau; *IATI*, Innotest Amyloid Tau Index; *NfL*, neurofilament light chain; *GFAP*, glial fibrillary acidic protein; *n.a.*, not available; *NfL*, neurofilament light chain; *GFAP*, glial fibrillary acidic protein.

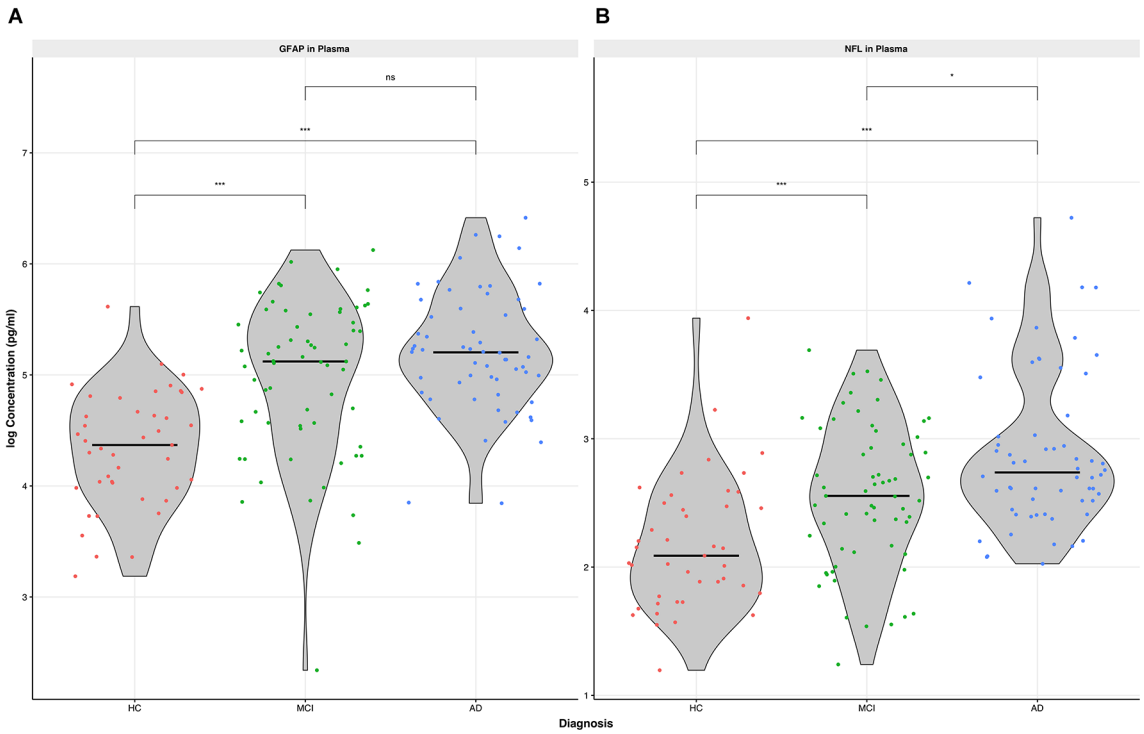

FIGURE 1
Concentration of GFAP **(A)** and NfL **(B)** in plasma among the three cohorts (HC, MCI, AD). Differences of biomarker concentration were calculated using Kruskal-Wallis Test, p value is displayed as *$p < 0.05$, ***$p < 0.001$, *ns*, not significant. *HC*, healthy controls; *MCI*, mild cognitive impairment; *AD*, Alzheimer's disease; *CSF*, cerebrospinal fluid; *NfL*, neurofilament light chain; *GFAP*, glial fibrillary acidic protein.

MCI (Figure 3B) and an AUC of 66.4% (95%CI = 0.56–0.77) for MCI vs. AD (Figure 3C). Regarding the diagnostic accuracy in predicting amyloid status and the distinction of amyloid-negative (Aβ-) from amyloid-positive (Aβ+) individuals, the AUC was 75% (95% CI = 0.62–0.88, Figure 3D).

By adding NfL to the panel (age+sex+*APOE4*+NfL panel), the discrimination between HC vs. AD reached a significantly higher AUC of 84.5% (95%CI = 0.76–0.93, Figure 3A) compared to the age+sex+*APOE4* panel alone (p = 0.003), while the other calculations failed to achieve significantly better results (HC vs. MCI AUC 68.8%, 95%CI = 0.58–0.80, MCI vs. AD

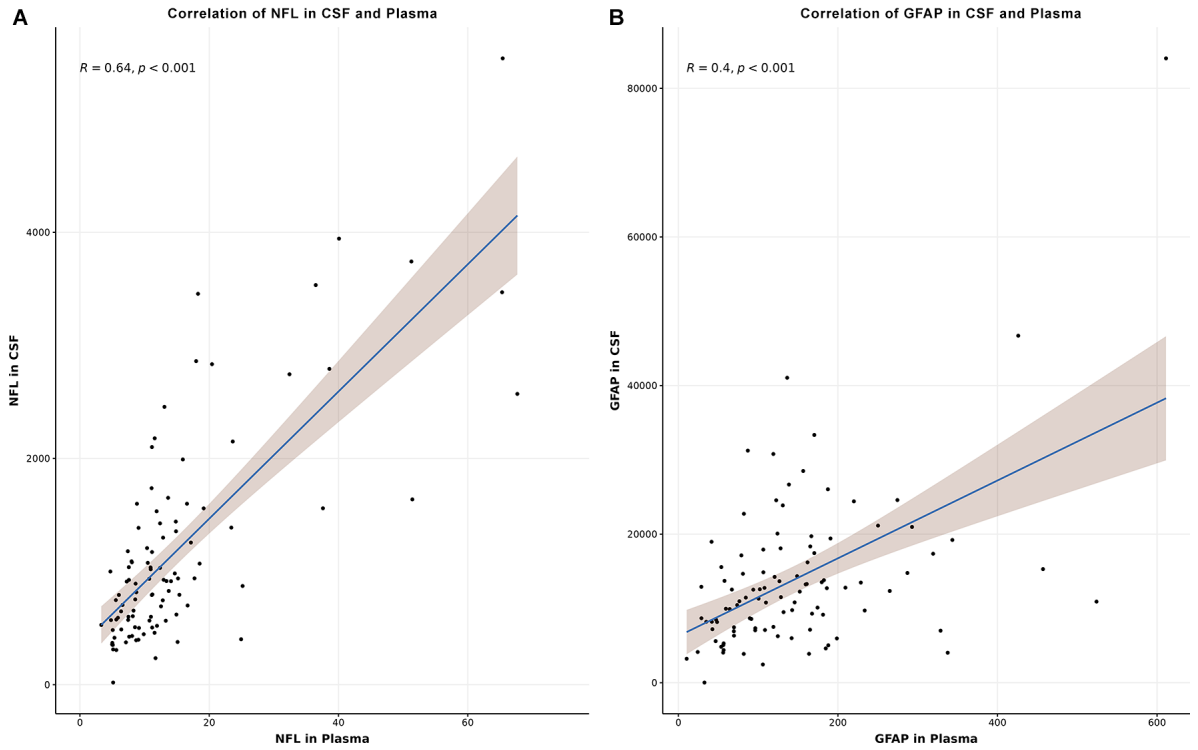

FIGURE 2
Correlation of NfL in CSF and plasma **(A)** and GFAP in CSF and plasma **(B)**. Correlation was assessed using Spearman's rank correlation coefficient. *CSF*, cerebrospinal fluid; *NfL*, neurofilament light chain; *GFAP*, glial fibrillary acidic protein.

AUC 72%, 95%CI = 0.63–0.82), amyloid positivity (AUC 76.5%, 95%CI = 0.61–0.87, Figures 3B–D).

The combination of GFAP with the age+sex+*APOE4* panel (age+sex+*APOE4*+GFAP panel) obtained an AUC of 91.3% (95%CI = 0.85–0.97) for HC vs. AD ($p < 0.001$, Figure 3A) and AUC of 81.3% (95% CI = 0.72–0.90) for HC vs. MCI ($p < 0.01$, Figure 3B) compared to the age+sex+*APOE4* panel. The prediction of amyloid positivity demonstrated an AUC of 86% (95%CI = 0.70–0.97, Figure 3D), but missed statistical significance as well as the differentiation between MCI vs. AD (AUC 66.7%, 95%CI = 0.57–0.77, Figure 3C).

When combining the two biomarkers with the age+sex+*APOE4* panel (combination panel: age+sex+*APOE4*+GFAP+NfL), the AUC of HC vs. AD reached 91.6% (95%CI = 0.85–0.98, $p < 0.001$, Figure 3A), AUC of HC vs. MCI 81.7% (95%CI = 0.73–0.90, $p < 0.01$, Figure 3B) and for amyloid positivity 87.5% (95%CI = 0.73–0.96, $p < 0.05$, Figure 3D), therefore, significantly outperforming the age+sex+*APOE4* panel alone. Similar to the other two panels (age+sex+*APOE4*+GFAP panel and age+sex+*APOE4*+NfL panel), the combination panel could not improve the distinction between MCI vs. AD (AUC 72.3%, 95%CI = 0.63–0.82, Figure 3C).

Discussion

In this outpatient memory clinic-based study, we examined the performance of two promising biomarkers of neurodegeneration and neuroinflammation, NfL, and GFAP, for the diagnostic work-up of patients along the continuum of AD-related cognitive decline. We aimed to develop a practical and reproducible model for a quick and accurate patient at-risk identification in a routine clinical practice.

A combination of demographic factors with *APOE4* status and blood biomarkers, such as GFAP and NfL, might offer a reliable differentiation between healthy controls and patients with an objective cognitive decline, particularly between healthy controls and patients with AD. In terms of predicting amyloid positivity in a cognitively impaired cohort, an integrated approach of history and blood analysis could also serve as a feasible and accessible tool, especially in screening those patients, who might need a more detailed and effortful diagnostic approach. By additional assessment of these two plasma biomarkers, the diagnostic accuracy as well as the prediction of cerebral amyloid accumulation could be majorly improved. Interestingly, this effect was more pronounced for plasma GFAP than plasma NfL. This could be explained by the fact, that GFAP seems to be a marker of the earliest AD

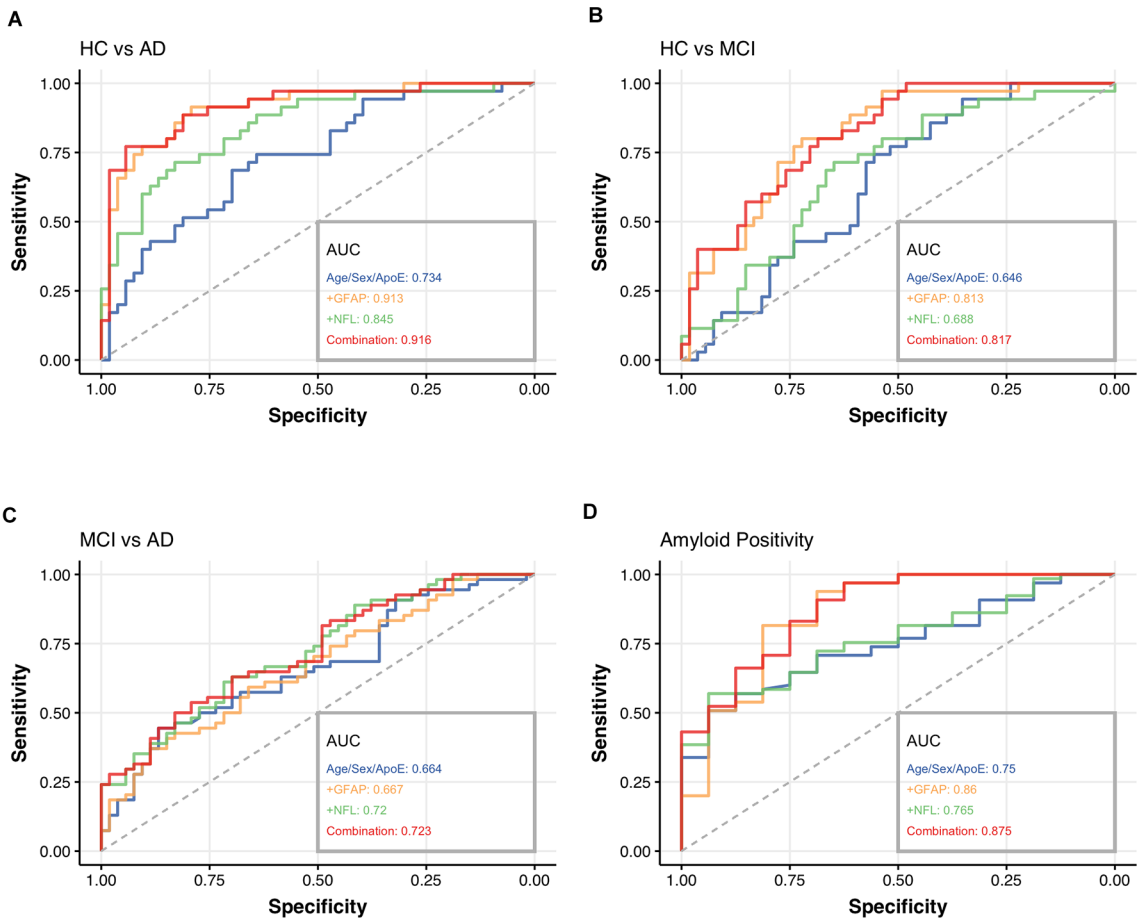

FIGURE 3
Receiver operating characteristic (ROC) curves for the diagnostic performance in distinguishing HC from AD **(A)**, HC from MCI **(B)**, MCI from AD **(C)**, the differentiation between amyloid positive and negative patients in our cohort **(D)**. The area under the curve (AUC) of each model was compared using DeLong's test for correlated AUC curves. The four panels analyzed were called age+sex+*APOE4* (blue), GFAP+ (age+sex+*APOE4*+GFAP, orange), NfL+ (age+sex+*APOE4*+NfL, green), and Combination panel (age+sex+*APOE4*+GFAF+NfL, red) in this figure. *HC*, healthy controls; *MCI*, mild cognitive impairment; *AD*, Alzheimer's disease; *NfL*, neurofilament light chain; *GFAP*, glial fibrillary acidic protein; *AUC*, area under the curve.

pathology with an association between GFAP levels and amyloid load, while NfL could be more useful in terms of disease monitoring and progression (Verberk et al., 2021; Ebenau et al., 2022). Unfortunately, for discriminating the disease states of MCI and AD, none of the three biomarker-based panels could add a significant benefit to the age+sex+*APOE4* panel. However, due to the better understanding of AD as a continuum, this clear distinction is getting more and more ambiguous (Jack et al., 2018).

Focusing on plasma GFAP alone, its levels showed a gradual increase along the three cohorts, with the highest concentration in patients with AD, thereby allowing a good biological interpretation of a gradual rise of this biomarker along the progressing neuropathological process. The most prominent discrimination was achieved between HC and patients with an objective cognitive decline (MCI and AD). However, in contrast to NfL alone, plasma GFAP could not differentiate between MCI vs. AD.

Regarding CSF biomarkers in our cohort, we found the highest concentration of CSF GFAP in patients with AD followed by the HC group and the lowest concentration in MCI, therefore, these results must be interpreted cautiously. CSF NfL demonstrated a gradual increase over the three cohorts with the lowest levels in HC and the highest in AD. Nevertheless, both measurements—CSF GFAP and CSF NfL—allowed a good discrimination between HC and AD as well as MCI and AD, with better results for CSF NfL. The concentration of NfL in CSF and plasma correlated well with each other, which is in line with already published data (Kuhle et al., 2016; Rojas et al., 2016; Mattsson et al., 2017), suggesting that plasma levels might be considered as an acceptable proxy for CSF levels. In contrast to NfL, levels of GFAP in CSF and plasma showed

a lower correlation, which was already described by another study (Oeckl et al., 2019). Recently published data indicated higher effect sizes of the increase of plasma GFAP compared to CSF GFAP and a more accurate distinction between Aβ+ and Aβ- individuals for plasma GFAP. Potential explanations could be preanalytical factors or different clearance mechanisms regarding the disrupted blood-brain barrier in patients with AD (Benedet et al., 2021). Thus, further investigations are needed to better determine the role of CSF GFAP and its correlation with GFAP levels in blood in these patient cohorts.

Diagnosis of the early phases of AD is crucial in regard to detecting patients at risk as early as possible in the development of the neuropathological cascade. Furthermore, due to the limited resources of *in vivo* biomarker testing in the general population, the establishment of a screening tool to select those patients, who would benefit from a more thorough testing, is of great importance. Besides the abnormal aggregation of Aβ peptide and tau protein, neuroinflammation and neurodegeneration represent major components in the pathophysiology of AD (Jack et al., 2018). In recent years, the role of neuroinflammation in the pathogenesis of AD has been increasingly focused on in the literature. Neuropathological data have shown a close spatial relationship between Aβ plaques and reactive astrocytes, which along with microglia, may trigger a pro-inflammatory cascade and eventually lead to neurodegeneration, which in turn activates astrocytes and microglia (Frost and Li, 2017; Garwood et al., 2017). As a cytoskeletal component of astrocytes, GFAP could serve as a promising biomarker reflecting astrocytic activation and proliferation during the neurodegenerative processes, including AD, particularly in its earliest stages (Chatterjee et al., 2021; Verberk et al., 2021). On the other hand, NfL represents a rather unspecific biomarker for neurodegeneration, as it is released by axonal damage in multiple neurological disorders (Forgrave et al., 2019; Thebault et al., 2020). While the importance of NfL as a blood-based biomarker has been already reported in several studies (Mattsson et al., 2017, 2019; Benedet et al., 2019), the significance of GFAP is currently still evolving. To our knowledge, only a few studies have evaluated the combination of GFAP with other biomarkers so far and presented the utility of plasma GFAP not just in discriminating healthy controls from patients with AD but also in distinguishing Aβ+ from Aβ- individuals (Oeckl et al., 2019; Asken et al., 2020; Verberk et al., 2020). Furthermore, higher GFAP levels have been associated with an increased risk for future progression to dementia and a steeper cognitive decline (Cicognola et al., 2021; Verberk et al., 2021).

Regarding the heterogeneity of AD pathology, a panel of well-combined blood-based biomarkers could aid in early detection as well as disease monitoring in the future. Emerging data have proposed plasma-derived pTau 181 and pTau 217 as highly specific biomarkers for AD pathology, which are currently investigated in ongoing studies (Moscoso et al., 2020; Rodriguez et al., 2020; Thijssen et al., 2021). Additional biomarkers, such as GFAP and NfL, could on one side potentially aid in detecting these patients at risk early in the neuropathological cascade and on the other side give further information about disease progression.

While our study population is rather heterogeneous, i.e., more closely resembles a real-world setting, where some patients will not undergo biomarker testing for various reasons, we believe that this adds to the existing literature and confirms the practical usefulness of these biomarkers. As patients undergo a detailed history taking, neurological examination, and blood sampling at the first patient visit, the collection of plasma samples for further biomarker analysis may be easily implemented. Since *APOE* genotyping can be derived from these blood samples and performed in-house in a quick and inexpensive manner, we have added this marker to our proposed panel. In a routine memory clinical setting, the analysis of a panel of blood-derived markers in combination with known risk factors could be of great value concerning the identification of those patients at risk who would need further biomarker testing. This approach could further substantially reduce the number of patients who would otherwise undergo expensive PET imaging or invasive lumbar puncture.

Limitations

Due to the retrospective nature of this study, established AD biomarkers were not available for the whole study cohort. Positive amyloid status and *APOE4* carriership were significantly less common in the MCI group, which might lead to the notion, that at least some of the MCI patients were not along the AD continuum. Since the patients in the HC group were enrolled based on their clinical performance, we cannot exclude that some of these patients had an underlying AD pathology. Healthy controls were significantly younger than the patient groups, which might influence the results of these biomarkers and their corresponding analysis. To counteract this potential bias in our data, ROC analyses were adjusted for sex and age.

Conclusion

Blood-based biomarkers for AD may represent a valuable complementary tool for clinical diagnosis and patient management in the near future. We suggest that plasma GFAP could aid in a better distinction of patients along different predementia stages and that the combination of GFAP and NfL plasma levels with conventional risk factors could serve as a good "at-risk" model for selecting those patients, who might need a more invasive or expensive diagnostic approach.

Data availability statement

The raw data supporting the conclusions of this article will be made available by the authors, without undue reservation.

Ethics statement

The studies involving human participants were reviewed and approved by Ethics Committee of the Medical University of Vienna. Written informed consent for participation was not required for this study in accordance with the national legislation and the institutional requirements.

Author contributions

TP, RW, and ES devised the protocol. TP collected and managed the data with contribution of RW, SS, and ES. TP and TK performed SIMOA analyses in CSF and plasma. TP and RW performed the statistical analysis. TP and ES interpreted the data and prepared the manuscript. RW, TK, PR, SK, EG, PA, TT-W, and JF provided feedback and major contribution to the manuscript. All authors contributed to the article and approved the submitted version.

Acknowledgments

We would like to thank the patients and their families whose help and participation made this work possible. In addition, we thank contributors who collected samples used in this study.

Conflict of interest

The authors declare that the research was conducted in the absence of any commercial or financial relationships that could be construed as a potential conflict of interest.

Publisher's note

References

Abdelhak, A., Foschi, M., Abu-Rumeileh, S., Yue, J. K., D'Anna, L., Huss, A., et al. (2022). Blood GFAP as an emerging biomarker in brain and spinal cord disorders. *Nat. Rev. Neurol.* 18, 158–172. doi: 10.1038/s41582-021-00616-3

Albert, M. S., DeKosky, S. T., Dickson, D., Dubois, B., Feldman, H. H., Fox, N. C., et al. (2011). The diagnosis of mild cognitive impairment due to Alzheimer's disease: recommendations from the national institute on aging-Alzheimer's association workgroups on diagnostic guidelines for Alzheimer's disease. *Alzheimers Dementia* 7, 270–279. doi: 10.1016/j.jalz.2011.03.008

Altmann, P., Leutmezer, F., Zach, H., Wurm, R., Stattmann, M., Ponleitner, M., et al. (2020). Serum neurofilament light chain withstands delayed freezing and repeated thawing. *Sci. Rep.* 10:19982. doi: 10.1038/s41598-020-77098-8

Ashton, N. J., Janelidze, S., Khleifat, A. A., Leuzy, A., van der Ende, E. L., Karikari, T. K., et al. (2021). A multicentre validation study of the diagnostic value of plasma neurofilament light. *Nat. Commun.* 12:3400. doi: 10.1038/s41467-021-23620-z

Asken, B. M., Elahi, F. M., Joie, R. L., Strom, A., Staffaroni, A. M., Lindbergh, C. A., et al. (2020). Plasma glial fibrillary acidic protein levels differ along the spectra of amyloid burden and clinical disease stage. *J. Alzheimers Dis.* 78, 265–276. doi: 10.3233/JAD-200755

Barro, C., Chitnis, T., and Weiner, H. L. (2020). Blood neurofilament light: a critical review of its application to neurologic disease. *Ann. Clin. Transl. Neurol.* 7, 2508–2523. doi: 10.1002/acn3.51234

Bateman, R. J., Xiong, C., Benzinger, T. L. S., Fagan, A. M., Goate, A., Fox, N. C., et al. (2012). Clinical and biomarker changes in dominantly inherited Alzheimer's disease. *New Engl. J. Med.* 367, 795–804. doi: 10.1056/NEJMoa1202753

Benedet, A. L., Ashton, N. J., Pascoal, T. A., Leuzy, A., Mathotaarachchi, S., Kang, M. S., et al. (2019). Plasma neurofilament light associates with Alzheimer's disease metabolic decline in amyloid-positive individuals. *Alzheimers Dementia (Amst)* 11, 679–689. doi: 10.1016/j.dadm.2019.08.002

Benedet, A. L., Milà-Alomà, M., Vrillon, A., Ashton, N. J., Pascoal, T. A., Lussier, F., et al. (2021). Differences between plasma and cerebrospinal fluid glial fibrillary acidic protein levels across the Alzheimer disease continuum. *JAMA Neurol.* 78, 1471–1483. doi: 10.1001/jamaneurol.2021.3671

Bridel, C., van Wieringen, W. N., Zetterberg, H., Tijms, B. M., Teunissen, C. E., the NFL Group (2019). Diagnostic value of cerebrospinal fluid neurofilament light protein in neurology. *JAMA Neurol.* 76, 1035–1048. doi: 10.1001/jamaneurol.2019.1534

Chatterjee, P., Pedrini, S., Stoops, E., Goozee, K., Villemagne, V. L., Asih, P. R., et al. (2021). Plasma glial fibrillary acidic protein is elevated in cognitively normal older adults at risk of Alzheimer's disease. *Transl. Psychiatry* 11:27. doi: 10.1038/s41398-020-01137-1

Chouliaras, L., Thomas, A., Malpetti, M., Donaghy, P., Kane, J., Mak, E., et al. (2022). Differential levels of plasma biomarkers of neurodegeneration in Lewy body dementia, Alzheimer's disease, frontotemporal dementia and progressive supranuclear palsy. *J. Neurol. Neurosurg. Psychiatry* 93, 651–658. doi: 10.1136/jnnp-2021-327788

Cicognola, C., Janelidze, S., Hertze, J., Zetterberg, H., Blennow, K., Mattsson-Carlgren, N., et al. (2021). Plasma glial fibrillary acidic protein detects Alzheimer pathology and predicts future conversion to Alzheimer dementia in patients with mild cognitive impairment. *Alzheimers Res. Ther.* 13:68. doi: 10.1186/s13195-021-00804-9

Delcoigne, B., Manouchehrinia, A., Barro, C., Benkert, P., Michalak, Z., Kappos, L., et al. (2020). Blood neurofilament light levels segregate treatment effects in multiple sclerosis. *Neurology* 94, e1201–e1212. doi: 10.1212/WNL.0000000000009097

DeLong, E. R., DeLong, D. M., and Clarke-Pearson, D. L. (1988). Comparing the areas under two or more correlated receiver operating characteristic curves: a nonparametric approach. *Biometrics* 44, 837–845.

Duits, F. H., Prins, N. D., Lemstra, A. W., Pijnenburg, Y. A. L., Bouwman, F. H., Teunissen, C. E., et al. (2015). Diagnostic impact of CSF biomarkers for

Alzheimer's disease in a tertiary memory clinic. *Alzheimers Dement.* 11, 523–532. doi: 10.1016/j.jalz.2014.05.1753

Ebenau, J. L., Pelkmans, W., Verberk, I. M. W., Verfaillie, S. C. J., van den Bosch, K. A., van Leeuwenstijn, M., et al. (2022). Association of CSF, plasma and imaging markers of neurodegeneration with clinical progression in people with subjective cognitive decline. *Neurology* 98, e1315–e1326. doi: 10.1212/WNL.0000000000200035

Elahi, F. M., Casaletto, K. B., Joie, R. L., Walters, S. M., Harvey, D., Wolf, A., et al. (2019). Plasma biomarkers of astrocytic and neuronal dysfunction in early- and late-onset Alzheimer's disease. *Alzheimers Dementia* 16, 681–695. doi: 10.1016/j.jalz.2019.09.004

Forgrave, L. M., Ma, M., Best, J. R., and DeMarco, M. L. (2019). The diagnostic performance of neurofilament light chain in CSF and blood for Alzheimer's disease, frontotemporal dementia and amyotrophic lateral sclerosis: a systematic review and meta-analysis. *Alzheimers Dementia (Amst)* 11, 730–743. doi: 10.1016/j.dadm.2019.08.009

Frost, G. R., and Li, Y.-M. (2017). The role of astrocytes in amyloid production and Alzheimer's disease. *Open Biol.* 7:170228. doi: 10.1098/rsob.170228

Garwood, C. J., Ratcliffe, L. E., Simpson, J. E., Heath, P. R., Ince, P. G., and Wharton, S. B. (2017). Review: Astrocytes in Alzheimer's disease and other age-associated dementias: a supporting player with a central role. *Neuropathol. Appl. Neurobiol.* 43, 281–298. doi: 10.1111/nan.12338

Heller, C., Foiani, M. S., Moore, K., Convery, R., Bocchetta, M., Neason, M., et al. (2020). Plasma glial fibrillary acidic protein is raised in progranulin-associated frontotemporal dementia. *J. Neurol. Neurosurg. Psychiatry* 91, 263–270. doi: 10.1136/jnnp-2019-321954

Hulstaert, F., Blennow, K., Ivanoiu, A., Schoonderwaldt, H. C., Riemenschneider, M., de Deyn, P. P., et al. (1999). Improved discrimination of AD patients using β-amyloid$_{(1-42)}$ and tau levels in CSF. *Neurology* 52, 1555–1562. doi: 10.1212/wnl.52.8.1555

Jack, C. R., Bennett, D. A., Blennow, K., Carrillo, M. C., Dunn, B., Haeberlein, S. B., et al. (2018). NIA-AA research framework: toward a biological definition of Alzheimer's disease. *Alzheimers Dement.* 14, 535–562. doi: 10.1016/j.jalz.2018.02.018

Kühner, C., Bürger, C., Keller, F., and Hautzinger, M. (2007). Reliabilität und validität des revidierten Beck-Depressionsinventars (BDI-II). *Der. Nervenarz.* 78, 651–656. doi: 10.1007/s00115-006-2098-7

Kamphuis, W., Middeldorp, J., Kooijman, L., Sluijs, J. A., Kooi, E.-J., Moeton, M., et al. (2014). Glial fibrillary acidic protein isoform expression in plaque related astrogliosis in Alzheimer's disease. *Neurobiol. Aging* 35, 492–510. doi: 10.1016/j.neurobiolaging.2013.09.035

Katisko, K., Cajanus, A., Huber, N., Jääskeläinen, O., Kokkola, T., Kärkkäinen, V., et al. (2021). GFAP as a biomarker in frontotemporal dementia and primary psychiatric disorders: diagnostic and prognostic performance. *J. Neurol. Neurosurg. Psychiatry* 92, 1305–1312. doi: 10.1136/jnnp-2021-326487

Kuhle, J., Barro, C., Andreasson, U., Derfuss, T., Lindberg, R., Sandelius, Å., et al. (2016). Comparison of three analytical platforms for quantification of the neurofilament light chain in blood samples: ELISA, electrochemiluminescence immunoassay and Simoa. *Clin. Chem. Lab. Med.* 54, 1655–1661. doi: 10.1515/cclm-2015-1195

Lehrner, J., Kogler, S., Lamm, C., Moser, D., Klug, S., Pusswald, G., et al. (2015a). Awareness of memory deficits in subjective cognitive decline, mild cognitive impairment, Alzheimer's disease and Parkinson's disease. *Int. Psychogeriatr.* 27, 357–366. doi: 10.1017/S1041610214002245

Lehrner, J., Krakhofer, H., Lamm, C., Macher, S., Moser, D., Klug, S., et al. (2015b). Visuo-constructional functions in patients with mild cognitive impairment, Alzheimer's disease and Parkinson's disease. *Neuropsychiatry* 29, 112–119. doi: 10.1007/s40211-015-0141-2

Lewczuk, P., Ermann, N., Andreasson, U., Schultheis, C., Podhorna, J., Spitzer, P., et al. (2018). Plasma neurofilament light as a potential biomarker of neurodegeneration in Alzheimer's disease. *Alzheimers Res. Ther.* 10:71. doi: 10.1186/s13195-018-0404-9

Mattsson, N., Andreasson, U., Zetterberg, H., Blennow, K., and for the Alzheimer's Disease Neuroimaging Initiative (2017). Association of plasma neurofilament light with neurodegeneration in patients with Alzheimer disease. *JAMA Neurol.* 74:557. doi: 10.1001/jamaneurol.2016.6117

Mattsson, N., Cullen, N. C., Andreasson, U., Zetterberg, H., and Blennow, K. (2019). Association between longitudinal plasma neurofilament light and neurodegeneration in patients with Alzheimer disease. *JAMA Neurol.* 76, 791–799. doi: 10.1001/jamaneurol.2019.0765

McKhann, G., Drachman, D., Folstein, M., Katzman, R., Price, D., and Stadlan, E. M. (1984). Clinical diagnosis of Alzheimer's disease Report of the NINCDS-ADRDA Work Group* under the auspices of department of health and human services task force on Alzheimer's disease. *Neurology* 34, 939–939. doi: 10.1212/wnl.34.7.939

McKhann, G. M., Knopman, D. S., Chertkow, H., Hyman, B. T., Jack, C. R., Kawas, C. H., et al. (2011). The diagnosis of dementia due to Alzheimer's disease: recommendations from the national institute on Aging-Alzheimer's association workgroups on diagnostic guidelines for Alzheimer's disease. *Alzheimers Dement.* 7, 263–269. doi: 10.1016/j.jalz.2011.03.005

Moscoso, A., Grothe, M. J., Ashton, N. J., Karikari, T. K., Rodriguez, J. L., Snellman, A., et al. (2020). Time course of phosphorylated-tau181 in blood across the Alzheimer's disease spectrum. *Brain* 144, 325–339. doi: 10.1093/brain/awaa399

Oeckl, P., Halbgebauer, S., Anderl-Straub, S., Steinacker, P., Huss, A. M., Neugebauer, H., et al. (2019). Glial fibrillary acidic protein in serum is increased in Alzheimer's disease and correlates with cognitive impairment. *J. Alzheimers Dis.* 67, 481–488. doi: 10.3233/JAD-180325

Olsson, B., Alberg, L., Cullen, N. C., Michael, E., Wahlgren, L., Kroksmark, A.-K., et al. (2019). NFL is a marker of treatment response in children with SMA treated with nusinersen. *J. Neurol.* 266, 2129–2136. doi: 10.1007/s00415-019-09389-8

Philippe, C., Haeusler, D., Mitterhauser, M., Ungersboeck, J., Viernstein, H., Dudczak, R., et al. (2011). Optimization of the radiosynthesis of the Alzheimer tracer 2-(4-N-[^{11}C]methylaminophenyl).-6-hydroxybenzothiazole ([^{11}C]PIB). *Appl. Radiat. Isot.* 69, 1212–1217. doi: 10.1016/j.apradiso.2011.04.010

Preische, O., Schultz, S. A., Apel, A., Kuhle, J., Kaeser, S. A., Barro, C., et al. (2019). Serum neurofilament dynamics predicts neurodegeneration and clinical progression in presymptomatic Alzheimer's disease. *Nat. Med.* 25, 277–283. doi: 10.1038/s41591-018-0304-3

Pusswald, G., Moser, D., GleiSS, A., Janzek-Hawlat, S., Auff, E., Dal-Bianco, P., et al. (2013). Prevalence of mild cognitive impairment subtypes in patients attending a memory outpatient clinic—comparison of two modes of mild cognitive impairment classification. results of the vienna conversion to dementia study. *Alzheimers Dement.* 9, 366–376. doi: 10.1016/j.jalz.2011.12.009

Robin, X., Turck, N., Hainard, A., Tiberti, N., Lisacek, F., Sanchez, J.-C., et al. (2011). pROC: an open-source package for R and S+ to analyze and compare ROC curves. *BMC Bioinform.* 12:77. doi: 10.1186/1471-2105-12-77

Rodriguez, J. L., Karikari, T. K., Suárez-Calvet, M., Troakes, C., King, A., Emersic, A., et al. (2020). Plasma p-tau181 accurately predicts Alzheimer's disease pathology at least 8 years prior to post-mortem and improves the clinical characterisation of cognitive decline. *Acta Neuropathol.* 140, 267–278. doi: 10.1007/s00401-020-02195-x

Rojas, J. C., Karydas, A., Bang, J., Tsai, R. M., Blennow, K., Liman, V., et al. (2016). Plasma neurofilament light chain predicts progression in progressive supranuclear palsy. *Ann. Clin. Transl. Neur.* 3, 216–225. doi: 10.1002/acn3.290

Schmidt, K.-H., and Metzler, P. (1992). *Wortschatztest, WST*. Weinheim: Beltz.

Sperling, R. A., Aisen, P. S., Beckett, L. A., Bennett, D. A., Craft, S., Fagan, A. M., et al. (2011). Toward defining the preclinical stages of Alzheimer's disease: recommendations from the national institute on aging-Alzheimer's association workgroups on diagnostic guidelines for Alzheimer's disease. *Alzheimers Dement.* 7, 280–292. doi: 10.1016/j.jalz.2011.03.003

Tabaraud, F., Leman, J. P., Milor, A. M., Roussie, J. M., Barrière, G., Tartary, M., et al. (2012). Alzheimer CSF biomarkers in routine clinical setting. *Acta Neurol. Scand.* 125, 416–423. doi: 10.1111/j.1600-0404.2011.01592.x

Teunissen, C. E., Tumani, H., Engelborghs, S., and Mollenhauer, B. (2014). Biobanking of CSF: international standardization to optimize biomarker development. *Clin. Biochem.* 47, 288–292. doi: 10.1016/j.clinbiochem.2013.12.024

Thebault, S., Booth, R. A., and Freedman, M. S. (2020). Blood neurofilament light chain: the neurologist's troponin. *Biomedicines* 8:523. doi: 10.3390/biomedicines8110523

Thijssen, E. H., Joie, R. L., Strom, A., Fonseca, C., Iaccarino, L., Wolf, A., et al. (2021). Plasma phosphorylated tau 217 and phosphorylated tau 181 as biomarkers in Alzheimer's disease and frontotemporal lobar degeneration: a retrospective diagnostic performance study. *Lancet Neurol.* 20, 739–752. doi: 10.1016/S1474-4422(21)00214-3

Vanderstichele, H., van Kerschaver, E., Hesse, C., Davidsson, P., Buyse, M.-A., Andreasen, N., et al. (2009). Standardization of measurement of β-amyloid$_{(1-42)}$ in cerebrospinal fluid and plasma. *Amyloid* 7, 245–258. doi: 10.3109/13506120009146438

Vanmechelen, E., Vanderstichele, H., Davidsson, P., van Kerschaver, E., van der Perre, B., Sjögren, M., et al. (2000). Quantification of tau phosphorylated at threonine 181 in human cerebrospinal fluid: a sandwich ELISA with a synthetic phosphopeptide for standardization. *Neurosci. Lett.* 285, 49–52. doi: 10.1016/s0304-3940(00)01036-3

Verberk, I. M. W., Laarhuis, M. B., van den Bosch, K. A., Ebenau, J. L., van Leeuwenstijn, M., Prins, N. D., et al. (2021). Serum markers glial fibrillary acidic protein and neurofilament light for prognosis and monitoring in cognitively normal older people: a prospective memory clinic-based cohort study. *Lancet Heal. Longev.* 2, e87–e95. doi: 10.1016/s2666-7568(20)30061-1

Verberk, I. M. W., Thijssen, E., Koelewijn, J., Mauroo, K., Vanbrabant, J., de Wilde, A., et al. (2020). Combination of plasma amyloid $\beta_{(1-42/1-40)}$ and glial fibrillary acidic protein strongly associates with cerebral amyloid pathology. *Alzheimers Res. Ther.* 12:118. doi: 10.1186/s13195-020-00682-7

Verkhratsky, A., Olabarria, M., Noristani, H. N., Yeh, C.-Y., and Rodriguez, J. J. (2010). Astrocytes in Alzheimer's disease. *Neurotherapeutics* 7, 399–412. doi: 10.1016/j.nurt.2010.05.017

Youden, W. J. (1950). Index for rating diagnostic tests. *Cancer* 3, 32–35. doi: 10.1002/1097-0142(1950)3:1<32::aid-cncr2820030106>3.0.co;2-3

Zhu, N., Santos-Santos, M., Illán-Gala, I., Montal, V., Estellés, T., Barroeta, I., et al. (2021). Plasma glial fibrillary acidic protein and neurofilament light chain for the diagnostic and prognostic evaluation of frontotemporal dementia. *Transl. Neurodegener.* 10:50. doi: 10.1186/s40035-021-00275-w

frontiers | Frontiers in Aging Neuroscience

TYPE Review
PUBLISHED 15 September 2022
DOI 10.3389/fnagi.2022.987174

OPEN ACCESS

EDITED BY
Suman Dutta,
University of California, Los Angeles, United States

REVIEWED BY
Karolina Pircs,
Lund University, Sweden
Shunliang Xu,
The Second Hospital of Shandong University, China

*CORRESPONDENCE
Kaveh Ebrahimzadeh
dr.kavehmay1980@gmail.com
Rezvan Noroozi
Rezvan.noroozi@uj.edu.pl

SPECIALTY SECTION
This article was submitted to Cellular and Molecular Mechanisms of Brain-aging, a section of the journal Frontiers in Aging Neuroscience

RECEIVED 05 July 2022
ACCEPTED 31 August 2022
PUBLISHED 15 September 2022

CITATION
Ghafouri-Fard S, Khoshbakht T, Hussen BM, Taheri M, Ebrahimzadeh K and Noroozi R (2022) The emerging role of long non-coding RNAs, microRNAs, and an accelerated epigenetic age in Huntington's disease. *Front. Aging Neurosci.* 14:987174. doi: 10.3389/fnagi.2022.987174

The emerging role of long non-coding RNAs, microRNAs, and an accelerated epigenetic age in Huntington's disease

Soudeh Ghafouri-Fard[1], Tayyebeh Khoshbakht[2], Bashdar Mahmud Hussen[3,4], Mohammad Taheri[5,6], Kaveh Ebrahimzadeh[7]* and Rezvan Noroozi[8]*

[1]Department of Medical Genetics, School of Medicine, Shahid Beheshti University of Medical Sciences, Tehran, Iran, [2]Phytochemistry Research Center, Shahid Beheshti University of Medical Sciences, Tehran, Iran, [3]Department of Pharmacognosy, College of Pharmacy, Hawler Medical University, Erbil, Iraq, [4]Center of Research and Strategic Studies, Lebanese French University, Erbil, Iraq, [5]Institute of Human Genetics, Jena University Hospital, Jena, Germany, [6]Urology and Nephrology Research Center, Shahid Beheshti University of Medical Sciences, Tehran, Iran, [7]Skull Base Research Center, Loghman Hakim Hospital, Shahid Beheshti University of Medical Sciences, Tehran, Iran, [8]Malopolska Centre of Biotechnology, Jagiellonian University, Krakow, Poland

Huntington's disease (HD) is a dominantly inherited neurodegenerative disease with variable clinical manifestations. Recent studies highlighted the contribution of epigenetic alterations to HD progress and onset. The potential crosstalk between different epigenetic layers and players such as aberrant expression of non-coding RNAs and methylation alterations has been found to affect the pathogenesis of HD or mediate the effects of trinucleotide expansion in its pathophysiology. Also, microRNAs have been assessed for their roles in the modulation of HD manifestations, among them are miR-124, miR-128a, hsa-miR-323b-3p, miR-432, miR-146a, miR-19a, miR-27a, miR-101, miR-9*, miR-22, miR-132, and miR-214. Moreover, long non-coding RNAs such as DNM3OS, NEAT1, Meg3, and Abhd11os are suggested to be involved in the pathogenesis of HD. An accelerated DNA methylation age is another epigenetic signature reported recently for HD. The current literature search collected recent findings of dysregulation of miRNAs or lncRNAs as well as methylation changes and epigenetic age in HD.

KEYWORDS

Huntington's disease, miRNA, lncRNA, DNA methylation, epigenetic age

Introduction

Huntington's disease (HD) is a neurodegenerative condition that is inherited in a Mendelian dominant fashion. This disorder has a wide variation in the age of onset. The disease is usually manifested in the 40 s with uncontrolled choreiform movements, cognitive defects, mood disorder, and behavioral alterations. HD is classified as a

trinucleotide repeat disorder, resulting from increased numbers of CAG repeats in the *Huntingtin* gene (Myers, 2004). This disorder has variable clinical manifestations in terms of age of onset and severity of movement and cognitive functions. More than 50% of the variability in age of onset of HD is attributed to the size of the CAG repeat (Tabrizi et al., 2009). Persons with longer repeats usually have an earlier onset (Tabrizi et al., 2009). Nevertheless, subclinical alterations occur before the initiation of evident clinical manifestations. These changes include alterations in cognitive functions (Paulsen et al., 2006) as well as motor and oculomotor assessments (Gordon et al., 2000; Kirkwood et al., 2000).

Non-coding RNAs have been found to affect the pathobiology of HD or mediate the effects of trinucleotide expansion in its pathophysiology (Dubois et al., 2021; Tan et al., 2021). Particularly, two classes of non-coding RNAs, namely microRNAs (miRNAs) and long non-coding RNAs (lncRNAs) have been verified to be abnormally expressed in HD (Johnson, 2012; Dong and Cong, 2021b; Tan et al., 2021). These two classes of non-coding RNAs have been classified based on their size using the cutoff value of 200 nt. There are approximately 50,000 lncRNAs in the human genome (Cabili et al., 2011; Iyer et al., 2015). These transcripts partake in epigenetic mechanisms that influence chromatin configuration. Moreover, they are involved in the regulation of mRNA stability and imprinting processes (Managadze et al., 2013). LncRNAs are classified into five distinct groups, namely long intergenic non-coding RNAs, bidirectional, intronic, sense, and antisense lncRNAs (Ma et al., 2013). miRNAs are a distinct group of non-coding RNAs with sizes of about 22 nucleotides, regulatory roles in the expression of genes, and a high level of conservation among species (Bushati and Cohen, 2007). Both classes of non-coding RNAs are expressed in the brain and have important functions in the pathophysiology of neurodegenerative disorders (Sattari et al., 2020; Zhou et al., 2021).

Also, several studies explored different aspects of methylation alterations related to HD status (Vashishtha et al., 2013; Villar-Menéndez et al., 2013; Valor and Guiretti, 2014; Glajch and Sadri-Vakili, 2015; De Souza et al., 2016). Investigating the methylation signature of HD revealed the impact of specific methylation changes on disease progression and onset which can be caused by mutation or act through altering gene expressions (Vashishtha et al., 2013; Villar-Menéndez et al., 2013; Valor and Guiretti, 2014; Glajch and Sadri-Vakili, 2015; De Souza et al., 2016). DNA methylation estimated biological age (DNAm Age) of HD brain is reported to be accelerated in affected or non-affected regions. But the mechanisms underlying these methylation alterations are unclear which might be through a lncRNA-dependent manner (Vashishtha et al., 2013; Villar-Menéndez et al., 2013; Valor and Guiretti, 2014; Glajch and Sadri-Vakili, 2015; De Souza et al., 2016).

We designed the current study to collect information about the dysregulation of miRNAs and lncRNAs as well as DNA methylation changes in HD.

MicroRNAs in Huntington's disease

RNA-sequencing has enabled researchers to quantify miRNA expression in different brain regions (Langfelder et al., 2018). A similar experiment in the mice model of HD has revealed CAG length-dependent alterations in miRNA expression profile in the brain. Notably, selective alterations in expression profiles have been identified in 159, 102, 51, and 45 miRNAs in the striatum, cerebellum, hippocampus, and cortex, respectively (Langfelder et al., 2018).

miR-124 is among dysregulated miRNAs in HD. This miRNA has an important role in neurogenesis by regulating a few target genes (Cheng et al., 2009). Expression of miR-124 is decreased in the brain tissue of the HDR6/2 mice, expressing mHTT as well as in affected human subjects (Das et al., 2013). Expression of this miRNA has also been shown to be reduced in the cell and animal models of HD which express mutant HTT. Consistently, both models have exhibited up-regulation of levels of CCNA2, a predicted target of miR-124 (Das et al., 2013). Cumulatively, down-regulation of miR-124 can result in enhancement of expression of CCNA2 in these models of HD and subsequent deregulation of the cell cycle in affected cells (Das et al., 2013).

Experiments in HD transgenic mice (R6/2 HD mice) have shown that miR-124 injection improves behavioral phenotype as evident by an increase in the latency to fall in the rotarod test (Liu et al., 2015). Furthermore, injection of this miRNA into bilateral striata has resulted in up-regulation of the neuroprotective factors PGC-1α and BDNF (Liu et al., 2015). Moreover, it has led to down-regulation of the repressor of cell differentiation SOX9 (Liu et al., 2015). Taken together, miR-124 can slow down HD course most probably *via* its vital functions in the differentiation and survival of neurons (Liu et al., 2015). Based on the important role of this miRNA in neurogenesis, Lee et al. have established an exosome-based delivery system to up-regulate miR-124 levels. Injection of Exo-124 into the striatum of R6/2 HD animal models has resulted in the reduction of expression of its target gene, REST. Yet, this strategy has not improved HD-related behavioral changes (Lee et al., 2017). **Figure 1** illustrates the role of several miRNAs in regulating HD.

Accumulating evidence has illustrated that various miRNAs are an important regulatory factor in the pathoetiology of HD. It has been reported that miR-302 could play a crucial role in attenuating mHtt-induced cytotoxicity by promoting insulin sensitivity, resulting in a diminution of mHtt aggregates *via* the improvement of autophagy (Chang et al., 2021). Furthermore, miR-302 could also enhance the expression levels of silent information regulator 1 (Sirt1), AMP-activated

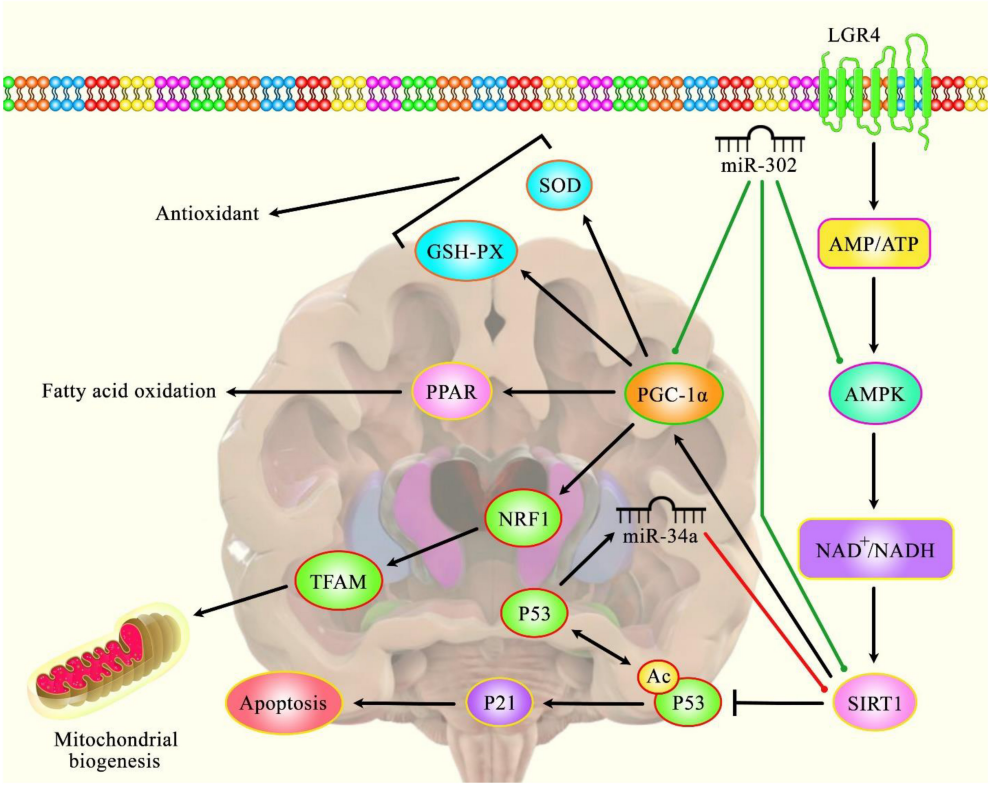

FIGURE 1
A schematic diagram of the role of several miRNAs in the modulation of Huntington's disease.

protein kinase (AMPK), and PPARγ coactivator-1α (PGC-1α), therefore preserving mitochondrial function (Chang et al., 2021). The effect of the AMPK-SIRT1-PGC1α signaling pathway on antagonizing oxidative stress and maintaining mitochondrial function revealed an enhanced cognitive function in Sevo-anesthetized aged rats (Yang et al., 2020). SIRT1 as an NAD+ -dependent deacetylase has been investigated for its regulatory role in the regulation of cellular senescence and aging (Chen et al., 2020) and its association with lifespan elongation suggested it as a longevity gene (Bonkowski and Sinclair, 2016; Elibol and Kilic, 2018; Kim D. H. et al., 2019). Moreover, another research has figured out that dysregulation of p53/miR-34a/SIRT1 cascade could have an important role in HD-associated pathogenic mechanisms. Downregulation of miR-34a-5p could lead to the upregulation of SIRT1 and p53 protein levels in brain tissue (Reynolds et al., 2018). Green lines indicate the positive regulatory effect among miRNAs and their targets, and red lines depict the negative one among them. All the information regarding the role of these miRNAs participating in the pathobiology of Huntington's disease can be seen in **Table 1**.

Another experiment in a monkey model of HD has shown dysregulation of 11 miRNAs in the frontal cortex of these animals among them being the down-regulated miRNA miR-128a. This miRNA has also been found to be down-regulated in the brain tissues obtained from both pre-symptomatic and post-symptomatic affected persons (Kocerha et al., 2014).

A study on the human subject has shown down-regulation of hsa-miR-98 and over-expression of hsa-miR-323b-3p in HD cases compared with healthy subjects and psychiatric patients (Ferraldeschi et al., 2021). Additional expression assays in an independent cohort of HD cases have validated up-regulation of hsa-miR-323b-3p in HD cases even before disease manifestations (Ferraldeschi et al., 2021). However, authors have reported no significant difference in expression of hsa-miR-98 in the second cohort. Further bioinformatics evaluations have shown overconnectivity between the hsa-miR-323b-3p targetome and the HTT interactome. Besides, these investigations have shown transcriptional regulation of the HTT interactome by the targetome of this miRNA (Ferraldeschi et al., 2021).

Experiments in a cell model of HD have confirmed the delay in the S and G2-M phases of cell cycles in these cells compared to control cells (Das et al., 2015). Consistent with this finding, expressions of PCNA, CHEK1, and CCNA2 are elevated in primary cortical neurons expressing mutant Huntingtin (mHTT) as well as animal and cell models of

TABLE 1 MicroRNAs and Huntington's disease (HD, Huntington's disease; UHDRS, Unified Huntington's Disease Rating Scales).

miRNA	Pattern of expression	Samples/ Animals	Cell lines	Targets/ Regulators/ Signaling pathways	Function	References
miR-124	decreased	R6/2 HD mice and their wild-type littermates	–	–	miR-124 reduces the progression of HD *via* promoting neurogenesis in the striatum.	Liu et al., 2015
	–	R6/2 HD mice	HEK 293 cells	REST	Overexpression of miR-124 reduced REST levels. But Exo-124 treatment did not lead to significant behavioral improvement.	Lee et al., 2017
	Decreased	R6/2 HD mice	STHdh(Q111)/Hdh(Q111) and STHdh(Q7)/Hdh(Q7) cells	CCNA2	Low levels of miR-124 could lead to high levels of CCNA2 in the cell and animal model of HD, thus it participates in the deregulation of the cell cycle.	Das et al., 2013
miR-128a	decreased	control, pre-symptomatic HD, and post-symptomatic HD human striatum samples/HD monkeys	–	HTT, HIP1	miR-128a has a role in regulation of HTT and HIP1.	Kocerha et al., 2014
hsa-miR-323b-3p	Increased	33 HD patients and 49 matched controls	–	HTT	A significant overconnectivity has been found between hsa-miR-323b-3p and HTT.	Ferraldeschi et al., 2021
miR-432 miR-146a miR-146a and miR-19a	Decreased	–	STHdh(Q111)/Hdh(Q111) and control STHdhQ7/HdhQ7cells	PCNA CHEK1 CCNA2	High expressions of these miRNAs in STHdh(Q111)/Hdh(Q111) cells relieved the irregularities in the cell cycle and apoptosis.	Das et al., 2015
miR-27a	Decreased	R6/2 HD mice	Primary neurosphere cells from C57BL/6 mice	mHtt, MDR-1	miR-27a could decrease mHtt levels of the HD cell by increasing MDR-1 function, thus playing a role in the reduction of mHtt aggregation in HD cells.	Ban et al., 2017
miR-34a	Decreased	R6/2 HD mice	–	SIRT1, p53	miR-34a was down-regulated and SIRT1 and p53 were up-regulated in HD, but, there were no known interactions between these factors.	Reynolds et al., 2018
miR-101	–	–	HEK293 cells	Rhes	miR-101 was found to target Rhes which plays an important role in HD development caused by striatal anomalies.	Mizuno and Taketomi, 2018
miR-9*	Decreased	36 HD patients and 28 healthy controls	–	–	miR-9* levels in peripheral leukocyte may be an indicator neurodegeneration in HD patients.	Chang et al., 2017
miR-22	Decreased	–	Primary cortical and striatal neuron cultures from striata or cerebral cortices of E16 rat embryos	HDAC4, Rcor1, and Rgs2	miR-22 has multipartite anti-neurodegenerative activities such as the inhibition of apoptosis *via* targeting HDAC4, Rcor1, and Rgs2.	Jovicic et al., 2013

(Continued)

TABLE 1 (Continued)

miRNA	Pattern of expression	Samples/ Animals	Cell lines	Targets/ Regulators/ Signaling pathways	Function	References
miR-132	Decreased	R6/2 HD mice	–	–	miR-132 has a role in neuronal maturation and function in HD.	Fukuoka et al., 2018
miR-214	Increased	–	HD cell models	MFN2	miR-214 could increase the distribution of fragmented mitochondria and change the distribution of cells in different phases of the cell cycle by targeting MFN2.	Bucha et al., 2015
	Increased	–	Q7 and Q111 cells	Beta-catenin	Gain-of-function of mutant Htt could reduce beta-catenin levels *via* upregulating miR-214.	Ghatak and Raha, 2018
	Increased	_	STHdhQ7/Q7 and STHdhQ111/Q111 cells	Beta-catenin	miR-214 could reduce Beta-catenin post-transcriptionally, thus transcriptional activity of wnt/β-catenin signaling was decreased.	Ghatak and Raha, 2015
miR-196a	Decreased	R6/2 HD mice	N2a mouse neuroblastoma cells and primary neurons	RANBP10	miR-196a could increase neuronal morphology to provide neuroprotection in HD *via* targeting RANBP10.	Her et al., 2017
	Decreased	Analysis of different bioinformatics tools, including DAVID, MSigDB, TargetScan, and MetaCore	–	–	miR-196a could have beneficial functions *via* the alteration of cytoskeleton structures.	Fu et al., 2015
	Increased	Eight HD patients and four controls	WT-NPCs, HD-NPCs, and HD-NCs	–	miR-196a could reduce cytotoxicity and apoptosis in HD-NHP neural progenitor cells and differentiated neural cells.	Kunkanjanawan et al., 2016
	Decreased	D-Tg mice, GHD mice, 196a transgenic mice, and WT mice	293 FT cells, N2a cells, and HD-iPSCs	HTT	miR-196a could reduce mHTT in the brain and also improve neuropathological progression.	Cheng et al., 2013
hsa-miR-4324 and hsa-miR-4756-5p	–	HD patients	HEK293T cells and derived fibroblast from HD patients	–	hsa-miR-4324 and hsa-miR-4756-5p could reduce HTT 3'-UTR reporter activity and endogenous HTT protein levels.	Kim K. H. et al., 2019
miR-302	Decreased	–	SK-N-MC neuroblastoma cells	Sirt1/AMPK-PGC1α pathway	miR-302 could reduce mHtt-induced cytotoxicity by increasing insulin sensitivity, leading to a reduction of mHtt aggregates *via* the increasing autophagy, besides it could upregulate Sirt1/AMPK-PGC1α pathway.	Chang et al., 2021
miR-10b-5p	Increased	12 HD patients and nine control samples	–	BDNF	miR-10b-5p could reduce BDNF expression which is associated with neuronal dysfunction and death.	Müller, 2014
miR-10b-5p	Increased	prefrontal cortex samples of 26 HD patients and 36 controls	–	–	miR-10b-5p expression in brain tissues is correlated with to age of onset and the severity of striatal pathology.	Hoss et al., 2015

HD. Over-expression of these genes has resulted from down-regulation of miR-432, miR-146a, and miR-19a, and miR-146a, respectively (Das et al., 2015).

miR-27a is another down-regulated miRNA in the brain tissues of the HD mice model. This miRNA can regulate the expression of MDR-1 (Ban et al., 2017). Transfection of miR-27a into the differentiated neuronal stem cells originating from the R6/2 HD mouse model has led to decreased mHtt aggregation. Furthermore, the level of MDR-1, as a transporter of mHtt, has been enhanced by this miRNA. Thus, miR-27a can decrease mHtt levels in the HD cells through increasing MDR-1 efflux function (Ban et al., 2017).

Figure 2 summarizes the impact of down-regulated miRNAs in the pathogenesis of HD.

On the other hand, a quantity of miRNAs has been reported to be up-regulated in HD. For instance, miR-214 has been found to be increased in HD cell model (Bucha et al., 2015). This miRNA can target HTT mRNA. Moreover, expression levels of numerous HTT co-expressed genes have been demonstrated to be affected by exogenous expression of mutant or wildtype miR-214. MFN2 is an example of HTT co-expressed genes which is directly targeted by miR-214 (Bucha et al., 2015). Over-expression of miR-214 could result in repression of MFN2 expression, increase in the dispersal of fragmented mitochondria and changes in the distribution of cells in diverse stages of the cell cycle. Taken together, up-regulation of miR-214 can affect the morphology of mitochondria and disturb cell cycle regulation in HD models (Bucha et al., 2015). Another study has shown up-regulation of miR-214 following gain-of-function mutation in Htt in Q7 and Q111 HD cells. This miRNA could also decrease β-catenin levels and its transcriptional activity (Ghatak and Raha, 2018).

Re-analysis of the high throughput expression data has shown dysregulation of several miRNAs in HD. Further studies have shown that up-regulated miRNAs, miR-10b-5p, and miR-30a-5p can regulate the expression of BDNF (Müller, 2014). Down-regulation of BDNF is correlated with dysfunction and death of neurons in HD (Müller, 2014). Besides, these two miRNAs have been predicted to target CREB1, a down-regulated gene in HD whose up-regulation can decrease susceptibility to 3-NP-induced toxicity (Chaturvedi et al., 2012). Contradictory to these results, it is supposed that up-regulation of miR-10b-5p plays a neuroprotective role against *HTT* mutation (Müller, 2014). Thus, the functional role of miR-10b-5p and its impact on the expression of BDNF in HD need additional investigations (Müller, 2014). **Figure 3** shows up-regulated miRNAs in HD.

Soldati et al. (2013) have assessed the impact of up-regulation of nuclear REST on the expression of miRNAs in the presence of mHTT. Comparison of expression levels of 41 miRNAs in $Hdh^{109/109}$ cells and $Hdh^{7/7}$ cells has led to the identification of 15 down-regulation miRNAs in the former group, including miR-9, miR-9*, and miR-23b. The expression of 12 miRNAs among these down-regulated miRNAs (including the three mentioned miRNAs) have been enhanced after REST knock-down. Notably, miR-137, miR-153, and miR-455 are mouse homologs of human miRNAs with predicted REST binding sites. Authors have concluded that several miRNAs with abnormal expression in HD are presumably suppressed by over-expressed REST (Soldati et al., 2013).

Analysis of expression of miRNAs in the postmortem brain samples of HD patients has resulted in the identification of differential expression of 54 miRNAs, including 30 upregulated and 24 downregulated miRNAs. Expressions of 26 miRNAs have been found by several number of transcription factors, namely TP53, E2F1, REST, and GATA4 (Sinha et al., 2012).

In fact, repression of expression of important neuronal miRNAs such as mir-9/9*, mir-124, and mir-132-is in the brain regions of HD patients and animal models occurs downstream of REST, possibly due to interruption of mRNA regulation and neuron functions. In this study, we will discuss these findings and their implications for our understanding of HD. An *in silico* assessment has led to the prediction of 21 novel candidate miRNAs in HD. This study has indicated that HD is associated with a large-scale suppression of neural genes in the caudate and motor cortex. Moreover, it has been concluded that cooperation between REST, miRNAs and probably other non-coding RNAs can significantly affect the transcriptome of neurons in HD (Johnson and Buckley, 2009). Mechanistically, polyglutamine expansion in huntingtin has been shown to abrogate REST-huntingtin binding. This leads to nuclear translocation of REST (Zuccato et al., 2003) where it lodges RE1 repressor sequences and reduces gene expression in neurons (Zuccato et al., 2003). Packer et al. (2008) have reported the reduction of expression of numerous miRNAs with upstream RE1 sites in cortex samples of HD patients compared with healthy controls. Notably, among these miRNAs has been the bifunctional brain enriched miR-9/miR-9* which targets two constituents of the REST complex (Packer et al., 2008).

Another experiment in post-mortem tissues of HD patients has demonstrated accumulation of Argonaute-2 (AGO2) in the presence of neuronal protein aggregates as a result of impairment of autophagy. Since AGO2 is an important constituent of the RISC complex that implements miRNA functions, its accumulation leads to global changes in the miRNA levels and activity (Pircs et al., 2018).

Finally, experiments in the 3NP-induced animal model of HD have shown distinct miRNA profiles compared with the transgenic mice. This observation is possibly due to the effects of mHtt on the activity of HTT in extra-mitochondrial energy metabolism (Lee et al., 2007).

Table 1 lists miRNAs that are possibly involved in the pathogenesis of HD.

Most notably, investigations in animal models of HD have demonstrated that artificial miRNAs are able to reduce levels of mHTT. Pfister et al. (2018) have performed an experiment in HD transgenic sheep model that expresses the full-length

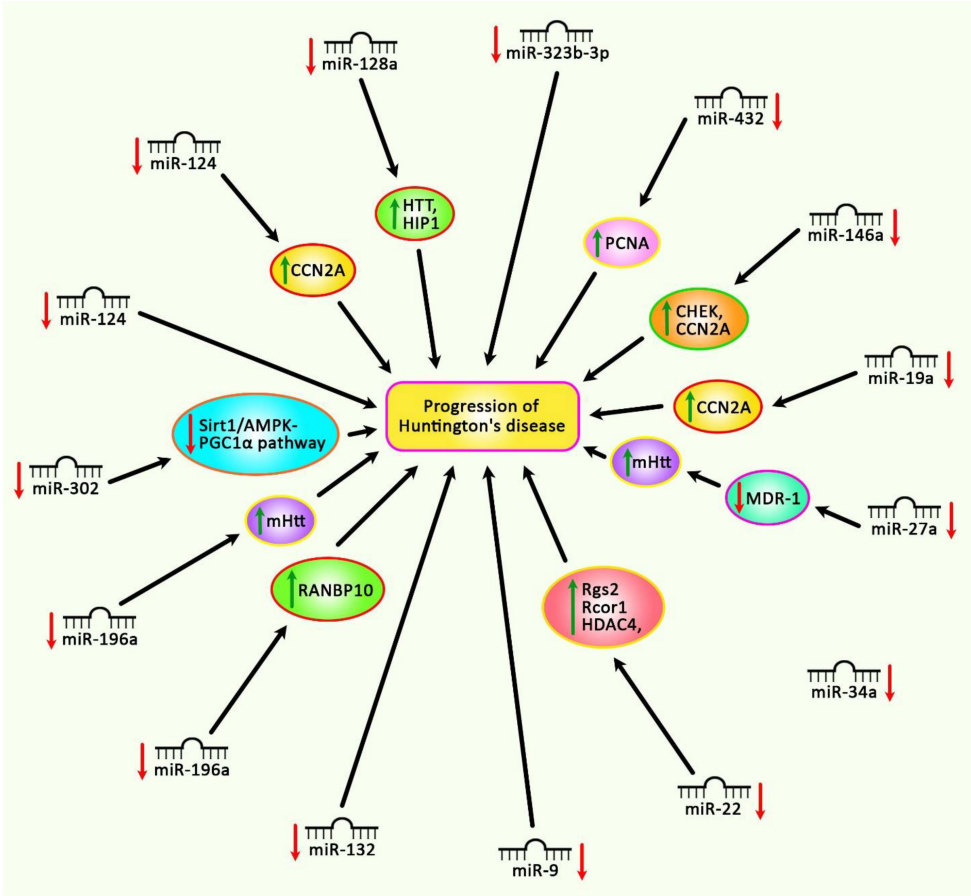

FIGURE 2
Different experiments have shown the down-regulation of miRNAs in Huntington's disease. Subsequent up-regulation of mRNA targets of these miRNAs can lead to the progression of Huntington's disease.

human HTT with 73 CAG repeats. Treatment of these animals with AAV9-expressing an artificial miRNA targeting exon 48 of the human HTT transcript has led to a reduction of human mHTT transcript and protein in the striatum without any significant neuron loss. This study has revealed the safety and efficiency of silencing human mHTT protein using an AAV-mediated transfer of an artificial miRNA (Pfister et al., 2018).

Long non-coding RNAs in Huntington's disease

Few lncRNAs are dysregulated in HD (**Table 2**). Expression of lncRNA-DNM3OS has been assessed in a rat pheochromocytoma cell line induced by *Huntingtin* gene exon 1 fragment containing either 23 or 74 CAG repeats. This intervention has led to up-regulation of GAPDH and DNM3OS. Down-regulation of these genes has resulted in suppression of aggregate formation, reduction of apoptosis and enhancement of cell survival. Furthermore, up-regulation of DNM3OS in HD PC12 cells can decrease miR-196b-5p levels by sponging. GAPDH is a direct target of this miRNA which contributes in the development of aggregates (Dong and Cong, 2021a).

Sunwoo et al. (2017) have performed a microarray-based study to evaluate the expression profile of lncRNAs in HD. They have reported up-regulation of NEAT1 (Sunwoo et al., 2017). Further studies in brain tissues of R6/2 HD models as well as postmortem brain tissues of human HD subjects have validated the up-regulation of this lncRNA (Sunwoo et al., 2017). Functional studies have shown increased viability of cells in oxidative stress conditions following transfection of cells with NEAT1. Taken together, up-regulation of NEAT1 in HD can be regarded as a neuroprotective strategy against neuronal damage instead of being a pathological event (Sunwoo et al., 2017). Another study has revealed up-regulation of the long isoform of NEAT1 in the brain tissues of mice model of HD. This transcript has also been up-regulated in differentiated striatal neurons originating from HD knock-in mice as well as brain tissues of affected individuals. Up-regulation of this

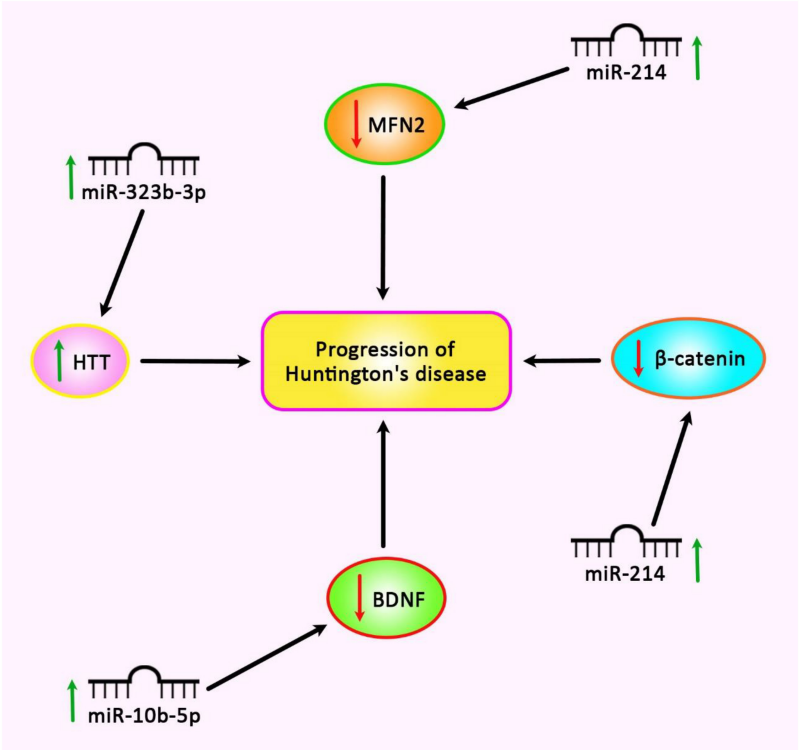

FIGURE 3
Up-regulation of miR-214, miR-322b-3p, and miR-10b-5p is involved in the pathogenesis of Huntington's disease.

isoform has been found to be dependent on mHTT. MeCP2 could repress expression of this isoform of Neat1 through a molecular interaction outside its promoter. Up-regulation of this isoform exerts a protective effect against mHTT-induced cytotoxicity. On the other hand, its down-regulation results in impairment of several cellular processes such as those related with cell proliferation and development. Interestingly, dysregulated genes in HD human brain tissues overlap with pathways influenced by down-regulation of NEAT1 (**Figure 4**; Cheng et al., 2018).

Mounting evidence has demonstrated that aberrant expression of various lncRNAs could be correlated with dysfunction and death of neurons in HD (Cheng et al., 2018). As an illustration, a recent study has detected that the expression of NEAT1L could be inhibited by mHTT as well as MeCP2 *via* RNA-protein interaction, thereby NEAT1L may play a protective role in CAG-repeat expansion diseases, such as HD (Cheng et al., 2018).

Chanda et al. (2018) have used small RNA sequencing and PCR array techniques to find dysregulated RNAs in R6/2 HD mice brains. They have detected alteration in 12 non-coding RNAs in these samples eight of them having human homologs. Three lncRNAs, namely Meg3, Neat1, and Xist have exhibited a constant and substantial over-expression in cell and animal models of HD. Silencing of Meg3 and Neat1 in cell models of HD has resulted in the reduction of aggregate formation by mHTT and a significant decrease in the endogenous levels of Tp53 (Chanda et al., 2018).

Abhd11os is another lncRNA that is down-regulated in various animal models of HD. Up-regulation of Abhd11os has a neuroprotective effect against an N-terminal fragment of mHTT, while its silencing has a toxic effect. Thus, loss of Abhd11os contributes to striatal susceptibility in HD (Francelle et al., 2015). **Figure 5** depicts up-regulated lncRNAs in HD.

DNA methylation age acceleration in Huntington's disease

The crosstalk among different epigenetic players such as histone modification, non-coding RNA action, and DNA methylation, ensures stable regulation of gene expression required for the maintenance of cell-type-specific identity. However, environmentally induced alterations in the epigenome may lead to chromatin remodeling, and as a result, the abnormal gene expression can affect the state of differentiated cells (Boland et al., 2014). In the case of neuronal cells, the interplay between epigenetic mechanisms and transcriptional changes controls neuronal cell identity as well, but it also regulates neuronal activation and consequent brain functions such as cognitive and

TABLE 2 Long non-coding RNAs and Huntington's disease (HD, Huntington's disease; mHTT, mutant Huntingtin).

lncRNA	Pattern of expression	Samples/ Animals	Cell lines	Targets/ Regulators/ Signaling pathways	Description	References
DNM3OS	increased	–	HD PC12 cells (httex1p−Q23 and httex1p−Q74)	miR-196b-5p/GAPDH	Downregulation of DNM3OS leads to suppression of aggregate formation accompanied by a reduced apoptosis and augmented relative ROS levels and cell viability.	Dong and Cong, 2021a
NEAT1	Increased	R6/2 HD mice	neuro2A cells	–	Upregulation of NEAT1 could increase viability under oxidative stress.	Sunwoo et al., 2017
	Increased	HD mice	STHdhQ7/Q7 cells and STHdhQ111/Q111	mHTT, MeCP2	The elevation of NEAT1 was mHTT dependent, as knockdown of mHTT restored Neat1L to normal levels. It was found that Neat1L is suppressed by MeCP2 *via* RNA-protein interaction.	Cheng et al., 2018
Meg3 and NEAT1	Increased	R6/2 HD mice	STHdhQ7/HdhQ7 cells and STHdhQ111/HdhQ111 cells	–	Downregulation of Meg3 and NEAT1 could decrease aggregate formation by mHTT and downregulation of Tp53 expression.	Chanda et al., 2018
Abhd11os	Decreased	male C57BL/6J mice	HEK293T cells	–	Upregulation of Abhd11os protects neurons against an N-terminal fragment of mHTT, while Abhd11os downregulation is protoxic.	Francelle et al., 2015

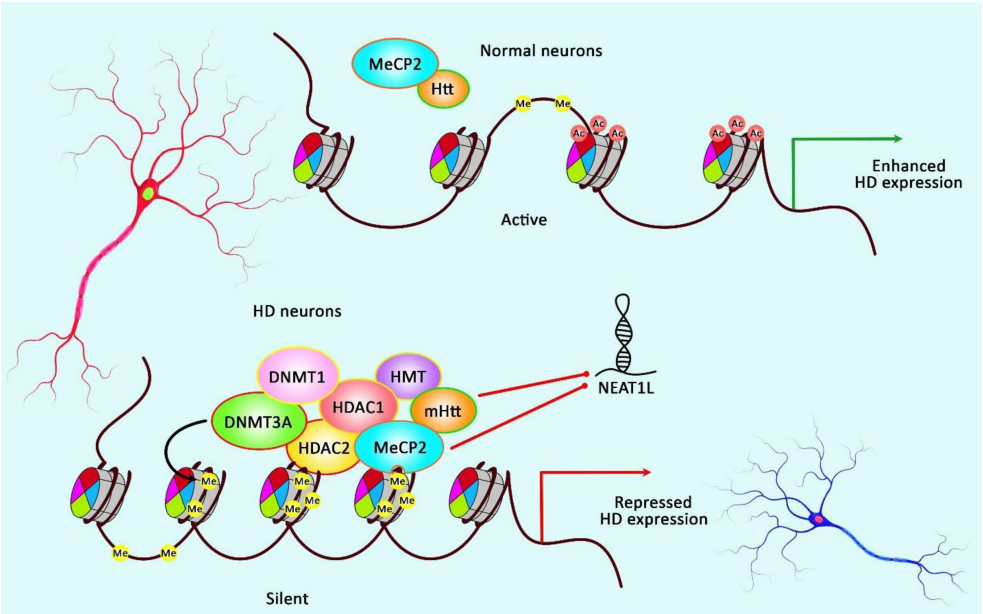

FIGURE 4
A schematic illustration of the role of NEAT1L in HD.

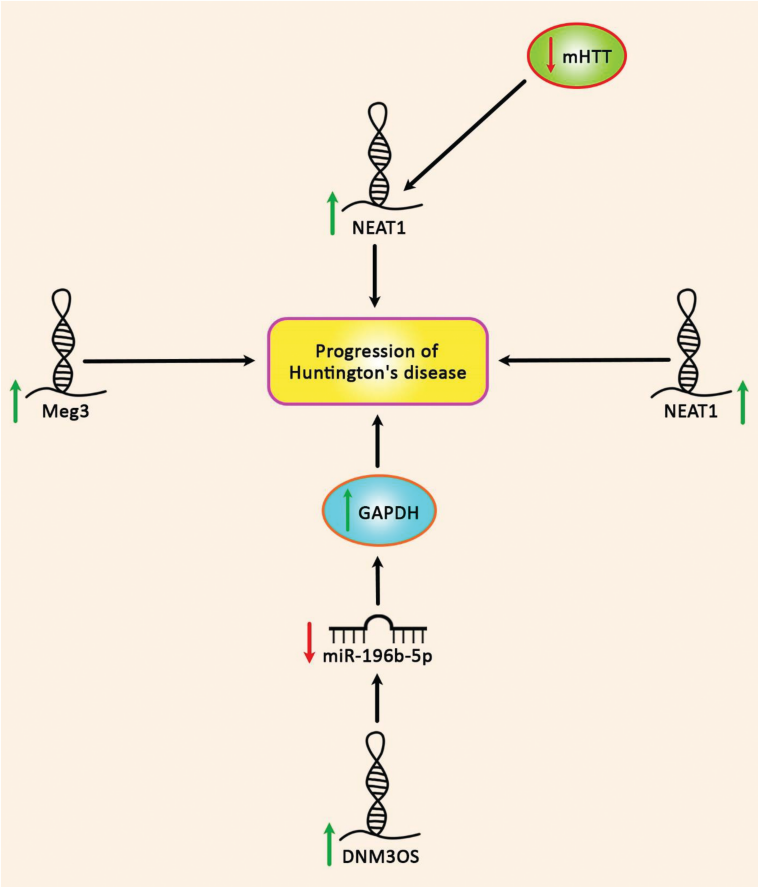

FIGURE 5
Up-regulation of DNM3OS, NEAT1, and Meg3 in Huntington's disease.

motor functions in response to environmental signals (Francelle et al., 2017).

One of the main epigenetic mechanisms that have profound effects on the DNA packaging, gene expression, and maintenance of the cellular identity, is DNA methylation, the addition of a methyl group (CH3), particularly to the fifth position of carbon in the cytosine ring, which results in the formation of 5-methylcytosine (5mC), and creates a mutational hotspot in the genome which may finally affect the susceptibility to different diseases (Denissenko et al., 1997).

Recently, the DNA methylation levels of CpG markers, correlated with age or age-related physiological dysregulation, have been used to develop different DNA methylation-based age estimators, also known as DNA methylation biological age clocks (Horvath, 2013). Tissue-specific DNA methylation variability has been correlated with the differences in biological ages of individuals and the estimated biological age is reported to be accelerated in different diseases including cognitive and neurodegenerative disorders (Noroozi et al., 2021). The aging-related systematic decline and biological aging have been shown to play an active role in HD pathogenesis, its onset, and progression (Machiela and Southwell, 2020). And recent research studies aim to reveal the role of methylation modifications in HD pathogenesis (Lee et al., 2013; Valor and Guiretti, 2014). The unstable CAG trinucleotide expansion in HD is suggested to be affected by the biological age and the methylation pattern of the tissue. The transcriptional dysregulation observed in the HD brain tissue is reported to be influenced by aberrant DNA methylation (De Souza et al., 2016) which modulates the expression levels of *HTT* and other neuronal identity genes (Hyeon et al., 2021). DNA methylation alterations in response to polyglutamine-expanded *HTT* were observed in HD cell models at both promoter-proximal and distal regulatory regions (Ng et al., 2013). A tissue-specific methylation pattern of the *HTT* gene was reported by analyzing post-mortem cortex and liver tissues of HD patients (De Souza et al., 2016).

Investigation of the DNA methylation changes in the post-mortem brain tissues of HD patients demonstrates accelerated epigenetic aging (Horvath et al., 2016). The recent epigenome-wide association study (EWAS) of HD gene-expansion carriers (HDGECs) in multiple tissues from three species, reported

33 genome-wide significant CpGs for HD status and the most significant locus was *HTT* and the EWAS results of motor progression in manifest HD cases indicate significant associations with methylation levels at three loci. Also, a higher blood epigenetic age acceleration (calculated discrepancy between chronological age and DNA methylation age) was reported in manifest HD in comparison to controls (Lu et al., 2020). Most recently, exploration of the HD-associated epigenetic signatures using the slowly progressing knockin (KI) mouse model of HD, revealed that even before the onset of HD motor problems, age-related epigenetic remodeling and transcriptional alteration of neuronal and glial-specific genes are accelerated. This might suggest that the progressive HD striatal epigenetic signatures develop from the earliest stages of HD (Alcalá-Vida et al., 2021).

Discussion

Neurodegenerative processes in the brains of HD patients are associated with extensive alterations in gene regulatory networks. These alterations have been detected in both protein-coding genes and non-coding RNAs (ncRNAs) (Johnson, 2012). Among non-coding RNAs, the impacts of miRNAs in HD pathogenesis have been investigated more than lncRNAs. LncRNAs can inhibit or stimulate the neurodegenerative processes through epigenetically modulating expression of genes critically implicated in the pathoetiology of these disorders (Zhou et al., 2021). Thus, further high throughput studies are needed to find other HD-related lncRNAs.

The functional effects of dysregulation of non-coding RNAs in the development of HD have been assessed in cell and animal models of HD. These transcripts mostly affect the survival of neurons through influencing apoptotic pathways or cell cycle transition.

The expression profile of non-coding RNAs in the circulation of suspected persons might be used to predict HD course. Thus, these transcripts can be used as biomarkers for HD. They can also be targeted by siRNAs or antisense oligonucleotides. Therefore, they represent potential targets for gene therapy of HD. It is worth mentioning that altered expression of non-coding RNAs in HD might be either a part of pathogenic processes in this disorder or a compensatory mechanism for increasing the viability of neurons. This note should be considered in the design of therapeutic modalities.

In addition, the pathophysiology of HD is affected by epigenetic modulations and the methylation levels of selected genes are related to HD progress and onset. Accelerated epigenetic age of HD brain suggested association of the older biological age of the affected tissue with the disease which is not affected by sex, age, or the abundance of neuronal cells. Enrichment analysis on the methylation modules of HD highlights the association of genes involved in olfactory receptor activity and sensory perception of chemical stimulus with HD status.

The crosstalk between DNAm and non-coding RNAs, and most interestingly regulation of DNA methylation by lncRNAs is an important factor that can declare the underlying mechanisms of neurodegenerative disorders. The association analysis of the methylation levels of different age-related loci in blood and buccal swab samples showed a significant association between the hypomethylation of a lncRNA MIR29B2CHG with age, suggesting it is a marker for the development of DNAm based age prediction models in these tissues (Tharakan et al., 2020; Woźniak et al., 2021).

Several miRNAs have been shown to affect the expression of mHTT, thus they can be used as modulators of HD pathogenic events. Moreover, several panels of miRNAs are dysregulated in the course of HD, thus having the potential to be used as predictive markers in this disorder. Several number of dysregulated miRNAs in HD are regarded as specific markers for this disorder, thus being promising biomarkers for diagnostic purposes as well as monitoring HD progression and therapeutic response.

Besides, lncRNAs have been suggested to play an active role in specifying the pattern of histone modifications of target genes by serving as scaffolds for histone modification enzymes. For example, the binding of LSD1 enzyme to target genes, mediated by *HOTAIR*, has been shown to affect the repression of target genes by changing the methylation level of the histone H3 lysine 27 (H3K27) (Tsai et al., 2010). While, decreased acetylation of H3K27 showed an association with the downregulation of neuronal identity genes in the striatum of HD patients and mice (Achour et al., 2015; Alcalá-Vida et al., 2021). Also, an association is shown between aberrant DNA methylation levels correlated with aberrant expression of different lncRNAs with susceptibility to different diseases. For instance, altered expression of *FMR4* lncRNA is reported to change genome-wide histone methylations and play an active role in the development of repeat expansion-associated disorders such as fragile X (Peschansky et al., 2016).

Although investigating the epigenetic signatures of the HD suggested these alterations to be the consequent rather than cause of the underlying genetic structure of the HD (Zimmer-Bensch, 2020), potential interactions between different layers of epigenome for instance the lncRNA-dependent methylation alterations related to HD progress and onset should be investigated with much rigor.

Author contributions

SG-F wrote the manuscript and revised it. MT and KE supervised and designed the study. TK, RN, and BH collected the data and designed the figures and tables. All authors have read and approved the submitted version.

Acknowledgments

We would like to thank the Clinical Research Development Unit (CRDU) of Loghman Hakim Hospital, Shahid Beheshti University of Medical Sciences, Tehran, Iran for their support, cooperation and assistance throughout the period of study (Grant Number: 43002792).

Conflict of interest

The authors declare that the research was conducted in the absence of any commercial or financial relationships that could be construed as a potential conflict of interest.

Publisher's note

All claims expressed in this article are solely those of the authors and do not necessarily represent those of their affiliated organizations, or those of the publisher, the editors and the reviewers. Any product that may be evaluated in this article, or claim that may be made by its manufacturer, is not guaranteed or endorsed by the publisher.

References

Achour, M., Le Gras, S., Keime, C., Parmentier, F., Lejeune, F.-X., Boutillier, A.-L., et al. (2015). Neuronal identity genes regulated by super-enhancers are preferentially down-regulated in the striatum of Huntington's disease mice. *Hum. Mol. Genet.* 24, 3481–3496. doi: 10.1093/hmg/ddv099

Alcalá-Vida, R., Seguin, J., Lotz, C., Molitor, A. M., Irastorza-Azcarate, I., Awada, A., et al. (2021). Age-related and disease locus-specific mechanisms contribute to early remodelling of chromatin structure in Huntington's disease mice. *Nat. Commun.* 12:364. doi: 10.1038/s41467-020-20605-2

Ban, J.-J., Chung, J.-Y., Lee, M., Im, W., and Kim, M. (2017). MicroRNA-27a reduces mutant hutingtin aggregation in an *in vitro* model of Huntington's disease. *Biochem. Biophys. Res. Commun.* 488, 316–321. doi: 10.1016/j.bbrc.2017.05.040

Boland, M. J., Nazor, K. L., and Loring, J. F. (2014). Epigenetic regulation of pluripotency and differentiation. *Circ. Res.* 115, 311–324.

Bonkowski, M. S., and Sinclair, D. A. (2016). Slowing ageing by design: The rise of NAD+ and sirtuin-activating compounds. *Nat. Rev. Mol. Cell Biol.* 17, 679–690. doi: 10.1038/nrm.2016.93

Bucha, S., Mukhopadhyay, D., and Bhattacharyya, N. P. (2015). Regulation of mitochondrial morphology and cell cycle by microRNA-214 targeting Mitofusin2. *Biochem. Biophys. Res. Commun.* 465, 797–802. doi: 10.1016/j.bbrc.2015.08.090

Bushati, N., and Cohen, S. M. (2007). microRNA functions. *Annu. Rev. Cell Dev. Biol.* 23, 175–205.

Cabili, M. N., Trapnell, C., Goff, L., Koziol, M., Tazon-Vega, B., Regev, A., et al. (2011). Integrative annotation of human large intergenic noncoding RNAs reveals global properties and specific subclasses. *Genes Dev.* 25, 1915–1927. doi: 10.1101/gad.17446611

Chanda, K., Das, S., Chakraborty, J., Bucha, S., Maitra, A., Chatterjee, R., et al. (2018). Altered levels of long NcRNAs Meg3 and Neat1 in cell and animal models of Huntington's disease. *RNA Biol.* 15, 1348–1363. doi: 10.1080/15476286.2018.1534524

Chang, C.-C., Tsou, S.-H., Chen, W.-J., Ho, Y.-J., Hung, H.-C., Liu, G.-Y., et al. (2021). miR-302 Attenuates Mutant Huntingtin-Induced Cytotoxicity through Restoration of Autophagy and Insulin Sensitivity. *Int. J. Mol. Sci.* 22:8424. doi: 10.3390/ijms22168424

Chang, K.-H., Wu, Y.-R., and Chen, C.-M. (2017). Down-regulation of miR-9* in the peripheral leukocytes of Huntington's disease patients. *Orphanet J. Rare Dis.* 12:185. doi: 10.1186/s13023-017-0742-x

Chaturvedi, R. K., Hennessey, T., Johri, A., Tiwari, S. K., Mishra, D., Agarwal, S., et al. (2012). Transducer of regulated CREB-binding proteins (TORCs) transcription and function is impaired in Huntington's disease. *Hum. Mol. Genet.* 21, 3474–3488. doi: 10.1093/hmg/dds178

Chen, C., Zhou, M., Ge, Y., and Wang, X. (2020). SIRT1 and aging related signaling pathways. *Mech. Ageing Dev.* 187:111215.

Cheng, C., Spengler, R. M., Keiser, M. S., Monteys, A. M., Rieders, J. M., Ramachandran, S., et al. (2018). The long non-coding RNA NEAT1 is elevated in polyglutamine repeat expansion diseases and protects from disease gene-dependent toxicities. *Hum. Mol. Genet.* 27, 4303–4314. doi: 10.1093/hmg/ddy331

Cheng, L.-C., Pastrana, E., Tavazoie, M., and Doetsch, F. (2009). miR-124 regulates adult neurogenesis in the subventricular zone stem cell niche. *Nat. Neurosci.* 12, 399–408. doi: 10.1038/nn.2294

Cheng, P.-H., Li, C.-L., Chang, Y.-F., Tsai, S.-J., Lai, Y.-Y., Chan, A. W., et al. (2013). miR-196a ameliorates phenotypes of Huntington disease in cell, transgenic mouse, and induced pluripotent stem cell models. *Am. J. Hum. Genet.* 93, 306–312. doi: 10.1016/j.ajhg.2013.05.025

Das, E., Jana, N. R., and Bhattacharyya, N. P. (2013). MicroRNA-124 targets CCNA2 and regulates cell cycle in STHdhQ111/HdhQ111 cells. *Biochem. Biophys. Res. Commun.* 437, 217–224.

Das, E., Jana, N. R., and Pada Bhattacharyya, N. (2015). Delayed Cell Cycle Progression in STHdhQ111/HdhQ111 Cells, a Cell Model for Huntington's Disease Mediated by microRNA-19a, microRNA-146a and microRNA-432. *Microrna* 4, 86–100. doi: 10.2174/2211536604666150713105606

De Souza, R. A., Islam, S. A., McEwen, L. M., Mathelier, A., Hill, A., Mah, S. M., et al. (2016). DNA methylation profiling in human Huntington's disease brain. *Hum. Mol. Genet.* 25, 2013–2030.

Denissenko, M. F., Chen, J. X., Tang, M.-S., and Pfeifer, G. P. (1997). Cytosine methylation determines hot spots of DNA damage in the human P53 gene. *Proc. Natl. Acad. Sci. U.S.A.* 94, 3893–3898.

Dong, X., and Cong, S. (2021b). MicroRNAs in Huntington's disease: Diagnostic biomarkers or therapeutic agents? *Front. Cell. Neurosci.* 15:705348. doi: 10.3389/fncel.2021.705348

Dong, X., and Cong, S. (2021a). DNM3OS regulates GAPDH expression and influences the molecular pathogenesis of Huntington's disease. *J. Cell. Mol. Med.* 25, 9066–9071. doi: 10.1111/jcmm.16838

Dubois, C., Kong, G., Tran, H., Li, S., Pang, T. Y., Hannan, A. J., et al. (2021). Small Non-coding RNAs Are Dysregulated in Huntington's Disease Transgenic Mice Independently of the Therapeutic Effects of an Environmental Intervention. *Mol. Neurobiol.* 58, 3308–3318. doi: 10.1007/s12035-021-02342-9

Elibol, B., and Kilic, U. (2018). High levels of SIRT1 expression as a protective mechanism against disease-related conditions. *Front. Endocrinol.* 9:614. doi: 10.3389/fendo.2018.00614

Ferraldeschi, M., Romano, S., Giglio, S., Romano, C., Morena, E., Mechelli, R., et al. (2021). Circulating hsa-miR-323b-3p in Huntington's Disease: A Pilot Study. *Front. Neurol.* 12:657973. doi: 10.3389/fneur.2021.657973

Francelle, L., Galvan, L., Gaillard, M.-C., Petit, F., Bernay, B., Guillermier, M., et al. (2015). The striatal long noncoding RNA Abhd11os is neuroprotective against an N-terminal fragment of mutant huntingtin *in vivo*. *Neurobiol. Aging* 36, 1601.e7–1601.e16. doi: 10.1016/j.neurobiolaging.2014.11.014

Francelle, L., Lotz, C., Outeiro, T., Brouillet, E., and Merienne, K. (2017). Contribution of neuroepigenetics to Huntington's disease. *Front. Hum. Neurosci.* 11:17. doi: 10.3389/fnhum.2017.00017

Fu, M.-H., Li, C.-L., Lin, H.-L., Tsai, S.-J., Lai, Y.-Y., Chang, Y.-F., et al. (2015). The potential regulatory mechanisms of miR-196a in Huntington's disease through bioinformatic analyses. *PLoS One* 10:e0137637. doi: 10.1371/journal.pone.0137637

Fukuoka, M., Takahashi, M., Fujita, H., Chiyo, T., Popiel, H. A., Watanabe, S., et al. (2018). Supplemental treatment for Huntington's disease with miR-132 that is deficient in Huntington's disease brain. *Mol. Ther. Nucl. Acids* 11, 79–90. doi: 10.1016/j.omtn.2018.01.007

Ghatak, S., and Raha, S. (2015). Micro RNA-214 contributes to proteasome independent downregulation of beta catenin in Huntington's disease knock-in striatal cell model STHdhQ111/Q111. *Biochem. Biophys. Res. Commun.* 459, 509–514. doi: 10.1016/j.bbrc.2015.02.137

Ghatak, S., and Raha, S. (2018). Beta catenin is regulated by its subcellular distribution and mutant huntingtin status in Huntington's disease cell STHdhQ111/HdhQ111. *Biochem. Biophys. Res. Commun.* 503, 359–364. doi: 10.1016/j.bbrc.2018.06.034

Glajch, K. E., and Sadri-Vakili, G. (2015). Epigenetic mechanisms involved in Huntington's disease pathogenesis. *J. Huntington's Dis.* 4, 1–15.

Gordon, A. M., Quinn, L., Reilmann, R., and Marder, K. (2000). Coordination of prehensile forces during precision grip in Huntington's disease. *Exp. Neurol.* 163, 136–148. doi: 10.1006/exnr.2000.7348

Her, L.-S., Mao, S.-H., Chang, C.-Y., Cheng, P.-H., Chang, Y.-F., Yang, H.-I., et al. (2017). miR-196a enhances neuronal morphology through suppressing RANBP10 to provide Neuroprotection in Huntington's disease. *Theranostics* 7:2452. doi: 10.7150/thno.18813

Horvath, S. (2013). DNA methylation age of human tissues and cell types. *Genome Biol.* 14:R115.

Horvath, S., Langfelder, P., Kwak, S., Aaronson, J., Rosinski, J., Vogt, T. F., et al. (2016). Huntington's disease accelerates epigenetic aging of human brain and disrupts DNA methylation levels. *Aging* 8:1485. doi: 10.18632/aging.101005

Hoss, A. G., Labadorf, A., Latourelle, J. C., Kartha, V. K., Hadzi, T. C., Gusella, J. F., et al. (2015). miR-10b-5p expression in Huntington's disease brain relates to age of onset and the extent of striatal involvement. *BMC Med. Genom.* 8:10. doi: 10.1186/s12920-015-0083-3

Hyeon, J. W., Kim, A. H., and Yano, H. (2021). Epigenetic regulation in Huntington's disease. *Neurochem. Int.* 148:105074.

Iyer, M. K., Niknafs, Y. S., Malik, R., Singhal, U., Sahu, A., Hosono, Y., et al. (2015). The landscape of long noncoding RNAs in the human transcriptome. *Nature genetics* 47, 199–208.

Johnson, R. (2012). Long non-coding RNAs in Huntington's disease neurodegeneration. *Neurobiol. Dis.* 46, 245–254.

Johnson, R., and Buckley, N. J. (2009). Gene dysregulation in Huntington's disease: REST, microRNAs and beyond. *Neuromolecular Med.* 11, 183–199. doi: 10.1007/s12017-009-8063-4

Jovicic, A., Zaldivar Jolissaint, J. F., Moser, R., Silva Santos Mde, F., and Luthi-Carter, R. (2013). MicroRNA-22 (miR-22) overexpression is neuroprotective via general anti-apoptotic effects and may also target specific Huntington's disease-related mechanisms. *PLoS One* 8:e54222. doi: 10.1371/journal.pone.0054222

Kim, D. H., Jung, I. H., Kim, D. H., and Park, S. W. (2019). Knockout of longevity gene Sirt1 in zebrafish leads to oxidative injury, chronic inflammation, and reduced life span. *PLoS One* 14:e0220581. doi: 10.1371/journal.pone.0220581

Kim, K.-H., Abu Elneel, K., Shin, J. W., Keum, J. W., Seong, D., Kwak, S., et al. (2019). Full sequence of mutant huntingtin 3'-untranslated region and modulation of its gene regulatory activity by endogenous microRNA. *J. Hum. Genet.* 64, 995–1004. doi: 10.1038/s10038-019-0639-8

Kirkwood, S. C., Siemers, E., Hodes, M. E., Conneally, P. M., Christian, J. C., and Foroud, T. (2000). Subtle changes among presymptomatic carriers of the Huntington's disease gene. *J. Neurol. Neurosurg. Psychiatry* 69, 773–779.

Kocerha, J., Xu, Y., Prucha, M. S., Zhao, D., and Chan, A. W. (2014). microRNA-128a dysregulation in transgenic Huntington's disease monkeys. *Mol. Brain* 7:46. doi: 10.1186/1756-6606-7-46

Kunkanjanawan, T., Carter, R. L., Prucha, M. S., Yang, J., Parnpai, R., and Chan, A. W. (2016). miR-196a ameliorates cytotoxicity and cellular phenotype in transgenic Huntington's disease monkey neural cells. *PLoS One* 11:e0162788. doi: 10.1371/journal.pone.0162788

Langfelder, P., Gao, F., Wang, N., Howland, D., Kwak, S., Vogt, T. F., et al. (2018). MicroRNA signatures of endogenous Huntingtin CAG repeat expansion in mice. *PLoS One* 13:e0190550. doi: 10.1371/journal.pone.0190550

Lee, J. M., Ivanova, E. V., Seong, I. S., Cashorali, T., Kohane, I., Gusella, J. F., et al. (2007). Unbiased gene expression analysis implicates the huntingtin polyglutamine tract in extra-mitochondrial energy metabolism. *PLoS Genet.* 3:e135. doi: 10.1371/journal.pgen.0030135

Lee, J., Hwang, Y. J., Kim, K. Y., Kowall, N. W., and Ryu, H. (2013). Epigenetic mechanisms of neurodegeneration in Huntington's disease. *Neurotherapeutics* 10, 664–676.

Lee, S.-T., Im, W., Ban, J.-J., Lee, M., Jung, K.-H., Lee, S. K., et al. (2017). Exosome-based delivery of miR-124 in a Huntington's disease model. *J. Mov. Disord.* 10:45. doi: 10.14802/jmd.16054

Liu, T., Im, W., Mook-Jung, I., and Kim, M. (2015). MicroRNA-124 slows down the progression of Huntington's disease by promoting neurogenesis in the striatum. *Neural Regen. Res.* 10:786. doi: 10.4103/1673-5374.156978

Lu, A. T., Narayan, P., Grant, M. J., Langfelder, P., Wang, N., Kwak, S., et al. (2020). DNA methylation study of Huntington's disease and motor progression in patients and in animal models. *Nat. Commun.* 11:4529.

Ma, L., Bajic, V. B., and Zhang, Z. (2013). On the classification of long non-coding RNAs. *RNA Biol.* 10, 924–933.

Machiela, E., and Southwell, A. L. (2020). Biological aging and the cellular pathogenesis of Huntington's disease. *J. Huntington's Dis.* 9, 115–128.

Managadze, D., Lobkovsky, A. E., Wolf, Y. I., Shabalina, S. A., Rogozin, I. B., and Koonin, E. V. (2013). The vast, conserved mammalian lincRNome. *PLoS Comput. Biol.* 9:e1002917. doi: 10.1371/journal.pcbi.1002917

Mizuno, H., and Taketomi, A. (2018). MicroRNA-101 inhibits the expression of Rhes, a striatal-enriched small G-protein, at the post-transcriptional level *in vitro*. *BMC Res. Notes* 11:528. doi: 10.1186/s13104-018-3654-5

Müller, S. (2014). In silico analysis of regulatory networks underlines the role of miR-10b-5p and its target BDNF in huntington's disease. *Transl. Neurodegener.* 3:17. doi: 10.1186/2047-9158-3-17

Myers, R. H. (2004). Huntington's disease genetics. *NeuroRx* 1, 255–262.

Ng, C. W., Yildirim, F., Yap, Y. S., Dalin, S., Matthews, B. J., Velez, P. J., et al. (2013). Extensive changes in DNA methylation are associated with expression of mutant huntingtin. *Proc. Natl. Acad. Sci. U.S.A.* 110, 2354–2359. doi: 10.1073/pnas.1221292110

Noroozi, R., Ghafouri-Fard, S., Pisarek, A., Rudnicka, J., Spólnicka, M., Branicki, W., et al. (2021). DNA methylation-based age clocks: From age prediction to age reversion. *Ageing Res. Rev.* 68:101314.

Packer, A. N., Xing, Y., Harper, S. Q., Jones, L., and Davidson, B. L. (2008). The bifunctional microRNA miR-9/miR-9* regulates REST and CoREST and is downregulated in Huntington's disease. *J. Neurosci.* 28, 14341–14346. doi: 10.1523/JNEUROSCI.2390-08.2008

Paulsen, J. S., Hayden, M., Stout, J. C., Langbehn, D. R., Aylward, E., Ross, C. A., et al. (2006). Preparing for preventive clinical trials: The Predict-HD study. *Arch. Neurol.* 63, 883–890. doi: 10.1001/archneur.63.6.883

Peschansky, V. J., Pastori, C., Zeier, Z., Wentzel, K., Velmeshev, D., Magistri, M., et al. (2016). The long non-coding RNA FMR4 promotes proliferation of human neural precursor cells and epigenetic regulation of gene expression in trans. *Mol. Cell. Neurosci.* 74, 49–57. doi: 10.1016/j.mcn.2016.03.008

Pfister, E. L., DiNardo, N., Mondo, E., Borel, F., Conroy, F., Fraser, C., et al. (2018). Artificial miRNAs Reduce Human Mutant Huntingtin Throughout the Striatum in a Transgenic Sheep Model of Huntington's Disease. *Hum. Gene Ther.* 29, 663–673. doi: 10.1089/hum.2017.199

Pircs, K., Petri, R., Madsen, S., Brattås, P. L., Vuono, R., Ottosson, D. R., et al. (2018). Huntingtin Aggregation Impairs Autophagy, Leading to Argonaute-2 Accumulation and Global MicroRNA Dysregulation. *Cell Rep.* 24, 1397–1406. doi: 10.1016/j.celrep.2018.07.017

Reynolds, R. H., Petersen, M. H., Willert, C. W., Heinrich, M., Nymann, N., Dall, M., et al. (2018). Perturbations in the p53/miR-34a/SIRT1 pathway in the R6/2 Huntington's disease model. *Mol. Cell. Neurosci.* 88, 118–129. doi: 10.1016/j.mcn.2017.12.009

Sattari, A., Nicknafs, F., and Noroozi, R. (2020). The role of single nucleotide polymorphisms within long non-coding RNAs in susceptibility to human disorders. *Ecol. Genet. Genom.* 17:100071.

Sinha, M., Mukhopadhyay, S., and Bhattacharyya, N. P. (2012). Mechanism(s) of alteration of micro RNA expressions in Huntington's disease and their possible contributions to the observed cellular and molecular dysfunctions in the disease. *Neuromolecular Med.* 14, 221–243. doi: 10.1007/s12017-012-8183-0

Soldati, C., Bithell, A., Johnston, C., Wong, K. Y., Stanton, L. W., and Buckley, N. J. (2013). Dysregulation of REST-regulated coding and non-coding RNAs in a cellular model of Huntington's disease. *J. Neurochem.* 124, 418–430. doi: 10.1111/jnc.12090

Sunwoo, J.-S., Lee, S.-T., Im, W., Lee, M., Byun, J.-I., Jung, K.-H., et al. (2017). Altered expression of the long noncoding RNA NEAT1 in Huntington's disease. *Mol. Neurobiol.* 54, 1577–1586. doi: 10.1007/s12035-016-9928-9

Tabrizi, S. J., Langbehn, D. R., Leavitt, B. R., Roos, R. A., Durr, A., Craufurd, D., et al. (2009). Biological and clinical manifestations of Huntington's disease in the longitudinal TRACK-HD study: Cross-sectional analysis of baseline data. *Lancet Neurol.* 8, 791–801. doi: 10.1016/S1474-4422(09)70170-X

Tan, X., Liu, Y., Liu, Y., Zhang, T., and Cong, S. (2021). Dysregulation of long non-coding RNAs and their mechanisms in Huntington's disease. *J. Neurosci. Res.* 99, 2074–2090.

Tharakan, R., Ubaida-Mohien, C., Moore, A. Z., Hernandez, D., Tanaka, T., and Ferrucci, L. (2020). Blood DNA methylation and aging: A cross-sectional analysis and longitudinal validation in the InCHIANTI study. *J. Gerontol.* 75, 2051–2055. doi: 10.1093/gerona/glaa052

Tsai, M.-C., Manor, O., Wan, Y., Mosammaparast, N., Wang, J. K., Lan, F., et al. (2010). Long noncoding RNA as modular scaffold of histone modification complexes. *Science* 329, 689–693.

Valor, L. M., and Guiretti, D. (2014). What's wrong with epigenetics in Huntington's disease? *Neuropharmacology* 80, 103–114. doi: 10.1016/j.neuropharm.2013.10.025

Vashishtha, M., Ng, C. W., Yildirim, F., Gipson, T. A., Kratter, I. H., Bodai, L., et al. (2013). Targeting H3K4 trimethylation in Huntington disease. *Proc. Natl. Acad. Sci. U.S.A.* 110:E3027–E3036. doi: 10.1073/pnas.1311323110

Villar-Menéndez, I., Blanch, M., Tyebji, S., Pereira-Veiga, T., Albasanz, J. L., Martín, M., et al. (2013). Increased 5-methylcytosine and decreased 5-hydroxymethylcytosine levels are associated with reduced striatal A2AR levels in Huntington's disease. *Neuromolecular Med.* 15, 295–309. doi: 10.1007/s12017-013-8219-0

Woźniak, A., Heidegger, A., Piniewska-Róg, D., Pośpiech, E., Xavier, C., Pisarek, A., et al. (2021). Development of the VISAGE enhanced tool and statistical models for epigenetic age estimation in blood, buccal cells and bones. *Aging* 13:6459. doi: 10.18632/aging.202783

Yang, X.-Y., Li, Q.-J., Zhang, W.-C., Zheng, S.-Q., Qu, Z.-J., Xi, Y., et al. (2020). AMPK-SIRT1-PGC1α signal pathway influences the cognitive function of aged rats in sevoflurane-induced anesthesia. *J. Mol. Neurosci.* 70, 2058–2067. doi: 10.1007/s12031-020-01612-w

Zhou, S., Yu, X., Wang, M., Meng, Y., Song, D., Yang, H., et al. (2021). Long non-coding RNAs in pathogenesis of neurodegenerative diseases. *Front. Cell Dev. Biol.* 9:719247. doi: 10.3389/fcell.2021.719247

Zimmer-Bensch, G. (2020). Epigenomic remodeling in Huntington's disease—master or servant? *Epigenomes* 4:15.

Zuccato, C., Tartari, M., Crotti, A., Goffredo, D., Valenza, M., Conti, L., et al. (2003). Huntingtin interacts with REST/NRSF to modulate the transcription of NRSE-controlled neuronal genes. *Nat. Genet.* 35, 76–83. doi: 10.1038/ng1219

frontiers | Frontiers in Aging Neuroscience

TYPE Original Research
PUBLISHED 04 October 2022
DOI 10.3389/fnagi.2022.981632

OPEN ACCESS

EDITED BY
Helena Blumen,
Albert Einstein College of Medicine,
United States

REVIEWED BY
Chaur-Jong Hu,
Taipei Medical University, Taiwan
Gabriel Gonzalez-Escamilla,
Johannes Gutenberg University Mainz,
Germany

*CORRESPONDENCE
Fang-Yu Cheng
fycheng@mmc.edu.tw

SPECIALTY SECTION
This article was submitted to Neurocognitive Aging and Behavior, a section of the journal Frontiers in Aging Neuroscience

RECEIVED 29 June 2022
ACCEPTED 20 September 2022
PUBLISHED 04 October 2022

CITATION
Chen P-H, Lin S-I, Liao Y-Y, Hsu W-L and Cheng F-Y (2022) Associations between blood-based biomarkers of Alzheimer's disease with cognition in motoric cognitive risk syndrome: A pilot study using plasma Aβ42 and total tau.
Front. Aging Neurosci. 14:981632.
doi: 10.3389/fnagi.2022.981632

Associations between blood-based biomarkers of Alzheimer's disease with cognition in motoric cognitive risk syndrome: A pilot study using plasma Aβ42 and total tau

Pei-Hao Chen[1,2,3], Sang-I Lin[4], Ying-Yi Liao[5], Wei-Ling Hsu[4,6] and Fang-Yu Cheng[4]*

[1]Department of Neurology, MacKay Memorial Hospital, Taipei, Taiwan, [2]Department of Medicine, MacKay Medical College, New Taipei City, Taiwan, [3]Graduate Institute of Mechanical and Electrical Engineering, National Taipei University of Technology, Taipei, Taiwan, [4]Institute of Long-Term Care, MacKay Medical College, New Taipei City, Taiwan, [5]Department of Gerontological Health Care, National Taipei University of Nursing and Health Sciences, Taipei, Taiwan, [6]Center of Dementia Care, MacKay Memorial Hospital, New Taipei City, Taiwan

Background: Motoric cognitive risk (MCR) syndrome is a conceptual construct that combines slow gait speed with subjective cognitive complaints and has been shown to be associated with an increased risk of developing dementia. However, the relationships between the pathology of Alzheimer's disease (AD) and MCR syndrome remain uncertain. Therefore, the purpose of this study was to determine the levels of plasma AD biomarkers (Aβ42 and total tau) and their relationships with cognition in individuals with MCR.

Materials and methods: This was a cross-sectional pilot study that enrolled 25 individuals with normal cognition (NC), 27 with MCR, and 16 with AD. Plasma Aβ42 and total tau (t-tau) levels were measured using immunomagnetic reduction (IMR) assays. A comprehensive neuropsychological assessment was also performed.

Results: The levels of plasma t-tau proteins did not differ significantly between the MCR and AD groups, but that of plasma t-tau was significantly increased in the MCR and AD groups, compared to the NC group. Visuospatial performance was significantly lower in the MCR group than in the NC group. The levels of plasma t-tau correlated significantly with the Montreal Cognitive Assessment (MoCA) and Boston naming test scores in the MCR group.

Conclusion: In this pilot study, we found significantly increased plasma t-tau proteins in the MCR and AD groups, compared with the NC group. The plasma

t-tau levels were also significantly correlated with the cognitive function of older adults with MCR. These results implied that MCR and AD may share similar pathology. However, these findings need further confirmation in longitudinal studies.

KEYWORDS

plasma biomarker, cognition, gait speed, Alzheimer's disease, motoric cognitive risk syndrome

Introduction

Motoric cognitive risk (MCR) syndrome is a conceptual construct that combines slow gait speed with subjective cognitive complaints (Verghese et al., 2013). Motoric cognitive risk syndrome is easy to screen in the community and is associated with an increased risk of developing dementia, such as Alzheimer's disease (AD) or vascular dementia (Verghese et al., 2013, 2014a). This syndrome is presented in approximately 10% of the older population and has been shown to be associated with an increased risk of falls and disability (Verghese et al., 2014b). The pathophysiological mechanisms underlying MCR have not yet been fully established. Previous studies revealed that MCR could be related to cortical atrophy (Blumen et al., 2021), lacunar infarction (Wang et al., 2016), or increased levels of systematic inflammatory biomarkers (Bortone et al., 2021). A cross-sectional study using MRI found that gray matter volumes, hippocampal volumes, and white matter hyperintensities were worse in individuals with MCR (Yaqub et al., 2022). Meiner et al. (2021) also reported that Apolipoprotein E ε4 allele (APOE ε4) was associated with the conversion to dementia in older adults with MCR. On the contrary, although MCR has good predictive validity for the incidence of AD, the relationships between AD pathology and MCR remain uncertain. Alzheimer's disease is characterized by two major pathological lesions in the brain, amyloid β plaques and tau neurofibrillary tangles (Avila, 2006; Capetillo-Zarate et al., 2012). Alzheimer's disease pathology has been found to have a strong association with gait disorder in older adults without dementia and can predict cognitive decline and incident dementia (Del Campo et al., 2016; Tian et al., 2017). Recently, in a study investigating the relationships between MCR and AD pathology using imaging biomarkers, no significant differences in the biomarkers of AD, such as amyloid, tau deposition, or white matter hyperintensities, were found between individuals with MCR and without MCR (Bommarito et al., 2022). Although the findings of this study were informative, the sample size was relatively small, and no comparisons were made with the normal cognition (NC) group, making it difficult to determine whether the physiological changes in MCR were caused by normal aging or the pathological changes related to AD.

Amyloid β and tau protein are presented in the cerebrospinal fluid (CSF) and the brain and can be measured by lumbar puncture (Olsson et al., 2016) or positron emission tomography (PET), respectively (Johnson et al., 2013). However, their clinical applications are often limited because CSF sampling is invasive and PET scans are costly. Recently, blood-based biomarkers have been used cost-effectively to assist in the diagnosis of neurodegenerative diseases and the estimation of prognosis clinically (Hansson, 2021). Immunomagnetic reduction (IMR) is a highly sensitive assay technology for the analysis of biomarkers in blood samples, and can accurately quantify plasma Aβ and tau (Baird et al., 2015; Yang et al., 2017). A review article including 15 studies using the IMR assay indicated that significant increases in the plasma levels of Aβ42 and tau in persons with amnestic mild cognitive impairment (aMCI) and AD, and the levels of Aβ42 and tau are related to the severity of AD (Lee et al., 2022). These findings suggested that assays of plasma Aβ42 or tau using IMR may be promising tools for facilitating an early diagnosis of AD. Therefore, measuring plasma Aβ42 or tau protein concentrations *via* IMR assay in individuals with MCR may also reveal its associated physiological changes.

In this pilot study, we compared the levels of plasma Aβ42 and total tau (t-tau), and their associations with global and specific cognitive functions among older adults with NC, individuals with MCR, and those with AD. We aimed to determine the levels of plasma AD biomarkers (Aβ42 and total tau) and their relationships with cognition in individuals with MCR.

Materials and methods

Participants and study design

This work was a cross-sectional study conducted in Taiwan between June 2021 and April 2022. Participants were recruited from a medical center in Taipei. All participants met the following criteria: (a) aged 60 years or older, (b) could walk 10 m

independently, and (c) living in the community. The exclusion criteria were as follows: (a) unstable medical conditions, for example, the presence of major visual or hearing loss, and (b) a recent or planned surgery leading to limitations in walking or participation in this study. A total of 68 participants provided informed consent, and the study procedures were approved by the Institutional Review Board of Mackay Memorial Hospital (number: 21MMHIS078e). We confirmed that the experimental procedures were performed in accordance with the relevant guidelines and regulations. Of these participants, 16 suffered from mild to moderate AD, with the disease courses longer than 2 years. There were 27 participants with MCR, with the symptoms courses longer than 3 months. There were 25 NC controls. Clinical diagnosis was based on physical and neurological examinations, laboratory tests, and comprehensive neuropsychological tests.

Demographic and clinical measures

Information about age, sex, history of metabolic disease, and level of education was obtained from interviews and medical charts. All the participants completed the comprehensive neuropsychological testing, including the Mini-Mental State Examination (MMSE), Montreal Cognitive Assessment (MoCA), clinical dementia rating (CDR), the Chinese version of Parts A and B of the trail making test (TMT) (Wu et al., 2015), category fluency test (Rosen, 1980), digital symbol modality test, the Chinese version of the California Verbal Learning Test (CVLT-SF) (Chang et al., 2010), Judgment of Line Orientation test (Mitrushina et al., 2005), Boston naming test (del Toro et al., 2011), and the Chinese version of the Geriatric Depression Scale-15 (GDS-15) (Liu et al., 1997) to evaluate global cognitive function, executive function, attention and working memory, episodic memory, visuospatial performance, language, and depression. All the neuropsychological tests were assessed by experienced neurologists who have received professional neuropsychological scale training.

Motoric cognitive risk syndrome group

This study mainly adopted the diagnostic criteria of Verghese et al. (2014b). The inclusion criteria for the MCR group were as follows: (1) subjective cognitive complaints, (2) slow gait speed, (3) absence of dementia, and (4) a consistent level of independence in the activities of daily living. The presence of subjective cognitive complaints was determined by a "yes" response to the memory item on the Geriatric Depression Scale (Yesavage et al., 1982; Ayers and Verghese, 2019). Slow gait speed was defined as a walking speed of one or more standard deviations (SDs) below the mean age- and sex-specific gait speed (Verghese et al., 2013, 2014b). The exclusion criteria were (1) consumption of any medications causing cognitive complaints during the past 3 months, (2) inability to cooperate with the procedures and tests in this study, and (3) other significant neurological or psychiatric conditions, such as Parkinson's disease, stroke, Parkinsonism, other movement disorder, or major depression.

Alzheimer's disease group

The presence of AD was based on the diagnostic criteria defined by the National Institute on Aging (NIA) and the Alzheimer's Association (AA) in McKhann et al. (2011). The inclusion criteria were as follows: (1) fulfilled the core clinical criteria proposed by the NIA-AA workgroup, and (2) clinical dementia rating (CDR) = 1 (Morris, 1997). The exclusion criteria were as follows: (1) other significant neurological or psychiatric conditions that might cause cognitive impairments, such as frontotemporal dementia, dementia with Lewy bodies, vascular dementia, Parkinson's disease, stroke, vitamin B12 deficiency, alcoholism, or major depression.

Normal cognition group

Older adults with NC were screened and recruited from the neurology outpatient department. The inclusion criteria were as follows: (1) no subjective or objective memory deficits or declines in cognitive performance, (2) no mental or neurological disease, and (3) CDR = 0 (Morris, 1997). The exclusion criteria were the same as those for the MCR group.

Blood sample processing and immunomagnetic reduction assays

Ten milliliters of venous blood were collected from each participant, and then the blood sample was centrifuged at room temperature for 15 min at 1,500–2,500 xg. Pure serum was drained and immediately frozen in test tubes at −80°C. Frozen plasma was dry ice delivered to MagQu Co., Ltd. (New Taipei City, Taiwan) for IMR assay processing. The technical information and the validation accuracy of the IMR assay were previously described (Chiu et al., 2013; Lue et al., 2017). The volumes of the t-tau magnetic reagents and the to-be-detected samples were 80 and 40 μl, respectively. The volumes of the Aβ42 magnetic reagents and the to-be-detected samples were 60 and 60 μl, respectively. After mixing, superconducting quantum interference device (SQID)-based alternative current magnetosusceptometer (model XacPro-S, MagQu Co., New Taipei City, Taiwan) to determine the time-dependent alternative current magnetic susceptibility. Because of the association between the antibody-functionalized magnetic nanoparticles and the target biomarkers, the alternative current magnetic susceptibility of the mixture was reduced. This

reduction in magnetic susceptibility is referred to as the IMR signal. For each to-be-detected sample, the sample was divided into three parts, and the IMR signals of each part were detected individually. Therefore, three IMR signals were obtained for each sample. The mean value, standard deviation, and coefficient of variation (interrun) of the IMR signals were analyzed.

Statistical analysis

Analysis was conducted using Statistical Product and Service Solutions (SPSS) version 26.0 (SPSS Inc., Chicago, IL, USA). The participants' characteristics are summarized using the means, SDs, or numbers, as appropriate. Between-group comparisons were performed using one-way analysis of covariance (ANCOVA) (continuous variables) (age and sex as covariate variables), followed by Bonferroni *post-hoc* tests, or chi-square tests (categorical variables). Spearman's rank correlation coefficient was used to examine the correlations between plasma neurodegenerative biomarkers and cognitive functions in the NC, MCR, and AD groups. In this study, the within-group Spearman's rank correlations were examined 10 times. Although such multiple tests might inflate the type I error, previous studies have shown that correlation coefficients larger than 0.3 could indicate meaningful correlations without correction for multiple comparisons (Hinkle et al., 2003; Mukaka, 2012). Thus, for the correlational analysis, a correlation coefficient greater than 0.3 or a p-value less than 0.05 would be considered significant.

Results

Baseline demographics and biomarkers

Sixty-eight participants were recruited for the study. Table 1 presents the characteristics and plasma biomarkers of the participants in the NC (N = 25), MCR (n = 27), and AD (n = 16) groups. The mean ages of the participants in the NC, MCR, and AD groups were 74.3 ± 7.4, 75.2 ± 6.4, and 78.2 ± 6.6 years, respectively. There were no differences in age, body mass index, educational level, or the prevalence of medical conditions (hypertension, diabetes, and heart disease) among the three groups. However, the AD group had a higher proportion of women than the other groups (NC: 36%, MCR: 52%, AD: 81%, p = 0.018). The MCR and AD groups had poorer general cognitive functions (MMSE, F = 25.740, η^2 = 0.450, p < 0.001; MoCA, F = 11.911, η^2 = 0.274, p < 0.001; CDR, F = 156.595, η^2 = 0.833, p < 0.001) and lower gait speed (F = 29.422, η^2 = 0.487, p < 0.001) than the NC group. The AD group had significantly lower MMSE (Cohen's d = 1.675, p < 0.001), MoCA (Cohen's d = 1.058, p = 0.014), and CDR (Cohen's d = 3.299, p < 0.001) scores but a faster gait speed (Cohen's d = 0.784, p = 0.032) than the MCR group. Compared to the NC group, the AD group had higher levels of plasma t-tau

TABLE 1 Comparison of participants' characteristics among the three groups (n = 68).

	Normal cognition (n = 25)	Motoric cognitive risk syndrome (n = 27)	Alzheimer's disease (n = 16)	F	P-value	Partial eta squared
Age (years)	74.3 ± 7.4	75.2 ± 6.4	78.2 ± 6.6		0.204	
Sex (male/female), n	16/9	13/14	3/13		0.018	
BMI	24.9 ± 2.6	24.2 ± 3.4	23.9 ± 3.9		0.586	
Education level	7.8 ± 4.7	6.4 ± 4.9	5.2 ± 4.8		0.489	
0 years, n	3	5	4			
1–6 years, n	12	17	7			
7–12 years, n	7	2	4			
13 or more years, n	3	3	1			
Hypertension, n	10	17	7		0.216	
Diabetes mellitus, n	6	13	5		0.177	
Heart disease, n	3	6	2		0.546	
MMSE	26.6 ± 2.8	23.7 ± 4.6	15.3 ± 5.4$^{**\#\#}$	25.745	<0.001[a]	0.450
MoCA	22.2 ± 4.5	17.9 ± 6.2*	11.6 ± 5.7$^{**\#}$	11.911	<0.001[a]	0.274
CDR	0.0 ± 0.0	0.3 ± 0.3**	1.0 ± 0.0$^{**\#\#}$	156.595	<0.001[a]	0.833
Gait speed, m/s	1.1 ± 0.2	0.6 ± 0.2**	0.8 ± 0.3$^{*\#}$	29.422	<0.001[a]	0.487
Aβ42, pg/ml	16.4 ± 0.5	16.6 ± 0.6	16.8 ± 0.5	2.328	0.106[a]	0.069
t-tau, pg/ml	20.6 ± 1.7	22.7 ± 3.4*	24.2 ± 3.6**	9.583	<0.001[a]	0.233

BMI, body mass index; MMSE, Mini-Mental State Examination; MoCA, Montreal Cognitive Assessment; CDR, clinical dementia rating; Aβ42, amyloid beta 42; t-tau, total tau.
[a]Adjusted for age and sex.
* and **: Significance levels of <0.05 and <0.001 for intergroup comparisons between the normal cognition (NC) group and other groups.
# and ##: Significance levels of <0.05 and <0.001 for intergroup comparisons between the motoric cognitive risk (MCR) syndrome group and the Alzheimer's disease (AD) group.

(Cohen's d = 1.279, $p < 0.001$). The levels of plasma Aβ42 did not differ significantly between the MCR and NC groups, but the former had significantly higher levels of t-tau (Cohen's d = 0.781, p = 0.018).

Cognitive function

The cognitive function of the participants is shown in Table 2. The MCR and AD groups had poorer visuospatial performance (Judgment of Line Orientation, F = 7.591, η^2 = 0.194, p = 0.001) than the NC group. The AD group had significantly poorer executive function (TMT-A, Cohen's d = 1.265, p = 0.013), attention and working memory (Digital symbol modality test, Cohen's d = 1.318, p = 0.025), episodic memory (CVLT-SF, Cohen's d = 0.945, p = 0.015), and language ability (Boston naming test, Cohen's d = 1.831, $p < 0.001$) than the NC group. The AD group had significantly poorer language performance (Boston naming test, Cohen's d = 1.523, $p < 0.001$) than the MCR group.

Association of cognitive function and biomarkers in motoric cognitive risk "Syndrome"

Table 3 shows the correlations between cognitive function and plasma Aβ42 in the NC, MCR, and AD groups. In the AD group, the levels of plasma Aβ42 were positively correlated with the TMT-B scores (r_s = 0.572, p = 0.020), which indicated that higher plasma Aβ42 levels were associated with lower cognitive function (Figure 1). However, there were no significant correlations between the levels of plasma Aβ42 and cognitive function in the NC and MCR groups. Table 4 shows the correlations between cognitive function and plasma t-tau in the NC, MCR, and AD groups. In the NC group, the levels of plasma t-tau were positively correlated with the GDS-15 scores (r_s = 0.456, p = 0.022), which indicated that higher plasma t-tau levels were associated with higher levels of depression (Figure 2). In the MCR group, the levels of plasma t-tau were negatively correlated with the MoCA and Boston naming test scores [MoCA, r_s = (−0.484), p = 0.011; Boston naming test, r_s = (−0.444), p = 0.020], which indicated that higher plasma t-tau levels were associated with lower cognitive function (Figure 3). However, there were no significant correlations between the levels of plasma t-tau and cognitive function in the AD group.

Discussion

To our knowledge, this is the first study to use plasma biomarkers to examine Aβ42 and t-tau in relation to cognitive function in older adults with MCR and the first to report that plasma t-tau is related to cognitive function in individuals with MCR. We found that the levels of plasma Aβ42 and t-tau did not differ between older adults with MCR and AD, but the levels of plasma t-tau in older adults with MCR and AD were significantly higher than those in older adults with NC. In addition, the levels of plasma t-tau in individuals with MCR were related to MoCA and Boston naming test scores.

The accumulation of Aβ plaques and tau neurofibrillary tangles in the brain are two pathological hallmarks of AD (Avila, 2006; Capetillo-Zarate et al., 2012). These biomarkers can cause neural damage and lead to hippocampal atrophy, cortical shrinkage, and brain damage (Pini et al., 2016; Pereira et al., 2017). In the present study, the AD group had higher levels of plasma t-tau, compared with the NC group. These findings reconfirmed the above statement. MCR is a symptomatic predementia phase and has good predictive validity for the incidence of dementia (Verghese et al., 2013, 2014a). However, previous studies have presented inconsistent results regarding whether MCR would increase the risk of AD. In the Einstein Aging Study, MCR was a strong predictor of vascular dementia (hazard ratio = 12.81) but not AD dementia (hazard ratio = 0.66) (Verghese et al., 2013). In another multicountry study, samples from multiple cohorts were pooled, and it was found that MCR was associated with an increased risk of AD in two cohorts (hazard ratio = 1.79–2.10) (Verghese et al., 2014a). Therefore, clarifying the relationship between AD pathology and MCR may aid clinical diagnosis and the planning of prevention strategies. To date, only one study has investigated the relationship between MCR and AD pathology using imaging biomarkers (Bommarito et al., 2022) and reported findings inconsistent with the present study. In the above mentioned study, 20 patients with cognitive complaints (8 individuals with MCR and 12 without MCR) were recruited from the Memory Center of the Geneva University Hospitals, and no significant differences in the deposition of amyloid and tau protein in the brain between older adults with MCR and without MCR were found. The individuals without MCR in Bommarito et al. (2022) had subjective cognitive complaints and a CDR scale score of 0.5, which might have affected the results of the study. The strength of our study was that NC and AD groups were included for comparison. We found that the levels of plasma t-tau were higher in the participants with MCR and AD than in the older adults with NC. However, plasma t-tau did not differ between the individuals with MCR and those with AD. MCR is a predementia syndrome similar to mild cognitive impairment (MCI). A review of 15 clinical studies demonstrated an increase in the plasma t-tau levels in older adults with MCI and AD (Lee et al., 2022). The elevated levels of plasma t-tau in individuals with MCR suggested that MCR might share a similar pathology with AD.

For cognitively normal individuals, earlier studies have reported significant correlations between slow gait speed

TABLE 2 Comparison of participants' cognitive performance and physical function among the three groups (n = 68).

	Normal cognition (n = 25)	Motoric cognitive risk syndrome (n = 27)	Alzheimer's disease (n = 16)	F	P-value	Partial eta squared
Executive function						
TMT-A, s	23.1 ± 15.1	42.6 ± 32.1	61.5 ± 40.2*	4.679	0.013[a]	0.129
TMT-B, s	62.0 ± 36.0	83.6 ± 35.5	89.9 ± 37.2	1.892	0.159[a]	0.057
Category fluency test	11.3 ± 3.6	10.0 ± 3.8	7.8 ± 4.4	2.060	0.136[a]	0.061
Attention and working memory						
Digital symbol modality test	34.0 ± 13.3	23.7 ± 15.6	15.1 ± 15.3*	4.284	0.018[a]	0.120
Episodic memory						
CVLT-SF	18.8 ± 5.3	15.9 ± 5.3	13.3 ± 6.3*	4.393	0.016[a]	0.122
Visuospatial performance						
Judgment of line orientation	13.6 ± 3.6	9.4 ± 4.3*	7.3 ± 5.1*	7.591	0.001[a]	0.194
Language						
Boston naming test	23.5 ± 5.1	21.3 ± 4.5	12.7 ± 6.6**##	15.175	<0.001[a]	0.325
Depression						
Geriatric Depression Scale-15	3.1 ± 2.8	3.8 ± 3.2	2.6 ± 2.7	0.698	0.501[a]	0.022

TMT, trail making test; CVLT-SF, California Verbal Language Test-Short Form.

[a]Adjusted for age and sex.

* and **: Significance levels of <0.05 and <0.001 for intergroup comparisons between the normal cognition (NC) group and other groups.

##: Significance level of <0.001 for intergroup comparisons between the motoric cognitive risk (MCR) syndrome group and the Alzheimer's disease (AD) group.

TABLE 3 Associations between plasma Aβ42 and cognitive function in the three groups.

	Normal cognition (n = 25)		Motoric cognitive risk syndrome (n = 27)		Alzheimer's disease (n = 16)	
Outcomes	r_s	p	r_s	p	r_s	P
MMSE	0.232	0.264	−0.096	0.633	−0.221	0.412
MoCA	−0.151	0.472	0.034	0.865	−0.105	0.699
TMT-A	0.038	0.855	0.067	0.741	0.353	0.180
TMT-B	0.042	0.842	−0.011	0.958	0.572	0.020*
Category fluency test	−0.156	0.457	0.227	0.254	0.341	0.197
CVLT-SF	−0.020	0.926	−0.052	0.795	−0.246	0.359
Digital symbol modality test	−0.260	0.210	−0.068	0.737	−0.387	0.139
Judgment of line orientation	0.053	0.801	−0.258	0.193	−0.006	0.983
Boston naming test	−0.340	0.096	−0.091	0.653	−0.289	0.278
Geriatric Depression Scale-15	−0.017	0.935	0.145	0.471	0.408	0.116

Aβ42, amyloid beta 42; t-tau, total tau; MoCA, Montreal Cognitive Assessment; TMT, trail making test; CVLT-SF, California Verbal Language Test-Short Form; *$p < 0.05$.

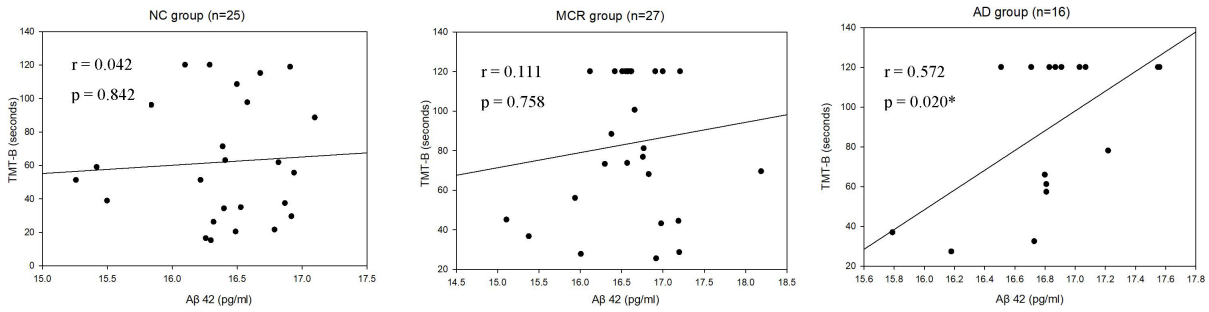

FIGURE 1
Scatterplots of the associations between TMT-B and plasma Aβ42 levels (pg/ml) in the three groups. NC, normal cognition; MCR, Motoric Cognitive Risk syndrome; AD, Alzheimer's disease; Aβ42, amyloid beta 42; TMT-B, trail making test-part B; *$p < 0.05$.

TABLE 4 Associations between plasma t-tau and cognitive function in the three groups.

Outcomes	Normal cognition (n = 25)		Motoric cognitive risk syndrome (n = 27)		Alzheimer's disease (n = 16)	
	r_s	p	r_s	p	r_s	p
MMSE	−0.121	0.564	−0.359	0.066	0.006	0.983
MoCA	0.008	0.972	−0.484	0.011*	0.263	0.326
TMT-A	0.073	0.730	0.338	0.085	−0.287	0.280
TMT-B	0.001	0.999	0.194	0.332	−0.143	0.598
Category fluency test	−0.260	0.210	−0.061	0.764	0.163	0.545
CVLT-SF	0.055	0.793	−0.064	0.750	0.244	0.362
Digital symbol modality test	−0.163	0.436	−0.356	0.068	−0.074	0.786
Judgment of line orientation	−0.317	0.122	−0.358	0.067	0.091	0.736
Boston naming test	0.132	0.528	−0.444*	0.020	0.104	0.703
Geriatric Depression Scale-15	0.456	0.022*	0.141	0.483	−0.252	0.346

Aβ42, amyloid beta 42; t-tau, total tau; MoCA, Montreal Cognitive Assessment; TMT, trail making test; CVLT-SF, California Verbal Language Test-Short Form; *$p < 0.05$.

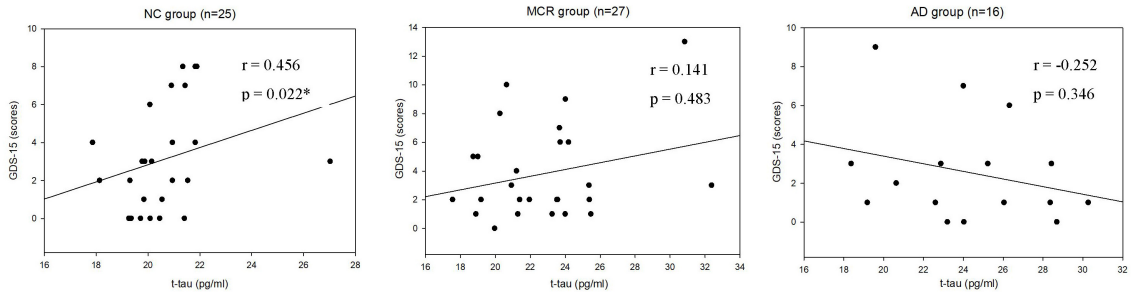

FIGURE 2
Scatterplots of the associations between Geriatric Depression Scale-15 (GDS-15) scores and plasma t-tau levels (pg/ml) in the three groups. NC, normal cognition; MCR, Motoric Cognitive Risk syndrome; AD, Alzheimer's disease; t-tau, total tau; GDS-15, Geriatric Depression Scale-15; *$p < 0.05$.

and amyloid deposition in the subcortical and cortical areas (Del Campo et al., 2016; Wennberg et al., 2017). However, recent studies did not find increased amyloid deposition in older adults with MCR (Bommarito et al., 2022; Gomez et al., 2022). In this study, for the first time, we compared plasma Aβ42 among older adults with NC, individuals with MCR and those with AD. It was found that, compared to the NC group, there were no significantly increased levels of plasma Aβ42 in the MCR group. We also noted that there were no significant correlations between the level of plasma Aβ42 and cognitive function in the MCR group. Previous studies suggested that the pathophysiological mechanisms underlying MCR were probably heterogeneous (Bommarito et al., 2022). Gomez et al. (2022) recruited 204 participants with MCR and noted that MCR was associated with prominent white matter abnormalities and frontoparietal atrophy. A cross-sectional study recruited 38 participants with MCR and reported that lacunar infarcts in the frontal lobe were associated with MCR in older adults (Wang et al., 2016). In the present exploratory study, the absence of an increase in the plasma Aβ42 in older adults with MCR suggested that MCR was probably not due to a pure AD pathology.

In this study, we further reported that higher levels of plasma t-tau were correlated with lower cognitive function in the MCR group. Mattsson et al. (2016) enrolled 1,284 participants, including healthy older adults, participants with cognitive impairment, and individuals with AD, in an exploratory study. They found that MMSE scores were negatively correlated with plasma t-tau concentrations. Another cross-sectional study using IMR assays to measure the plasma t-tau levels in participants with AD found that t-tau levels and MMSE scores had a strong negative correlation (Jiao et al., 2020). Chen et al. (2019) recruited 22 participants with amnestic MCI in a cohort study. They found that higher levels of t-tau were correlated with lower cognitive performance at the baseline and greater cognitive decline in 1.5 years follow-up. Tsai et al. (2019) enrolled 13 older adults with NC, 40 participants with amnestic MCI, and 37 individuals with AD, in a cross-sectional study. They found that MMSE scores were negatively correlated with plasma levels of t-tau. A retrospective case study noted that

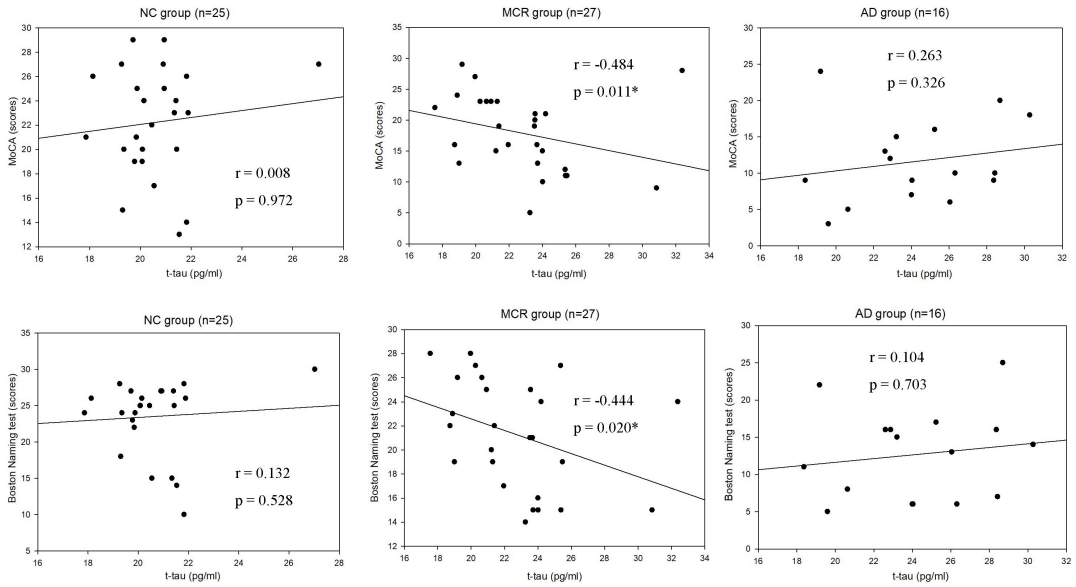

FIGURE 3
Scatterplots of the associations between Montreal Cognitive Assessment (MoCA) scores, Boston Naming test scores, and plasma t-tau levels (pg/ml) in the three group. NC, normal cognition; MCR, Motoric Cognitive Risk syndrome; AD, Alzheimer's disease; t-tau, total tau; MoCA, Montreal Cognitive Assessment; *$p < 0.05$.

the MoCA scores in the lowest CSF tau quartile group were significantly higher than those in the highest quartile group (Pillai et al., 2019). Our results were in line with the findings of these studies, suggesting that cognitive performance might be correlated with the level of t-tau.

Prior studies have indicated that depression is not only a risk factor for AD (Gallagher et al., 2018), but also a symptom of AD (Van der Mussele et al., 2013). Many studies have investigated the relationship between depression and AD biomarkers. A systematic review including 15 studies reported significant differences in the Aβ levels between depressed and non-depressed older adults (Harrington et al., 2015). Babulal et al. (2020) enrolled 301 cognitively normal older adults in a cross-sectional study. They found that tau was associated with a depression diagnosis. In the present study, we observed a significant relationship between plasma t-tau and depression in the NC group. These findings were in line with the results from the previous studies.

There are some study limitations that should be addressed in this study. The first limitation was small sample size, which limits the statistical power. Studies with a larger sample size should be conducted in the future to confirm our results. A second limitation of this study is the cross-sectional study design, which prevented us from investigating the changes in plasma biomarkers and cognitive function in the MCR group over time. A large cohort study is warranted and encouraged. Third, the current study did not provide neuroimaging data. Therefore, we were unable to test the relationship between plasma biomarkers and brain pathology.

In conclusion, we found significantly higher plasma t-tau proteins in the MCR and AD groups, compared to the NC group, and correlations between the levels of plasma t-tau and cognitive function in individuals with MCR. These results implied that MCR and AD may share similar pathology. However, these findings need further confirmation in longitudinal studies.

Data availability statement

The raw data supporting the conclusions of this article will be made available by the authors, without undue reservation.

Ethics statement

The studies involving human participants were reviewed and approved by Institutional Review Board of MacKay Memorial Hospital. The patients/participants provided their written informed consent to participate in this study.

Author contributions

P-HC and F-YC conceived and designed the experiments and wrote the manuscript. P-HC, Y-YL, and W-LH performed the experiments. F-YC and S-IL analyzed the data. All authors reviewed the manuscript and approved the submitted version.

Funding

This study was supported by a grant from the Ministry of Science and Technology (MOST 110-2314-B-715-006-MY3), MacKay Memorial Hospital (MMH-MM-11011), and MacKay Medical College (MMC-RD-110-1B-P026). The funders had no role in the design of the study, data collection, analysis, interpretation of data, or writing of the manuscript.

Acknowledgments

We would like to thank all the participants, as well as the research assistants, Wen-Chun Wu and Jhih-Yu Huang, for participating in the assessment.

Conflict of interest

The authors declare that the research was conducted in the absence of any commercial or financial relationships that could be construed as a potential conflict of interest.

Publisher's note

All claims expressed in this article are solely those of the authors and do not necessarily represent those of their affiliated organizations, or those of the publisher, the editors and the reviewers. Any product that may be evaluated in this article, or claim that may be made by its manufacturer, is not guaranteed or endorsed by the publisher.

References

Avila, J. (2006). Tau phosphorylation and aggregation in Alzheimer's disease pathology. *FEBS Lett.* 580, 2922–2927. doi: 10.1016/j.febslet.2006.02.067

Ayers, E., and Verghese, J. (2019). Gait dysfunction in motoric cognitive risk syndrome. *J. Alzheimers Dis.* 71, S95–S103. doi: 10.3233/JAD-181227

Babulal, G. M., Roe, C. M., Stout, S. H., Rajasekar, G., Wisch, J. K., Benzinger, T. L. S., et al. (2020). Depression is associated with tau and not amyloid positron emission tomography in cognitively normal adults. *J. Alzheimers Dis.* 74, 1045–1055. doi: 10.3233/JAD-191078

Baird, A. L., Westwood, S., and Lovestone, S. (2015). Blood-Based proteomic biomarkers of Alzheimer's disease pathology. *Front. Neurol.* 6:236. doi: 10.3389/fneur.2015.00236

Blumen, H. M., Schwartz, E., Allali, G., Beauchet, O., Callisaya, M., Doi, T., et al. (2021). Cortical thickness, volume, and surface area in the motoric cognitive risk syndrome. *J. Alzheimers Dis.* 81, 651–665. doi: 10.3233/JAD-201576

Bommarito, G., Garibotto, V., Frisoni, G. B., Ribaldi, F., Stampacchia, S., Assal, F., et al. (2022). The biological substrate of the motoric cognitive risk syndrome: A pilot study using amyloid-/Tau-PET and MR imaging. *J. Alzheimers Dis.* 87, 1483–1490. doi: 10.3233/JAD-215461

Bortone, I., Griseta, C., Battista, P., Castellana, F., Lampignano, L., Zupo, R., et al. (2021). Physical and cognitive profiles in motoric cognitive risk syndrome in an older population from Southern Italy. *Eur. J. Neurol.* 28, 2565–2573. doi: 10.1111/ene.14882

Capetillo-Zarate, E., Gracia, L., Tampellini, D., and Gouras, G. K. (2012). Intraneuronal Aβ accumulation, amyloid plaques, and synapse pathology in Alzheimer's disease. *Neuro Degener. Dis.* 10, 56–59. doi: 10.1159/000334762

Chang, C. C., Kramer, J. H., Lin, K. N., Chang, W. N., Wang, Y. L., Huang, C. W., et al. (2010). Validating the Chinese version of the verbal learning test for screening Alzheimer's disease. *J. Int. Neuropsychol. Soc.* 16, 244–251. doi: 10.1017/S1355617709991184

Chen, T. B., Lee, Y. J., Lin, S. Y., Chen, J. P., Hu, C. J., Wang, P. N., et al. (2019). Plasma Aβ42 and total tau predict cognitive decline in amnestic mild cognitive impairment. *Sci. Rep.* 9:13984. doi: 10.1038/s41598-019-50315-9

Chiu, M. J., Yang, S. Y., Horng, H. E., Yang, C. C., Chen, T. F., Chieh, J. J., et al. (2013). Combined plasma biomarkers for diagnosing mild cognition impairment and Alzheimer's disease. *ACS Chem. Neurosci.* 4, 1530–1536. doi: 10.1021/cn400129p

Del Campo, N., Payoux, P., Djilali, A., Delrieu, J., Hoogendijk, E. O., Rolland, Y., et al. (2016). Relationship of regional brain β-amyloid to gait speed. *Neurology* 86, 36–43. doi: 10.1212/WNL.0000000000002235

del Toro, C. M., Bislick, L. P., Comer, M., Velozo, C., Romero, S., Gonzalez Rothi, L. J., et al. (2011). Development of a short form of the Boston naming test for individuals with aphasia. *J. Speech Lang. Hear. Res.* 54, 1089–1100. doi: 10.1044/1092-4388(2010/09-0119)

Gallagher, D., Kiss, A., Lanctot, K., and Herrmann, N. (2018). Depression and risk of Alzheimer dementia: A longitudinal analysis to determine predictors of increased risk among older adults with depression. *Am. J. Geriatr. Psychiatry* 26, 819–827. doi: 10.1016/j.jagp.2018.05.002

Gomez, G. T., Gottesman, R. F., Gabriel, K. P., Palta, P., Gross, A. L., Soldan, A., et al. (2022). The association of motoric cognitive risk with incident dementia and neuroimaging characteristics: The Atherosclerosis Risk in Communities Study. *Alzheimers Dement.* 18, 434–444. doi: 10.1002/alz.12412

Hansson, O. (2021). Biomarkers for neurodegenerative diseases. *Nat. Med.* 27, 954–963. doi: 10.1038/s41591-021-01382-x

Harrington, K. D., Lim, Y. Y., Gould, E., and Maruff, P. (2015). Amyloid-beta and depression in healthy older adults: A systematic review. *Aust. N. Z. J. Psychiatry* 49, 36–46. doi: 10.1177/0004867414557161

Hinkle, D. E., Wiersma, W., and Jurs, S. G. (2003). *Applied statistics for the behavioral sciences*. Boston, MA: Houghton Mifflin College Division.

Jiao, F., Yi, F., Wang, Y., Zhang, S., Guo, Y., Du, W., et al. (2020). The validation of multifactor model of plasma Aβ (42) and total-tau in combination with MoCA for diagnosing probable Alzheimer disease. *Front. Aging Neurosci.* 12:212. doi: 10.3389/fnagi.2020.00212

Johnson, K. A., Sperling, R. A., Gidicsin, C. M., Carmasin, J. S., Maye, J. E., Coleman, R. E., et al. (2013). Florbetapir (F18-AV-45) PET to assess amyloid burden in Alzheimer's disease dementia, mild cognitive impairment, and normal aging. *Alzheimers Dement.* 9(Suppl. 5), S72–S83. doi: 10.1016/j.jalz.2012.10.007

Lee, P. J., Tsai, C. L., Liang, C. S., Peng, G. S., Lee, J. T., Tsai, C. K., et al. (2022). Biomarkers with plasma amyloid β and tau protein assayed by immunomagnetic reduction in patients with amnestic mild cognitive impairment and Alzheimer's disease. *Acta Neurol. Taiwan.* 31, 53–60.

Liu, C. Y., Wang, S. J., Teng, E. L., Fuh, J. L., Lin, C. C., Lin, K. N., et al. (1997). Depressive disorders among older residents in a Chinese rural community. *Psychol. Med.* 27, 943–949. doi: 10.1017/S0033291797005230

Lue, L. F., Sabbagh, M. N., Chiu, M. J., Jing, N., Snyder, N. L., Schmitz, C., et al. (2017). Plasma levels of Aβ42 and tau identified probable Alzheimer's dementia: Findings in two cohorts. *Front. Aging Neurosci.* 9:226. doi: 10.3389/fnagi.2017.00226

Mattsson, N., Zetterberg, H., Janelidze, S., Insel, P. S., Andreasson, U., Stomrud, E., et al. (2016). Plasma tau in Alzheimer disease. *Neurology* 87, 1827–1835. doi: 10.1212/WNL.0000000000003246

McKhann, G. M., Knopman, D. S., Chertkow, H., Hyman, B. T., Jack, C. R. Jr., Kawas, C. H., et al. (2011). The diagnosis of dementia due to Alzheimer's disease: Recommendations from the National Institute on Aging-Alzheimer's Association workgroups on diagnostic guidelines for Alzheimer's disease. *Alzheimers Dement.* 7, 263–269. doi: 10.1016/j.jalz.2011.03.005

Meiner, Z., Ayers, E., Bennett, D. A., Wang, C., and Verghese, J. (2021). Risk factors for the progression of motoric cognitive risk syndrome to dementia:

Retrospective cohort analysis of two populations. *Eur. J. Neurol.* 28, 1859–1867. doi: 10.1111/ene.14841

Mitrushina, M., Boone, K. B., Razani, J., and D'Elia, L. F. (2005). *Handbook of normative data for neuropsychological assessment*, 2nd Edn. New York, NY: US: Oxford University Press, xxii.

Morris, J. C. (1997). Clinical dementia rating: A reliable and valid diagnostic and staging measure for dementia of the Alzheimer type. *Int. Psychogeriatr.* 9(Suppl. 1), 173–176; discussion 7–8. doi: 10.1017/S1041610297004870

Mukaka, M. M. (2012). Statistics corner: A guide to appropriate use of correlation coefficient in medical research. *Malawi Med. J.* 24, 69–71.

Olsson, B., Lautner, R., Andreasson, U., Öhrfelt, A., Portelius, E., Bjerke, M., et al. (2016). CSF and blood biomarkers for the diagnosis of Alzheimer's disease: A systematic review and meta-analysis. *Lancet Neurol.* 15, 673–684. doi: 10.1016/S1474-4422(16)00070-3

Pereira, J. B., Westman, E., and Hansson, O. (2017). Association between cerebrospinal fluid and plasma neurodegeneration biomarkers with brain atrophy in Alzheimer's disease. *Neurobiol. Aging* 58, 14–29. doi: 10.1016/j.neurobiolaging.2017.06.002

Pillai, J. A., Bonner-Jackson, A., Bekris, L. M., Safar, J., Bena, J., and Leverenz, J. B. (2019). Highly elevated cerebrospinal fluid total tau level reflects higher likelihood of non-amnestic subtype of Alzheimer's disease. *J. Alzheimers Dis.* 70, 1051–1058. doi: 10.3233/JAD-190519

Pini, L., Pievani, M., Bocchetta, M., Altomare, D., Bosco, P., Cavedo, E., et al. (2016). Brain atrophy in Alzheimer's disease and aging. *Ageing Res. Rev.* 30, 25–48. doi: 10.1016/j.arr.2016.01.002

Rosen, W. G. (1980). Verbal fluency in aging and dementia. *J. Clin. Neuropsychol.* 2, 135–146. doi: 10.1080/01688638008403788

Tian, Q., Resnick, S. M., Bilgel, M., Wong, D. F., Ferrucci, L., and Studenski, S. A. (2017). β-amyloid burden predicts lower extremity performance decline in cognitively unimpaired older adults. *J. Gerontol. Ser. A Biol. Sci. Med. Sci.* 72, 716–723. doi: 10.1093/gerona/glw183

Tsai, C. L., Liang, C. S., Lee, J. T., Su, M. W., Lin, C. C., Chu, H. T., et al. (2019). Associations between plasma biomarkers and cognition in patients with Alzheimer's disease and amnestic mild cognitive impairment: A cross-sectional and longitudinal study. *J. Clin. Med.* 8:1893. doi: 10.3390/jcm8111893

Van der Mussele, S., Bekelaar, K., Le Bastard, N., Vermeiren, Y., Saerens, J., Somers, N., et al. (2013). Prevalence and associated behavioral symptoms of depression in mild cognitive impairment and dementia due to Alzheimer's disease. *Int. J. Geriatr. Psychiatry* 28, 947–958. doi: 10.1002/gps.3909

Verghese, J., Annweiler, C., Ayers, E., Barzilai, N., Beauchet, O., Bennett, D. A., et al. (2014a). Motoric cognitive risk syndrome: Multicountry prevalence and dementia risk. *Neurology* 83, 718–726. doi: 10.1212/WNL.0000000000000717

Verghese, J., Ayers, E., Barzilai, N., Bennett, D. A., Buchman, A. S., Holtzer, R., et al. (2014b). Motoric cognitive risk syndrome: Multicenter incidence study. *Neurology* 83, 2278–2284. doi: 10.1212/WNL.0000000000001084

Verghese, J., Wang, C., Lipton, R. B., and Holtzer, R. (2013). Motoric cognitive risk syndrome and the risk of dementia. *J. Gerontol. A Biol. Sci. Med. Sci.* 68, 412–418. doi: 10.1093/gerona/gls191

Wang, N., Allali, G., Kesavadas, C., Noone, M. L., Pradeep, V. G., Blumen, H. M., et al. (2016). Cerebral small vessel disease and motoric cognitive risk syndrome: Results from the Kerala-Einstein study. *J. Alzheimers Dis.* 50, 699–707. doi: 10.3233/JAD-150523

Wennberg, A. M. V., Savica, R., Hagen, C. E., Roberts, R. O., Knopman, D. S., Hollman, J. H., et al. (2017). Cerebral amyloid deposition is associated with gait parameters in the mayo clinic study of aging. *J. Am. Geriatr. Soc.* 65, 792–799. doi: 10.1111/jgs.14670

Wu, Y. H., Liu, L. K., Chen, W. T., Lee, W. J., Peng, L. N., Wang, P. N., et al. (2015). Cognitive function in individuals with physical frailty but without dementia or cognitive complaints: Results from the I-Lan longitudinal aging study. *J. Am. Med. Dir. Assoc.* 16, 899.e9–899.16. doi: 10.1016/j.jamda.2015.07.013

Yang, S. Y., Chiu, M. J., Chen, T. F., and Horng, H. E. (2017). Detection of plasma biomarkers using immunomagnetic reduction: A promising method for the early diagnosis of Alzheimer's disease. *Neurol. Ther.* 6(Suppl. 1), 37–56. doi: 10.1007/s40120-017-0075-7

Yaqub, A., Darweesh, S. K. L., Dommershuijsen, L. J., Vernooij, M. W., Ikram, M. K., Wolters, F. J., et al. (2022). Risk factors, neuroimaging correlates and prognosis of the motoric cognitive risk syndrome: A population-based comparison with mild cognitive impairment. *Eur. J. Neurol.* 29, 1587–1599. doi: 10.1111/ene.15281

Yesavage, J. A., Brink, T. L., Rose, T. L., Lum, O., Huang, V., Adey, M., et al. (1982). Development and validation of a geriatric depression screening scale: A preliminary report. *J. Psychiatr. Res.* 17, 37–49. doi: 10.1016/0022-3956(82)90033-4

frontiers | Frontiers in Aging Neuroscience

TYPE Review
PUBLISHED 04 October 2022
DOI 10.3389/fnagi.2022.1020092

OPEN ACCESS

EDITED BY
Suman Dutta,
University of California, Los Angeles, United States

REVIEWED BY
Seong Lin Teoh,
National University of Malaysia, Malaysia
Subodh Kumar,
Texas Tech University Health Sciences Center, United States

*CORRESPONDENCE
Sneha S. Pillai
pillais@marshall.edu

†These authors have contributed equally to this work

SPECIALTY SECTION
This article was submitted to Cellular and Molecular Mechanisms of Brain-aging, a section of the journal Frontiers in Aging Neuroscience

RECEIVED 15 August 2022
ACCEPTED 13 September 2022
PUBLISHED 04 October 2022

CITATION
Alvarez M, Trent E, Goncalves BDS, Pereira DG, Puri R, Frazier NA, Sodhi K and Pillai SS (2022) Cognitive dysfunction associated with COVID-19: Prognostic role of circulating biomarkers and microRNAs. *Front. Aging Neurosci.* 14:1020092. doi: 10.3389/fnagi.2022.1020092

Cognitive dysfunction associated with COVID-19: Prognostic role of circulating biomarkers and microRNAs

Marissa Alvarez†, Erick Trent†, Bruno De Souza Goncalves, Duane G. Pereira, Raghav Puri, Nicolas Anthony Frazier, Komal Sodhi and Sneha S. Pillai*

Department of Surgery, Biomedical Sciences and Medicine, Joan C. Edwards School of Medicine, Marshall University, Huntington, WV, United States

COVID-19 is renowned as a multi-organ disease having subacute and long-term effects with a broad spectrum of clinical manifestations. The evolving scientific and clinical evidence demonstrates that the frequency of cognitive impairment after COVID-19 is high and it is crucial to explore more clinical research and implement proper diagnostic and treatment strategies. Several central nervous system complications have been reported as comorbidities of COVID-19. The changes in cognitive function associated with neurodegenerative diseases develop slowly over time and are only diagnosed at an already advanced stage of molecular pathology. Hence, understanding the common links between COVID-19 and neurodegenerative diseases will broaden our knowledge and help in strategizing prognostic and therapeutic approaches. The present review focuses on the diverse neurodegenerative changes associated with COVID-19 and will highlight the importance of major circulating biomarkers and microRNAs (miRNAs) associated with the disease progression and severity. The literature analysis showed that major proteins associated with central nervous system function, such as Glial fibrillary acidic protein, neurofilament light chain, p-tau 181, Ubiquitin C-terminal hydrolase L1, S100 calcium-binding protein B, Neuron-specific enolase and various inflammatory cytokines, were significantly altered in COVID-19 patients. Furthermore, among various miRNAs that are having pivotal roles in various neurodegenerative diseases, miR-146a, miR-155, Let-7b, miR-31, miR-16 and miR-21 have shown significant dysregulation in COVID-19 patients. Thus the review consolidates the important findings from the numerous studies to unravel the underlying mechanism of neurological sequelae in COVID-19 and the possible association of circulatory biomarkers, which may serve as prognostic predictors and therapeutic targets in future research.

KEYWORDS

COVID-19, cognitive impairment, neurodegenerative diseases, circulating biomarkers, microRNAs

Introduction

Coronavirus disease 2019 (COVID-19), the disease caused by severe acute respiratory syndrome coronavirus 2 (SARS-CoV-2), has created morbidity and mortality at an unprecedented scale globally and was declared a pandemic by the World Health Organization (WHO) in March 2020 (Nalbandian et al., 2021). It was initially detected in Wuhan, China, which triggered a severe acute respiratory syndrome, contaminating more than 175 million people after one year and leading to the death of 3.8 million people worldwide (Huang et al., 2020; Hui et al., 2020; Wu et al., 2020a; Lopez-Leon et al., 2021). SARS-CoV-2 is a betacoronavirus, a member of the subfamily *Coronavirinae,* having a single-stranded positive-sense RNA genome (Wang et al., 2020b). SARS-CoV-2 is made up of at least 29 proteins, four of which are structural proteins, and the others are non-structural proteins (Yao et al., 2020). SARS-CoV-2 is prone to genetic evolution through mutations over time in human hosts. This leads to the generation of mutant variants having diverse characteristics than their ancestral strains. Several variants of SARS-CoV-2 have been described during the course of this pandemic and WHO has classified them based on their impact on public health. Currently, there are five SARS-CoV-2 variants of concern (VOC), Alpha, Beta, Gamma, Delta, and Omicron, and two SARS-CoV-2 variants of interest (VOI), Lambda and Mu (WHO SARS-CoV-2 Variants) (Liu et al., 2022). The emergence of these new SARS-CoV-2 variants are posing threats to vaccine development and other therapeutic options.

Several scientific and clinical studies have shown that subacute and long-term effects of COVID-19 can affect multiple organ systems (Gupta et al., 2020a). It is reported that the mechanism of infection and replication of SARS-CoV-2 is similar to that of SARS-CoV and MERS-CoV. The angiotensin-converting enzyme-2 (ACE-2) receptors are the primary binding receptors for the viral particle and are found highly expressed in alveolar epithelial cells of lungs, vascular endothelial cells, and enterocytes but can also be found in other organs, such as kidney, liver, and gastrointestinal tract (Azer, 2020; Bhavana et al., 2020; Harrison et al., 2020; Parasher, 2021). The internalization of the virus in host cells results in different inflammatory changes such as edema, necrosis, and tissue dysfunction. These changes can cause a cytokine storm, promoting changes in the immune response that cause excessive damage to the lung, gastrointestinal, neurological, and cardiopulmonary systems (Azer, 2020; Bhavana et al., 2020; Harrison et al., 2020; Rizzo et al., 2020; Xu et al., 2020; Anka et al., 2021).

As SARS-CoV-2 has the ability to affect different organs, recent clinical studies have demonstrated that there is an increased risk of long-term health problems in patients who have survived infection with SARS-CoV-2 (Seyedalinaghi et al., 2021). The most recurrent long-term complication is respiratory problems that may further develop pulmonary fibrosis, arterial complications, venous thrombo-embolic late complications associated with a hyperinflammatory and hypercoagulable state (Lodigiani et al., 2020; Puntmann et al., 2020). Likewise, cardiac dysfunction can be caused due to structural damage to the myocardium, pericardium, and conduction system, triggering arrhythmias in a large proportion of patients (Lindner et al., 2020; Liu et al., 2020). Renal lesions have also been reported in approximately 20-31% of patients who developed the severe form of COVID-19. The reduced glomerular filtration was related to extensive acute tubular necrosis observed in renal biopsies (Kudose et al., 2020). Diabetic ketoacidosis, liver dysfunction, joint pain, muscle weekness and dermatologic manifestations were also observed in post-covid patients (Freeman et al., 2020; Suwanwongse and Shabarek, 2021). In addition, late complications are reported in the central and peripheral nervous system, promoting decreased awareness and absorption, difficulties with concentration, disturbed memory, difficulty in communication, anxiety, depression, sleep problems, and olfactory and taste losses (Paybast et al., 2020; Varatharaj et al., 2020; Huang et al., 2021a). **Figure 1** demonstrates the various complications associated with COVID-19.

The present review aims to elucidate the underlying mechanism that links COVID-19 with neurodegenerative changes that lead to cognitive dysfunction. As patients infected with SARS-CoV-2 are stratified according to their clinical manifestations, such as symptoms, oxygen saturation, and blood pressure (Malik et al., 2021), these manifestations are apparent at the late stages of infection, especially for neurological complications. Identifying factors that can lead to complications during the disease early is extremely important since it can significantly influence the quality of care and adequate treatment. It would be valuable to reveal the alterations of plasma biomarkers in various cognitive impairment stages since the cognitive manifestations are one of the most concerned post covid complications. Hence, based on recent literature, we will provide clinicians with updated and practical information on the role of circulating biomarkers and miRNAs in COVID-19-associated cognitive dysfunction that may act as possible therapeutic targets and prognostic predictors in future studies.

Materials and methods

The purpose of this review is to highlight the importance of cognitive dysfunction and neurodegenerative changes associated with COVID-19 and the dysregulation of circulating biomarkers and miRNAs in the clinical condition being studied. A systematic search of relevant research articles was performed using the databases, namely, PubMed, ProQuest, Science Direct, and Google Scholar. The electronic search was conducted using a combination of search terms related to the

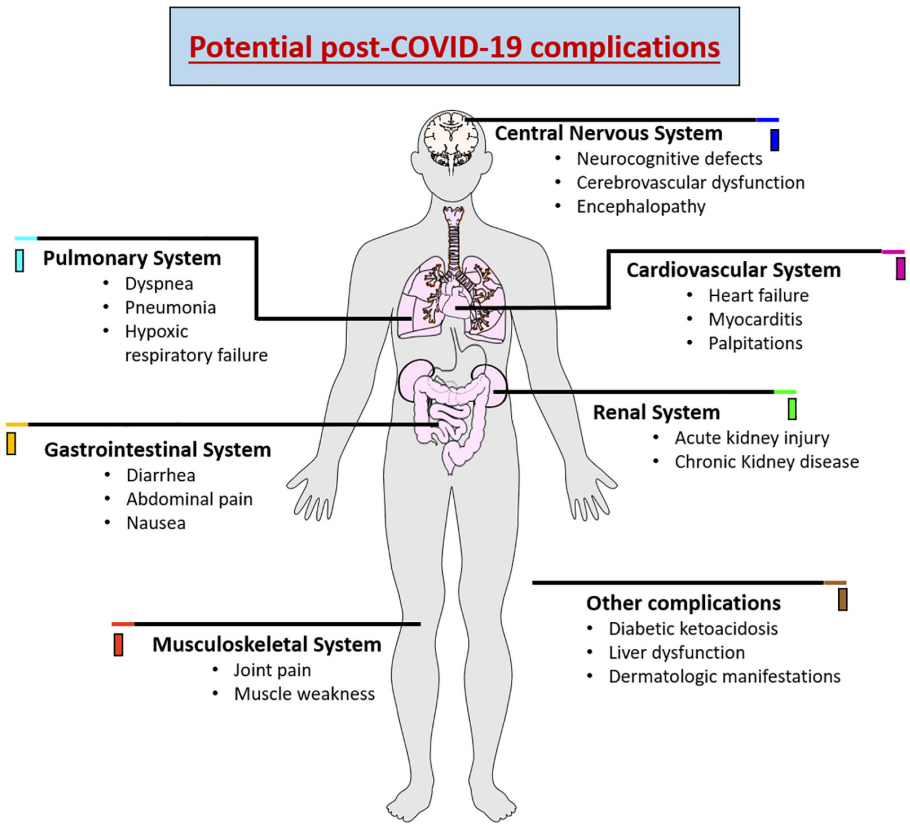

FIGURE 1
Schematic representation showing the potential complications of COVID-19 causing wide range of complications in various organ systems.

following keywords: "COVID-19" OR "SARS-CoV-2" OR " Post COVID-19 complications" OR "Cognitive dysfunction" OR "Neurodegeneration" OR "Circulating Biomarkers" OR "miRNAs". The articles retrieved from our search were further distinguished for relevancy. The inclusion and exclusion criteria were set to only evaluate articles published from 2000 to 2022 in order to limit this search. Moreover, articles that contain only abstracts without their full text and published in languages other than English were excluded.

COVID-19-associated cognitive dysfunction and neurodegeneration

COVID-19-associated cognitive dysfunction

As the population of patients recovering from COVID-19 grows, it is important to establish an understanding of the multi-organ dysfunction associated with post- COVID-19 complications. Of note, neurological manifestations in COVID-19 patients have been reported, showing a close correlation between COVID-19 and future development of neurodegenerative diseases (Wu et al., 2020b; Taquet et al., 2021; Frontera et al., 2022; Li et al., 2022a). It has also been established that the likelihood of developing COVID-19-associated cognitive impairment and the severity of these deficits is associated with the severity of the SARS-CoV-2 infection and the subsequent increases in specific circulating inflammatory mediators and biomarkers (Becker et al., 2021; Miskowiak et al., 2021; Zeng et al., 2022). Alternatively, some studies have demonstrated that even non-hospitalized COVID-19 patients have developed cognitive-associated post-COVID-19 symptoms, suggesting that regardless of illness severity, cognitive dysfunction can arise (Graham et al., 2021; Hadad et al., 2022; Van Kessel et al., 2022). Report shows that COVID-19-associated cognitive impairment can arise during post-acute COVID-19 infection 3 weeks following diagnosis, and 31.2% of participants experience cognitive dysfunction within the first week of symptoms (Davis et al., 2021). Another study found that 22% of individuals infected with SARS-CoV-2 developed symptoms of cognitive impairment, which remained after 12 weeks following their diagnosis (Ceban et al., 2022). These deficits can last for a prolonged period of time and clinically

relevant cognitive impairments in verbal learning and executive function were found in 48% of patients 1 year following the onset of symptoms (Miskowiak et al., 2022).

Likewise, another report identified abnormalities in executive function, attention, and phonemic fluency in post-COVID-19 patients (Hadad et al., 2022). The results of a systemic review showed a high frequency of cognitive impairment after COVID-19 infection with defects in processing speed, inattention, or executive dysfunction (Tavares-Junior et al., 2022). A post-COVID-19 community clinic compared Montreal Cognitive Assessment (MoCA) index scores of participants who reported cognitive symptoms and found that index scores were significantly worse in language, executive function, and attention (Crivelli et al., 2022). With increasing severity of infection with SARS-CoV-2, there are corresponding increases in both the likelihood of developing cognitive dysfunction as well as the severity of the cognitive dysfunction in those who develop these sequelae (Wang et al., 2021). For these reasons, it is imperative to understand the underlying mechanisms by which covid-associated cognitive dysfunction and neurodegeneration occur.

COVID-19-associated neurodegeneration

The neurological complications of COVID-19 include damage to the central and the peripheral nervous system that consists of neuronal damage, neuroinflammation, rupture of the blood brain barrier, microvasculitis and hypoxia (Ellul et al., 2020; Boldrini et al., 2021). ACE2 receptors within the central nervous system (CNS) are most highly concentrated within the substantia nigra, ventricles, middle temporal gyrus, posterior cingulate cortex, olfactory bulb, motor cortex, and brainstem (Iodice et al., 2021). The disruption of the normal physiological functions of these areas due to infection with SARS-CoV-2 has been postulated to be a potential explanation for many of the reported symptoms associated with the long-Covid syndrome. This was validated by an observational study that examined cortical metabolism in the subacute and chronic (>6 months) stages of illness and found that hypometabolism in the frontoparietal and temporal cortex was associated with cognitive impairment (Hosp et al., 2021). Long- COVID-19 brain fog in patients has presented with abnormal FDG-PET scan results, with hypometabolic regions localized mostly to the anterior and posterior cingulate cortices (Hugon et al., 2022). The cingulate cortex plays a role in a variety of neurological functions including memory, emotions, and decisive action taking. The abundance of ACE2 receptors in this area could additionally provide some insight into their experience of brain fog (Hugon et al., 2022).

There are numerous potential mechanisms by which SARS-CoV-2 could access the CNS to elicit these pathologies, which can be broadly classified into direct invasion and indirect hematological entry following inflammatory mediated neurodegeneration of the blood-brain-barrier (BBB) (Iodice et al., 2021). Direct neurological invasion is hypothesized to occur through the olfactory epithelium and the cribriform plate into the olfactory bulbs following nasal inhalation of aerosolized droplets containing the infectious viral load. Additionally, it has been suggested that SARS-CoV-2 penetration into the CNS can result in heightened neuroinflammation which may cause neurodegeneration or exacerbate existing neuroinflammation from preexisting comorbidities such as Alzheimer's dementia and Parkinson's disease, leading to the development of neuropsychological symptoms (Iodice et al., 2021).

Hematological spread is another proposed mechanism by which SARS-CoV-2 can gain access to the CNS. One possible mechanism involves the attachment of SARS-CoV-2 to ACE2 expressed on BBB endothelial cells and the induction of neuroinflammation, which weakens the protective barrier of the brain and thus provides access for the virus. It is also hypothesized that it is possible that the virus may circumvent BBB altogether by infecting CNS-infiltrating macrophages and monocytes (Zhou et al., 2020b). Furthermore, astrocytes, a vital component of the BBB, can receive signals from circulating pro-inflammatory cytokines, generated in response to viral infection in the lungs, which in turn cause SARS-CoV-2 to enter the CNS and induce neuroinflammation (Murta et al., 2020). Moreover, SARS-CoV-2 can elicit the pro-inflammatory phenotype of microglia, the native immune cells in the CNS, which up-regulate the expression of genes involved in neuroinflammation (Amruta et al., 2021). In addition, it has been demonstrated that SARS-CoV-2 infection can facilitate neuronal injury, encephalitis, fibrosis, thrombosis and axonal damage (Bradley et al., 2020; Turski et al., 2020; Wang et al., 2020a). As, COVID-19-associated pathological changes are characterized by distinct changes in the levels of specific circulating biomarkers, the expression profile of these biomarkers may demonstrate a link between various disease states. The Schematic representation of various neurodegenerative changes associated with COVID-19 is shown in **Figure 2**. Understanding the changes in expression of these circulating biomarkers may provide insights into the holistic understanding of the underlying process by which COVID-19 long-haulers experience their cognitive dysfunction.

Role of circulating biomarkers in COVID-19-associated cognitive dysfunction

Circulating biomarkers present a promising approach in the research and clinical practice of various diseases including neurodegenerative diseases as they are minimally invasive, highly cost-effective and provide high specificity (Solfrizzi et al., 2006; Pillai et al., 2020; Lakhani et al., 2021; Kivisakk et al., 2022). The prognostic utility of plasma biomarkers in

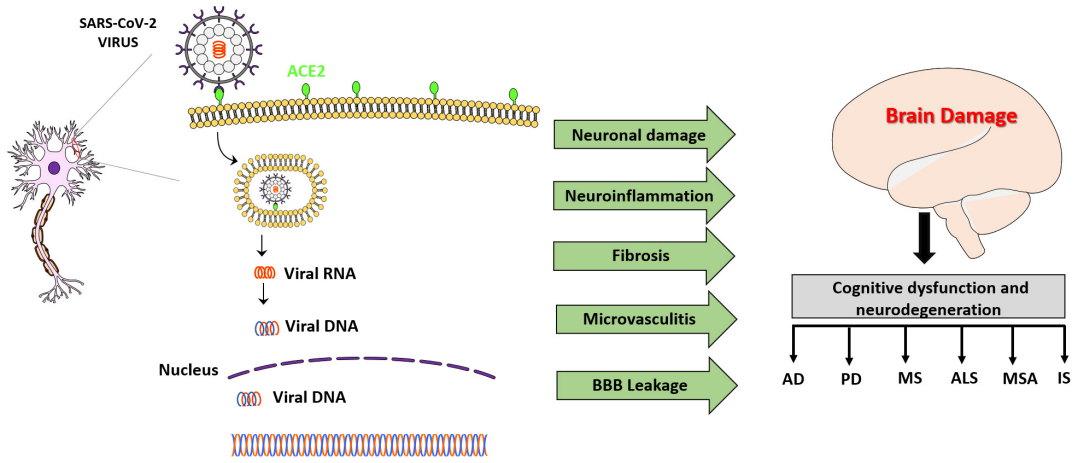

FIGURE 2
Schematic representation showing the neuronal infection of SARS-CoV-2 virus and CNS damage caused by the infection that leads to cognitive dysfunction and neurodegenerative diseases. Angiotensin-converting enzyme-2 (ACE-2), Alzheimer's disease (AD), Parkinson's disease (PD), Multiple sclerosis (MS), Amyotrophic lateral sclerosis (ALS), Multiple system atrophy (MSA), Ischemia stroke (IS).

neuroinflammation, vascular injury, and cognitive dysfunction may aid in the management of clinical care and treatment strategies. Hence in this section, we are highlighting the importance of some key biomarkers of cognitive decline and neurodegeneration that are altered in COVID-19 for their future application in research on therapeutic targets and prognostic deliberations of COVID-19- associated cognitive dysfunction. A summary of the findings are illustrated in **Table 1**.

Glial fibrillary acidic protein

Astrocytes are the most abundant cell type throughout the CNS and have many roles including but not limited to maintenance of BBB, neurotransmitter homeostasis, synaptogenesis, neurogenesis, ion and water homeostasis, and neuronal cholesterol synthesis (Cabezas et al., 2014; Liu et al., 2018). When neurological insult occurs, astrocytes become activated through reactive gliosis that involves the upregulation of glial fibrillary acidic protein (GFAP), a widely known biomarker of brain injury (Pekny and Pekna, 2014). As a structural protein that is unique to astrocytes, GFAP provides stability to astrocytes, thereby influencing their shape and movement (Eng et al., 2000; Hol and Capetanaki, 2017). Therefore, GFAP has been regarded as a biomarker of reactive astrocytes in a variety of neuropathological conditions (Eng et al., 2000). Elevated circulating levels of GFAP have been linked to a number of such neurological conditions including traumatic brain injury (TBI), spinal cord injury, multiple sclerosis (MS), Alzheimer's Disease (AD), Alexander disease, Parkinson's disease (PD), and neuromyelitis optica spectrum disorder (Elahi et al., 2020; Abdelhak et al., 2022; Heimfarth et al., 2022; Kim et al., 2022; Newcombe et al., 2022). It is evident that GFAP has been and continues to be explored as a potential biomarker of neurological injury across several neurodegenerative and inflammatory CNS diseases.

Recent studies have found elevated levels of GFAP in serum and/or plasma of COVID-19 patients (Kanberg et al., 2020, 2021; Frontera et al., 2022; Hanson et al., 2022; Sahin et al., 2022). This supports that GFAP correlates with disease severity, as it was found at significantly higher levels in COVID-19 patients who died during hospitalization when compared to those who survived (Frontera et al., 2022). Other results have supported elevated GFAP levels with disease severity but did not find a significant correlation with the presence of neurological symptoms (Sahin et al., 2022). One study found that GFAP levels normalized in all COVID-19 patients despite disease severity and the persistence of reported cognitive symptoms suggesting that the symptoms of COVID-19-associated cognitive impairment linger without the presence of active CNS injury (Kanberg et al., 2021). These findings may also further support the proposed mechanism that reactive gliosis following SARS-CoV-2 infection causes COVID-19-associated cognitive dysfunction by spreading hematogenously, infecting endothelial cells, and disrupting the BBB (Johansson et al., 2021; Mohamed et al., 2022). Taken together, these findings suggest that additional studies with larger sample sizes and standardized protocols should be explored to determine exactly how useful plasma or serum GFAP can be as a biomarker for COVID-19-associated cognitive impairment.

Neurofilament light chain

Neurofilaments (Nfs) are classified as type IV intermediate filaments that provide cytoskeletal stability and allow for radial

TABLE 1 Summary of circulating biomarkers associated with neurological dysfunction showing potential dysregulation in COVID-19.

Biomarker	Source	Function	Pathophysiology	Status in neurodegenerative diseases	Patients' information	Status in COVID-19	References
GFAP	Serum/ plasma	Provides stability to astrocytes influencing their shape and movement.	Astrocytes damage and inflammation	AD- increased PD- increased MS- increased	1. 47 COVID-19 patients divided into 3 groups related to systemic disease severity. 2. 100 COVID-19 patients classified into three main groups: mild, moderate and severe patients. 3. 58 COVID-19 patients divided into 3 groups related to disease severity. 4. 251 hospitalized COVID-19 patients aged between 60-83 years without a history of dementia	Significantly increased	Eng et al., 2000; Elahi et al., 2020; Kanberg et al., 2020, 2021; Frontera et al., 2022; Heimfarth et al., 2022; Kim et al., 2022; Sahin et al., 2022
NFL	Serum/ plasma	Provide cytoskeletal stability and allow for radial growth of neurons.	Neuroaxonal injury	AD- increased PD- increased ALS- increased HD- increased LBD- increased	1. 104 COVID-19 patients 2. COVID-19 Patients classified into 3 groups according to the disease severity: mild (n = 24), moderate (n = 28), and severe (n = 48). 3. 142 hospitalized COVID-19 4. 251 hospitalized COVID-19 patients aged between 60-83 years without a history of dementia 5. 57 hospitalized Covid-19 patients without major neurological manifestations	Significantly increased	Yuan et al., 2017; Gaetani et al., 2019; Palermo et al., 2020; Rajan et al., 2020; De Lorenzo et al., 2021; Kanberg et al., 2021; Prudencio et al., 2021; Verde et al., 2021, 2022; Chouliaras et al., 2022; Frontera et al., 2022; Thijssen et al., 2022; Zanella et al., 2022
P-tau 181	Serum/ plasma	Maintaining neuronal microtubule integrity by providing stability and encouraging assembly.	Form neurofibrillary tangles	AD- increased	1. 16 COVID-19 volunteers without neurological symptoms and 8 COVID-19 volunteers with neurological symptoms 2. 251 hospitalized COVID-19 patients aged between 60-83 years without a history of dementia	Significantly increased	Metaxas and Kempf, 2016; Wang and Mandelkow, 2016; Moscoso et al., 2021; Sun et al., 2021; Frontera et al., 2022; Smirnov et al., 2022
UCH-L1	Plasma	Removing ubiquitin from their target proteins maintaining the nervous system integrity.	Changes in regulating the function of various synapses influencing their maintenance, transmission, and plasticity.	PD- increased AD-increased FA- increased	1. 27 hospitalized COVID-19 patients aged 54-76 years without major neurological manifestations 2. 251 hospitalized COVID-19 patients aged between 60-83 years without a history of dementia 3. 104 COVID-19 patients aged 49-67	Significantly increased	Bishop et al., 2016; Zeitlberger et al., 2018; Cooper et al., 2020; Ng et al., 2020; De Lorenzo et al., 2021; Bogdan et al., 2022; Frontera et al., 2022
S100B	Serum	Regulation of cell proliferation and cytoskeletal structure	Cause astrocyte damage and injury	AD- increased PD- increased ALS- increased MS- increased	1. 74 hospitalized COVID-19 patients 2. 64 COVID-19 patients (34 mild cases; 30 severe cases) 3. 57 patients hospitalized with COVID-19 4. 58 COVID-19 Patients classified into mild (n = 17), moderate (n = 18), and severe (n = 23).	Significantly increased	Steiner et al., 2007; Lam et al., 2013; Barateiro et al., 2016; Serrano et al., 2017; Cristovao and Gomes, 2019; Aceti et al., 2020; Angelopoulou et al., 2021; Mete et al., 2021; Savarraj et al., 2021; Sahin et al., 2022

(Continued)

10.3389/fnagi.2022.1020092

TABLE 1 (Continued)

Biomarker	Source	Function	Pathophysiology	Status in neurodegenerative diseases	Patients' information	Status in COVID-19	References
NSE	Serum/ plasma	Regulating neuronal growth, differentiation, survival.	Cause axonal injury and neuroinflammation	AD-increased HD-increased BPAN-increased	1. 252 COVID-19 patients classified into 3 groups according to the disease severity. 2. 128 hospitalized COVID-19 patients 3. 57 COVID-19 hospitalized patients	Significantly increased	Chaves et al., 2010; Ciancarelli et al., 2014; Polcyn et al., 2017; Takano et al., 2017; Haque et al., 2018; Wei et al., 2020; Cione et al., 2021; Savarraj et al., 2021
Inflammatory cytokines	Serum	Mobilization of immune cells	Cytokine storm implicated in neurotoxicity, disruption of the integrity of BBB, neuroglial cells activation, and neuroinflammation	AD-increased	1. 57 COVID-19 hospitalized patients 2. 43 COVID-19 patients with mild-moderate ($n = 39$) and severe ($n = 14$) 3. 33 COVID-19 patients 4. 60 COVID-19 patients divided in to two subgroup, clinical group ($n = 32$), participants seeking care for post-acute cognitive complaints and a non-clinical group ($n = 28$), participants patients who did not seek care for post-acute COVID-19.	Significantly increased	Gupta et al., 2020b; Xin et al., 2021; Acosta-Ampudia et al., 2022; Ferrando et al., 2022; Hirzel et al., 2022; Lu et al., 2022; Schultheiss et al., 2022; Zhang et al., 2022b

Ischemia stroke (IS), Alzheimer's disease (AD), Parkinson's disease (PD), Amyotrophic lateral sclerosis (ALS), Multiple sclerosis (MS), Multiple system atrophy (MSA), mild cognitive impairment (MIC), Huntington's Disease (HD), Lewy body dementia (LBD), Friedreich's Ataxia (FA), beta-propeller protein-associated neurodegeneration (BPAN).

growth of neurons (Yuan et al., 2017; Gaetani et al., 2019). Under normal conditions, axons release neurofilament light chain (NfL), the most abundant subunit of Nfs, into the blood at low levels, and this has been found to increase with age (Yuan et al., 2017; Gaetani et al., 2019; Zanella et al., 2022). Moreover, during neurological degeneration or injury, these levels increase significantly indicating its potential use as a biomarker of neuroaxonal injury (Zanella et al., 2022). Elevated levels of NfL in serum have been associated with various neuropathologies such as cognitive decline, TBI, AD, PD, MS, Lewy body dementia (LBD), frontotemporal dementia (FTD), Amyotrophic Lateral Sclerosis (ALS), and Huntington Disease (HD) (Palermo et al., 2020; Rajan et al., 2020; Verde et al., 2021; Chouliaras et al., 2022; Ebenau et al., 2022; Newcombe et al., 2022; Thijssen et al., 2022).

Studies examining various COVID-19 patient populations have also found elevated plasma and or serum levels of NfL (Ameres et al., 2020; Kanberg et al., 2020, 2021; Aamodt et al., 2021; De Lorenzo et al., 2021; Prudencio et al., 2021; Frontera et al., 2022; Hanson et al., 2022; Verde et al., 2022). Similarly to GFAP, NfL was elevated in hospitalized patients who had COVID-19 encephalopathy (Hanson et al., 2022). NfL also correlates with disease severity as elevated plasma levels were found in COVID-19 patients that died during hospitalization (Aamodt et al., 2021; Frontera et al., 2022). When compared to the control group consisting of non-COVID-19 AD patients, the COVID-19 patients exhibited higher levels of NfL (Frontera et al., 2022). COVID-19 patients who did not have obvious signs or symptoms of cognitive dysfunction also had elevated levels of serum NfL (Prudencio et al., 2021; Verde et al., 2022). In another group of intensive care unit (ICU) COVID-19 patients, those who did not survive the infection had higher levels of NfL when compared to those who survived (Aamodt et al., 2021). Report shows that after 30-70 days, plasma NfL levels increased persistently and then normalized after six months in COVID-19 patients who continued to report the presence of neurological symptoms (Kanberg et al., 2021). Also plasma NfL levels were found to be increased from the first follow-up to the last in the severe group (Kanberg et al., 2020). Both studies support their shared hypothesis of delayed axonal injury occurring in severe COVID-19 patients, while astrocyte activation occurs earlier and is not limited to the severe COVID-19 patient population (Kanberg et al., 2020, 2021). The elevated concentrations of plasma NfL found in these COVID-19 patient populations warrants further investigation to explore its neuropathological mechanism causing neuroaxonal injury to determine whether it can be a contributing factor to the cognitive sequelae that arises in post-COVID-19 infections.

Phosphorylated tau at threonine-181

The soluble tau proteins are important for maintaining neuronal microtubule integrity by providing stability and

encouraging assembly (Wang and Mandelkow, 2016). The post-translational phosphorylation of tau is necessary for the protein to change its confirmation to operate under physiological conditions (Wang and Mandelkow, 2016; Kent et al., 2020). However, when phosphorylated excessively, the tau proteins dissociate from microtubules and aggregate with one another becoming insoluble and ultimately leading to extensive networks of neurofibrillary tangles (NFTs), which are characteristic of AD pathology (Metaxas and Kempf, 2016). The neurogenerative diseases distinctively express the hyperphosphorylation of Tau and subsequent aggregation are altogether known as tauopathies (Wang and Mandelkow, 2016). The role of p-tau 181 has been explored extensively in AD pathology and has been found to predict cognitive decline and AD several years before diagnosis and/or death (Guo et al., 2017; Lantero Rodriguez et al., 2020; Moscoso et al., 2021; Smirnov et al., 2022). These findings support p-tau 181 as a promising blood biomarker for AD and the potential for its application in other tauopathies.

Elevated levels of serum and/or plasma p-tau 181 have been found in COVID-19 patients (Sun et al., 2021; Frontera et al., 2022). COVID-19 patients who did not survive the infection and those who developed COVID-encephalopathy had elevated levels of p-tau 181, along with NfL and GFAP as mentioned previously. The study also found that hospitalized COVID-19 patients who experienced new cognitively related symptoms also had elevated levels p-tau 181 when compared to patients who did not experience additional cognitive sequelae (Frontera et al., 2022). In a study that examined the contents of neuronal-enriched extracellular vesicles (nEVs) in the plasma of COVID-19 patients, elevated levels of p-tau 181 were found and these levels also had a significant correlation with NfL in patients who reported neurological sequelae (Sun et al., 2021). There is some evidence suggesting that COVID-19 worsens pathology that has been implicated in AD such as tau, β-amyloid aggregation, neuroinflammation cerebral ischemia, and disruption of the BBB (Miners et al., 2020; Shen et al., 2022). Therefore, these findings suggest that p-tau 181 is yet another neurodegenerative biomarker correlated with COVID-19 disease severity during and/or following SARS-CoV-2 infection.

Ubiquitin Carboxy-Terminal Hydrolase L1

Ubiquitin is a regulatory protein that is widely known for its role in the ubiquitin-proteasome system (UPS), which is involved in cellular processes including protein degradation, DNA repair and cell trafficking (Bishop et al., 2016; Guo and Tadi, 2022). In neurons, ubiquitination is involved in regulating the function of various synapses influencing their maintenance, transmission, and plasticity by altering the quantity of proteins at each synapse (Mabb and Ehlers, 2010). Deubiquinating enzymes known as deubiquitinases (DUBs) are responsible for removing ubiquitin from their target proteins (Bishop et al., 2016). Ubiquitin C-terminal hydrolase L1 (UCH-L1) is a specific member of this group that is highly expressed in neurons (Bishop et al., 2016). Higher levels of plasma UCH-L1 have been associated with PD (Ng et al., 2020), AD (Bogdan et al., 2022), Friedreich's Ataxia (Zeitlberger et al., 2018), TBI (Wang et al., 2018), and general cognitive capabilities (Zhang et al., 2022a). The loss of UCH-L1 has resulted in the loss of neurons and instability of axons, while in some cases oxidatively modified UCH-L1 may aggregate (Bishop et al., 2016). These findings support that UCH-L1 is utilized as a general marker of neurodegeneration and other CNS-related complications.

Various COVID-19 patient populations have also experienced elevated levels of plasma UCH-L1 (Cooper et al., 2020; Frontera et al., 2022). It was found to correlate with COVID-19 disease severity as it was significantly higher in COVID-19 patients with encephalopathy (Frontera et al., 2022). As mentioned previously, hospitalized COVID-19 patients who experienced new neurological symptoms during admission had elevated plasma levels of UCH-L1, p-tau 181, and NfL, when compared to the control group consisting of non-COVID AD patients (Frontera et al., 2022). A group of ICU COVID-19 patients were also found to have higher levels of UCH-L1 that was also associated with delirium (Cooper et al., 2020). In another group of COVID-19 patients, UCH-L1 and NfL yielded predictive values on whether patients required a transfer to the ICU (De Lorenzo et al., 2021). Hence, it remains a possibility that UCH-L1 may be used as a prognostic biomarker when combined with others in providing potential clinical outcomes in COVID-19 patients (De Lorenzo et al., 2021).

S100 calcium-binding protein B

The S100 protein family consists of proteins that principally bind Ca^{2+} and are named S100 because they dissolve in a neutral pH solution consisting of 100% saturated ammonium sulfate (Sedaghat and Notopoulos, 2008). A frequently investigated member of this protein family, S100 calcium-binding protein B (S100B), is used to describe levels of both the heterodimer S100AB and homodimer S100BB (Thelin et al., 2017). Serum levels of S100B may indicate astrocyte damage or injury, though with less accuracy than GFAP due to its more extensive distribution throughout different cell types of the CNS (Steiner et al., 2007). The function of S100B also differs depending on the concentration, having cytotoxic effects when increased (micromolar) and neuroprotective effects when at lower levels (nanomolar) in serum (Lam et al., 2013). S100B has been implicated in several neurological disorders including TBI (Thelin et al., 2017; Mondello et al., 2021), AD (Cristovao and Gomes, 2019), PD (Angelopoulou et al., 2021), ALS (Serrano et al., 2017), and MS (Barateiro et al., 2016). Micromolar levels

of S100B is reported to cause such disorders by activating astrocytes and microglia, inducing nitric oxide (NO) release, increasing reactive oxygen species (ROS) and ultimately leading to neuroinflammation and loss of neurons (Michetti et al., 2019). These findings support that S100B is continuing to be explored as a potential blood biomarker across neurological disorders.

Elevated levels of circulating S100B has also been found in different groups of COVID-19 patients (Aceti et al., 2020; Mete et al., 2021; Savarraj et al., 2021; Sahin et al., 2022). As mentioned with previous brain injury biomarkers, serum S100B has also been associated with disease severity in COVID-19 patients (Aceti et al., 2020; Mete et al., 2021). Report show that levels of serum S100B were not correlated with neurological symptoms overall in acute phase COVID-19 patients, but did find marginally elevated levels of S100B in patients with more than one neurological symptom (Sahin et al., 2022). This may suggest that the elevated levels of S100B represents CNS injury to some extent during the acute phase of COVID-19, but it is unclear what implications this may have both clinically and in long-COVID patients. S100B has also been described as a pro-inflammatory ligand by binding to the Receptor for Advanced Glycation Endproducts (RAGE), which itself has been associated with neuroinflammation following neurological insult (Michetti et al., 2019). These findings may partly explain the association of elevated levels S100B with both disease severity and cognitive sequelae in COVID-19 infection. The exact role of S100B in COVID-associated cognitive dysfunction remains to be discovered to confirm whether it is directly contributing to neuropathological damage and/or it is a reaction of downstream inflammatory processes.

Neuron specific enolase

Neuron specific enolase (NSE) is the gamma isozyme named due to its specificity for neuronal and neuroendocrine cells (Haque et al., 2018). NSE itself can be expressed as two different isozymes in neurons as either γγ or αγ (Polcyn et al., 2017). In astrocytes, NSE is expressed as γγ and in oligodendrocytes and microglia it is found as the αγ subunits (Polcyn et al., 2017). NSE has therefore been linked to both neurological and non-neurological pathologies due to its tissue specificity and upregulation following axonal injury (Polcyn et al., 2017). Similar to S100B, NSE can be both neuroprotective or neuroinflammatory depending on surrounding conditions such as the typical homeostatic environment, disease state, or presence of injury (Polcyn et al., 2017). The neuropathological conditions that have been associated with altered levels of plasma or serum NSE include AD (Chaves et al., 2010), HD (Ciancarelli et al., 2014), postoperative cognitive dysfunction (POCD) (Wan et al., 2021), and beta-propeller protein-associated neurodegeneration (BPAN) (Takano et al., 2017).

Neuron specific enolase levels have also been found at higher concentrations in the serum or plasma of COVID-19 patients (Wei et al., 2020; Cione et al., 2021; Savarraj et al., 2021). Increased levels of serum NSE has also been associated with disease severity as mentioned previously with other biomarkers specifically in a cohort of COVID-19 patients who developed dyspnea (Cione et al., 2021), in critical cases of COVID-19 patients (Wei et al., 2020), and in patients immediately following hospital admission for COVID-19 infection (Savarraj et al., 2021). A unique observation found was that serum NSE was found at significantly higher levels in men when compared to women, which may support increased susceptibility to COVID-associated cognitive dysfunction in men (Savarraj et al., 2021). NSE may be elevated in COVID-19 due to the potential presence of axonal injury (Polcyn et al., 2017), lung injury (Cione et al., 2021), neuroinflammation (Haque et al., 2018), or a combination of all. There is not enough data at this time to concretely validate the use of serum NSE as a biomarker of only neurodegeneration and/or prognosis in COVID-19 infection. Further investigation are required to support these findings and uncover the exact role of NSE in COVID-29 infection.

Inflammatory cytokines

Pro-inflammatory cytokines, such as interleukin (IL)-6, IL-1β, and tumor necrosis factor-α (TNF-α) are well established as major contributing factors to neuropathological diseases (Wang et al., 2015; Gupta et al., 2020b; Xin et al., 2021; Lu et al., 2022). Anti-inflammatory cytokines such as IL-10 also play crucial roles in brain injury and neuroinflammation due to its ability to suppress inflammatory responses (Garcia et al., 2017; Burmeister and Marriott, 2018; Lu et al., 2022; Sanchez-Molina et al., 2022). C-reactive protein (CRP), a non-specific marker of systemic inflammation, is induced by pro-inflammatory cytokines such as IL-6, and has been associated with chronic inflammation, and various degrees of cognitive dysfunction (Watanabe et al., 2016; Luan and Yao, 2018; Vintimilla et al., 2019; Gupta et al., 2020b; Xin et al., 2021). A cascade of events, referred to as "cytokine storm" or "cytokine release syndrome (CRS)," has been implicated in neurotoxicity, disruption of the integrity of BBB, neuroglial cells activation, and ultimately neuroinflammation (Gupta et al., 2020b; Zhang et al., 2022b).

In COVID-19 patients, elevated serum levels of IL-6, IL-1β, TNF- α, IL-10, and CRP have been measured and discussed (Chen et al., 2020; Han et al., 2020; Islam et al., 2021a; Lavillegrand et al., 2021; Lu et al., 2021; Acosta-Ampudia et al., 2022; Ferrando et al., 2022; Hirzel et al., 2022; Leretter et al., 2022; Montazersaheb et al., 2022; Peluso et al., 2022; PHOSP-COVID Collaborative Group, 2022; Schultheiss et al., 2022). IL-6, CRP, and IL-10 and have also been associated with disease severity amongst COVID-19 patients, correlating with severe clinical outcomes and fatality (Han et al., 2020; Lavillegrand et al., 2021; Alshammary et al., 2022; Ashktorab et al., 2022; Azaiz et al., 2022; Galliera et al., 2022; Jafrin et al., 2022; Mainous et al., 2022). CRP was found specifically to be positively

correlated with two parts of a Continuous Performance Test (CPT) conducted in patients who had resolved COVID-19 infections (Zhou et al., 2020a) and was found at significantly elevated concentration in COVID-19 patients with moderate to severe cognitive dysfunction (Arica-Polat et al., 2022). Even though vast amount of evidence continues to validate the role of hyperinflammation in SARS-CoV-2 infection, there is a clear need for additional studies to explore the role of these inflammation in the CNS in COVID-19 patient populations.

Role of circulating micro RNAs in COVID-19-associated cognitive dysfunction

Growing evidence suggests that as post-transcriptional regulators of gene expression, miRNAs are involved in physiological and pathological processes and their dysregulation in function is synonymous with a multiplicity of diseases (Condrat et al., 2020; Carini et al., 2021). The prominent role of non-coding microRNAs in CNS and their signature in the circulation has been well established in various neurodegenerative diseases (Thounaojam et al., 2013; Bahlakeh et al., 2021; Islam et al., 2021c; Perdoncin et al., 2021; Blount et al., 2022). Hence, miRNAs as possible therapeutic targets and disease markers for early diagnosis have strongly been advocated because of their stability and convenience in extraction from biological fluids (Szelenberger et al., 2019). In this section of the review, we are showcasing the importance of some dysregulated miRNAs in COVID-19 and their possible correlation with CNS to further explore the mechanism of COVID-19- associated cognitive dysfunction. A summary of the findings are illustrated in **Table 2**.

miR-146a

miR-146a is produced by bone marrow mesenchymal stem cells and released in exosome granules, then it is taken up by activated astrocytes, particularly in the hippocampal region, indicating it may serve a neuroprotective role in seizure-related cognitive dysfunction (Kong et al., 2015). miR-146a exerts an anti-inflammatory effect by inactivating NF-κB activity through a reduction of interleukin-1 receptor-associated kinase 1 (IRAK1) and tumor necrosis factor associated factor 6 (TRAF6) (Nakano et al., 2020a,b). This will further lead to the supression of NF-κB's target genes such as the interleukins IL-6, IL-8, IL-1β, and TNF alpha (TNF-α) (Saba et al., 2014; Fan et al., 2020). Increased expression of miR-146a in brain endothelial cells alters cytokine signaling and reduces NF-κB activity by reducing its nuclear translocation and thus decreasing the number of expressed T-cell adhesion molecules and limiting their entry into the CNS in the development of neuroinflammation (Wu et al., 2015). Circulating miR-146a is reduced in the blood of AD (Kumar and Reddy, 2016; Swarbrick et al., 2019), reducing the capability to deal with neurodegenerative inflammation. Overexpression of miR146a in microglia has been shown to reduce cognitive deficits in learning and memory, attenuate neuroinflammation, reduce beta-amyloid levels, and alleviate plaque-associated neuritic pathologies. miR-146a also influences microglial phenotype switching, allowing for the reduction of pro-inflammatory cytokine production and improved phagocytic functions in the clearance of beta-amyloid and tau (Liang et al., 2021). Thus, serum miR-146a levels are being considered for clinical use as a biomarker for neurodegenerative diseases (Kumar and Reddy, 2016; Mai et al., 2019; Swarbrick et al., 2019; Sabbatinelli et al., 2021).

Cumulative evidences suggest that decreased expression of miR-146a is associated with SARS-CoV-2 infection (Keikha and Jebali, 2021; Roganovic, 2021; Sabbatinelli et al., 2021). Furthermore, individuals with pre-existing inflammatory conditions which cause a decreased expression of miR-146a are thus predisposed to COVID-19 infection, and at risk for more serious progression of the illness (Roganovic, 2021; Sudhakar et al., 2022). Interestingly, COVID-19 patients showed a down-regulation of this anti-neuroinflammatory miRNA, which in turn causes an increase in expression of IL-6, IL-8, IL-17, and other inflammatory cytokines (Arghiani et al., 2021; Roganovic, 2021). Increased levels of the inflammatory cytokine IL-6 thus reduce the effectiveness of many drugs being currently tested for use against COVID, such as tocilizumab, because they act as antibodies against these inflammatory cytokines (Arghiani et al., 2021; Sabbatinelli et al., 2021). Conversely, some studies have shown that the expression of miR-146a is increased in COVID-19 patients when compared to healthy controls (Donyavi et al., 2021; Pinacchio et al., 2022). miR-146a is therefore uniquely can be positioned as one of a handful of micro-RNAs suited for use as a biomarker for cognitive dysfunction and SARS-CoV-2 infection and as a potential therapeutic for the treatment of those disease states. Given the altered expression of miR-146a in neurodegenerative diseases as well as in SARS-CoV-2 infection, and its role as an anti-neuroinflammatory microRNA, future studies with large populations may help to elucidate the actual mechanism of action of miR-146a in COVID-19 mediated cognitive decline and its importance as a circulating prognostic marker.

miR-155

CNS upregulation of miR-155 has been associated cognitive dysfunction and is the most expressed chromosome 21 miRNA in Down's Syndrome dementia, as it is co-expressed with hyperphosphorylated tau protein (Tili et al., 2018). miR-155 act as a prevalent CNS pro-inflammatory mediator and

TABLE 2 Summary of circulating miRNAs associated with neurological dysfunction showing potential dysregulation in COVID-19.

miRNA	Source	Target genes	Status in neurodegenerative diseases	Patients' information	Status in COVID-19	References
miR-146a	Serum	IRAK1, TRAF6	IS- decreased AD- decreased PD- decreased	1.Different grades of COVID-19 patients (n = 103) 2. 13 COVID-19 patients, characterized by multifocal interstitial pneumonia confirmed by CT-scan and requiring oxygen therapy.	Significantly decreased	Fan et al., 2020; Nakano et al., 2020a,b; Keikha and Jebali, 2021; Keikha et al., 2021; Sabbatinelli et al., 2021
miR-155	Serum	SOCS1, SHIP1, STAT5, IL13Ra1, claudin-1, annexin-2, syntenin-1, DOCK-1	IS- increased AD- increased PD- increased ALS- increased MS- increased	1. 18 patients after diagnosis of Covid-19 and in the recovery period. 2. 20 patients with COVID-19 infection in the acute period and in the recovery period. 3. 150 COVID-19 patients classified into two main groups: moderate patients and severe patients.	Significantly increased	Lopez-Ramirez et al., 2014; Song and Lee, 2015; Donyavi et al., 2021; Zingale et al., 2021; Abbasi-Kolli et al., 2022; Haroun et al., 2022
Let-7b	PBMC	TLR7, HMGA2	AD- increased PD-increased MIC-increased	1. 18 patients after diagnosis of COVID-19 and in the recovery period. 2. 31 COVID-19 positive obese female participants.	Significantly increased	Coleman et al., 2017; Donyavi et al., 2021; Huang et al., 2021b; Qin et al., 2021; Bellae Papannarao et al., 2022
miR-31	Serum	RhoA, APP, BACE1, PARK2, GIGYF2	AD- decreased PD- decreased MSA- decreased	1.Different grades of COVID-19 patients (n = 103) 2. 122 COVID-19 patients with different severity of illness. 3. 10 COVID-19 patients 2–15 days (average 8 days) post symptomatic disease onset.	Significantly decreased	Pearn et al., 2018; Barros-Viegas et al., 2020; Li et al., 2020; Tang et al., 2020; Yan et al., 2020; Bautista-Becerril et al., 2021; Farr et al., 2021; Keikha and Jebali, 2021; Keikha et al., 2021
miR-16	Plasma	APP, BACE1, Tau	AD- decreased	1. 84 COVID-19 patients divided according to the severity of the disease. 2. 94 COVID-19 patients	Significantly decreased	Liu et al., 2012; Parsi et al., 2015; De Gonzalo-Calvo et al., 2021; Li et al., 2022b
miR-21	Plasma/serum	NF-κB, PTEN/AKT,PI3K, GSK-3β, mTOR1, STAT3	AD- decreased PD- decreased IS-decreased	1. 10 COVID-19 patients 2. 13 COVID-19 patients, characterized by multifocal interstitial pneumonia confirmed by CT-scan and requiring oxygen therapy 3. 122 COVID-19 patients with different severity of illness. 4. 6 severe and 6 moderate COVID-19 patients	Significantly decreased	Ma et al., 2011; Feng et al., 2018; Gao et al., 2020; Bai and Bian, 2022; Blount et al., 2022

Ischemia stroke (IS), Alzheimer's disease (AD), Parkinson's disease (PD), Amyotrophic lateral sclerosis (ALS), Multiple sclerosis (MS), Multiple system atrophy (MSA), mild cognitive impairment (MIC), Peripheral blood mononuclear cell (PBMC), interleukin-1 receptor-associated kinase 1 (IRAK1), receptor-associated factor 6 (TRAF6), Suppressor of Cytokine Signaling 1 (SOCS1), SH2 Domain-Containing Inositol 5'-Phosphatase1 (SHIP1), Signal Transducers and Activators of Transcription 5 (STAT5) and IL-13 Receptor Alpha 1 (IL13Ra1), Dedicator of cytokinesis 1 (DOCK-1), toll-like receptor 7 (TLR7), High-mobility group AT-hook 2 (HMGA2), amyloid precursor protein (APP), β-secretase (BACE1), parkin E3 ubiquitin-protein ligase (PARK2), interacting GYF protein 2 (GIGYF2), Ras Homolog Family Member A (RhoA), tubulin associated unit protein (TAU protein), *Nuclear factor kappa*β (NF-κβ), Phosphatase and tensin homolog (PTEN), Phosphoinositide 3-kinase (PI3K), Mammalian target of rapamycin complex 1 (mTOR1), Glycogen Synthase Kinase 3 Beta (GSK-3β), toll-like receptor 4 (TLR4).

microglia activator by regulating inflammatory cytokines such as (IFN)-λ and IFN-β (Thounaojam et al., 2013). In the CNS, the action of miR-155 is mediated in microglia and macrophages through NF-κB following stimulation of the appropriate TLR and interferon-gamma release. It also causes a reduction in the anti-inflammatory response by targeting anti-inflammatory regulators such as Suppressor of Cytokine Signaling 1 (SOCS1), SH2 Domain-Containing Inositol 5'-Phosphatase1 (SHIP1), activator protein 1, Signal Transducers and Activators of Transcription 5 (STAT5) and IL-13 Receptor

Alpha 1 (IL13Ra1), further increasing inflammation (Song and Lee, 2015; Zingale et al., 2021). miR-155 increases BBB permeability by targeting cell–cell complex molecules including claudin-1 and annexin-2 and focal adhesion components such as syntenin-1 and dedicator of cytokinesis 1 (DOCK-1) (Lopez-Ramirez et al., 2014). miR-155 is also associated with promotion of CNS T cell responses and the subsequent development of cognitive dysfunction symptomology. Through regulation of interferon-gamma signaling, miR-155 can influence CD8 + T cell activation, T cell development, various cell to cell interactions, and macrophage activation. T cell activation and IFN-γ production, followed by infiltration into the CNS, results in the deposition of beta-amyloid and thus cognitive dysfunction (Song and Lee, 2015). The pro-neuroinflammatory role of miR-155 was affirmed through knockout studies which show reduced neuroinflammation, reduced cognitive impairment and better recovery in traumatic brain injury mouse models (Henry et al., 2019). Moreover, miR-155 overexpression is implicated in CCR2/CXCL2 translation disorders, causing impaired cell migration and clearance of beta-amyloid by blood-derived monocytes (BDMs) and monocyte-derived macrophages (MDMs) in AD (Guedes et al., 2016). The pro-inflammatory function of miR-155 also carries over into auto-immune conditions such as MS-associated cognitive dysfunction by promoting inflammatory damage to the neurovascular units of the blood-brain-barrier *via* down regulation of junctional proteins (Maciak et al., 2021). miR-155 contributes to CNS demyelination *via* microglia activation and subsequent production of TNF-a, IL-1, IL-6, interferon-inducible protein 10 (IP-10), macrophage inflammatory protein-1a (MIP-1a), monocyte chemoattractant protein-1 (MCP-1), and nitric oxide (NO) (Miller, 2012). It is reported that miR-155 mediated impairment to the BBB, damage of myelin and axons, synaptic dysfunction, and dysregulated neurotransmitter production due to acute inflammation can lead to brain atrophy and progressive cognitive impairment (Varma-Doyle et al., 2021).

Serum miR-155 levels are significantly increased during the acute and post-acute phases of SARS-CoV-2 infection (Bautista-Becerril et al., 2021; Abbasi-Kolli et al., 2022). The study which showed significantly increased expression of miR-155 in the peripheral blood mononuclear cell (PBMC) samples of patients with acute COVID-19 infection suggest it as a diagnostic marker for COVID-19 (Abbasi-Kolli et al., 2022). Similarly, another study demonstrates miR-155 as a biomarker to distinguish acute from post-acute phase of COVID-19 disease (Donyavi et al., 2021). Additionally, plasma miR-155 levels appear to be significantly correlated with chest CT findings, CRP and ferritin levels, mortality, d-dimer, WBC count and neutrophil percentage. miR-155 levels are 90% sensitive and 100% specific when used as a biomarker for the detection of COVID-19 and are 76% sensitive and specific for detection of severity of COVID-19 disease (Haroun et al., 2022). Overexpression of miR-155 in SARS-CoV-2 infection thus may partially explain the enhanced immune response that leads to CNS damage in the context of covid-associated cognitive dysfunction.

Let-7b

Let-7b a multifunctional miRNA that is differentially expressed in issues of cognitive dysfunction in comparison to healthy individuals (Rahman et al., 2020; Yuen et al., 2021). Levels of Let-7b appear to be increased in diseases of cognitive dysfunction such as MCI (Kenny et al., 2019), AD (Leidinger et al., 2013), and PD (Huang et al., 2021b). Overexpression of Let-7b in AD models was found to significantly reduce cell viability, inhibit autophagy and increase apoptosis through increased cleavage of caspase 3 and through increased expression levels of PI3K, p-AKT, and p-mTOR in upstream signaling pathways (Pang et al., 2022). Let-7b also appears to be involved in neurodegeneration through interaction with toll-like receptor 7 (TLR7) (Lehmann et al., 2012). TLR7 mediated pathway of Let-7b action is additionally seen in the postmortem hippocampal formations of alcoholics, where TLR7 and Let-7b expression was increased, leading to neuroinflammation and neurodegeneration (Coleman et al., 2017). Additional studies have also shown the role of Let-7b and TLR7 mediated mechanism of alcohol-associated cognitive dysfunction (Qin et al., 2021). Let-7b has been shown to regulate the function of high mobility group AT-hook 2 (HMGA2) protein in PD, causing a dysregulation of chromatin structure and transcription which leads to decreased self-renewal of neuronal stem cells, leading to neurodegeneration (Huang et al., 2021b).

Let-7b levels are elevated in peripheral blood samples in both the acute and post-acute stages of SARS-CoV-2 infection compared to healthy individuals (Donyavi et al., 2021; Nain et al., 2021), suggesting potential use as a clinical biomarker COVID-19 infection. Let-7b targets ACE2 causing dysregulation of ACE2 and potentially increasing susceptibility to SARS-CoV-2 infection, making it a potential target for therapeutic treatment of SARS-CoV-2 infection (Bellae Papannarao et al., 2022). Let-7b, in the context of SARS-CoV-2 infection, increases apoptosis through a reduction of BCL-2, an anti-apoptotic protein, and through modulation of immune responses, establishing a potential link between chronic inflammatory illness such as type 2 diabetes and COVID-19 (Islam et al., 2021b), which may have effect on cognitive dysfunction. Reports shows showcase Let-7b as a marker of lung disease which is highly prevalent in COVID-19 (Islam et al., 2021b; Nain et al., 2021). These reported upregulation of Let-7b in SARS-CoV-2 infection suggest its possible link with cognitive dysfunction that warrants future studies.

miR-31

miR-31 is decreased in the serum of AD individuals compared to healthy controls (Dong et al., 2015; Klyucherev et al., 2022) and can be used as part of a panel in conjunction with miR-93 and miR-146a to differentiate Alzheimer's Disease from Vascular Dementia (Dong et al., 2015). Expression of miR-31 was also decreased in the serum of PD and Multiple System Atrophy (MSA) individuals (Yan et al., 2020). Letiviral delivery of miR-31 was able to significantly ameliorate AD neuropathology by reducing Aβ deposition in both the hippocampus and subiculum of transgenic mice models (Barros-Viegas et al., 2020). The study shows that miRNA-31 targets amyloid precursor protein (APP) and β-secretase (BACE1), which further abolishes the pathogical aletrations in AD. The results showed improvements in memory deficits, reduced anxiety, and reduced cognitive inflexibility, suggesting future possibilities for miR-31 to be used as a therapeutic in the treatment of AD (Barros-Viegas et al., 2020). RhoA has been reported to modulate synaptic plasticity and inhibition of the RhoA pathway reduces cognitive impairment and deficits in synapses and dendritic spines (Pearn et al., 2018). miR-31 has been reported as a regulator of RhoA and decrease in miR-31 plays a role in the development of cognitive dysfunction in learning, memory, behavior, etc., patterns which are similarly seen in neurodegenerative disease (Qian et al., 2021). miRNA target prediction analysis have shown some PD- and MSA-related genes such as parkin E3 ubiquitin-protein ligase (PARK2), GRB10-interacting GYF protein 2 (GIGYF2) as potential target of miR-31 (Yan et al., 2020).

miR-31 is multifunctional in the context of COVID-19, particularly when discussing hypoxia and potential resultant neurodegenerative effects. miR-31 serum expression levels have been demonstrated to be decreased in COVID-19 infected patients (Bautista-Becerril et al., 2021). Expression levels of miR-31 appear to decrease with worsening severity of illness with COVID-19 infection also, making it a worthwhile candidate for use as a biomarker of COVID-19 infection and severity (Keikha et al., 2021). Decreased expression may play a role in the neurodegenerative pathologies seen with enhanced micro coagulation in SARS-CoV-2 infected individuals. Thus, decreased levels of miR-31 appear to have a multifactorial effect in cognitive dysfunction and in SARS-CoV-2 infection and presents as a potential link between the two disease processes. Conversely, microRNA expression profile analysis of another set of COVID-19 patients showed up-regulation of miR-31 expression (Farr et al., 2021). Hence, future studies with more population size and more detailed mechanistic approach may clarify the exact role of miR-31 in COVID-19-associated cognitive decline.

miR-16

miR-16 is differentially expressed in various neurodegenerative diseases, with its levels being significantly decreased in the serum of AD patients (Denk et al., 2018; Mckeever et al., 2018). miR-16 regulates cell death in AD by targeting APP (Liu et al., 2012; Zhang et al., 2015; Turk et al., 2021). Downregulation of miR-16 in hippocampal neurons has been associated with increases in APP eventual processing to beta-amyloid followed by deposition into neurons within the brain (Zhang et al., 2015; Grinan-Ferre et al., 2018). In cell culture studies, miR16 has been shown to regulate Aβ

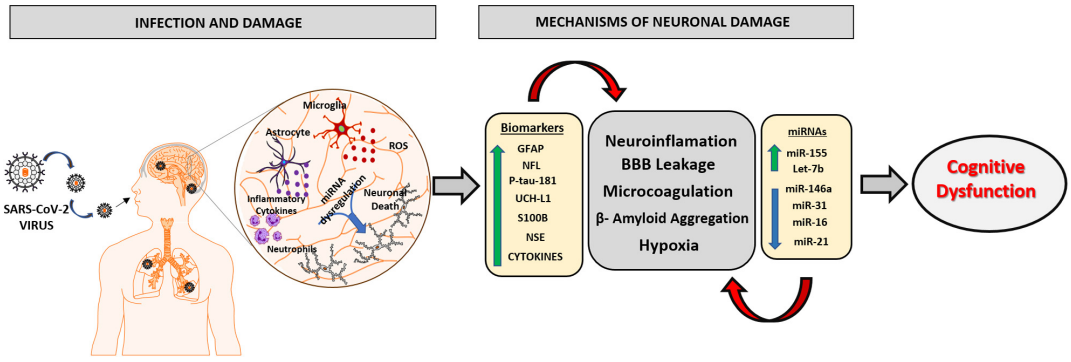

FIGURE 3
Schematic representation of the main mechanisms involved in the neurophysiology caused by SARS-CoV2 virus and the role of biomarkers and miRNAs in neuronal damage. The SARS-CoV2 virus has the ability to infect brain tissue by mechanisms involving the olfactory and hematological pathway, which will lead to an oxidative and inflammatory state in nervous tissue, due to the activation of neutrophils, astrocytes, and microglial cells releasing excessive ROS and pro-inflammatory molecules. The imbalance in brain homeostasis leads to a dysfunction in the expression pattern of different biomarkers and miRNAs, potentiating neuroinflammatory mechanisms, responsible for brain damage and the consequent progression of cognitive dysfunction and neurodegenerative disorders. GFAP, Glial fibrillary acid protein; NFL, Neurofilament light chain; P-tau-181, Phosphorylated tau at threonine-181; UCH-L1, Ubiquitin Carboxy-Terminal Hydrolase L1; S100B, S100 calcium-binding protein B; NSE, Neuron Specific Enolase.

production, and Tau phosphorylation (Hebert et al., 2012). Similarly report shows a reduction of the expression of a number of genes related to AD including APP, BACE1, tau, inflammation and oxidative stress through the delivery of miR-16 mimics directly to mouse brain (Parsi et al., 2015). The role of miR16 in targeting genes involved in neurite extension and branching in hippocampal neurons during presymptomatic prion disease has also been reported (Burak et al., 2018). miR-16 appears to have potential for future drug development because it simultaneously targets various endogenous targets of AD biomarkers. These findings suggest that further research is needed into the role of miR-16 in other forms of neurodegenerative diseases to evaluate its impact more completely on cognitive function.

Serum miR-16 levels are likewise reduced in COVID-19 infected patients suggesting a potential link between differential miR-16 expression and covid-associated cognitive dysfunction. miR-16 levels were established to be inversely correlated with length of ICU stay in COVID-19 infected patients as well, opening the possibility for its use as a biomarker of disease and severity (De Gonzalo-Calvo et al., 2021). Also, miR-16 has already been used as a biomarker for other viral respiratory illnesses such as community acquired pneumonia (Galvan-Roman et al., 2020). miR-16 is capable of high affinity binding to the SARS-CoV-2 genome, opening future avenues of potential drug research (Kim et al., 2020; Nersisyan et al., 2020). A single-cell RNA-sequencing based study identified miR-16 as a potential virus targeting miRNAs across multiple cell types from bronchoalveolar lavage fuid samples (Li et al., 2022b). Down regulation of miR-16 levels in individuals with SARS-CoV-2 suggests miR-16 may play a role in covid-associated cognitive dysfunction due to its previously defined role in other forms of neurodegenerative cognitive dysfunction.

miR-21

miR-21 is extensively involved in processes governing apoptosis and neuroinflammation in neurodegenerative diseases and thus in cognitive dysfunction (Bai and Bian, 2022). Serum and CSF levels of miR-21 are decreased in patients with AD compared to individuals with Lewy Body Dementia and healthy controls (Gamez-Valero et al., 2019). miR-21 acts as an anti-inflammatory microRNA by acting as a negative feedback regulator on NF-κB in response to pro-inflammatory signaling (Ma et al., 2011). miR-21 has been shown to ameliorate cognitive impairments associated with brain injury from subarachnoid hemorrhaging by modulation of the PTEN/AKT pathway and reducing apoptosis in the hippocampus and prefrontal cortex (Gao et al., 2020). Use of miR-21 mimics in cell culture studies of AD has shown that miR21 is capable of inhibiting beta-amyloid induced apoptosis by increasing expression of PI3K, AKT, and GSK-3B (Feng et al., 2018). Overexpression of miR-21 was demonstrated to protect neurons of the hippocampus in epileptic rat studies by inhibiting STAT3 (Bai and Bian, 2022). Microglial miR-21 has been reported to protect neurons from cell death under hypoxic conditions (Zhang et al., 2012). miR-21 has been shown to restore neurogenesis and reverse cellular senescence *via* inhibition of the mTOR1 pathway in models of vascular dementia, making a candidate as a potential therapeutic in the treatment of vascular dementia and its associated cognitive impairment (Blount et al., 2022).

Serum miR-21 levels have been reported to be decreased in COVID-19 infected individuals (Li et al., 2020; Sabbatinelli et al., 2021). The down-regulation in the relative expression of miR-21 in COVID-19 patients was concomitant with up-regulation of its target proinflammatory genes (Keikha and Jebali, 2021). The study also demonstrate miR-21 as an anti- neuroinflammatory miRNA, for correlating the disease grade from asymptomatic to critical illness in COVID-19. Down regulation of miR-21 in COVID-19 patients exacerbates systemic inflammation through hyperactive immune response, loss of T cell function, and immune dysregulation (Tang et al., 2020). Increased systemic inflammation can weaken the blood-brain-barrier, causing heightened neuroinflammation and resulting in neurodegeneration. Thus, decreases in expression of miR-21 could directly and indirectly contribute to the development and progression of covid-associated cognitive dysfunction, or worsening of pre-existing cognitive dysfunction after infection with SARS-CoV-2.

Conclusion

The different sequelae presented by post-COVID-19 patients are being increasingly studied from the improvement of clinical and laboratory experience. Cumulative evidences suggest that surviving patients of COVID-19 have a high risk of developing some neuropsychiatric impairment, which can occur in different forms, such as cases of depression, anxiety, and severe mental illness. The sequelae related to cognitive decline and neurodegeneration are diverse and there is a need for detailed assessments to identify new neurological conditions. An extremely relevant factor to be considered in the fight against COVID-19 is the use of biomarkers in the early recognition of patients susceptible to developing the severe form of the disease. The discovery of potential markers could be used to provide essential information that will assist in stratifying these patients, improving primary care, and developing optimal individualized therapy according to the patient's response to cognitive damage. The review summarizes the neuropathological changes associated with COVID-19 and signifies the importance of circulating biomarkers and miRNAs in these neurodegenerative changes (**Figure 3**).

Thus, the clinical use of the markers reported in this review will significantly improve the development of new policies to prevent, address and manage the neurological conditions caused by SARS-CoV-2 infection and may aid in future research exploring the mechanistic aspects of COVID-19 associated neurodegeneration and cognitive dysfunction.

Author contributions

SP: conceptualization, project administration, and writing—review and editing. KS: conceptualization and project administration. MA, ET, BG, DP, RP, and NF: writing—original draft preparation. All authors contributed to the article and approved the submitted version.

Conflict of interest

The authors declare that the research was conducted in the absence of any commercial or financial relationships that could be construed as a potential conflict of interest.

Publisher's note

All claims expressed in this article are solely those of the authors and do not necessarily represent those of their affiliated organizations, or those of the publisher, the editors and the reviewers. Any product that may be evaluated in this article, or claim that may be made by its manufacturer, is not guaranteed or endorsed by the publisher.

References

Aamodt, A. H., Hogestol, E. A., Popperud, T. H., Holter, J. C., Dyrhol-Riise, A. M., Tonby, K., et al. (2021). Blood neurofilament light concentration at admittance: A potential prognostic marker in COVID-19. *J. Neurol.* 268, 3574–3583. doi: 10.1007/s00415-021-10517-6

Abbasi-Kolli, M., Sadri Nahand, J., Kiani, S. J., Khanaliha, K., Khatami, A., Taghizadieh, M., et al. (2022). The expression patterns of MALAT-1, NEAT-1, THRIL, and miR-155-5p in the acute to the post-acute phase of COVID-19 disease. *Braz. J. Infect. Dis.* 26:102354. doi: 10.1016/j.bjid.2022.102354

Abdelhak, A., Foschi, M., Abu-Rumeileh, S., Yue, J. K., D'anna, L., Huss, A., et al. (2022). Blood GFAP as an emerging biomarker in brain and spinal cord disorders. *Nat. Rev. Neurol.* 18, 158–172. doi: 10.1038/s41582-021-00616-3

Aceti, A., Margarucci, L. M., Scaramucci, E., Orsini, M., Salerno, G., Di Sante, G., et al. (2020). Serum S100B protein as a marker of severity in Covid-19 patients. *Sci. Rep.* 10:18665. doi: 10.1038/s41598-020-75618-0

Acosta-Ampudia, Y., Monsalve, D. M., Rojas, M., Rodriguez, Y., Zapata, E., Ramirez-Santana, C., et al. (2022). Persistent autoimmune activation and proinflammatory state in post-coronavirus disease 2019 syndrome. *J. Infect. Dis.* 225, 2155–2162. doi: 10.1093/infdis/jiac017

Alshammary, A. F., Alsughayyir, J. M., Alharbi, K. K., Al-Sulaiman, A. M., Alshammary, H. F., and Alshammary, H. F. (2022). T-Cell subsets and interleukin-10 levels are predictors of severity and mortality in COVID-19: A systematic review and meta-analysis. *Front. Med. (Lausanne)* 9:852749. doi: 10.3389/fmed.2022.852749

Ameres, M., Brandstetter, S., Toncheva, A. A., Kabesch, M., Leppert, D., Kuhle, J., et al. (2020). Association of neuronal injury blood marker neurofilament light chain with mild-to-moderate COVID-19. *J. Neurol.* 267, 3476–3478. doi: 10.1007/s00415-020-10050-y

Amruta, N., Chastain, W. H., Paz, M., Solch, R. J., Murray-Brown, I. C., Befeler, J. B., et al. (2021). SARS-CoV-2 mediated neuroinflammation and the impact of COVID-19 in neurological disorders. *Cytokine Growth Factor Rev.* 58, 1–15. doi: 10.1016/j.cytogfr.2021.02.002

Angelopoulou, E., Paudel, Y. N., and Piperi, C. (2021). Emerging role of S100B protein implication in Parkinson's disease pathogenesis. *Cell Mol. Life Sci.* 78, 1445–1453. doi: 10.1007/s00018-020-03673-x

Anka, A. U., Tahir, M. I., Abubakar, S. D., Alsabbagh, M., Zian, Z., Hamedifar, H., et al. (2021). Coronavirus disease 2019 (COVID-19): An overview of the immunopathology, serological diagnosis and management. *Scand. J. Immunol.* 93:e12998. doi: 10.1111/sji.12998

Arghiani, N., Nissan, T., and Matin, M. M. (2021). Role of microRNAs in COVID-19 with implications for therapeutics. *Biomed. Pharmacother.* 144:112247. doi: 10.1016/j.biopha.2021.112247

Arica-Polat, B. S., Gundogdu, A. A., Cinar, N., Uncu, G., Ayas, Z. O., Iseri, P., et al. (2022). Evaluation of cognitive deficits in patients infected with COVID-19. *Eur. Rev. Med. Pharmacol. Sci.* 26, 678–685.

Ashktorab, H., Pizuorno, A., Adeleye, F., Laiyemo, A., Dalivand, M. M., Aduli, F., et al. (2022). Symptomatic, clinical and biomarker associations for mortality in hospitalized COVID-19 patients enriched for African Americans. *BMC Infect. Dis.* 22:552. doi: 10.1186/s12879-022-07520-1

Azaiz, M. B., Jemaa, A. B., Sellami, W., Romdhani, C., Ouslati, R., Gharsallah, H., et al. (2022). Deciphering the balance of IL-6/IL-10 cytokines in severe to critical COVID-19 patients. *Immunobiology* 227:152236. doi: 10.1016/j.imbio.2022.152236

Azer, S. A. (2020). COVID-19: Pathophysiology, diagnosis, complications and investigational therapeutics. *New Microbes New Infect.* 37:100738. doi: 10.1016/j.nmni.2020.100738

Bahlakeh, G., Gorji, A., Soltani, H., and Ghadiri, T. (2021). MicroRNA alterations in neuropathologic cognitive disorders with an emphasis on dementia: Lessons from animal models. *J. Cell Physiol.* 236, 806–823. doi: 10.1002/jcp.29908

Bai, X., and Bian, Z. (2022). MicroRNA-21 is a versatile regulator and potential treatment target in central nervous system disorders. *Front. Mol. Neurosci.* 15:842288. doi: 10.3389/fnmol.2022.842288

Barateiro, A., Afonso, V., Santos, G., Cerqueira, J. J., Brites, D., Van Horssen, J., et al. (2016). S100B as a potential biomarker and therapeutic target in multiple sclerosis. *Mol. Neurobiol.* 53, 3976–3991. doi: 10.1007/s12035-015-9336-6

Barros-Viegas, A. T., Carmona, V., Ferreiro, E., Guedes, J., Cardoso, A. M., Cunha, P., et al. (2020). miRNA-31 improves cognition and abolishes amyloid-beta pathology by targeting APP and BACE1 in an animal model of Alzheimer's disease. *Mol. Ther. Nucleic Acids* 19, 1219–1236. doi: 10.1016/j.omtn.2020.01.010

Bautista-Becerril, B., Perez-Dimas, G., Sommerhalder-Nava, P. C., Hanono, A., Martinez-Cisneros, J. A., Zarate-Maldonado, B., et al. (2021). miRNAs, from evolutionary junk to possible prognostic markers and therapeutic targets in COVID-19. *Viruses* 14:41. doi: 10.3390/v14010041

Becker, J. H., Lin, J. J., Doernberg, M., Stone, K., Navis, A., Festa, J. R., et al. (2021). Assessment of cognitive function in patients after COVID-19 infection. *JAMA Netw. Open* 4:e2130645. doi: 10.1001/jamanetworkopen.2021.30645

Bellae Papannarao, J., Schwenke, D. O., Manning, P., and Katare, R. (2022). Upregulated miR-200c is associated with downregulation of the functional receptor for severe acute respiratory syndrome coronavirus 2 ACE2 in individuals with obesity. *Int. J. Obes. (Lond)* 46, 238–241. doi: 10.1038/s41366-021-00984-2

Bhavana, V., Thakor, P., Singh, S. B., and Mehra, N. K. (2020). COVID-19: Pathophysiology, treatment options, nanotechnology approaches, and research agenda to combating the SARS-CoV2 pandemic. *Life Sci.* 261:118336. doi: 10.1016/j.lfs.2020.118336

Bishop, P., Rocca, D., and Henley, J. M. (2016). Ubiquitin C-terminal hydrolase L1 (UCH-L1): Structure, distribution and roles in brain function and dysfunction. *Biochem. J.* 473, 2453–2462. doi: 10.1042/BCJ20160082

Blount, G. S., Coursey, L., and Kocerha, J. (2022). MicroRNA networks in cognition and dementia. *Cells* 11:1882. doi: 10.3390/cells11121882

Bogdan, S., Puscion-Jakubik, A., Klimiuk, K., Socha, K., Kochanowicz, J., and Gorodkiewicz, E. (2022). UCHL1 and proteasome in blood serum in relation to dietary habits, concentration of selected antioxidant minerals and total antioxidant status among patients with Alzheimer's disease. *J. Clin. Med.* 11:412. doi: 10.3390/jcm11020412

Boldrini, M., Canoll, P. D., and Klein, R. S. (2021). How COVID-19 Affects the Brain. *JAMA Psychiatry* 78, 682–683. doi: 10.1001/jamapsychiatry.2021.0500

Bradley, B. T., Maioli, H., Johnston, R., Chaudhry, I., Fink, S. L., Xu, H., et al. (2020). Histopathology and ultrastructural findings of fatal COVID-19 infections in Washington State: A case series. *Lancet* 396, 320–332. doi: 10.1016/S0140-6736(20)31305-2

Burak, K., Lamoureux, L., Boese, A., Majer, A., Saba, R., Niu, Y., et al. (2018). MicroRNA-16 targets mRNA involved in neurite extension and branching in hippocampal neurons during presymptomatic prion disease. *Neurobiol. Dis.* 112, 1–13. doi: 10.1016/j.nbd.2017.12.011

Burmeister, A. R., and Marriott, I. (2018). The interleukin-10 family of cytokines and their role in the CNS. *Front. Cell Neurosci.* 12:458. doi: 10.3389/fncel.2018.00458

Cabezas, R., Avila, M., Gonzalez, J., El-Bacha, R. S., Baez, E., Garcia-Segura, L. M., et al. (2014). Astrocytic modulation of blood brain barrier: Perspectives on Parkinson's disease. *Front. Cell Neurosci.* 8:211. doi: 10.3389/fncel.2014.00211

Carini, G., Musazzi, L., Bolzetta, F., Cester, A., Fiorentini, C., Ieraci, A., et al. (2021). The potential role of miRNAs in cognitive frailty. *Front. Aging Neurosci.* 13:763110. doi: 10.3389/fnagi.2021.763110

Ceban, F., Ling, S., Lui, L. M. W., Lee, Y., Gill, H., Teopiz, K. M., et al. (2022). Fatigue and cognitive impairment in Post-COVID-19 Syndrome: A systematic review and meta-analysis. *Brain Behav. Immun.* 101, 93–135. doi: 10.1016/j.bbi.2021.12.020

Chaves, M. L., Camozzato, A. L., Ferreira, E. D., Piazenski, I., Kochhann, R., Dall'igna, O., et al. (2010). Serum levels of S100B and NSE proteins in Alzheimer's disease patients. *J. Neuroinflamm.* 7:6. doi: 10.1186/1742-2094-7-6

Chen, X., Zhao, B., Qu, Y., Chen, Y., Xiong, J., Feng, Y., et al. (2020). Detectable serum severe acute respiratory syndrome coronavirus 2 viral load (RNAemia) is closely correlated with drastically elevated interleukin 6 level in critically ill patients with coronavirus disease 2019. *Clin. Infect. Dis.* 71, 1937–1942. doi: 10.1093/cid/ciaa449

Chouliaras, L., Thomas, A., Malpetti, M., Donaghy, P., Kane, J., Mak, E., et al. (2022). Differential levels of plasma biomarkers of neurodegeneration in Lewy body dementia. Alzheimer's disease, frontotemporal dementia and progressive supranuclear palsy. *J. Neurol. Neurosurg. Psychiatry* 93, 651–658. doi: 10.1136/jnnp-2021-327788

Ciancarelli, I., De Amicis, D., Di Massimo, C., Di Scanno, C., Pistarini, C., D'orazio, N., et al. (2014). Peripheral biomarkers of oxidative stress and their limited potential in evaluation of clinical features of Huntington's patients. *Biomarkers* 19, 452–456. doi: 10.3109/1354750X.2014.935955

Cione, E., Siniscalchi, A., Gangemi, P., Cosco, L., Colosimo, M., Longhini, F., et al. (2021). Neuron-specific enolase serum levels in COVID-19 are related to the severity of lung injury. *PLoS One* 16:e0251819. doi: 10.1371/journal.pone.0251819

Coleman, L. G. Jr., Zou, J., and Crews, F. T. (2017). Microglial-derived miRNA let-7 and HMGB1 contribute to ethanol-induced neurotoxicity *via* TLR7. *J. Neuroinflamm.* 14:22. doi: 10.1186/s12974-017-0799-4

Condrat, C. E., Thompson, D. C., Barbu, M. G., Bugnar, O. L., Boboc, A., Cretoiu, D., et al. (2020). miRNAs as biomarkers in disease: Latest findings regarding their role in diagnosis and prognosis. *Cells* 9:276. doi: 10.3390/cells9020276

Cooper, J., Stukas, S., Hoiland, R. L., Fergusson, N. A., Thiara, S., Foster, D., et al. (2020). Quantification of neurological blood-based biomarkers in critically Ill patients with coronavirus disease 2019. *Crit. Care Explor.* 2:e0238. doi: 10.1097/CCE.0000000000000238

Cristovao, J. S., and Gomes, C. M. (2019). S100 proteins in Alzheimer's disease. *Front. Neurosci.* 13:463. doi: 10.3389/fnins.2019.00463

Crivelli, L., Palmer, K., Calandri, I., Guekht, A., Beghi, E., Carroll, W., et al. (2022). Changes in cognitive functioning after COVID-19: A systematic review and meta-analysis. *Alzheimers Dement.* 18, 1047–1066. doi: 10.1002/alz.12644

Davis, H. E., Assaf, G. S., Mccorkell, L., Wei, H., Low, R. J., Re'em, Y., et al. (2021). Characterizing long COVID in an international cohort: 7 months of symptoms and their impact. *E Clin.Med.* 38:101019. doi: 10.1016/j.eclinm.2021.101019

De Gonzalo-Calvo, D., Benitez, I. D., Pinilla, L., Carratala, A., Moncusi-Moix, A., Gort-Paniello, C., et al. (2021). Circulating microRNA profiles predict the severity of COVID-19 in hospitalized patients. *Transl. Res.* 236, 147–159. doi: 10.1016/j.trsl.2021.05.004

De Lorenzo, R., Lore, N. I., Finardi, A., Mandelli, A., Cirillo, D. M., Tresoldi, C., et al. (2021). Blood neurofilament light chain and total tau levels at admission predict death in COVID-19 patients. *J. Neurol.* 268, 4436–4442. doi: 10.1007/s00415-021-10595-6

Denk, J., Oberhauser, F., Kornhuber, J., Wiltfang, J., Fassbender, K., Schroeter, M. L., et al. (2018). Specific serum and CSF microRNA profiles distinguish sporadic behavioural variant of frontotemporal dementia compared with Alzheimer patients and cognitively healthy controls. *PLoS One* 13:e0197329. doi: 10.1371/journal.pone.0197329

Dong, H., Li, J., Huang, L., Chen, X., Li, D., Wang, T., et al. (2015). Serum MicroRNA profiles serve as novel biomarkers for the diagnosis of Alzheimer's disease. *Dis. Markers* 2015:625659. doi: 10.1155/2015/625659

Donyavi, T., Bokharaei-Salim, F., Baghi, H. B., Khanaliha, K., Alaei Janat-Makan, M., Karimi, B., et al. (2021). Acute and post-acute phase of COVID-19: Analyzing expression patterns of miRNA-29a-3p, 146a-3p, 155-5p, and let-7b-3p in PBMC. *Int. Immunopharmacol.* 97:107641. doi: 10.1016/j.intimp.2021.107641

Ebenau, J. L., Pelkmans, W., Verberk, I. M. W., Verfaillie, S. C. J., Van Den Bosch, K. A., Van Leeuwenstijn, M., et al. (2022). Association of CSF, plasma, and imaging markers of neurodegeneration with clinical progression in people with subjective cognitive decline. *Neurology* 98, e1315–e1326. doi: 10.1212/WNL.0000000000200035

Elahi, F. M., Casaletto, K. B., La Joie, R., Walters, S. M., Harvey, D., Wolf, A., et al. (2020). Plasma biomarkers of astrocytic and neuronal dysfunction in early- and late-onset Alzheimer's disease. *Alzheimers Dement.* 16, 681–695. doi: 10.1016/j.jalz.2019.09.004

Ellul, M. A., Benjamin, L., Singh, B., Lant, S., Michael, B. D., Easton, A., et al. (2020). Neurological associations of COVID-19. *Lancet Neurol.* 19, 767–783. doi: 10.1016/S1474-4422(20)30221-0

Eng, L. F., Ghirnikar, R. S., and Lee, Y. L. (2000). Glial fibrillary acidic protein: GFAP-thirty-one years (1969-2000). *Neurochem. Res.* 25, 1439–1451. doi: 10.1023/A:1007677003387

Fan, W., Liang, C., Ou, M., Zou, T., Sun, F., Zhou, H., et al. (2020). MicroRNA-146a is a wide-reaching neuroinflammatory regulator and potential treatment target in neurological diseases. *Front. Mol. Neurosci.* 13:90. doi: 10.3389/fnmol.2020.00090

Farr, R. J., Rootes, C. L., Rowntree, L. C., Nguyen, T. H. O., Hensen, L., Kedzierski, L., et al. (2021). Altered microRNA expression in COVID-19 patients enables identification of SARS-CoV-2 infection. *PLoS Pathog.* 17:e1009759. doi: 10.1371/journal.ppat.1009759

Feng, M. G., Liu, C. F., Chen, L., Feng, W. B., Liu, M., Hai, H., et al. (2018). MiR-21 attenuates apoptosis-triggered by amyloid-beta *via* modulating PDCD4/PI3K/AKT/GSK-3beta pathway in SH-SY5Y cells. *Biomed. Pharmacother.* 101, 1003–1007. doi: 10.1016/j.biopha.2018.02.043

Ferrando, S. J., Dornbush, R., Lynch, S., Shahar, S., Klepacz, L., Karmen, C. L., et al. (2022). Neuropsychological, medical, and psychiatric findings after recovery from acute COVID-19: A cross-sectional study. *J. Acad. Consult Liaison Psychiatry* 63, 474–484. doi: 10.1016/j.jaclp.2022.01.003

Freeman, E. E., Mcmahon, D. E., Lipoff, J. B., Rosenbach, M., Kovarik, C., Desai, S. R., et al. (2020). The spectrum of COVID-19-associated dermatologic manifestations: An international registry of 716 patients from 31 countries. *J. Am. Acad. Dermatol.* 83, 1118–1129. doi: 10.1016/j.jaad.2020.06.1016

Frontera, J. A., Boutajangout, A., Masurkar, A. V., Betensky, R. A., Ge, Y., Vedvyas, A., et al. (2022). Comparison of serum neurodegenerative biomarkers among hospitalized COVID-19 patients versus non-COVID subjects with normal cognition, mild cognitive impairment, or Alzheimer's dementia. *Alzheimers Dement.* 18, 899–910. doi: 10.1002/alz.12556

Gaetani, L., Blennow, K., Calabresi, P., Di Filippo, M., Parnetti, L., and Zetterberg, H. (2019). Neurofilament light chain as a biomarker in neurological disorders. *J. Neurol. Neurosurg. Psychiatry* 90, 870–881. doi: 10.1136/jnnp-2018-320106

Galliera, E., Massaccesi, L., Yu, L., He, J., Ranucci, M., and Corsi Romanelli, M. M. (2022). SCD14-ST and new generation inflammatory biomarkers in the prediction of COVID-19 outcome. *Biomolecules* 12:826. doi: 10.3390/biom12060826

Galvan-Roman, J. M., Lancho-Sanchez, A., Luquero-Bueno, S., Vega-Piris, L., Curbelo, J., Manzaneque-Pradales, M., et al. (2020). Usefulness of circulating

microRNAs miR-146a and miR-16-5p as prognostic biomarkers in community-acquired pneumonia. *PLoS One* 15:e0240926. doi: 10.1371/journal.pone.0240926

Gamez-Valero, A., Campdelacreu, J., Vilas, D., Ispierto, L., Rene, R., Alvarez, R., et al. (2019). Exploratory study on microRNA profiles from plasma-derived extracellular vesicles in Alzheimer's disease and dementia with Lewy bodies. *Transl. Neurodegener.* 8:31. doi: 10.1186/s40035-019-0169-5

Gao, X., Xiong, Y., Li, Q., Han, M., Shan, D., Yang, G., et al. (2020). Extracellular vesicle-mediated transfer of miR-21-5p from mesenchymal stromal cells to neurons alleviates early brain injury to improve cognitive function *via* the PTEN/Akt pathway after subarachnoid hemorrhage. *Cell Death Dis.* 11:363. doi: 10.1038/s41419-020-2530-0

Garcia, J. M., Stillings, S. A., Leclerc, J. L., Phillips, H., Edwards, N. J., Robicsek, S. A., et al. (2017). Role of interleukin-10 in acute brain injuries. *Front. Neurol.* 8:244. doi: 10.3389/fneur.2017.00244

Graham, E. L., Clark, J. R., Orban, Z. S., Lim, P. H., Szymanski, A. L., Taylor, C., et al. (2021). Persistent neurologic symptoms and cognitive dysfunction in non-hospitalized Covid-19 "long haulers". *Ann. Clin. Transl. Neurol.* 8, 1073–1085. doi: 10.1002/acn3.51350

Grinan-Ferre, C., Corpas, R., Puigoriol-Illamola, D., Palomera-Avalos, V., Sanfeliu, C., and Pallas, M. (2018). Understanding epigenetics in the neurodegeneration of Alzheimer's disease: SAMP8 mouse model. *J. Alzheimers Dis.* 62, 943–963. doi: 10.3233/JAD-170664

Guedes, J. R., Santana, I., Cunha, C., Duro, D., Almeida, M. R., Cardoso, A. M., et al. (2016). MicroRNA deregulation and chemotaxis and phagocytosis impairment in Alzheimer's disease. *Alzheimers Dement. (Amst)* 3, 7–17. doi: 10.1016/j.dadm.2015.11.004

Guo, H. J., and Tadi, P. (2022). *Biochemistry, ubiquitination*. Treasure Island (FL): StatPearls.

Guo, T., Noble, W., and Hanger, D. P. (2017). Roles of tau protein in health and disease. *Acta Neuropathol.* 133, 665–704. doi: 10.1007/s00401-017-1707-9

Gupta, K. K., Khan, M. A., and Singh, S. K. (2020b). Constitutive inflammatory cytokine storm: A major threat to human health. *J. Interferon Cytokine Res.* 40, 19–23. doi: 10.1089/jir.2019.0085

Gupta, A., Madhavan, M. V., Sehgal, K., Nair, N., Mahajan, S., Sehrawat, T. S., et al. (2020a). Extrapulmonary manifestations of COVID-19. *Nat. Med.* 26, 1017–1032. doi: 10.1038/s41591-020-0968-3

Hadad, R., Khoury, J., Stanger, C., Fisher, T., Schneer, S., Ben-Hayun, R., et al. (2022). Cognitive dysfunction following COVID-19 infection. *J. Neurovirol.* 28, 430–437. doi: 10.1007/s13365-022-01079-y

Han, H., Ma, Q., Li, C., Liu, R., Zhao, L., Wang, W., et al. (2020). Profiling serum cytokines in COVID-19 patients reveals IL-6 and IL-10 are disease severity predictors. *Emerg. Microbes Infect.* 9, 1123–1130. doi: 10.1080/22221751.2020.1770129

Hanson, B. A., Visvabharathy, L., Ali, S. T., Kang, A. K., Patel, T. R., Clark, J. R., et al. (2022). Plasma biomarkers of neuropathogenesis in hospitalized patients with COVID-19 and those with postacute sequelae of SARS-CoV-2 infection. *Neurol. Neuroimmunol. Neuroinflamm.* 9:e1151. doi: 10.1212/NXI.0000000000001151

Haque, A., Polcyn, R., Matzelle, D., and Banik, N. L. (2018). New insights into the role of neuron-specific enolase in neuro-inflammation, neurodegeneration, and neuroprotection. *Brain Sci.* 8:33. doi: 10.3390/brainsci8020033

Haroun, R. A., Osman, W. H., Amin, R. E., Hassan, A. K., Abo-Shanab, W. S., and Eessa, A. M. (2022). Circulating plasma miR-155 is a potential biomarker for the detection of SARS-CoV-2 infection. *Pathology* 54, 104–110. doi: 10.1016/j.pathol.2021.09.006

Harrison, A. G., Lin, T., and Wang, P. (2020). Mechanisms of SARS-CoV-2 transmission and pathogenesis. *Trends Immunol.* 41, 1100–1115. doi: 10.1016/j.it.2020.10.004

Hebert, S. S., Sergeant, N., and Buee, L. (2012). MicroRNAs and the regulation of tau metabolism. *Int. J. Alzheimers Dis.* 2012:406561. doi: 10.1155/2012/406561

Heimfarth, L., Passos, F. R. S., Monteiro, B. S., Araujo, A.A.S, Quintans Junior, L. J., and Quintans, J. S. S. (2022). Serum glial fibrillary acidic protein is a body fluid biomarker: A valuable prognostic for neurological disease–A systematic review. *Int. Immunopharmacol.* 107:108624. doi: 10.1016/j.intimp.2022.108624

Henry, R. J., Doran, S. J., Barrett, J. P., Meadows, V. E., Sabirzhanov, B., Stoica, B. A., et al. (2019). Inhibition of miR-155 limits neuroinflammation and improves functional recovery after experimental traumatic brain injury in mice. *Neurotherapeutics* 16, 216–230. doi: 10.1007/s13311-018-0665-9

Hirzel, C., Grandgirard, D., Surial, B., Wider, M. F., Leppert, D., Kuhle, J., et al. (2022). Neuro-axonal injury in COVID-19: The role of systemic inflammation and SARS-CoV-2 specific immune response. *Ther. Adv. Neurol. Disord.* 15:17562864221080528. doi: 10.1177/17562864221080528

Hol, E. M., and Capetanaki, Y. (2017). Type III intermediate filaments desmin, glial fibrillary acidic protein (GFAP), vimentin, and peripherin. *Cold Spring Harb. Perspect. Biol.* 9:a021642. doi: 10.1101/cshperspect.a021642

Hosp, J. A., Dressing, A., Blazhenets, G., Bormann, T., Rau, A., Schwabenland, M., et al. (2021). Cognitive impairment and altered cerebral glucose metabolism in the subacute stage of COVID-19. *Brain* 144, 1263–1276. doi: 10.1093/brain/awab009

Huang, Y., Liu, Y., Huang, J., Gao, L., Wu, Z., Wang, L., et al. (2021b). Let7b5p promotes cell apoptosis in Parkinson's disease by targeting HMGA2. *Mol. Med. Rep.* 24:820. doi: 10.3892/mmr.2021.12461

Huang, C., Huang, L., Wang, Y., Li, X., Ren, L., Gu, X., et al. (2021a). 6-month consequences of COVID-19 in patients discharged from hospital: A cohort study. *Lancet* 397, 220–232. doi: 10.1016/S0140-6736(20)32656-8

Huang, C., Wang, Y., Li, X., Ren, L., Zhao, J., Hu, Y., et al. (2020). Clinical features of patients infected with 2019 novel coronavirus in Wuhan. *China Lancet* 395, 497–506. doi: 10.1016/S0140-6736(20)30183-5

Hugon, J., Msika, E. F., Queneau, M., Farid, K., and Paquet, C. (2022). Long COVID: Cognitive complaints (brain fog) and dysfunction of the cingulate cortex. *J. Neurol.* 269, 44–46. doi: 10.1007/s00415-021-10655-x

Hui, D. S., I Azhar, E., Madani, T. A., Ntoumi, F., Kock, R., Dar, O., et al. (2020). The continuing 2019-nCoV epidemic threat of novel coronaviruses to global health–The latest 2019 novel coronavirus outbreak in Wuhan, China. *Int. J. Infect. Dis.* 91, 264–266. doi: 10.1016/j.ijid.2020.01.009

Iodice, F., Cassano, V., and Rossini, P. M. (2021). Direct and indirect neurological, cognitive, and behavioral effects of COVID-19 on the healthy elderly, mild-cognitive-impairment, and Alzheimer's disease populations. *Neurol. Sci.* 42, 455–465. doi: 10.1007/s10072-020-04902-8

Islam, H., Chamberlain, T. C., Mui, A. L., and Little, J. P. (2021a). Elevated interleukin-10 Levels in COVID-19: Potentiation of pro-inflammatory responses or impaired anti-inflammatory action? *Front. Immunol.* 12:677008. doi: 10.3389/fimmu.2021.677008

Islam, M. B., Chowdhury, U. N., Nain, Z., Uddin, S., Ahmed, M. B., and Moni, M. A. (2021b). Identifying molecular insight of synergistic complexities for SARS-CoV-2 infection with pre-existing type 2 diabetes. *Comput. Biol. Med.* 136:104668. doi: 10.1016/j.compbiomed.2021.104668

Islam, M. R., Kaurani, L., Berulava, T., Heilbronner, U., Budde, M., Centeno, T. P., et al. (2021c). A microRNA signature that correlates with cognition and is a target against cognitive decline. *EMBO Mol. Med.* 13:e13659. doi: 10.15252/emmm.202013659

Jafrin, S., Aziz, M. A., and Islam, M. S. (2022). Elevated levels of pleiotropic interleukin-6 (IL-6) and interleukin-10 (IL-10) are critically involved with the severity and mortality of COVID-19: An updated longitudinal meta-analysis and systematic review on 147 studies. *Biomark. Insights* 17:11772719221106600. doi: 10.1177/11772719221106600

Johansson, A., Mohamed, M. S., Moulin, T. C., and Schioth, H. B. (2021). Neurological manifestations of COVID-19: A comprehensive literature review and discussion of mechanisms. *J. Neuroimmunol.* 358:577658. doi: 10.1016/j.jneuroim.2021.577658

Kanberg, N., Ashton, N. J., Andersson, L. M., Yilmaz, A., Lindh, M., Nilsson, S., et al. (2020). Neurochemical evidence of astrocytic and neuronal injury commonly found in COVID-19. *Neurology* 95, e1754–e1759. doi: 10.1212/WNL.0000000000010111

Kanberg, N., Simren, J., Eden, A., Andersson, L. M., Nilsson, S., Ashton, N. J., et al. (2021). Neurochemical signs of astrocytic and neuronal injury in acute COVID-19 normalizes during long-term follow-up. *EBioMedicine* 70:103512. doi: 10.1016/j.ebiom.2021.103512

Keikha, R., and Jebali, A. (2021). [The miRNA neuroinflammatory biomarkers in COVID-19 patients with different severity of illness]. *Neurologia (Engl Ed).* doi: 10.1016/j.nrl.2021.06.005 [Epub ahead of print].

Keikha, R., Hashemi-Shahri, S. M., and Jebali, A. (2021). The relative expression of miR-31, miR-29, miR-126, and miR-17 and their mRNA targets in the serum of COVID-19 patients with different grades during hospitalization. *Eur. J. Med. Res.* 26:75. doi: 10.1186/s40001-021-00544-4

Kenny, A., Mcardle, H., Calero, M., Rabano, A., Madden, S. F., Adamson, K., et al. (2019). Elevated plasma microRNA-206 levels predict cognitive decline and progression to dementia from mild cognitive impairment. *Biomolecules* 9:734. doi: 10.3390/biom9110734

Kent, S. A., Spires-Jones, T. L., and Durrant, C. S. (2020). The physiological roles of tau and Abeta: Implications for Alzheimer's disease pathology and therapeutics. *Acta Neuropathol.* 140, 417–447. doi: 10.1007/s00401-020-02196-w

Kim, H., Lee, E. J., Lim, Y. M., and Kim, K. K. (2022). Glial fibrillary acidic protein in blood as a disease biomarker of neuromyelitis optica spectrum disorders. *Front. Neurol.* 13:865730. doi: 10.3389/fneur.2022.865730

Kim, W. R., Park, E. G., Kang, K. W., Lee, S. M., Kim, B., and Kim, H. S. (2020). Expression analyses of MicroRNAs in hamster lung tissues infected by SARS-CoV-2. *Mol. Cells* 43, 953–963. doi: 10.14348/molcells.2020.0177

Kivisakk, P., Magdamo, C., Trombetta, B. A., Noori, A., Kuo, Y. K. E., Chibnik, L. B., et al. (2022). Plasma biomarkers for prognosis of cognitive decline in patients with mild cognitive impairment. *Brain Commun.* 4:fcac155. doi: 10.1093/braincomms/fcac155

Klyucherev, T. O., Olszewski, P., Shalimova, A. A., Chubarev, V. N., Tarasov, V. V., Attwood, M. M., et al. (2022). Advances in the development of new biomarkers for Alzheimer's disease. *Transl. Neurodegener.* 11:25. doi: 10.1186/s40035-022-00296-z

Kong, H., Yin, F., He, F., Omran, A., Li, L., Wu, T., et al. (2015). The effect of miR-132, miR-146a, and miR-155 on MRP8/TLR4-induced astrocyte-related inflammation. *J Mol Neurosci* 57, 28–37. doi: 10.1007/s12031-015-0574-x

Kudose, S., Batal, I., Santoriello, D., Xu, K., Barasch, J., Peleg, Y., et al. (2020). Kidney biopsy findings in patients with COVID-19. *J. Am. Soc. Nephrol.* 31, 1959–1968. doi: 10.1681/ASN.2020060802

Kumar, S., and Reddy, P. H. (2016). Are circulating microRNAs peripheral biomarkers for Alzheimer's disease? *Biochim. Biophys. Acta* 1862, 1617–1627. doi: 10.1016/j.bbadis.2016.06.001

Lakhani, H. V., Pillai, S. S., Zehra, M., Dao, B., Tirona, M. T., Thompson, E., et al. (2021). Detecting early onset of anthracyclines-induced cardiotoxicity using a novel panel of biomarkers in West-Virginian population with breast cancer. *Sci. Rep.* 11:7954. doi: 10.1038/s41598-021-87209-8

Lam, V., Albrecht, M. A., Takechi, R., Giles, C., James, A. P., Foster, J. K., et al. (2013). The serum concentration of the calcium binding protein S100B is positively associated with cognitive performance in older adults. *Front. Aging Neurosci.* 5:61. doi: 10.3389/fnagi.2013.00061

Lantero Rodriguez, J., Karikari, T. K., Suarez-Calvet, M., Troakes, C., King, A., Emersic, A., et al. (2020). Plasma p-tau181 accurately predicts Alzheimer's disease pathology at least 8 years prior to post-mortem and improves the clinical characterisation of cognitive decline. *Acta Neuropathol.* 140, 267–278. doi: 10.1007/s00401-020-02195-x

Lavillegrand, J. R., Garnier, M., Spaeth, A., Mario, N., Hariri, G., Pilon, A., et al. (2021). Elevated plasma IL-6 and CRP levels are associated with adverse clinical outcomes and death in critically ill SARS-CoV-2 patients: Inflammatory response of SARS-CoV-2 patients. *Ann. Intensive Care* 11:9. doi: 10.1186/s13613-020-00798-x

Lehmann, S. M., Kruger, C., Park, B., Derkow, K., Rosenberger, K., Baumgart, J., et al. (2012). An unconventional role for miRNA: Let-7 activates Toll-like receptor 7 and causes neurodegeneration. *Nat. Neurosci.* 15, 827–835. doi: 10.1038/nn.3113

Leidinger, P., Backes, C., Deutscher, S., Schmitt, K., Mueller, S. C., Frese, K., et al. (2013). A blood based 12-miRNA signature of Alzheimer disease patients. *Genome Biol.* 14:R78. doi: 10.1186/gb-2013-14-7-r78

Leretter, M. T., Vulcanescu, D. D., Horhat, F. G., Matichescu, A., Rivis, M., Rusu, L. C., et al. (2022). COVID-19: Main findings after a year and half of unease and the proper scientific progress (Review). *Exp. Ther. Med.* 23:424. doi: 10.3892/etm.2022.11350

Li, C., Hu, X., Li, L., and Li, J. H. (2020). Differential microRNA expression in the peripheral blood from human patients with COVID-19. *J. Clin. Lab. Anal.* 34:e23590. doi: 10.1002/jcla.23590

Li, C., Wang, R., Wu, A., Yuan, T., Song, K., Bai, Y., et al. (2022b). SARS-COV-2 as potential microRNA sponge in COVID-19 patients. *BMC Med. Genomics* 15:94. doi: 10.1186/s12920-022-01243-7

Li, C., Liu, J., Lin, J., and Shang, H. (2022a). COVID-19 and risk of neurodegenerative disorders: A mendelian randomization study. *Transl. Psychiatry* 12:283. doi: 10.1038/s41398-022-02052-3

Liang, C., Zou, T., Zhang, M., Fan, W., Zhang, T., Jiang, Y., et al. (2021). MicroRNA-146a switches microglial phenotypes to resist the pathological processes and cognitive degradation of Alzheimer's disease. *Theranostics* 11, 4103–4121. doi: 10.7150/thno.53418

Lindner, D., Fitzek, A., Brauninger, H., Aleshcheva, G., Edler, C., Meissner, K., et al. (2020). Association of cardiac infection with SARS-CoV-2 in confirmed COVID-19 autopsy cases. *JAMA Cardiol.* 5, 1281–1285. doi: 10.1001/jamacardio.2020.3551

Liu, C. Y., Yang, Y., Ju, W. N., Wang, X., and Zhang, H. L. (2018). Emerging roles of astrocytes in neuro-vascular unit and the tripartite synapse with emphasis on reactive gliosis in the context of Alzheimer's disease. *Front. Cell Neurosci.* 12:193. doi: 10.3389/fncel.2018.00193

Liu, H., Wei, P., Kappler, J. W., Marrack, P., and Zhang, G. (2022). SARS-CoV-2 variants of concern and variants of interest receptor binding domain mutations and virus infectivity. *F. Immunol.* 13:825256. doi: 10.3389/fimmu.2022.825256

Liu, P. P., Blet, A., Smyth, D., and Li, H. (2020). The science underlying COVID-19: Implications for the cardiovascular system. *Circulation* 142, 68–78. doi: 10.1161/CIRCULATIONAHA.120.047549

Liu, W., Liu, C., Zhu, J., Shu, P., Yin, B., Gong, Y., et al. (2012). MicroRNA-16 targets amyloid precursor protein to potentially modulate Alzheimer's-associated pathogenesis in SAMP8 mice. *Neurobiol. Aging* 33, 522–534. doi: 10.1016/j.neurobiolaging.2010.04.034

Lodigiani, C., Iapichino, G., Carenzo, L., Cecconi, M., Ferrazzi, P., Sebastian, T., et al. (2020). Venous and arterial thromboembolic complications in COVID-19 patients admitted to an academic hospital in Milan. *Italy. Thromb. Res.* 191, 9–14. doi: 10.1016/j.thromres.2020.04.024

Lopez-Leon, S., Wegman-Ostrosky, T., Perelman, C., Sepulveda, R., Rebolledo, P. A., Cuapio, A., et al. (2021). More than 50 Long-term effects of COVID-19: A systematic review and meta-analysis. *medRxiv* [Preprint]. doi: 10.1101/2021.01.27.21250617

Lopez-Ramirez, M. A., Wu, D., Pryce, G., Simpson, J. E., Reijerkerk, A., King-Robson, J., et al. (2014). MicroRNA-155 negatively affects blood-brain barrier function during neuroinflammation. *FASEB J.* 28, 2551–2565. doi: 10.1096/fj.13-248880

Lu, Q., Zhu, Z., Tan, C., Zhou, H., Hu, Y., Shen, G., et al. (2021). Changes of serum IL-10. IL-1beta, IL-6, MCP-1, TNF-alpha, IP-10 and IL-4 in COVID-19 patients. *Int. J. Clin. Pract.* 75:e14462. doi: 10.1111/ijcp.14462

Lu, Y., Li, J., and Hu, T. (2022). Analysis of Correlation between Serum Inflammatory Factors and Cognitive Function. Language, and Memory in Alzheimer's Disease and Its Clinical Significance. *Comput. Math. Methods Med.* 2022:2701748. doi: 10.1155/2022/2701748

Luan, Y. Y., and Yao, Y. M. (2018). The clinical significance and potential role of c-reactive protein in chronic inflammatory and neurodegenerative diseases. *Front. Immunol.* 9:1302. doi: 10.3389/fimmu.2018.01302

Ma, X., Becker Buscaglia, L. E., Barker, J. R., and Li, Y. (2011). MicroRNAs in NF-kappaB signaling. *J. Mol. Cell Biol.* 3, 159–166. doi: 10.1093/jmcb/mjr007

Mabb, A. M., and Ehlers, M. D. (2010). Ubiquitination in postsynaptic function and plasticity. *Annu. Rev. Cell Dev. Biol.* 26, 179–210. doi: 10.1146/annurev-cellbio-100109-104129

Maciak, K., Dziedzic, A., Miller, E., and Saluk-Bijak, J. (2021). miR-155 as an Important regulator of multiple sclerosis pathogenesis. A review. *Int. J. Mol. Sci.* 22:4332. doi: 10.3390/ijms22094332

Mai, H., Fan, W., Wang, Y., Cai, Y., Li, X., Chen, F., et al. (2019). Intranasal administration of miR-146a agomir rescued the pathological process and cognitive impairment in an AD mouse model. *Mol. Ther. Nucleic Acids* 18, 681–695. doi: 10.1016/j.omtn.2019.10.002

Mainous, A. G. III, Rooks, B. J., and Orlando, F. A. (2022). The impact of initial COVID-19 episode inflammation among adults on mortality within 12 months post-hospital discharge. *Front. Med. (Lausanne)* 9:891375. doi: 10.3389/fmed.2022.891375

Malik, P., Patel, U., Mehta, D., Patel, N., Kelkar, R., Akrmah, M., et al. (2021). Biomarkers and outcomes of COVID-19 hospitalisations: Systematic review and meta-analysis. *BMJ Evid. Based Med.* 26, 107–108. doi: 10.1136/bmjebm-2020-111536

Mckeever, P. M., Schneider, R., Taghdiri, F., Weichert, A., Multani, N., Brown, R. A., et al. (2018). MicroRNA expression levels are altered in the cerebrospinal fluid of patients with young-onset Alzheimer's Disease. *Mol. Neurobiol.* 55, 8826–8841. doi: 10.1007/s12035-018-1032-x

Metaxas, A., and Kempf, S. J. (2016). Neurofibrillary tangles in Alzheimer's disease: Elucidation of the molecular mechanism by immunohistochemistry and tau protein phospho-proteomics. *Neural Regen. Res.* 11, 1579–1581. doi: 10.4103/1673-5374.193234

Mete, E., Sabirli, R., Goren, T., Turkcuer, I., Kurt, O., and Koseler, A. (2021). Association Between S100b Levels and COVID-19 Pneumonia: A Case Control Study. *In. Vivo* 35, 2923–2928. doi: 10.21873/invivo.12583

Michetti, F., D'ambrosi, N., Toesca, A., Puglisi, M. A., Serrano, A., Marchese, E., et al. (2019). The S100B story: From biomarker to active factor in neural injury. *J. Neurochem.* 148, 168–187. doi: 10.1111/jnc.14574

Miller, E. (2012). Multiple sclerosis. *Adv. Exp. Med. Biol.* 724, 222–238. doi: 10.1007/978-1-4614-0653-2_17

Miners, S., Kehoe, P. G., and Love, S. (2020). Cognitive impact of COVID-19: Looking beyond the short term. *Alzheimers Res. Ther.* 12:170. doi: 10.1186/s13195-020-00744-w

Miskowiak, K. W., Fugledalen, L., Jespersen, A. E., Sattler, S. M., Podlekareva, D., Rungby, J., et al. (2022). Trajectory of cognitive impairments over 1 year after COVID-19 hospitalisation: Pattern, severity, and functional implications. *Eur. Neuropsychopharmacol.* 59, 82–92. doi: 10.1016/j.euroneuro.2022.04.004

Miskowiak, K. W., Johnsen, S., Sattler, S. M., Nielsen, S., Kunalan, K., Rungby, J., et al. (2021). Cognitive impairments four months after COVID-19 hospital discharge: Pattern, severity and association with illness variables. *Eur. Neuropsychopharmacol.* 46, 39–48. doi: 10.1016/j.euroneuro.2021.03.019

Mohamed, M. S., Johansson, A., Jonsson, J., and Schioth, H. B. (2022). Dissecting the molecular mechanisms surrounding post-COVID-19 syndrome and neurological features. *Int. J. Mol. Sci.* 23:4275. doi: 10.3390/ijms23084275

Mondello, S., Sorinola, A., Czeiter, E., Vamos, Z., Amrein, K., Synnot, A., et al. (2021). Blood-based protein biomarkers for the management of traumatic brain injuries in adults presenting to emergency departments with mild brain injury: A living systematic review and meta-analysis. *J. Neurotrauma.* 38, 1086–1106. doi: 10.1089/neu.2017.5182

Montazersaheb, S., Hosseiniyan Khatibi, S. M., Hejazi, M. S., Tarhriz, V., Farjami, A., Ghasemian Sorbeni, F., et al. (2022). COVID-19 infection: An overview on cytokine storm and related interventions. *Virol. J.* 19:92. doi: 10.1186/s12985-022-01814-1

Moscoso, A., Grothe, M. J., Ashton, N. J., Karikari, T. K., Rodriguez, J. L., Snellman, A., et al. (2021). Time course of phosphorylated-tau181 in blood across the Alzheimer's disease spectrum. *Brain* 144, 325–339. doi: 10.1093/brain/awaa399

Murta, V., Villarreal, A., and Ramos, A. J. (2020). Severe acute respiratory syndrome coronavirus 2 impact on the central nervous system: Are astrocytes and microglia main players or merely bystanders? *ASN Neuro* 12:1759091420954960. doi: 10.1177/1759091420954960

Nain, Z., Rana, H. K., Lio, P., Islam, S. M. S., Summers, M. A., and Moni, M. A. (2021). Pathogenetic profiling of COVID-19 and SARS-like viruses. *Brief. Bioinform.* 22, 1175–1196. doi: 10.1093/bib/bbaa173

Nakano, M., Kubota, K., Kobayashi, E., Chikenji, T. S., Saito, Y., Konari, N., et al. (2020b). Bone marrow-derived mesenchymal stem cells improve cognitive impairment in an Alzheimer's disease model by increasing the expression of microRNA-146a in hippocampus. *Sci. Rep.* 10:10772. doi: 10.1038/s41598-020-67460-1

Nakano, M., Kubota, K., Hashizume, S., Kobayashi, E., Chikenji, T. S., Saito, Y., et al. (2020a). An enriched environment prevents cognitive impairment in an Alzheimer's disease model by enhancing the secretion of exosomal microRNA-146a from the choroid plexus. *Brain Behav. Immun. Health* 9:100149. doi: 10.1016/j.bbih.2020.100149

Nalbandian, A., Sehgal, K., Gupta, A., Madhavan, M. V., Mcgroder, C., Stevens, J. S., et al. (2021). Post-acute COVID-19 syndrome. *Nat. Med.* 27, 601–615. doi: 10.1038/s41591-021-01283-z

Nersisyan, S., Engibaryan, N., Gorbonos, A., Kirdey, K., Makhonin, A., and Tonevitsky, A. (2020). Potential role of cellular miRNAs in coronavirus-host interplay. *PeerJ* 8:e9994. doi: 10.7717/peerj.9994

Newcombe, V. F. J., Ashton, N. J., Posti, J. P., Glocker, B., Manktelow, A., Chatfield, D. A., et al. (2022). Post-acute blood biomarkers and disease progression in traumatic brain injury. *Brain* 145, 2064–2076. doi: 10.1093/brain/awac126

Ng, A. S. L., Tan, Y. J., Lu, Z., Ng, E. Y., Ng, S. Y. E., Chia, N. S. Y., et al. (2020). Plasma ubiquitin C-terminal hydrolase L1 levels reflect disease stage and motor severity in Parkinson's disease. *Aging (Albany NY)* 12, 1488–1495. doi: 10.18632/aging.102695

Palermo, G., Mazzucchi, S., Della Vecchia, A., Siciliano, G., Bonuccelli, U., Azuar, C., et al. (2020). Different clinical contexts of use of blood neurofilament light chain protein in the spectrum of neurodegenerative diseases. *Mol. Neurobiol.* 57, 4667–4691. doi: 10.1007/s12035-020-02035-9

Pang, Y., Lin, W., Zhan, L., Zhang, J., Zhang, S., Jin, H., et al. (2022). Inhibiting autophagy pathway of PI3K/AKT/mTOR promotes apoptosis in SK-N-SH cell model of Alzheimer's Disease. *J. Healthc. Eng.* 2022:6069682. doi: 10.1155/2022/6069682

Parasher, A. (2021). COVID-19: Current understanding of its Pathophysiology. Clinical presentation and Treatment. *Postgrad, Med. J.* 97, 312–320. doi: 10.1136/postgradmedj-2020-138577

Parsi, S., Smith, P. Y., Goupil, C., Dorval, V., and Hebert, S. S. (2015). Preclinical evaluation of miR-15/107 family members as multifactorial drug targets for Alzheimer's disease. *Mol. Ther. Nucleic Acids* 4:e256. doi: 10.1038/mtna.2015.33

Paybast, S., Emami, A., Koosha, M., and Baghalha, F. (2020). Novel coronavirus disease (COVID-19) and central nervous system complications: What neurologist need to know. *Acta Neurol. Taiwan.* 29, 24–31.

Pearn, M. L., Schilling, J. M., Jian, M., Egawa, J., Wu, C., Mandyam, C. D., et al. (2018). Inhibition of RhoA reduces propofol-mediated growth cone collapse, axonal transport impairment, loss of synaptic connectivity, and behavioural deficits. *Br. J. Anaesth.* 120, 745–760. doi: 10.1016/j.bja.2017.12.033

Pekny, M., and Pekna, M. (2014). Astrocyte reactivity and reactive astrogliosis: Costs and benefits. *Physiol. Rev.* 94, 1077–1098. doi: 10.1152/physrev.00041.2013

Peluso, M. J., Sans, H. M., Forman, C. A., Nylander, A. N., Ho, H. E., Lu, S., et al. (2022). Plasma markers of neurologic injury and inflammation in people with self-reported neurologic postacute sequelae of SARS-CoV-2 infection. *Neurol. Neuroimmunol. Neuroinflamm.* 9:e200003. doi: 10.1212/NXI.0000000000200003

Perdoncin, M., Konrad, A., Wyner, J. R., Lohana, S., Pillai, S. S., Pereira, D. G., et al. (2021). A review of miRNAs as biomarkers and effect of dietary modulation in obesity associated cognitive decline and neurodegenerative disorders. *Front. Mol. Neurosci.* 14:756499. doi: 10.3389/fnmol.2021.756499

PHOSP-COVID Collaborative Group (2022). Clinical characteristics with inflammation profiling of long COVID and association with 1-year recovery following hospitalisation in the UK: A prospective observational study. *Lancet Respir. Med.* 10, 761–775.

Pillai, S. S., Lakhani, H. V., Zehra, M., Wang, J., Dilip, A., Puri, N., et al. (2020). Predicting nonalcoholic fatty liver disease through a panel of plasma biomarkers and MicroRNAs in female west virginia population. *Int. J. Mol. Sci.* 21:6698. doi: 10.3390/ijms21186698

Pinacchio, C., Scordio, M., Santinelli, L., Frasca, F., Sorrentino, L., Bitossi, C., et al. (2022). Analysis of serum microRNAs and rs2910164 GC single-nucleotide polymorphism of miRNA-146a in COVID-19 patients. *J. Immunoassay Immunochem.* 43, 347–364. doi: 10.1080/15321819.2022.2035394

Polcyn, R., Capone, M., Hossain, A., Matzelle, D., Banik, N. L., and Haque, A. (2017). Neuron specific enolase is a potential target for regulating neuronal cell survival and death: Implications in neurodegeneration and regeneration. *Neuroimmunol. Neuroinflamm.* 4, 254–257. doi: 10.20517/2347-8659.2017.59

Prudencio, M., Erben, Y., Marquez, C. P., Jansen-West, K. R., Franco-Mesa, C., Heckman, M. G., et al. (2021). Serum neurofilament light protein correlates with unfavorable clinical outcomes in hospitalized patients with COVID-19. *Sci. Transl. Med.* 13:eabi7643. doi: 10.1126/scitranslmed.abi7643

Puntmann, V. O., Carerj, M. L., Wieters, I., Fahim, M., Arendt, C., Hoffmann, J., et al. (2020). Outcomes of cardiovascular magnetic resonance imaging in patients recently recovered from coronavirus disease 2019 (COVID-19). *JAMA Cardiol.* 5, 1265–1273. doi: 10.1001/jamacardio.2020.3557

Qian, H., Shang, Q., Liang, M., Gao, B., Xiao, J., Wang, J., et al. (2021). MicroRNA-31-3p/RhoA signaling in the dorsal hippocampus modulates methamphetamine-induced conditioned place preference in mice. *Psychopharmacology (Berl)* 238, 3207–3219. doi: 10.1007/s00213-021-05936-2

Qin, L., Zou, J., Barnett, A., Vetreno, R. P., Crews, F. T., and Coleman, L. G. Jr. (2021). TRAIL mediates neuronal death in AUD: A link between neuroinflammation and neurodegeneration. *Int. J. Mol. Sci.* 22:2547. doi: 10.3390/ijms22052547

Rahman, M. R., Islam, T., Zaman, T., Shahjaman, M., Karim, M. R., Huq, F., et al. (2020). Identification of molecular signatures and pathways to identify novel therapeutic targets in Alzheimer's disease: Insights from a systems biomedicine perspective. *Genomics* 112, 1290–1299. doi: 10.1016/j.ygeno.2019.07.018

Rajan, K. B., Aggarwal, N. T., Mcaninch, E. A., Weuve, J., Barnes, L. L., Wilson, R. S., et al. (2020). Remote blood biomarkers of longitudinal cognitive outcomes in a population study. *Ann. Neurol.* 88, 1065–1076. doi: 10.1002/ana.25874

Rizzo, P., Vieceli Dalla Sega, F., Fortini, F., Marracino, L., Rapezzi, C., and Ferrari, R. (2020). COVID-19 in the heart and the lungs: Could we "Notch" the inflammatory storm? *Basic Res. Cardiol.* 115:31. doi: 10.1007/s00395-020-0791-5

Roganovic, J. (2021). Downregulation of microRNA-146a in diabetes, obesity and hypertension may contribute to severe COVID-19. *Med. Hypotheses* 146:110448. doi: 10.1016/j.mehy.2020.110448

Saba, R., Sorensen, D. L., and Booth, S. A. (2014). MicroRNA-146a: A Dominant. Negative regulator of the innate immune response. *Front. Immunol.* 5:578. doi: 10.3389/fimmu.2014.00578

Sabbatinelli, J., Giuliani, A., Matacchione, G., Latini, S., Laprovitera, N., Pomponio, G., et al. (2021). Decreased serum levels of the inflammaging marker miR-146a are associated with clinical non-response to tocilizumab in COVID-19 patients. *Mech. Ageing Dev.* 193:111413. doi: 10.1016/j.mad.2020.111413

Sahin, B. E., Celikbilek, A., Kocak, Y., Saltoglu, G. T., Konar, N. M., and Hizmali, L. (2022). Plasma biomarkers of brain injury in COVID-19 patients with neurological symptoms. *J. Neurol. Sci.* 439:120324. doi: 10.1016/j.jns.2022.120324

Sanchez-Molina, P., Almolda, B., Gimenez-Llort, L., Gonzalez, B., and Castellano, B. (2022). Chronic IL-10 overproduction disrupts microglia-neuron dialogue similar to aging, resulting in impaired hippocampal neurogenesis and spatial memory. *Brain Behav. Immun.* 101, 231–245. doi: 10.1016/j.bbi.2021.12.026

Savarraj, J., Park, E. S., Colpo, G. D., Hinds, S. N., Morales, D., Ahnstedt, H., et al. (2021). Brain injury, endothelial injury and inflammatory markers are elevated and express sex-specific alterations after COVID-19. *J. Neuroinflamm.* 18:277. doi: 10.1186/s12974-021-02323-8

Schultheiss, C., Willscher, E., Paschold, L., Gottschick, C., Klee, B., Henkes, S. S., et al. (2022). The IL-1beta. IL-6, and TNF cytokine triad is associated with post-acute sequelae of COVID-19. *Cell Rep. Med.* 3:100663. doi: 10.1016/j.xcrm.2022.100663

Sedaghat, F., and Notopoulos, A. (2008). S100 protein family and its application in clinical practice. *Hippokratia* 12, 198–204.

Serrano, A., Donno, C., Giannetti, S., Peric, M., Andjus, P., D'ambrosi, N., et al. (2017). The Astrocytic S100B protein with its receptor rage is aberrantly expressed in SOD1(G93A) models, and its inhibition decreases the expression of proinflammatory genes. *Mediators Inflamm.* 2017:1626204. doi: 10.1155/2017/1626204

Seyedalinaghi, S., Afsahi, A. M., Mohssenipour, M., Behnezhad, F., Salehi, M. A., Barzegary, A., et al. (2021). Late complications of COVID-19; a systematic review of current evidence. *Arch. Acad. Emerg. Med.* 9:e14. doi: 10.5501/wjv.v9.i5.79

Shen, W. B., Logue, J., Yang, P., Baracco, L., Elahi, M., Reece, E. A., et al. (2022). SARS-CoV-2 invades cognitive centers of the brain and induces Alzheimer's-like neuropathology. *bioRxiv* [Preprint]. doi: 10.1101/2022.01.31.478476

Smirnov, D. S., Ashton, N. J., Blennow, K., Zetterberg, H., Simren, J., Lantero-Rodriguez, J., et al. (2022). Plasma biomarkers for Alzheimer's Disease in relation to neuropathology and cognitive change. *Acta Neuropathol.* 143, 487–503. doi: 10.1007/s00401-022-02408-5

Solfrizzi, V., D'introno, A., Colacicco, A. M., Capurso, C., Todarello, O., Pellicani, V., et al. (2006). Circulating biomarkers of cognitive decline and dementia. *Clin. Chim. Acta* 364, 91–112. doi: 10.1016/j.cca.2005.06.015

Song, J., and Lee, J. E. (2015). miR-155 is involved in Alzheimer's disease by regulating T lymphocyte function. *Front. Aging Neurosci.* 7:61. doi: 10.3389/fnagi.2015.00061

Steiner, J., Bernstein, H. G., Bielau, H., Berndt, A., Brisch, R., Mawrin, C., et al. (2007). Evidence for a wide extra-astrocytic distribution of S100B in human brain. *BMC Neurosci.* 8:2. doi: 10.1186/1471-2202-8-2

Sudhakar, M., Winfred, S. B., Meiyazhagan, G., and Venkatachalam, D. P. (2022). Mechanisms contributing to adverse outcomes of COVID-19 in obesity. *Mol. Cell Biochem.* 477, 1155–1193. doi: 10.1007/s11010-022-04356-w

Sun, B., Tang, N., Peluso, M. J., Iyer, N. S., Torres, L., Donatelli, J. L., et al. (2021). Characterization and biomarker analyses of Post-COVID-19 complications and neurological manifestations. *Cells* 10:386. doi: 10.3390/cells10020386

Suwanwongse, K., and Shabarek, N. (2021). Newly diagnosed diabetes mellitus. DKA, and COVID-19: Causality or coincidence? A report of three cases. *J. Med. Virol.* 93, 1150–1153. doi: 10.1002/jmv.26339

Swarbrick, S., Wragg, N., Ghosh, S., and Stolzing, A. (2019). Systematic review of miRNA as biomarkers in Alzheimer's Disease. *Mol. Neurobiol.* 56, 6156–6167. doi: 10.1007/s12035-019-1500-y

Szelenberger, R., Kacprzak, M., Saluk-Bijak, J., Zielinska, M., and Bijak, M. (2019). Plasma MicroRNA as a novel diagnostic. *Clin. Chim. Acta* 499, 98–107. doi: 10.1016/j.cca.2019.09.005

Takano, K., Goto, K., Motobayashi, M., Wakui, K., Kawamura, R., Yamaguchi, T., et al. (2017). Early manifestations of epileptic encephalopathy, brain atrophy, and elevation of serum neuron specific enolase in a boy with beta-propeller protein-associated neurodegeneration. *Eur. J. Med. Genet.* 60, 521–526. doi: 10.1016/j.ejmg.2017.07.008

Tang, H., Gao, Y., Li, Z., Miao, Y., Huang, Z., Liu, X., et al. (2020). The noncoding and coding transcriptional landscape of the peripheral immune response in patients with COVID-19. *Clin. Transl. Med.* 10:e200. doi: 10.1002/ctm2.200

Taquet, M., Geddes, J. R., Husain, M., Luciano, S., and Harrison, P. J. (2021). 6-month neurological and psychiatric outcomes in 236 379 survivors of COVID-19: A retrospective cohort study using electronic health records. *Lancet Psychiatry* 8, 416–427. doi: 10.1016/S2215-0366(21)00084-5

Tavares-Junior, J. W. L., De Souza, A. C. C., Borges, J. W. P., Oliveira, D. N., Siqueira-Neto, J. I., Sobreira-Neto, M. A., et al. (2022). COVID-19 associated cognitive impairment: A systematic review. *Cortex* 152, 77–97. doi: 10.1016/j.cortex.2022.04.006

Thelin, E. P., Nelson, D. W., and Bellander, B. M. (2017). A review of the clinical utility of serum S100B protein levels in the assessment of traumatic brain injury. *Acta Neurochir. (Wien)* 159, 209–225. doi: 10.1007/s00701-016-3046-3

Thijssen, E. H., Verberk, I. M. W., Kindermans, J., Abramian, A., Vanbrabant, J., Ball, A. J., et al. (2022). Differential diagnostic performance of a panel of plasma biomarkers for different types of dementia. *Alzheimers Dement. (Amst)* 14:e12285. doi: 10.1002/dad2.12285

Thounaojam, M. C., Kaushik, D. K., and Basu, A. (2013). MicroRNAs in the brain: It's regulatory role in neuroinflammation. *Mol. Neurobiol.* 47, 1034–1044. doi: 10.1007/s12035-013-8400-3

Tili, E., Mezache, L., Michaille, J. J., Amann, V., Williams, J., Vandiver, P., et al. (2018). microRNA 155 up regulation in the CNS is strongly correlated to Down's syndrome dementia. *Ann. Diagn. Pathol.* 34, 103–109. doi: 10.1016/j.anndiagpath.2018.03.006

Turk, A., Kunej, T., and Peterlin, B. (2021). MicroRNA-target interaction regulatory network in Alzheimer's disease. *J. Pers. Med.* 11:1275. doi: 10.3390/jpm11121275

Turski, W. A., Wnorowski, A., Turski, G. N., Turski, C. A., and Turski, L. (2020). AhR and IDO1 in pathogenesis of Covid-19 and the "Systemic AhR Activation Syndrome:" a translational review and therapeutic perspectives. *Restor. Neurol. Neurosci.* 38, 343–354. doi: 10.3233/RNN-201042

Van Kessel, S. A. M, Olde Hartman, T. C., Lucassen, P., and Van Jaarsveld, C. H. M. (2022). Post-acute and long-COVID-19 symptoms in patients with mild diseases: A systematic review. *Fam. Pract.* 39, 159–167. doi: 10.1093/fampra/cmab076

Varatharaj, A., Thomas, N., Ellul, M. A., Davies, N. W. S., Pollak, T. A., Tenorio, E. L., et al. (2020). Neurological and neuropsychiatric complications of COVID-19 in 153 patients: A UK-wide surveillance study. *Lancet Psychiatry* 7, 875–882. doi: 10.1016/S2215-0366(20)30287-X

Varma-Doyle, A. V., Lukiw, W. J., Zhao, Y., Lovera, J., and Devier, D. (2021). A hypothesis-generating scoping review of miRs identified in both multiple sclerosis and dementia, their protein targets, and miR signaling pathways. *J. Neurol. Sci.* 420:117202. doi: 10.1016/j.jns.2020.117202

Verde, F., Milone, I., Bulgarelli, I., Peverelli, S., Colombrita, C., Maranzano, A., et al. (2022). Serum neurofilament light chain levels in Covid-19 patients without major neurological manifestations. *J. Neurol.* 1–11. doi: 10.1007/s00415-022-11233-5 [Epub ahead of print].

Verde, F., Otto, M., and Silani, V. (2021). Neurofilament light chain as biomarker for amyotrophic lateral sclerosis and frontotemporal dementia. *Front. Neurosci.* 15:679199. doi: 10.3389/fnins.2021.679199

Vintimilla, R., Hall, J., Johnson, L., and O'bryant, S. (2019). The relationship of CRP and cognition in cognitively normal older Mexican Americans: A cross-sectional study of the HABLE cohort. *Medicine (Baltimore)* 98:e15605. doi: 10.1097/MD.0000000000015605

Wan, Z., Li, Y., Ye, H., Zi, Y., Zhang, G., and Wang, X. (2021). Plasma S100beta and neuron-specific enolase, but not neuroglobin, are associated with early cognitive dysfunction after total arch replacement surgery: A pilot study. *Medicine (Baltimore)* 100:e25446. doi: 10.1097/MD.0000000000025446

Wang, M. Y., Zhao, R., Gao, L. J., Gao, X. F., Wang, D. P., and Cao, J. M. (2020b). SARS-CoV-2: Structure. Biology, and Structure-Based Therapeutics Development. *Front. Cell Infect. Microbiol.* 10:587269. doi: 10.3389/fcimb.2020.587269

Wang, F., Kream, R. M., and Stefano, G. B. (2020a). Long-term respiratory and neurological sequelae of COVID-19. *Med. Sci. Monit.* 26:e928996. doi: 10.12659/MSM.928996

Wang, K. K., Yang, Z., Zhu, T., Shi, Y., Rubenstein, R., Tyndall, J. A., et al. (2018). An update on diagnostic and prognostic biomarkers for traumatic brain injury. *Expert. Rev. Mol. Diagn.* 18, 165–180. doi: 10.1080/14737159.2018.1428089

Wang, Q., Davis, P. B., Gurney, M. E., and Xu, R. (2021). COVID-19 and dementia: Analyses of risk, disparity, and outcomes from electronic health records in the US. *Alzheimers Dement.* 17, 1297–1306. doi: 10.1002/alz.12296

Wang, W. Y., Tan, M. S., Yu, J. T., and Tan, L. (2015). Role of pro-inflammatory cytokines released from microglia in Alzheimer's disease. *Ann. Transl. Med.* 3:136.

Wang, Y., and Mandelkow, E. (2016). Tau in physiology and pathology. *Nat. Rev. Neurosci.* 17, 5–21. doi: 10.1038/nrn.2015.1

Watanabe, Y., Kitamura, K., Nakamura, K., Sanpei, K., Wakasugi, M., Yokoseki, A., et al. (2016). Elevated C-reactive protein is associated with cognitive decline in outpatients of a general hospital: The project in sado for total health (PROST). *Dement. Geriatr. Cogn. Dis. Extra* 6, 10–19. doi: 10.1159/000442585

Wei, X., Su, J., Yang, K., Wei, J., Wan, H., Cao, X., et al. (2020). Elevations of serum cancer biomarkers correlate with severity of COVID-19. *J. Med. Virol.* 92, 2036–2041. doi: 10.1002/jmv.25957

Wu, D., Cerutti, C., Lopez-Ramirez, M. A., Pryce, G., King-Robson, J., Simpson, J. E., et al. (2015). Brain endothelial miR-146a negatively modulates T-cell adhesion through repressing multiple targets to inhibit NF-kappaB activation. *J. Cereb. Blood Flow Metab.* 35, 412–423. doi: 10.1038/jcbfm.2014.207

Wu, J. T., Leung, K., and Leung, G. M. (2020a). Nowcasting and forecasting the potential domestic and international spread of the 2019-nCoV outbreak originating in Wuhan, China: A modelling study. *Lancet* 395, 689–697. doi: 10.1016/S0140-6736(20)30260-9

Wu, Y., Xu, X., Chen, Z., Duan, J., Hashimoto, K., Yang, L., et al. (2020b). Nervous system involvement after infection with COVID-19 and other coronaviruses. *Brain Behav. Immun.* 87, 18–22. doi: 10.1016/j.bbi.2020.03.031

Xin, Y., Zhang, L., Hu, J., Gao, H., and Zhang, B. (2021). Correlation of early cognitive dysfunction with inflammatory factors and metabolic indicators in patients with Alzheimer's disease. *Am. J. Transl. Res.* 13, 9208–9215. doi: 10.3389/fneur.2022.944205

Xu, Y., Li, X., Zhu, B., Liang, H., Fang, C., Gong, Y., et al. (2020). Characteristics of pediatric SARS-CoV-2 infection and potential evidence for persistent fecal viral shedding. *Nat. Med.* 26, 502–505. doi: 10.1038/s41591-020-0817-4

Yan, J. H., Hua, P., Chen, Y., Li, L. T., Yu, C. Y., Yan, L., et al. (2020). Identification of microRNAs for the early diagnosis of Parkinson's disease and multiple system atrophy. *J. Integr. Neurosci.* 19, 429–436. doi: 10.31083/j.jin.2020.03.163

Yao, H., Song, Y., Chen, Y., Wu, N., Xu, J., Sun, C., et al. (2020). Molecular architecture of the SARS-CoV-2 Virus. *Cell* 183, 730–738e713. doi: 10.1016/j.cell.2020.09.018

Yuan, A., Rao, M. V., Veeranna, and Nixon, R. A. (2017). Neurofilaments and neurofilament proteins in health and disease. *Cold Spring Harb. Perspect. Biol.* 9:a018309. doi: 10.1101/cshperspect.a018309

Yuen, S. C., Liang, X., Zhu, H., Jia, Y., and Leung, S. W. (2021). Prediction of differentially expressed microRNAs in blood as potential biomarkers for Alzheimer's disease by meta-analysis and adaptive boosting ensemble learning. *Alzheimers Res. Ther.* 13:126. doi: 10.1186/s13195-021-00862-z

Zanella, I., Blasco, H., Filosto, M., and Biasiotto, G. (2022). Editorial: The impact of neurofilament light chain (NFL) quantification in serum and cerebrospinal fluid in neurodegenerative diseases. *Front. Neurosci.* 16:915115. doi: 10.3389/fnins.2022.915115

Zeitlberger, A. M., Thomas-Black, G., Garcia-Moreno, H., Foiani, M., Heslegrave, A. J., Zetterberg, H., et al. (2018). Plasma markers of neurodegeneration are raised in friedreich's ataxia. *Front. Cell Neurosci.* 12:366. doi: 10.3389/fncel.2018.00366

Zeng, N., Zhao, Y. M., Yan, W., Li, C., Lu, Q. D., Liu, L., et al. (2022). A systematic review and meta-analysis of long term physical and mental sequelae of COVID-19 pandemic: Call for research priority and action. *Mol. Psychiatry* 1–11. doi: 10.1038/s41380-022-01614-7 [Epub ahead of print].

Zhang, B., Chen, C. F., Wang, A. H., and Lin, Q. F. (2015). MiR-16 regulates cell death in Alzheimer's disease by targeting amyloid precursor protein. *Eur. Rev. Med. Pharmacol. Sci.* 19, 4020–4027.

Zhang, L., Dong, L. Y., Li, Y. J., Hong, Z., and Wei, W. S. (2012). miR-21 represses FasL in microglia and protects against microglia-mediated neuronal cell death following hypoxia/ischemia. *Glia* 60, 1888–1895. doi: 10.1002/glia.22404

Zhang, M., Chen, M. Y., Wang, S. L., Ding, X. M., Yang, R., Li, J., et al. (2022a). Association of Ubiquitin C-Terminal Hydrolase-L1 (Uch-L1) serum levels with cognition and brain energy metabolism. *Eur. Rev. Med. Pharmacol. Sci.* 26, 3656–3663.

Zhang, Y., Chen, X., Jia, L., and Zhang, Y. (2022b). Potential mechanism of SARS-CoV-2-associated central and peripheral nervous system impairment. *Acta Neurol. Scand.* 146, 225–236. doi: 10.1111/ane.13657

Zhou, Z., Kang, H., Li, S., and Zhao, X. (2020b). Understanding the neurotropic characteristics of SARS-CoV-2: From neurological manifestations of COVID-19 to potential neurotropic mechanisms. *J. Neurol.* 267, 2179–2184. doi: 10.1007/s00415-020-09929-7

Zhou, H., Lu, S., Chen, J., Wei, N., Wang, D., Lyu, H., et al. (2020a). The landscape of cognitive function in recovered COVID-19 patients. *J. Psychiatr. Res.* 129, 98–102. doi: 10.1016/j.jpsychires.2020.06.022

Zingale, V. D., Gugliandolo, A., and Mazzon, E. (2021). MiR-155: An Important Regulator of Neuroinflammation. *Int. J. Mol. Sci.* 23:90. doi: 10.3390/ijms23010090

frontiers | Frontiers in Neuroscience

TYPE Original Research
PUBLISHED 06 October 2022
DOI 10.3389/fnins.2022.964715

OPEN ACCESS

EDITED BY
Miriam Sklerov,
University of North Carolina at Chapel Hill, United States

REVIEWED BY
Anna Behler,
University of Ulm, Germany
Alexander Ulrich Brandt,
University of California, Irvine, United States

*CORRESPONDENCE
Bryan M. Wong
bryanm.wong@mail.utoronto.ca

†These authors have contributed equally to this work and share senior authorship

SPECIALTY SECTION
This article was submitted to Neurodegeneration, a section of the journal Frontiers in Neuroscience

RECEIVED 08 June 2022
ACCEPTED 31 August 2022
PUBLISHED 06 October 2022

CITATION
Wong BM, Hudson C, Snook E, Tayyari F, Jung H, Binns MA, Samet S, Cheng RW, Balian C, Mandelcorn ED, Margolin E, Finger E, Black SE, Tang-Wai DF, Zinman L, Tan B, Lou W, Masellis M, Abrahao A, Frank A, Beaton D, Sunderland KM, Arnott SR, ONDRI Investigators, Tartaglia MC and Hatch WV (2022) Retinal nerve fiber layer in frontotemporal lobar degeneration and amyotrophic lateral sclerosis.
Front. Neurosci. 16:964715.
doi: 10.3389/fnins.2022.964715

Retinal nerve fiber layer in frontotemporal lobar degeneration and amyotrophic lateral sclerosis

Bryan M. Wong[1,2]*, Christopher Hudson[2,3], Emily Snook[1], Faryan Tayyari[3,4], Hyejung Jung[5], Malcolm A. Binns[5,6], Saba Samet[2], Richard W. Cheng[4], Carmen Balian[3,4], Efrem D. Mandelcorn[2,4], Edward Margolin[2,4], Elizabeth Finger[7], Sandra E. Black[8,9], David F. Tang-Wai[9,10], Lorne Zinman[8,9], Brian Tan[6], Wendy Lou[5], Mario Masellis[8,9], Agessandro Abrahao[8,9], Andrew Frank[11], Derek Beaton[6], Kelly M. Sunderland[6], Stephen R. Arnott[6], ONDRI Investigators, Maria Carmela Tartaglia[9,10†] and Wendy V. Hatch[2,4†]

[1]Faculty of Medicine, University of Toronto, Toronto, ON, Canada, [2]Department of Ophthalmology and Vision Sciences, University of Toronto, Toronto, ON, Canada, [3]School of Optometry and Vision Science, University of Waterloo, Waterloo, ON, Canada, [4]Kensington Eye Institute, Toronto, ON, Canada, [5]Dalla Lana School of Public Health, University of Toronto, Toronto, ON, Canada, [6]Rotman Research Institute, Baycrest Health Sciences, Toronto, ON, Canada, [7]Department of Clinical Neurological Sciences, Western University, London, ON, Canada, [8]Department of Medicine (Neurology), Sunnybrook Health Sciences Centre, Hurvitz Brain Sciences Research Program, Sunnybrook Research Institute, University of Toronto, Toronto, ON, Canada, [9]Department of Medicine, Division of Neurology, University of Toronto, Toronto, ON, Canada, [10]Krembil Brain Institute, University Health Network Memory Clinic, Toronto, ON, Canada, [11]Bruyere Research Institute, University of Ottawa, Ottawa, ON, Canada

Purpose: Tauopathy and transactive response DNA binding protein 43 (TDP-43) proteinopathy are associated with neurodegenerative diseases. These proteinopathies are difficult to detect *in vivo*. This study examined if spectral-domain optical coherence tomography (SD-OCT) can differentiate *in vivo* the difference in peripapillary retinal nerve fibre layer (pRNFL) thickness and macular retinal thickness between participants with presumed tauopathy (progressive supranuclear palsy) and those with presumed TDP-43 proteinopathy (amyotrophic lateral sclerosis and semantic variant primary progressive aphasia).

Study design: Prospective, multi-centre, observational study.

Materials and methods: pRNFL and macular SD-OCT images were acquired in both eyes of each participant using Heidelberg Spectralis SD-OCT. Global and pRNFL thickness in 6 sectors were analyzed, as well as macular thickness in a central 1 mm diameter zone and 4 surrounding sectors. Linear mixed model methods adjusting for baseline differences between groups were used to compare the two groups with respect to pRNFL and macular thickness.

Results: A significant difference was found in mean pRNFL thickness between groups, with the TDP-43 group (n = 28 eyes) having a significantly thinner pRNFL in the temporal sector than the tauopathy group (n = 9 eyes; mean difference = 15.46 μm, SE = 6.98, p = 0.046), which was not significant after adjusting for multiple comparisons. No other significant differences were found between groups for pRNFL or macular thickness.

Conclusion: The finding that the temporal pRNFL in the TDP-43 group was on average 15.46 μm thinner could potentially have clinical significance. Future work with larger sample sizes, longitudinal studies, and at the level of retinal sublayers will help to determine the utility of SD-OCT to differentiate between these two proteinopathies.

KEYWORDS

retinal nerve fibre layer, optical coherence tomography, tauopathy, TDP-43 proteinopathy, frontotemporal lobar degeneration, amyotrophic lateral sclerosis

Introduction

Frontotemporal dementia (FTD) encompasses a heterogeneous group of clinical syndromes characterized by frontotemporal lobar degeneration (FTLD) and prominent changes in cognition, behavior and motor function. After Alzheimer's disease (AD), it is the second-most common form of dementia in people under 65 years of age (Hodges et al., 2003; Knopman and Roberts, 2011). Pathologically, FTLD is associated with two predominant proteinopathies: tauopathy and transactive response DNA-binding protein 43 (TDP-43) proteinopathy (Irwin et al., 2015). Some FTLD-related syndromes, such as progressive supranuclear palsy (PSP), are reliably associated with tauopathy (Höglinger et al., 2017; Kim et al., 2019), while semantic variant primary progressive aphasia (svPPA) is almost always associated with TDP-43 proteinopathy (Irwin et al., 2015). Additional subtypes such as behavioral variant FTD (bvFTD), non-fluent variant PPA (nfvPPA) and corticobasal syndrome (CBS) are associated with both proteinopathies (Olney et al., 2017). FTLD-tau and FTLD-TDP-43 are difficult to detect *in vivo* (Irwin et al., 2015).

Amyotrophic lateral sclerosis (ALS) is a motor neuron degenerative disorder characterized by muscle weakness and paralysis (Rojas et al., 2020). It can also be associated with cognitive and behavioral alterations. ALS is also reliably associated with TDP-43 as its main pathological mechanism (Brettschneider et al., 2013; Neumann, 2013; Masala et al., 2018). ALS and some forms of FTLD have overlapping pathology and so are considered to be on the same disease spectrum (Mackenzie and Feldman, 2005).

Spectral-domain optical coherence tomography (SD-OCT) is a clinical tool routinely used to obtain rapid, non-invasive three-dimensional scans of ocular structures including the retina and optic nerve. Since the retina and optic nerve extend from the diencephalon, they are considered parts of the central nervous system. Accordingly, the potential for SD-OCT to detect biomarkers of neurodegenerative disease has been explored (Kirbas et al., 2013; Doustar et al., 2017; Ferrari et al., 2017; Wong et al., 2019).

Although some studies have found thinning in the peripapillary retinal nerve fiber layer (pRNFL; Stemplewitz et al., 2017; Sevim et al., 2018), macula (Stemplewitz et al., 2017; Sevim et al., 2018), and macular sublayers (Kim et al., 2017, 2019; Sevim et al., 2018) in patients with FTD and its subtypes, there is no current consensus on how specifically these structures are affected. Similarly in patients with ALS, although several studies reported a thinner global (average) pRNFL compared to controls (Ringelstein et al., 2014; Mukherjee et al., 2017; Rohani et al., 2018; Rojas et al., 2020), their results differ with respect to how the macula and pRNFL sectors are affected (Roth et al., 2013; Mukherjee et al., 2017; Rohani et al., 2018; Rojas et al., 2019). Furthermore, there is a paucity of research that compares retinal biomarkers based on proteinopathy rather than clinical phenotypes.

Previous studies have emphasized the need to investigate biomarkers to help differentiate tauopathy from TDP-43 proteinopathy (Irwin et al., 2015; Kim et al., 2017). Since PSP is usually associated with tauopathy, while svPPA and ALS are associated with TDP-43 proteinopathy, in this study, pRNFL and macular thickness were used to compare patients with PSP (presumed tauopathy) to those with svPPA or ALS (presumed TDP-43 proteinopathy). Hereafter, presumed tauopathy and presumed TDP-43 proteinopathy will be referred to as tauopathy and TDP-43 proteinopathy, respectively. We hypothesize differences in pRNFL and macular thickness could

support the use of SD-OCT to differentiate between these two proteinopathies.

Materials and methods

This was an analysis of a prospective, multi-center, observational study known as the Ontario Neurodegenerative Disease Research Initiative (ONDRI; Farhan et al., 2017). Baseline characteristics of the full ONDRI cohort are summarized in a study by Sunderland and colleagues (Sunderland et al., 2022). Participants diagnosed with FTLD-related syndromes or ALS were recruited from the Toronto Western Hospital (Toronto, Canada), Sunnybrook Hospital (Toronto, Canada), Baycrest Hospital (Toronto, Canada), Parkwood Institute (London, Canada), and Élisabeth Bruyère Continuing Care (Ottawa, Canada), between 2014 and 2018. This study was approved by the Research Ethics Boards at the University Health Network, Sunnybrook Research Institute, University of Waterloo, and the University of Western Ontario. The study protocol followed the tenets of the Declaration of Helsinki and participants provided informed consent.

Inclusion and exclusion criteria

General inclusion and exclusion criteria for the ONDRI cohort were outlined by Farhan and co-workers (Farhan et al., 2017). The study included four neurodegenerative diseases (FTLD-related syndromes (PSP, svPPA, bvFTD, nfvPPA, and CBS), ALS, AD/mild cognitive impairment, Parkinson's disease) and cerebrovascular disease (Farhan et al., 2017). Exclusion criteria specific to the SD-OCT retinal imaging platform within ONDRI included poorly controlled diabetes mellitus, glaucoma or glaucoma suspect (defined as intraocular pressure (IOP) greater than 22 mmHg in either eye, IOP difference between eyes $>$ 5 mmHg, optic nerve head cup-to-disk ratio (C/D) $\geq$ 0.7, or C/D difference between eyes $>$ 0.2), and other optic neuropathies or maculopathies (such as exudative age related macular degeneration) identified on inspection of fundus photographs by an ophthalmologist (EM, EDM) masked to the participant's underlying diagnosis. SD-OCT images with a quality score of less than 20 were excluded. Upon inspection by expert observers (WVH, FT, CH, CB, RC) and consultation with ophthalmologists when necessary, SD-OCT images were excluded if macular thickness or pRNFL thickness could be affected by pathologies or structural anomalies including tilted optic disks. Participants with a history of stroke were also excluded from the analysis as potential retrograde degeneration in the retina could affect thickness measurements.

Procedure

Peripapillary RNFL and macular SD-OCT scans were acquired in both eyes of each participant using the Heidelberg Spectralis SD-OCT, acquisition software version 6.0.13.0 (Heidelberg Engineering GmbH, Heidelberg, Germany), and analyzed with the Heidelberg Eye Explorer software (HEYEX version 6.3.4.0). Prior to analyses, each scan was inspected for any software-generated retinal segmentation lines that did not accurately delineate the internal limiting membrane and Bruch's membrane, and were manually corrected by a trained observer.

For each pRNFL OCT scan, seven pRNFL thickness measurements were captured: global (average) and 6 sectors (temporal, superior-temporal, inferior-temporal, nasal, superior-nasal, and inferior-nasal) using a B-scan with a diameter of 3.5 mm centered on the middle of the optic nerve head (**Figure 1**). For each macular (posterior pole) OCT image, a grid with concentric circles of 1 and 3 mm diameters was centered on the fovea (**Figure 2**). Average retinal thickness was measured in the central 1 mm diameter zone, as well as 4 surrounding sectors (superior, inferior, temporal, and nasal) within the 3 mm diameter circular grid.

Analysis

PSP is usually associated with tauopathy, while svPPA and ALS are associated with TDP-43 (Irwin et al., 2015; Höglinger et al., 2017; Kim et al., 2019). Any participants with other clinical subtypes of FTD that involve both tauopathy and TDP-43 proteinopathies (i.e., CBS, bvFTD, and nfPPA) were excluded.

A linear mixed model adjusting for fixed effects of eye, age, and sex, and accounting for within-subject correlation, was used to compare both pRNFL thickness and macular retinal thickness between eyes in subjects with tauopathy to those with TDP-43 proteinopathy. The unstructured covariance matrix was used for errors. A Bonferroni adjustment was employed to control for multiple comparisons which yielded a threshold of significance of 0.05/12 = 0.0042, and controls the familywise error rate at the level of 0.05. SAS statistical software (version 9.4, SAS Institute, Cary, NC) was used for analysis.

A sensitivity analysis with a linear mixed repeated measures model adjusting for age, sex, and eye was also performed, excluding the 3 svPPA participants in the TDP43 group, leaving only those with ALS in the group.

An outlier analysis was also performed on the svPPA group to assess whether it could influence the results of the TDP43 group.

Furthermore, in the 11 subjects with ALS, a Wilcoxon signed rank test was performed to compare the left and right eyes.

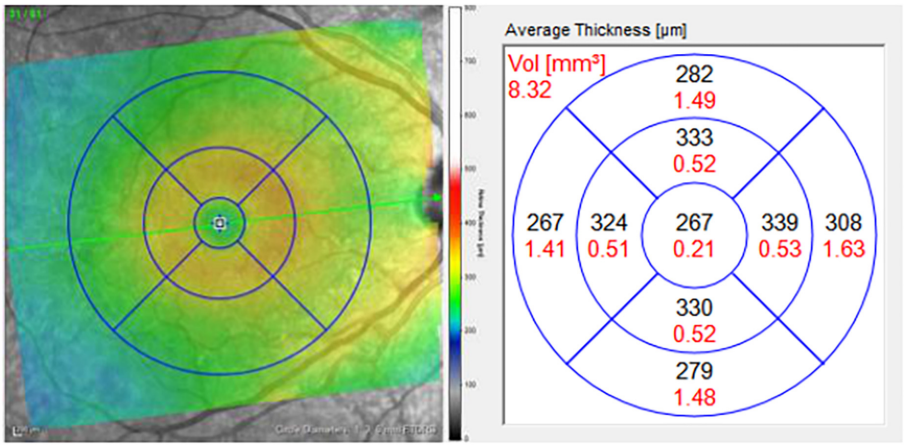

FIGURE 1
Macular grid with 1, 3, and 6 mm diameter circles centered on the foveola **(left)**. Measurements for average thickness (black) in areas of each sector of the macula **(right)**. Only the central five macular sectors were analyzed in this study: central macula, and the inner superior, inferior, nasal, and temporal sectors, bordered by the 3 mm diameter circle.

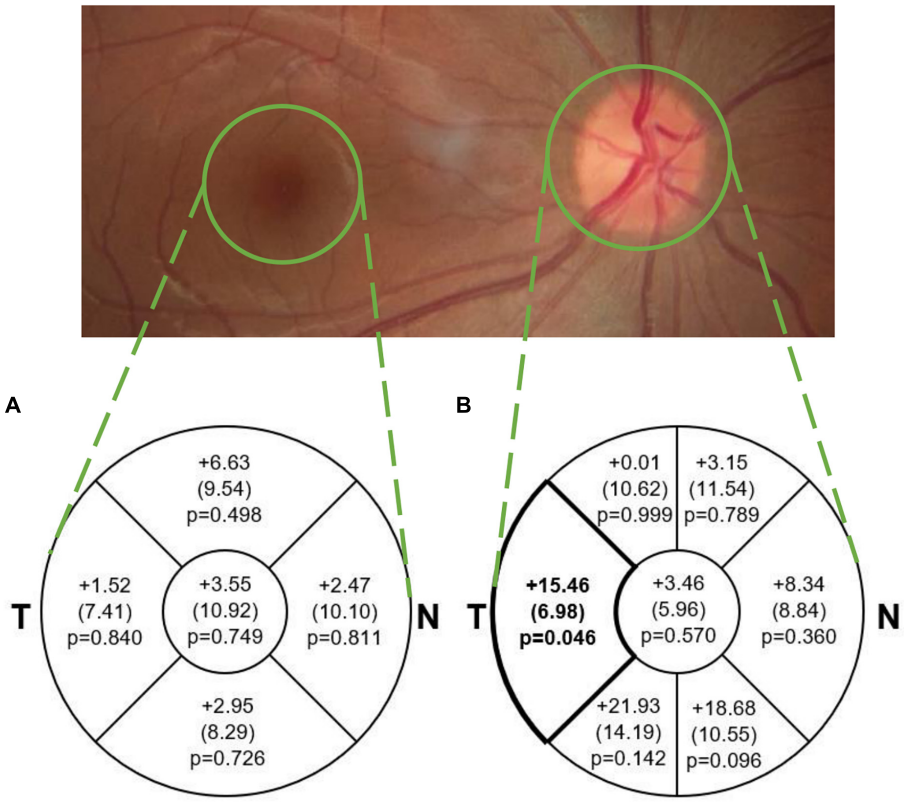

FIGURE 2
Mean (SE) difference (tauopathy – TDP43, μm) in average **(A)** macular sectoral thickness and **(B)** pRNFL sectoral and global thickness. The difference in pRNFL thickness between groups in the temporal sector ($p < 0.05$; medium effect size of 0.61) is illustrated in bold. This difference was not significant after adjusting for multiple comparisons. Note that average thickness in the macular scan is *within the area* of each sector and represents total retinal thickness, while in the pRNFL scan it is *along the circular line* of each sector and represents RNFL thickness only. T, Temporal; N, Nasal.

Results

The final dataset included 9 eyes of 5 subjects (3 female) in the tauopathy group (with a clinical diagnosis of PSP) and 28 eyes of 14 subjects (4 female) in the TDP-43 group (3 with a clinical diagnosis of svPPA and 11 with ALS). Baseline characteristics are described in Table 1. The groups were not matched for age or sex. There were 9 eyes in the tauopathy group; there were 8 eyes with pRNFL scans, and a different 8 eyes with macular scans.

For the retinal thickness (RT) scan in subjects with FTLD, 23 eyes in 12 subjects were excluded due to fixation difficulties during their scan, and 9 eyes in 5 subjects were excluded due to pathologies including AMD, macular hole, lamellar hole, glaucoma, and uncontrolled diabetes (HbA1c > 7.5).

For the pRNFL scan in subjects with FTLD, 15 eyes in 8 subjects were excluded due to fixation difficulties during their scan, and 6 eyes in 3 subjects were excluded due to pathologies including AMD, lamellar hole, cupped optic disk, and uncontrolled diabetes (HbA1c > 7.5).

Of the 30 subjects who met criteria In the FTLD group, only 8 subjects were used (5 in the PSP and 3 in the svPPA group), as the other FTLD subjects did not meet the criteria for a diagnosis of PSP or svPPA.

For the RT and pRNFL scans in subjects with ALS, in a *post hoc* analysis, 2 subjects (4 eyes) with tilted nerves and 1 subject (2 eyes) with a history of stroke were excluded since they could potentially exhibit abnormal pRNFL thicknesses.

Mean pRNFL and macular thickness values in each group are described in Table 2, and mean differences between groups are illustrated in Figure 2. The TDP-43 group demonstrated a thinner pRNFL in the temporal sector than the tauopathy group (mean difference = 15.46 μm, SE = 6.98 (95% CI: 0.32, 30.60), $p = 0.046$) with a medium effect size of 0.61. Based on adjustment for multiple comparisons, this difference is not statistically significant. The differences in global pRNFL thickness between groups and for the other sectors were not significantly different (Figure 2).

No statistically significant differences were found between the groups for mean retinal thickness in the central 1 mm diameter macular zone between the tauopathy (275.04 μm, SE = 9.06) and TDP-43 (271.49 μm, SE = 5.05) groups ($p = 0.749$). Similarly, no significant differences were found in the surrounding 4 sectors within the 3 mm diameter grid of the macula between the groups.

The *post hoc* sensitivity analysis that excluded the svPPA participants, allowing for a comparison of the tauopathy group to the ALS group, did not yield any new findings that were significant after controlling for multiple comparisons. Additionally, the outlier analysis found no outliers in the 3 svPPA participants in terms of age, macular, or pRNFL thickness. Comparison of the left and right eyes in those with ALS showed that the temporal pRNFL was thinner in the left eye compared to the right eye.

TABLE 1 Participant demographics.

	Tauopathy ($n = 9$ eyes, 5 subjects)	TDP-43 Proteinopathy ($n = 28$ eyes, 14 subjects)
Clinical diagnosis, *n*		
PSP	5	N/A
svPPA	N/A	3
ALS	N/A	11
Mean age, years (SD)	72.7 (5.2)	62.1 (9.8)
Sex, *n* (%)		
Male	2 (40%)	10 (71.4%)
Female	3 (60%)	4 (28.6%)
Eyes with pRNFL scans	8	27
Eyes with macular scans	8	28

PSP, progressive supranuclear palsy; svPPA, semantic variant primary progressive aphasia; ALS, amyotrophic lateral sclerosis.

Discussion

This study found that the pRNFL in the temporal sector in the presumed TDP-43 proteinopathy group was on average approximately 15 μm thinner than the presumed tauopathy group ($p = 0.046$). However, this difference was not statistically significant after applying a conservative adjustment for multiple comparisons.

To our knowledge, no studies have compared pRNFL or macular thickness between FTLD-tau and FTLD-TDP-43 proteinopathies. PSP is usually associated with tauopathy, while svPPA and ALS are associated with TDP-43 proteinopathy (Irwin et al., 2015; Höglinger et al., 2017; Kim et al., 2019). Based on this, we compared a group with tauopathy to a group with TDP-43 proteinopathy. Since the pRNFL and retina thins with age even in healthy normal eyes, we adjusted for age in our analysis (Eriksson and Alm, 2009; Celebi and Mirza, 2013). A summary of the findings of previous related studies is shown in Supplementary Table 1. One study found thinning in the temporal pRNFL in ALS subjects compared to healthy controls (Mukherjee et al., 2017). This temporal sector is the same area that was thinner in our TDP-43 group compared to the tau group. Compared to healthy controls, pRNFL thinning has also been reported in subjects with PSP (Stemplewitz et al., 2017), TDP-43 (Ward et al., 2014), a pathologically heterogeneous group of subjects with FTD (Ferrari et al., 2017), and ALS (Ringelstein et al., 2014; Mukherjee et al., 2017; Rohani et al., 2018). In contrast, two groups reported no significant differences in pRNFL thickness between ALS subjects and controls (Roth et al., 2013; Rojas et al., 2019). Our finding in the ALS group of the left pRNFL being thinner than the right is consistent with two studies that found either pRNFL or

TABLE 2 Mean peripapillary retinal nerve fibre layer and macular thickness values in tauopathy and TDP-43 proteinopathy groups, adjusted for age and sex.

	Adjusted model*				Non-adjusted model
	Tauopathy (n = 9 eyes, 5 subjects)	TDP-43 proteinopathy (n = 28 eyes, 14 subjects)	Difference		
	Adjusted mean (95% CI)	Adjusted mean (95% CI)	Coefficient for group (95% CI)	*P*-value**	*P*-value
pRNFL thickness [μm]					
Global	104.16 (93.53,114.80)	100.71 (94.77,106.64)	3.46 (−9.23, 16.15)	0.5703	0.6438
Temporal	85.77 (72.98, 98.55)	70.31 (62.42, 78.20)	15.46 (0.32, 30.60)	0.0461	0.0064
Superior-temporal	137.83 (119.12,156.55)	137.83 (127.51,148.14)	0.01 (−22.52, 22.54)	0.9994	0.7989
Inferior-temporal	162.88 (137.70,188.06)	140.95 (125.76,156.15)	21.93 (−8.25, 52.10)	0.1426	0.7864
Nasal	85.97 (70.33,101.61)	77.63 (69.00, 86.25)	8.34 (−10.43, 27.11)	0.3598	0.6358
Superior-nasal	108.27 (86.93,129.60)	105.12 (91.67,118.56)	3.15 (−21.36, 27.66)	0.7885	0.7078
Inferior-nasal	132.13 (113.54,150.72)	113.45 (102.88,124.02)	18.68 (−3.68, 41.04)	0.0956	0.5725
Macular thickness [μm]					
Central	275.04 (255.85,294.23)	271.49 (260.73,282.25)	3.55 (−19.61, 26.71)	0.7493	0.7070
Superior	344.08 (327.37,360.79)	337.45 (328.10,346.80)	6.63 (−13.66, 26.91)	0.4976	0.8315
Inferior	337.93 (323.16,352.70)	334.98 (326.54,343.42)	2.95 (−14.62, 20.52)	0.7264	0.9516
Temporal	326.66 (313.46,339.85)	325.13 (317.44,332.83)	1.52 (−14.10, 17.15)	0.8397	0.6632
Nasal	344.06 (325.98,362.13)	341.59 (331.38,351.79)	2.47 (−19.33, 24.26)	0.8106	0.7918

*Model was adjusted for age, sex, and eye.
**Significance level after adjusting for multiple comparisons (Bonferroni correction) is 0.004 (=0.05/12). None of the differences were significant at the 0.4% level.

ganglion cell complex (GCC) thinning in the left eye compared to the right in ALS subjects, which may suggest asymmetric CNS involvement in the disease (Rohani et al., 2018; Rojas et al., 2019).

With regards to macular thickness, this study found no differences between the groups. Kim and co-workers (Kim et al., 2017, 2019) reported no differences in total retinal thickness in the central 3 mm diameter macular zone between participants with FTD and healthy controls. However, they did find the outer retina sublayer to be significantly thinner in the FTD group overall and in the FTLD-Tau subtype (with PSP, CBS or nfPPA) compared to controls (Kim et al., 2017). With longitudinal analysis, they found this outer retina thinning to persist and correlate with disease progression in participants with probable tauopathy (Kim et al., 2019). In this study, only the central macular sectors were analyzed because the density of the retinal ganglion cells (RGCs) is the highest in this area. Degeneration of neurons in these central sectors would be more pronounced compared to sectors that are relatively more peripheral (Wässle et al., 1989).

Three groups reported significant macular changes in proteinopathies compared to healthy controls (Ward et al., 2014; Stemplewitz et al., 2017; Rojas et al., 2019), including reduced macular volume in subjects with progranulin (GRN) mutations (which are associated with TDP-43 neuropathology), and thinning in six macular sectors in subjects with PSP (Stemplewitz et al., 2017). Rojas' group (Rojas et al., 2019) reported greater macular thicknesses in the inferior and temporal 3 mm sectors in subjects with ALS compared to controls. However, 6 months later, the inferior 3 and 6 mm sectors were both significantly thinner than at baseline. Because the participants in Rojas' study were at a similar early stage of disease (within 18 months of motor symptom onset) and were then followed over time, this captured a potential evolution of macular thickening followed by thinning, which may illustrate the disease course of ALS in the macula. Furthermore, since previous studies have reported changes to macular sublayers (including the ganglion cell layer, inner nuclear layer, and outer plexiform layer) in these proteinopathies (Ringelstein et al., 2014; Ward et al., 2014; Sevim et al., 2018), differences in sublayer thicknesses between these groups also warrants further investigation.

This study has several strengths. This is the first study to use SD-OCT to compare participants with tauopathy and TDP-43 proteinopathy by using clinical phenotypes (Kim et al., 2017, 2019). The ability to find non-invasive biomarkers to differentiate between tauopathy and TDP-43 pathology is important as proteinopathy-targeted therapies are being developed (Liscic et al., 2020; Yang et al., 2020). A second strength of this study was the rigorous inspection of SD-OCT images and fundus photographs to exclude pathologies unrelated to neurodegeneration that could affect retinal or pRNFL thickness. Large delineation errors on SD-OCT images were corrected to prevent spurious thickness measurements.

Images were also inspected for non-pathological structural anomalies that could potentially affect pRNFL thickness measurements, such as tilted optic disks (Brito et al., 2015), and subjects with these anomalies were excluded. Additionally, subjects with a history of stroke were excluded from the analysis as potential retrograde degeneration in the retina could affect thickness measurements. This rigorous inspection and data curation provided a dataset to reliably identify changes in thickness due to these neurodegenerative diseases.

There are limitations to consider in this study. First, the sample size was small, which may make the findings less generalizable. Despite this, we found a non-significant, but medium effect size difference in the temporal pRNFL thickness between groups. This difference of 15.46 μm may be considered clinically significant. Based on this observed difference, a future study with larger sample size will be able to provide sufficient evidence of statistical significance. For example, a future balanced-design study could recruit 152 patients in total that will likely provide a desirable 80% power to detect significant difference in temporal pRNFL thickness at 5% level. Second, there is a need to consider that the various sectors of pRNFL contain retinal arterioles and venules that typically enter and exit the optic nerve head near the 6 and 12 o'clock positions. At this point on the nerve head, the vessel lumen diameters typically range from 80 to 140 μm for arterioles and 100–150 μm for venules. These vessels can pulse and change in diameter and position with the cardiac cycle. Another limitation is that the disease staging for ALS and PSP are classified using different scales. As such, it is difficult to compare the severity of participants with these different diseases from a clinical standpoint. Consequently, variations in retinal vessel diameter and pulsation will add noise to any structural measurement of pRNFL thickness. Furthermore, the clinical subgroup diagnoses of FTLD and ALS were used to define the pathological groups of tauopathy and TDP-43 proteinopathy. Although the clinical subgroups included were reliably associated with either tau or TDP-43, and any subgroups that were known to involve both pathological mechanisms were eliminated to reduce confounding factors, future studies would hopefully include only biomarker proven proteinopathies. Lastly, if ALS progression consists of a change from pRNFL thickening to thinning with an intermediate stage of normal thickness, as Rojas and co-workers suggested, measurements may be affected by including subjects with different disease severities (Rojas et al., 2019). Future work should involve assessing this cohort over time.

In conclusion, this was the first study to compare pRNFL and macular thickness between participants with PSP (tauopathy) and svPPA and ALS (TDP-43 proteinopathy). The thinning in the temporal pRNFL of the TDP-43 group compared to the tau group warrants further investigation to determine whether retinal imaging can help identify and differentiate proteinopathies in neurodegenerative disease. Future work should assess changes in thickness over time and retinal sub-layer thicknesses to assess whether they are also factors that can help differentiate these two pathological mechanisms.

Data availability statement

The raw data supporting the conclusions of this article will be made available by the authors through request from the Ontario Brain Institute (see ondri.ca).

Ethics statement

The studies involving human participants were reviewed and approved by the Research Ethics Boards at the University Health Network, Sunnybrook Research Institute, University of Waterloo, and the University of Western Ontario. The patients/participants provided their written informed consent to participate in this study.

The ONDRI investigators

Sabrina Adamo, Stephen Arnott, Rob Bartha, Derek Beaton, Courtney Berezuk, Alanna Black, Alisia Bonnick, David Breen, Don Brien, Susan Bronskill, Dennis Bulman, Leanne Casaubon, Ying Chen, Marvin Chum, Brian Coe, Ben Cornish, Jane Lawrence Dewar, Roger A. Dixon, Sherif El-Defrawy, Sali M.K. Farhan, Frederico Faria, Julia Fraser, Mahdi Ghani, Barry Greenberg, Hassan Haddad, Wendy Hatch, Melissa Holmes, Chris Hudson, Peter Kleinstiver, Donna Kwan, Elena Leontieva, Brian Levine, Wendy Lou, Efrem D. Mandelcorn, Ed Margolin, Connie Marras, Bill McIlroy, Paula McLaughlin, Manuel Montero Odasso, Doug Munoz, David Munoz, Nuwan Nanayakkara, JB Orange, Miracle Ozzoude, Alicia Peltsch, Pradeep Raamana, Joel Ramirez, Natalie Rashkovan, Angela Roberts, Yanina Sarquis Adamson, Christopher Scott, Michael Strong, Stephen Strothers, Sujeevini Sujanthan, Kelly M. Sunderland, Sean Symons, Faryan Tayyari, Athena Theyers, Angela Troyer, Abiramy Uthirakumaran, Karen Van Ooteghem, John Woulfe, Mojdeh Zamyadi, and Guangyong (GY) Zou.

Author contributions

BW, CH, ES, FT, HJ, MB, SS, RC, MT, and WH contributed to conception and design of the study. EF, SB, DT-W, LZ, MM, AA, AF, and MT contributed to participant recruitment. BW, CH, FT, CB, MB, RC, EDM, EM, BT, DB, KS, SA, and WH contributed to curation, processing, and/or quality control of the data. BW, CH, HJ, MB, WL, and WH contributed to the

statistical analysis. BW wrote the first draft of the manuscript. BW, CH, HJ, MT, and WH wrote sections of the manuscript. All authors contributed to manuscript revision, read, and approved the submitted version.

Funding

This study was supported by grants from the Ontario Neurodegenerative Disease Research Initiative (ONDRI) through the Ontario Brain Institute, an independent non-profit corporation, funded partially by the Ontario government. Funding was also received from the Toronto Western Hospital Practice Plan.

Conflict of interest

EM received honoraria for speaking engagements from Bayer and Novartis, none of which are relevant to this study. SB was a consultant for Roche and Pfizer. SB obtained funding and has funding pending (through institutions) from GE Healthcare, Eli Lilly, Biogen Idec, Genentech, Optina, Roche, and Novartis. SA was a consultant for Indoc Research Canada (not relevant to this study).

The remaining authors declare that the research was conducted in the absence of any commercial or financial relationships that could be construed as a potential conflict of interest.

Publisher's note

Supplementary material

The Supplementary Material for this article can be found online at: https://www.frontiersin.org/articles/10.3389/fnins.2022.964715/full#supplementary-material

References

Brettschneider, J., Del Tredici, K., Toledo, J. B., Robinson, J. L., Irwin, D. J., Grossman, M., et al. (2013). Stages of pTDP-43 pathology in amyotrophic lateral sclerosis. *Ann. Neurol.* 74, 20–38. doi: 10.1002/ana.23937

Brito, P. N., Vieira, M. P., Falcão, M. S., Faria, O. S., and Falcão-Reis, F. (2015). Optical coherence tomography study of peripapillary retinal nerve fiber layer and choroidal thickness in eyes with tilted optic disc. *J. Glaucoma* 24, 45–50. doi: 10.1097/IJG.0b013e3182883c29

Celebi, A. R. C., and Mirza, G. E. (2013). Age-related change in retinal nerve fiber layer thickness measured with spectral domain optical coherence tomography. *Invest. Ophthalmol. Vis. Sci.* 54, 8095–8103. doi: 10.1167/iovs.13-12634

Doustar, J., Torbati, T., Black, K. L., Koronyo, Y., and Koronyo-Hamaoui, M. (2017). Optical coherence tomography in Alzheimer's disease and other neurodegenerative diseases. *Front. Neurol.* 8:701. doi: 10.3389/fneur.2017.00701

Eriksson, U., and Alm, A. (2009). Macular thickness decreases with age in normal eyes: A study on the macular thickness map protocol in the Stratus OCT. *Br. J. Ophthalmol.* 93, 1448–1452. doi: 10.1136/bjo.2007.131094

Farhan, S. M. K., Bartha, R., Black, S. E., Corbett, D., Finger, E., Freedman, M., et al. (2017). The Ontario Neurodegenerative Disease Research Initiative (ONDRI). *Can. J. Neurol. Sci.* 44, 196–202. doi: 10.1017/cjn.2016.415

Ferrari, L., Huang, S. C., Magnani, G., Ambrosi, A., Comi, G., and Leocani, L. (2017). Optical coherence tomography reveals retinal neuroaxonal thinning in frontotemporal dementia as in Alzheimer's disease. *J. Alzheimers Dis.* 56, 1101–1107. doi: 10.3233/JAD-160886

Hodges, J. R., Davies, R., Xuereb, J., Kril, J., and Halliday, G. (2003). Survival in frontotemporal dementia. *Neurology* 61, 349–354. doi: 10.1212/01.wnl.0000078928.20107.52

Höglinger, G. U., Respondek, G., Stamelou, M., Kurz, C., Josephs, K. A., Lang, A. E., et al. (2017). Clinical diagnosis of progressive supranuclear palsy: The movement disorder society criteria. *Mov. Disord.* 32, 853–864. doi: 10.1002/mds.26987

Irwin, D. J., Cairns, N. J., Grossman, M., McMillan, C. T., Lee, E. B., Van Deerlin, V. M., et al. (2015). Frontotemporal lobar degeneration: Defining phenotypic diversity through personalized medicine. *Acta Neuropathol.* 129, 469–491. doi: 10.1007/s00401-014-1380-1

Kim, B. J., Grossman, M., Song, D., Saludades, S., Pan, W., Dominguez-Perez, S., et al. (2019). Persistent and progressive outer retina thinning in frontotemporal degeneration. *Front. Neurosci.* 13:298. doi: 10.3389/fnins.2019.00298

Kim, B. J., Irwin, D. J., Song, D., Daniel, E., Leveque, J. D., Raquib, A. R., et al. (2017). Optical coherence tomography identifies outer retina thinning in frontotemporal degeneration. *Neurology* 89, 1604–1611. doi: 10.1212/WNL.0000000000004500

Kirbas, S., Turkyilmaz, K., Tufekci, A., and Durmus, M. (2013). Retinal nerve fiber layer thickness in Parkinson disease. *J. Neuroophthalmol.* 33, 62–65. doi: 10.1097/WNO.0b013e3182701745

Knopman, D. S., and Roberts, R. O. (2011). Estimating the number of persons with frontemporal lobar degeneration in the US population. *J. Mol. Neurosci.* 45, 330–335. doi: 10.1007/s12031-011-9538-y.Estimating

Liscic, R. M., Alberici, A., Cairns, N. J., Romano, M., and Buratti, E. (2020). From basic research to the clinic: Innovative therapies for ALS and FTD in the pipeline. *Mol. Neurodegener.* 15:31. doi: 10.1186/s13024-020-00373-9

Mackenzie, I. R. A., and Feldman, H. H. (2005). Ubiquitin immunohistochemistry suggests classic motor neuron disease, motor neuron disease with dementia, and frontotemporal dementia of the motor neuron disease type represent a clinicopathologic spectrum. *J. Neuropathol. Exp. Neurol.* 64, 730–739. doi: 10.1097/01.jnen.0000174335.27708.0a

Masala, A., Sanna, S., Esposito, S., Rassu, M., Galioto, M., Zinellu, A., et al. (2018). Epigenetic changes associated with the expression of amyotrophic lateral aclerosis (ALS) causing genes. *Neuroscience* 390, 1–11. doi: 10.1016/j.neuroscience.2018.08.009

Mukherjee, N., McBurney-Lin, S., Kuo, A., Bedlack, R., and Tseng, H. (2017). Retinal thinning in amyotrophic lateral sclerosis patients without

ophthalmic disease. *PLoS One* 12:e0185242. doi: 10.1371/journal.pone.0185242

Neumann, M. (2013). Frontotemporal lobar degeneration and amyotrophic lateral sclerosis: Molecular similarities and differences. *Rev. Neurol.* 169, 793–798. doi: 10.1016/j.neurol.2013.07.019

Olney, N. T., Spina, S., and Miller, B. L. (2017). Frontotemporal Dementia. *Neurol. Clin.* 35, 339–374. doi: 10.1016/j.ncl.2017.01.008

Ringelstein, M., Albrecht, P., Südmeyer, M., Harmel, J., Müller, A. K., Keser, N., et al. (2014). Subtle retinal pathology in amyotrophic lateral sclerosis. *Ann. Clin. Transl. Neurol.* 1, 290–297. doi: 10.1002/acn3.46

Rohani, M., Meysamie, A., Zamani, B., Sowlat, M. M., and Akhoundi, F. H. (2018). Reduced retinal nerve fiber layer (RNFL) thickness in ALS patients: A window to disease progression. *J. Neurol.* 265, 1557–1562. doi: 10.1007/s00415-018-8863-2

Rojas, P., de Hoz, R., Ramírez, A. I., Ferreras, A., Salobrar-Garcia, E., Muñoz-Blanco, J. L., et al. (2019). Changes in retinal OCT and their correlations with neurological disability in early ALS patients, a follow-up study. *Brain Sci.* 9:337. doi: 10.3390/brainsci9120337

Rojas, P., Ramírez, A. I., Fernández-Albarral, J. A., López-Cuenca, I., Salobrar-García, E., Cadena, M., et al. (2020). Amyotrophic lateral sclerosis: A neurodegenerative motor neuron disease with ocular involvement. *Front. Neurosci.* 14:566858. doi: 10.3389/fnins.2020.566858

Roth, N. M., Saidha, S., Zimmermann, H., Brandt, A. U., Oberwahrenbrock, T., Maragakis, N. J., et al. (2013). Optical coherence tomography does not support optic nerve involvement in amyotrophic lateral sclerosis. *Eur. J. Neurol.* 20, 1170–1176. doi: 10.1111/ene.12146

Sevim, D. G., Unlu, M., Gultekin, M., Karaca, C., Mirza, M., and Mirza, G. E. (2018). Evaluation of retinal changes in progressive supranuclear palsy and Parkinson disease. *J. Neuroophthalmol.* 38, 151–155. doi: 10.1097/WNO.0000000000000591

Stemplewitz, B., Kromer, R., Vettorazzi, E., Hidding, U., Frings, A., and Buhmann, C. (2017). Retinal degeneration in progressive supranuclear palsy measured by optical coherence tomography and scanning laser polarimetry. *Sci. Rep.* 7:5357. doi: 10.1038/s41598-017-05575-8

Sunderland, K. M., Beaton, D., Arnott, S. R., Ramirez, J., Borrie, M., Kleinstiver, P., et al. (2022). Characteristics of the Ontario Neurodegenerative Disease Research Initiative cohort. *Alzheimers Dement*. doi: 10.1002/alz.12632 [Epub ahead of print].

Ward, M. E., Taubes, A., Chen, R., Miller, B. L., Sephton, C. F., Gelfand, J. M., et al. (2014). Early retinal neurodegeneration and impaired Ran-mediated nuclear import of TDP-43 in progranulin-deficient FTLD. *J. Exp. Med.* 211, 1937–1945. doi: 10.1084/jem.20140214

Wässle, H., Grünert, U., Röhrenbeck, J., and Boycott, B. B. (1989). Cortical magnification factor and the ganglion cell density of the primate retina. *Nature* 341, 643–646. doi: 10.1038/341643a0

Wong, B. M., Cheng, R. W., Mandelcorn, E. D., Margolin, E., El-Defrawy, S., Yan, P., et al. (2019). Validation of optical coherence tomography retinal segmentation in neurodegenerative disease. *Transl. Vis. Sci. Technol.* 8:6. doi: 10.1167/tvst.8.5.6

Yang, Q., Jiao, B., and Shen, L. (2020). The development of C9orf72-related amyotrophic lateral sclerosis and frontotemporal dementia disorders. *Front. Genet.* 11:562758. doi: 10.3389/fgene.2020.562758

frontiers | Frontiers in Aging Neuroscience

TYPE Original Research
PUBLISHED 11 October 2022
DOI 10.3389/fnagi.2022.1010064

OPEN ACCESS

EDITED BY
Weidong Le,
Dalian Medical University,
China

REVIEWED BY
Giorgio Vivacqua,
Campus Bio-Medico University,
Italy
Nian Xiong,
Huazhong University of Science and Technology, China

*CORRESPONDENCE
Zhenwei Yu
jasonyzw@163.com
Tao Feng
bxbkyjs@sina.com

†These authors have contributed equally to this work

SPECIALTY SECTION
This article was submitted to Parkinson's Disease and Aging-related Movement Disorders, a section of the journal Frontiers in Aging Neuroscience

RECEIVED 02 August 2022
ACCEPTED 26 September 2022
PUBLISHED 11 October 2022

CITATION
Zheng Y, Cai H, Zhao J, Yu Z and Feng T (2022) Alpha-Synuclein species in oral mucosa as potential biomarkers for multiple system atrophy. *Front. Aging Neurosci.* 14:1010064. doi: 10.3389/fnagi.2022.1010064

Alpha-Synuclein species in oral mucosa as potential biomarkers for multiple system atrophy

Yuanchu Zheng[1†], Huihui Cai[1†], Jiajia Zhao[1], Zhenwei Yu[2*] and Tao Feng[1,3*]

[1]Department of Neurology, Center for Movement Disorders, Beijing Tiantan Hospital, Capital Medical University, Beijing, China, [2]Department of Pathophysiology, Beijing Neurosurgical Institute, Beijing, China, [3]China National Clinical Research Center for Neurological Diseases, Beijing, China

Background: The definitive diagnosis of Multiple system atrophy (MSA) requires the evidence of abnormal deposition of α-Synuclein (α-Syn) through brain pathology which is unable to achieve *in vivo*. Deposition of α-Syn is not limited to the central nervous system (CNS), but also extended to peripheral tissues. Detection of pathological α-Syn deposition in extracerebral tissues also contributes to the diagnosis of MSA. We recently reported the increased expressions of α-Syn, phosphorylated α-Synuclein at Ser129 (pS129), and α-Syn aggregates in oral mucosal cells of Parkinson's disease (PD), which serve as potential biomarkers for PD. To date, little is known about the α-Syn expression pattern in oral mucosa of MSA which is also a synucleinopathy. Here, we intend to investigate whether abnormal α-Syn deposition occurs in oral mucosal cells of MSA, and to determine whether α-Syn, pS129, and α-Syn aggregates in oral mucosa are potential biomarkers for MSA.

Methods: The oral mucosal cells were collected by using cytobrush from 42 MSA patients (23 MSA-P and 19 MSA-C) and 47 age-matched healthy controls (HCs). Immunofluorescence analysis was used to investigate the presence of α-Syn, pS129, and α-Syn aggregates in the oral mucosal cells. Then, the concentrations of α-Syn species in oral mucosa samples were measured using electrochemiluminescence assays.

Results: Immunofluorescence images indicated elevated α-Syn, pS129, and α-Syn aggregates levels in oral mucosal cells of MSA than HCs. The concentrations of three α-Syn species were significantly higher in oral mucosal cells of MSA than HCs (α-Syn, $p<0.001$; pS129, $p=0.042$; α-Syn aggregates, $p<0.0001$). In MSA patients, the oral mucosa α-Syn levels negatively correlated with disease duration ($r=-0.398$, $p=0.009$). The area under curve (AUC) of receiver operating characteristic (ROC) analysis using an integrative model including age, gender, α-Syn, pS129, and α-Syn aggregates for MSA diagnosis was 0.825, with 73.8% sensitivity and 78.7% specificity.

Conclusion: The α-Syn levels in oral mucosal cells elevated in patients with MSA, which may be promising biomarkers for MSA.

KEYWORDS

multiple system atrophy, alpha-synuclein, oral mucosal cells, immunofluorescence, electrochemiluminescence

Introduction

Multiple system atrophy (MSA) is a rare and rapidly progressive neurodegenerative disease, that clinically presents with variable combination of autonomic failure, levodopa-unresponsive parkinsonism, and cerebellar ataxia (Fanciulli and Wenning, 2015). MSA can be clinically divided into two subtypes: MSA with predominant parkinsonism (MSA-P) and predominant cerebellar ataxia (MSA-C) according to their predominant clinical manifestations (Gilman et al., 2008). Currently, the diagnosis of MSA is mainly based on clinical symptoms, supplemented by magnetic resonance imaging (MRI) evidence. MRI markers of MSA are as follows: atrophy of putamen, middle cerebellar peduncle, pons, and cerebellum; "hot cross bun" sign; increased diffusivity of putamen and middle cerebellar peduncle. Due to overlapping characteristics with other synucleinopathies such as Parkinson's disease (PD) and dementia with Lewy bodies (DLB), the misdiagnosis rate of MSA is high, particularly in the early stages (Joutsa et al., 2014; Cong et al., 2021). In the brain of MSA patients, the α-Synuclein (α-Syn) accumulates in the cytoplasm of oligodendrocytes and forms insoluble inclusion bodies, namely glial cytoplasmic inclusions (GCIs; Marmion et al., 2021). The definitive diagnosis of MSA requires the evidence of abnormal deposition of α-Syn in the brain through autopsy. α-Syn abnormal deposition in MSA patients is not limited to the central nervous system (CNS), but also extended to peripheral tissues, biofluids, and cells. Detection of α-Syn abnormal deposition in peripheral tissues may be a promising biomarker for MSA.

Studies reported α-Syn abnormal deposition in blood, olfactory mucosa, saliva, salivary glands, skin, colon, and sural nerves of MSA patients. Liu et al. found the increased α-Syn and α-Syn aggregates levels in erythrocyte membranes of MSA patient than those in healthy controls (HCs; Liu et al., 2019). Recently, Luan et al. used alpha-synuclein real-time quaking-induced conversion (α-syn RT-QuIC) assay to detect the seeding activity of pathological α-syn in the saliva (Luan et al., 2022). 11 of 18 patients with clinical probable MSA displayed positive seeding activity, whereas 2 of 36 controls showed positive seeding activity. MSA patients showed higher seeding activity of pathological α-syn in the saliva than controls. Some groups also found the positive seeding activity of α-Syn in olfactory mucosa of MSA patients (De Luca et al., 2019; Bargar et al., 2021). Skin and colon biopsies revealed the abnormal deposition of phosphorylated α-Syn in MSA patients (Pouclet et al., 2012; Donadio et al., 2018). However, most of the sampling methods are either invasive or of poor compliance. A non-invasive sampling assay with high diagnostic efficiency is in urgent need for the diagnosis of MSA. We recently reported the increased expressions of α-Syn, phosphorylated α-Synuclein at Ser129 (pS129), and α-Syn aggregates in oral mucosal cells of PD, which serve as potential non-invasive biomarkers (Zheng et al., 2022). These results suggested that oral mucosal cells may be the ideal source of biomarker for synucleinopathies including MSA. To date, little is known about the α-Syn expression pattern in oral mucosa of MSA. Whether there are differential α-Syn species expressions in oral mucosal cells between MSA patients and HCs deserves further study.

In the current study, we intend to explore the expressions of α-Syn, pS129, and α-Syn aggregates in oral mucosal cells from MSA patients and age-matched HCs, and to determine the diagnostic performance of α-Syn species in oral mucosa for MSA. We also aim to determine the relationship between oral mucosal α-Syn levels and disease severity.

Materials and methods

Study design and subjects

Patients with MSA and age-matched HCs were recruited from Beijing Tiantan Hospital, Capital Medical University between November 2021 and May 2022. All patients were diagnosed by a movement disorders specialist (T. F) and fulfilled the MSA criteria (Gilman et al., 2008). The exclusion criteria were as follows: (1) secondary parkinsonism due to cerebrovascular, hypoxia, trauma, infection, metabolic or systemic disease affecting the CNS; (2) other Parkinson-plus syndromes, such as DLB, PSP, and corticobasal degeneration (CBD); (3) severe systemic disorders and oral mucosa diseases. According to the dominant clinical manifestations, MSA patients were divided into MSA-P and MSA-C subtypes. HCs were excluded if they had a diagnosis of the neurological disease, a family history of movement disorders, severe psychiatric disorders, severe systemic disorders, or oral mucosa diseases.

We collected clinical and demographic data including age, gender, disease duration, predominant motor symptoms, MMSE, MoCA and orthostatic hypotension (OH). Neurogenic orthostatic hypotension is defined as a 30 mmHg systolic blood pressure (BP) decrease usually accompanied by a 15 mmHg diastolic BP drop and a heart rate (HR)/SBP ratio 0.5 bpm/mmHg within 3 min of standing or head-up tilt (HUT; Gilman et al., 2008). For MSA patients, disease duration and MDS-UPDRS III (Carmona-Abellan et al., 2021) were used to assess the disease severity. The study was approved by the Ethics Committee of Beijing Tiantan Hospital, Capital Medical University. All participants provided written informed consent.

Oral mucosa sampling and preparation

Participants rinsed their mouths with sterile saline before sampling to exclude the effects of oral food debris and saliva contamination. Immediately after rinsing, small-headed cytobrush (2 cm head length; Thomas et al., 2009) was used to collect oral mucosa samples from bilateral inner buccal mucosa, respectively. The right-sided oral mucosa samples were used for electrochemiluminescence immunoassays, and the left-sided oral mucosa samples were used for immunofluorescence stains.

The collection and procession of oral mucosal cell samples for electrochemiluminescence (ECL) assay: the operator holds the cytobrush and makes 30 circular motions of the brush head, then immerses the brush head in a 1.5 ml tube filled with 200 µl RIPA buffer (Applygen, cat. no. C1053 +). The cytobrush head was removed after vortexing for 1 min. Then, the oral mucosal cell suspension was sonicated for 1 min and centrifuged at 12,000*g* and 4°C for 10 min. Transfer the supernatant to a new tube and discard the pellet at the bottom. Samples were stored at −80°C. The bicinchoninic acid (BCA) protein assay kit (Pierce/Thermo Fisher Scientific, Rockford, IL, United States) was used to assess the total protein levels of oral mucosal cell samples.

The collection and procession of oral mucosal cell samples for immunofluorescence stains: the operator holds the cytobrush and makes 5 circular motions of the brush head, then immerses the brush head in a 1.5 ml tube with 1 ml Phosphate-buffered saline (PBS). The cytobrush was removed after vortexing tubes for 1 min. The tube was centrifuged at 2,000*g* and 4°C for 20 min. Remove the supernatant, then resuspend the cell mass with 1.5 ml PBS. Add 70 µl cell resuspension to each funnel, mount the slide and funnel, then cytocentrifuge cell suspension onto microscope slides by cytospin (CYTOSPIN IV, AHSI, Italy) at 700 rpm for 6 min. The slides were then stored at −20°C.

Oral mucosal cell immunofluorescence staining

Immunofluorescence staining with α-Syn species antibodies

The slide was fixed in 4% paraformaldehyde for 10 min and then washed with PBS. After rinsing, the slide was permeabilized in 1% Triton X-100 for 10 min and then incubated in 5% Bovine serum albumin blocking solution (Sigma, Poole, United Kingdom). We evaluated the expression of α-Syn species in oral mucosa samples using MJFR1 (ab138501, Abcam, Cambridge, MA, United States), which is specific for full-length human α-Syn protein. PS129 antibody (cat825701, BioLegend, San Diego, CA, United States) is a synthetic peptide-specific antibody, which corresponds to the α-Syn phosphorylated at serine 129. Using MJFR-14-6-4-2(ab209538, Abcam, Cambridge, MA, United States), the expression of α-Syn aggregates was determined. Primary antibodies were diluted 1:500 in blocking solution and incubated overnight at 4°C. After incubation, the slide was washed with PBST buffer (PBS with 0.05% Tween® 20). The sections were then incubated with Alexa-conjugated secondary antibodies for α-Syn, pS129, and α-Syn aggregates, respectively: donkey anti-rabbit Alexa Fluor 488 (diluted 1:500, ab150077, Abcam, Cambridge, MA, United States), donkey anti-mouse Alexa Fluor 647 (diluted 1:500, ab150107, Abcam, Cambridge, MA, United States) and donkey anti-rabbit Alexa Fluor 647 (diluted 1:500, ab150075, Abcam, Cambridge, MA, United States) for 1 h at room temperature. Sealed with a DAPI-containing anti-fluorescence quencher (S2110 Solarbio, Beijing, CHINA) and imaged with Zeiss LSM 700 confocal microscope (Carl Zeiss Microscopy GmbH, Oberkochen, Germany) using 40 × objective.

Double immunofluorescence staining with ThT and MJFR-14-6-4-2

The slides were fixed in 4% paraformaldehyde for 10 min and then washed with PBS for three times. After rinsing, slides were permeabilized in 1% Triton X-100 for 15 min. After three washings of 5 min each, slides were incubated in 5% Bovine serum albumin blocking solution (Sigma, Poole, United Kingdom) for 2 h. After blocking, the slides were incubated overnight with 0.05% Thioflavin T (ThT) and MJFR-14-6-4-2 (diluted 1:500, ab209538, Abcam, Cambridge, MA, United States). After overnight incubation, the slides were incubated with donkey anti-rabbit Alexa Fluor 647 (diluted 1:500, ab150075, Abcam, Cambridge, MA, United States) for 1 h at room temperature. Nuclei were stained with DAPI (0.2 µg/ml) for 5 min. Slides observation was performed with a Zeiss LSM 880 confocal microscope (Carl Zeiss Microscopy GmbH, Oberkochen, Germany) using 40 × objective.

Electrochemiluminescence immunoassays

The ECL assay of oral mucosal cells was made as described previously (Zheng et al., 2022), with minor modifications. The Meso Scale Discovery (MSD, Rockville, MD, United States) U-Plex plates were used for the quantification of oral mucosa-derived α-Syn, pS129, and α-Syn aggregates. Recombinant unphosphorylated a-Syn monomers (RP-001, Proteos, Inc., Kalamazoo, MI, United States), phosphorylated α-Syn monomers (RP-004, Proteos, Inc.) and filaments (RP-002, Proteos, Inc.) were used as the standard proteins for three a-Syn species assay, respectively. The NanoDrop OneC spectrophotometer (Thermo Scientific, Waltham, MA, United States) is used to measure the standard protein concentration. Standard protein was then diluted between 1,000 pg./ml and 1.37 pg./ml in 3-fold serial dilutions with Diluent 35 (D35, MSD, Rockville, MD, United States). Anti-α-Syn clone 42 (624096, BD Bioscience, San Jose, CA, United States) was labeled with Sulfo-TAG and used as detection antibodies for all a-Syn species. Recombinant anti-α-Syn MJFR-1 (ab 138,501, Abcam, Cambridge, MA, United States), recombinant anti-α-Syn aggregate MJFR-14 (ab209538, Abcam, Cambridge, MA, United States), and anti-phosphorylated α-Synuclein at Ser129 (825,701, BioLegend, San Diego, CA, United States) antibodies were biotinylated and used as capture antibodies. Capture antibodies were coated on plates and incubated for 1 h with 600 rpm shaking at room temperature. After rinsing three times with 150 µl wash buffer (MSD, Rockville, MD, United States), plates were blocked with 150 µl D35 for 1 h with 600 rpm shaking at room temperature and then rinsed. The oral mucosal cell protein-containing samples were

diluted in D35 (protein-containing samples: D35, 25 µl:30 µl). Diluted samples together with standard proteins were loaded 50 µl/well and incubated for 1 h while shaking at 600 rpm. For α-Syn, pS129 detection, overnight incubation at 4°C is needed. After incubation, the detection antibody solution (1 µg/ml) was loaded and incubated for 1 h with 600 rpm shaking and then rinsing with wash buffer for three times. Immediately after rinsing, 150 µl 2 × Reading Buffer (MSD, Rockville, MD, United States) was loaded and the plates were analyzed in a Sector Imager 6000 (MSD, Rockville, MD, United States).

Statistical analysis

The statistical analysis was conducted with SPSS 26.0 (IBM, Chicago, IL, United States) and GraphPad Prism 8 software (GraphPad Software, La Jolla California United States). Prior to analysis, α-Syn, pS129, and α-Syn aggregates concentrations were normalized to total oral mucosal cell protein levels. Non-parametric Mann–Whitney *U* test was performed to compare group difference. The chi-square test was used to compare the gender ratio between the two groups. Spearman's rank correlation coefficient was employed to test the correlation between α-Syn species levels and disease severity. $p < 0.05$ was considered significant. Binary logistic regression was used to create a multivariable logistic regression model suited for MSA diagnosis. We evaluated the area under the ROC curve and derived the Youden index maxima (sensitivity + specificity −1) to determine the optimal cutoff value for MSA patients and HCs.

Results

Demographic and clinical features

A total of 89 subjects were included in this study. The cohort consisted of 42 MSA patients (23 patients with MSA-P and 19 patients with MSA-C) and 47 age-matched HCs. The demographic and clinical features of all subjects were listed in Table 1. There were no statistically significant differences in gender distribution and age between total MSA and HCs. While there were significant differences in Mini-mental State Examination (MMSE) and Montreal Cognitive Assessment (MoCA) scores between MSA and HCs ($p_{MMSE} < 0.001$, $p_{MoCA} < 0.001$). The median disease duration of MSA patients was 2 years (range 4 months–7.5 years) and median Movement Disorder Society Unified Parkinson's Disease Rating Scale Part III (MDS-UPDRS III) score was 40.5 (range 21–83). For the MSA subtypes, the age and MDS-UPDRS III scores were higher in MSA-P patients compared with MSA-C ($p_{age} = 0.023$, $p_{MDS\text{-}UPDRS\ III} = 0.020$). There were no significant differences in gender distribution, disease duration, MoCA, MMSE scores, and orthostatic hypotension between MSA-C and MSA-P.

Immunofluorescence stains

We evaluated the expression of α-Syn in oral mucosa using MJFR1, which is specific for recombinant full-length human α-Syn protein. PS129 antibody is a synthetic peptide directed toward phosphorylated serine 129 of α-Syn, which corresponds to amino acids 124–134. Using MJFR-14-6-4-2, the expression of α-Syn aggregates was determined. In oral mucosal cells of both MSA patients and HCs, α-Syn (Figure 1A), pS129 (Figure 1B), and α-Syn aggregates (Figure 1C) immunoreactive signals were detectable through confocal microscopy. Immunofluorescence imaging revealed that immunoreactive signals of α-Syn and α-Syn aggregates significantly increased in the oral mucosal cells of MSA patients compared to those of HCs, while ps129 showed a slightly higher intensity in the oral mucosal cells of MSA patients. The morphological pattern of a-syn species varies in oral mucosal cells. A-Syn aggregates showed a large granular pattern, whereas α-Syn and pS129 showed diffused or small dotted patterns.

TABLE 1 Demographic and clinical features.

Group	MSA, $n = 42$	MSA-C, $n = 19$	MSA-P, $n = 23$	HCs, $n = 47$	*p*	
					MSA vs HCs	MSA-C vs MSA-P
Females/Males	21/21	8/11	13 /10	33/14	0.051	0.352
Age (year)	62 [54.75, 69]	56 [52, 67]	65 [57, 70]	57 [53, 66]	0.082	0.023*
Duration (year)	2 [1, 3.125]	1.5 [1, 2]	2.5 [2, 4]	NA	NA	0.067
MDS-UPDRS III	40.5 [31, 48.5]	36 [29, 43]	43 [36, 57]	NA	NA	0.020*
MoCA	21 [19, 25]	22 [19, 26]	21 [19, 24]	25 [24, 27]	<0.001*	0.395
MMSE	26 [24, 28]	26 [25, 27]	26 [23,28]	28 [28, 30]	<0.001*	0.721
OH/NOH	16/26	9/10	7/16	NA	NA	0.266

MSA, Multiple System Atrophy; HCs, Healthy Controls; MSA-P, Multiple System Atrophy with predominant parkinsonism; MSA-C, Multiple System Atrophy with predominant cerebellar ataxia; MMSE, Mini-mental State Examination; MoCA, Montreal Cognitive Assessment; MDS-UPDRS III, Movement Disorder Society Unified Parkinson's Disease Rating Scale Part III; OH, Orthostatic Hypotension; NOH, No Orthostatic Hypotension; NA, not applicable. Data is represented as median [25%–75%]. *This value of *p* indicates a statistically significant difference.

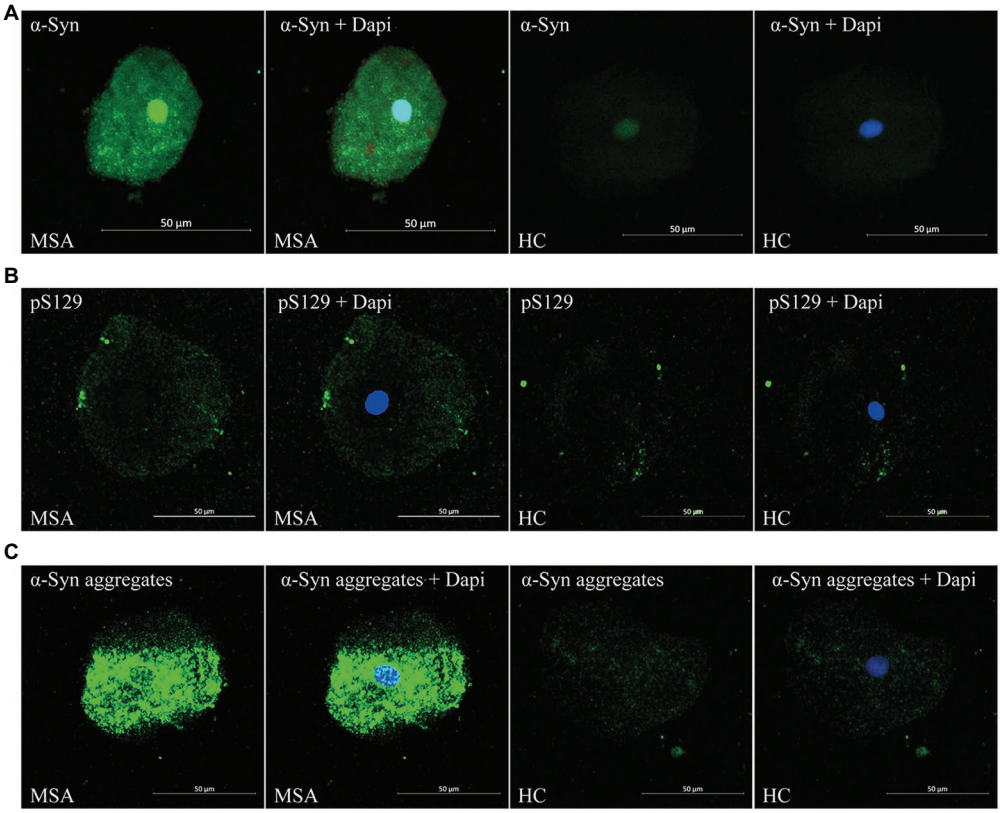

FIGURE 1
Confocal microscopy (×40) study of α-Syn **(A)**, pS129 **(B)**, and α-Syn aggregates **(C)** expression pattern in oral mucosal cells of MSA patients and controls. DAPI: bule. α-Syn: green. Scale bar: 50μm. MSA, Multiple System Atrophy; α-Syn, α-synuclein; pS129, phosphorylated α-Syn at Ser129.

There was no significant difference between MSA patients and HCs in the immunoreactive signal pattern or the intracellular distribution of α-Syn species. More specifically, in oral mucosal cells of both MSA patients and HCs, α-Syn showed a diffuse distribution in the nucleus and cytoplasm of oral mucosal cells. PS129 showed a dotted positivity mainly located in the cytoplasm of oral mucosal cells. A-Syn aggregates showed a predominantly granular positivity in the nucleus and perinuclear cytoplasm of oral mucosal cells.

Through confocal microscopy analysis, ThT immunoreactive signals were visible in oral mucosa cells of both MSA (Figure 2A) and control groups (Figure 2B). ThT immunoreactive signals were slightly higher in MSA group than the control group. Double immunofluorescence staining with ThT and MJFR-14-6-4-2 antibody revealed that MJFR-14-6-4-2 immunoreactive signals mainly colocalized with ThT immunoreactive signals in the cytoplasm of oral mucosal cells in MSA group (Figure 2A).

Electrochemiluminescence assay

The concentrations of α-Syn species in oral mucosal cells between MSA and HCs

Before analysis, the concentrations of α-Syn, pS129, and α-Syn aggregates were all standardized to the total protein levels of oral mucosa samples. Compared with HCs, the concentration of α-Syn in oral mucosal cells was significantly higher of MSA patients ($p < 0.001$, Figure 3A; Table 2). The pS129 and α-Syn aggregates levels also increased in MSA patients compared with those in HCs ($p = 0.042$, $p < 0.0001$, Figures 3B,C; Table 2).

The concentrations of α-Syn species in oral mucosal cells between MSA subgroups

The MSA group was further divided into MSA-C/MSA-P and MSA-OH/MSA-NOH subgroups according to clinical manifestations. There was no significant difference in α-Syn, pS129, or α-Syn aggregates levels between MSA-C and MSA-P patients ($p_{\alpha\text{-Syn}} = 0.294$, $p_{\text{pS129}} = 0.185$, $p_{\alpha\text{-Syn aggregates}} = 0.426$). There was neither a significant difference of α-Syn, pS129, nor α-Syn aggregates levels between MSA patients with or without orthostatic hypotension ($p_{\alpha\text{-Syn}} = 0.422$, $p_{\text{pS129}} = 0.756$, $p_{\alpha\text{-Syn aggregates}} = 0.856$; Table 2).

The correlations of α-Syn species concentrations with disease severity in MSA

In MSA group, there was a significantly negative correlation between α-syn levels in oral mucosal cells and disease duration ($r = -0.398$, $p = 0.009$; Figure 4). However, α-Syn and pS129 levels in oral mucosal cells did not significantly correlate with disease duration in MSA group. The α-Syn species levels did not correlate

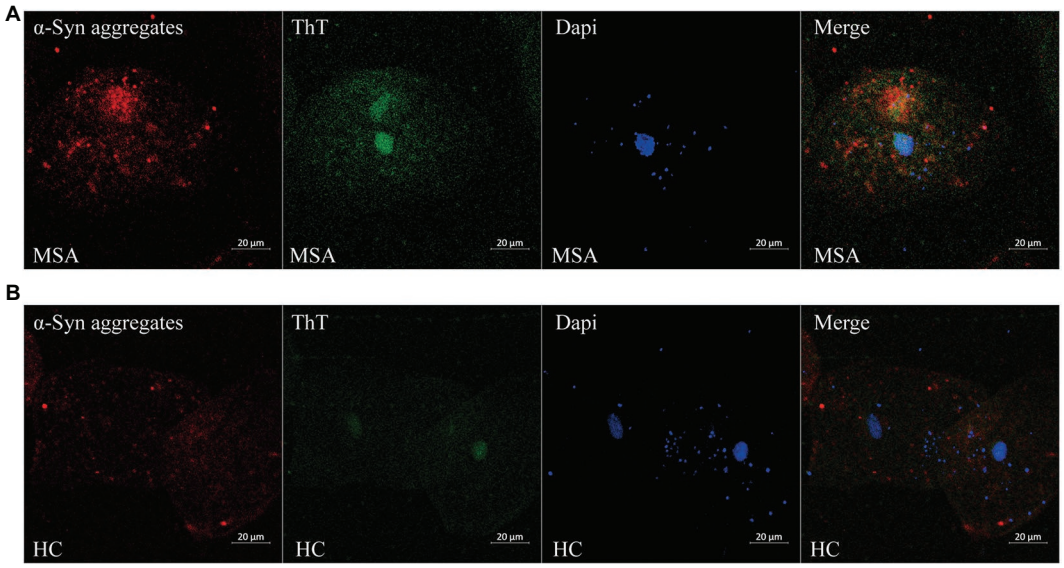

FIGURE 2
Confocal microscopy (×40) study of double immunofluorescence staining with ThT and MJFR-14-6-4-2 antibody in oral mucosal cells of MSA patients **(A)** and controls **(B)**. DAPI: bule. α-Syn aggregates: red. ThT: green. Scale bar: 20μm. MSA, Multiple System Atrophy; α-Syn, α-synuclein; ThT, Thioflavin T.

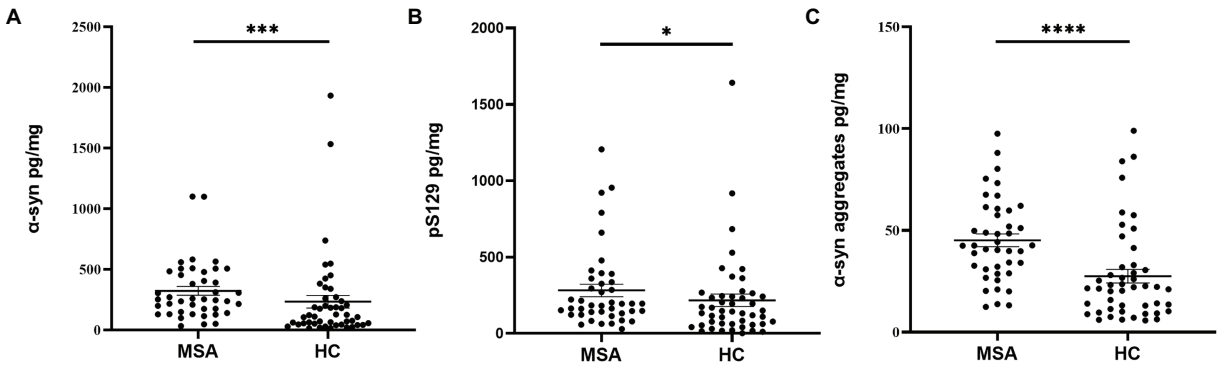

FIGURE 3
The concentrations of α-Syn, pS129, and α-Syn aggregates in oral mucosa samples of MSA patients and controls. **(A)** α-Syn, normalized to total oral mucosal cell proteins (pg/mg); ***p<0.001 (Mann–Whitney U test); **(B)** pS129, normalized to total oral mucosal cell proteins (pg/mg); *p=0.042 (Mann–Whitney U test); **(C)** α-Syn aggregates, normalized to total oral mucosal cell proteins (pg/mg); ****p<0.0001 (Mann–Whitney U test).

with MDS-UPDRS III scores or cognitive scores in patients with MSA.

ROC curve analysis of α-Syn species in oral mucosal cells between MSA and HCs

Receiver operating characteristic (ROC) analysis was performed to assess the diagnostic performance of α-Syn species in oral mucosal cells for MSA. α-syn levels discriminated MSA from HCs with a sensitivity of 88.1% and a specificity of 55.3%, and the area under curve (AUC) was 0.718. PS129 levels discriminated MSA from HCs with a sensitivity of 81.0% and a specificity of 44.7% (AUC = 0.625). A-Syn aggregates discriminated MSA from HCs with a sensitivity of 69.0% and a specificity of 76.6% (AUC = 0.763). The binary logistic regression with forward like ratio was used to create a multivariable logistic regression model based on age, gender, and levels of α-Syn species in oral mucosal cells. The AUC of this integrative model was 0.825, with 73.8% sensitivity and 78.7% specificity (Figure 5).

10.3389/fnagi.2022.1010064

TABLE 2 The concentrations of α-Syn in oral mucosal cells of MSA and HCs.

Group	MSA	MSA-C	MSA-P	MSA-OH	MSA-NOH	HCs	*p*		
							MSA vs HCs	MSA-C vs MSA-P	MSA-OH vs MSA-NOH
α-Syn	253.69 [147.47, 481.28]	304.65 [176.13, 507.72]	239.11 [130.97, 454.33]	288.31 [182.30, 500.93]	250.06 [130.64, 462.04]	112.39 [47.40, 261.64]	<0.001*	0.294	0.422
pS129	188.92 [129.57, 342.38]	203.13 [131.96, 412.13]	163.59 [122.17, 270.60]	188.55 [124.77, 343.46]	188.92 [135.78, 350.01]	142.96 [61.88, 245.39]	0.042*	0.185	0.756
A-Syn aggregates	42.53 [30.40, 60.04]	42.63 [30.90, 61.43]	40.32 [28.73, 59.8]	42.61 [29.40, 58.29]	41.60 [30.82, 60.22]	21.53 [10.29, 31.97]	<0.0001*	0.426	0.856

MSA; Multiple System Atrophy; HCs; Healthy Controls; MSA-P, Multiple System Atrophy with predominant parkinsonism; MSA-C, Multiple System Atrophy with predominant cerebellar ataxia; MSA-OH, MSA with orthostatic hypotension; MSA-NOH, MSA without orthostatic hypotension; α-Syn, α-synuclein; pS129, Phosphorylated α-Syn at Ser129; Data is represented as median [25%–75%]. *This value of *p* indicates a statistically significant difference.

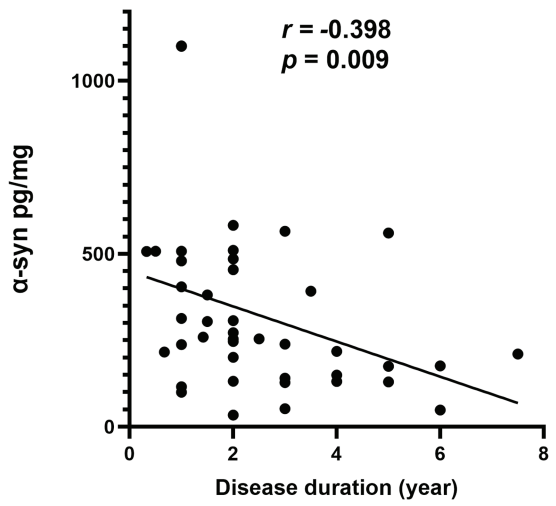

FIGURE 4
Correlation of α-syn in oral mucosa with disease duration in patients with MSA.

Discussion

The current study demonstrated the differential expression of α-Syn, pS129, and α-Syn aggregates in oral mucosal cells between MSA patients and HCs. The main results are as follows: (1) immunofluorescence images showed detectable α-Syn species immunoreactive signals in oral mucosal cells of both MSA patients and HCs, with higher immunoreactive signals of α-Syn, pS129, and α-Syn aggregates in oral mucosal cells of MSA patients; (2) ECL assays demonstrated that the α-Syn, pS129, and α-Syn aggregates levels in oral mucosal cells were increased in MSA group compared with HCs, further supporting the immunofluorescence results; (3) the level of α-Syn in oral mucosal cells negatively correlated with the disease duration in MSA patients.

α-Syn is a small (14 kDa) and highly conserved acidic protein normally expressed in neurons (Rcom-H'cheo-Gauthier et al., 2016). Abnormal deposition of α-Syn plays a critical role in the pathogenesis of MSA (Clayton and George, 1999; Serratos et al., 2022). In MSA patients, α-Syn mainly accumulates in the cytoplasm of oligodendrocytes of the CNS and forms glial cell inclusion bodies. In fact, α-Syn not only deposits in the CNS of MSA, but also deposits in peripheral nervous system. Zhe Rong et al. reported the deposition of phosphorylated α-syn in the Schwann cells (SCs), a kind of peripheral glial cells, of sural nerves in MSA patients (Rong et al., 2021). Donadio et al. reported the abnormal deposition of pS129 in cutaneous nerve fibers of MSA patients, mainly in the somatosensory fibers of the subcutaneous plexus (Donadio et al., 2018). Some studies also reported the deposition of α-Syn in peripheral non-nervous tissues, biofluids, and cells of MSA (Lee et al., 2017; Ma et al., 2019). Liu et al. found that MSA patients had higher α-Syn and α-Syn aggregates levels in the erythrocyte membranes than HCs (Liu et al., 2019). A meta-analysis revealed that MSA patients had higher plasma α-Syn level than controls (Yang et al., 2018). Several studies also reported the depositions of α-Syn in the salivary glands and olfactory mucosal cells of MSA patients (De Luca et al., 2019; Cao et al., 2020; Bargar et al., 2021). These studies suggest that α-Syn not only exists in the CNS, but also exits in peripheral biofluids, tissues, and cells of MSA patients, which is consistent with the current study.

In the current study, pS129 and α-Syn aggregates immunoreactive signals were also detectable in control group, indicating that pS129 and α-Syn aggregates were expressed in normal controls' oral mucosal cells. Several recent studies also reported the detectable pS129 immunoreactive signals in normal controls' peripheral tissues of healthy controls, such as submucosal plexus and skin (Barrenschee et al., 2017; Wang et al., 2020). As for the α-Syn aggregates expression in controls, Mazzetti et al. recently found that PD patients showed higher α-Syn aggregates expression in skin than healthy controls. Using proximity ligation assay, skin α-Syn aggregates expression was detectable in about 2/3 of the included healthy controls (Mazzetti et al., 2020). These previous studies suggested that pathological α-Syn, pS129, and α-Syn aggregates were detectable in peripheral tissues of normal controls but with a lower level, which was consistent with the current study.

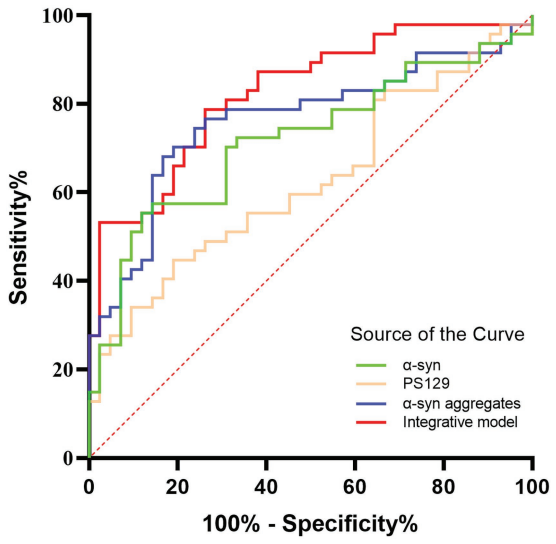

FIGURE 5
The ROC curves for α-Syn, pS129, α-Syn aggregates, and the integrative model. Green curve: α-Syn (AUC=0.718); Yellow curve: pS129 (AUC=0.625); Blue curve: α-Syn aggregates (AUC=0.763); Red curve: the integrative model including α-Syn, pS129, and α-Syn aggregates (AUC=0.825).

ThT is a benzothiazole dye that exhibits enhanced fluorescence upon binding to β-sheet-rich protein aggregate including Abeta fibrils, α-Syn filaments, PrP (Sc) (Khurana et al., 2005), which does not specifically demonstrate the enrich of α-Syn fibrillar aggregates. Through confocal microscopy analysis, ThT immunoreactive signals were detectable in oral mucosal cells, which indicates the potential protein aggregation in oral mucosal cells. Colocation of ThT and MJFR-14-6-4-2 immunoreactive signals indicates the presence of the α-Syn fibrils in oral mucosal cells. However, due to the minimal level of intracellular α-Syn aggregate in the mucosal cells and the lack of α-Syn oligomer or fibril-specific antibody, it is very difficult to in-depth investigate the differences between soluble oligomers and the presence of fibrils in oral mucosal cells in the current study.

The mechanism of the increased α-Syn expression in oral mucosal cells of MSA is currently unknown. In order to avoid contamination with saliva, included participants were asked to rinse their mouths with sterile saline 3 times in the current study. Immediately after rinsing, cytobrush was used to collect oral mucosa samples. Also, before the placement of cells on the slides, oral mucosa cells were washed with PBS and centrifuged at 2,000*g*. Then, the supernatant was removed, so that only mucosa cells were placed onto slides. The method of oral mucosa cell sampling used in the current study was based on the buccal micronucleus cytome assay (Thomas et al., 2009). Through confocal microscopy, the detected a-syn species were located in buccal micronucleus cells. Therefore, we believe that a-syn species detected were derived from oral mucosa cell rather than saliva gland cells or nervous fibers. Numerous researchers have focused on the alterations of oral mucosal cells in neurodegenerative disorders. As for the DNA content, DNA content of oral mucosal cells in certain neurodegenerative disorders, such as AD, is significantly higher than the control group (Francois et al., 2014). Some researchers reported that the levels of the Tau protein and the transcripts of p-Tau and Tau are increased in the oral mucosal cells of patients with cognitive impairment (Hattori et al., 2002; Arredondo et al., 2017). The above studies indicated that α-Syn may also have increased expression in oral mucosal cells in synucleinopathies. Our previous study reported the increased expressions of α-Syn species in oral mucosal cells of PD patients. In the present study, we demonstrated that abnormal α-Syn species deposition also occurred in oral mucosal cells of MSA. The meaning of abnormal deposition of α-Syn species in oral mucosal cells of synucleinopathies remains unknown, mainly because the physiological role of α-Syn in oral mucosal cell is uncertain. It is now widely accepted that abnormal α-Syn deposition in the CNS causes neurodegeneration (Burmann et al., 2020). Whether the increased level of α-Syn in oral mucosal cells of synucleinopathies is the cause or consequence of neurodegeneration requires further study.

The current study showed that the level of α-Syn in oral mucosal cells negatively correlated with the disease duration in MSA patients ($r = -0.398$, $p = 0.009$). However, α-Syn in oral mucosal cells did not correlate with age or MDS-UPDRS III scores. This is the first study on α-Syn expression levels in oral mucosal cells of MSA, the relationship between α-Syn levels in oral mucosal cells and disease progression remains inconclusive. A previous study revealed that α-syn oligomers/protein ratio in erythrocyte membrane negatively correlated with disease duration in MSA ($r = -0.336$; $p = 0.009$). One possible explanation is that the majority of the α-syn transferred to glial cell inclusions as MSA progresses, while lesser α-syn diffuses from the brain to the peripheral oral mucosal cells (Motter et al., 1995; Sun et al., 2014). We presume that α-Syn levels may decrease in peripheral tissues with the progression of MSA. Our findings should be confirmed by future larger and longitudinal studies.

The ECL assays used for detecting α-Syn, pS129, and α-Syn aggregates of oral mucosa were established previously (Zheng et al., 2022) and have been applied to detect α-Syn, pS129, and α-Syn aggregates in erythrocytes (Tian et al., 2019; Yu et al., 2022). Previous studies have validated the high sensitivity and reproducibility of ECL detection of disease-associated proteins on CSF samples (Kruse et al., 2017). As the signal generated is highly proportional to the large number of detection antibodies conjugated to the Sulfo-TAG marker, the ECL system has the advantage of a wide dynamic range and high sensitivity. Also, it has the advantage of shorter experiment time and the lower clinical sample volumes required. The above makes ECL an appropriate technique for detecting the trace proteins in peripheral biological specimens.

Recent developed ultrasensitive protein amplification assays, such as RT-QuIC and protein misfolding cyclic

amplification (PMCA), offered an ultrasensitive approach for pathological α-syn assays (Parnetti et al., 2019; Koga et al., 2021). This assay induces conversion of normal α-syn in samples to misfolded α-syn, allowing amplification and detection of trace amounts of pathological α-syn in tissues or biofluids (Nakagaki et al., 2021). Previous studies showed that the CSF α-syn RT-QuIC had high specificity (82.3%–100%) and sensitivity (84%–100%) for the diagnosis of PD and other synucleinopathies (Nakagaki et al., 2021). Subsequent studies used RT-QuIC for the detection of pathological α-syn in various biospecimens, such as submandibular gland (sensitivity: 100%; specificity: 94%; Manne et al., 2020a), olfactory mucosa (sensitivity: 46%–69%; specificity: 90%–91%; De Luca et al., 2019; Bargar et al., 2021; Stefani et al., 2021), skin (sensitivity: 75%–100%; specificity: 83%–100%; Hong et al., 2010; Manne et al., 2020b; Donadio et al., 2021; Kuzkina et al., 2021), and saliva (sensitivity: 61.1%–76.0%; specificity: 94.4%; Luan et al., 2022). The detection of pathological α-Syn using RT-QuIC yielded high sensitivity and specificity in both synucleinopathies and the prodromal stage of synucleinopathies. The seeding activity of pathological α-syn in oral mucosa cells should be further studied by RT-QuIC or PMCA assays which might be ideal approaches to the detection of trace amounts of pathological α-syn in oral mucosal cells.

Detecting α-Syn species in the oral mucosa as the biomarkers for MSA have several advantages over other peripheral samples. First of all, compared with invasive procedures such as lumbar puncture, blood drawing, skin, salivary gland, and gastrointestinal biopsies, sampling of oral mucosal cells is a noninvasive and safe procedure. Moreover, the oral mucosal cells renew every 7–21 days, repeated sampling in a short period of time can be achieved (Thomas et al., 2009).

As a relatively easy-to-obtain biospecimen, there were numbers of studies focused on salivary α-Syn species as biomarkers for synucleinopathies. Devic et al. reported that the salivary α-Syn tends to decrease in PD patients compared with controls (Devic et al., 2011). While, Goldman et al. reported that salivary α-Syn did not differ between PD and controls (Goldman et al., 2018). Vivacqua et al. detected lower α-Syn and higher oligomeric α-Syn in saliva of PD patients than in healthy controls, the sensitivity and the specificity of salivary oligomeric α-Syn/α-Syn ratio ware 69.77% and 95.16% in distinguishing PD from healthy controls (Vivacqua et al., 2016, 2019). Cao et al. reported the higher level of α-Syn in salivary extracellular vesicles (EVs) of PD patients than that of HCs (Cao et al., 2020). Oligomeric α-Syn in salivary EVs distinguished PD from HCs with sensitivity of 92% and specificity of 86%. Recently, Luan et al. used alpha-synuclein real-time quaking-induced conversion (α-Syn RT-QuIC) assay to detect the seeding activity of pathological α-Syn in the saliva. MSA patients showed higher seeding activity of pathological α-Syn in the saliva than controls (Luan et al., 2022). Salivary α-syn RT-QuIC displayed a sensitivity of 61.1% and specificity of 94.4% in distinguishing MSA from controls. In the current study, the sensitivity and specificity of α-Syn in oral mucosal cells for MSA diagnosis were 73.8% and 78.7%, separately. Further study is needed to determine the optimal biomarker for PD: α-Syn in saliva or oral mucosal cells. In my opinion, the salivary α-Syn may not derive from oral mucosa cells. In the previous studies focused on salivary α-syn, saliva was always centrifuged after sampling and only supernatant was reserved. Oral mucosal cells as well as debris and other tissues were removed. The main contribution on salivary a-syn may be secreted α-syn from salivary glands. Cause abnormal deposition of α-syn has been reported by many groups (Andréasson and Svenningsson, 2021). The origins of salivary a-syn still need further validation. As is known, PD predominantly affects the elderly. Salivary gland atrophy in the elderly could reduce saliva production. Trihexyphenidyl, a commonly used PD drugs, can also cause side effects of reduced saliva production. Thus, oral mucosal cells may have an advantage over saliva in terms of sampling.

This study has some limitations. Above all, we did not include patients with PD or DLB in the current study because of the lack of other synucleinopathies patients. We are now accelerating our efforts to collect enough samples to explore the expression patterns of oral mucosal α-Syn among PD, MSA, and DLB patients. Furthermore, the current study was a cross-sectional study, and prospective studies are required to determine whether α-Syn in oral mucosal cells was a biomarker of disease progression for MSA.

Conclusion

The current study demonstrated the differential expression of α-Syn, pS129, and α-Syn aggregates in oral mucosal cells between MSA patients and HCs, which may potentially serve as a diagnostic biomarker for MSA. Moreover, α-Syn level in oral mucosa is inversely correlated with disease progression. Further longitudinal cohort studies are needed to validate α-Syn in oral mucosal cells as a progression biomarker for MSA.

Data availability statement

The raw data supporting the conclusions of this article will be made available by the authors, without undue reservation.

Ethics statement

The studies involving human participants were reviewed and approved by the Ethics Committee of Beijing Tiantan Hospital, Capital Medical University. The patients/participants provided their written informed consent to participate in this study.

Author contributions

TF and ZY designed the study. HC and YZ performed the measurements and data analysis and wrote the manuscript. JZ and HC contributed to sample collection and preparation. All authors contributed to the article and approved the submitted version.

Funding

This research was funded by the National Natural Science Foundation of China (grant numbers 82071422, 81901151, and 82020108012) and Beijing Municipal Natural Science Foundation (grant number 7212031).

Conflict of interest

The authors declare that the research was conducted in the absence of any commercial or financial relationships that could be construed as a potential conflict of interest.

Publisher's note

References

Andréasson, M., and Svenningsson, P. (2021). Update on alpha-synuclein-based biomarker approaches in the skin, submandibular gland, gastrointestinal tract, and biofluids. *Curr. Opin. Neurol.* 34, 572–577. doi: 10.1097/wco.0000000000000948

Arredondo, L. F., Aranda-Romo, S., Rodríguez-Leyva, I., Chi-Ahumada, E., Saikaly, S. K., Portales-Pérez, D. P., et al. (2017). Tau protein in Oral mucosa and cognitive state: a cross-sectional study. *Front. Neurol.* 8:554. doi: 10.3389/fneur.2017.00554

Bargar, C., De Luca, C. M. G., Devigili, G., Elia, A. E., Cilia, R., Portaleone, S. M., et al. (2021). Discrimination of MSA-P and MSA-C by RT-QuIC analysis of olfactory mucosa: the first assessment of assay reproducibility between two specialized laboratories. *Mol. Neurodegener.* 16:82. doi: 10.1186/s13024-021-00491-y

Barrenschee, M., Zorenkov, D., Böttner, M., Lange, C., Cossais, F., Scharf, A. B., et al. (2017). Distinct pattern of enteric phospho-alpha-synuclein aggregates and gene expression profiles in patients with Parkinson's disease. *Acta Neuropathol. Commun.* 5:1. doi: 10.1186/s40478-016-0408-2

Burmann, B. M., Gerez, J. A., Matečko-Burmann, I., Campioni, S., Kumari, P., Ghosh, D., et al. (2020). Regulation of α-synuclein by chaperones in mammalian cells. *Nature* 577, 127–132. doi: 10.1038/s41586-019-1808-9

Cao, Z., Wu, Y., Liu, G., Jiang, Y., Wang, X., Wang, Z., et al. (2020). Differential diagnosis of multiple system atrophy-parkinsonism and Parkinson's disease using α-Synuclein and external anal sphincter electromyography. *Front. Neurol.* 11:1043. doi: 10.3389/fneur.2020.01043

Carmona-Abellan, M., Del Pino, R., Murueta-Goyena, A., Acera, M., Tijero, B., Berganzo, K., et al. (2021). Multiple system atrophy: clinical, evolutive and histopathological characteristics of a series of cases. *Neurologia (Engl Ed).* S0213:4853. doi: 10.1016/j.nrl.2021.04.007

Clayton, D. F., and George, J. M. (1999). Synucleins in synaptic plasticity and neurodegenerative disorders. *J. Neurosci. Res.* 58, 120–129. doi: 10.1002/(SICI)1097-4547(19991001)58:1<120::AID-JNR12>3.0.CO;2-E

Cong, S., Xiang, C., Wang, H., and Cong, S. (2021). Diagnostic utility of fluid biomarkers in multiple system atrophy: a systematic review and meta-analysis. *J. Neurol.* 268, 2703–2712. doi: 10.1007/s00415-020-09781-9

De Luca, C. M. G., Elia, A. E., Portaleone, S. M., Cazzaniga, F. A., Rossi, M., Bistaffa, E., et al. (2019). Efficient RT-QuIC seeding activity for α-synuclein in olfactory mucosa samples of patients with Parkinson's disease and multiple system atrophy. *Transl. Neurodegener* 8:24. doi: 10.1186/s40035-019-0164-x

Devic, I., Hwang, H., Edgar, J. S., Izutsu, K., Presland, R., Pan, C., et al. (2011). Salivary α-synuclein and DJ-1: potential biomarkers for Parkinson's disease. *Brain* 134:e178. doi: 10.1093/brain/awr015

Donadio, V., Incensi, A., El-Agnaf, O., Rizzo, G., Vaikath, N., Del Sorbo, F., et al. (2018). Skin α-synuclein deposits differ in clinical variants of synucleinopathy: an in vivo study. *Sci. Rep.* 8:14246. doi: 10.1038/s41598-018-32588-8

Donadio, V., Wang, Z., Incensi, A., Rizzo, G., Fileccia, E., Vacchiano, V., et al. (2021). In vivo diagnosis of Synucleinopathies: a comparative study of skin biopsy and RT-QuIC. *Neurology* 96, e2513–e2524. doi: 10.1212/wnl.0000000000011935

Fanciulli, A., and Wenning, G. K. (2015). Multiple-system atrophy. *N. Engl. J. Med.* 372, 249–263. doi: 10.1056/NEJMra1311488

Francois, M., Leifert, W., Hecker, J., Faunt, J., Martins, R., Thomas, P., et al. (2014). Altered cytological parameters in buccal cells from individuals with mild cognitive impairment and Alzheimer's disease. *Cytometry A* 85, 698–708. doi: 10.1002/cyto.a.22453

Gilman, S., Wenning, G. K., Low, P. A., Brooks, D. J., Mathias, C. J., Trojanowski, J. Q., et al. (2008). Second consensus statement on the diagnosis of multiple system atrophy. *Neurology* 71, 670–676. doi: 10.1212/01.wnl.0000324625.00404.15

Goldman, J. G., Andrews, H., Amara, A., Naito, A., Alcalay, R. N., Shaw, L. M., et al. (2018). Cerebrospinal fluid, plasma, and saliva in the BioFIND study: relationships among biomarkers and Parkinson's disease features. *Mov. Disord.* 33, 282–288. doi: 10.1002/mds.27232

Hattori, H., Matsumoto, M., Iwai, K., Tsuchiya, H., Miyauchi, E., Takasaki, M., et al. (2002). The tau protein of oral epithelium increases in Alzheimer's disease. *J. Gerontol. A Biol. Sci. Med. Sci.* 57, M64–M70. doi: 10.1093/gerona/57.1.m64

Hong, Z., Shi, M., Chung, K. A., Quinn, J. F., Peskind, E. R., Galasko, D., et al. (2010). DJ-1 and alpha-synuclein in human cerebrospinal fluid as biomarkers of Parkinson's disease. *Brain* 133, 713–726. doi: 10.1093/brain/awq008

Joutsa, J., Gardberg, M., Röyttä, M., and Kaasinen, V. (2014). Diagnostic accuracy of parkinsonism syndromes by general neurologists. *Parkinsonism Relat. Disord.* 20, 840–844. doi: 10.1016/j.parkreldis.2014.04.019

Khurana, R., Coleman, C., Ionescu-Zanetti, C., Carter, S. A., Krishna, V., Grover, R. K., et al. (2005). Mechanism of thioflavin T binding to amyloid fibrils. *J. Struct. Biol.* 151, 229–238. doi: 10.1016/j.jsb.2005.06.006

Koga, S., Sekiya, H., Kondru, N., Ross, O. A., and Dickson, D. W. (2021). Neuropathology and molecular diagnosis of Synucleinopathies. *Mol. Neurodegener.* 16:83. doi: 10.1186/s13024-021-00501-z

Kruse, N., El-Agnaf, O. M., and Mollenhauer, B. (2017). Validation of electrochemiluminescence assays for highly sensitive and reproducible quantification of alpha-synuclein in cerebrospinal fluid. *Bioanalysis* 9, 621–630. doi: 10.4155/bio-2017-0005

Kuzkina, A., Bargar, C., Schmitt, D., Rößle, J., Wang, W., Schubert, A. L., et al. (2021). Diagnostic value of skin RT-QuIC in Parkinson's disease: a two-laboratory study. *NPJ Parkinsons Dis* 7:99. doi: 10.1038/s41531-021-00242-2

Lee, J. M., Derkinderen, P., Kordower, J. H., Freeman, R., Munoz, D. G., Kremer, T., et al. (2017). The search for a peripheral biopsy indicator of alpha-Synuclein pathology for Parkinson disease. *J. Neuropathol. Exp. Neurol.* 76, 2–15. doi: 10.1093/jnen/nlw103

Liu, G., Tian, C., Gao, L., Cao, Z., and Feng, T. (2019). Alpha-synuclein in erythrocyte membrane of patients with multiple system atrophy: a pilot study. *Parkinsonism Relat. Disord.* 60, 105–110. doi: 10.1016/j.parkreldis.2018.09.012

Luan, M., Sun, Y., Chen, J., Jiang, Y., Li, F., Wei, L., et al. (2022). Diagnostic value of salivary real-time quaking-induced conversion in Parkinson's disease and multiple system atrophy. *Mov. Disord.* 37, 1059–1063. doi: 10.1002/mds.28976

Ma, L. Y., Liu, G. L., Wang, D. X., Zhang, M. M., Kou, W. Y., and Feng, T. (2019). Alpha-Synuclein in peripheral tissues in Parkinson's disease. *ACS Chem. Neurosci.* 10, 812–823. doi: 10.1021/acschemneuro.8b00383

Manne, S., Kondru, N., Jin, H., Anantharam, V., Huang, X., Kanthasamy, A., et al. (2020a). α-Synuclein real-time quaking-induced conversion in the submandibular glands of Parkinson's disease patients. *Mov. Disord.* 35, 268–278. doi: 10.1002/mds.27907

Manne, S., Kondru, N., Jin, H., Serrano, G. E., Anantharam, V., Kanthasamy, A., et al. (2020b). Blinded RT-QuIC analysis of α-Synuclein biomarker in skin tissue from Parkinson's disease patients. *Mov. Disord.* 35, 2230–2239. doi: 10.1002/mds.28242

Marmion, D. J., Peelaerts, W., and Kordower, J. H. (2021). A historical review of multiple system atrophy with a critical appraisal of cellular and animal models. *J. Neural Transm. (Vienna)* 128, 1507–1527. doi: 10.1007/s00702-021-02419-8

Mazzetti, S., Basellini, M. J., Ferri, V., Cassani, E., Cereda, E., Paolini, M., et al. (2020). α-Synuclein oligomers in skin biopsy of idiopathic and monozygotic twin patients with Parkinson's disease. *Brain* 143, 920–931. doi: 10.1093/brain/awaa008

Motter, R., Vigo-Pelfrey, C., Kholodenko, D., Barbour, R., Johnson-Wood, K., Galasko, D., et al. (1995). Reduction of beta-amyloid peptide42 in the cerebrospinal fluid of patients with Alzheimer's disease. *Ann. Neurol.* 38, 643–648. doi: 10.1002/ana.410380413

Nakagaki, T., Nishida, N., and Satoh, K. (2021). Development of α-Synuclein real-time quaking-induced conversion as a diagnostic method for α-Synucleinopathies. *Front. Aging Neurosci.* 13:703984. doi: 10.3389/fnagi.2021.703984

Parnetti, L., Gaetani, L., Eusebi, P., Paciotti, S., Hansson, O., El-Agnaf, O., et al. (2019). CSF and blood biomarkers for Parkinson's disease. *Lancet Neurol.* 18, 573–586. doi: 10.1016/s1474-4422(19)30024-9

Pouclet, H., Lebouvier, T., Coron, E., Rouaud, T., Flamant, M., Toulgoat, F., et al. (2012). Analysis of colonic alpha-synuclein pathology in multiple system atrophy. *Parkinsonism Relat. Disord.* 18, 893–895. doi: 10.1016/j.parkreldis.2012.04.020

Rcom-H'cheo-Gauthier, A. N., Osborne, S. L., Meedeniya, A. C., and Pountney, D. L. (2016). Calcium: alpha-Synuclein interactions in alpha-Synucleinopathies. *Front. Neurosci.* 10:570. doi: 10.3389/fnins.2016.00570

Rong, Z., Shen, F., Wang, Y., Sun, L., Wu, J., Zhang, H., et al. (2021). Phosphorylated α-synuclein and phosphorylated tau-protein in sural nerves may contribute to differentiate Parkinson's disease from multiple system atrophy and progressive supranuclear paralysis. *Neurosci. Lett.* 756:135964. doi: 10.1016/j.neulet.2021.135964

Serratos, I. N., Hernandez-Perez, E., Campos, C., Aschner, M., and Santamaria, A. (2022). An update on the critical role of alpha-Synuclein in Parkinson's disease and other Synucleinopathies: from tissue to cellular and molecular levels. *Mol. Neurobiol.* 59, 620–642. doi: 10.1007/s12035-021-02596-3

Stefani, A., Iranzo, A., Holzknecht, E., Perra, D., Bongianni, M., Gaig, C., et al. (2021). Alpha-synuclein seeds in olfactory mucosa of patients with isolated REM sleep behaviour disorder. *Brain* 144, 1118–1126. doi: 10.1093/brain/awab005

Sun, Z. F., Xiang, X. S., Chen, Z., Zhang, L., Tang, B. S., Xia, K., et al. (2014). Increase of the plasma α-synuclein levels in patients with multiple system atrophy. *Mov. Disord.* 29, 375–379. doi: 10.1002/mds.25688

Thomas, P., Holland, N., Bolognesi, C., Kirsch-Volders, M., Bonassi, S., Zeiger, E., et al. (2009). Buccal micronucleus cytome assay. *Nat. Protoc.* 4, 825–837. doi: 10.1038/nprot.2009.53

Tian, C., Liu, G., Gao, L., Soltys, D., Pan, C., Stewart, T., et al. (2019). Erythrocytic α-Synuclein as a potential biomarker for Parkinson's disease. *Transl. Neurodegener* 8:15. doi: 10.1186/s40035-019-0155-y

Vivacqua, G., Latorre, A., Suppa, A., Nardi, M., Pietracupa, S., Mancinelli, R., et al. (2016). Abnormal salivary Total and oligomeric alpha-Synuclein in Parkinson's disease. *PLoS One* 11:e0151156. doi: 10.1371/journal.pone.0151156

Vivacqua, G., Suppa, A., Mancinelli, R., Belvisi, D., Fabbrini, A., Costanzo, M., et al. (2019). Salivary alpha-synuclein in the diagnosis of Parkinson's disease and progressive Supranuclear palsy. *Parkinsonism Relat. Disord.* 63, 143–148. doi: 10.1016/j.parkreldis.2019.02.014

Wang, Z., Becker, K., Donadio, V., Siedlak, S., Yuan, J., Rezaee, M., et al. (2020). Skin α-Synuclein aggregation seeding activity as a novel biomarker for Parkinson disease. *JAMA Neurol.* 78, 30–11. doi: 10.1001/jamaneurol.2020.3311

Yang, F., Li, W. J., and Huang, X. S. (2018). Alpha-synuclein levels in patients with multiple system atrophy: a meta-analysis. *Int. J. Neurosci.* 128, 477–486. doi: 10.1080/00207454.2017.1394851

Yu, Z., Liu, G., Li, Y., Arkin, E., Zheng, Y., and Feng, T. (2022). Erythrocytic alpha-Synuclein species for Parkinson's disease diagnosis and the correlations with clinical characteristics. *Front. Aging Neurosci.* 14:827493. doi: 10.3389/fnagi.2022.827493

Zheng, Y., Yu, Z., Zhao, J., Cai, H., Wang, Z., Wang, X., et al. (2022). Oral mucosa derived alpha-Synuclein as a potential diagnostic biomarker for Parkinson's disease. *Front. Aging Neurosci.* 14:867528. doi: 10.3389/fnagi.2022.867528

frontiers | Frontiers in Aging Neuroscience

TYPE Original Research
PUBLISHED 31 October 2022
DOI 10.3389/fnagi.2022.981451

OPEN ACCESS

EDITED BY
Nilton Custodio,
Peruvian Institute of Neurosciences (IPN), Peru

REVIEWED BY
Mehmet Ilyas Cosacak,
Helmholtz Association of German Research Centers, Germany
Victor Montal,
Sant Pau Institute for Biomedical Research, Spain

*CORRESPONDENCE
Pan Li
doc_panpan@163.com

SPECIALTY SECTION
This article was submitted to Alzheimer's Disease and Related Dementias, a section of the journal Frontiers in Aging Neuroscience

RECEIVED 30 June 2022
ACCEPTED 10 October 2022
PUBLISHED 31 October 2022

CITATION
Li P, Quan W, Wang Z, Liu Y, Cai H, Chen Y, Wang Y, Zhang M, Tian Z, Zhang H and Zhou Y (2022) Early-stage differentiation between Alzheimer's disease and frontotemporal lobe degeneration: Clinical, neuropsychology, and neuroimaging features.
Front. Aging Neurosci. 14:981451.
doi: 10.3389/fnagi.2022.981451

Early-stage differentiation between Alzheimer's disease and frontotemporal lobe degeneration: Clinical, neuropsychology, and neuroimaging features

Pan Li [1,2,3]*, Wei Quan[4,5], Zengguang Wang[4,5], Ying Liu[1,2,3], Hao Cai[1,2,3], Yuan Chen[1,2,3], Yan Wang[1,2,3], Miao Zhang[1,2,3], Zhiyan Tian[1,2,3], Huihong Zhang[1,2,3] and Yuying Zhou[1,2,3]

[1]Department of Neurology, Tianjin Huanhu Hospital, Tianjin, China, [2]Department of Neurology, Tianjin Huanhu Hospital Affiliated to Tianjin Medical University, Tianjin Huanhu Hospital Affiliated to Nankai University, Tianjin University Huanhu Hospital, Tianjin, China, [3]Tianjin Key Laboratory of Cerebral Vascular and Neurodegenerative Diseases, Tianjin Neurosurgery Institute, Tianjin Huanhu Hospital, Tianjin, China, [4]Department of Neurosurgery, General Hospital of Tianjin Medical University, Tianjin, China, [5]Tianjin Key Laboratory of Injuries, Variations and Regeneration of Nervous System, Tianjin Neurological Institute, Tianjin, China

Background: Alzheimer's disease (AD) and frontotemporal lobar degeneration (FTLD) are the two most common forms of neurodegenerative dementia. Although both of them have well-established diagnostic criteria, achieving early diagnosis remains challenging. Here, we aimed to make the differential diagnosis of AD and FTLD from clinical, neuropsychological, and neuroimaging features.

Materials and methods: In this retrospective study, we selected 95 patients with PET-CT defined AD and 106 patients with PET-CT/biomarker-defined FTLD. We performed structured chart examination to collect clinical data and ascertain clinical features. A series of neuropsychological scales were used to assess the neuropsychological characteristics of patients. Automatic tissue segmentation of brain by Dr. Brain tool was used to collect multi-parameter volumetric measurements from different brain areas. All patients' structural neuroimage data were analyzed to obtain brain structure and white matter hyperintensities (WMH) quantitative data.

Results: The prevalence of vascular disease associated factors was higher in AD patients than that in FTLD group. 56.84% of patients with AD carried at least one APOE ε4 allele, which is much high than that in FTLD patients. The first symptoms of AD patients were mostly cognitive impairment rather than behavioral abnormalities. In contrast, behavioral abnormalities were the prominent early manifestations of FTLD, and few patients may be accompanied by memory impairment and motor symptoms. In direct comparison, patients with AD had slightly more posterior lesions and less

frontal atrophy, whereas patients with FTLD had more frontotemporal atrophy and less posterior lesions. The WMH burden of AD was significantly higher, especially in cortical areas, while the WMH burden of FTLD was higher in periventricular areas.

Conclusion: These results indicate that dynamic evaluation of cognitive function, behavioral and psychological symptoms, and multimodal neuroimaging are helpful for the early diagnosis and differentiation between AD and FTLD.

KEYWORDS

Alzheimer's disease, frontotemporal lobar degeneration, differential diagnosis, neuropsychology, multimodal neuroimaging

Introduction

Alzheimer's disease (AD) and frontotemporal lobar degeneration (FTLD) are two entities of major neurodegenerative disorders, leading to dementia, especially among young patients (<65 years old) (Neary et al., 1998; Dubois et al., 2014). Episodic memory impairment is usually the first symptom in the course of AD, however, variants of AD characterized by visual and language impairments have been well described and are termed as posterior cortical atrophy (PCA) (Benson et al., 1988; Crutch et al., 2012; Dubois et al., 2014) and logopenic variant primary progressive aphasia (lvPPA) (Mesulam, 2008; Gorno-Tempini et al., 2011; Dubois et al., 2014). A less common phenotype is the "frontal variant" of AD (fv-AD), with a clinical manifestations of mainly behavioral and/or executive disorders, which is easily misdiagnosed as FTLD (Dubois et al., 2014). Frontotemporal dementia (FTD) is a series of clinically heterogeneous disease, mainly manifested by behavioral abnormalities, language disorders, and executive function deficits. At present, it is classified into three major clinical types, including behavioral variant frontotemporal dementia (bvFTD) (Rascovsky et al., 2011), semantic variant of primary progressive aphasia (svPPA), and non-fluent variant primary progressive aphasia (nfvPPA) (Gorno-Tempini et al., 2011). Behavioral and executive disorders are predominant in bvFTD, while PPAs have severe language deficits. In addition, parkinsonism and motor neuron disease can be noted in many cases (Liu et al., 2019). No matter what symptoms appear, these disorders will develop overtime, and the symptoms will change with the course of the disease. Thereby, it may be difficult to establish an accurate diagnosis in the early stage of both diseases.

Since the clinical heterogeneity of the two disease spectrums, the early symptoms may be ambiguous and overlapping. The current clinical standard requires qualitative examination of clinical core symptoms and neuroimaging features, but due to the lack of high sensitivity and specificity, it is impossible to accurately differentiate AD from FTLD. Some clinical observational studies have shown that early episodic memory impairment should be the exclusion criteria for FTLD, but, actually, it is not absolutely (Katisko et al., 2019). Similarly, it is reported that behavioral and psychological symptoms are the characteristic manifestations of patients with FTLD, but some studies have shown that the proportion of neuropsychiatric symptoms in patients with AD can be as high as 93.4% (Laakso et al., 2000). Traditional visual assessment of brain MRI requires the time of an well-experienced neuroradiologist and provides only moderate sensitivity and specificity (Harper et al., 2016). Early diagnosis requires techniques, such as fluorodeoxyglucose-positron emission tomography (FDG-PET), to detect early brain changes, whereas its availability is limited and the costs is relatively high (Smailagic et al., 2015; Minoshima et al., 2021). When it is difficult to distinguish between AD and FTLD, the ways of computer-aided diagnosis may be useful. These methods utilize multivariate data analysis techniques to train models (classifiers) based on neuroimaging or related data, so as to realize objective diagnosis. Moreover, computer-aided diagnosis can take advantage of subtle between-group differences, which is more accurate than using only clinical criteria (Kloppel et al., 2012). Using structural MRI to discover characteristic patterns of brain atrophy, the accuracy of computer-aided diagnosis in the differentiation of AD and FTLD was yielded up to 84% (Raamana et al., 2014; Moller et al., 2016).

In addition to using structural MRI, evidence of neurodegeneration can also be surveyed by using advanced T2-weighted MRI sequences to detect the white matter hypersignal (WMH) changes, which have emerged as a potential biomarker of neurodegenerative diseases (Desmarais et al., 2021). Regional WMH is related to the clinical manifestation of AD and FTLD. In prospective longitudinal studies of elderly with normal cognition and AD patients, periventricular WMH was

negatively correlated with mental processing speed, and WMH in left temporal lobe was negatively correlated with memory performance (Smith et al., 2011; Ramirez et al., 2014). However, the neural correlates of WMH have not been extensively and rigorously studied in AD and FTLD. Mapping the distribution and burden of WMH in AD and FTLD can provide further insight into the underlying pathological mechanisms.

Although both diseases and their subtypes have been well incorporated into new diagnostic criteria (Gorno-Tempini et al., 2011; Rascovsky et al., 2011; Dubois et al., 2014), little is known about the initial symptoms, risk factors, genetic susceptibility, behavioral and neuropsychological characteristics and common pathological characteristics of these phenotype. It is necessary for better understanding of neurodegenerative diseases across the boundaries of different clinical entities, as it likely improves the ability of clinicians to identify the histopathological cause of dementia. We enrolled a large number of patients with AD or FTLD defined by biomarkers or neuroimaging in this retrospective study. In the present study, we aimed to better represent the clinical, neuropsychological, and neuroimaging features. We attempted to present a framework that contains a series of volume measurements of different brain tissues to supply clinical information for differential diagnosis of AD and FTLD. We also investigated the burden and distribution of WMH in these neurodegenerative diseases and studied the correlation of neuropsychiatric manifestations with brain WMH.

Materials and methods

Subjects and inclusion criteria

Two hundred one subjects were screened and included in the study, and a case-control clinical-imaging observational prospective study was conducted by the Dementia Research Institute (DRG) at Tianjin Huanhu Hospital between 2012 and 2021. All enrolled patients completed a standardized research battery of validated tests and multisequence imaging by a 3.0-T MRI scanner (MAGNETOM ESSENZA, Siemens Healthineers, Germany and Signa HDxt, GE Healthcare, USA) and partially by 18-fluorodeoxyglucose-positron emission computed tomography (^{18}FDG-PET-CT) and Pittsburgh compound B-positron emission computed tomography (^{11}C-PET-CT). All of them were assessed by at least 2 experienced specialists in the field of dementia. Patients who were clinically diagnosed with typical AD fulfilled the criteria for probable AD dementia as defined by the National Institute on Aging-Alzheimer's Association (NIA-AA) (McKhann et al., 2011) and the variants of AD fitted the International Working Group (IWG) –2 criteria (Dubois et al., 2014). FTLD patients met the clinical criteria for the FTLD disease spectrum (Gorno-Tempini et al., 2011; Rascovsky et al., 2011). Exclusion criteria: (1) those with disturbance of consciousness, severe aphasia or serious illness, unable to complete the evaluation of neuropsychological scale; (2) symptoms caused by other systemic diseases or non-degenerative diseases of nervous system; (3) patients with heart, lung, liver, kidney, endocrine system diseases, or serious medical diseases such as connective tissue disease, hematopathy, and malnutrition; (4) patients with a history of brain or other tumors, brain trauma, gas poisoning, long-term alcoholism, epilepsy, etc.; (5) abnormal behavior conforms to psychiatric diagnosis; (6) biomarkers indicate other neurodegenerative diseases (non-AD or FTLD).

Ethical considerations

All the subjects were accompanied by reliable caregivers, and the subjects and their families signed the informed consent form. All procedures are carried out according to the ethical standards specified by Tianjin Human trial Committee and approved by Ethics Committee of Tianjin Huanhu Hospital.

Clinical evaluation and procedures

Baseline demographics and clinical data were collected through comprehensive geriatric assessment to ensure confidentiality. Participants underwent a series of detailed neurological examinations to evaluate their clinic symptomatic status, cognitive and both behavioral and neuropsychiatric performances at baseline by the experienced, board-certified neurologist. The Mini-Mental State Examination (MMSE) (Molloy and Standish, 1997) and Montreal cognitive assessment scale (MoCA) (Hu et al., 2013) were applied to assess subjects' cognitive function, and the scores of each sub-item were recorded in detail. The Clinical Dementia Rating (CDR) (Morris, 1993) was used to estimate the grade of dementia. Behavioral and psychological symptoms evaluation: Neuropsychiatric Inventory Questionnaire (NPI) (Wang et al., 2012) and Frontal Behavioral Inventory (FBI) (Kertesz et al., 2000) were applied to evaluate the psychobehavioral symptoms of the subjects. Daily activity ability and emotional state of patients were evaluated by Activities of Daily Living (ADL) Scale (Eto et al., 1992) and Hamilton Depression scale 21 (HAMD-21), respectively (Faries et al., 2000).

Neuroimaging and biochemical assessment

Positron emission tomography (PET) and CSF estimation of each diagnostic group were shown in **Table 1**. ^{18}F-FDG-PET-CT was performed to assess patterns of hypometabolism across the brain. Amyloid PET using ^{11}C-Pittsburgh compound B (PiB)

TABLE 1 Baseline demographics and clinical characteristics of AD and FTLD groups.

Variables	AD	FTLD	Statistic value	*P*-value
Enrolled patients (n)	95	106	—	—
Age (mean ± SE, yrs.)	68.23 ± 0.95	63.24 ± 0.80	7.295 [b]	0.000*
Gender (M/F)	51/44	45/61	2.533 [a]	0.111
Course of disease (mean ± SE yrs.)	3.05 ± 0.31	2.03 ± 0.21	2.344 [b]	0.021*
Age of onset (mean ± SE, yrs.)	64.84 ± 1.17	59.94 ± 0.94	3.239 [b]	0.002*
Marital status (n [%])				
Married	95	106		
Not married	0	0	2.425 [a]	0.297
Widow (er)	7	15		
Dwelling state				
Living with Family	86	101		
Solitary	9	5	1.749 [a]	0.186
BMI (Mean ± SE, kg/m^2)	22.89 ± 0.45	23.89 ± 0.36	−1.744 [b]	0.083
Education (Mean ± SE, yrs.)	10.68 ± 0.42	9.93 ± 0.41	1.204 [b]	0.230
Smoking (n [%])	29 (30.52)	13 (12.26)	10.108 [a]	0.001*
Drinking (n [%])	23 (24.21)	9 (8.49)	9.249 [a]	0.002*
Dementia family history (n [%])	13 (13.68)	29 (27.36)	70.426 [a]	0.000*
Vascular diseases				
Hypertension (n [%])	35 (36.84)	28 (26.41)	2.531 [a]	0.112
Heart disease (n [%])	20 (21.05)	15 (14.16)	1.659 [a]	0.198
Diabetes (n [%])	24 (25.26)	15 (14.15)	3.956 [a]	0.047 *
Hyperlipemia (n [%])	14 (14.74)	6 (5.66)	4.606 [a]	0.032 *
Stroke history (n [%])	5 (5.26)	6 (5.66)	0.015 [a]	0.902
TC (Mean ± SE, mmol/l)	5.85 ± 0.25	5.29 ± 0.16	1.773 [b]	0.080
LDL-C (Mean ± SE, mmol/l)	3.43 ± 0.11	2.77 ± 0.20	1.553 [b]	0.125
TG (Mean ± SE, mmol/l)	1.37 ± 0.07	1.30 ± 0.11	0.542 [b]	0.590
HDL-C (Mean ± SE, mmol/l)	1.45 ± 0.05	1.39 ± 0.06	0.807 [b]	0.422
APOE ε4 carriers (n [%])	54 (56.84)	16 (15.09)	38.470 [a]	0.000*
AD7c-NTP (Mean ± SE, ng/ml)	3.36 ± 0.24	2.82 ± 0.35	1.283 [b]	0.205
^{18}FDG-PET-CT/^{11}C-PET-CT/CSF $A\beta_{42/40}$ biomarker (n)	95/11/44	82/9/26	—	—
Structural MRI	35	54	—	—
MMSE	17.47 ± 0.63	18.91 ± 0.60	−1.639 [b]	0.103
CDR	1.39 ± 0.11	1.36 ± 0.15	0.187 [b]	0.852
MoCA	18.64 ± 0.74	15.56 ± 1.17	2.348 [b]	0.022 *
NPI	8.93 ± 0.87	15.75 ± 2.51	−3.15 [b]	0.002 *
FBI	16.83 ± 1.44	24.05 ± 2.45	−2.649 [b]	0.010 *
FBI-A	9.15 ± 0.81	13.30 ± 1.36	−2.734 [b]	0.008 *
FBI-B	7.94 ± 0.76	10.75 ± 1.19	−2.004 [b]	0.049 *
ADL	32.27 ± 1.41	37.21 ± 1.65	−2.116 [b]	0.036
BADL	13.43 ± 0.65	14.84 ± 0.69	−1.417 [b]	*0.159
IADL	18.37 ± 0.87	21.91 ± 0.99	−2.536 [b]	0.012 *
HADM-21	6.51 ± 0.56	9.21 ± 0.80	−2.738 [b]	0.007 *

[a] is χ^2 statistic value and analyzed with Chi-square test, [b] is *t* statistic value and analyzed with independent sample *t*-tests; * $P < 0.05$ vs. FTLD group.
AD, Alzheimer's disease; AD7c-NTP, Alzheimers disease associated neural filament protein; ADL, Activity of Daily Life; BADL, Basic Activity of Daily Life; IADL, Instrumental Activity of Daily Life; APOE, Apolipoprotein E; BMI, Body Mass Index; CDR, Clinical Dementia Rating Scale; F, female; FBI, Frontal Behavioral Inventory; FBI-A, Frontal Behavioral Inventory, Positive term subscale; FBI-B, Frontal Behavioral Inventory, Negative term subscale; FTLD, Frontotemporal Lobar Degeneration; HADM-21, The 21-items Hamilton Depression Rating Scale; HDL-C, High density Lipoprotein Cholesterol; LDL-C, Low density Lipoprotein Cholesterol; M, male; MMSE, Mini-Mental State Examination; MoCA, Montreal Cognitive Assessment; NPI, Neuropsychiatric Inventory Questionnaire; PET, Positron Emission Computed Tomography; TC, Total Cholesterol; TG, Triglyceride.

(Klunk et al., 2004) and/or amyloid-$\beta_{42/40}$ biomarkers in CSF were applied for pathological evaluation.

On the second day after admission, morning blood or serum specimen was gathered after fasting at night. The levels of total cholesterol (TC), triglyceride (TG), high-density lipoprotein cholesterol (HDL-C), and low-density lipoprotein cholesterol (LDL-C) were gauged by ADVIA 2400 automatic biochemical analyzer (Siemens, Germany). The urine of AD-associated neural filament protein (AD7c-NTP) was also assessed.

Magnetic resonance imaging gathering and processing

Structural MRI scans were collected in our study: (1) T1-weighted MR images were obtained by a 3D magnetization-prepared rapid spin-echo (MPRAGE) sequence: repetition time/echo time (TR/TE) = 2530/3.43 ms; FA = 90°, matrix size = 256 × 256; field of view (FOV) = 265 × 224 mm^2; slice thickness = 1.0 mm; gap = 1.2 mm; (2) T2 fluid attenuated inversion recovery (T2 FLAIR) image: TR/TE = 8000/120 ms; matrix size = 512 × 512; field of view (FOV) = 240 × 240 mm^2; slice thickness = 1.2 mm; gap = 1.2 mm. The proposed method was preceded following the previously published description (Jiang et al., 2020; Wei et al., 2020). First, skull dissection was performed on T1W and T2 FLAIR images using FMRIB software library.[1] Then, based on rigid transformation and normalized mutual information, the T2 FLAIR images of skull dissection were aligned and registered to T1WI images through SPM12 (Ashburner and Friston, 2011). N4 deviation correction was then operated on T1W and T2 FLAIR images to eliminate low-frequency intensity heterogeneity.[2]

Brain structure and WMH quantitative data were analyzed using Dr. Brain analysis system ([3]registration number: 20212210359), which has its own standard healthy population database platform as a control. All patients' T1WI and T2 FLAIR DICOM data were compressed into Zip files and simultaneously uploaded to Dr. Brain cloud system for image analysis. This system is an automatic segmentation based on multi-template segmentation. A patient image is processed in the Dr. Brain cloud system for approximately 25 min to automatically generate a PDF report containing the information of absolute and relative (that is, the percentage of absolute volume of WMH in the total intracranial volume) volume of WMH of each brain region and brain regional volume (the total volume, parenchyma and brain white matter of more than 100 brain regions were recorded). Statistical parameter mapping (SPM)-voxel-based morphological analysis (VBM) and surface-based morphometry (SBM) were applied to quantify changes in gray matter structure under pathophysiological conditions. The differences of gray matter density (GMD) between groups were analyzed and implemented by VBM8 toolbox[4] and SPM8 (Wellcome Trust Centre for Neuroimaging, London, UK). Data were pre-treated on the basis of VBM8 toolbox. The results were controlled by potential confounding factors, including age, gender, total intracranial volume, and MRI equipment. For family-wise error on the cluster level, *P* value less than 0.01 was set as analysis threshold.

We observed four parameters in SBM: cortical thickness, sulcus depth, gyrification index, and fractal dimension of cortical complexity. The cerebral cortex is a highly folded sheet of gray matter (GM), with areas that fold inward called sulci and areas that fold outward called gyri. There are three commonly used surfaces to describe this sheet: outer surface, inner surface, and central surface (CS). Cortical thickness describes the distance between the inner and outer surfaces (Dahnke et al., 2013). Sulcal depth computation will be processed according to the following procedures (Lyu et al., 2018): first, interiors of the cortical surface are filled in the volumetric space. Then, the cerebral hull is obtained by closing sulci through a three-dimensional spherical morphological closing operation. Next, the volumetric Boolean operation defines the intersection between the exterior of the cortical surface and the interior of the cerebral hull, which is severed as a medium between those two interfaces. Finally, the geodesic distance is calculated inside the medium by solving an Eikonal equation. The actual depth calculation (wavefront propagation) is performed on multiple slices of the volume. The gyrification index is extracted from central surface data, based on absolute mean curvature, which is the mean curvature calculated from the average between the minimum and maximum curvatures of the surface in each vertex in mm^{-1} – the mean curvature maps will, hereafter, referred to as the gyrification index (Chaudhary et al., 2021). Fractal dimension is a quantitative indicator of the morphological complexity and variability of an object. The different metrics for measuring fractal dimension are Hausdoff dimension, box counting dimension, capacity dimension, and mass radius dimension. There is increasing evidence that shape analysis using fractal dimension provides better information about structural changes induced by neurological conditions, which can supplement the information obtained by conventional volumetric analysis (Sheelakumari et al., 2018).

Positron emission tomography image acquisition and processing

The acquisition and processing protocols for 18F-FDG and 11C-PIB PET imaging have been described in our previous

1 http://fsl.fmrib.ox.ac.uk/fsl/fslwiki/FSL

2 http://stnava.github.io/ANTs/

3 https://cloud.drbrain.net

4 https://neuro-jena.github.io/software.html#vbm

study (Zhang et al., 2017; Wang et al., 2019). Briefly, PET images were acquired in the three-dimensional scanning mode on a GE Discovery LS PET/CT 710 scanner. 11C-PIB was administered intravenously at a dose of 370-555MBq, and a 90-min dynamic PET scan was performed according to a predetermined protocol. One hour after the 11C-PiB PET scan, 185-259 MBq of 18F-FDG was then injected intravenously, A 10-min static PET emission scan was performed 40 min after FDG injection with the same scanning mode. FDG PET and PiB PET images were preprocessed using MRI data for partial volume effect correction and spatial normalization. PiB PET imaging analysis was performed using Statistical Parameter Mapping 8 (SPM8) software on MATLAB 2010b for Windows (Mathworks, Natick, MA, USA) or PMOD software (version 3.7, PMOD Technologies Ltd., Zurich, Switzerland), as described in our previous study. The average of all specific regions was calculated from the PiB integral image. FDG frames for each subject were summed and normalized to mean pons activity. It is then displayed on the NIH color scale and can be windowed and viewed on three planes according to the rater's discretion.

Visual rating for Pittsburgh compound B positron emission tomography and fluorodeoxyglucose-positron emission tomography

The PiB PET and FDG PET imaging results were evaluated by two experienced nuclear medicine physicians. The positivity or negativity of PiB PET was determined by the mean value of target regions to cerebellum ratio with a cutoff value of 1.5 (the upper 95% confidence interval from a cluster analysis of healthy individuals). 18F-FDG PET images were read with color scale and standard to preferably route clinical brain FDG PET reports. FDG PET images were graded and dichotomized as follows: temporoparietal cortex dominant hypometabolism, other brain regions dominant hypometabolism or non-specific and mild hypometabolism.

Statistical analysis

Chi-square test was used to examine the baseline demographic qualitative variables, described as the relative abundance ratio (%) or rate (%). Normally distributed quantitative variables were calculated using two independent sample *t*-tests or one-way analysis of variance (ANOVA). All values were presented as mean ± standard (SD) deviation. All statistical analyses were performed with SPSS 26.0 (SPSS, Inc., USA). A P value <0.05 was considered statistically significant.

Data availability

Anonymized data can be obtained from the corresponding author upon request from any qualified researcher to replicate protocols and results.

Results

Demographic, biomarker measurements, and neuroimaging of the study population

Demographic, clinical characteristic data, and biomarker measurements were summarized in Table 1. We recruited 95 AD patients (51 men and 44 women) and 106 FTLD patients (45 men and 61 women). All the diagnoses of the participants were confirmed by ^{18}FDG-PET-CT or ^{11}C-PET-CT combined with cerebrospinal fluid amyloid-β 42 ratio 40 ($A\beta_{42/40}$) biomarker results. Patients with FTLD were relatively young at time of disease onset and diagnosis (mean age: age at onset, 59.94 ± 0.94 years; age at diagnosis, 63.24 ± 0.80 years) and had more shorter time to diagnosis (mean time, 2.03 ± 0.21 years) compared with AD patients (mean age: age at onset, 64.84 ± 1.17 years; age at diagnosis, 68.23 ± 0.9 years; course of disease, 3.05 ± 0.31). Smoking, drinking, and risk factors associated with vascular disease (diabetes, hyperlipemia) were more frequent in AD patients; however, the genetic predisposition in FTLD families is more pronounced than in patients with AD. Apolipoprotein E (APOE) ε4 allele was more common in the AD group. APOE ε4 alleles occurred in 56.84% of patients in the AD group and 15.09% of patients in the FTLD group.

Cognitive function analysis showed that there was no remarkable difference in the total score of MMSE and CDR between the two groups, but the MoCA scores of FTLD patients were lower than that of AD patients. FTLD patients had more severe psychobehavioral symptoms, mood disorders, and executive dysfunction as compared with AD patients. Although not statistically significant, patients with FTLD tended to decrease in the ability to perform daily activities and had higher scores on the instrumental activity of daily life (IADL).

Typical neuroimaging features of ^{18}FDG-PET-CT in different subtypes of two disease groups are summarized in Figure 1. Typical AD patients exhibit a typical default network pattern, with hypometabolic effects in the temporoparietal junction areas including precuneus and posterior cingulate cortex. Frontal variant in AD group was more frequently involved in the frontal cortical areas (such as anterior cingulate, orbitofrontal cortex, middle and superior frontal gyrus) compared with typical AD patients. Logopenic variant of AD displayed predominant posterior perisylvian or parietal hypometabolism. In FTLD groups, behavioral variant FTD

patients showed frontal and anterior temporal hypometabolism on PET, svPPA patients showed more frequently relative involvement in the anterior temporal, and nfvPPA patients showed more involvement in the posterior fronto-insular.

Clinical presentations comparison among diagnostic groups

In the study population, hypertension, diabetes, heart disease, sleeping disorder, hyperlipemia, stroke history, and traumatic cerebral injury were the most frequently noted diseases in the history of medicine. The incidences of diabetes and hyperlipemia histories in AD were remarkably higher than that in FTLD (confounding factors were corrected by logisitc regression analysis). The proportions of AD patients with smoking and drinking habits were also higher than those with FTLD patients. However, the incidence of thyroid disease is higher in FTLD than in AD (Figure 2A).

The frequency of cognitive impairment (91.6%) was higher than that of behavioral changes (6.3%) in AD patients. Conversely, patients with FTLD predominantly presented with behavioral deficits (67.9%) or both behavioral and motor dysfunction (10.4%) as the first symptoms of the disease (Figure 2B). Although all of the FTLD patients were satisfied, the diagnostic criteria of $\geq$3 of 6 core behavioral/cognitive symptoms required to diagnose possible behavioral variability FTD at the time of diagnosis, most patients were only near the threshold value of diagnostic criteria at the onset of symptoms [0 feature: 18/106 (16.98%), 1 feature: 23/106 (21.70%) or 2 features: 29/106 (27.35%), (Figure 2C)], and had more behavioral symptoms compared with AD patients. Among the neuropsychiatric list fields frequently mentioned in FTLD population, apathy, disinhibition, and appetite were the most prominent, followed by agitation and irritability, which were less common (Figure 2D).

Changes in neuropsychological and neuropsychiatric symptoms among diagnostic groups

In order to avoid the influence of the severity of dementia, patients in AD group and FTLD group were divided into three grades: CDR1 stage (AD 33 cases, FTLD 27 cases), CDR2 stage (AD 45 cases, FTLD 57 cases), and CDR3 stage (AD 17 cases, FTLD 22 cases). In the evaluation of cognitive function, AD patients mainly showed decreased delayed recall ability in the early stage, problems in attention, orientation, executive function, and language became more and more obvious as the disease progressed (Figures 3A–D). However, in FTLD patient group, attention, executive and language dysfunction, and decreased abstraction were always the earliest symptoms. In the late stage, overall cognitive decline and memory impairment were observed (Figures 3A–D). In neuropsychiatric behavior evaluation, patient group with FTLD showed worse neuropsychiatric functions than AD group, almost in all subdomains. Patients with AD generally developed behavioral abnormalities in the middle and later stages of the disease, mainly manifested as depression, anxiety, and irritability. In patients with mild-to-moderate FTLD, agitation, disinhibition, and appetite were the first prominent behavioral symptoms, then followed by euphoria, apathy, and irritability, and finally developed into a comprehensive spectrum involved. Hallucination was the least common symptom, even in the advanced stages of FTLD (Figure 3E).

Volumetric feature differences of brain regions among diagnostic groups

Volumetric differences between AD and FTLD, as well as the differences between each group with healthy controls, are summarized in Figure 4. The structural changes of brain regions in patients with AD and FTLD were obvious. Compared with FLTD, AD patients have a larger frontal lobe volume and a tendency to have larger superior frontal gyrus and frontal pole volume in their subdomains. Although there were no significant difference in the overall volume of temporal lobe, occipital lobe, parietal lobe, basal ganglia, and cerebellum between the two groups, subfields analysis showed that the volumes of temporal polar and transtemporal region were more preserved in AD patients, and the volumes of parietal, occipital lobe and cerebellum subareas were relatively less. There was no difference in hippocampal volume between the two groups, however, bilateral parahippocampal gyrus and entorhinal cortex volumes decreased in AD patients. In FTLD individuals, there is asymmetric atrophy of the right putamen and left caudate nuclei in the subcortical basal ganglia region.

We performed VBM comparisons between the different patients and control groups (Figure 5), and trimmed for age, gender, disease severity, and total intracranial volume. Compared with the healthy control group, the characteristic pattern of brain atrophy in AD patients involved a large area of the temporoparietal cortex, posterior cingulate gyrus, precuneus, and part of the occipital lobes. The frontal cortex is also partially involved in AD patients (Figure 5A). In FTLD group, the affected atrophy areas were mainly concentrated in the frontal pole, orbito-frontal lobe, frontal insula, anterior cingulate gyrus, and bilateral anterior temporal lobes comparing to healthy control group. It also affects the parietal part of the posterior central gyrus (Figure 5B). Direct comparison between patient groups showed the posterior involvement of AD patients and the anterior involvement in FTLD patients had significantly different atrophy patterns, which mainly survived the correction of family-wise error (FWE) with $P > 0.05$. FTLD patients showed asymmetry in the affected brain regions (Figure 5C).

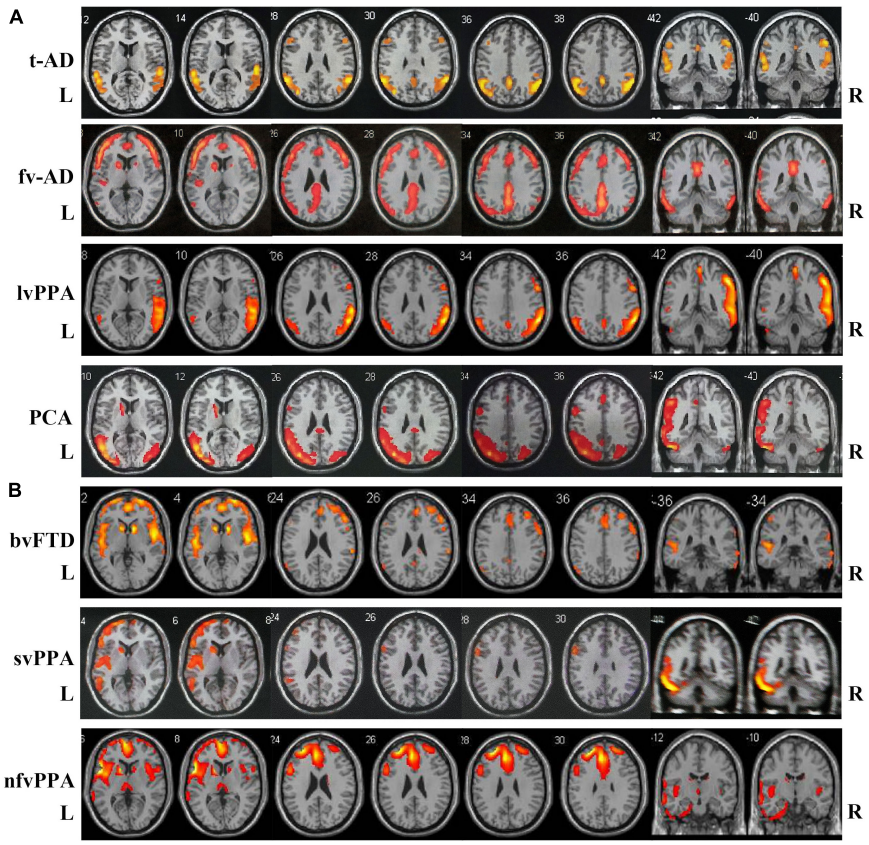

FIGURE 1
Atrophy maps in different clinical subtypes of AD and FTLD disease groups analyzed by ^{18}FDG-PET-CT. **(A)** Typical AD is characterized by predominant temporoparietal cortex atrophy, fv-AD will partially spread to frontal cortical regions. LvPPA displayed predominant posterior perisylvian or parietal atrophy. PCA mainly involved temporo-occipital cortex atrophy. **(B)** In FTLD disease group, bv-FTD showed frontal and anterior temporal atrophy, svPPA was more frequent with involvement of anterior temporal, and nfvPPA patient showed more posterior fronto-insular atrophy. t-AD, typical Alzheimer's disease; fv-AD, frontal variant Alzheimer's disease; lvPPA, logopenic variant primary progressive aphasia; PCA, posterior cortical atrophy; bv-FTD, behavioral variant frontotemporal dementia; svPPA, semantic variant of primary progressive aphasia; nfvPPA, non-fluent variant primary progressive aphasia.

In the SBM-based structural brain characterization, differences in cortical thickness (Figure 6), sulcus depth, gyrification index, and fractal dimension (Supplementary Figure 1) between the two disease groups of patients and healthy controls were analyzed. The results showed that there were disease-specific alterations in brain structure in both AD and FTLD groups compared with the control group (Figures 6A,B). In the AD group, cortical thickness in the superior parietal lobe, inferior parietal, superior temporal, lateral occipital, fusiform, and rostral middle frontal lobe decreased symmetrically (Figure 6A). However, in FTLD patient group, the cortical thickness of the supramarginal, caudal middle frontal, pars triangularis, superior frontal, and superior temporal decreased significantly, and the distribution tended to be asymmetrical (Figure 6B). As compared to AD patients, the FTLD patient group showed a reduction in pars triangularis, rostral middle frontal, lateral orbitofrontal (Figure 6C), whereas AD exhibited a significant reduction in the superior parietal, lateral occipital, precuneus cortex as compared to FTLD patient group (Figure 6D) (voxel significance set to $P < 0.01$ or 0.001, corrected significance set to $P < 0.01$). The AD and FTLD patient groups exhibited characteristic changes in sulcus depth, gyrification index, and fractal dimension (Supplementary Figure 1) between the AD and FTLD patient groups as compared to the healthy controls and intercomparison. Specific brain areas involved are shown in the Supplementary Table 1.

White matter hyperintensities volumetrics and characteristics among diagnostic groups

According to different brain regions, white matter signals can be divided into cortical, periventricular, deep white matter, and subatentorial regions. There was no significant difference

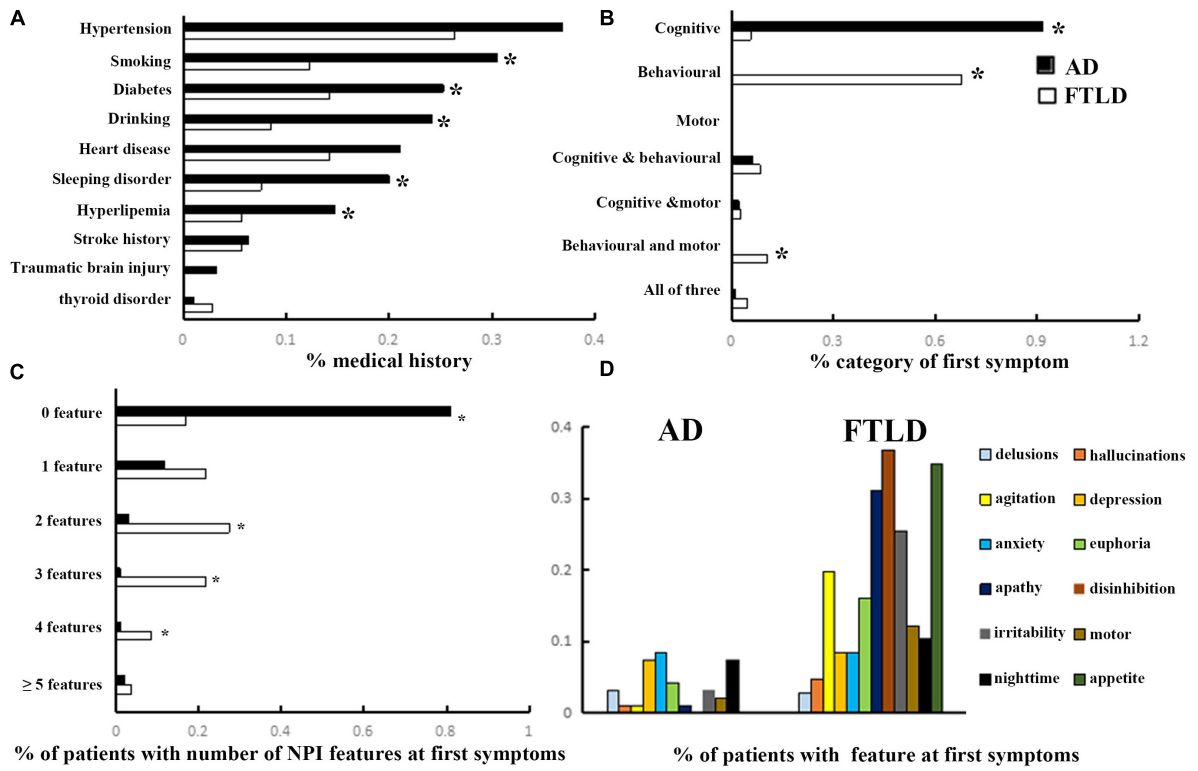

FIGURE 2
Clinical features comparison between AD and FTLD disease groups. **(A)** Past medical conditions in self-reported or supplied by caregivers. **(B)** Rate of first symptoms informed by patients and caregivers. **(C)** Frequency of psychobehavioral abnormalities in the first episode. **(D)** Clinical features of psychobehavioral abnormalities in the first symptom.

in total cerebral capacity between the two groups after checking for blood vascular hazard factors and age at the time of imaging (Figure 7A), but there were significant differences in WMH load and brain distribution between the study groups (Figures 7B–E). There were significant differences between groups in the total burden of WMH, and the average volume of AD group (8.05 ± 3.25 ml) was higher than that of FTLD group (0.60 ± 0.030 ml) (Figures 7B,C). The average volume of WMH in cerebral cortex of AD group was the highest. For FTLD group, results revealed that the WMH burden in the periventricular region was significantly higher than that in AD (Figures 7D,E). Neither AD group nor FTLD group had subatentorial white matter lesions (Figures 7D,E).

Discussion

Frontotemporal lobar degeneration (FTLD) and AD are the two main neurodegenerative diseases that cause dementia. Despite recent progress in the early characterization of both disorders, early clinical diagnosis remains a challenge. In this retrospective study, we evaluated the neuropsychological and multimodal neuroimaging properties of the clinical syndromes of AD and FTLD in a Chinese population. We compared biomarker or PET-CT-defined patients and analyzed the first-episode clinical features, the evolution of cognitive function and behavioral and psychological symptoms of these two diseases. Patients with AD often showed cognitive rather than behavioral symptoms at the initial symptoms. As the disease progresses, attention and orientation dysfunction become prominent and gradually accompanied by psychiatric and behavioral symptoms. However, in FTLD group, dysexecutive and language dysfunction features presented as the primarily cognitive phenotypes, accompanied by a certain degree of behavioral abnormalities, and memory deterioration from middle-to-late stage (Figures 3, 4). The prevalence of vascular disease associated factors and APOE ε4 were higher in AD patients than that in FTLD group (Table 1). AD patients were characterized by major atrophy of temporal parietal and relatively sparse of frontal gray matter, whereas FTLD patients typically present with frontal and temporal lobe involvement (Figures 4–6). In addition, we found differences in the burden and distribution of WMH on T2-weighted MRI between AD patients and FTLD patients. The WMH burden of the former was significantly higher than that of the latter, especially in cortical area, while the WMH burden in the periventricular

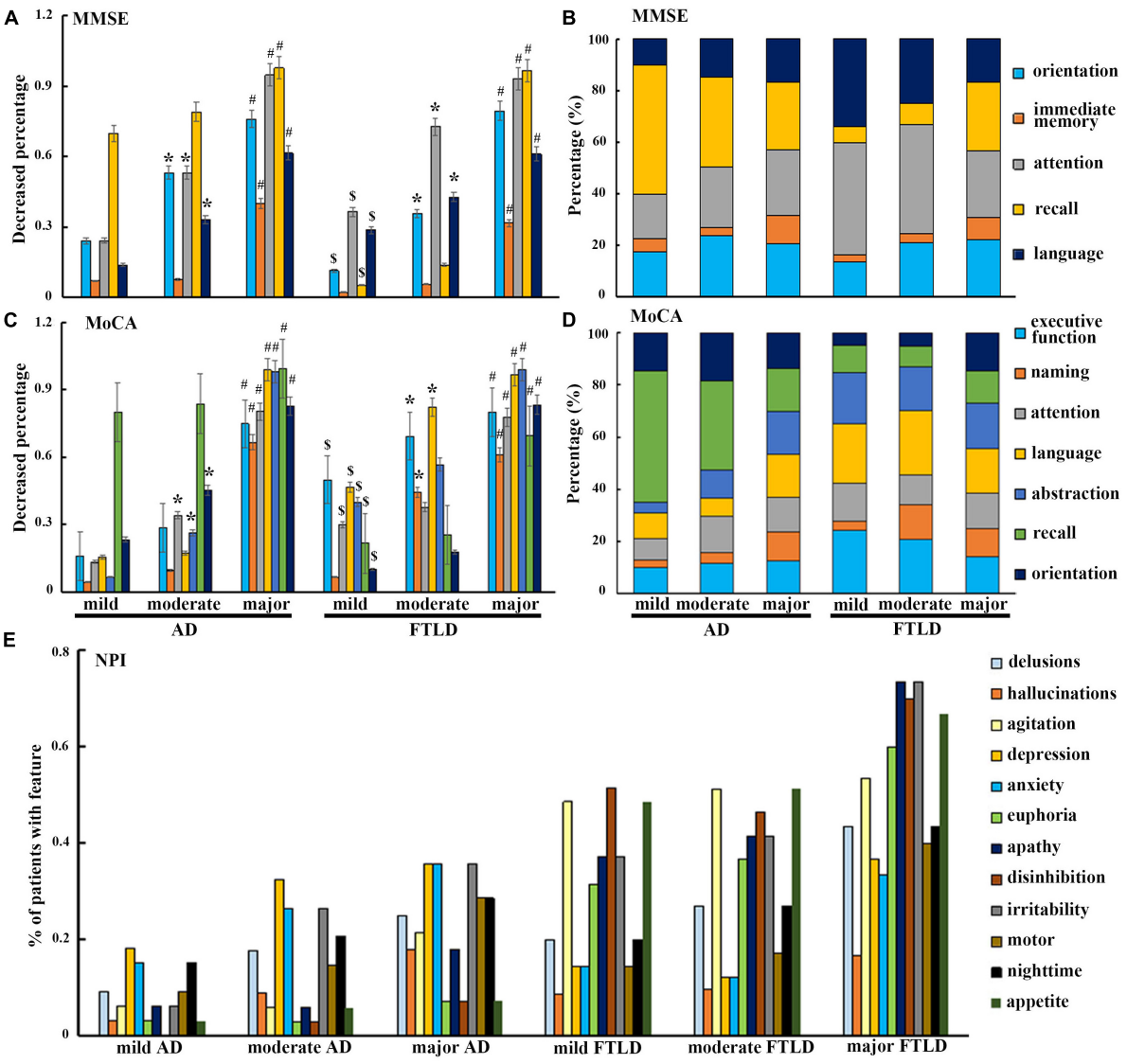

FIGURE 3
Neuropsychological characteristics comparison between AD and FTLD disease groups with disease progression. **(A–D)** Decreased degree of subscale items in MMSE and MoCA assessment with disease progression. **(E)** Frequency of neuropsychiatric symptoms in different stages of disease measured by NPI.

areas of the FTLD patients was higher than that of AD patient (Figure 7), suggesting potentially different underlying neuropathological processes.

Clinical features and neuropsychological profiles

Some progress has been made in using neuropsychological methods to analyze the differences between FTLD and AD from different manifestations in the cognitive field, but the different stages of the disease are poorly understood. The time sequence of clinical symptoms in the course of disease is the most reliable basis for the correct diagnosis. According to current criteria, memory impairment is not required for the early diagnosis of FTLD, or even as an exclusion criterion of early disease. However, memory loss and visuospatial orientation problems are usually the diagnostic criteria for early symptoms in AD patients, including core clinical symptoms (Gorno-Tempini et al., 2011; Rascovsky et al., 2011; Dubois et al., 2014). By comparison, FTLD patients may develop early neuropsychiatric symptoms, such as agitation and psychosis, consistent with a range of neurological and mental disorders (Rascovsky et al., 2011). Our observational data showed that although all patients with bvFTD met

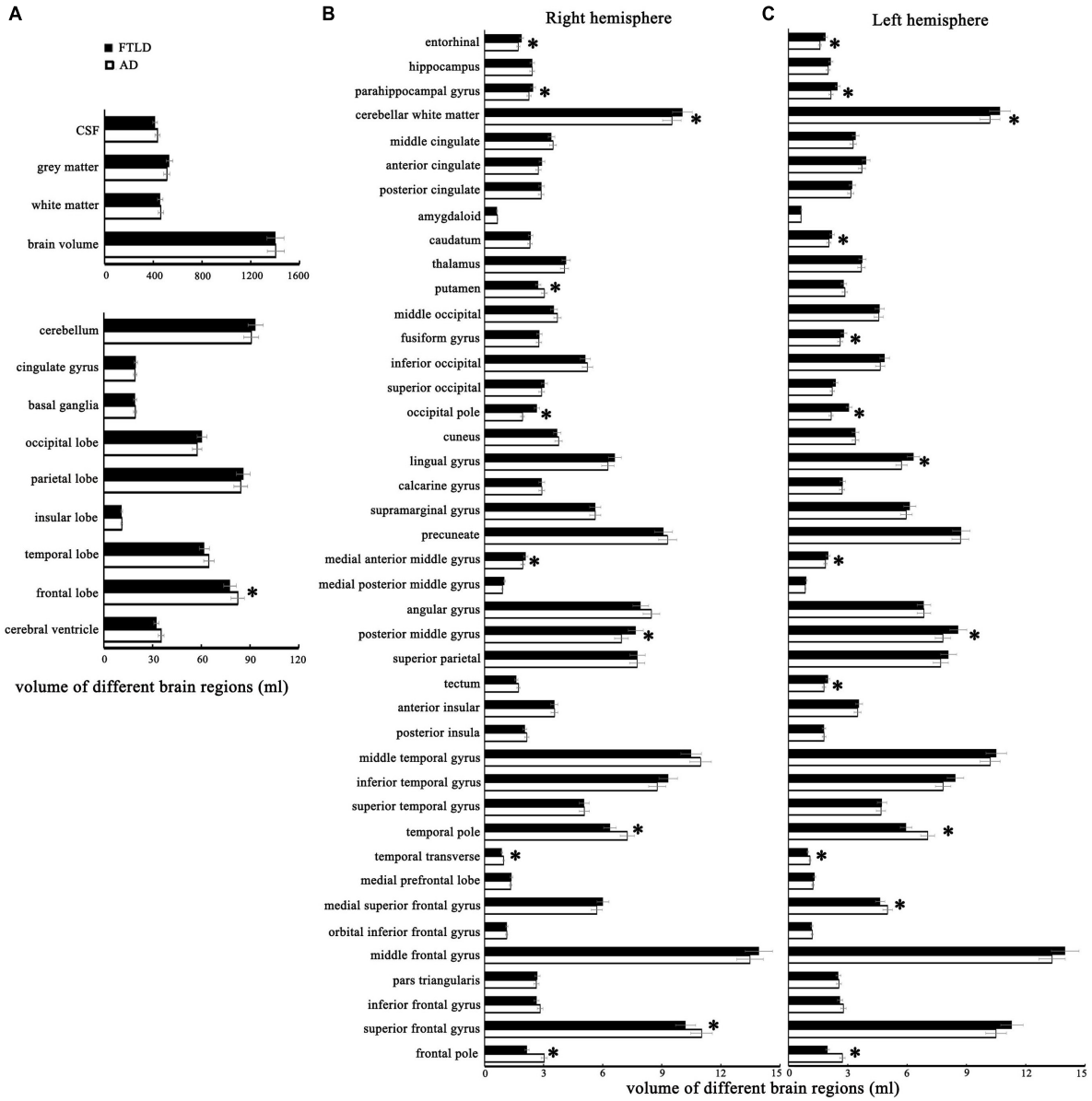

FIGURE 4
The structural MRI features with statistical differences between patients with AD and FTLD. **(A)** Comparison of different brain structures between the two groups. **(B)** Comparison of the cortical volume of different brain regions in the right cerebral hemisphere between the two groups. **(C)** Comparison of the cortical volume of different brain regions in the left cerebral hemisphere between the two groups.

the core clinical symptoms of possible diagnostic criteria at admission, most patients were just close to the threshold of diagnostic criteria at the onset of symptoms [0 feature: 18/106 (16.98%), 1 feature: 23/106 (21.70%) or 2 features: 29/106 (27.35%), Figure 2C], and some patients even have cognitive impairment [20/106 (18.87%), Figure 2B], or accompanied by motor disorders [10/106 (9.43%), Figure 2B] as the onset of symptoms. As a result, these patients are often initially misdiagnosed as psychiatric and other neurological diseases, most commonly AD. Therefore, misconceptions about the early symptoms of both diseases often delay a correct diagnosis.

In this study, through the subitem analysis of MMSE and MoCA, we found that both FTLD and AD patients had memory impairment, but AD patients showed more significant impairment, accompanied by obvious disorientation. However, orientation was relatively preserved in FTLD patients, which was related to the reservation of temporal-parietal lobe combined cortex, anterior cuneate lobe, and posterior cingulate gyrus in early FTLD patients (Figures 4–6). Through the clinical

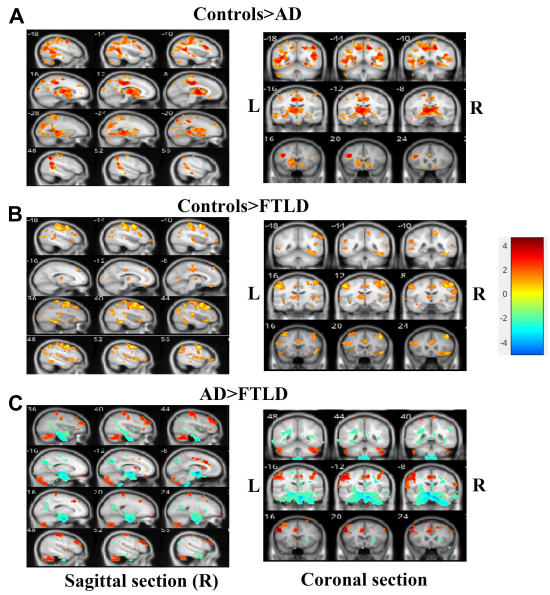

FIGURE 5
Voxel-based morphometry comparisons of gray matter volumes in AD or FTLD patients compared with healthy controls. The contrasts were adjusted according to age, gender, total intracranial volume and scanner type. **(A)** Comparison between AD patients and healthy controls; **(B)** Comparison between FTLD patients and healthy controls; **(C)** FTLD patients compared with AD patients. Color overlay shows $p_{unc} < 0.001$ for family-wise error = 0.05. The warm color of the color bar representing gray matter volume of controls lager than AD or FTLD, and cold color denoting gray matter volume of controls smaller than AD or FTLD **(A, B)**. The warm color of the color bar representing gray matter volume of AD lager than FTLD, and cold color denoting gray matter volume of AD smaller than FTLD **(C)**.

observation of patients with FTLD, it was found that the impairment of executive function was earlier and more severe than memory loss, but the orientation ability and visuospatial ability were preserved to a certain extent (Figures 3A–D). By stratifying the severity of dementia, we found that the degree of cognitive impairment was directly proportional to the severity of dementia in both groups. AD patients almost spread to cognitive areas such as attention, orientation, and language in the middle and later stages of the disease, while FTLD patients mainly showed executive function, attention and language dysfunction, and gradually appeared orientation and memory domains, which was basically consistent with the dynamic manifestations of clinical symptoms (Figures 3A–D).

It is worth noting that, there were remarkable differences between MMSE scores and MoCA scores in FTLD patients; however, the total score of MMSE and MoCA was almost identical in the AD population (Table 1). This is because the MMSE examination focuses more on the detection of memory and visuospatial ability, and these two cognitive areas are the main manifestations of cognitive impairment in AD patients. Therefore, MMSE can accurately reflect the actual degree of cognitive impairment in AD patients. However, due to lack of in-depth monitoring of executive function and language, clinical findings are not very sensitive to FTLD screening. In some patients with FTLD, MMSE is in normal range, but MoCA examination has indicated moderate damage. In the early stage of FTLD, executive ability and language dysfunction are the main cognitive manifestations, and both cognitive areas are reflected in the MoCA subscales, such as Trail Making Test and complex sentence repetition. Freitas et al. (2012) proposed that MoCA had better identification ability than MMSE through comparative study of AD and FTLD. When MoCA score is below 17 points, the sensitivity and specificity for FTLD were 78% and 98%, which were significantly higher than MMSE.

Potential risk factors

It is suggested that, at the onset of dementia, some clinical and demographic data can be used as predictors of differential diagnosis and future progression. In this study, we have investigated some of the demographic factors most relevant to the cognitive traits, such as age at disease onset, disease duration, and education (Table 1); clinical features as motor signs and behavioral disorders (Figure 2); APOE genotype (Table 1) and vascular diseases and medical histories (Figure 2 and Table 1). In recent years, it has been suggested that AD and FTLD might be kinds of cognitive disorder caused by both vascular pathological changes and neurodegenerative damage, especially in the AD spectrum (Nichols et al., 2021). Many previous longitudinal studies have also shown that vascular risk factors (VRFs) are hazard factors for AD, such as middle-age hypertension, hypercholesteremia, diabetes, obesity, stroke, atrial fibrillation, and lack of exercise (Yu et al., 2020). Our study was consistent with previous reports that the incidence of vascular disease-related histories such as hypertension, diabetes, hyperlipemia, and stroke history seemed over-represented in AD compared to FTLD. Currently, well-controlled VRFs may be one of the reasons for the decline in the prevalence and incidence rate of dementia in some countries (Wu et al., 2017). At the same time, recent researches have shown that VRFs-induced hypoperfusion and hypoxia can lead to amyloid-β accumulation by producing or restraining its degradation, which ultimately impairs neuronal and synaptic plasticity (Pluta et al., 2020; Babusikova et al., 2021). AD patients without VRFs in this study may also have mixed dementia and asymptomatic vasculopathy (Esiri et al., 1999).

Consistent with previous research, the prevalence of APOE ε4 carriers in AD patients (56.84%) was much higher than that in FTLD group (15.09%) in the Chinese cohort. ApoE ε4 has been identified as the strongest genetic predictor of the development of sporadic AD (Ferrari et al., 2018). Furthermore, APOE ε4 carrier status is another key factor of cognitive decline in AD patients with VRFs. APOE ε4 of AD patients are particularly

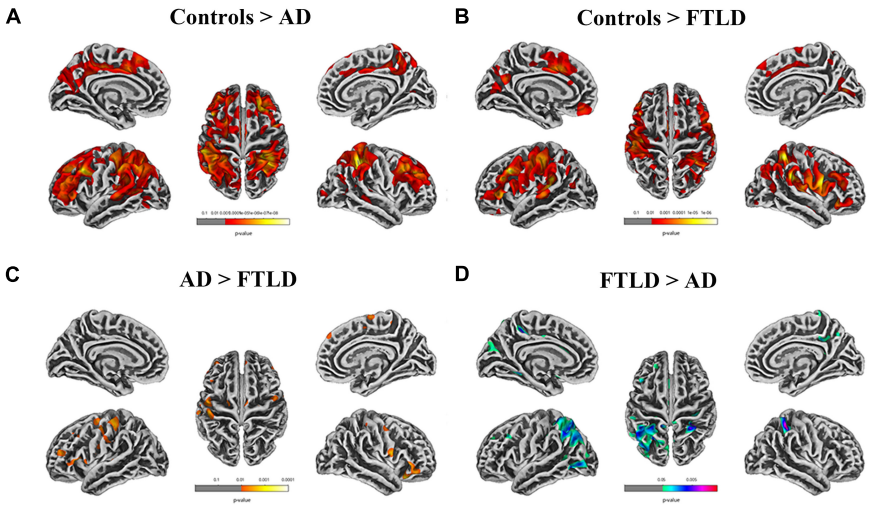

FIGURE 6
Cortical thickness alterations in different groups assessed by surface-based morphometry. **(A)** Comparison between AD patients and healthy controls; **(B)** Comparison between FTLD patients and healthy controls; **(C, D)** FTLD patients compared with AD patients. Color overlay shows $p_{unc} < 0.001$ for family-wise error = 0.05.

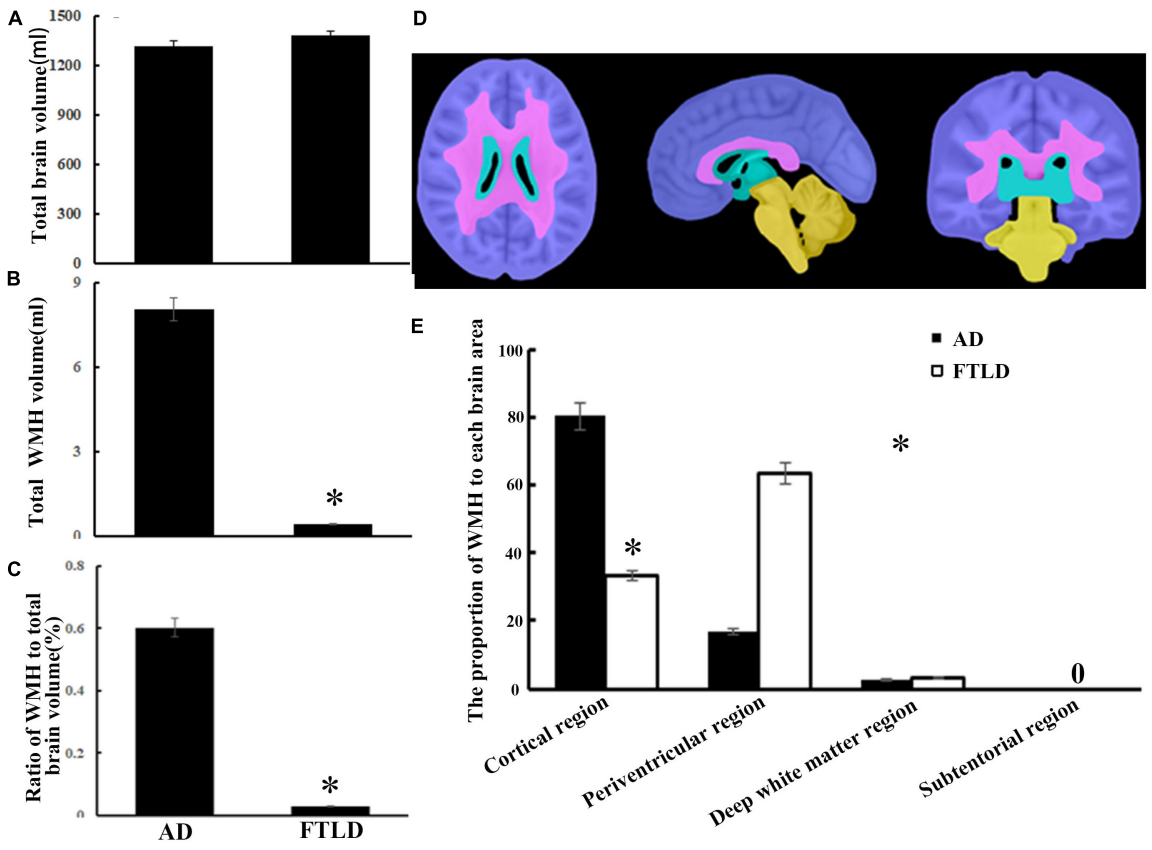

FIGURE 7
White matter hyperintensity volumes and distribution comparison between AD and FTLD disease groups. **(A)** Total brain volume comparison. **(B)** Total WMH volume comparison. **(C)** Total WMH ratio comparison. **(D)** Diagram of white matter region division supplied by semi-automatic brain region extraction. **(E)** Comparison of the proportion of WMH in different brain regions.

sensitive to VRFs (Lee et al., 2020). Accordingly, APOE ε4 carriage and VRFs may synergistically affect cognitive outcomes in patients with increased genetic and vascular risk (Lee et al., 2020). Functional imaging studies have shown that APOE ε4 carriers not only exhibit substantial reductions in regional cerebral blood flow over time (Thambisetty et al., 2010) but also reduced glucose metabolic rates in posterior cingulate and/or precuneus and lateral parietal lobe (Knopman et al., 2014). Another plausible explanation is that ApoE ε4 allele carriers would disturb the biochemical pathways of neurofibrillary tangle and affect amyloid-β accumulation (Cosentino et al., 2008).

Neuroimaging distinction between Alzheimer's disease and frontotemporal lobar degeneration

We identified neuroimaging differences in our study. The current results indicated that symmetry and volume differences in different brain domains, parahippocampal gyrus, entorhinal cortex, and asymmetrical atrophy in putamen and caudate nucleus may distinguish FTLD from AD (**Figure 4**). Notably, a voxel-based morphometric analysis comparison between the two groups showed a slight effect in the frontal lobe (traditionally supposed to be the core monitor of behavior and executive function) over classical AD, but not as prominent as we observed in FTLD individuals (**Figure 4**). Although previous cases and our clinical experience have shown that deep prefrontal involvement can be surveyed in patients with frontal variant of AD (Li et al., 2016), these single-subject effects may have been washed in group-level voxel-based morphometric analysis. The discrepancy in frontal atrophy partly explains why psychiatric symptoms, such as hallucinations anxiety and depression are always present in AD patients, but rare in FTLD patients. Complete destruction of frontal lobe function will result in a complete loss of disease awareness in FTLD patients, whereas some of this self-awareness is preserved in AD patients. SBM with non-linearly aligned cortical folding patterns provides precise standardization of participant brains, which may be useful in examining cortical morphology. By measuring cortical thickness, gray to white matter contrast (GWC), surface area, cortical volume, cortical microstructure and macrostructure, SBM provides the possibility to reveal the mechanisms of brain changes and elucidate neurological problems associated with neurodegenerative disease (Singh et al., 2022).

Mapping the distribution and burden of WMH in AD and FTLD will contribute further understand the underlying pathological mechanisms of these diseases. Indeed, previous studies have suggested that the preferential distribution of WMH in cortical regions of AD patients was related to tissue characteristics. For example, as it was located in the watershed areas, normal perfusion in this region was relatively low (Keith et al., 2017). Furthermore, hypersignal of white matter in the paraventricular area is due to periventricular small-vessel disease and neurodegenerative changes, such as amyloid deposition in arteries, arterioles, and veins, leading to brain atrophy and the onset of AD (Keith et al., 2017; Alosco et al., 2018). Conversely, the extensive white matter involvement in cortical and periventricular regions in our FTLD cases has always been without obvious vascular hazard factors or related illness. It has been reported that raised WMH load in symptomatic GRN mutant FTLD patients mainly existed in the frontal and occipital lobes (Sudre et al., 2017).

Although the exact mechanisms of white matter injury in the absence of progranulocyte precursor protein are unclear, it has been hypothesized that the functions of granulocyte precursor protein may play a critical role in neuroinflammation and vascular protection (Ahmed et al., 2007). In addition, other common pathological elements, such as Wallerian degeneration, may be the potential mechanism leading to preferential participation in the distribution of white matter lesions. As a disease with a strong genetic background, we will further analyze the relationship between genotype, neuropathology, neuroimaging, and clinical phenotype, as well as the underlying mechanisms in the subsequent research work.

Strengths and limitations

To the best of our knowledge, this is the only one of the largest series of direct comparison against well-characterized AD and FTLD patients in a Chinese Han population cohort. The detailed clinical, neuropsychiatric, and multimodal neuroimaging comparisons between these two patient populations would be crucial for future clinical trials. Our rigorous criteria based on detailed clinical examination, neuropsychological, and multimodal neuroimaging with FDG-PET, 3.0T structural MRI, and PiB PET amyloid assays, which enabled us to investigate relationships between neuroanatomical locations of atrophy or WMH, with neuropsychological and neuropsychiatric manifestations, facilitating early diagnosis of neurodegenerative disease. There are also some limitations. **First**, this is a case-selective clinical retrospective study, the recording of clinical data is inevitably incomplete, although we often make a decision with two experienced neurologists, sometimes the subjective judgment of clinicians is inevitable. Therefore, selective bias in clinical data should be taken into account. In addition, our enrolled patients were not racially diverse, therefore, enlarged samples from multi-centers and multi-ethnic are required for comparative analysis of different clinical subtypes. **Second**, the fact that not all patients had PiB PET, thereby the likelihood of mixed clinical superposition cannot be ruled out, because of the clinical and pathological heterogeneity of these two types of neurodegenerative dementia. **Finally**, it is worth mentioning that when we summarized

the multimodal imaging features, we did not stratify the different subtypes and different disease stages of the two groups. The heterogeneous composition of populations with different disease stages and baseline levels will partly affect the parameter analysis between clinical characteristics and neuroimaging biomarkers. Since the cross-sectional approach is not conducive to establishing a direct correlation between each clinical scale and neuroimaging changes, longitudinal studies are needed to reflect the direct correlation between the longitudinal performance of each scale, as well as the longitudinal neuroimaging evaluation of MRI parameters during the course of the disease and disease severity.

Conclusion

We performed a detailed clinical, neuropsychiatric, and multimodal neuroimaging analysis of AD patients compared with FTLD patients. We identified several differences, most importantly, the initial symptoms of the disease and clinical features in the progression of the disease. In addition, medical history, especially vascular disease and associated risk factors, involved brain regions and WMH burden and regional distribution gained from multimodal neuroimaging, may provide valuable supplements for early differential diagnosis. Further studies are warranted to investigate the genetics, neuropathology, biomarkers, and mechanistic pathways to track the course of the disease.

Data availability statement

The original contributions presented in this study are included in the article/**Supplementary material**, further inquiries can be directed to the corresponding author.

Ethics statement

All the subjects were accompanied by reliable caregivers, and the subjects and their families signed the informed consent form. All procedures are carried out according to the ethical standards specified by Tianjin Human trial Committee and approved by Ethics Committee of Tianjin Huanhu Hospital. The patients/participants provided their written informed consent to participate in this study.

Author contributions

PL conceived and monitored the research. HC, YC, and ZT performed the data collection. PL and WQ analyzed the data, wrote the original manuscript, and made modified. YZ, YW, and MZ participated in clinic diagnosis. YL and HZ were responsible for patient care and scales assessment. All authors examined the results and authorized the final version of the manuscript.

Funding

This study was supported by Tianjin Natural Science Foundation (820JCYBJC01380), the Youth Fund of the National Nature Science Foundation of China (81801076), the National Nature Science Foundation of China (82071402), Tianjin Municipal Health Commission Project (TJWJ2021MS029), and Tianjin Key Medical Discipline (Specialty) Construction Project (No. TJYXZDXK-052B).

Acknowledgments

We thank all our colleagues in the institute for their assistance and propose throughout the research.

Conflict of interest

The authors declare that the research was conducted in the absence of any commercial or financial relationships that could be construed as a potential conflict of interest.

Publisher's note

Supplementary material

The Supplementary Material for this article can be found online at: https://www.frontiersin.org/articles/10.3389/fnagi.2022.981451/full#supplementary-material

SUPPLEMENTARY FIGURE 1
Sulcus depth, gyrification index and fractal dimension alterations in different groups assessed by surface-based morphometry. **(A)** Comparison between AD patients and healthy controls; **(B)** Comparison between FTLD patients and healthy controls; **(C, D)** FTLD patients compared with AD patients. Color overlay shows $p_{unc} < 0.001$ for family-wise error = 0.05.

References

Ahmed, Z., Mackenzie, I. R., Hutton, M. L., and Dickson, D. W. (2007). Progranulin in frontotemporal lobar degeneration and neuroinflammation. *J. Neuroinflammation* 4:7. doi: 10.1186/1742-2094-4-7

Alosco, M. L., Sugarman, M. A., Besser, L. M., Tripodis, Y., Martin, B., Palmisano, J. N., et al. (2018). A Clinicopathological Investigation of White Matter Hyperintensities and Alzheimer's Disease Neuropathology. *J. Alzheimers Dis.* 63, 1347–1360. doi: 10.3233/JAD-180017

Ashburner, J., and Friston, K. J. (2011). Diffeomorphic registration using geodesic shooting and Gauss-Newton optimisation. *Neuroimage* 55, 954–967. doi: 10.1016/j.neuroimage.2010.12.049

Babusikova, E., Dobrota, D., Turner, A. J., and Nalivaeva, N. N. (2021). Effect of Global Brain Ischemia on Amyloid Precursor Protein Metabolism and Expression of Amyloid-Degrading Enzymes in Rat Cortex: Role in Pathogenesis of Alzheimer's Disease. *Biochemistry* 86, 680–692. doi: 10.1134/S0006297921060067

Benson, D. F., Davis, R. J., and Snyder, B. D. (1988). Posterior cortical atrophy. *Arch. Neurol.* 45, 789–793. doi: 10.1001/archneur.1988.00520310107024

Chaudhary, S., Kumaran, S. S., Goyal, V., Kaloiya, G. S., Kalaivani, M., Jagannathan, N. R., et al. (2021). Cortical thickness and gyrification index measuring cognition in Parkinson's disease. *Int. J. Neurosci.* 131, 984–993. doi: 10.1080/00207454.2020.1766459

Cosentino, S., Scarmeas, N., Helzner, E., Glymour, M. M., Brandt, J., Albert, M., et al. (2008). APOE epsilon 4 allele predicts faster cognitive decline in mild Alzheimer disease. *Neurology* 70, 1842–1849. doi: 10.1212/01.wnl.0000304038.37421.cc

Crutch, S. J., Lehmann, M., Schott, J. M., Rabinovici, G. D., Rossor, M. N., and Fox, N. C. (2012). Posterior cortical atrophy. *Lancet Neurol.* 11, 170–178. doi: 10.1016/S1474-4422(11)70289-7

Dahnke, R., Yotter, R. A., and Gaser, C. (2013). Cortical thickness and central surface estimation. *Neuroimage* 65, 336–348. doi: 10.1016/j.neuroimage.2012.09.050

Desmarais, P., Gao, A. F., Lanctot, K., Rogaeva, E., Ramirez, J., Herrmann, N., et al. (2021). White matter hyperintensities in autopsy-confirmed frontotemporal lobar degeneration and Alzheimer's disease. *Alzheimers Res. Ther.* 13:129. doi: 10.1186/s13195-021-00869-6

Dubois, B., Feldman, H. H., Jacova, C., Hampel, H., Molinuevo, J. L., Blennow, K., et al. (2014). Advancing research diagnostic criteria for Alzheimer's disease: The IWG-2 criteria. *Lancet Neurol.* 13, 614–629. doi: 10.1016/S1474-4422(14)70090-0

Esiri, M. M., Nagy, Z., Smith, M. Z., Barnetson, L., and Smith, A. D. (1999). Cerebrovascular disease and threshold for dementia in the early stages of Alzheimer's disease. *Lancet* 354, 919–920. doi: 10.1016/S0140-6736(99)02355-7

Eto, F., Tanaka, M., Chishima, M., Igarashi, M., Mizoguchi, T., Wada, H., et al. (1992). [Comprehensive activities of daily living (ADL) index for the elderly]. *Nihon Ronen Igakkai Zasshi* 29, 841–848. doi: 10.3143/geriatrics.29.841

Faries, D., Herrera, J., Rayamajhi, J., DeBrota, D., Demitrack, M., and Potter, W. Z. (2000). The responsiveness of the Hamilton Depression Rating Scale. *J. Psychiatr. Res.* 34, 3–10. doi: 10.1016/s0022-3956(99)00037-0

Ferrari, C., Lombardi, G., Polito, C., Lucidi, G., Bagnoli, S., Piaceri, I., et al. (2018). Alzheimer's Disease Progression: Factors Influencing Cognitive Decline. *J. Alzheimers Dis.* 61, 785–791. doi: 10.3233/JAD-170665

Freitas, S., Simoes, M. R., Alves, L., Duro, D., and Santana, I. (2012). Montreal Cognitive Assessment (MoCA): Validation study for frontotemporal dementia. *J. Geriatr. Psychiatry Neurol.* 25, 146–154. doi: 10.1177/0891988712455235

Gorno-Tempini, M. L., Hillis, A. E., Weintraub, S., Kertesz, A., Mendez, M., Cappa, S. F., et al. (2011). Classification of primary progressive aphasia and its variants. *Neurology* 76, 1006–1014. doi: 10.1212/WNL.0b013e31821103e6

Harper, L., Fumagalli, G. G., Barkhof, F., Scheltens, P., O'Brien, J. T., Bouwman, F., et al. (2016). MRI visual rating scales in the diagnosis of dementia: Evaluation in 184 post-mortem confirmed cases. *Brain* 139, 1211–1225. doi: 10.1093/brain/aww005

Hu, J. B., Zhou, W. H., Hu, S. H., Huang, M. L., Wei, N., Qi, H. L., et al. (2013). Cross-cultural difference and validation of the Chinese version of Montreal Cognitive Assessment in older adults residing in Eastern China: Preliminary findings. *Arch. Gerontol. Geriatr.* 56, 38–43. doi: 10.1016/j.archger.2012.05.008

Jiang, W., Lin, F., Zhang, J., Zhan, T., Cao, P., and Wang, S. (2020). Deep-Learning-Based Segmentation and Localization of White Matter Hyperintensities on Magnetic Resonance Images. *Interdiscip. Sci.* 12, 438–446. doi: 10.1007/s12539-020-00398-0

Katisko, K., Cajanus, A., Korhonen, T., Remes, A. M., Haapasalo, A., and Solje, E. (2019). Prodromal and Early bvFTD: Evaluating Clinical Features and Current Biomarkers. *Front. Neurosci.* 13:658. doi: 10.3389/fnins.2019.00658

Keith, J., Gao, F. Q., Noor, R., Kiss, A., Balasubramaniam, G., Au, K., et al. (2017). Collagenosis of the Deep Medullary Veins: An Underrecognized Pathologic Correlate of White Matter Hyperintensities and Periventricular Infarction? *J. Neuropathol. Exp. Neurol.* 76, 299–312. doi: 10.1093/jnen/nlx009

Kertesz, A., Nadkarni, N., Davidson, W., and Thomas, A. W. (2000). The Frontal Behavioral Inventory in the differential diagnosis of frontotemporal dementia. *J. Int. Neuropsychol. Soc.* 6, 460–468. doi: 10.1017/s1355617700644041

Kloppel, S., Abdulkadir, A., Jack, C. R. Jr., Koutsouleris, N., Mourao-Miranda, J., and Vemuri, P. (2012). Diagnostic neuroimaging across diseases. *Neuroimage* 61, 457–463. doi: 10.1016/j.neuroimage.2011.11.002

Klunk, W. E., Engler, H., Nordberg, A., Wang, Y., Blomqvist, G., Holt, D. P., et al. (2004). Imaging brain amyloid in Alzheimer's disease with Pittsburgh Compound-B. *Ann. Neurol.* 55, 306–319. doi: 10.1002/ana.20009

Knopman, D. S., Jack, C. R. Jr., Wiste, H. J., Lundt, E. S., Weigand, S. D., Vemuri, P., et al. (2014). 18F-fluorodeoxyglucose positron emission tomography, aging, and apolipoprotein E genotype in cognitively normal persons. *Neurobiol. Aging* 35, 2096–2106. doi: 10.1016/j.neurobiolaging.2014.03.006

Laakso, M. P., Hallikainen, M., Hanninen, T., Partanen, K., and Soininen, H. (2000). Diagnosis of Alzheimer's disease: MRI of the hippocampus vs delayed recall. *Neuropsychologia* 38, 579–584. doi: 10.1016/s0028-3932(99)00111-6

Lee, W. J., Liao, Y. C., Wang, Y. F., Lin, Y. S., Wang, S. J., and Fuh, J. L. (2020). Summative Effects of Vascular Risk Factors on the Progression of Alzheimer Disease. *J. Am. Geriatr. Soc.* 68, 129–136. doi: 10.1111/jgs.16181

Li, P., Zhou, Y. Y., Lu, D., Wang, Y., and Zhang, H. H. (2016). Correlated patterns of neuropsychological and behavioral symptoms in frontal variant of Alzheimer disease and behavioral variant frontotemporal dementia: A comparative case study. *Neurol. Sci.* 37, 797–803. doi: 10.1007/s10072-015-2405-9

Liu, M. N., Lau, C. I., and Lin, C. P. (2019). Precision Medicine for Frontotemporal Dementia. *Front. Psychiatry* 10:75. doi: 10.3389/fpsyt.2019.00075

Lyu, I., Kang, H., Woodward, N. D., and Landman, B. A. (2018). Sulcal Depth-based Cortical Shape Analysis in Normal Healthy Control and Schizophrenia Groups. *Proc. SPIE Int. Soc. Opt. Eng.* 10574:1057402. doi: 10.1117/12.2293275

McKhann, G. M., Knopman, D. S., Chertkow, H., Hyman, B. T., Jack, C. R. Jr., Kawas, C. H., et al. (2011). The diagnosis of dementia due to Alzheimer's disease: Recommendations from the National Institute on Aging-Alzheimer's Association workgroups on diagnostic guidelines for Alzheimer's disease. *Alzheimers Dement.* 7, 263–269. doi: 10.1016/j.jalz.2011.03.005

Mesulam, M. (2008). Primary progressive aphasia pathology. *Ann. Neurol.* 63, 124–125. doi: 10.1002/ana.20940

Minoshima, S., Mosci, K., Cross, D., and Thientunyakit, T. (2021). Brain [F-18)FDG PET for Clinical Dementia Workup: Differential Diagnosis of Alzheimer's Disease and Other Types of Dementing Disorders. *Semin. Nucl. Med.* 51, 230–240. doi: 10.1053/j.semnuclmed.2021.01.002

Moller, C., Pijnenburg, Y. A., van der Flier, W. M., Versteeg, A., Tijms, B., de Munck, J. C., et al. (2016). Alzheimer Disease and Behavioral Variant Frontotemporal Dementia: Automatic Classification Based on Cortical Atrophy for Single-Subject Diagnosis. *Radiology* 279, 838–848. doi: 10.1148/radiol.2015150220

Molloy, D. W., and Standish, T. I. (1997). A guide to the standardized Mini-Mental State Examination. *Int. Psychogeriatr.* 9, 87–94. doi: 10.1017/s1041610297004754

Morris, J. C. (1993). The Clinical Dementia Rating (CDR): Current version and scoring rules. *Neurology* 43, 2412–2414. doi: 10.1212/wnl.43.11.2412-a

Neary, D., Snowden, J. S., Gustafson, L., Passant, U., Stuss, D., Black, S., et al. (1998). Frontotemporal lobar degeneration: A consensus on clinical diagnostic criteria. *Neurology* 51, 1546–1554. doi: 10.1212/wnl.51.6.1546

Nichols, J. B., Malek-Ahmadi, M., Tariot, P. N., Serrano, G. E., Sue, L. I., and Beach, T. G. (2021). Vascular Lesions, APOE epsilon4, and Tau Pathology in Alzheimer Disease. *J. Neuropathol. Exp. Neurol.* 80, 240–246. doi: 10.1093/jnen/nlaa160

Pluta, R., Ulamek-Koziol, M., Kocki, J., Bogucki, J., Januszewski, S., Bogucka-Kocka, A., et al. (2020). Expression of the Tau Protein and Amyloid Protein Precursor Processing Genes in the CA3 Area of the Hippocampus in the Ischemic Model of Alzheimer's Disease in the Rat. *Mol. Neurobiol.* 57, 1281–1290. doi: 10.1007/s12035-019-01799-z

Raamana, P. R., Rosen, H., Miller, B., Weiner, M. W., Wang, L., and Beg, M. F. (2014). Three-Class Differential Diagnosis among Alzheimer Disease, Frontotemporal Dementia, and Controls. *Front. Neurol.* 5:71. doi: 10.3389/fneur.2014.00071

Ramirez, J., McNeely, A. A., Scott, C. J., Stuss, D. T., and Black, S. E. (2014). Subcortical hyperintensity volumetrics in Alzheimer's disease and normal elderly in the Sunnybrook Dementia Study: Correlations with atrophy, executive function, mental processing speed, and verbal memory. *Alzheimers Res. Ther.* 6:49. doi: 10.1186/alzrt279

Rascovsky, K., Hodges, J. R., Knopman, D., Mendez, M. F., Kramer, J. H., Neuhaus, J., et al. (2011). Sensitivity of revised diagnostic criteria for the behavioural variant of frontotemporal dementia. *Brain* 134, 2456–2477. doi: 10.1093/brain/awr179

Sheelakumari, R., Venkateswaran, R., Chandran, A., Varghese, T., Zhang, L., Yue, G. H., et al. (2018). Quantitative analysis of grey matter degeneration in FTD patients using fractal dimension analysis. *Brain Imaging Behav.* 12, 1221–1228. doi: 10.1007/s11682-017-9784-x

Singh, A., Arya, A., Agarwal, V., Shree, R., and Kumar, U. (2022). Grey and white matter alteration in euthymic children with bipolar disorder: A combined source-based morphometry (SBM) and voxel-based morphometry (VBM) study. *Brain Imaging Behav.* 16, 22–30. doi: 10.1007/s11682-021-00473-0

Smailagic, N., Vacante, M., Hyde, C., Martin, S., Ukoumunne, O., and Sachpekidis, C. (2015). (1)(8)F-FDG PET for the early diagnosis of Alzheimer's disease dementia and other dementias in people with mild cognitive impairment (MCI). *Cochrane Database Syst. Rev.* 1:CD010632. doi: 10.1002/14651858.CD010632.pub2

Smith, E. E., Salat, D. H., Jeng, J., McCreary, C. R., Fischl, B., Schmahmann, J. D., et al. (2011). Correlations between MRI white matter lesion location and executive function and episodic memory. *Neurology* 76, 1492–1499. doi: 10.1212/WNL.0b013e318217e7c8

Sudre, C. H., Bocchetta, M., Cash, D., Thomas, D. L., Woollacott, I., Dick, K. M., et al. (2017). White matter hyperintensities are seen only in GRN mutation carriers in the GENFI cohort. *Neuroimage Clin.* 15, 171–180. doi: 10.1016/j.nicl.2017.04.015

Thambisetty, M., Beason-Held, L., An, Y., Kraut, M. A., and Resnick, S. M. (2010). APOE epsilon4 genotype and longitudinal changes in cerebral blood flow in normal aging. *Arch. Neurol.* 67, 93–98. doi: 10.1001/archneurol.2009.913

Wang, T., Xiao, S., Li, X., Wang, H., Liu, Y., Su, N., et al. (2012). Reliability and validity of the Chinese version of the neuropsychiatric inventory in mainland China. *Int. J. Geriatr. Psychiatry* 27, 539–544. doi: 10.1002/gps.2757

Wang, Y., Shi, Z., Zhang, N., Cai, L., Li, Y., Yang, H., et al. (2019). Spatial Patterns of Hypometabolism and Amyloid Deposition in Variants of Alzheimer's Disease Corresponding to Brain Networks: A Prospective Cohort Study. *Mol. Imaging Biol.* 21, 140–148. doi: 10.1007/s11307-018-1219-6

Wei, Y., Huang, N., Liu, Y., Zhang, X., Wang, S., and Tang, X. (2020). Hippocampal and Amygdalar Morphological Abnormalities in Alzheimer's Disease Based on Three Chinese MRI Datasets. *Curr. Alzheimer Res.* 17, 1221–1231. doi: 10.2174/1567205018666210218150223

Wu, Y. T., Beiser, A. S., Breteler, M. M. B., Fratiglioni, L., Helmer, C., Hendrie, H. C., et al. (2017). The changing prevalence and incidence of dementia over time - current evidence. *Nat. Rev. Neurol.* 13, 327–339. doi: 10.1038/nrneurol.2017.63

Yu, J. T., Xu, W., Tan, C. C., Andrieu, S., Suckling, J., Evangelou, E., et al. (2020). Evidence-based prevention of Alzheimer's disease: Systematic review and meta-analysis of 243 observational prospective studies and 153 randomised controlled trials. *J. Neurol. Neurosurg. Psychiatry* 91, 1201–1209. doi: 10.1136/jnnp-2019-321913

Zhang, N., Zhang, L., Li, Y., Gordon, M. L., Cai, L., Wang, Y., et al. (2017). Urine AD7c-NTP Predicts Amyloid Deposition and Symptom of Agitation in Patients with Alzheimer's Disease and Mild Cognitive Impairment. *J. Alzheimers Dis.* 60, 87–95. doi: 10.3233/JAD-170383

frontiers | Frontiers in Aging Neuroscience

TYPE Review
PUBLISHED 01 November 2022
DOI 10.3389/fnagi.2022.1034684

OPEN ACCESS

EDITED BY
Miriam Sklerov,
University of North Carolina at Chapel Hill, United States

REVIEWED BY
Chiara Fenoglio,
University of Milan, Italy
Francesca Gilli,
Dartmouth College, United States

*CORRESPONDENCE
Sylvain Lehmann
s-lehmann@chu-montpellier.fr

SPECIALTY SECTION
This article was submitted to Cellular and Molecular Mechanisms of Brain-aging, a section of the journal Frontiers in Aging Neuroscience

RECEIVED 01 September 2022
ACCEPTED 10 October 2022
PUBLISHED 01 November 2022

CITATION
Delaby C, Bousiges O, Bouvier D, Fillée C, Fourier A, Mondésert E, Nezry N, Omar S, Quadrio I, Rucheton B, Schraen-Maschke S, van Pesch V, Vicca S, Lehmann S and Bedel A (2022) Neurofilaments contribution in clinic: state of the art. Front. Aging Neurosci. 14:1034684. doi: 10.3389/fnagi.2022.1034684

Neurofilaments contribution in clinic: state of the art

Constance Delaby[1,2], Olivier Bousiges[3], Damien Bouvier[4], Catherine Fillée[5], Anthony Fourier[6], Etienne Mondésert[1], Nicolas Nezry[7], Souheil Omar[8], Isabelle Quadrio[6], Benoit Rucheton[9], Susanna Schraen-Maschke[7], Vincent van Pesch[10], Stéphanie Vicca[11], Sylvain Lehmann[1]* and Aurelie Bedel[12]

[1]Université de Montpellier, IRMB, INM, INSERM, CHU de Montpellier, Laboratoire Biochimie-Protéomique clinique, Montpellier, France, [2]Sant Pau Memory Unit, Hospital de la Santa Creu i Sant Pau—Biomedical Research Institute Sant Pau—Universitat Autònoma de Barcelona, Barcelona, Spain, [3]Laboratoire de biochimie et biologie moléculaire (LBBM)—Pôle de biologie Hôpital de Hautepierre—CHU de Strasbourg, CNRS, laboratoire ICube UMR 7357 et FMTS (Fédération de Médecine Translationnelle de Strasbourg), équipe IMIS, Strasbourg, France, [4]Service de Biochimie et Génétique Moléculaire, CHU de Clermont-Ferrand, Clermont-Ferrand, France, [5]Cliniques universitaires Saint-Luc UCLouvain, Service de Biochimie Médicale, Brussels, Belgium, [6]Biochimie et Biologie Moléculaire—LBMMS, Unité de diagnostic des pathologies dégénératives, Centre de Biologie et Pathologie Est, Groupement Hospitalier Est, Lyon, France, [7]Univ. Lille, Inserm, CHU Lille, UMR-S-U1172, LiCEND, Lille Neuroscience & Cognition, LabEx DISTALZ, Lille, France, [8]Laboratoire de biologie médicale de l'Institut de Neurologie de Tunis, Tunis, Tunisia, [9]Laboratoire de Biologie, Institut Bergonié, Bordeaux, France, [10]Cliniques universitaires Saint-Luc UCLouvain, Service de Neurologie, Brussels, Belgium, [11]Hôpital Necker-Enfants malades, Paris, Laboratoire de Biochimie générale, DMU BioPhyGen, AP-HP.Centre—Université de Paris, Paris, France, [12]Service de Biochimie, CHU Pellegrin, Bordeaux, France

Neurological biomarkers are particularly valuable to clinicians as they can be used for diagnosis, prognosis, or response to treatment. This field of neurology has evolved considerably in recent years with the improvement of analytical methods, allowing the detection of biomarkers not only in cerebrospinal fluid (CSF) but also in less invasive fluids like blood. These advances greatly facilitate the repeated quantification of biomarkers, including at asymptomatic stages of the disease. Among the various informative biomarkers of neurological disorders, neurofilaments (NfL) have proven to be of particular interest in many contexts, such as neurodegenerative diseases, traumatic brain injury, multiple sclerosis, stroke, and cancer. Here we discuss these different pathologies and the potential value of NfL assay in the management of these patients, both for diagnosis and prognosis. We also describe the added value of NfL compared to other biomarkers currently used to monitor the diseases described in this review.

KEYWORDS

neurofilament, biomarkers, neurological and neurodegenerative diseases, cut-off, biological fluids

Abbreviations: AD, Alzheimer's disease; AUC, area under the curve; CBD, corticobasal degeneration; CJD, Creutzfeldt Jakob disease; CNS, central nervous system; CSF, cerebrospinal fluid; FTD, fronto-temporal dementia; Gd+ , gadolinium lesions; GRN, progranulin; HTT, hungtintin; ICANS, Immune Cell Associated Neurotoxicity Syndrome; LBD, Lewy body disease; MCI, mild cognitive impairment; MS, multiple sclerosis; MSA, multisystem atrophy; NfL, neurofilament light; OCB, oligoclonal bande in the CSF; PD, Parkinson's disease; PPD, primary psychiatric disorders; PS, Parkinson's syndromes; PSP, progressive supranuclear palsy; ROC, receiver operating characteristic; TBI, traumatic brain injury.

10.3389/fnagi.2022.1034684

Introduction

Neurofilaments (Nf) belong to the family of intermediate filaments and their localization is exclusively neuronal. Nf differ from other types of intermediate filaments by the complexity of their structure and the composition of their subunits. Three subunits of Nf can be identified (and differentiated on SDS gel according to their molecular weight): NfH (heavy chain, 200 kDa), NfM (medium chain, 160 kDa), and NfL (light chain, 68 kDa; Yuan et al., 2017; **Figure 1**). Each protein subunit consists of a globular head, an alpha helix portion and a C-terminal domain of variable length, thus determining the molecular weight of each of these subunits (Yuan et al., 2006, 2012). Nf are involved in the radial growth of the axon during neuron development and in the maintenance of its structure and diameter, which are necessary for the transmission of nerve impulses. Nf are also involved in the organization and docking of the different components of the axon to the microtubule network.

Because of their enrichment in axons and their release into blood and cerebrospinal fluid (CSF) during neuronal damage, the measurement of NfL in these biological fluids as potential biomarkers of axonal damage, axonal loss and neuronal death raises many hopes in terms of diagnosis and prognosis (**Figure 2**).

NfL thus appears as one of the biomarkers of neurodegeneration, non-specific, but indirectly involved in the pathogenesis of many neurological diseases. These biomarkers are therefore being actively investigated and several assays for their quantification are currently available: the first one is based on an ELISA immunoassay (marketed by Uman Diagnostic, Umeå, Sweden), the second one is based on Simoa (single molecule array) technology and is implemented on the Quanterix® (Billerica, MA, USA) Simoa™ device, and the third one is an immunoassay, based on a microfluidic approach, which can be implemented on the Ella™ device from the Protein Simple® company. These three approaches use the same detection antibodies. A fourth approach, based on electro-chemiluminescence, can be implemented on the Mesoscale Discovery (MSD) devices (Rockville, MD, USA). However, the cut-offs for NfL measurement remain to be homogenized, or even defined, depending on the method, the clinical contexts and the physiological parameters influencing the concentrations such as age, body mass index or renal function (see **Table 1**). The objective of this article is to overview the interest of NfL in various neurodegenerative diseases and in other contexts of neurological impairment. We present the prognostic or diagnostic implications of measuring this biomarker in biological fluids. We also discuss the place and informative value of NfL in relation to other biomarkers commonly used to monitor the described pathologies.

NfL and neurodegenerative diseases

Alzheimer's disease

Background and state of the art

Alzheimer's disease (AD) is the most prevalent cognitive neurodegenerative disease with approximately 900,000 people affected in France and more than 225,000 new cases per year (Helmer et al., 2006). From a pathophysiological point of view, AD is characterized by neurodegeneration due to the development of neurofibrillary tangles (NFTs, formed by aggregates of hyperphosphorylated tau protein) and amyloid plaques [formed by agglomerates of amyloid peptides Aβ produced by the cleavage of amyloid precursor protein (APP)]. The diagnosis of AD is based on clinical examination, interview with the patient and relatives, neuropsychological tests (e.g., mini-mental state examination, MMSE), imaging (structural Magnetic Resonance Imaging, MRI, FDG-PET, amyloid PET), and finally lumbar puncture with the quantification of CSF biomarkers Aβ42, Aβ40 (together with the ratio of Aβ42/Aβ40), total tau (t-tau), and phosphorylated tau on threonine 181 (p-tau). These CSF biomarkers perform well in the diagnosis of AD at the dementia stage (Hansson et al., 2006) but also allow diagnosis of the disease at early stage (MCI, mild cognitive impairment; Jack et al., 2013).

The number of publications related to the determination of NfL in AD is very high, both in CSF and in blood (546 referenced in Pubmed on 01/06/2022). As for almost all neurodegenerative diseases, NfL is increased in blood and CSF of AD patients (Gaetani et al., 2019; Mattsson et al., 2019; Delaby et al., 2020). Thus, AD patients can be differentiated from healthy controls with very good accuracy, by measuring NfL in both the CSF (Lista et al., 2017) and the blood (Forgrave et al., 2019; Mattsson et al., 2019). However, several studies reported absence of direct correlation between NfL concentrations in CSF or plasma and amyloid pathology (Aβ+ and Aβ−) as assessed by amyloid PET (Dhiman et al., 2020; Verberk et al., 2020). This suggests that changes in NfL concentration are independent of amyloid pathology in AD, whereas they are correlated with neurodegeneration and tauopathy (Dhiman et al., 2020).

Diagnostic and prognostic values

This almost systematic increase of NfL in neurodegenerative diseases limits the diagnostic interest of this biomarker in AD. However, it is noteworthy that the increase in NfL levels (both in blood and CSF) of AD patients remains more moderate than in most other neurodegenerative diseases (Gaetani et al., 2019). NfL may be differentially involved in the pathological processes

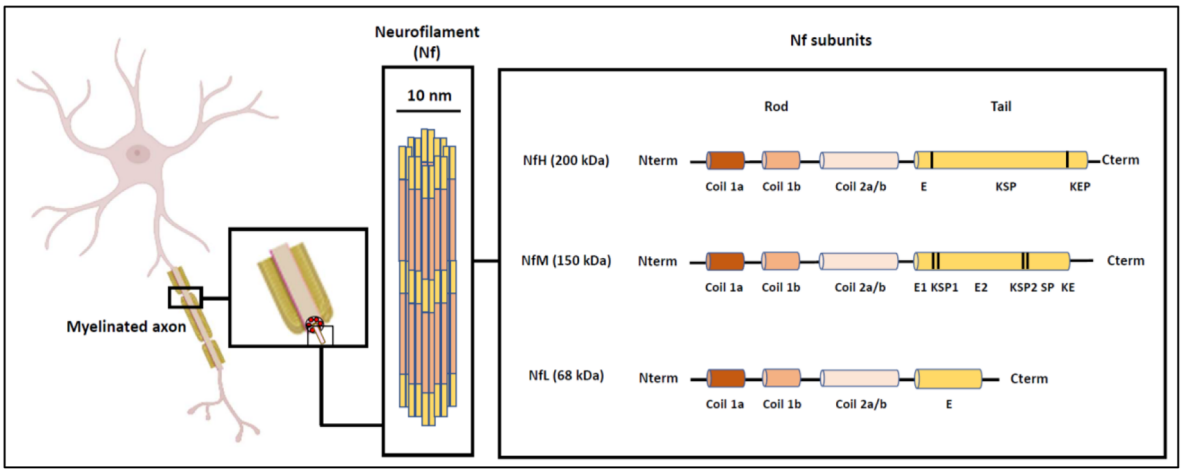

FIGURE 1
Structure and organization of neurofilaments (Nf), adapted from Gaetani et al. (2019).

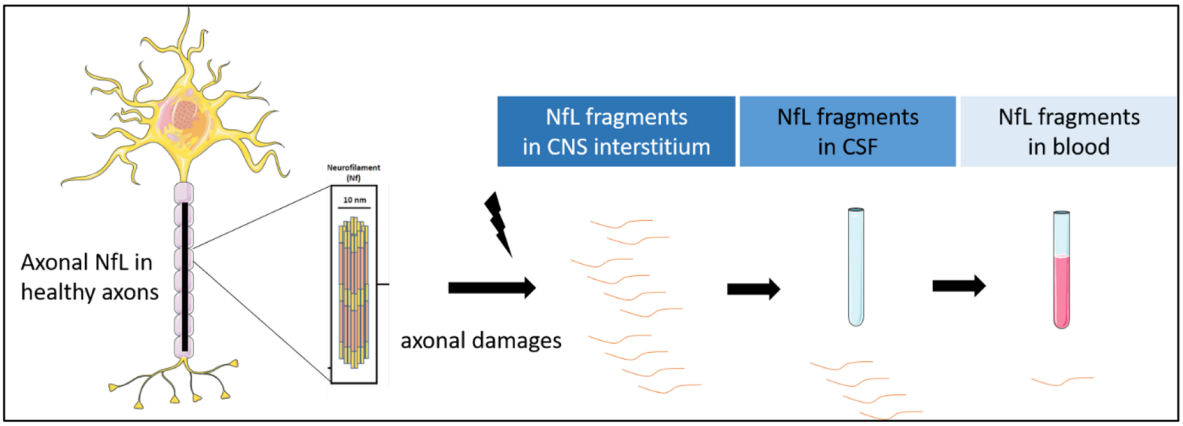

FIGURE 2
NfL release after axonal damages. NfL are detectable in CSF and blood.

of these disorders, in particular, neuronal death may be greater in some of them than in AD (which is chronic), thus generating higher levels of sNfL. In addition, pathologies associated with motor neuron death, such as ALS, might also exhibit higher levels of NfL than others.

Thus, for frontal forms of AD (e.g., primary progressive logopenic aphasia), the measurement of NfL could be of interest in the differential diagnosis with other primary progressive aphasias and, more generally, with frontotemporal lobar degeneration (FTLD), where NfL levels are higher (Pijnenburg et al., 2015; Disanto et al., 2016; Steinacker et al., 2017a; Paterson et al., 2018; Lleó A et al., 2019). The elevated levels of NfL in prion diseases would also allow a differential diagnosis between prions and AD (Steinacker et al., 2016; Thompson et al., 2018).

Changes in blood NfL appear to precede the first clinical manifestations of AD by about 16 years, as shown in longitudinal studies of AD mutation carriers (Preische et al., 2019): NfL could thus be used to monitor subjects with genetic risk factors for AD. Indeed, serum NfL has been shown to correlate with the estimated number of years before symptoms appear in carriers of autosomal dominant AD mutations (Sánchez-Valle et al., 2018) or in Down syndrome (Fortea et al., 2018, 2020).

Elevated CSF NfL is also associated with faster brain atrophy and cognitive decline in AD patients followed up longitudinally (Zetterberg et al., 2016; Osborn et al., 2019; Dhiman et al., 2020). Therefore, elevated CSF NfL in the early clinical stages of AD may predict accelerated cognitive decline and conversion to dementia in AD (Zetterberg et al., 2016; Lim et al., 2021).

TABLE 1 Diagnostic/prognostic blood NfL's threshold in neurological pathological context, according to various technological approaches.

	Clinical contexts	sNfL cut-off value (pg/ml)	Technological approach used for cut-off definition	Reference
Neurodegenerative Diseases				
Alzheimer's Disease (AD)	AD vs. control subjects	37.0	Simoa	Ashton et al. (2021) and Smirnov et al. (2022)
		19.3	Ella	Oeckl et al. (2022)
		26.6	MSD	Gaiottino et al. (2013)
	AD vs. FTD	42.7	Ella	Oeckl et al. (2022)
Parkinson's syndrome (PS)	PS vs. control subjects	21.0	Simoa	Zhang et al. (2022)
	PD vs. atypical forms of parkinsonism (MSA, PSP)	14.8	Simoa	Marques et al. (2019)
	PD vs. atypical forms of parkinsonism (MSA, PSP, CBD)	17.2	Simoa	Quadalti et al. (2021)
	PD vs. PSP/CBD	16.6	Simoa	Quadalti et al. (2021)
	PD vs. MSA	17.2	Simoa	Quadalti et al. (2021)
	Atypical forms of parkinsonism vs. control subjects	13.6	Simoa	Marques et al. (2019)
Fronto-temporal dementia	Fronto-temporal dementia vs. PPD	19.5–33.0	Simoa	Forgrave et al. (2019)
Amyotrophic lateral sclerosis (ALS)	ALS vs. control subjects	500	Elisa	Shi et al. (2022)
	ALS vs. non-ALS patients	32.7	Simoa	Vacchiano et al. (2021)
Multiple sclerosis (MS)	OCB/Gd + occurence	31.0	Simoa	Bittner et al. (2020)
	Prognosis clinical disease activity	1.5 (z-score)	Simoa	Benkert et al. (2022)
Neurological Damages				
Traumatic brain injury (TBI)	TBI diagnosis	20.0	Simoa	Thelin et al. (2017)
	Prediction of intracranial lesions	8.38	Simoa	Kahouadji et al. (2022)
Stroke	Stroke prognosis	46.12	Simoa	Wang Z. et al. (2021)
Oncology	Response to cancer therapy	28.0–60.0	Simoa	Schoeberl et al. (2022)
	Brain metastasis diagnosis	>22.0	Simoa	Kim et al. (2021)
	Chemotherapy toxicity	>36.0	Simoa	Huehnchen et al. (2022)
	ICANS occurence	75.0	Simoa	Schoeberl et al. (2022)

AD, Alzheimer's disease; PS, Parkinson's syndromes; PD, Parkinson's disease; FTD, fronto-temporal dementia; MSA, multisystem atrophy; PSP, progressive supranuclear palsy; CBD, corticobasal degeneration; PPD, primary psychiatric disorders; TBI, traumatic brain injury; MS, multiple sclerosis; ICANS, Immune Cell Associated Neurotoxicity Syndrome; OCB, oligoclonal bande in the CSF; Gd +, gadolinium lesions.

Thus, NfL assay could serve as a prognostic marker of worsening cognitive function in AD.

Position of NfL compared to other biomarkers and cut-off value

NfL measurement in CSF does not seem to provide further information to the amyloid biomarkers, t-tau and p-tau, already used to predict conversion to dementia in AD (Fortea et al., 2018).

Measurement of NfL in blood could be useful as a first line, i.e., screening test for AD and other neurodegenerative diseases. This would indeed be a straightforward implement due to the less invasive nature of blood collection compared to lumbar puncture.

Thresholds for the use of the blood NfL for diagnosis have been proposed in some studies, although the areas under the curve never reach 0.8. Two large studies found similar cut-off values with the Simoa technique, around 37 pg/ml: the first study being based on the comparison of amyloid+ vs. amyloid− subjects (defined on the basis of $A\beta_{1-42}$ assays in CSF or amyloid PET imaging, $N = 805$; Ashton et al., 2021) and the second being based on a pathology cohort ($N = 312$) comparing Braak 0_II vs. Thal 4–5 and Braak V–VI subjects (Braak being the scale measuring DNF pathology and Thal amyloid pathology by brain region immunohistochemistry techniques; Smirnov et al., 2022). Using Ella technique, thresholds of 19.3 pg/ml and 42.7 pg/ml were reported to differentiate AD from controls and AD from FTD, respectively (Oeckl et al., 2022). When using the MSD technique, a threshold of 26.6 pg/ml was found to discriminate AD from controls (Gaiottino et al., 2013). These cut-offs are not comparable since the techniques are not standardized, but all studies agree in finding areas under the curve in the range of 0.7, which is insufficient for diagnostic use. But these blood thresholds might however be of interest for a first screening step. In addition, age-dependent cut-offs should increase the performance of the test. Finally, the combination of this test with blood measurements of amyloid and tau could also be interesting.

Parkinson's syndromes and synucleopathies

Background and state of the art

Parkinson's disease (PD) is the second most common neurodegenerative disease in France (after AD) and the first leading cause of motor disorders. In France, 150,000 people are affected and 25,000 new cases are diagnosed every

year (Elbaz et al., 2016). PD is due to the progressive loss of dopaminergic neurons of the nigro-striatal pathway in association with the formation of Lewy bodies corresponding to alpha-synuclein aggregation (Elbaz et al., 2016). Other neurodegenerative pathologies present alpha-synuclein aggregates, such as Lewy body disease (LBD), Parkinson's dementia, multisystem atrophy (MSA) or idiopathic orthostatic hypotension (IOH). All these pathologies are part of the so-called synucleinopathies. The differential diagnosis between these synucleinopathies is complex and is compounded by diseases with atypical Parkinsonian syndromes, such as progressive supranuclear palsy (PSP) or corticobasal degeneration (CBD), making the differential diagnosis sometimes challenging. To date, no specific biomarkers can be used for such differential diagnosis.

The determination of NfL, both in CSF and in blood, has been intensively studied in the context of PD (156 results in Pubmed as of 01/06/2022). Interestingly, NfL levels do not seem to increase in the CSF of PD patients and several publications have reported similar levels to those of healthy controls (Gaetani et al., 2019).

Diagnostic and prognostic values

While NfL levels are not increased in either blood or CSF of parkinsonian patients, it is noteworthy that they rise in atypical forms of parkinsonian syndromes such as PSP, MSA, and CBD in both CSF (Bäckström et al., 2015; Herbert et al., 2015) and blood (Hansson et al., 2017; Lin et al., 2018; Marques et al., 2019; Ashton et al., 2021). This discrepancy could be due in part to milder and less extensive axonal degeneration in PD than in these atypical forms of parkinsonian syndromes. NfL levels are indeed related to severity, motor neurons scores, and stratification of PD.

Of note, while LBD patients (or those with parkinsonian dementia) also have significant elevated levels of NfL in CSF compared to healthy and PD patients, they have lower levels than PSP, MSA, and CBD patients (Hall et al., 2012). On the other hand, NfL levels in CSF are not very specific and do not differentiate LBD and AD patients (de Jong et al., 2007). The assessment of NfL in CSF or blood could thus be useful for the differential diagnosis of PD vs. atypical parkinsonian syndromes.

The prognostic value of NfL has been evaluated in PD and PSP, but no data are available on its prognostic value in MSA and CBD. In PD, baseline CSF NfL values are associated with mean change per year in *Dementia rating scale scores* (Olsson et al., 2019; Aamodt et al., 2021). The determination of NfL in CSF (Bäckström et al., 2015) and blood (Aamodt et al., 2021) thus predicts the risk of conversion to parkinsonian dementia in the following years, with not only cognitive but also motor impairment (Lerche et al., 2020; Mollenhauer et al., 2020). In PSP, higher baseline NfL values in CSF and blood appear to be associated with accelerated worsening of motor and cognitive symptoms (Rojas et al., 2016). Furthermore, some patients with HOI evolve to synucleinopathies with motor or cognitive impairment such as PD, LBD or MSA and the level of NfL in the CSF could help predict this conversion (Singer et al., 2021).

Position of NfL compared to other biomarkers and cut-off value

NfL assessed alone appears to have modest performance in predicting conversion from normal cognition to MCI or parkinsonian dementia individually, suggesting that NfL should be integrated into a multi-marker panel to improve prediction of clinical conversion to dementia. Some studies propose to incorporate, for example, $A\beta_{1-42}$ assay in CSF for this purpose (Bäckström et al., 2015). Some articles have attempted to determine a threshold value using ROC curve to support the differential diagnosis of parkinsonian syndromes. Interestingly, all these studies achieved NfL quantification using the Simoa technique. Thus, a cut-off value of NfL at 21 pg/ml in plasma would allow a satisfactory discrimination of MSA patients and healthy subjects, with a sensitivity of 81% and a specificity of 93% (AUC = 0.912; Zhang et al., 2022). Similarly, NfL cut-off value in serum of 14.8 pg/ml (assessed by the Simoa approach) allows a clear discrimination (AUC = 0.91) between PD patients and those with atypical forms of parkinsonism (MSA and PSP), yielding a sensitivity of 86% and a specificity of 85% (Marques et al., 2019). Thus, among patients whose serum NfL concentration is above the cut-off value, the probability of having an atypical parkinsonism syndrome is 76% (positive predictive value), and patients whose serum NfL amount is below this cut-off value have a 92% probability of having PD (negative predictive value). In the same study, a cut-off value of 13.6 ng/L was used to differentiate patients with atypical parkinsonism from control subjects with a sensitivity of 93% and a specificity of 71% (AUC = 0.88; Marques et al., 2019). One study further detailed the differences in threshold values (assessed by Simoa) according to parkinsonian syndromes (Quadalti et al., 2021): for example, to differentiate PD from MSA, the best cut-off value for plasma NfL is at 17.2 pg/ml for a sensitivity of 90.3% and specificity of 96.4% (AUC = 0.972), and to differentiate a group of PD patients from a group of PSP/DCB patients, the optimal cut-off value is 16.6 pg/ml with a sensitivity of 88.7% and specificity of 87.8% (AUC = 0.936). When grouping atypical parkinsonian syndromes (MSA, PSP, DCB) vs. PD, the cut-off value of plasma NfL is 17.2 pg/ml for a sensitivity of 90.3% and a specificity of 91.7% (Quadalti et al., 2021). These results highlight the interest of NfL measurement in clinical setting, however, prospective validation and real-life clinical use are still needed to confirm such value.

Fronto-temporal dementia (FTD)

Background and state of the art

Frontotemporal dementia (FTD) is a heterogeneous group of neurodegenerative diseases characterized by behavioral disorders and deficits in executive and language functions. It is the third most common cause of neurocognitive impairment after AD and LBD. In clinical practice, the challenge is to differentiate FTD patients with various primary psychiatric disorders (PPD), because of the overlap of some behavioral symptoms with FTD. To date, there is no validated biomarker to distinguish PPD from FTD but NfL, as a non-specific biomarker of neuronal death, appears to be promising to fill this gap in diagnosis.

Several studies have investigated NfL levels in FTD subjects: a total of 19 publications reporting NfL results in CSF (Goossens et al., 2018) and seven in serum were identified. Among these studies, three described NfL levels in patients with a definite diagnosis of FTD on *post-mortem* pathology analysis and 14 of them described this marker for an FTD population including also familial forms (Steinacker et al., 2018).

Diagnostic and prognostic values

The existing studies describe increased NfL concentrations in both matrices (CSF and serum) in FTD groups compared to PPD and control groups (Forgrave et al., 2019), with sensitivity and specificity values above 80%. The highest concentrations of NfL are observed in FTD associated with Amyotrophic Lateral Sclerosis (ALS, or Charcot disease; Pijnenburg et al., 2015). Thus, according to recently published international recommendations (Ducharme et al., 2020), NfL measurement in CSF or blood could be used in practice for the differential diagnosis between FTD and SPD, as long as validated thresholds are available.

Cut-off values found in studies comparing FTD vs. controls or FTD vs. PPD are similar (Davy et al., 2021), which suggests that NfL amounts are comparable in patients with PPD and healthy subjects; this is confirmed by studies comparing PPD and controls (Eratne et al., 2020).

Studies investigating the prognostic performance of NfL in the context of FTD described a 5-year survival estimate respectively at 36% in FTD patients with a high NfL concentration in the CSF (>3,675 pg/ml) and at 73% in patients whose NfL level was lower than 1,989 pg/ml (both measures determined by ELISA; Meeter et al., 2018). CSF NfL achieved an AUC of 0.87 (95% CI 0.81–0.92, $p < 0.001$), with a sensitivity of 79% and specificity of 89% (cutoff ≥1,613 pg/ml) to discriminate patients from controls (Meeter et al., 2018).

In a second study, high serum NfL concentrations were also associated with shorter patient survival and these concentrations were correlated with cortical atrophy of the prefrontal, temporal and parietal brain regions (Benussi et al., 2020). Interestingly, serum NfL concentrations showed a high accuracy in discriminating between FTD and healthy controls (area under the curve (AUC): 0.86, $p < 0.001$; Benussi et al., 2020). In subjects with genetic mutations in the *C9ORF72, GRN* or *MAPT* genes (pre-symptomatic subjects), increased serum NfL has been described during the conversion phase corresponding to the onset of symptoms (Wilke et al., 2022). Finally, as in ALS, serum NfL determination seems to be particularly relevant for monitoring future therapies in FTD (Toft et al., 2020; Saracino et al., 2021).

Position of NfL compared to other biomarkers and cut-off value

Low blood progranulin level is a validated biomarker used to predict the presence of GRN mutations for hereditary FTD (van Swieten and Heutink, 2008). Biomarkers are however lacking for the other etiologies and analysis of AD biomarkers in CSF (t-tau, p-tau, amyloid peptides) remains recommended to exclude this pathology as it is the main differential diagnosis for degenerative dementia (Ducharme et al., 2020). On the other hand, no difference in t-tau and p-tau concentrations was found between DFT and control groups (Abu-Rumeileh et al., 2018) and no difference in the concentration of other Nf subunits (NfM and NfH) is observed between FTD patients and PPD (Escal et al., 2022).

To date, no consensual NfL threshold value has been validated for the differential diagnosis between FTD and PPD. However, the studies mentioning cut-offs and using the UmanDiagnostics ELISA kit range from 1,063 pg/ml to 1,877 pg/ml in the CSF (Forgrave et al., 2019) and for the Simoa technique from 19.5 pg/ml to 33 pg/ml in blood (Forgrave et al., 2019). As the assay is not standardized, it is therefore necessary to assess and validate this threshold in each laboratory according to the technique used. This is not so easy, as it requires samples with a probable diagnosis, which is quite rare in this type of uncommon neurocognitive disorder.

Other neurodegenerative proteinopathies

Creutzfeld-Jakob disease (CJD), the most common form of prion disease, is responsible for extremely rapid cognitive decline. Its diagnosis is based on clinical criteria, EEG and the detection of the 14.3.3 protein in the CSF. Alternatively, a very large increase in t-tau concentration, with a high t-tau/p-tau ratio are strong arguments for the diagnosis. Recently, studies

have shown the interest of NfL measurement in CSF (Abu-Rumeileh and Parchi, 2021) and in blood (Schmitz et al., 2022) to help in the early diagnosis of the disease and to differentiate it from other causes of dementia, in particular from progressive forms of AD. Of note, CSF NfL, either alone or in combination with other biomarkers, yielded a performance similar to t-tau in the distinction of prion disease from other neurodegenerative diseases (AUC 0.926 vs. 0.939) and showed even a higher diagnostic value than t-tau in the specific comparisons between atypical prion disease and other rapidly progressive neurodegenerative dementias (AUC 0.839 vs. 0.722; Abu-Rumeileh and Parchi, 2021). As for the blood, NfL shows lower values compared to blood t-tau for the discrimination between CJD and non-prion rapidly progressive dementias (AUC 0.497–0.724 and AUC 0.722–0.837, respectively; Abu-Rumeileh and Parchi, 2021).

Huntington's disease is a rare, inherited disorder of the CNS. It is manifested by motor, cognitive, and psychiatric disorders. The mutated huntingtin (HTT) protein becomes abnormal and toxic to the neurons of the striatum when the number of CAG repeats is greater than 35. Mean concentrations of NfL in plasma at baseline were significantly higher in HTT mutation carriers than in controls [3.63 (SD 0.54) log pg/ml vs. 2.68 (0.52) log pg/ml, $p < 0.0001$] and the difference increased from one disease stage to the next, thus correlating with the severity of symptoms (Byrne et al., 2017, 2018; Rodrigues et al., 2020). Interestingly, the elevation of NfL precedes the clinic in children with the mutation (Byrne et al., 2018). Concentrations of NfL in CSF and plasma were correlated in mutation carriers ($r = 0.868$, $p < 0.0001$; Byrne et al., 2017).

Amyotrophic lateral sclerosis

Background and state of the art

Amyotrophic lateral sclerosis (ALS) is a neurodegenerative disease of central and peripheral motor neurons, resulting in rapidly progressive amyotrophy and a greatly reduced life expectancy. Diagnosis can be challenging due to the heterogeneity of clinical presentations and the criterion of evolutivity. Therefore, it is common for patients initially identified as having ALS to have their diagnosis reconsidered as a slowly evolving motor neuron disease. In recent years, the NfL assay has emerged as a promising biomarker for the diagnosis and prognosis of ALS.

Published studies first focused on the determination of NfL in CSF (Zetterberg et al., 2007), then in blood (Gaiottino et al., 2013) but also on drying blood or plasma spots (Lombardi et al., 2020). To our knowledge, 36 articles illustrating the interest of NfL blood determination in the context of ALS have been published since 2013.

Diagnostic and prognostic values

Increased blood and/or CSF NfL levels have been reported in ALS patients (Xu et al., 2016; Verde et al., 2019), reflecting axonal damage of motor neurons during disease progression. The mean increase of NfL is significantly greater in ALS patients compared to patients with slowly progressing amyotrophy (Gaiani et al., 2017).

More recently, the interest of blood NfL in predicting the course of the disease has become apparent due to the correlation of this biomarker with the severity of clinical signs (Kojima et al., 2021) and/or the course of the disease (Thouvenot et al., 2020). Monitoring NfL blood levels could also allow the detection of pre-symptomatic forms of ALS in subjects at risk (Benatar et al., 2018). Finally, although no cure for ALS is yet available, NfL blood levels have been suggested as a monitoring marker for potential future therapies (Benatar et al., 2018; Witzel et al., 2021).

Position of NfL compared to other biomarkers and cut-off value

Diagnostic performance of blood NfL for ALS is superior to other biomarkers of axonal degeneration [such as S100B and progranulin (Steinacker et al., 2017b) or neuroinflammation (Brodovitch et al., 2021)]. This can be partly explained by the severity of the disease, but also by the fact that the degeneration affects large myelinated axons that have a strong expression of NfL. The combination of NfL and C-reactive protein in blood (De Schaepdryver et al., 2020) or ferroptosis markers (Devos et al., 2019) have been proposed for the prognostic evaluation of ALS. Determination of TDP-43 and t-tau proteins levels in CSF has also been described in this context (Kojima et al., 2021). A recent study described optimal cut-off values to discriminate between ALS and controls at 500 pg/ml (a sensitivity of 88.5% and specificity of 83.3%), using ELISA assay (Shi et al., 2022). When evaluating the ROC curves in discriminating patients with ALS and subjects with an alternative ALS-mimicking disease, sNfL (measured through Simoa) yields a diagnostic value of 0.873 ± 0.036 (sensitivity 84.7%, specificity 83.3%), for a cut-off 32.7 pg/ml (Vacchiano et al., 2021).

Multiple sclerosis

Background and state of the art

Multiple sclerosis (MS) is a chronic inflammatory disease of the central nervous system (CNS), which can cause significant physical and cognitive disability and is responsible for a significant deterioration in quality of life. It is the most common neurological disease affecting young adults, three women for one

man, with onset occurring mainly between the ages of 20 and 40. It is a multifactorial disease linked to genetic susceptibility factors in association with environmental risk factors and epigenetic factors leading to immune dysfunction (Reich et al., 2018). Eighty-five percent of multiple sclerosis evolves in the form of relapses alternating with phases of remission (so-called relapsing-remitting MS or RRMS). After 10–15 years of disease, RRMS may progress, especially without treatment, to a phase where disability progresses (so-called secondarily progressive MS or SPMS). Fifteen percent of patients present a progressive form from the start (so-called primary progressive MS or PPMS). Relapses are related to CNS invasion by pro-inflammatory peripheral immune cells causing multifocal demyelinating lesions and secondary axonal degeneration. Later phases of the disease are associated with diffuse microglial activation and the formation of ectopic lymphoid meningeal follicles (Cree et al., 2021). Although great progress in the accuracy of diagnostic criteria and immunotherapies for RR forms of MS has been achieved, no blood or CSF biomarkers to monitor disease activity or prognosis or finally to monitor response to treatment are available to date. NfL could be a useful biomarker in these indications, and more than 300 studies related to the measurement of NfL in MS have been published in CSF and since 2016 in serum ($n = 178$) or plasma ($n = 49$).

Diagnostic and prognostic values

Measurement of NfL is not relevant for the differential diagnosis of neuroinflammatory CNS pathology. However, various parameters related to the neuro-axonal damage induced by the inflammatory activity of MS are correlated with increased NfL levels in the CSF and in the blood: presence of a relapse (Barro et al., 2018), presence and number of gadolinium-enhancing lesions on gadolinium injection on MRI (Gd+), indicating "active" lesions (Novakova et al., 2017; Varhaug et al., 2018), increase in the number of new lesions on MRI (Bittner et al., 2020), and the brain volume (Barro et al., 2018). Interestingly, sNfL levels were described to be higher in RRMS than in clinically isolated syndrome patients ($p = 0.001$), thus suggesting sNfL might serve as a biomarker from very early stages of MS (Bittner et al., 2020). Importantly, the prediction accuracy of OCB (presence of oligoclonal bands in the CSF) and/or Gd+ (sensitivity: 72%, specificity: 76%, accuracy: 79%) were increased by including the 90th percentile of sNfL in addition to the above two variables (sensitivity: 73%; specificity: 79%, accuracy: 84%). These findings pointed towards a potential value of especially high sNfL levels (>31 pg/ml) at time of first demyelinating event as indicators of ongoing chronic CNS neuroinflammation and may be considered for inclusion in a future refinement of the McDonald criteria (Bittner et al., 2020). In the context of relapse occurrence or so-called "active" lesions, this increase may persist for a few weeks to a few months. Blood NfL levels also seem to correlate with markers of B cell activity in the CSF, such as the $CD80^+$ marker or the $CD20^+/CD14^+$ ratio (Engel et al., 2019; Uher et al., 2021).

In the short term, elevation of NfL blood levels above the 80th percentile of measured samples correlates with worsening disability within 1 year, as measured by the Expanded Disability Status Scale (EDSS) score. This elevation is also predictive of the occurrence of relapses and progression of brain atrophy in the short term (Disanto et al., 2017; Barro et al., 2018; Calabresi et al., 2021a; Thebault et al., 2022). In the long term, elevated blood NfL levels seem to be predictive of increased brain atrophy at 5 or even 10 years (Kuhle et al., 2017; Barro et al., 2018; Chitnis et al., 2018; Cantó et al., 2019; Jakimovski et al., 2019; Srpova et al., 2021). Contrast enhancing and new/enlarging lesions were independently associated with increased serum neurofilament light chain (17.8% and 4.9% increase per lesion respectively; $P < 0.001$; Barro et al., 2018). The association with disability progression, however, is inconsistent across studies (Manouchehrinia et al., 2020a). One hypothesis that may explain the weaker long-term predictive value is that part of the increase in NfL blood levels related to chronic neurodegenerative processes (associated with the progression of disability in the long term) could be masked by neuro-axonal damage/injury due to the acute inflammatory activity of MS.

Blood NfL as a marker of treatment response

Numerous studies have reported decreased blood NfL levels following initiation of MS immunotherapies (Pop and Viuleț, 1985; Disanto et al., 2017; Novakova et al., 2017; Varhaug et al., 2018; Cantó et al., 2019; Bittner et al., 2020; Calabresi et al., 2021a,b), so that this assay is currently included in most pharmaceutical clinical trials as a secondary measure of treatment effectiveness. The decrease appears to be greater upon initiation of high efficacy therapy (Delcoigne et al., 2020), compared to moderate or basic therapy ($p < 0.05$). This indicates that longitudinal sNfL changes rather than absolute sNfL values at a given time point might be indicative of disease activity and treatment stratification (Bittner et al., 2020). Longitudinal and individual measurement of NfL blood levels to assess the effect of initiated treatment on MS inflammatory activity is therefore promising. Early detection of a suboptimal response to treatment could indeed help to individualize therapeutic decisions, and some treatment strategies are already proposed on the basis of measured NfL values (Bittner et al., 2021; Thebault et al., 2021).

Position of NfL compared to other biomarkers and cut-off value

Astrocytic biomarkers [such as GFAP and chitinase-3-like protein 1 (CHI3L1)] are currently being studied to discriminate RRMS from SPMS patients (Selner, 1988; Huss et al., 2020).

However their determination is not a substitute for other markers currently used in clinical routine (such as determination of the presence of CSF-specific IgG oligoclonal bands or visualization of lesion progression on MRI).

Comparison of ELISA and electrochemiluminescence techniques showed better sensitivity of the Simoa™ platform for the determination of blood NfL in this context (Kuhle et al., 2016) and comparison between Simoa and Ella technologies showed similar results (Gauthier et al., 2021).

NfL levels increase with age (Gauthier et al., 2021) and fluctuate with body mass index and total blood volume (Manouchehrinia et al., 2020b), but are not influenced by gender (Harp et al., 2022). Renal function only influences NfL levels when the glomerular filtration rate is below 60 ml/min/1.73 m^2 (Benkert et al., 2022). A meta-analysis in MS and independent cohort studies of young patients (between 18 and 50 years of age) did not show any association between CSF NfL level and age, in contrast to healthy subjects or those with other neurodegenerative diseases. This suggests that in younger patients, inflammatory activity may mask the effect of age on measured NfL levels (Bridel et al., 2019; Bittner et al., 2020; Manouchehrinia et al., 2020a; Rosso et al., 2021; Uher et al., 2021). Nevertheless, a recent study of more than 10,000 blood samples confirms that NfL level varies with age, with an increase of 2.5% per year, but that this increase is greater after 50 years of age (Benkert et al., 2022). This study enabled the determination and validation in independent cohorts of cut-off values expressed as percentile/Z-scores that quantify the deviation of serum NfL level from the control group, adjusted for age and body mass index: in this study, a sNfL Z score above 1.5 was associated with an increased risk of future clinical or MRI disease activity in all people with multiple sclerosis (odds ratio 3.15, 95% CI 2.35–4.23; $p < 0.0001$) and in people considered stable with no evidence of disease activity (2.66, 1.08–6.55; $p = 0.034$; Benkert et al., 2022). A freely available web application allows calculation of the adjusted percentile/Z-score from an individual NfL value[1].

NfL and neurological damages

Traumatic brain injuries

Background and state of the art

Traumatic brain injury (TBI) is a major public health problem (more than 500 per day in France). About 80% of cases of TBI are classified as mild head injury (also called concussions). The morbidity associated with head trauma is considerable. Nearly 50% of victims have residual disabilities that may include progressive neurodegeneration, cognitive impairment, and dementia. Head injuries must be carefully diagnosed to foresee, anticipate, and treat the medical and/or social after-effects they cause. Blood and CSF biomarkers of neurodegeneration, particularly NfL, could help in the diagnosis and prognosis assessment.

Diagnostic and prognostic values

The number of publications regarding the interest of NfL in TBI is growing rapidly (391 articles in PubMed as of 01/06/2022). An increase in NfL levels in the CSF and blood is found during TBI, reflecting the axonal damage suffered (Khalil et al., 2018). Following TBI, whether severe or mild in athletes, NfL is detectable from the first hour and continues in a linear fashion with a maximum at Day 12 in the CSF and blood (Zetterberg et al., 2013; Zetterberg and Blennow, 2016; Shahim et al., 2017; McDonald et al., 2021).

The 24-h assessment of this biomarker could also be of prognostic interest. The NfL increase seems to be correlated with the severity of the damage found on the brain scan and with the severity of the neurological sequelae at 1 year, as well as with the survival of the patients (Shahim et al., 2016, 2018; Graham et al., 2021). Measurement at 24 h allows prediction of the long-term evolution of patients and high values are observed in case of unfavorable evolution. In athletes, NfL blood levels are correlated with the number of concussions and their impact (Verduyn et al., 2021). A recent study in rugby players showed that those who have suffered more than three concussions in a year maintained high NfL levels after the off-season, indicating chronic suffering. Chronically elevated levels of this biomarker have also been associated with the development of frontotemporal cognitive deficits and damage to the blood-brain barrier (Verduyn et al., 2021). Thus, a persistent increase in NfL could indicate the presence of progressive post-traumatic neurodegeneration. These results have yet to be confirmed by larger studies but suggest that NfL blood determination may be useful to identify patients at risk of developing chronic traumatic encephalopathy and to adapt their follow-up.

Position of NfL compared to other biomarkers and cut-off value

The monitoring of serum biomarkers, such as S100B protein in TBI patients is of great interest for rapid and inexpensive diagnosis and prognostic evaluation. Other blood biomarkers are being studied and the NfL assay could be a complementary tool to enhance its diagnostic performance. Indeed, the cellular origin and the kinetics of these biomarkers are different (**Figure 3**): the determination of S100B must be performed within 3 h after the TBI [because of its half-life of 2 h (Jackson et al., 2000)], and the serum determination

1 https://shiny.dkfbasel.ch/baselnflreference

of NfL (whose half-life is longer and whose levels remain high several days after the TBI) would thus present a real informative added value in case of delayed patient management (Blomquist et al., 1997; Shahim et al., 2016; Thelin et al., 2017). A mean diagnostic serum threshold of 20 pg/ml is found in several studies in this context (Thelin et al., 2017). Other biomarkers of interest in this context are emerging, such as neuron-specific enolase (NSE), glial fibrillary acidic protein (GFAP), t-tau, and ubiquitin C-terminal hydrolase L1 (UCH-L1; **Figure 3**). Further studies comparing the diagnostic and prognostic performance of these markers are needed for their clinical use, alone or in combination, as well as for the advancement of CE and IVD labeling, which are essential for their use in clinical care. In the field of mild TBI (MTBI) and the interest of blood biomarkers in the reduction of unnecessary brain scans prescriptions, a recent study compared the diagnostic performances of S100B and NfL in the early management (blood samples within 3 h post-trauma) of 179 MTBI patients referred to an emergency department. S100B predicted intracranial lesions with a sensitivity of 100% and a 36% specificity. The NfL measurement did not enhance the predictive value. At a threshold of 8.38 ng/L, NfL predicted intracranial lesions with a 28% specificity. On the other hand, in the same population, NfL proved to be a high effective marker for the detection of patients with degenerative neurological pathologies, as shown by the data collected in this study (area under the ROC curve of 0.87 compared with only 0.57 for the S100B protein; Kahouadji et al., 2022).

Considering the extensive literature in this area, NfL is likely to be of greater interest for prognostic assessment. However, no cut-off value has yet been determined to predict the secondary occurrence of cognitive disorders.

Stroke

Background and state of the art

Stroke is the worldwide leading cause of death and long-term morbidity. NfL may be of interest as a predictive biomarker for the outcome of ischemic stroke, and for the long-term consequences. Indeed, only one third of patients recover with minimal or no deficit, whereas the majority remain moderately or severely disabled for life. As life expectancy and population ages increase, stroke management has become a societal issue and efforts are underway to identify appropriate prognostic indicators for optimizing patient management.

Diagnostic and prognostic values

CSF and blood NfL levels are both increased after stroke, involving both small and large vessels, and several studies have investigated the relationship between this increase and the prognosis of ischemic stroke (Gattringer et al., 2017; Pujol-Calderón et al., 2019; Peters et al., 2020). A recent meta-analysis confirmed existence of a correlation between serum NfL level

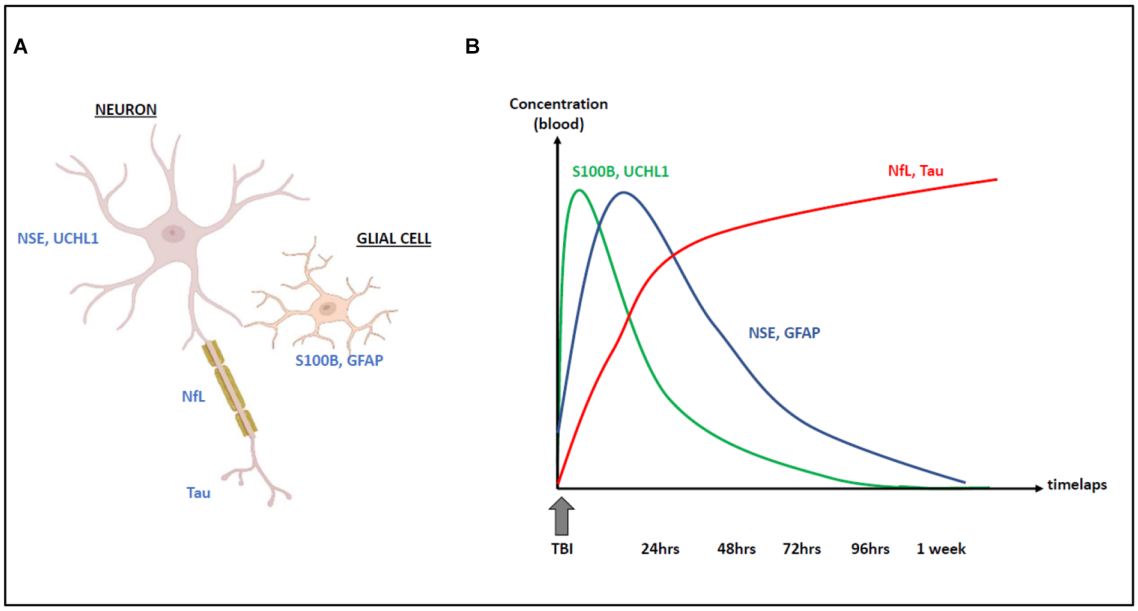

FIGURE 3
Cellular origin **(A)** and kinetics **(B)** of NfL increase following traumatic brain injury (TBI) compared with other biomarkers: S100B, UCH-L1, Tau, NSE, and GFAP.

and the volume of the cerebral infarct area (Liu et al., 2020), with a pool adjusted odds ratios (ORs) from multivariate regression models, = 1.71 (95% CI: 1.17–4.29), representing that the patients with higher sNfL had a 1.71 times higher risk of poor functional outcome during follow-up (compared with lower sNfL patients; Liu et al., 2020). Kinetic assays reveal that the highest concentration would be reached 1 week after stroke (Tiedt et al., 2018; Gendron et al., 2020). Patients with the highest levels between 1 and 7 days after stroke were 1.7 times more likely to have sequelae within 3 months than those with low NfL levels. A large prospective study (n = 1,694 patients) recently confirmed that NfL levels at 48 h were an independent risk factor for cognitive sequelae within 3 months after stroke (Wang Z. et al., 2021), $p < 0.001$. Levels also correlated with the Rankin score used to measure disability secondary to stroke in the acute phase. Other studies show that initial NfL levels predict longer-term patient outcomes, particularly cognitive decline at 1 year (Wang J.-H. et al., 2021) and mortality (Gendron et al., 2020), regardless of whether the stroke was ischemic or hemorrhagic. The optimal cut-off value of the sNfL concentration was 46.12 pg/ml, which yielded a sensitivity of 71.0% and a specificity of 81.5%, with the area under the curve (AUC) at 0.785 (95% CI 0.762–0.808, $p < 0.001$; Wang Z. et al., 2021). These results demonstrate the value of early NfL determination as a prognostic biomarker.

CSF NfL levels are also increased in subarachnoid hemorrhage due to aneurysm rupture (Nylén et al., 2006; Gendron et al., 2020). As in stroke, the levels correlate with a poor prognosis, and in particular with 3-month mortality (Gendron et al., 2020; Hviid et al., 2020). The area under the receiver operating characteristic curve (ROC AUC) for discrimination of day-30 mortality was significant on admission [AUC = 0.83, 95% confidence interval (CI): 0.56–1.0] and increased on 24-h follow-up (AUC = 0.93, 95% CI: 0.84–1.0; Hviid et al., 2020).

NfL levels may remain elevated for up to 6 months after stroke. The sustained high levels could be explained by secondary Wallerian degeneration affecting motor neurons and by the poststroke inflammatory and immune response. High 6-month NfL levels correlate with the presence of secondary lesions and quantitative measure of secondary neurodegeneration detected by MRI (Tiedt et al., 2018; Peng et al., 2021).

Position of NfL compared to other biomarkers and cut-off value

Other biomarkers are studied in the stroke context: GFAP and Tau levels increase after stroke and are correlated with lesion volume and the NIHSS clinical score used for diagnosis and severity assessment. The kinetics of these biomarkers are different from NfL with a much faster rise and fall. The time between stroke and the determination of each of these biomarkers should be evaluated for optimal use (Pujol-Calderón et al., 2022). Although the place of blood NfL remains to be confirmed, it will undoubtedly improve, in combination with the available tools (biomarkers, clinical, and imaging scores), a better assessment of the prognosis of stroke patients. After an acute stroke, prophylaxis is implemented to prevent or reduce subsequent events, and a blood biomarker that captures subclinical events would help both monitor and determine the best treatment for this purpose (Campbell et al., 2019). Thus, blood levels of NfL are related to the risk of developing stroke in the years after the acute event and low NfL could be a real-time biomarker of the effectiveness of prophylactic treatment (Uphaus et al., 2019).

There is no validated consensus cut-off value for the assessment of stroke prognosis by blood NfL. Only one study proposes a threshold value of 46 pg/ml, determined by the Simoa approach, to identify patients who will remain with cognitive sequelae at 3 months [sensitivity of 71% and specificity of 81.5% (AUC 0.79; Wang Z. et al., 2021)]. This value should be adjusted according to the assay technique used, the patient's history (neurodegenerative diseases) and age.

Neurological damages in oncology

Background and state of the art

Neurological disorders in cancerology are numerous and varied in terms of both their etiology and the symptoms observed. They can be due to the primary cerebral localization of a tumor (glioblastoma, oligodendroglioma, medulloblastoma...), to the cerebral or medullary localization of metastases of an extra-cerebral cancer (lung, breast, melanoma, digestive cancer, lymphoma...), to a carcinomatous meningitis (inflammation by meningeal invasion by cancerous cells) or to autoimmune reactions triggered (paraneoplastic neurological syndrome). The treatment of these cancers is also responsible for neurological complications, and this neurotoxicity is in most cases dose-dependent. Neurological damage may affect the central nervous system (CNS), the peripheral nervous system (PNS) or both simultaneously. Early diagnosis of these disorders can often reduce symptoms and prevent permanent neurological deficits. Imaging tests such as MRI or electromyography (EMG) are used to identify these disorders, but there are no blood biomarkers (except for anti-neuronal antibodies) that can be useful for the diagnosis of these pathologies. Moreover, the currently available markers do not allow the evaluation of lesion progression and response to treatment. Various studies have explored the use of NfL in these indications.

Diagnostic and prognostic values

Primary CNS tumors and brain metastases are major causes of morbidity and mortality. The earlier the diagnosis, the better the management of the patients and the survival rates, which are anyway low in these cases. Several publications have thus focused on the use of NfL as a diagnostic and prognostic blood marker. High blood levels of NfL in brain metastases (Hepner et al., 2019; Kim et al., 2021; Lin et al., 2022) was reported, these levels being correlated with the number and size of metastases (Lin et al., 2022). A decrease in levels of NfL was also detected following treatment (Kim et al., 2021).

Interestingly, Winther-Larsen et al. demonstrated an increase in NfL in the blood (35 vs. 16 pg/ml, $p = 0.001$) early, even before the diagnosis of brain metastases (median 3 months before; Winther-Larsen et al., 2020). sNfL discriminated these patients with an area under the curve of 0.77 (0.66–0.89; Winther-Larsen et al., 2020). An increase in NfL could be measured median 3 months (range: 1–5) before the brain metastasis diagnosis. A very high level of NfL at the time of diagnosis seemed to be correlated with a lower survival, with an inferior survival [hazard ratio: 2.10 (95% confidence interval: 1.11–3.98; Winther-Larsen et al., 2020)]. Of note, these findings were recently confirmed in a cohort of lung cancer patients (Lin et al., 2022).

NfL determination may also have prognostic value in primary CNS tumors. Thus, Hepner et al. showed in a cohort of glioma patients that blood levels of NfL varied closely with tumor activity (Hepner et al., 2019), and that patients with progressive disease had on average 10-fold higher levels than those with stable disease.

Response to cancer therapy

Iatrogenic neurological complications can appear as early as the first days of treatment or even years later. Some alkylating agents are well known to be responsible for adverse effects with neurological manifestations (e.g., neuropathy and platinum salts). The increase in treatment lines and the development of new therapeutic modalities increase the risk of neurotoxicity. It can be challenging to make the diagnosis, but it is essential to get it done as soon as possible. Several studies have shown that the concentration of NfL correlates with the development and severity of toxicity resulting from various treatments. Thus, patients treated with paclitaxel, known to induce peripheral neurological manifestations, show an increase in blood NfL concentration 4 weeks after chemotherapy (compared to controls), resulting in an 86% sensitivity and 87% specificity (Huehnchen et al., 2022). An increase of sNFL of +36 pg/ml from baseline was associated with a predicted CIPN probability of more than 0.5 (Huehnchen et al., 2022).

The increase correlated with the development and severity of polyneuropathy (Huehnchen et al., 2022; Karteri et al., 2022). However, no association between increased blood NfL and cognitive impairment could be demonstrated in this context (Argyriou et al., 2022).

Emerging therapies such as antibody immunotherapy and CAR-T cells may also induce neurotoxicity, particularly autoimmune encephalitis, and the Immune Cell Associated Neurotoxicity Syndrome (ICANS), 1 week after treatment. In the case of post-immunotherapy autoimmune encephalitis, blood and CSF NfL rises and this result might be useful for tolerance monitoring (Piepgras et al., 2021). A very recent study reports that patients with ICANS after CAR-T therapy had elevated NfL levels (Schoeberl et al., 2022) and increased levels correlated with severity of the symptoms [(ICANS grade 0–1: 28.4 pg/ml (IQR, 19.2–49.7 pg/ml); ICANS grade 2–4: 60.0 pg/ml (IQR, 31.7–109.0 pg/ml); $p < 0.01$; Schoeberl et al., 2022)]. More surprisingly, patients who developed this neurotoxicity had already elevated pre-transplant levels of NfL (60 pg/ml vs. 28 pg/ml in the group that developed no or little neurotoxicity, as assessed by Simoa technology; Schoeberl et al., 2022).

These initial results are promising in terms of the usefulness of NfL in oncology but remain to be validated on larger and longer-term cohorts for neurotoxicity.

Position of NfL compared to other biomarkers and cut-off value

For metastases diagnosis, NfL threshold values may be defined according to age: for example, NfL levels >22 pg/ml (measured by the Simoa approach) in cancer patients aged 51–60 years may predict the presence of brain metastases (Kim et al., 2021). Other biomarkers are also being evaluated, in particular the GFAP protein which would, according to Darlix et al. (2021) outperform NfL as a diagnostic and prognostic factor for brain metastases in breast cancer patients. Further studies will determine whether the combination of the two biomarkers is worthwhile, but studies have already described increased levels of sNfL and GFAP in patients with CNS tumors with disease in progression vs. CNS with stable disease ($p = 0.03$ and $p = 0.01$, respectively; Hepner et al., 2019). Regarding chemotherapy toxicity, an increase in serum NfL concentration (assessed by Simoa) of more than 36 pg/ml (Huehnchen et al., 2022) or an elevated level at 3 or 4 weeks (>50 pg/ml and >85 pg/ml) is associated with high risk of developing polyneuropathy (Huehnchen et al., 2022; Karteri et al., 2022). In addition, high level of blood NfL could predict the occurrence of ICANS in case of CAR-T cell treatment (a threshold value of 75 pg/ml determined by the Simoa approach has been proposed; Schoeberl et al., 2022).

Other NfL applications

It is difficult to be exhaustive on the use of NfL as this marker is in full expansion. For example, Nf could be of interest in other peripheral neuropathies, such as TTR amyloidosis (Ticau et al., 2021) and AL amyloidosis (Louwsma et al., 2021). Growing literature also highlights the predictive value of NfL concentrations in the intensive care setting, as it may be used to assess the risk of neurological events following either resuscitation (Fisse et al., 2021; Page et al., 2022) or cardiac arrest. Thus, high levels of blood NfL 48 h after cardiac arrest (>500 pg/ml) were described to predict neurological complications related to cerebral ischemia/hypoxia with high sensitivity (100%, 95%CI 70.0–100%) and specificity (91.7%, 95%CI 62.5–100%; Adler et al., 2022; Hoiland et al., 2022) and were correlated with EEG abnormalities, $p < 0.001$ (Grindegård et al., 2022).

Recent research has focused on the determination of NfL values in **children**, and norms could be proposed in the pediatric population (Nitz et al., 2021). Increased NfL is described to be correlated with the development of motor neurological disorders or retinopathy in premature infants (Goeral et al., 2021; Sjöbom et al., 2021). The value of NfL in CSF and blood also appears to be associated with the severity of inherited diseases with neurological impairment, such as SMA (Johannsen et al., 2021; Nitz et al., 2021), cerebral adrenoleukodystrophy (Wang et al., 2022) or mitochondrial diseases (Sofou et al., 2019). Finally, NfL could be relevant for monitoring treatment response (Ru et al., 2019).

Conclusion

Development of ultrasensitive immunoassays has made it possible to detect biomarkers of neuronal damage in easily collected blood samples, even though the concentrations are lower than in CSF. This opens a promising new avenue for the development of neurological biomarkers. Neurofilaments (Nf) are proteins selectively expressed in the cytoskeleton of neurons, the increase of which is a marker of neuronal damage. NfLs are highly specific to neurons but increase in many clinical settings and other candidates for neurological damage are currently under development. Indeed, neuronal damage is common and can be observed both during neurodegenerative diseases (such as AD, PD, FTD) but also in other neurological contexts (such as head injury, stroke or cancer). In this review, we have provided an overview of these different contexts, showing that the determination of NfL in biological fluids has a wide range of potential uses, sometimes for differential diagnosis, but more often for prognosis or monitoring of the therapeutic response of many neurological diseases (**Figure 4**). We discuss the place and informative added value of NfL compared to other commonly used biomarkers for monitoring neurodegenerative or no-neurodegenerative pathologies.

The NfL assay may be particularly relevant for the diagnosis of ALS or PD dementia for example. It would also be useful for the differential diagnosis between FTD and psychiatric disorders, between different Parkinsonian syndromes, or between Alzheimer's disease and Prion disease, for which the levels of circulating NfL are very different.

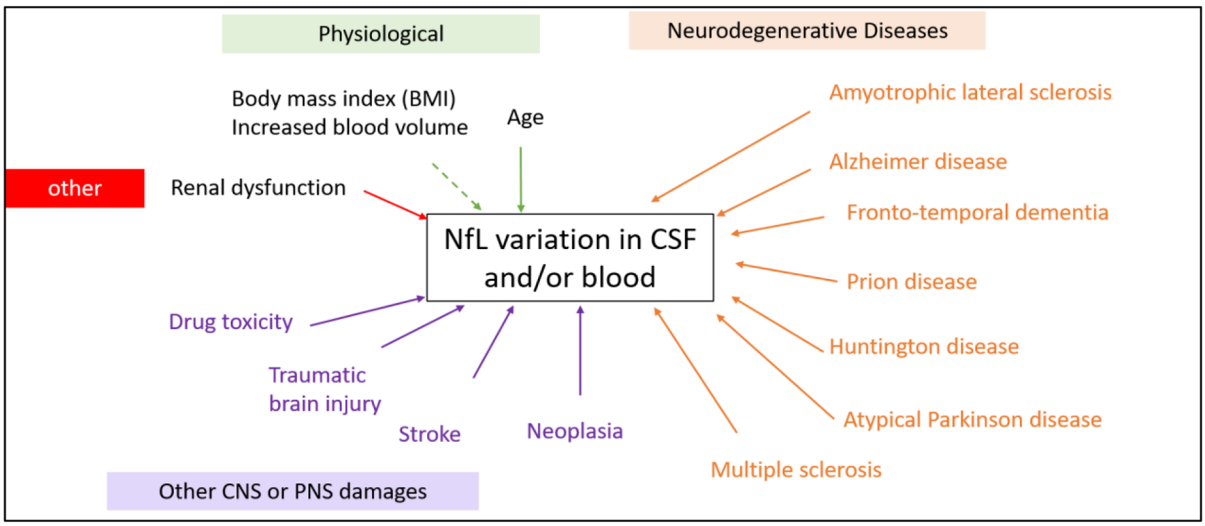

FIGURE 4
Physiological and pathological factors modifying the NfL levels in CSF and blood (non-exhaustive). A rise in NfL is not specific for a specific disease factor and may be caused by both neurodegenerative diseases or a head impact during sports for example.

It is important to note that the level of NfL is a good marker of severity: its level is indeed correlated with a poor prognosis in many neurodegenerative diseases (ALS, Parkinson's disease syndromes, MS, Huntington's,...) and predicts the cognitive decline following repeated head trauma and stroke. The signs and symptoms on which the clinical diagnosis is based sometimes appear late in the course of the disease compared to the time of onset; the dynamics of blood NfL in the preclinical phases of neurological diseases and the possibility of detecting blood levels of NfL in an ultrasensitive manner could be used to identify diseases at an earlier stage. Finally, NfL can also be used to monitor the response to therapies and the neurotoxicity that such treatments may cause.

Nonetheless, it is important to keep in mind that NfL is a marker of neuroaxonal destruction independent of the mechanism causing the neuronal damage. The specific diagnosis will require consideration of a great deal of information, including the patient's history, physical examination, imaging, and other laboratory tests. It seems essential to define reference ranges of normality for this biomarker, depending on the biological sample considered (CSF or blood), the analytical test performed, age and BMI for each medical indication in order to correctly interpret NfL results according to the context. Indeed, many factors other than the primary neurological disease, including age, BMI, cardiovascular risk factors, unrecognized head injury, etc., may be confounding factors that influence blood NfL and should therefore be taken into account when evaluating this biomarker in patients.

The homogenization of the thresholds of this biomarker according to the assay methods would allow a rapid development of its use in clinical routine for an optimized management of the patients. The extent of its use means that NfL could soon become a must for the clinical activity of the neurologist (Giovannoni, 2018; Lambertsen et al., 2020).

Author contributions

All authors contributed to the writing of the different parts of the article. SL, AB, and CD assembled the final version. All authors contributed to the article and approved the submitted version.

Funding

No funding was required for this study which was carried out within the "Neurofilaments" working group of the French Society of Clinical Biology (SFBC).

Conflict of interest

The authors declare that the research was conducted in the absence of any commercial or financial relationships that could be construed as a potential conflict of interest.

Publisher's note

All claims expressed in this article are solely those of the authors and do not necessarily represent those of their affiliated organizations, or those of the publisher, the editors and the reviewers. Any product that may be evaluated in this article, or claim that may be made by its manufacturer, is not guaranteed or endorsed by the publisher.

References

Aamodt, W. W., Waligorska, T., Shen, J., Tropea, T. F., Siderowf, A., Weintraub, D., et al. (2021). Neurofilament light chain as a biomarker for cognitive decline in Parkinson disease. *Mov. Disord.* 36, 2945–2950. doi: 10.1002/mds.28779

Abu-Rumeileh, S., Mometto, N., Bartoletti-Stella, A., Polischi, B., Oppi, F., Poda, R., et al. (2018). Cerebrospinal fluid biomarkers in patients with frontotemporal dementia spectrum: a single-center study. *J. Alzheimers Dis.* 66, 551–563. doi: 10.3233/JAD-180409

Abu-Rumeileh, S., and Parchi, P. (2021). Cerebrospinal fluid and blood neurofilament light chain protein in prion disease and other rapidly progressive dementias: current state of the art. *Front. Neurosci.* 15:648743. doi: 10.3389/fnins.2021.648743

Adler, C., Onur, O. A., Braumann, S., Gramespacher, H., Bittner, S., Falk, S., et al. (2022). Absolute serum neurofilament light chain levels and its early kinetics predict brain injury after out-of-hospital cardiac arrest. *J. Neurol.* 269, 1530–1537. doi: 10.1007/s00415-021-10722-3

Argyriou, A. A., Karteri, S., Bruna, J., Mariotto, S., Simo, M., Velissaris, D., et al. (2022). Serum neurofilament light chain levels as biomarker of paclitaxel-induced cognitive impairment in patients with breast cancer: a prospective study. *Support. Care Cancer* 30, 1807–1814. doi: 10.1007/s00520-021-06509-x

Ashton, N. J., Janelidze, S., Al Khleifat, A., Leuzy, A., van der Ende, E. L., Karikari, T. K., et al. (2021). A multicentre validation study of the diagnostic value of plasma neurofilament light. *Nat. Commun.* 12:3400. doi: 10.1038/s41467-021-23620-z

Bäckström, D. C., Eriksson Domellöf, M., Linder, J., Olsson, B., Öhrfelt, A., Trupp, M., et al. (2015). Cerebrospinal fluid patterns and the risk of future dementia in early, incident Parkinson disease. *JAMA Neurol.* 72, 1175–1182. doi: 10.1212/WNL.0000000000201124

Barro, C., Benkert, P., Disanto, G., Tsagkas, C., Amann, M., Naegelin, Y., et al. (2018). Serum neurofilament as a predictor of disease worsening and brain and spinal cord atrophy in multiple sclerosis. *Brain* 141, 2382–2391. doi: 10.1093/brain/awy154

Benatar, M., Wuu, J., Andersen, P. M., Lombardi, V., and Malaspina, A. (2018). Neurofilament light: a candidate biomarker of presymptomatic amyotrophic lateral sclerosis and phenoconversion. *Ann. Neurol.* 84, 130–139. doi: 10.1002/ana.25276

Benkert, P., Meier, S., Schaedelin, S., Manouchehrinia, A., Yaldizli, Ö., Maceski, A., et al. (2022). Serum neurofilament light chain for individual prognostication of disease activity in people with multiple sclerosis: a retrospective

modelling and validation study. *Lancet Neurol.* 21, 246–257. doi: 10.1016/S1474-4422(22)00009-6

Benussi, A., Karikari, T. K., Ashton, N., Gazzina, S., Premi, E., Benussi, L., et al. (2020). Diagnostic and prognostic value of serum NfL and p-Tau181 in frontotemporal lobar degeneration. *J. Neurol. Neurosurg. Psychiatry* 91, 960–967. doi: 10.1136/jnnp-2020-323487

Bittner, S., Oh, J., Havrdová, E. K., Tintoré, M., and Zipp, F. (2021). The potential of serum neurofilament as biomarker for multiple sclerosis. *Brain* 144, 2954–2963. doi: 10.1093/brain/awab241

Bittner, S., Steffen, F., Uphaus, T., Muthuraman, M., Fleischer, V., Salmen, A., et al. (2020). Clinical implications of serum neurofilament in newly diagnosed MS patients: a longitudinal multicentre cohort study. *EBioMedicine* 56:102807. doi: 10.1016/j.ebiom.2020.102807

Blomquist, S., Johnsson, P., Lührs, C., Malmkvist, G., Solem, J. O., Alling, C., et al. (1997). The appearance of S-100 protein in serum during and immediately after cardiopulmonary bypass surgery: a possible marker for cerebral injury. *J. Cardiothorac. Vasc. Anesth.* 11, 699–703. doi: 10.1016/s1053-0770(97)90160-9

Bridel, C., van Wieringen, W. N., Zetterberg, H., Tijms, B. M., Teunissen, C. E., and the NFL Group Alvarez-Cermeño, J. C., Andreasson, U., et al. (2019). Diagnostic value of cerebrospinal fluid neurofilament light protein in neurology: a systematic review and meta-analysis. *JAMA Neurol.* 76:1035. doi: 10.1001/jamaneurol.2019.1534

Brodovitch, A., Boucraut, J., Delmont, E., Parlanti, A., Grapperon, A.-M., Attarian, S., et al. (2021). Combination of serum and CSF neurofilament-light and neuroinflammatory biomarkers to evaluate ALS. *Sci. Rep.* 11:703. doi: 10.1038/s41598-020-80370-6

Byrne, L. M., Rodrigues, F. B., Blennow, K., Durr, A., Leavitt, B. R., Roos, R. A. C., Scahill, R. I., et al. (2017). Neurofilament light protein in blood as a potential biomarker of neurodegeneration in Huntington's disease: a retrospective cohort analysis. *Lancet Neurol.* 16, 601–609. doi: 10.1016/S1474-4422(17)30124-2

Byrne, L. M., Rodrigues, F. B., Johnson, E. B., Wijeratne, P. A., De Vita, E., Alexander, D. C., et al. (2018). Evaluation of mutant huntingtin and neurofilament proteins as potential markers in Huntington's disease. *Sci. Transl. Med.* 10:eaat7108. doi: 10.1126/scitranslmed.aat7108

Calabresi, P. A., Arnold, D. L., Sangurdekar, D., Singh, C. M., Altincatal, A., de Moor, C., et al. (2021a). Temporal profile of serum neurofilament light in multiple sclerosis: implications for patient monitoring. *Mult. Scler.* 27, 1497–1505. doi: 10.1177/1352458520972573

Calabresi, P. A., Kappos, L., Giovannoni, G., Plavina, T., Koulinska, I., Edwards, M. R., et al. (2021b). Measuring treatment response to advance precision medicine for multiple sclerosis. *Ann. Clin. Transl. Neurol.* 8, 2166–2173. doi: 10.1002/acn3.51471

Campbell, B. C. V., De Silva, D. A., Macleod, M. R., Coutts, S. B., Schwamm, L. H., Davis, S. M., et al. (2019). Ischaemic stroke. *Nat. Rev. Dis. Primers* 5:70. doi: 10.1038/s41572-019-0118-8

Cantó, E., Barro, C., Zhao, C., Caillier, S. J., Michalak, Z., Bove, R., et al. (2019). Association between serum neurofilament light chain levels and long-term disease course among patients with multiple sclerosis followed up for 12 years. *JAMA Neurol.* 76, 1359–1366. doi: 10.1177/10556656221131855

Chitnis, T., Gonzalez, C., Healy, B. C., Saxena, S., Rosso, M., Barro, C., et al. (2018). Neurofilament light chain serum levels correlate with 10-year MRI outcomes in multiple sclerosis. *Ann. Clin. Transl. Neurol.* 5, 1478–1491. doi: 10.1002/acn3.638

Cree, B. A. C., Arnold, D. L., Chataway, J., Chitnis, T., Fox, R. J., Pozo Ramajo, A., Murphy, N., et al. (2021). Secondary progressive multiple sclerosis: new insights. *Neurology* 97, 378–388. doi: 10.1212/WNL.0000000000012323

Darlix, A., Hirtz, C., Mollevi, C., Ginestet, N., Tiers, L., Jacot, W., et al. (2021). Serum glial fibrillary acidic protein is a predictor of brain metastases in patients with metastatic breast cancer. *Int. J. Cancer* 149, 1605–1618. doi: 10.1002/ijc.33724

Davy, V., Dumurgier, J., Fayosse, A., Paquet, C., and Cognat, E. (2021). Neurofilaments as emerging biomarkers of neuroaxonal damage to differentiate behavioral frontotemporal dementia from primary psychiatric disorders: a systematic review. *Diagnostics (Basel)* 11:754. doi: 10.3390/diagnostics11050754

de Jong, D., Jansen, R. W. M. M., Pijnenburg, Y. a. L, van Geel, W. J. A., Borm, G. F., Kremer, H. P. H., et al. (2007). CSF neurofilament proteins in the differential diagnosis of dementia. *J. Neurol. Neurosurg. Psychiatry* 78, 936–938. doi: 10.1136/jnnp.2006.107326

De Schaepdryver, M., Lunetta, C., Tarlarini, C., Mosca, L., Chio, A., Van Damme, P., et al. (2020). Neurofilament light chain and C reactive protein explored as predictors of survival in amyotrophic lateral sclerosis. *J. Neurol. Neurosurg. Psychiatry* 91, 436–437. doi: 10.1136/jnnp-2019-322309

Delaby, C., Alcolea, D., Carmona-Iragui, M., Illán-Gala, I., Morenas-Rodríguez, E., Barroeta, I., et al. (2020). Differential levels of neurofilament light protein in cerebrospinal fluid in patients with a wide range of neurodegenerative disorders. *Sci. Rep.* 10:9161. doi: 10.1038/s41598-020-66090-x

Delcoigne, B., Manouchehrinia, A., Barro, C., Benkert, P., Michalak, Z., Kappos, L., et al. (2020). Blood neurofilament light levels segregate treatment effects in multiple sclerosis. *Neurology* 94, e1201–e1212. doi: 10.1212/WNL.0000000000009097

Devos, D., Moreau, C., Kyheng, M., Garçon, G., Rolland, A. S., Blasco, H., et al. (2019). A ferroptosis-based panel of prognostic biomarkers for amyotrophic lateral sclerosis. *Sci. Rep.* 9:2918. doi: 10.1038/s41598-019-39739-5

Dhiman, K., Gupta, V. B., Villemagne, V. L., Eratne, D., Graham, P. L., Fowler, C., et al. (2020). Cerebrospinal fluid neurofilament light concentration predicts brain atrophy and cognition in Alzheimer's disease. *Alzheimers Dement. (Amst)* 12:e12005. doi: 10.1002/dad2.12005

Disanto, G., Adiutori, R., Dobson, R., Martinelli, V., Dalla Costa, G., Runia, T., et al. (2016). Serum neurofilament light chain levels are increased in patients with a clinically isolated syndrome. *J. Neurol. Neurosurg. Psychiatry* 87, 126–129. doi: 10.1136/jnnp-2014-309690

Disanto, G., Barro, C., Benkert, P., Naegelin, Y., Schädelin, S., Giardiello, A., et al. (2017). Serum neurofilament light: a biomarker of neuronal damage in multiple sclerosis. *Ann. Neurol.* 81, 857–870. doi: 10.1002/ana.24954

Ducharme, S., Dols, A., Laforce, R., Devenney, E., Kumfor, F., van den Stock, J., et al. (2020). Recommendations to distinguish behavioural variant frontotemporal dementia from psychiatric disorders. *Brain* 143, 1632–1650. doi: 10.1093/brain/awaa018

Elbaz, A., Carcaillon, L., Kab, S., and Moisan, F. (2016). Epidemiology of Parkinson's disease. *Rev. Neurol. (Paris)* 172, 14–26. doi: 10.1016/j.neurol.2015.09.012

Engel, S., Friedrich, M., Muthuraman, M., Steffen, F., Poplawski, A., Groppa, S., et al. (2019). Intrathecal B-cell accumulation and axonal damage distinguish MRI-based benign from aggressive onset in MS. *Neurol. Neuroimmunol. Neuroinflamm.* 6:e595. doi: 10.1212/NXI.0000000000000595

Eratne, D., Loi, S. M., Walia, N., Farrand, S., Li, Q.-X., Varghese, S., et al. (2020). A pilot study of the utility of cerebrospinal fluid neurofilament light chain in differentiating neurodegenerative from psychiatric disorders: a "C-reactive protein" for psychiatrists and neurologists. *Aust. N Z J. Psychiatry* 54, 57–67. doi: 10.1177/0004867419857811

Escal, J., Fourier, A., Formaglio, M., Zimmer, L., Bernard, E., Mollion, H., et al. (2022). Comparative diagnosis interest of NfL and pNfH in CSF and plasma in a context of FTD-ALS spectrum. *J. Neurol.* 269, 1522–1529. doi: 10.1007/s00415-021-10714-3

Fisse, A. L., Pitarokoili, K., Leppert, D., Motte, J., Pedreiturria, X., Kappos, L., et al. (2021). Serum neurofilament light chain as outcome marker for intensive care unit patients. *J. Neurol.* 268, 1323–1329. doi: 10.1007/s00415-020-10277-9

Forgrave, L. M., Ma, M., Best, J. R., and DeMarco, M. L. (2019). The diagnostic performance of neurofilament light chain in CSF and blood for Alzheimer's disease, frontotemporal dementia and amyotrophic lateral sclerosis: a systematic review and meta-analysis. *Alzheimers Dement.* 11, 730–743. doi: 10.1016/j.dadm.2019.08.009

Fortea, J., Carmona-Iragui, M., Benejam, B., Fernández, S., Videla, L., Barroeta, I., et al. (2018). Plasma and CSF biomarkers for the diagnosis of Alzheimer's disease in adults with Down syndrome: a cross-sectional study. *Lancet Neurol.* 17, 860–869. doi: 10.1016/S1474-4422(18)30285-0

Fortea, J., Vilaplana, E., Carmona-Iragui, M., Benejam, B., Videla, L., Barroeta, I., et al. (2020). Clinical and biomarker changes of Alzheimer's disease in adults with Down syndrome: a cross-sectional study. *Lancet* 395, 1988–1997. doi: 10.1016/S0140-6736(20)30689-9

Gaetani, L., Blennow, K., Calabresi, P., Di Filippo, M., Parnetti, L., and Zetterberg, H. (2019). Neurofilament light chain as a biomarker in neurological disorders. *J. Neurol. Neurosurg. Psychiatry* 90, 870–881. doi: 10.1136/jnnp-2018-320106

Gaiani, A., Martinelli, I., Bello, L., Querin, G., Puthenparampil, M., Ruggero, S., et al. (2017). Diagnostic and prognostic biomarkers in amyotrophic lateral sclerosis: neurofilament light chain levels in definite subtypes of disease. *JAMA Neurol.* 74, 525–532. doi: 10.1001/jamaneurol.2016.5398

Gaiottino, J., Norgren, N., Dobson, R., Topping, J., Nissim, A., Malaspina, A., et al. (2013). Increased neurofilament light chain blood levels in neurodegenerative neurological diseases. *PLoS One* 8:e75091. doi: 10.1371/journal.pone.0075091

Gattringer, T., Pinter, D., Enzinger, C., Seifert-Held, T., Kneihsl, M., Fandler, S., et al. (2017). Serum neurofilament light is sensitive to active cerebral small vessel disease. *Neurology* 89, 2108–2114. doi: 10.1212/WNL.0000000000004645

Gauthier, A., Viel, S., Perret, M., Brocard, G., Casey, R., Lombard, C., et al. (2021). Comparison of Simoa™ and Ella™ to assess serum neurofilament-light chain in multiple sclerosis. *Ann. Clin. Transl. Neurol.* 8, 1141–1150. doi: 10.1002/acn3.51355

Gendron, T. F., Badi, M. K., Heckman, M. G., Jansen-West, K. R., Vilanilam, G. K., Johnson, P. W., et al. (2020). Plasma neurofilament light predicts mortality in patients with stroke. *Sci. Transl. Med.* 12:eaay1913. doi: 10.1126/scitranslmed.aay1913

Giovannoni, G. (2018). Peripheral blood neurofilament light chain levels: the neurologist's C-reactive protein. *Brain* 141, 2235–2237. doi: 10.1093/brain/awy200

Goeral, K., Hauck, A., Atkinson, A., Wagner, M. B., Pimpel, B., Fuiko, R., et al. (2021). Early life serum neurofilament dynamics predict neurodevelopmental outcome of preterm infants. *J. Neurol.* 268, 2570–2577. doi: 10.1007/s00415-021-10429-5

Goossens, J., Bjerke, M., Van Mossevelde, S., Van den Bossche, T., Goeman, J., De Vil, B., et al. (2018). Diagnostic value of cerebrospinal fluid tau, neurofilament and progranulin in definite frontotemporal lobar degeneration. *Alzheimers Res. Ther.* 10:31. doi: 10.1186/s13195-018-0364-0

Graham, N. S. N., Zimmerman, K. A., Moro, F., Heslegrave, A., Maillard, S. A., Bernini, A., et al. (2021). Axonal marker neurofilament light predicts long-term outcomes and progressive neurodegeneration after traumatic brain injury. *Sci. Transl. Med.* 13:eabg9922. doi: 10.1126/scitranslmed.abg9922

Grindegård, L., Cronberg, T., Backman, S., Blennow, K., Dankiewicz, J., Friberg, H., et al. (2022). Association between EEG patterns and serum neurofilament light after cardiac arrest: a post hoc analysis of the TTM trial. *Neurology* 98, e2487–e2498. doi: 10.1212/WNL.0000000000200335

Hall, S., Öhrfelt, A., Constantinescu, R., Andreasson, U., Surova, Y., Bostrom, F., et al. (2012). Accuracy of a panel of 5 cerebrospinal fluid biomarkers in the differential diagnosis of patients with dementia and/or parkinsonian disorders. *Arch. Neurol.* 69, 1445–1452. doi: 10.1002/mds.29222

Hansson, O., Janelidze, S., Hall, S., Magdalinou, N., Lees, A. J., Andreasson, U., et al. (2017). Blood-based NfL: a biomarker for differential diagnosis of parkinsonian disorder. *Neurology* 88, 930–937. doi: 10.1212/WNL.0000000000003680

Hansson, O., Zetterberg, H., Buchhave, P., Londos, E., Blennow, K., and Minthon, L. (2006). Association between CSF biomarkers and incipient Alzheimer's disease in patients with mild cognitive impairment: a follow-up study. *Lancet Neurol.* 5, 228–234. doi: 10.1016/S1474-4422(06)70355-6

Harp, C., Thanei, G.-A., Jia, X., Kuhle, J., Leppert, D., Schaedelin, S., et al. (2022). Development of an age-adjusted model for blood neurofilament light chain. *Ann. Clin. Transl. Neurol.* 9, 444–453. doi: 10.1002/acn3.51524

Helmer, C., Pérès, K., Letenneur, L., Guttiérez-Robledo, L. M., Ramaroson, H., Barberger-Gateau, P., et al. (2006). Dementia in subjects aged 75 years or over within the PAQUID cohort: prevalence and burden by severity. *Dement. Geriatr. Cogn. Disord.* 22, 87–94. doi: 10.1159/000093459

Hepner, A., Porter, J., Hare, F., Nasir, S. S., Zetterberg, H., Blennow, K., et al. (2019). Serum neurofilament light, glial fibrillary acidic protein and tau are possible serum biomarkers for activity of brain metastases and gliomas. *World J. Oncol.* 10, 169–175. doi: 10.14740/wjon1228

Herbert, M. K., Aerts, M. B., Beenes, M., Norgren, N., Esselink, R. A. J., Bloem, B. R., et al. (2015). CSF neurofilament light chain but not FLT3 ligand discriminates Parkinsonian disorders. *Front. Neurol.* 6:91. doi: 10.3389/fneur.2015.00091

Hoiland, R. L., Rikhraj, K. J. K., Thiara, S., Fordyce, C., Kramer, A. H., Skrifvars, M. B., et al. (2022). Neurologic prognostication after cardiac arrest using brain biomarkers: a systematic review and meta-analysis. *JAMA Neurol.* 79, 390–398. doi: 10.1001/jamaneurol.2021.5598

Huehnchen, P., Schinke, C., Bangemann, N., Dordevic, A. D., Kern, J., Maierhof, S. K., et al. (2022). Neurofilament proteins as a potential biomarker in chemotherapy-induced polyneuropathy. *JCI Insight* 7:e154395. doi: 10.1172/jci.insight.154395

Huss, A., Otto, M., Senel, M., Ludolph, A. C., Abdelhak, A., and Tumani, H. (2020). A score based on NfL and glial markers may differentiate between relapsing-remitting and progressive MS course. *Front. Neurol.* 11:608. doi: 10.3389/fneur.2020.00608

Hviid, C. V. B., Gyldenholm, T., Lauridsen, S. V., Hjort, N., Hvas, A.-M., and Parkner, T. (2020). Plasma neurofilament light chain is associated with mortality after spontaneous intracerebral hemorrhage. *Clin. Chem. Lab. Med.* 58, 261–267. doi: 10.1515/cclm-2019-0532

Jack, C. R., Knopman, D. S., Jagust, W. J., Petersen, R. C., Weiner, M. W., Aisen, P. S., et al. (2013). Tracking pathophysiological processes in Alzheimer's disease: an updated hypothetical model of dynamic biomarkers. *Lancet Neurol.* 12, 207–216. doi: 10.1016/S1474-4422(12)70291-0

Jackson, R. G., Samra, G. S., Radcliffe, J., Clark, G. H., and Price, C. P. (2000). The early fall in levels of S-100 β in traumatic brain injury. *Clin. Chem. Lab. Med.* 38, 1165–1167. doi: 10.1515/CCLM.2000.179

Jakimovski, D., Kuhle, J., Ramanathan, M., Barro, C., Tomic, D., Hagemeier, J., et al. (2019). Serum neurofilament light chain levels associations with gray matter pathology: a 5-year longitudinal study. *Ann. Clin. Transl. Neurol.* 6, 1757–1770. doi: 10.1002/acn3.50872

Johannsen, J., Weiss, D., Daubmann, A., Schmitz, L., and Denecke, J. (2021). Evaluation of putative CSF biomarkers in paediatric spinal muscular atrophy (SMA) patients before and during treatment with nusinersen. *J. Cell Mol. Med.* 25, 8419–8431. doi: 10.1111/jcmm.16802

Kahouadji, S., Bouillon-Minois, J.-B., Oris, C., Durif, J., Pereira, B., Pinguet, J., et al. (2022). Evaluation of serum neurofilament light in the early management of mTBI patients. *Clin. Chem. Lab. Med.* 60, 1234–1241. doi: 10.1515/cclm-2022-0173

Karteri, S., Bruna, J., Argyriou, A. A., Mariotto, S., Velasco, R., Alemany, M., et al. (2022). Prospectively assessing serum neurofilament light chain levels as a biomarker of paclitaxel-induced peripheral neurotoxicity in breast cancer patients. *J. Peripher. Nerv. Syst.* 27, 166–174. doi: 10.1111/jns.12493

Khalil, M., Teunissen, C. E., Otto, M., Piehl, F., Sormani, M. P., Gattringer, T., et al. (2018). Neurofilaments as biomarkers in neurological disorders. *Nat. Rev. Neurol.* 14, 577–589. doi: 10.1038/s41582-018-0058-z

Kim, S.-H., Gwak, H.-S., Lee, Y., Park, N.-Y., Han, M., Kim, Y., et al. (2021). Evaluation of serum neurofilament light chain and glial fibrillary acidic protein as screening and monitoring biomarkers for brain metastases. *Cancers (Basel)* 13:2227. doi: 10.3390/cancers13092227

Kojima, Y., Kasai, T., Noto, Y.-I., Ohmichi, T., Tatebe, H., Kitaoji, T., et al. (2021). Amyotrophic lateral sclerosis: Correlations between fluid biomarkers of NfL, TDP-43 and tau and clinical characteristics. *PLoS One* 16:e0260323. doi: 10.1371/journal.pone.0260323

Kuhle, J., Barro, C., Andreasson, U., Derfuss, T., Lindberg, R., Sandelius, Å., et al. (2016). Comparison of three analytical platforms for quantification of the neurofilament light chain in blood samples: ELISA, electrochemiluminescence immunoassay and Simoa. *Clin. Chem. Lab. Med.* 54, 1655–1661. doi: 10.1515/cclm-2015-1195

Kuhle, J., Nourbakhsh, B., Grant, D., Morant, S., Barro, C., Yaldizli, Ö., et al. (2017). Serum neurofilament is associated with progression of brain atrophy and disability in early MS. *Neurology* 88, 826–831. doi: 10.1212/WNL.0000000000003653

Lambertsen, K. L., Soares, C. B., Gaist, D., and Nielsen, H. H. (2020). Neurofilaments: the C-reactive protein of neurology. *Brain Sci.* 10:E56. doi: 10.3390/brainsci10010056

Lerche, S., Wurster, I., Röben, B., Zimmermann, M., Machetanz, G., Wiethoff, S., et al. (2020). CSF NFL in a longitudinally assessed PD cohort: age effects and cognitive trajectories. *Mov. Disord.* 35, 1138–1144. doi: 10.1002/mds.28056

Lim, B., Grøntvedt, G. R., Bathala, P., Kale, S. S., Campbell, C. T., Stengelin, M., et al. (2021). CSF neurofilament light may predict progression from amnestic mild cognitive impairment to Alzheimer's disease dementia. *Neurobiol. Aging* 107, 78–85. doi: 10.1016/j.neurobiolaging.2021.07.013

Lin, Y.-S., Lee, W.-J., Wang, S.-J., and Fuh, J.-L. (2018). Levels of plasma neurofilament light chain and cognitive function in patients with Alzheimer or Parkinson disease. *Sci. Rep.* 8:17368. doi: 10.1038/s41598-018-35766-w

Lin, X., Lu, T., Deng, H., Liu, C., Yang, Y., Chen, T., et al. (2022). Serum neurofilament light chain or glial fibrillary acidic protein in the diagnosis and prognosis of brain metastases. *J. Neurol.* 269, 815–823. doi: 10.3881/j.issn.1000-503X.14472

Lista, S., Toschi, N., Baldacci, F., Zetterberg, H., Blennow, K., Kilimann, I., et al. (2017). Diagnostic accuracy of CSF neurofilament light chain protein in the biomarker-guided classification system for Alzheimer's disease. *Neurochem. Int.* 108, 355–360. doi: 10.1016/j.neuint.2017.05.010

Liu, D., Chen, J., Wang, X., Xin, J., Cao, R., and Liu, Z. (2020). Serum neurofilament light chain as a predictive biomarker for ischemic stroke outcome: a systematic review and meta-analysis. *J. Stroke Cerebrovasc. Dis.* 29:104813. doi: 10.1016/j.jstrokecerebrovasdis.2020.104813

Lleó A, Alcolea, D., Martínez-Lage, P., Scheltens, P., Parnetti, L., Poirier, J., Simonsen, A. H., et al. (2019). Longitudinal cerebrospinal fluid biomarker trajectories along the Alzheimer's disease continuum in the BIOMARKAPD study. *Alzheimers Dement.* 15, 742–753. doi: 10.1016/j.fochx.2022.100379

Lombardi, V., Carassiti, D., Giovannoni, G., Lu, C.-H., Adiutori, R., and Malaspina, A. (2020). The potential of neurofilaments analysis using dry-blood and plasma spots. *Sci. Rep.* 10:97. doi: 10.1038/s41598-019-54310-y

Louwsma, J., Brunger, A. F., Bijzet, J., Kroesen, B. J., Roeloffzen, W. W. H., Bischof, A., et al. (2021). Neurofilament light chain, a biomarker for polyneuropathy in systemic amyloidosis. *Amyloid* 28, 50–55. doi: 10.1080/13506129.2020.1815696

Manouchehrinia, A., Stridh, P., Khademi, M., Leppert, D., Barro, C., Michalak, Z., et al. (2020a). Plasma neurofilament light levels are associated with risk of disability in multiple sclerosis. *Neurology* 94, e2457–e2467. doi: 10.1212/WNL.0000000000009571

Manouchehrinia, A., Piehl, F., Hillert, J., Kuhle, J., Alfredsson, L., Olsson, T., et al. (2020b). Confounding effect of blood volume and body mass index on blood neurofilament light chain levels. *Ann. Clin. Transl. Neurol.* 7, 139–143. doi: 10.1002/acn3.50972

Marques, T. M., van Rumund, A., Oeckl, P., Kuiperij, H. B., Esselink, R. A. J., Bloem, B. R., et al. (2019). Serum NFL discriminates Parkinson disease from atypical parkinsonisms. *Neurology* 92, e1479–e1486. doi: 10.1212/WNL.0000000000007179

Mattsson, N., Cullen, N. C., Andreasson, U., Zetterberg, H., and Blennow, K. (2019). Association between longitudinal plasma neurofilament light and neurodegeneration in patients with Alzheimer disease. *JAMA Neurol.* 76, 791–799. doi: 10.1001/jamaneurol.2019.0765

McDonald, S. J., O'Brien, W. T., Symons, G. F., Chen, Z., Bain, J., Major, B. P., et al. (2021). Prolonged elevation of serum neurofilament light after concussion in male Australian football players. *Biomark. Res.* 9:4. doi: 10.1186/s40364-020-00256-7

Meeter, L. H. H., Vijverberg, E. G., Del Campo, M., Rozemuller, A. J. M., Donker Kaat, L., de Jong, F. J., et al. (2018). Clinical value of neurofilament and phospho-tau/tau ratio in the frontotemporal dementia spectrum. *Neurology* 90, e1231–e1239. doi: 10.1212/WNL.0000000000005261

Mollenhauer, B., Dakna, M., Kruse, N., Galasko, D., Foroud, T., Zetterberg, H., et al. (2020). Validation of serum neurofilament light chain as a biomarker of Parkinson's disease progression. *Mov. Disord.* 35, 1999–2008. doi: 10.1002/mds.28206

Nitz, E., Smitka, M., Schallner, J., Akgün, K., Ziemssen, T., von der Hagen, M., et al. (2021). Serum neurofilament light chain in pediatric spinal muscular atrophy patients and healthy children. *Ann. Clin. Transl. Neurol.* 8, 2013–2024. doi: 10.1002/acn3.51449

Novakova, L., Zetterberg, H., Sundström, P., Axelsson, M., Khademi, M., Gunnarsson, M., et al. (2017). Monitoring disease activity in multiple sclerosis using serum neurofilament light protein. *Neurology* 89, 2230–2237. doi: 10.1212/WNL.0000000000004683

Nylén, K., Csajbok, L. Z., Ost, M., Rashid, A., Karlsson, J.-E., Blennow, K., et al. (2006). CSF -neurofilament correlates with outcome after aneurysmal subarachnoid hemorrhage. *Neurosci. Lett.* 404, 132–136. doi: 10.1016/j.neulet.2006.05.029

Oeckl, P., Anderl-Straub, S., Von Arnim, C. A. F., Baldeiras, I., Diehl-Schmid, J., Grimmer, T., et al. (2022). Serum GFAP differentiates Alzheimer's disease from frontotemporal dementia and predicts MCI-to-dementia conversion. *J. Neurol. Neurosurg. Psychiatry*. doi: 10.1136/jnnp-2021-328547. [Online ahead of print].

Olsson, B., Portelius, E., Cullen, N. C., Sandelius, Å., Zetterberg, H., Andreasson, U., et al. (2019). Association of cerebrospinal fluid neurofilament light protein levels with cognition in patients with dementia, motor neuron disease and movement disorders. *JAMA Neurol.* 76, 318–325. doi: 10.1001/jamaneurol.2018.3746

Osborn, K. E., Khan, O. A., Kresge, H. A., Bown, C. W., Liu, D., Moore, E. E., et al. (2019). Cerebrospinal fluid and plasma neurofilament light relate to abnormal cognition. *Alzheimers Dement. (Amst)* 11, 700–709. doi: 10.1016/j.dadm.2019.08.008

Page, V. J., Watne, L. O., Heslegrave, A., Clark, A., McAuley, D. F., Sanders, R. D., et al. (2022). Plasma neurofilament light chain protein as a predictor of days in delirium and deep sedation, mortality and length of stay in critically ill patients. *EBioMedicine* 80:104043. doi: 10.1016/j.ebiom.2022.104043

Paterson, R. W., Slattery, C. F., Poole, T., Nicholas, J. M., Magdalinou, N. K., Toombs, J., et al. (2018). Cerebrospinal fluid in the differential diagnosis of Alzheimer's disease: clinical utility of an extended panel of biomarkers in a specialist cognitive clinic. *Alzheimers Res. Ther.* 10:32. doi: 10.1186/s13195-018-0361-3

Peng, Y., Li, Q., Qin, L., He, Y., Luo, X., Lan, Y., et al. (2021). Combination of serum neurofilament light chain levels and MRI markers to predict cognitive function in ischemic stroke. *Neurorehabil. Neural Repair* 35, 247–255. doi: 10.1177/1545968321989354

Peters, N., van Leijsen, E., Tuladhar, A. M., Barro, C., Konieczny, M. J., Ewers, M., et al. (2020). Serum neurofilament light chain is associated with incident lacunes in progressive cerebral small vessel disease. *J. Stroke* 22, 369–376. doi: 10.5853/jos.2019.02845

Piepgras, J., Müller, A., Steffen, F., Lotz, J., Loquai, C., Zipp, F., et al. (2021). Neurofilament light chain levels reflect outcome in a patient with glutamic acid decarboxylase 65 antibody-positive autoimmune encephalitis under immune checkpoint inhibitor therapy. *Eur. J. Neurol.* 28, 1086–1089. doi: 10.1111/ene.14692

Pijnenburg, Y. A. L., Verwey, N. A., van der Flier, W. M., Scheltens, P., and Teunissen, C. E. (2015). Discriminative and prognostic potential of cerebrospinal fluid phospho Tau/tau ratio and neurofilaments for frontotemporal dementia subtypes. *Alzheimers Dement. (Amst)* 1, 505–512. doi: 10.1016/j.dadm.2015.11.001

Pop, M., and Viuleț, V. (1985). [Results of a lens implant in unilateral cataract extracted intra- or extracapsularly]. *Rev. Chir. Oncol. Radiol. O R L Oftalmol. Stomatol. Ser. Oftalmol.* 29, 123–128.

Preische, O., Schultz, S. A., Apel, A., Kuhle, J., Kaeser, S. A., Barro, C., et al. (2019). Serum neurofilament dynamics predicts neurodegeneration and clinical progression in presymptomatic Alzheimer's disease. *Nat. Med.* 25, 277–283. doi: 10.1038/s41591-018-0304-3

Pujol-Calderón, F., Portelius, E., Zetterberg, H., Blennow, K., Rosengren, L. E., and Höglund, K. (2019). Neurofilament changes in serum and cerebrospinal fluid after acute ischemic stroke. *Neurosci. Lett.* 698, 58–63. doi: 10.1016/j.neulet.2018.12.042

Pujol-Calderón, F., Zetterberg, H., Portelius, E., Löwhagen Hendén, P., Rentzos, A., Karlsson, J.-E., et al. (2022). Prediction of outcome after endovascular embolectomy in anterior circulation stroke using biomarkers. *Transl. Stroke Res.* 13, 65–76. doi: 10.1007/s12975-021-00905-5

Quadalti, C., Calandra-Buonaura, G., Baiardi, S., Mastrangelo, A., Rossi, M., Zenesini, C., et al. (2021). Neurofilament light chain and α-synuclein RT-QuIC as differential diagnostic biomarkers in parkinsonisms and related syndromes. *NPJ Parkinsons Dis.* 7:93. doi: 10.1038/s41531-021-00232-4

Reich, D. S., Lucchinetti, C. F., and Calabresi, P. A. (2018). Multiple sclerosis. *N. Engl. J. Med.* 378, 169–180. doi: 10.1056/NEJMra1401483

Rodrigues, F. B., Byrne, L. M., Tortelli, R., Johnson, E. B., Wijeratne, P. A., Arridge, M., et al. (2020). Mutant huntingtin and neurofilament light have distinct longitudinal dynamics in Huntington's disease. *Sci. Transl. Med.* 12:eabc2888. doi: 10.1126/scitranslmed.abc2888

Rojas, J. C., Karydas, A., Bang, J., Tsai, R. M., Blennow, K., Liman, V., et al. (2016). Plasma neurofilament light chain predicts progression in progressive supranuclear palsy. *Ann. Clin. Transl. Neurol.* 3, 216–225. doi: 10.1002/acn3.290

Rosso, M., Healy, B. C., Saxena, S., Paul, A., Bjornevik, K., Kuhle, J., et al. (2021). MRI lesion state modulates the relationship between serum neurofilament light and age in multiple sclerosis. *J. Neuroimaging* 31, 388–393. doi: 10.1111/jon.12826

Ru, Y., Corado, C., Soon, R. K., Melton, A. C., Harris, A., Yu, G. K., et al. (2019). Neurofilament light is a treatment-responsive biomarker in CLN2 disease. *Ann. Clin. Transl. Neurol.* 6, 2437–2447. doi: 10.1002/acn3.50942

Sánchez-Valle, R., Heslegrave, A., Foiani, M. S., Bosch, B., Antonell, A., Balasa, M., et al. (2018). Serum neurofilament light levels correlate with severity measures and neurodegeneration markers in autosomal dominant Alzheimer's disease. *Alzheimers Res. Ther.* 10:113. doi: 10.1186/s13195-018-0439-y

Saracino, D., Dorgham, K., Camuzat, A., Rinaldi, D., Rametti-Lacroux, A., Houot, M., et al. (2021). Plasma NfL levels and longitudinal change rates in C9orf72 and GRN-associated diseases: from tailored references to clinical applications. *J. Neurol. Neurosurg. Psychiatry* 92, 1278–1288. doi: 10.1136/jnnp-2021-326914

Schmitz, M., Canaslan, S., Espinosa, J. C., Fernández-Borges, N., Villar-Piqué, A., Llorens, F., et al. (2022). Validation of plasma and CSF neurofilament light chain as an early marker for sporadic creutzfeldt-jakob disease. *Mol. Neurobiol.* 59, 1–9. doi: 10.1007/s12035-022-02891-7

Schoeberl, F., Tiedt, S., Schmitt, A., Blumenberg, V., Karschnia, P., Burbano, V. G., et al. (2022). Neurofilament light chain serum levels correlate with the severity of neurotoxicity after CAR T-cell treatment. *Blood Adv.* 6, 3022–3026. doi: 10.1182/bloodadvances.2021006144

Selner, J. C. (1988). Visualization techniques in the nasal airway: their role in the diagnosis of upper airway disease and measurement of therapeutic response. *J. Allergy Clin. Immunol.* 82, 909–916. doi: 10.1016/0091-6749(88)90033-4

Shahim, P., Gren, M., Liman, V., Andreasson, U., Norgren, N., Tegner, Y., et al. (2016). Serum neurofilament light protein predicts clinical outcome in traumatic brain injury. *Sci. Rep.* 6:36791. doi: 10.1038/srep36791

Shahim, P., Tegner, Y., Marklund, N., Blennow, K., and Zetterberg, H. (2018). Neurofilament light and tau as blood biomarkers for sports-related concussion. *Neurology* 90, e1780–e1788. doi: 10.1212/WNL.0000000000005518

Shahim, P., Zetterberg, H., Tegner, Y., and Blennow, K. (2017). Serum neurofilament light as a biomarker for mild traumatic brain injury in contact sports. *Neurology* 88, 1788–1794. doi: 10.1212/WNL.0000000000003912

Shi, J., Qin, X., Chang, X., Wang, H., Guo, J., and Zhang, W. (2022). Neurofilament markers in serum and cerebrospinal fluid of patients with amyotrophic lateral sclerosis. *J. Cell. Mol. Med.* 26, 583–587. doi: 10.1111/jcmm.17100

Singer, W., Schmeichel, A. M., Shahnawaz, M., Schmelzer, J. D., Sletten, D. M., Gehrking, T. L., et al. (2021). Alpha-synuclein oligomers and neurofilament light chain predict phenoconversion of pure autonomic failure. *Ann. Neurol.* 89, 1212–1220. doi: 10.1002/ana.26089

Sjöbom, U., Hellström, W., Löfqvist, C., Nilsson, A. K., Holmström, G., Pupp, I. H., et al. (2021). Analysis of brain injury biomarker neurofilament light and neurodevelopmental outcomes and retinopathy of prematurity among preterm infants. *JAMA Netw. Open* 4:e214138. doi: 10.1001/jamanetworkopen.2021.4138

Smirnov, D. S., Ashton, N. J., Blennow, K., Zetterberg, H., Simrén, J., Lantero-Rodriguez, J., et al. (2022). Plasma biomarkers for Alzheimer's disease in relation to neuropathology and cognitive change. *Acta Neuropathol.* 143, 487–503. doi: 10.1007/s00401-022-02408-5

Sofou, K., Shahim, P., Tulinius, M., Blennow, K., Zetterberg, H., Mattsson, N., et al. (2019). Cerebrospinal fluid neurofilament light is associated with survival in mitochondrial disease patients. *Mitochondrion* 46, 228–235. doi: 10.1016/j.mito.2018.07.002

Srpova, B., Uher, T., Hrnciarova, T., Barro, C., Andelova, M., Michalak, Z., et al. (2021). Serum neurofilament light chain reflects inflammation-driven neurodegeneration and predicts delayed brain volume loss in early stage of multiple sclerosis. *Mult. Scler.* 27, 52–60. doi: 10.1177/1352458519901272

Steinacker, P., Anderl-Straub, S., Diehl-Schmid, J., Semler, E., Uttner, I., von Arnim, C. A. F., et al. (2018). Serum neurofilament light chain in behavioral variant frontotemporal dementia. *Neurology* 91, e1390–e1401. doi: 10.1212/WNL.0000000000006318

Steinacker, P., Blennow, K., Halbgebauer, S., Shi, S., Ruf, V., Oeckl, P., et al. (2016). Neurofilaments in blood and CSF for diagnosis and prediction of onset in Creutzfeldt-Jakob disease. *Sci. Rep.* 6:38737. doi: 10.1038/srep38737

Steinacker, P., Semler, E., Anderl-Straub, S., Diehl-Schmid, J., Schroeter, M. L., Uttner, I., et al. (2017a). Neurofilament as a blood marker for diagnosis and monitoring of primary progressive aphasias. *Neurology* 88, 961–969. doi: 10.1212/WNL.0000000000003688

Steinacker, P., Huss, A., Mayer, B., Grehl, T., Grosskreutz, J., Borck, G., et al. (2017b). Diagnostic and prognostic significance of neurofilament light chain NF-L, but not progranulin and S100B, in the course of amyotrophic lateral sclerosis: data from the German MND-net. *Amyotroph. Lateral Scler. Frontotemporal Degener.* 18, 112–119. doi: 10.1080/21678421.2016.1241279

Thebault, S., Booth, R. A., Rush, C. A., MacLean, H., and Freedman, M. S. (2021). Serum neurofilament light chain measurement in MS: hurdles to clinical translation. *Front. Neurosci.* 15:654942. doi: 10.3389/fnins.2021.654942

Thebault, S., Reaume, M., Marrie, R. A., Marriott, J. J., Furlan, R., Laroni, A., et al. (2022). High or increasing serum NfL is predictive of impending multiple sclerosis relapses. *Mult. Scler. Relat. Disord.* 59:103535. doi: 10.1016/j.msard.2022.103535

Thelin, E. P., Zeiler, F. A., Ercole, A., Mondello, S., Büki, A., Bellander, B.-M., et al. (2017). Serial sampling of serum protein biomarkers for monitoring human traumatic brain injury dynamics: a systematic review. *Front. Neurol.* 8:300. doi: 10.3389/fneur.2017.00300

Thompson, A. G. B., Luk, C., Heslegrave, A. J., Zetterberg, H., Mead, S. H., Collinge, J., et al. (2018). Neurofilament light chain and tau concentrations are markedly increased in the serum of patients with sporadic Creutzfeldt-Jakob disease and tau correlates with rate of disease progression. *J. Neurol. Neurosurg. Psychiatry* 89, 955–961. doi: 10.1136/jnnp-2017-317793

Thouvenot, E., Demattei, C., Lehmann, S., Maceski-Maleska, A., Hirtz, C., Juntas-Morales, R., et al. (2020). Serum neurofilament light chain at time of diagnosis is an independent prognostic factor of survival in amyotrophic lateral sclerosis. *Eur. J. Neurol.* 27, 251–257. doi: 10.1111/ene.14063

Ticau, S., Sridharan, G. V., Tsour, S., Cantley, W. L., Chan, A., Gilbert, J. A., et al. (2021). Neurofilament light chain as a biomarker of hereditary transthyretin-mediated amyloidosis. *Neurology* 96, e412–e422. doi: 10.1212/WNL.0000000000011090

Tiedt, S., Duering, M., Barro, C., Kaya, A. G., Boeck, J., Bode, F. J., et al. (2018). Serum neurofilament light: a biomarker of neuroaxonal injury after ischemic stroke. *Neurology* 91, e1338–e1347. doi: 10.1212/WNL.0000000000006282

Toft, A., Roos, P., Jääskeläinen, O., Musaeus, C. S., Henriksen, E. E., Johannsen, P., et al. (2020). Serum neurofilament light in patients with frontotemporal dementia caused by CHMP2B mutation. *Dement. Geriatr. Cogn. Disord.* 49, 533–538. doi: 10.1159/000513877

Uher, T., McComb, M., Galkin, S., Srpova, B., Oechtering, J., Barro, C., et al. (2021). Neurofilament levels are associated with blood-brain barrier integrity, lymphocyte extravasation and risk factors following the first demyelinating event in multiple sclerosis. *Mult. Scler.* 27, 220–231. doi: 10.1177/1352458520912379

Uphaus, T., Bittner, S., Gröschel, S., Steffen, F., Muthuraman, M., Wasser, K., et al. (2019). NfL (Neurofilament Light Chain) levels as a predictive marker for long-term outcome after ischemic stroke. *Stroke* 50, 3077–3084. doi: 10.1161/STROKEAHA.119.026410

Vacchiano, V., Mastrangelo, A., Zenesini, C., Masullo, M., Quadalti, C., Avoni, P., et al. (2021). Plasma and CSF neurofilament light chain in amyotrophic lateral sclerosis: a cross-sectional and longitudinal study. *Front. Aging Neurosci.* 13:753242. doi: 10.3389/fnagi.2021.753242

van Swieten, J. C., and Heutink, P. (2008). Mutations in progranulin (GRN) within the spectrum of clinical and pathological phenotypes of frontotemporal dementia. *Lancet Neurol.* 7, 965–974. doi: 10.1016/S1474-4422(08)70194-7

Varhaug, K. N., Barro, C., Bjørnevik, K., Myhr, K.-M., Torkildsen, Ø., Wergeland, S., et al. (2018). Neurofilament light chain predicts disease activity in relapsing-remitting MS. *Neurol. Neuroimmunol. Neuroinflamm.* 5:e422. doi: 10.1212/NXI.0000000000000422

Verberk, I. M. W., Thijssen, E., Koelewijn, J., Mauroo, K., Vanbrabant, J., de Wilde, A., et al. (2020). Combination of plasma amyloid beta$_{(1-42/1-40)}$ and glial fibrillary acidic protein strongly associates with cerebral amyloid pathology. *Alzheimers Res. Ther.* 12:118. doi: 10.1186/s13195-020-00682-7

Verde, F., Silani, V., and Otto, M. (2019). Neurochemical biomarkers in amyotrophic lateral sclerosis. *Curr. Opin. Neurol.* 32, 747–757. doi: 10.1097/WCO.0000000000000744

Verduyn, C., Bjerke, M., Duerinck, J., Engelborghs, S., Peers, K., Versijpt, J., et al. (2021). CSF and blood neurofilament levels in athletes participating in physical contact sports: a systematic review. *Neurology* 96, 705–715. doi: 10.1212/WNL.0000000000011750

Wang, H., Davison, M. D., Kramer, M. L., Qiu, W., Gladysheva, T., Chiang, R. M. S., et al. (2022). Evaluation of neurofilament light chain as a biomarker of neurodegeneration in X-linked childhood cerebral adrenoleukodystrophy. *Cells* 11:913. doi: 10.3390/cells11050913

Wang, J.-H., Huang, J., Guo, F.-Q., Wang, F., Yang, S., Yu, N.-W., et al. (2021). Circulating neurofilament light predicts cognitive decline in patients with post-stroke subjective cognitive impairment. *Front. Aging Neurosci.* 13:665981. doi: 10.3389/fnagi.2021.665981

Wang, Z., Wang, R., Li, Y., Li, M., Zhang, Y., Jiang, L., et al. (2021). Plasma neurofilament light chain as a predictive biomarker for post-stroke cognitive impairment: a prospective cohort study. *Front. Aging Neurosci.* 13:631738. doi: 10.3389/fnagi.2021.631738

Wilke, C., Reich, S., van Swieten, J. C., Borroni, B., Sanchez-Valle, R., Moreno, F., et al. (2022). Stratifying the presymptomatic phase of genetic frontotemporal dementia by serum NfL and pNfH: a longitudinal multicentre study. *Ann. Neurol.* 91, 33–47. doi: 10.1002/ana.26265

Winther-Larsen, A., Hviid, C. V. B., Meldgaard, P., Sorensen, B. S., and Sandfeld-Paulsen, B. (2020). Neurofilament light chain as a biomarker for brain metastases. *Cancers (Basel)* 12:2852. doi: 10.3390/cancers12102852

Witzel, S., Frauhammer, F., Steinacker, P., Devos, D., Pradat, P.-F., Meininger, V., et al. (2021). Neurofilament light and heterogeneity of disease progression in amyotrophic lateral sclerosis: development and validation of a prediction model to improve interventional trials. *Transl. Neurodegener.* 10:31. doi: 10.1186/s40035-021-00257-y

Xu, Z., Henderson, R. D., David, M., and McCombe, P. A. (2016). Neurofilaments as biomarkers for amyotrophic lateral sclerosis: a systematic review and meta-analysis. *PLoS One* 11:e0164625. doi: 10.1371/journal.pone.0164625

Yuan, A., Rao, M. V., Sasaki, T., Chen, Y., Kumar, A., Veeranna, Liem, R. K. H., et al. (2006). α-internexin is structurally and functionally associated with the neurofilament triplet proteins in the mature CNS. *J. Neurosci.* 26, 10006–10019. doi: 10.1523/JNEUROSCI.2580-06.2006

Yuan, A., Rao, M. V., Veeranna, and Nixon, R. A. (2017). Neurofilaments and neurofilament proteins in health and disease. *Cold Spring Harb. Perspect. Biol.* 9:a018309. doi: 10.1101/cshperspect.a018309

Yuan, A., Sasaki, T., Kumar, A., Peterhoff, C. M., Rao, M. V., Liem, R. K., et al. (2012). Peripherin is a subunit of peripheral nerve neurofilaments: implications for differential vulnerability of CNS and peripheral nervous system axons. *J. Neurosci.* 32, 8501–8508. doi: 10.1523/JNEUROSCI.1081-12.2012

Zetterberg, H., and Blennow, K. (2016). Fluid biomarkers for mild traumatic brain injury and related conditions. *Nat. Rev. Neurol.* 12, 563–574. doi: 10.1038/nrneurol.2016.127

Zetterberg, H., Jacobsson, J., Rosengren, L., Blennow, K., and Andersen, P. M. (2007). Cerebrospinal fluid neurofilament light levels in amyotrophic lateral sclerosis: impact of SOD1 genotype. *Eur. J. Neurol.* 14, 1329–1333. doi: 10.1111/j.1468-1331.2007.01972.x

Zetterberg, H., Skillbäck, T., Mattsson, N., Trojanowski, J. Q., Portelius, E., Shaw, L. M., et al. (2016). Association of cerebrospinal fluid neurofilament light concentration with Alzheimer disease progression. *JAMA Neurol.* 73, 60–67. doi: 10.1001/jamaneurol.2015.3037

Zetterberg, H., Smith, D. H., and Blennow, K. (2013). Biomarkers of mild traumatic brain injury in cerebrospinal fluid and blood. *Nat. Rev. Neurol.* 9, 201–210. doi: 10.1038/nrneurol.2013.9

Zhang, L., Cao, B., Hou, Y., Gu, X., Wei, Q., Ou, R., et al. (2022). Neurofilament light chain predicts disease severity and progression in multiple system atrophy. *Mov. Disord.* 37, 421–426. doi: 10.1002/mds.28847

frontiers | Frontiers in Cellular Neuroscience

TYPE Original Research
PUBLISHED 07 November 2022
DOI 10.3389/fncel.2022.1013745

OPEN ACCESS

EDITED BY
Suman Dutta,
University of California, Los Angeles, United States

REVIEWED BY
Ye Zhou,
University of Toronto, Canada
Parisa Gazerani,
Oslo Metropolitan University, Norway
Anwesha Deb,
Presidency University, India

*CORRESPONDENCE
Jian Li
jian.li@suda.edu.cn
Wenxing Su
wenxingsu@126.com
Dazhuang Li
li13616279476@163.com

†These authors have contributed equally to this work

SPECIALTY SECTION
This article was submitted to Cellular Neuropathology, a section of the journal Frontiers in Cellular Neuroscience

RECEIVED 07 August 2022
ACCEPTED 18 October 2022
PUBLISHED 07 November 2022

CITATION
Heng H, Liu J, Hu M, Li D, Su W and Li J (2022) WDR43 is a potential diagnostic biomarker and therapeutic target for osteoarthritis complicated with Parkinson's disease.
Front. Cell. Neurosci. 16:1013745.
doi: 10.3389/fncel.2022.1013745

WDR43 is a potential diagnostic biomarker and therapeutic target for osteoarthritis complicated with Parkinson's disease

Hongquan Heng[1,2†], Jie Liu[3,4†], Mingwei Hu[5†], Dazhuang Li[4*], Wenxing Su[2*] and Jian Li[1*]

[1]Department of Orthopedics, The Second Affiliated Hospital of Soochow University, Suzhou, China, [2]Department of Plastic and Burn Surgery, The Second Affiliated Hospital of Chengdu Medical College, China National Nuclear Corporation 416 Hospital, Chengdu, China, [3]Department of Orthopedics, Liyang People's Hospital, Liyang, China, [4]Department of Orthopedics, The Affiliated Hospital of Yangzhou University, Yangzhou University, Yangzhou, China, [5]Department of Neurology, The First Affiliated Hospital of Anhui Medical University, Hefei, China

Osteoarthritis (OA) and Parkinson's disease (PD) are on the rise and greatly impact the quality of individuals' lives. Although accumulating evidence indicates a relationship between OA and PD, the particular interactions connecting the two diseases have not been thoroughly examined. Therefore, this study explored the association through genetic characterization and functional enrichment. Four datasets (GSE55235, GSE12021, GSE7621, and GSE42966) were chosen for assessment and validation from the Gene Expression Omnibus (GEO) database. Weighted Gene Co-Expression Network Analysis (WGCNA) was implemented to determine the most relevant genes for clinical features. Then, Gene Ontology (GO) and Kyoto Encyclopedia of Genes and Genomes (KEGG) were carried out to explore the biological processes of common genes, and to display the interrelationships between common genes, the STRING database and the application Molecular Complex Detection Algorithm (MCODE) of Cytoscape software were leveraged to get hub genes. By intersecting the common genes with the differentially expressed genes (DEGs) acquired from GSE12021 and GSE42966, the hub genes were identified. Finally, we validated the diagnostic efficacy of hub genes and explored their correlation with 22 immune infiltrating cells. As a consequence, we discovered 71 common genes, most of which were functionally enriched in antigen processing and presentation, mitochondrial translation, the mRNA surveillance pathway, and nucleocytoplasmic transport. Furthermore, WDR43 was found by intersecting eight hub genes with

Abbreviations: OA, Osteoarthritis; PD, Parkinson's disease; GEO, Gene Expression Omnibus; WGCNA, Weighted Gene Co-Expression Network Analysis; GO, Gene ontology; KEGG, Kyoto Encyclopedia of Genes and Genomes; MCODE, Molecular Complex Detection Algorithm; DEGs, differentially expressed genes; Tregs, T cell regulatory; TOM, topological overlap matrix; PPI, protein-protein interaction; IL-6, interleukin-6.

28 DEGs from the two validation datasets. Receiver Operating Characteristic (ROC) implied the diagnostic role of WDR43 in OA and PD. Immune infiltration research revealed that T-cell regulatory (Tregs), monocytes, and mast cells resting were associated with the pathogenesis of OA and PD. WDR43 may provide key insights into the relationship between OA and PD.

KEYWORDS

osteoarthritis, Parkinson's disease, weighted gene co-expression network analysis, immune cell infiltration, hub gene

Introduction

OA is a progressive and degenerative joint disease, which is a chronic disease and disability caused by various pathological changes such as synovial inflammation, cartilage degradation, and subchondral bone changes (McDonough and Jette, 2010; Neogi, 2013). OA has been reported in 10 percent of men and 18 percent of women over the age of 60 (Roseti et al., 2019). This degenerative disease primarily affects the weight-bearing joints of the lower extremities (hips, knees, and ankles). Patients with OA have a reduced quality of life due to limited joint mobility, pain, swelling, and deformity (Ma et al., 2014). A complex interplay between many genetic and environmental risk factors (developmental disorders, obesity, metabolic factors, and pre-existing joint damage) accelerates the onset and progression of OA (Egloff et al., 2012). Furthermore, one of the important risk factors for the degenerative process of OA is the inflammatory response. Elevated levels of inflammatory mediators have been detected in almost every OA joint tissue (synovium, subchondral bone, and cartilage, etc.; Orlowsky and Kraus, 2015).

PD is a progressive neurodegenerative disease caused by the loss of dopaminergic neurons (Bhat et al., 2018) and is characterized by motor (e.g., resting tremor, muscle stiffness, and bradykinesia) and nonmotor symptoms (e.g., apathy, orthostatic hypotension, and olfactory dysfunction; Modugno et al., 2013; DeMaagd and Philip, 2015). The global prevalence of PD is 0.1%–0.2% (Tysnes and Storstein, 2017), and the prevalence has gradually increased over the past few decades (Aktas et al., 2007; Aid and Bosetti, 2011). PD is often characterized by neuroinflammation, with glia-mediated responses and increased expression of proinflammatory substances (Cebrian et al., 2015).

Recent studies have shown that arthritis is the most common comorbidity of PD (Jones et al., 2012). OA significantly affects the joints of the hip, knee, and spine, resulting in joint inflammation, wear, and stiffness (Loeser et al., 2012; Jacob et al., 2021). Neurologically healthy individuals with lower extremity OA frequently exhibit slower pace, shortened stride length, reduced single-limb support, and reduced mobility compared with healthy controls (Brandes et al., 2008; Zasadzka et al., 2015). Similar to patients with PD, patients with OA also show increases in falls, disease severity, gait dysfunction, and mobility impairment throughout aging (Guideline for the prevention of falls in older persons, 2001; Astephen et al., 2008; Centers for Disease Control and Prevention, 2013). Furthermore, a growing body of literature reports that peripheral inflammation may induce neuroinflammation in the brain, leading to neurodegeneration (Perry, 2004; Träger and Tabrizi, 2013; Wang J. et al., 2018). Therefore, we hypothesized that having OA might increase the risk of developing PD.

In this study, on the basis of previous studies, we used bioinformatics methods to gradually identify common genes related to OA and PD, and preliminarily confirmed the relationship between OA and PD. The correlation between the occurrence and development of diseases, and the correlation between the two in terms of function and immune infiltration were found, thus providing new targets and references for the clinical research of OA and PD in the later stage.

Materials and methods

Data collection

GSE55235 (Woetzel et al., 2014) and GSE7621 (Lesnick et al., 2007) gene expression profiles were obtained from the GEO database[1] (Edgar et al., 2002), which is a comprehensive microarray and high-throughput sequencing dataset encompassing all research submissions. The two datasets were based on the GPL96 platform (Affymetrix Human Genome U133A Array) and the GPL570 platform (Affymetrix Human Genome U133 Plus 2.0 Array). The GSE55235 dataset contains synovial tissue samples from 10 patients with OA and 10 normal volunteers. The GSE7621 dataset contains 16 samples from Parkinsonian patients with postmortem human substantia nigra and nine samples from normal volunteers.

1 http://www.ncbi.nlm.nih.gov/geo

Data transformation and visualization

The "limma" R package was used to screen significative genes between OA and PD samples (Ritchie et al., 2015). The DEGs with an adjusted $p < 0.05$ and $|\log2FC| > 1$ were considered statistically significant. Then, the "ggplot2" (Lott et al., 2009) and "pheatmap" R package were used to plot the volcano diagram and heatmap.

WGCNA-based module and gene screening

To identify common genes linked with OA and PD, the "WGCNA" R package (Langfelder and Horvath, 2008) was used to generate two weighted gene co-expression networks from the two expression matrices. First, merging all the samples ensured a trustworthy network. Second, we computed Pearson correlation coefficients between each pair of genes to measure expression similarity and create a correlation matrix. We also utilized the soft threshold method to create a weighted neighborhood matrix. We utilized a soft connectivity technique to identify the best soft threshold to guarantee gene correlations were scale-free. The neighborhood matrix becomes a topological overlap matrix (TOM). Using dynamic tree cutting and a minimum of 50 genes per module, co-expression modules were produced. Gene significance (GS) and module membership (MM) were computed to link modules to clinical characteristics. Finally, we mapped eigengenes. Venn diagram was carried out by R (version 4.2.0) to overlap the genes between OA and PD.

Analysis of the enrichment of function in common genes

To get a deeper understanding of the principal biological functions of common genes for OA and PD, we analyzed the GO and KEGG pathways *via* the "ClusterProfiler" R package (Wu et al., 2021), $P < 0.05$ was deemed statistically significant.

Identification of hub genes in OA-related PD

Search Tool for the Retrieval of Interacting Genes (STRING[2]; version 11.5; Franceschini et al., 2013) may search for interactions between proteins of interest, such as direct binding associations, to form a protein-protein interaction (PPI) network with complicated regulatory linkages. Interactions with a combined score over 0.4 were considered statistically significant. Cytoscape[3] (version 3.9.1; Shannon et al., 2003) was used to visualize this PPI network of DEGs. And the MCODE (Bader and Hogue, 2003) was executed to build PPI network modules with the following parameters: degree cutoff = 2, node score cutoff = 0.2, k-core = 2, and max. depth = 100. The GeneCards database[4] was then applied to uncover further information on the hub genes by identifying the related genes, proteins, and disease interactions.

Validation of hub genes and prediction of diagnostic efficiency

To verify the hub genes, we investigated the expression variation of these genes in other OA and PD datasets (GSE12021 and GSE42966; Huber et al., 2008; Quan et al., 2021). Data from two datasets were compared using "limma" R package to find the DEGs. The cutoff value was $|\log2FC| > 0.8$, P value < 0.01. Cluster analysis with the R package "pheatmap." DEGs from the OA and PD datasets were merged using the web tool draw Venn diagram[5]. Moreover, ROC analysis of GSE55235, GSE12021, GSE7621, and GSE42966 was performed to evaluate whether hub genes could differentiate OA and PD samples from their control samples by using the "pROC" R package (Robin et al., 2011).

Analysis of immune infiltration

Analysis of integrated gene expression data (GSE55235 and GSE7621) using the CIBERSORT algorithm reveals the proportion of 22 immune cell types (Xue et al., 2021). Correlation heatmap was generated after detection of association between immune cells in OA and PD samples with the "corrplot" R package (Serang et al., 2017). Then, the "vioplot" R package was used to illustrate the expression differences of 22 immune cell types in two datasets.

WDR43 and infiltrating immune cells correlation analysis

The Spearman correlation analysis on WDR43 and Infiltrating immune cells was performed with the use of the "ggpubr," "ggExtra" and "reshape2" (Zhang, 2016) R packages. The above results were then visualized using the barplot function in R (version 4.2.0).

2 http://string-db.org

3 http://www.cytoscape.org

4 http://www.genecards.org/

5 http://bioinformatics.psb.ugent.be/webtools/Venn/

Results

Visualization of data variance analysis results

Figure 1 depicts the flowchart for this study. After standardizing the microarray results, the "pheatmap" and "ggplot2" R packages were chosen to generate heatmaps and volcano maps of top 30 significantly changed genes (Figures 2A–D).

Identification of co-expression gene modules

We applied WGCNA to discover gene modules co-expressed in OA and PD datasets. Following the exclusion of sample outliers from both datasets, the remaining data were grouped into control and disease groups. Then, nine and three were selected as the soft threshold power for GSE55235 and GSE7621 based on scale independence greater than 0.90 to assure physiologically significant scale-free networks (Figures 3A,B). Using the dynamic branching cut method on GSE55235 and GSE7621, the genes were put into 40 and 44 modules, respectively (Figures 3C,D).

Acquisition of common genes

Key modules related to OA and PD were found by calculating GS and MM to connect modules with clinical characteristics. The association of clinical characteristics in the control and disease groups was represented in the figures. The module eigengene (ME)black and MEivory modules were strongly associated with OA (Figure 4A), whereas the MEpurple and MEthistle2 modules were significantly associated with PD (Figure 4B). Then, we overlapped the genes of those modules to get 71 common genes (Figure 4C).

Investigation of the biological functions of common genes

The functional expression distribution of common genes was studied by looking at the GO and KEGG pathways. At first, GO analysis showed these common genes were mainly involved in intestinal epithelial cell differentiation, mitochondrial translation, positive regulation of cell cycle G2/M phase transition, and nuclear-transcribed mRNA catabolic process of the biological process. Moreover, these common genes were mainly associated with the RNA polymerase II transcription regulator complex, transcription regulator complex and intercellular bridge of the cellular component (Figure 5A). Furthermore, the findings of the KEGG analysis demonstrated that these common genes were enriched in antigen processing and presentation, mRNA surveillance pathway, and nucleocytoplasmic transport (Figure 5B).

Protein-protein interaction (PPI) network analysis of common genes in OA-associated PD

Cytoscape was used to generate the PPI network of common genes with a composite score larger than 0.4. After we explored the upstream and downstream genes. In the PPI network, there were 124 nodes and 163 edges, where nodes represent genes and edges represent their interactions, and the MCODE algorithm identified eight hub genes, including PRS11, UTP25, RPS15A, RPS13, DDX52, NOP58, SKIV2L2, and WDR43 (Figure 6). Based on the GeneCards database, Table 1 shows their full names and related disorders.

Validation of the core hub gene

First, we validated hub genes using the GEO datasets GSE12021 for OA and GSE42966 for PD. The clustering heatmaps of DEGs from the GS12021 and GSE42966 datasets were shown in Figures 7A,B. Second, after using Venn diagrams to compare the DEGs from the OA and PD datasets, we found that WDR43, a common gene, was still different (Figure 7C). Moreover, the core hub gene of WDR43 may play a significant role in OA and PD. Finally, this study examined diagnostic performance of WDR43 in four datasets by applying the "pROC" R package, the result as follows: AUC = 0.880 in GSE55235, AUC = 0.826, AUC = 0.911, and AUC = 0.778 (Figures 8A–D).

Immune infiltration in OA and PD

The CIBERSORT technique was used to construct the infiltration abundance matrix of 22 immune cell types from the dataset. On the one hand, the heatmap of 22 immune cell types in GSE55235 indicated: Eosinophils and NK cells activated had a crucial positive correlation, T cells CD4 naive were emphatically correlated with Eosinophils, Dendritic cells resting and B cells memory also had a vital positive correlation, and T cells regulatory and Mast cells resting also positively correlated. While T cells CD4 memory resting and T cells regulatory had a passive correction. Mast cells activated and Mast cells resting also negatively correlate (Figure 9A). Moreover, the heatmap of 22 immune cell types included in the dataset GSE7621 revealed that the relationship between B cells naive and Eosinophils was favorable, T cells gamma delta and T cells memory activated had

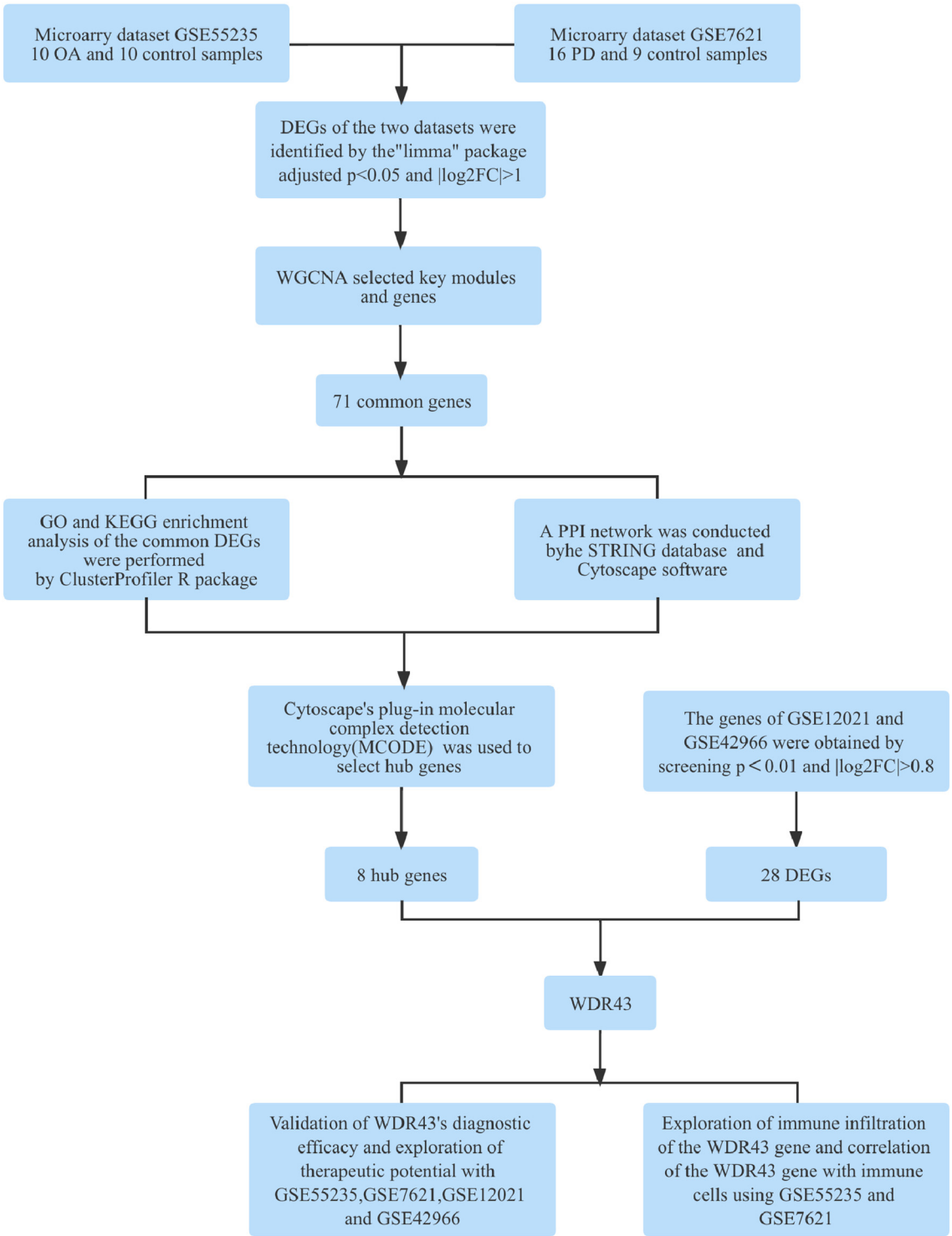

FIGURE 1
Research design flow chart.

an actively corrected. While T cells CD4 memory resting and T cells CD8 were negatively relevant, eosinophils and monocytes had a passively correlated, and T cells follicular helper and NK cells resting were contrasted (**Figure 9B**). On the other hand, T

10.3389/fncel.2022.1013745

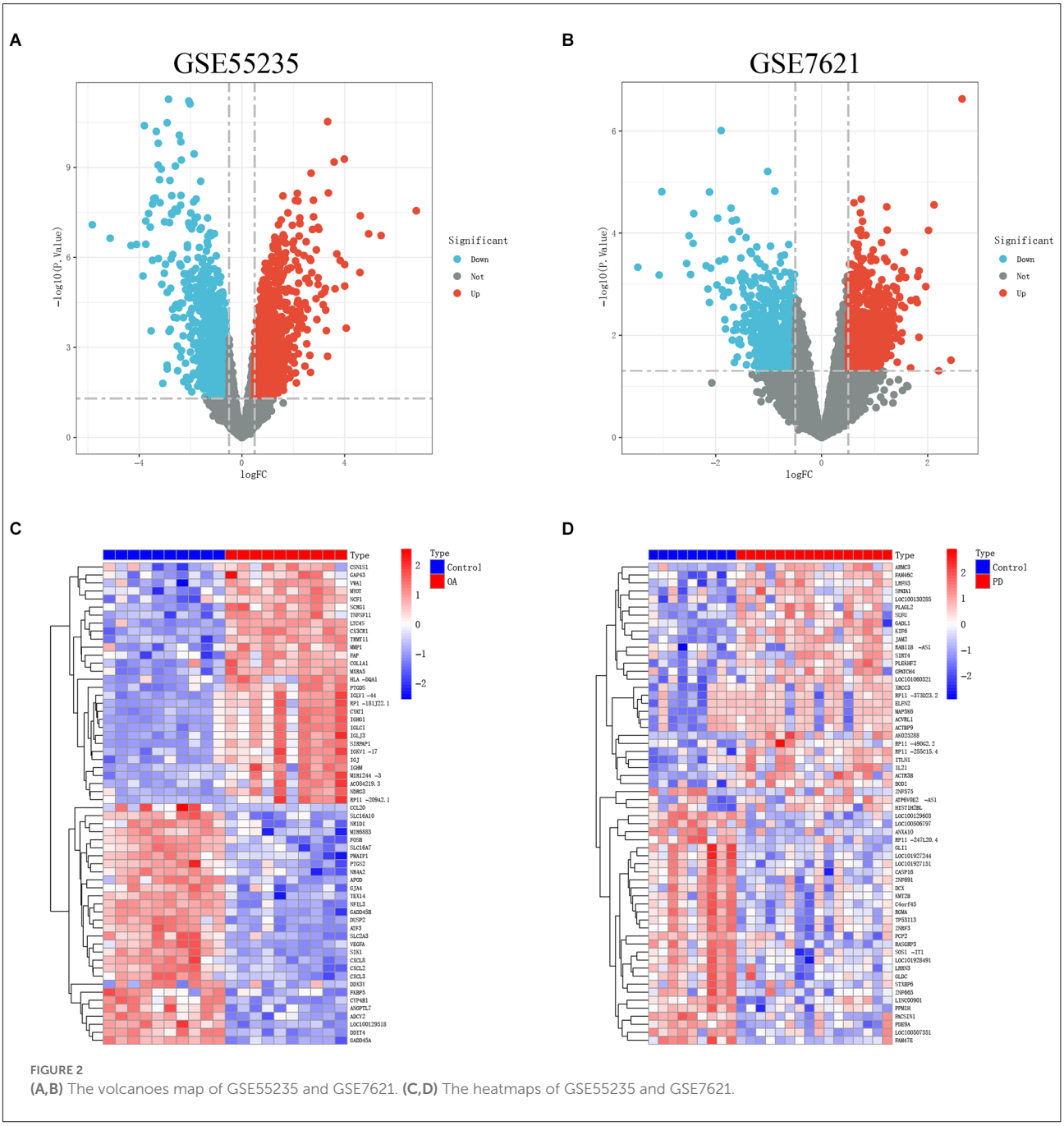

FIGURE 2
(A,B) The volcanoes map of GSE55235 and GSE7621. **(C,D)** The heatmaps of GSE55235 and GSE7621.

cells follicular helper, T cells regulatory, Macrophages M0 and Mast cells resting were highly expressed and significant in the OA group, T cells CD4 memory resting, Mast cells activated and eosinophils were low expression and meaningful in control group (Figure 9C). At the same time, Monocytes demonstrated statistically significant and strong expression in PD groups. Eosinophil immune cells' expression was low in control groups (Figure 9D).

Analysis of WDR43 and immune infiltrating cells for correlation

The correlation study indicated that WDR43 was positively connected with Mast cells activated (r = 0.574, p = 0.008), T cells CD4 memory resting (r = 0.466, p = 0.040). Moreover, WDR43 was negatively associated with T cells follicular helper (r = −0.520, p = 0.019), Mast cells resting (r = −0.560, p = 0.010),

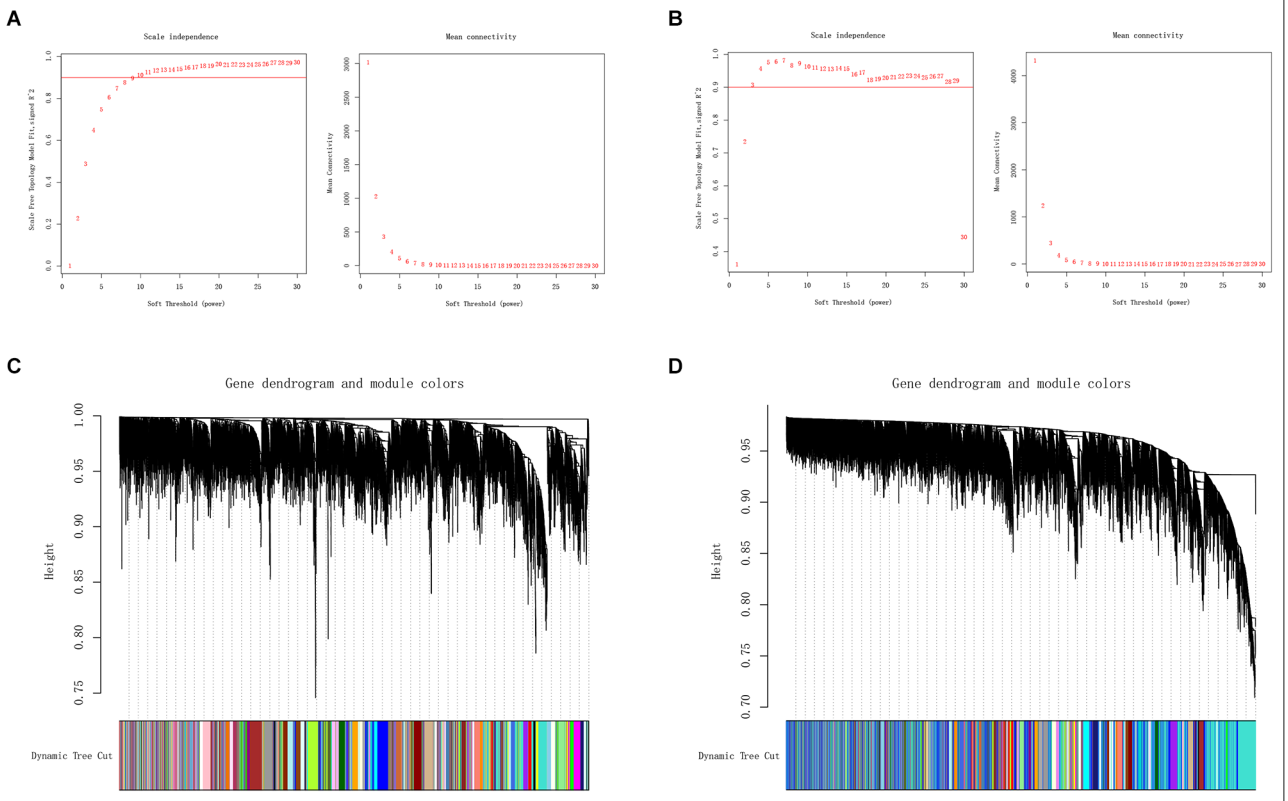

FIGURE 3
(A,B) Definition of soft threshold power through Weighted Gene Co-Expression Network Analysis (WGCNA). Scale-free indices and mean connectivity were analyzed for various soft threshold powers (β). **(C,D)** A gene dendrogram was created by averaging the results of a chain hierarchy clustering algorithm. The colorful rows underneath the tree diagram indicated the assignment of modules based on dynamic tree cutting.

and T cells regulatory ($r = -0.627$, $p = 0.003$) in the dataset of GSE55235 (**Figures 10A,B**).

Discussion

The current study has initially confirmed that the risk of PD in patients with OA is 41% higher than that in patients without OA. The relationship between OA and PD may involve common risk factors, such as inflammation (Scanzello, 2017; Pajares et al., 2020) and vitamin D deficiency (Zhang et al., 2014; Garfinkel et al., 2017; Sleeman et al., 2017), as well as several mediating factors, such as physical inactivity (Shih et al., 2006; Fang et al., 2018), hypertension (Veronese et al., 2018; Chen et al., 2019), and depression (Veronese et al., 2017; Wang S. et al., 2018).

Recent studies have shown that inflammatory mediators play a key role in the development of OA (Goldring and Otero, 2011; Berenbaum, 2013). Levels of interleukin-6 (IL-6) and tumor necrosis factor-α (TNF-α), both key pro-inflammatory cytokines that induce cartilage catabolism, are elevated in OA patients (Chow and Chin, 2020; Osteoarthritis linked to higher parkinson's disease risk, 2021). In addition, IL-6 and TNF-α can also activate microglia in the brain to produce pro-inflammatory cytokines in the brain, which may lead to further neuroinflammation in the brain, thereby accelerating neurodegeneration (Dufek et al., 2015; Le et al., 2016; Roper et al., 2020). Studies have found that a large number of microglia are present in the substantia nigra, and that midbrain dopaminergic neurons are particularly susceptible to inflammatory stimulation (Obeso et al., 2010; Tansey and Goldberg, 2010; Teder-Braschinsky et al., 2019). Therefore, we hypothesized that the higher PD risk observed in OA patients might be mediated through cytokine-induced neuroinflammation.

Furthermore, lower vitamin D levels are associated with the development of PD (Lv et al., 2014). Recent studies have shown that vitamin D can promote dopamine synthesis by increasing tyrosine hydroxylase activity. Vitamin D also promotes the production of glial cell-derived neurotrophic factor, a key protein for dopaminergic neuron survival (Pertile et al., 2018). In addition, high levels of vitamin D receptors are found in dopaminergic neurons within the substantia nigra (Cui et al.,

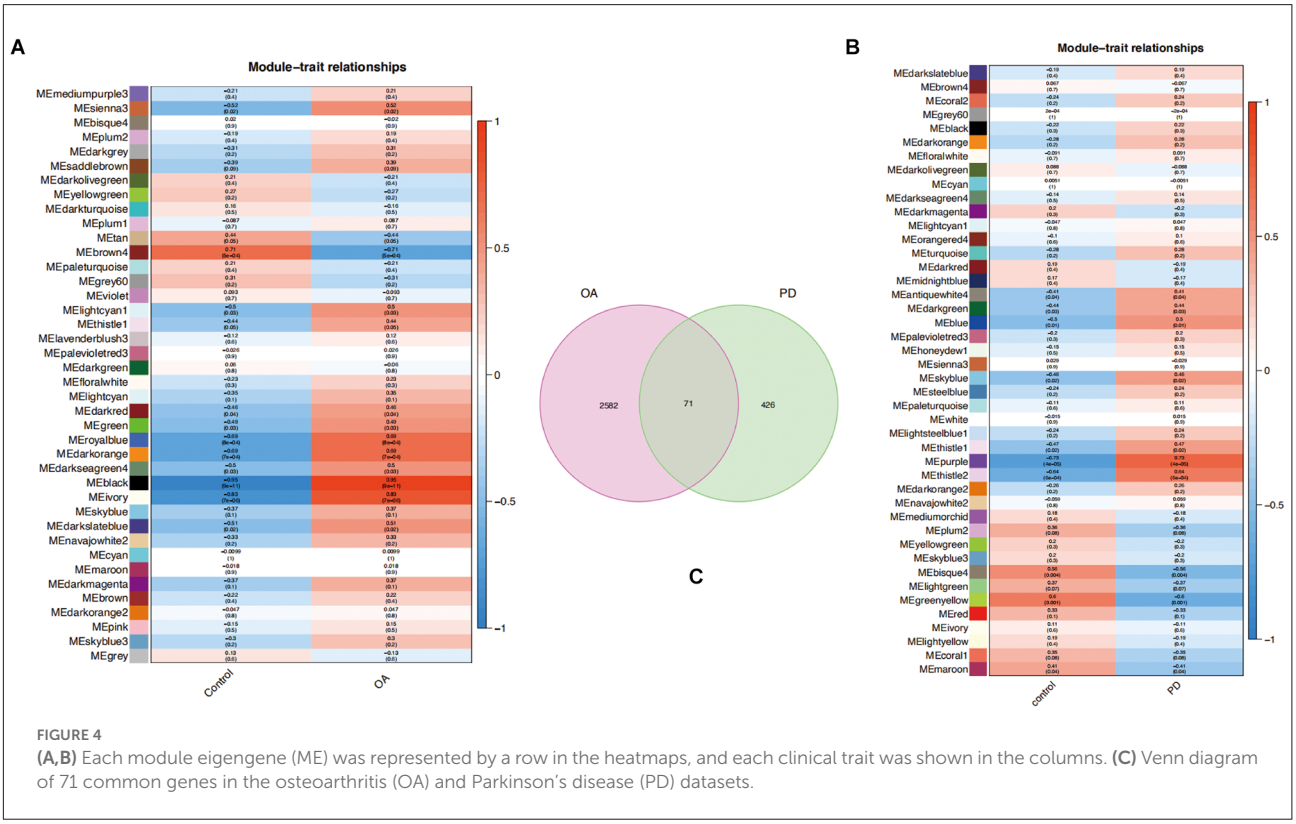

FIGURE 4
(A,B) Each module eigengene (ME) was represented by a row in the heatmaps, and each clinical trait was shown in the columns. **(C)** Venn diagram of 71 common genes in the osteoarthritis (OA) and Parkinson's disease (PD) datasets.

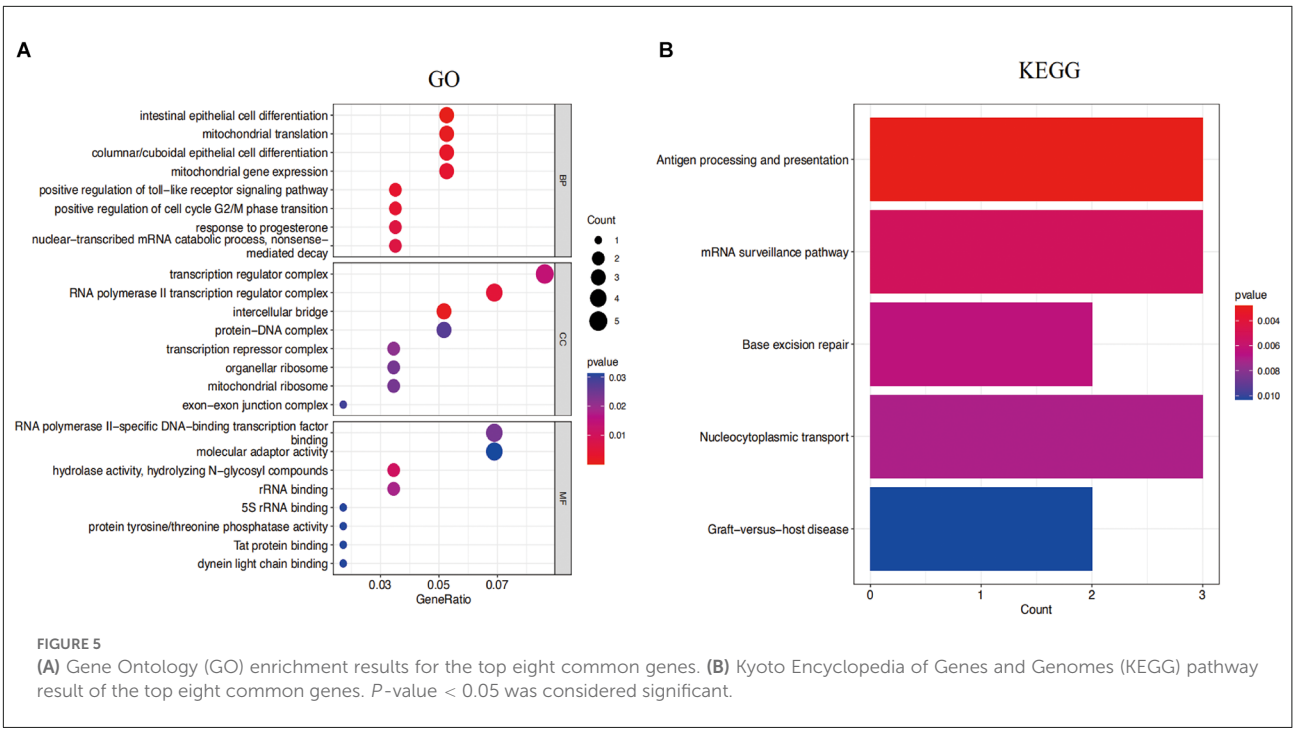

FIGURE 5
(A) Gene Ontology (GO) enrichment results for the top eight common genes. **(B)** Kyoto Encyclopedia of Genes and Genomes (KEGG) pathway result of the top eight common genes. *P*-value < 0.05 was considered significant.

2013; Feng et al., 2021). Therefore, chronic insufficiency of vitamin D may accelerate the degeneration of dopaminergic neurons, especially in the substantia nigra region, thereby promoting the development of PD. Studies have shown that patients with OA have lower serum vitamin D levels (Veronese et al., 2015; Bassiouni et al., 2017) and a higher prevalence

10.3389/fncel.2022.1013745

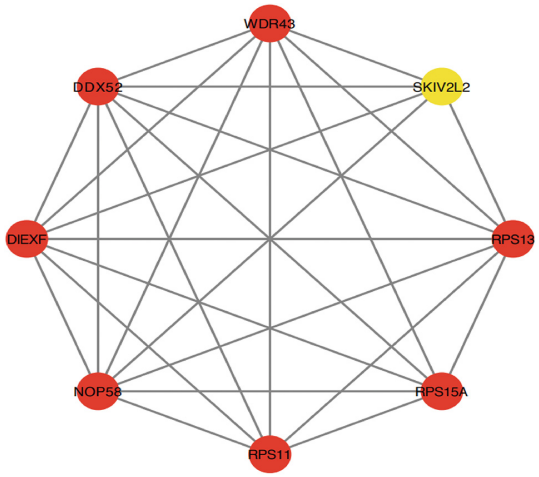

FIGURE 6
Protein-protein interaction (PPI) network constructed using the STRING database. The eight genes with the most connectivity under Molecular Complex Detection Algorithm (MCODE) were visualized using Cytoscape software.

TABLE 1 Details of the hub genes.

No.	Gene symbol	Full name	Gene-related diseases
1	RPS11	Ribosomal Protein S11	Cyclosporiasis, Diamond-Blackfan Anemia
2	UTP25	UTP25 Small Subunit Processome Component	Tetraamelia Syndrome
3	RPS15A	Ribosomal Protein S15a	Diamond-Blackfan Anemia 20, Diamond-Blackfan Anemia, Macrocytic Anemia
4	PRS13	Ribosomal Protein S13	Gaucher Disease, Type Ii, Sphingolipidosis, Gaucher's Disease, Neuroblastoma
5	DDX52	DExD-Box Helicase 52	Chromosome 17q12 Deletion Syndrome
6	NOP58	NOP58 Ribonucleoprotein	Dyskeratosis Congenita
7	SKIV2L2	Ski2 like RNA helicase 2	Trichohepatoenteric Syndrome, Diarrhea, Diarrhea 5, With Tufting Enteropathy, Congenital, Optic Disc Anomalies with Retinal and/or Macular Dystrophy
8	WDR43	WD Repeat Domain 43	3 mc Syndrome, Treacher Collins Syndrome 1

of vitamin D deficiency (24%–81%; Jansen and Haddad, 2013; Goula et al., 2015). Therefore, OA-related vitamin D deficiency may also increase the risk of PD.

In addition to these two common risk factors, the relationship between OA and PD may involve several mediators, such as physical inactivity, high blood pressure, and depression. Because physical activity may temporarily increase pain and disability, patients with OA are less likely to receive physical activity recommendations than the general population (Herbolsheimer et al., 2016). At the same time, studies have

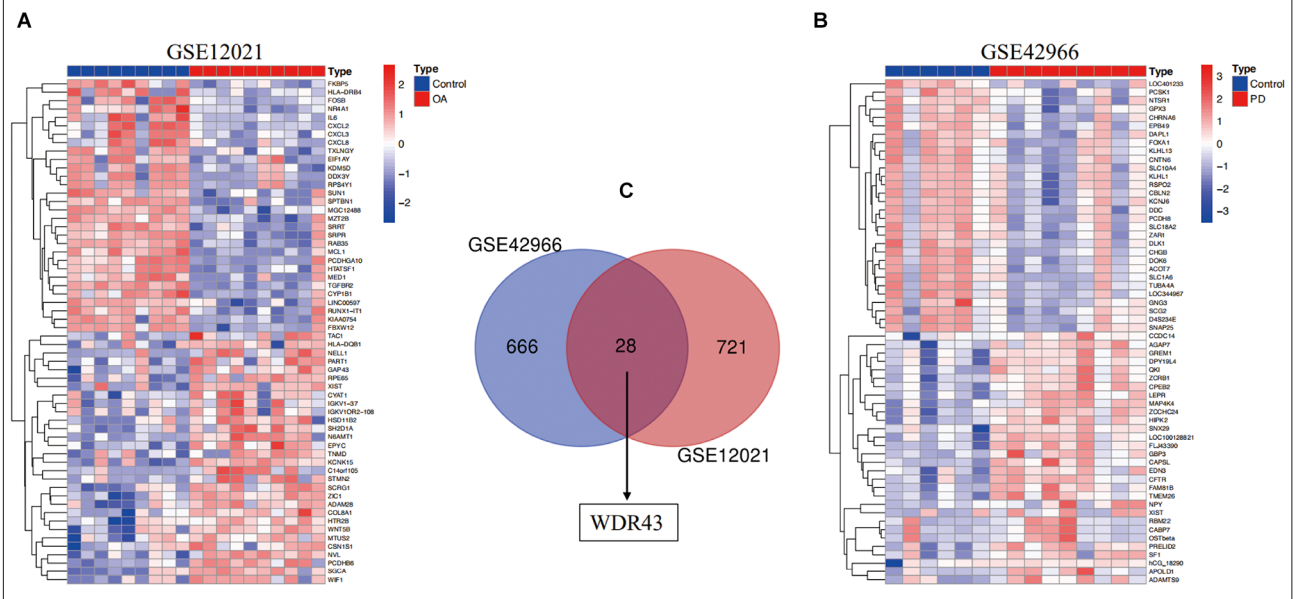

FIGURE 7
(A) A heat map illustrating the hierarchical clustering of differentially expressed genes (DEGs) within the GSE12021 datasets. **(B)** A heat map illustrating the hierarchical clustering of DEGs within the GSE42966 datasets. **(C)** The GSE12021 and GSE42966 datasets were analyzed for the overlap of DEGs. WDR43 were also DEGs in genes shared by the GSE42966 (blue) and GSE12021 (red) datasets.

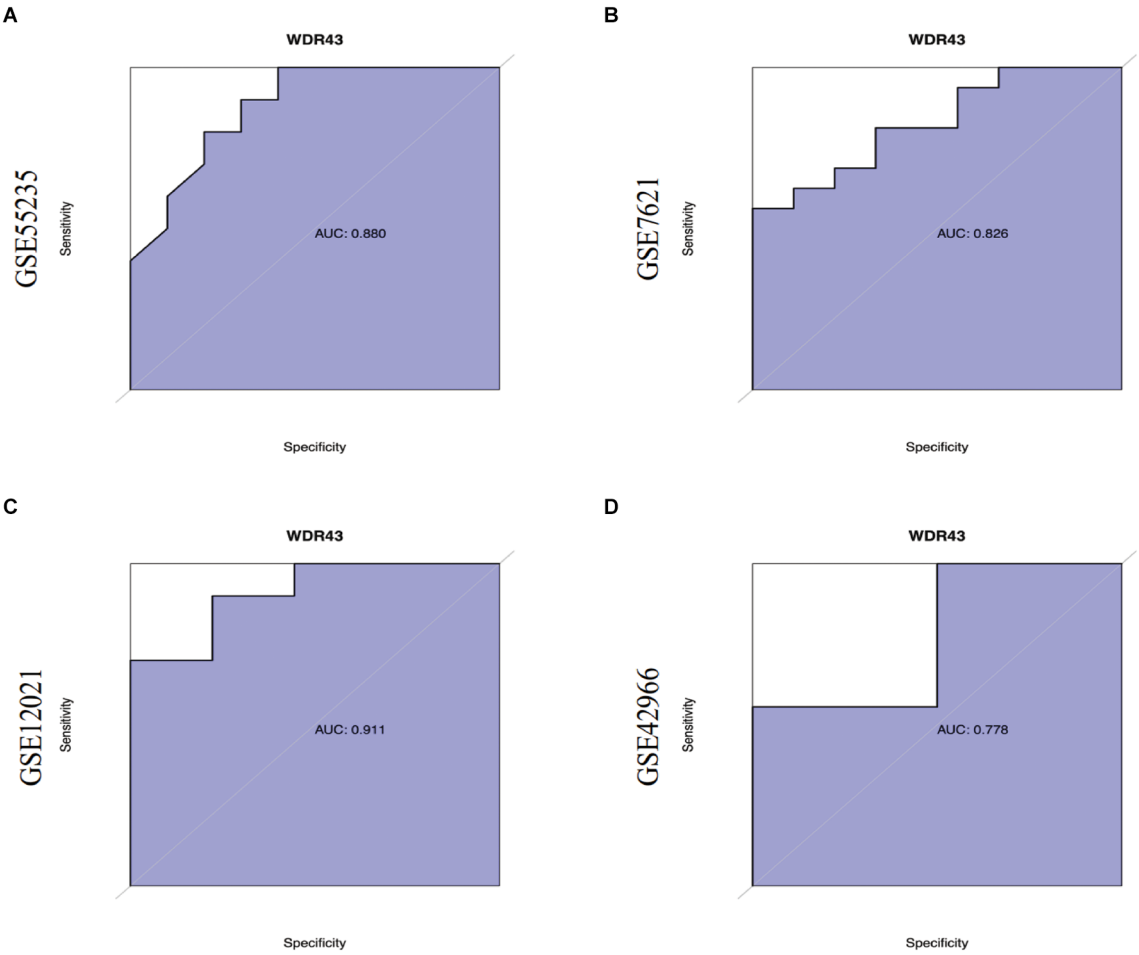

FIGURE 8
(A–D) Receiver Operating Characteristic (ROC) curves of WDR43 in GSE55235, GSE7621, GSE12021, and GSE42966 datasets.

shown that there is a dose-response negative correlation between physical activity and PD, which may be caused by the increased production of various growth factors and reduced oxidative stress caused by physical activity (Fang et al., 2018). Interestingly, some data suggest that OA is also a risk factor for hypertension (Veronese et al., 2018), and hypertensive patients may contribute to PD through basal ganglia hypertensive vascular disease (Chen et al., 2019). Finally, patients diagnosed with OA have a significantly higher risk of depression compared with patients without OA (Veronese et al., 2017). At the same time, there is a significant correlation between depression and the incidence of PD because they share common physiopathological features (e.g., brain atrophy and decreased GABA levels; Wang S. et al., 2018).

Through PPI network analysis of OA-related PD common genes and hub gene identification analysis, we found that WDR43 may play an important role in OA and PD. WDR43 is associated with congenital growth disorder 3-M syndrome, which causes mutations in three proteins (CUL7, OBSL1, and CCDC8), a congenital short stature disorder with a head deformity that exhibits only growth-related defects (Hanson et al., 2014). Some studies have used siRNA and shRNA virus to silence WDR43 to confirm the function of WDR43 in nucleolar fusion. After mitosis, multiple small nucleoli are formed around transcriptionally active NOR. As the cell cycle progresses, these small nucleoli fuse to form larger nucleoli (Hernandez-Verdun et al., 2010; Moore et al., 2022). Although the mechanism of action of WDR43 in nucleolar fusion is unclear, based on the fact that inhibition of NOL11 results in the formation of a large nucleolus, preventing nucleolar fusion may not be a common phenomenon in all ribosomal biogenesis protein mutations (Freed et al., 2012). One possible explanation is that WDR43 deletion might lead to structural changes in rDNA, which in turn might interfere with nucleolar fusion. In addition, studies have shown that WDR43/UTP5 is required for the proper formation of the nucleolus and for the organization and function of the subnucleolus (Sullivan et al., 2001).

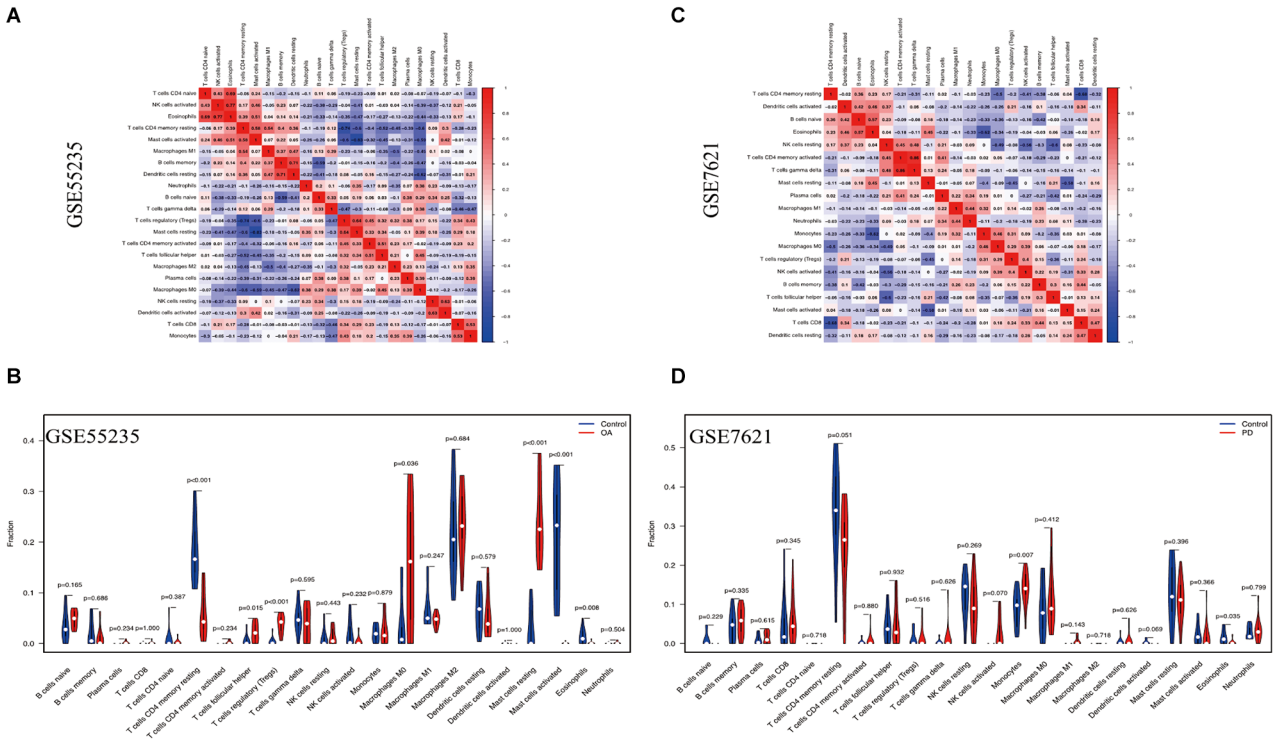

FIGURE 9
Immune cell infiltration analysis. **(A,B)** The correlation heat map depicted the link between 22 invading immune cells. Red squares indicate positive correlations, while blue squares indicated negative correlations. The size of the squares indicated the strength of the association. **(C,D)** The violin plot showed the distinction of 22 infiltrating immune cells among the OA and PD samples.

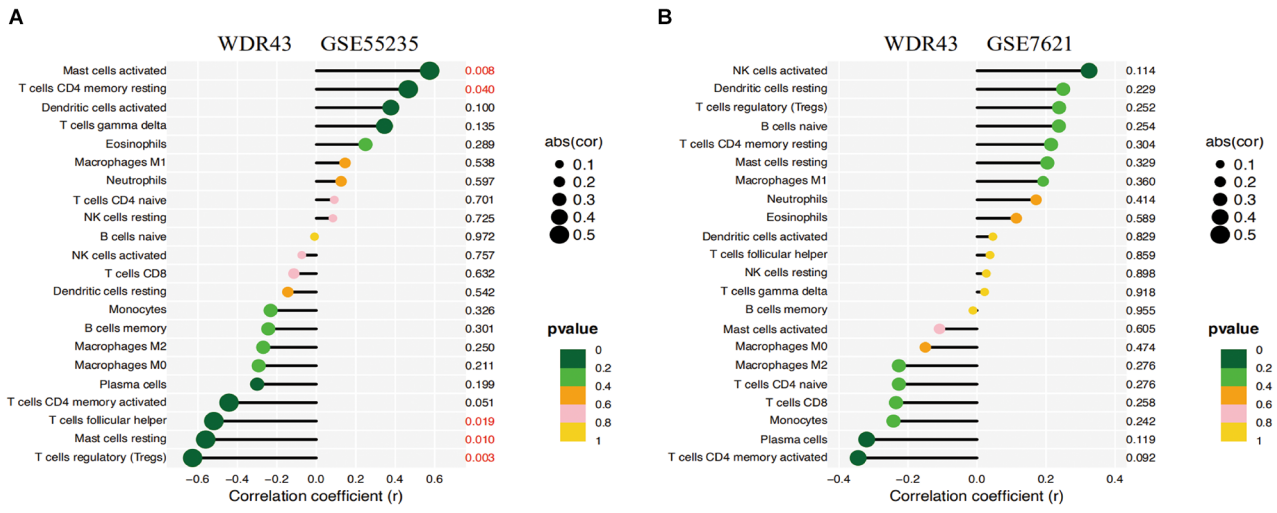

FIGURE 10
(A,B) Correlation analysis of WDR43 and immune infiltrating cells, the size of the circle determined the intensity of the correlation's absolute value. *P* values less than 0.05 was highlighted in red, with smaller and smaller *P* values progressing from yellow to dark green.

We found differential expression of a variety of immune cells through immune infiltration in OA and PD, suggesting that immune regulation plays a crucial role in the occurrence and development of OA and PD. The cells distributed in the OA synovium are mainly T lymphocytes and macrophages, which, together with activated synovial cells, are responsible

for the production of cytokines and increased angiogenesis, inducing the secretion of metalloproteinases and proteolytic enzymes, and sustaining cartilage degradation (Kapoor et al., 2011; Wojdasiewicz et al., 2014; Prieto-Potin et al., 2015; Klein-Wieringa et al., 2016). Synovial macrophage activation is a prerequisite for the overexpression of matrix metalloproteinases and an important step prior to the upregulation of cytokine production and subsequent cartilage degradation and destruction (Blom et al., 2007; Haseeb and Haqqi, 2013). *In vitro* experiments have shown that depletion of synovial macrophages can significantly reduce the synthesis and release of MMP-1 and MMP-3, as well as the synthesis and release of IL-1β as well as TNF-α, IL-6, and IL-8 (Bondeson et al., 2006). Synthesis of cartilage-specific collagens (e.g., types II and IX) by chondrocytes is inhibited by IL-1β, while proteolytic enzymes (e.g., MMP-13 and ADAMTS-4) are upregulated (Mengshol et al., 2000; Moore et al., 2022). In addition, lower numbers of T cells and B cells were also detected in synovial mononuclear cell infiltration in patients with OA.

Neurovascular units in PD patients are altered to not only activate innate immune responses but also recruit and activate adaptive responses (Bartels et al., 2008; Brochard et al., 2009). Oxidative modification of specific proteins associated with PD (α-Syn nitration) generates novel epitopes capable of initiating peripherally driven $CD4^+$ and $CD8^+$ T cell responses (Benner et al., 2008). Furthermore, activated microglia induce the expression of MHC class I molecules in human catecholaminergic neurons, making them susceptible to cell death in the presence of cytotoxic T lymphocytes (Cebrian et al., 2014). Notably, elevated levels of cytokines, including IL-1β, IL-2, IL-6, IFN-γ, and TNF-α, as well as $CD4^+$ lymphocyte counts, have been detected in the serum and cerebrospinal fluid of PD patients (Brodacki et al., 2008; Reale et al., 2009). The ratio of $CD4^+$ to $CD8^+$ lymphocytes and the number of Treg lymphocytes were reduced in patients compared with controls (Baba et al., 2005). In mouse models of PD, in addition to microglia and astrocyte activation, there is a marked infiltration of B cells, $CD4^+$ T cells, $CD8^+$ T cells, and natural killer cells (Kustrimovic et al., 2019).

In this study, we analyzed immune cell infiltration and core genes that may play key roles in OA and PD tissues. However, our study also has certain limitations. This is a bioinformatics study that has not been experimentally validated. Although the results of some previous studies are consistent with our analysis, the reliability of the results of this study needs further experimental verification. In order to deeply understand the relationship between OA and PD, further animal experiments and clinical studies are very necessary. Through bioinformatics research, we have discovered target gene from the dataset that is simultaneously related to OA and PD. In the following investigations, we will examine the impact of the target gene on the survival and function of brain nigrostriatal dopaminergic neurons and articular chondrocytes, as well as establish the correlation between target gene and these two diseases. Furthermore, by establishing mouse models of PD and OA (control and target gene deficient groups), the key regulatory roles of target genes in the development of the two diseases were clarified. Finally, clinical trials are organized to finally clarify the diagnostic and therapeutic value of the target gene.

Conclusions

Chronic inflammation can directly or indirectly contribute to the progression of OA and PD. However, therapeutic intervention for OA and PD remains an urgent challenge. Due to the central role of inflammation in OA and PD, immunomodulatory therapy is a major target of current research. But this may not alter the underlying cause of the disease, only by reducing the production of inflammatory mediators, resulting in clinical benefit. In this study, we used a variety of bioinformatics methods to unearth the common genes between the pathogenic mechanisms of OA and PD, thus providing a new research direction for future clinical interventions.

Data availability statement

The datasets presented in this study can be found in online repositories. The names of the repository and accession numbers can be found in the article.

Author contributions

JLi, WS, and DL developed a major research plan. HH, MH, and JLiu analyzed data, drew charts, and wrote manuscripts. HH and MH helped collect data and references. All authors contributed to the article and approved the submitted version.

Funding

This work was supported by Suzhou Science and Technology Project (SLJ2021013) and Natural Science Project of Chengdu Medical College (CYZYB21-07).

Conflict of interest

The authors declare that the research was conducted in the absence of any commercial or financial relationships that could be construed as a potential conflict of interest.

Publisher's note

References

Aid, S., and Bosetti, F. (2011). Targeting cyclooxygenases-1 and -2 in neuroinflammation: therapeutic implications. *Biochimie* 93, 46–51. doi: 10.1016/j.biochi.2010.09.009

Aktas, O., Ullrich, O., Infante-Duarte, C., Nitsch, R., and Zipp, F. (2007). Neuronal damage in brain inflammation. *Arch. Neurol.* 64, 185–189. doi: 10.1001/archneur.64.2.185

Astephen, J. L., Deluzio, K. J., Caldwell, G. E., Dunbar, M. J., and Hubley-Kozey, C. L. (2008). Gait and neuromuscular pattern changes are associated with differences in knee osteoarthritis severity levels. *J. Biomech.* 41, 868–876. doi: 10.1016/j.jbiomech.2007.10.016

Baba, Y., Kuroiwa, A., Uitti, R. J., Wszolek, Z. K., and Yamada, T. (2005). Alterations of T-lymphocyte populations in Parkinson disease. *Parkinsonism Relat. Disord.* 11, 493–498. doi: 10.1016/j.parkreldis.2005.07.005

Bader, G. D., and Hogue, C. W. (2003). An automated method for finding molecular complexes in large protein interaction networks. *BMC Bioinformatics* 4:2. doi: 10.1186/1471-2105-4-2

Bartels, A. L., Willemsen, A. T., Kortekaas, R., de Jong, B. M., de Vries, R., de Klerk, O., et al. (2008). Decreased blood-brain barrier P-glycoprotein function in the progression of Parkinson's disease, PSP and MSA. *J. Neural Transm. (Vienna)* 115, 1001–1009. doi: 10.1007/s00702-008-0030-y

Bassiouni, H., Aly, H., Zaky, K., Abaza, N., and Bardin, T. (2017). Probing the relation between vitamin D deficiency and progression of medial femoro-tibial osteoarthritis of the knee. *Curr. Rheumatol. Rev.* 13, 65–71. doi: 10.2174/1573397112666160404124532

Benner, E. J., Banerjee, R., Reynolds, A. D., Sherman, S., Pisarev, V. M., Tsiperson, V., et al. (2008). Nitrated alpha-synuclein immunity accelerates degeneration of nigral dopaminergic neurons. *PLoS One* 3:e1376. doi: 10.1371/journal.pone.0001376

Berenbaum, F. (2013). Osteoarthritis as an inflammatory disease (osteoarthritis is not osteoarthrosis!). *Osteoarthritis Cartilage* 21, 16–21. doi: 10.1016/j.joca.2012.11.012

Bhat, S., Acharya, U. R., Hagiwara, Y., Dadmehr, N., and Adeli, H. (2018). Parkinson's disease: cause factors, measurable indicators and early diagnosis. *Comput. Biol. Med.* 102, 234–241. doi: 10.1016/j.compbiomed.2018.09.008

Blom, A. B., Libregts, S., and Holthuysen, A. E. (2007). Crucial role of macrophages in matrix metalloproteinase-mediated cartilage destruction during experimental osteoarthritis: involvement of matrix metalloproteinase 3. *Arthritis Rheum.* 56, 147–157. doi: 10.1002/art.22337

Bondeson, J., Wainwright, S. D., Lauder, S., Amos, N., and Hughes, C. E. (2006). The role of synovial macrophages and macrophage-produced cytokines in driving aggrecanases, matrix metalloproteinases and other destructive and inflammatory responses in osteoarthritis. *Arthritis Res. Ther.* 8:R187. doi: 10.1186/ar2099

Brandes, M., Schomaker, R., Möllenhoff, G., and Rosenbaum, D. (2008). Quantity versus quality of gait and quality of life in patients with osteoarthritis. *Gait Posture* 28, 74–79. doi: 10.1016/j.gaitpost.2007.10.004

Brochard, V., CombadiÃĺre, B., Prigent, A., Laouar, Y., Perrin, A., Beray-Berthat, V., et al (2009). Infiltration of $CD4^+$ lymphocytes into the brain contributes to neurodegeneration in a mouse model of Parkinson disease. *J. Clin. Invest.* 119, 182–192. doi: 10.1172/JCI36470

Brodacki, B., Staszewski, J., Toczyłowska, B., Kozłowska, E., Drela, N., Chalimoniuk, M., et al. (2008). Serum interleukin (IL-2, IL-10, IL-6, IL-4), TNFalpha and INFgamma concentrations are elevated in patients with atypical and idiopathic parkinsonism. *Neurosci. Lett.* 441, 158–162. doi: 10.1016/j.neulet.2008.06.040

Cebrian, C., Banerjee, R., Reynolds, A. D., Sherman, S., Pisarev, V. M., Tsiperson, V., et al (2014). MHC-I expression renders catecholaminergic neurons susceptible to T-cell-mediated degeneration. *Nat. Commun.* 5:3633. doi: 10.1038/ncomms4633

Cebrian, C., Loike, J. D., and Sulzer, D. (2015). Neuroinflammation in Parkinson's disease animal models: a cell stress response or a step in neurodegeneration? *Curr. Top. Behav. Neurosci.* 22, 237–270. doi: 10.1007/7854_2014_356

Centers for Disease Control and Prevention (2013). Prevalence of doctor-diagnosed arthritis and arthritis-attributable activity limitation–United States, 20102012. *MMWR Morb. Mortal. Wkly. Rep.* 62, 869–873.

Chen, J., Zhang, C., Wu, Y., and Zhang, D. (2019). Association between hypertension and the risk of Parkinson's disease: a meta-analysis of analytical studies. *Neuroepidemiology* 52, 181–192. doi: 10.1159/000496977

Chow, Y. Y., and Chin, K. Y. (2020). The role of inflammation in the pathogenesis of osteoarthritis. *Mediators Inflamm.* 23:8293921. doi: 10.1155/2020/8293921

Cui, X., Pelekanos, M., Liu, P. Y., Burne, T. H., McGrath, J. J., Eyles, D. W., et al. (2013). The vitamin D receptor in dopamine neurons; its presence in human substantia nigra and its ontogenesis in rat midbrain. *Neuroscience* 236, 77–87. doi: 10.1016/j.neuroscience.2013.01.035

DeMaagd, G., and Philip, A. (2015). Parkinson's disease and its management: part 1: disease entity, risk factors, pathophysiology, clinical presentation and diagnosis. *P T* 40, 504–532.

Dufek, M., Rektorova, I., Thon, V., Lokaj, J., and Rektor, I. (2015). Interleukin-6 may contribute to mortality in Parkinson's disease patients: a 4-year prospective study. *Parkinsons Dis.* 2015:898192. doi: 10.1155/2015/898192

Edgar, R., Domrachev, M., and Lash, A. E. (2002). Gene expression omnibus: NCBI gene expression and hybridization array data repository. *Nucleic Acids Res.* 30:20710. doi: 10.1093/nar/30.1.207

Egloff, C., Hugle, T., and Valderrabano, V. (2012). Biomechanics and pathomechanisms of osteoarthritis. *Swiss Med. Wkly.* 142:w13583. doi: 10.4414/smw.2012.13583

Fang, X., Han, D., Cheng, Q., Zhang, P., Zhao, C., Min, J., et al. (2018). Association of levels of physical activity with risk of Parkinson disease: a systematic review and meta-analysis. *JAMA Netw. Open* 1:e182421. doi: 10.1001/jamanetworkopen.2018.2421

Feng, S. H., Chuang, H. J., Yeh, K. C., and Pan, S. L. (2021). Association of osteoarthritis with increased risk of Parkinson's disease: a population-based, longitudinal follow-up study. *Arthritis Care Res. (Hoboken)*. doi: 10.1002/acr.24708. [Online ahead of print].

Franceschini, A., Szklarczyk, D., Frankild, S., Kuhn, M., Simonovic, M., Roth, A., et al. (2013). STRING v9.1: protein-protein interaction networks, with increased coverage and integration. *Nucleic Acids Res.* 41, D808–D815. doi: 10.1093/nar/gks1094

Freed, E.F., Prieto, J. L., McCann, K. L., McStay, B., and Baserga, S. J. (2012). NOL11, implicated in the pathogenesis of North American Indian childhood cirrhosis, is required for pre-rRNA transcription and processing. *PLoS Genet.* 8:e1002892. doi: 10.1371/journal.pgen.1002892

Garfinkel, R. J., Dilisio, M. F., and Agrawal, D. K. (2017). Vitamin D and its effects on articular cartilage and osteoarthritis. *Orthop. J. Sports Med.* 5:2325967117711376. doi: 10.1177/2325967117711376

Goldring, M. B., and Otero, M. (2011). Inflammation in osteoarthritis. *Curr. Opin. Rheumatol.* 23, 471–478. doi: 10.1097/BOR.0b013e328349c2b1

Goula, T., Kouskoukis, A., Drosos, G., Tselepis, A. S., Ververidis, A., Valkanis, C., et al. (2015). Vitamin D status in patients with knee or hip osteoarthritis in a Mediterranean country. *J. Orthop. Traumatol.* 16, 35–39. doi: 10.1007/s10195-014-0322-y

Guideline for the prevention of falls in older persons (2001). American geriatrics society, british geriatrics society and american academy of orthopaedic surgeons panel on falls prevention. *J. Am. Geriatr. Soc.* 49, 664–672.

Hanson, D., Stevens, A., Murray, P. G., Black, G. C., and Clayton, P. E. (2014). Identifying biological pathways that underlie primordial short stature using network analysis. *J. Mol. Endocrinol.* 52, 333–344. doi: 10.1530/JME-14-0029

Haseeb, A., and Haqqi, T. M. (2013). Immunopathogenesis of osteoarthritis. *Clin. Immunol.* 146, 185–196. doi: 10.1016/j.clim.2012.12.011

Herbolsheimer, F., Schaap, L. A., Edwards, M. H., Maggi, S., Otero, Á., Timmermans, E. J., et al. (2016). Physical activity patterns among older adults with and without knee osteoarthritis in six european countries. *Arthritis Care Res. (Hoboken)* 68, 228–236. doi: 10.1002/acr.22669

Hernandez-Verdun, D., Roussel, P., Thiry, M., Sirri, V., and Lafontaine, D. L. (2010). The nucleolus: structure/function relationship in RNA metabolism. *Wiley Interdiscip. Rev. RNA* 1, 415–431. doi: 10.1002/wrna.39

Huber, R., Hummert, C., Gausmann, U., Pohlers, D., Koczan, D., Guthke, R., et al. (2008). Identification of intra-group, inter-individual and gene-specific variances in mRNA expression profiles in the rheumatoid arthritis synovial membrane. *Arthritis Res. Ther.* 10:R98. doi: 10.1186/ar2485

Jacob, L., Loeser, R. F., Goldring, S. R., Scanzello, C. R., and Goldring, M. B. (2021). Association between osteoarthritis and the incidence of Parkinson's disease in the United Kingdom. *Clin. Parkinsonism Relat. Disord.* 5:100120. doi: 10.1016/j.prdoa.2021.100120

Jansen, J. A., and Haddad, F. S. (2013). Haddad, high prevalence of vitamin d deficiency in elderly patients with advanced osteoarthritis scheduled for total knee replacement associated with poorer preoperative functional state. *Ann. R Coll. Surg. Engl.* 95, 569–572. doi: 10.1308/003588413x13781990150374

Jones, J. D., Malaty, I., Price, C. C., Okun, M. S., and Bowers, D. (2012). Health comorbidities and cognition in 1948 patients with idiopathic Parkinson's disease. *Parkinsonism Relat. Disord.* 18, 1073–1078. doi: 10.1016/j.parkreldis.2012.06.004

Kapoor, M., Martel-Pelletier, J., Lajeunesse, D., Pelletier, J. P., and Fahmi, H. (2011). Role of proinflammatory cytokines in the pathophysiology of osteoarthritis. *Nat. Rev. Rheumatol.* 7, 33–42. doi: 10.1038/nrrheum.2010.196

Klein-Wieringa, I. R., de Lange-Brokaar, B. J. E., Yusuf, E., Andersen, S. N., Kwekkeboom, J. C., Kroon, H. M., et al (2016). Inflammatory cells in patients with endstage knee osteoarthritis: a comparison between the synovium and the infrapatellar fat pad. *J. Rheumatol.* 43, 771–778. doi: 10.3899/jrheum.151068

Kustrimovic, N., Marino, F., and Cosentino, M. (2019). Peripheral immunity, immunoaging and neuroinflammation in Parkinson's disease. *Curr. Med. Chem.* 26, 3719–3753. doi: 10.2174/0929867325666181009161048

Langfelder, P., and Horvath, S. (2008). WGCNA: an R package for weighted correlation network analysis. *BMC Bioinformatics* 9:559. doi: 10.1186/1471-2105-9-559

Le, W., Wu, J., and Tang, Y. (2016). Protective microglia and their regulation in Parkinson's disease. *Front. Mol. Neurosci.* 9:89. doi: 10.3389/fnmol.2016.00089

Lesnick, T. G., Huber, R., Kupfer, P., Pohlers, D., Pfaff, M., Driesch, D., et al. (2007). A genomic pathway approach to a complex disease: axon guidance and Parkinson disease. *PLoS Genet.* 3:e98. doi: 10.1371/journal.pgen.0030098

Loeser, R. F., Goldring, S. R., Scanzello, C. R., and Goldring, M. B. (2012). Osteoarthritis: a disease of the joint as an organ. *Arthritis Rheum.* 64, 1697–1707. doi: 10.1002/art.34453

Lott, G. K., 3rd, Johnson, B. R., Bonow, R. H., Land, B. R., and Hoy, R. R. (2009). g-PRIME: a free, windows based data acquisition and event analysis software package for physiology in classrooms and research labs. *J. Undergrad. Neurosci. Educ.* 8, A50–A54.

Lv, Z., Qi, H., Wang, L., Fan, X., Han, F., and Wang, H. (2014). Vitamin D status and Parkinson's disease: a systematic review and meta-analysis. *Neurol. Sci.* 35, 1723–1730. doi: 10.1007/s10072-014-1821-6

Ma, V. Y., Chan, L., and Carruthers, K. J. (2014). Incidence, prevalence, costs and impact on disability of common conditions requiring rehabilitation in the United States: stroke, spinal cord injury, traumatic brain injury, multiple sclerosis, osteoarthritis, rheumatoid arthritis, limb loss and back pain. *Arch. Phys. Med. Rehabil.* 95, 986–995.e1. doi: 10.1016/j.apmr.2013.10.032

McDonough, C. M., and Jette, A. M. (2010). The contribution of osteoarthritis to functional limitations and disability. *Clin. Geriatr. Med.* 26, 387–399. doi: 10.1016/j.cger.2010.04.001

Mengshol, J. A., Vincenti, M. P., Coon, C. I., Barchowsky, A., and Brinckerhoff, C. E. (2000). Interleukin-1 induction of collagenase 3 (matrix metalloproteinase 13) gene expression in chondrocytes requires p38, c-Jun N-terminal kinase and nuclear factor kappaB: differential regulation of collagenase 1 and collagenase 3. *Arthritis Rheum.* 43, 801–811. doi: 10.1002/1529-0131(200004)43:4<801::AID-ANR10>3.0.CO;2-4

Modugno, N., Lena, F., Di Biasio, F., Cerrone, G., Ruggieri, S., and Fornai, F. (2013). A clinical overview of non-motor symptoms in Parkinson's disease. *Arch. Ital. Biol.* 151, 148–468.

Moore, H. G., Kahan, J. B., Sherman, J. J. Z., Burroughs, P. J., Donohue, K. W., and Grauer, J. N. (2022). Total shoulder arthroplasty for osteoarthritis in patients with Parkinson's disease: a matched comparison of 90-day adverse events and 5-year implant survival. *J. Shoulder Elbow Surg.* 31, 1436–1441. doi: 10.1016/j.jse.2022.01.113

Neogi, T. (2013). The epidemiology and impact of pain in osteoarthritis. *Osteoarthritis Cartilage* 21, 1145–1153. doi: 10.1016/j.joca.2013.03.018

Obeso, J. A., Rodriguez-Oroz, M. C., Goetz, C. G., Marin, C., Kordower, J. H., and Rodriguez, M. (2010). Missing pieces in the Parkinson's disease puzzle. *Nat. Med.* 16, 653–661. doi: 10.1038/nm.2165

Orlowsky, E. W., and Kraus, V. B. (2015). The role of innate immunity in osteoarthritis: when our first line of defense goes on the offensive. *J. Rheumatol.* 42, 363–371. doi: 10.3899/jrheum.140382

Osteoarthritis linked to higher parkinson's disease risk (2021). *Saudi Med. J.* 42:921.

Pajares, M., Rojo, A. I., Manda, G., Boscá, L., and Cuadrado, A. (2020). Inflammation in Parkinson's disease: mechanisms and therapeutic implications. *Cells* 9:1687. doi: 10.3390/cells9071687

Perry, V. H. (2004). The influence of systemic inflammation on inflammation in the brain: implications for chronic neurodegenerative disease. *Brain Behav. Immun.* 18, 407–413. doi: 10.1016/j.bbi.2004.01.004

Pertile, R. A. N., Cui, X., Hammond, L., and Eyles, D. W. (2018). Vitamin D regulation of GDNF/ret signaling in dopaminergic neurons. *FASEB J.* 32, 819–828. doi: 10.1096/fj.201700713R

Prieto-Potin, I., Largo, R., Roman-Blas, J. A., Herrero-Beaumont, G., and Walsh, D. A. (2015). Characterization of multinucleated giant cells in synovium and subchondral bone in knee osteoarthritis and rheumatoid arthritis. *BMC Musculoskelet. Disord.* 16:226. doi: 10.1186/s12891-015-0664-5

Quan, W., Li, J., Jin, X., Liu, L., Zhang, Q., Qin, Y., et al. (2021). Identification of potential core genes in Parkinson's disease using bioinformatics analysis. *Parkinsons Dis.* 2021:1690341. doi: 10.1155/2021/1690341

Reale, M., Iarlori, C., Thomas, A., Gambi, D., Perfetti, B., Nicola, M. D., et al. (2009). Peripheral cytokines profile in Parkinson's disease. *Brain Behav. Immun.* 23, 55–63. doi: 10.1016/j.bbi.2008.07.003

Ritchie, M. E., Phipson, B., Wu, D., Hu, Y., Law, C. W., Shi, W., et al. (2015). limma powers differential expression analyses for RNA-sequencing and microarray studies. *Nucleic Acids Res.* 43:e47. doi: 10.1093/nar/gkv007

Robin, X., Turck, N., Hainard, A., Tiberti, N., Lisacek, F., Sanchez, J.-C., et al. (2011). pROC: an open-source package for R and S+ to analyze and compare ROC curves. *BMC Bioinformatics* 12:77. doi: 10.1186/1471-2105-12-77

Roper, J. A., Schmitt, A. C., Gao, H., He, Y., Wu, S., Schmidt, P., et al. (2020). Coexistent osteoarthritis and Parkinson's disease: data from the Parkinson's foundation outcomes project. *J. Parkinsons Dis.* 10, 1601–1610. doi: 10.3233/JPD-202170

Roseti, L., Desando, G., Cavallo, C., Petretta, M., and Grigolo, B. (2019). Articular cartilage regeneration in osteoarthritis. *Cells* 8:1305. doi: 10.3390/cells8111305

Scanzello, C. R. (2017). Role of low-grade inflammation in osteoarthritis. *Curr. Opin. Rheumatol.* 29, 79–85. doi: 10.1097/BOR.0000000000000353

Serang, S., Jacobucci, R., Brimhall, K. C., and Grimm, K. J. (2017). Exploratory mediation analysis via regularization. *Struct. Equation Modeling* 24, 733–744. doi: 10.1080/10705511.2017.1311775

Shannon, P., Markiel, A., Ozier, O., Baliga, N. S., Wang, J. T., Ramage, D., et al. (2003). Cytoscape: a software environment for integrated models of biomolecular interaction networks. *Genome Res.* 13, 2498–2504. doi: 10.1101/gr.1239303

Shih, M., Hootman, J. M., Kruger, J., and Helmick, C. G. (2006). Physical activity in men and women with arthritis national health interview survey, 2002. *Am. J. Prev. Med.* 30, 385–393. doi: 10.1016/j.amepre.2005.12.005

Sleeman, I., Aspray, T., Lawson, R., Coleman, S., Duncan, G., Khoo, T. K., et al. (2017). The role of vitamin D in disease progression in early Parkinson's disease. *J. Parkinsons Dis.* 7, 669–675. doi: 10.3233/JPD-171122

Sullivan, G. J., Bridger, J. M., Cuthbert, A. P., Newbold, R. F., Bickmore, W. A., and McStay, B. (2001). Human acrocentric chromosomes with transcriptionally silent nucleolar organizer regions associate with nucleoli. *EMBO J.* 20, 2867–2874. doi: 10.1093/emboj/20.11.2867

Tansey, M. G., and Goldberg, M. S. (2010). Neuroinflammation in Parkinson's disease: its role in neuronal death and implications for therapeutic intervention. *Neurobiol. Dis.* 37, 510–518. doi: 10.1016/j.nbd.2009.11.004

Teder-Braschinsky, A., Märtson, A., Rosenthal, M., and Taba, P. (2019). Parkinson's disease and symptomatic osteoarthritis are independent risk factors of falls in the elderly. *Clin. Med. Insights Arthritis Musculoskelet. Disord.* 12:1179544119884936. doi: 10.1177/1179544119884936

Träger, U., and Tabrizi, S. J. (2013). Peripheral inflammation in neurodegeneration. *J. Mol. Med. (Berl)* 91, 673–681. doi: 10.1007/s00109-013-1026-0

Tysnes, O. B., and Storstein, A. (2017). Epidemiology of Parkinson's disease. *J. Neural Transm. (Vienna)* 124, 901–905. doi: 10.1007/s00702-017-1686-y

Veronese, N., Maggi, S., Noale, M., Bolzetta, F., Zambon, S., Corti, M. C., et al. (2015). Serum 25-Hydroxyvitamin D and osteoarthritis in older people: the progetto veneto anziani study. *Rejuvenation Res.* 18, 543–553. doi: 10.1089/rej.2015.1671

Veronese, N., Stubbs, B., Solmi, M., Smith, T. O., Noale, M., Cooper, C., et al. (2017). Association between lower limb osteoarthritis and incidence of depressive symptoms: data from the osteoarthritis initiative. *Age Ageing* 46, 470–476. doi: 10.1093/ageing/afw216

Veronese, N., Stubbs, B., Solmi, M., Smith, T. O., Noale, M., Schofield, P., et al. (2018). Knee osteoarthritis and risk of hypertension: a longitudinal cohort study. *Rejuvenation Res.* 21, 15–21. doi: 10.1089/rej.2017.1917

Wang, S., Mao, S., Xiang, D., and Fang, C. (2018). Association between depression and the subsequent risk of Parkinson's disease: a meta-analysis. *Prog. Neuropsychopharmacol. Biol. Psychiatry* 86, 186–192. doi: 10.1016/j.pnpbp.2018.05.025

Wang, J., Song, Y., Chen, Z., and Leng, S. X. (2018). Connection between systemic inflammation and neuroinflammation underlies neuroprotective mechanism of several phytochemicals in neurodegenerative diseases. *Oxid. Med. Cell. Longev.* 2018:1972714. doi: 10.1155/2018/1972714

Woetzel, D., Huber, R., Kupfer, P., Pohlers, D., Pfaff, M., Driesch, D., et al. (2014). Identification of rheumatoid arthritis and osteoarthritis patients by transcriptome-based rule set generation. *Arthritis Res. Ther.* 16:R84. doi: 10.1186/ar4526

Wojdasiewicz, P., Poniatowski, L. A., and Szukiewicz, D. (2014). The role of inflammatory and anti-inflammatory cytokines in the pathogenesis of osteoarthritis. *Mediators Inflamm.* 2014:561459. doi: 10.1155/2014/561459

Wu, T., Hu, E., Xu, S., Chen, M., Guo, P., Dai, Z., et al. (2021). clusterProfiler 4.0: a universal enrichment tool for interpreting omics data. *Innovation (Camb)* 2:100141. doi: 10.1016/j.xinn.2021.100141

Xue, G., Hua, L., Zhou, N., and Li, J. (2021). Characteristics of immune cell infiltration and associated diagnostic biomarkers in ulcerative colitis: results from bioinformatics analysis. *Bioengineered* 2, 252–265. doi: 10.1080/21655979.2020.1863016

Zasadzka, E., Borowicz, A. M., Roszak, M., and Pawlaczyk, M. (2015). Assessment of the risk of falling with the use of timed up and go test in the elderly with lower extremity osteoarthritis. *Clin. Interv. Aging* 10, 1289–1298. doi: 10.2147/CIA.S86001

Zhang, F. F., Driban, J. B., Lo, G. H., Price, L. L., Booth, S., Eaton, C. B., et al. (2014). Vitamin D deficiency is associated with progression of knee osteoarthritis. *J. Nutr.* 144, 2002–2008. doi: 10.3945/jn.114.193227

Zhang, Z. (2016). Reshaping and aggregating data: an introduction to reshape package. *Ann. Transl. Med.* 4:78. doi: 10.3978/j.issn.2305-5839.2016.01.33

frontiers | Frontiers in Aging Neuroscience

TYPE Original Research
PUBLISHED 29 November 2022
DOI 10.3389/fnagi.2022.1040001

OPEN ACCESS

EDITED BY
Gal Bitan,
David Geffen School of Medicine (UC), Los Angeles, United States

REVIEWED BY
Marcia H. Ratner,
Boston University School of Medicine, United States
Hao Wang,
Shanghai Jiao Tong University, China

*CORRESPONDENCE
Alejo J. Nevado-Holgado
alejo.nevado-holgado@psych.ox.ac.uk
Liu Shi
shiliuswgch@gmail.com

SPECIALTY SECTION
This article was submitted to Cellular and Molecular Mechanisms of Brain-aging, a section of the journal Frontiers in Aging Neuroscience

RECEIVED 08 September 2022
ACCEPTED 04 November 2022
PUBLISHED 29 November 2022

CITATION
Zhang Y, Ghose U, Buckley NJ, Engelborghs S, Sleegers K, Frisoni GB, Wallin A, Lleó A, Popp J, Martinez-Lage P, Legido-Quigley C, Barkhof F, Zetterberg H, Visser PJ, Bertram L, Lovestone S, Nevado-Holgado AJ and Shi L (2022) Predicting AT(N) pathologies in Alzheimer's disease from blood-based proteomic data using neural networks.
Front. Aging Neurosci. 14:1040001.
doi: 10.3389/fnagi.2022.1040001

Predicting AT(N) pathologies in Alzheimer's disease from blood-based proteomic data using neural networks

Yuting Zhang[1], Upamanyu Ghose[1], Noel J. Buckley[1], Sebastiaan Engelborghs[2,3,4], Kristel Sleegers[5,6], Giovanni B. Frisoni[7], Anders Wallin[8], Alberto Lleó[9], Julius Popp[10,11], Pablo Martinez-Lage[12], Cristina Legido-Quigley[13,14], Frederik Barkhof[15,16], Henrik Zetterberg[8,17,18,19,20], Pieter Jelle Visser[21,22], Lars Bertram[23,24], Simon Lovestone[1,25], Alejo J. Nevado-Holgado[1]* and Liu Shi[1]*

[1]Department of Psychiatry, University of Oxford, Oxford, United Kingdom, [2]Department of Biomedical Sciences, Reference Center for Biological Markers of Dementia (BIODEM), Institute Born-Bunge, University of Antwerp, Antwerp, Belgium, [3]Department of Neurology, Universitair Ziekenhuis Brussel, Brussels, Belgium, [4]Center for Neurosciences (C4N), Vrije Universiteit Brussel, Brussels, Belgium, [5]Complex Genetics Group, VIB Center for Molecular Neurology, Antwerp, Belgium, [6]Department of Biomedical Sciences, University of Antwerp, Antwerp, Belgium, [7]Department of Psychiatry, University of Geneva, Geneva, Switzerland, [8]Department of Psychiatry and Neurochemistry, Institute of Neuroscience and Physiology, The Sahlgrenska Academy at the University of Gothenburg, Mölndal, Sweden, [9]Centro de Investigación Biomédica en Red de Enfermedades Neurodegenerativas (CIBERNED), Hospital de la Santa Creu i Sant Pau, Barcelona, Spain, [10]Department of Psychiatry, University Hospital of Lausanne, Lausanne, Switzerland, [11]Department of Geriatric Psychiatry, University Hospital of Psychiatry and University of Zürich, Zürich, Switzerland, [12]CITA-Alzheimer Foundation, San Sebastian, Spain, [13]Kings College London, London, United Kingdom, [14]The Systems Medicine Group, Steno Diabetes Center, Gentofte, Denmark, [15]Department of Radiology and Nuclear Medicine, VU University Medical Center, Amsterdam, Netherlands, [16]University College London (UCL) Institutes of Neurology and Healthcare Engineering, London, United Kingdom, [17]Clinical Neurochemistry Laboratory, Sahlgrenska University Hospital, Mölndal, Sweden, [18]UK Dementia Research Institute at UCL, London, United Kingdom, [19]Department of Neurodegenerative Disease, UCL Institute of Neurology, London, United Kingdom, [20]Hong Kong Center for Neurodegenerative Diseases, Hong Kong, China, [21]Department of Psychiatry and Neuropsychology, School for Mental Health and Neuroscience, Alzheimer Centrum Limburg, Maastricht University, Maastricht, Netherlands, [22]Alzheimer Center, VU University Medical Center, Amsterdam, Netherlands, [23]Lübeck Interdisciplinary Platform for Genome Analytics, University of Lübeck, Lübeck, Germany, [24]Department of Psychology, University of Oslo, Oslo, Norway, [25]Janssen R&D, High Wycombe, United Kingdom

Background and objective: Blood-based biomarkers represent a promising approach to help identify early Alzheimer's disease (AD). Previous research has applied traditional machine learning (ML) to analyze plasma omics data and search for potential biomarkers, but the most modern ML methods based on deep learning has however been scarcely explored. In the current study, we aim to harness the power of state-of-the-art deep learning neural networks (NNs) to identify plasma proteins that predict amyloid, tau, and neurodegeneration (AT[N]) pathologies in AD.

Methods: We measured 3,635 proteins using SOMAscan in 881 participants from the European Medical Information Framework for AD Multimodal Biomarker

Discovery study (EMIF-AD MBD). Participants underwent measurements of brain amyloid β (Aβ) burden, phosphorylated tau (p-tau) burden, and total tau (t-tau) burden to determine their AT(N) statuses. We ranked proteins by their association with Aβ, p-tau, t-tau, and AT(N), and fed the top 100 proteins along with age and apolipoprotein E (*APOE*) status into NN classifiers as input features to predict these four outcomes relevant to AD. We compared NN performance of using proteins, age, and *APOE* genotype with performance of using age and *APOE* status alone to identify protein panels that optimally improved the prediction over these main risk factors. Proteins that improved the prediction for each outcome were aggregated and nominated for pathway enrichment and protein–protein interaction enrichment analysis.

Results: Age and *APOE* alone predicted Aβ, p-tau, t-tau, and AT(N) burden with area under the curve (AUC) scores of 0.748, 0.662, 0.710, and 0.795. The addition of proteins significantly improved AUCs to 0.782, 0.674, 0.734, and 0.831, respectively. The identified proteins were enriched in five clusters of AD-associated pathways including human immunodeficiency virus 1 infection, p53 signaling pathway, and phosphoinositide-3-kinase–protein kinase B/Akt signaling pathway.

Conclusion: Combined with age and *APOE* genotype, the proteins identified have the potential to serve as blood-based biomarkers for AD and await validation in future studies. While the NNs did not achieve better scores than the support vector machine model used in our previous study, their performances were likely limited by small sample size.

KEYWORDS

Alzheimer's disease, plasma proteomics, amyloid β, tau, neurodegeneration, machine learning, artificial neural networks

Introduction

Alzheimer's disease (AD) is a growing public health concern with no disease-modifying treatment available (Apostolova, 2016). The core criteria for clinical diagnosis of AD are based on behavioral and cognitive symptoms, but neuropathological changes in the central nervous system initiate years before the onset of cognitive impairment (Jack et al., 2013). The preclinical stage when pathologies develop in the absence of clinical symptoms presents an opportunity for early intervention with drugs to slow down or even halt disease progression. Currently, the well-established biomarkers for AD are cerebrospinal fluid (CSF) amyloid-β peptide (Aβ) and amyloid positron emission tomography (PET). They both highly correlate with pathologies found in brain autopsy (Strozyk et al., 2003; Curtis et al., 2015) and can identify early AD with high accuracy (Palmqvist et al., 2015). However, collecting CSF requires a lumbar puncture, an invasive practice that could lead to complications including post-dural puncture headache (de Almeida et al., 2011). PET imaging is expensive and requires specialist equipment that is not easily available. Thus, these two approaches have limited clinical utility. Blood-based biomarkers offer a desirable strategy to aid early diagnosis of AD. As blood-based test is minimally invasive, economical, and widely available, they can serve as efficient prescreening tools in a multi-stage diagnostic process (O'Bryant et al., 2016). Earlier research has provided evidence of alterations of proteomic profiles in blood samples associated with AD state (Hye et al., 2006; Ray et al., 2007), validating the feasibility of blood-based biomarkers.

The development of blood-based biomarkers is facilitated by advances in not only targeted approaches (e.g., plasma phosphorylated tau measurements; Ashton et al., 2021; Milà-Alomà et al., 2022) but also untargeted large-scale omics technologies. Researchers have adopted high-resolution mass spectrometry for proteomic profiling of blood and discovery of AD protein signatures (Lopez et al., 2005; Dey et al., 2019). Highly sensitive multiplexed immunoassay platforms, such as Olink (Whelan et al., 2019; Jiang et al., 2022), and aptamer-based assay platforms, such as SOMAscan (Kiddle et al., 2014; Sattlecker et al., 2014), have further allowed researchers to capture the complexity of plasma proteome and identify prospective biomarkers by measuring thousands of proteins simultaneously in thousands of individuals with a single platform. In analyzing the rich omics data, machine learning (ML), a subdomain of artificial intelligence, has proven an invaluable tool (Li et al., 2021). Previous studies have had great success in finding blood analytes that predict

AD-related measures using traditional ML algorithms such as support vector machines (Voyle et al., 2015; Shi L. et al., 2019; Karaglani et al., 2020), decision trees (Pérez-Grijalba et al., 2019; Shi Y. et al., 2019), and random forests (Goudey et al., 2019; Beltrán et al., 2020; Lin et al., 2020; Zhao et al., 2020).

Deep learning neural networks (NNs) are the last iteration of ML methods and have significant advantages when compared to the older ML methods both in terms of classification accuracy and versatility, yet fewer studies have explored their utility in blood-based AD biomarker discovery. As they are capable of learning data representations in multiple hierarchies, they have often outperformed conventional models in various applications including predicting clinical diagnoses (Durstewitz et al., 2019). Thus, in the current study, we implement deep NNs to analyze plasma proteomics measured by SOMAscan. Our objective is to identify candidate plasma protein panels to detect amyloid, tau, and neurodegeneration (AT[N]) pathologies in AD.

Materials and methods

Participants

European Medical Information Framework (EMIF, www.emif.eu) is funded by the Innovative Medicines Initiative to support the reuse of existing healthcare data. As part of this project, EMIF-AD set up the Multimodal Biomarker Discovery (MBD) study by integrating multi-omics data to facilitate the development of AD biomarkers. Participants of the current study were from the EMIF 1000 sub-cohort assembled in a previous study (Bos et al., 2018). The original sub-cohort included 1,221 participants from 11 single- or multi-center studies across Europe. In the current study, we included only subjects who had available plasma samples, resulting in a subset of 881 participants from 10 studies. Among them, 311 had normal cognition (CN), 386 had mild cognitive impairment (MCI), and 184 had a diagnosis of AD dementia.

All 881 participants underwent measurement of the concentration of the 42 amino acid-long Aβ protein, $A\beta_{42}$, in CSF, sometimes in a ratio with the 40 amino acid-long form, $A\beta_{40}$, or amyloid PET as the primary AD outcome. A previous study has classified the amyloid burden of each participant as high or low based on z-score cutoffs (Bos et al., 2018). In addition, a subgroup of 787 subjects underwent measurement of CSF phosphorylated tau (p-tau), and a subgroup of 791 subjects underwent measurement of CSF total tau (t-tau). CSF p-tau and t-tau levels were both measured locally, and their statuses were classified as high or low with local cutoffs. Mini-mental state examination (MMSE) was administered to a majority of participants to assess cognitive function. All participants were genotyped to determine whether they were apolipoprotein E (*APOE*) risk allele ε4 carriers or non-carriers. Lastly, proteins in plasma samples were measured by the SOMAscan assay (SomaLogic Inc.) in a previous study (Shi L. et al., 2019). SOMAscan is an aptamer-based platform which transforms individual protein signals into corresponding chemically-modified nucleotide signals that can be quantified by relative fluorescence on DNA microarrays (Gold et al., 2010). Plasma samples were divided into two groups, and each group was processed independently. Forty samples were tested in both batches to normalize the measurements across assay runs. A total of 3,635 plasma proteins were quantified.

Statistical analysis

All statistical analyses were performed using Python (version 3.9.7). We compared the demographic and clinical characteristics of patients with different diagnoses. Continuous variables were compared between groups by the Kruskal-Wallis one-way ANOVA test followed by Mann–Whitney *U*-tests for pairwise comparisons. Categorical variables were compared between groups by Chi-square test.

Building NNs

NNs were implemented using the Python package PyTorch (version 1.10.1). The network (Figure 1) consisted of three fully connected hidden layers with sizes 8, 16, and 8. Dimension of the input layer varied depending on the number of features: one for age, one for *APOE* status, and one for each protein. The output layer had one dimension to encode the binary outcome. Dropout was applied to the output of the first hidden layer at a rate of 0.5. Each hidden layer was followed by a rectified linear unit (ReLU) activation function. The loss function was binary cross-entropy with sigmoid. Learning was implemented using the Adam stochastic optimization algorithm with a learning rate of 0.01.

Training and testing were implemented with 5-fold cross-validation. The dataset was shuffled across samples before splitting between training and testing. On each training/testing split, the parameters of the NN (i.e., weights) were reinitialized, and the NN was trained for 15 epochs. In each epoch, data was fed into NN in minibatches of size 128. The outputs were transformed by a sigmoid function to compare with the binary ground-truth values.

Discrimination of AT(N)

The dataset was preprocessed for analysis. Age was power-transformed and z-scored. All protein levels were power-transformed and z-scored to have zero mean and unit variance. The effects of study and blood freeze–thaw cycles on proteins were removed by linear regression, and the resulting residuals replaced raw protein levels.

We aim to predict Aβ burden (high vs. low), p-tau burden (high vs. low), t-tau burden (high vs. low), and AT(N) profile (high

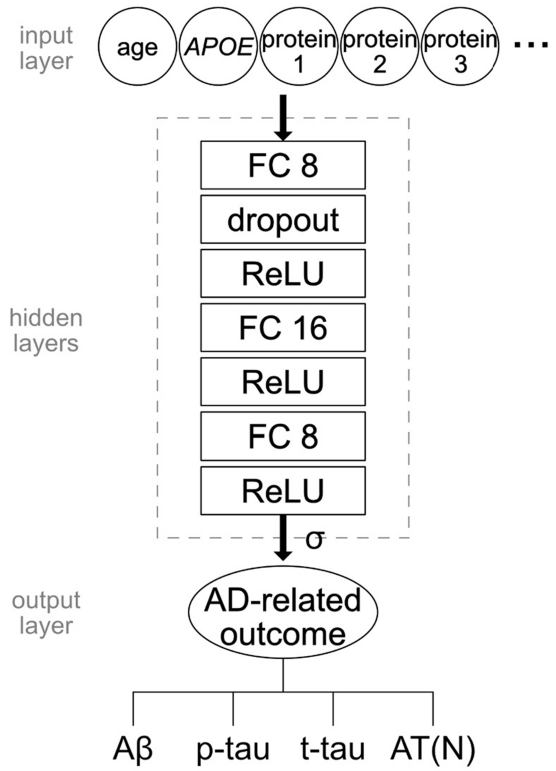

FIGURE 1
Structure of the NN model. The dimension of the input layer was determined by the number of features including age, *APOE* status, and/or protein levels. The hidden layers consisted of three fully connected layers of size 8, 16, and 8 connected by ReLU activation function. Dropout of rate 0.5 was applied to the output of the first hidden layer. The final output was transformed by a sigmoid function. Four AD-related measures were independently tested as outcomes: Aβ, p-tau, t-tau, and AT(N).

Aβ/p-tau/t-tau vs. low Aβ/p-tau/t-tau) from plasma proteins along with age and *APOE* genotype. For each of these classification objectives, we first performed logistic regression analysis to measure the linear association between each protein and the target and ranked the proteins by ascending *p* values. We then selected from 1 to 100 top-ranked proteins along with age and *APOE* status as input features for NN classification and compared their performance with that of age and *APOE* ε4 status alone. For each unique set of features and the target, we repeated training–testing 10 times to obtain the average receiver operating characteristic (ROC) curve and the area under the curve (AUC). AUC ROC scores resulting from different features were compared using independent t-tests.

Enrichment analysis

The proteins that achieved the best performance in NN classification along with age and *APOE* status in differentiating high and low Aβ, p-tau, t-tau, and AT(N) were aggregated and nominated for pathway enrichment and protein–protein interaction enrichment analysis. The analysis was performed using the Metascape software (Zhou et al., 2019). The complete set of proteins was provided as "background." The inputs were searched against KEGG Pathway database for pathway enrichment analysis and STRING, BioGrid, OmniPath, and InWeb_IM databases for protein–protein interaction analysis.

TABLE 1 Demographic and clinical characteristics of the study population.

Characteristic	Sample size	CN	MCI	AD	*P*-value
N	881	311	386	184	
Age, median (IQR)	881	66.0 (58.9–70.0)	70.5 (65.1–75.5)	71.0 (63.4–77.0)	<0.001*
Male sex, *N* (%)	881	133 (42.8%)	181 (46.9%)	86 (46.7%)	0.509
MMSE, median (IQR)	878	29.0 (28.0–30.0)	26.5 (25.0–28.0)	22.0 (18.0–25.0)	<0.001*
APOE ε4+, *N* (%)	881	118 (37.9%)	186 (48.2%)	112 (60.9%)	<0.001*
Aβ+, *N* (%)	881	93 (30.0%)	245 (63.5%)	165 (89.7%)	<0.001*
P-tau+, *N* (%)	787	42 (19.1%)	203 (53.0%)	128 (69.6%)	<0.001*
T-tau+, *N* (%)	791	45 (20.1%)	221 (57.6%)	149 (81.4%)	<0.001*

CN, normal cognition; MCI, mild cognitive impairment; AD, Alzheimer's disease; IQR, interquartile range; MMSE, mini-mental state examination; APOE, apolipoprotein E; Aβ, amyloid-β; p-tau, phosphorylated-tau; t-tau, total tau. *$p < 0.05$.

Results

Demographic and clinical variables

The current study included 881 participants from the EMIF 1000 sub-cohort. The demographic and clinical variables for each diagnostic group are described in Table 1. Patients with AD or MCI were older than CN subjects (AD vs. CN: odds ratio [OR] = 1.08, $p < 0.001$; MCI vs. CN: OR = 1.08, $p < 0.001$). CN subjects had higher MMSE scores than MCI subjects (OR = 2.08, $p < 0.001$), and MCI subjects had higher MMSE scores than AD subjects (OR = 1.44, $p < 0.001$). AD patients also had a higher prevalence of *APOE* ε4 carriers (AD vs. MCI: OR = 1.67, $p < 0.001$; AD vs. CN: OR = 2.54, $p < 0.01$). There was no statistical difference in sex distribution between diagnostic groups (AD vs. MCI: OR = 1.01, $p = 1.00$; MCI vs. CN: OR = 0.85, $p = 0.31$; AD vs. CN: OR = 1.01, $p = 0.44$). For AT(N) biomarkers, AD subjects had a higher prevalence of low CSF $A\beta_{42}$ or $A\beta_{42/40}$ or positive amyloid PET, high CSF p-tau, and high CSF t-tau than MCI subjects (Aβ: OR = 5.00; p-tau: OR = 2.03; t-tau: OR = 3.23; all $p < 0.001$) and CN subjects (Aβ: OR = 20.36; p-tau: OR = 9.69; t-tau: OR = 17.43; all $p < 0.001$).

Discrimination of AT(N) markers using NNs

We first used regression analysis to find the linear association between each protein and Aβ. Binary Aβ burden (high: $N = 503$; low: $N = 378$) was defined by z-score cutoff of CSF $A\beta_{42/40}$ at 0.061 or local cutoffs of CSF $A\beta_{42}$ and amyloid PET. Out of all proteins, 1,793 reached statistical significance (uncorrected $p < 0.05$), and 1,492 of them reached the false discovery rate after correction for multiple comparisons (corrected $p < 0.05$). We then sought to find the optimal set of proteins that differentiate high vs. low Aβ burden using NNs. The combination of age and *APOE* ε4 alone achieved an AUC of 0.748 (95% confidence interval [CI] 0.745–0.750). With protein features alone, a panel of 15 proteins achieved the highest AUC of 0.727 (95% CI 0.722–0.732). After the combination of age, *APOE* ε4, and proteins as input features, we found a panel of 11 proteins (see Supplementary Table 1) that achieved the highest predictive value with an AUC of 0.782 (95% CI 0.779–0.785). This was significantly higher than AUCs from using only age and *APOE* ε4 status ($p < 0.001$; Figure 2A).

Binary p-tau burden (high: $N = 373$; low: $N = 414$) was defined by local cutoffs of CSF p-tau levels. For p-tau, 690 proteins reached statistical significance (uncorrected $p < 0.05$) while none passed the false discovery rate (corrected $p < 0.05$). In classifying high and low p-tau, age and *APOE* ε4 alone achieved an AUC of 0.662 (95% CI 0.658–0.666). With protein features alone, the set of 99 proteins achieved the highest AUC of 0.626 (95% CI 0.615–0.636). After the combination of age, *APOE* ε4, and proteins, we found that the addition of 2 proteins (see Supplementary Table 1) achieved the highest AUC of 0.674 (95% CI 0.669–0.678), which was significantly greater than the AUCs from age and *APOE* alone ($p < 0.001$; Figure 2B).

Binary t-tau burden (high: $N = 415$; low: $N = 376$) was defined by local cutoffs of CSF t-tau levels. For t-tau, 1,437 out

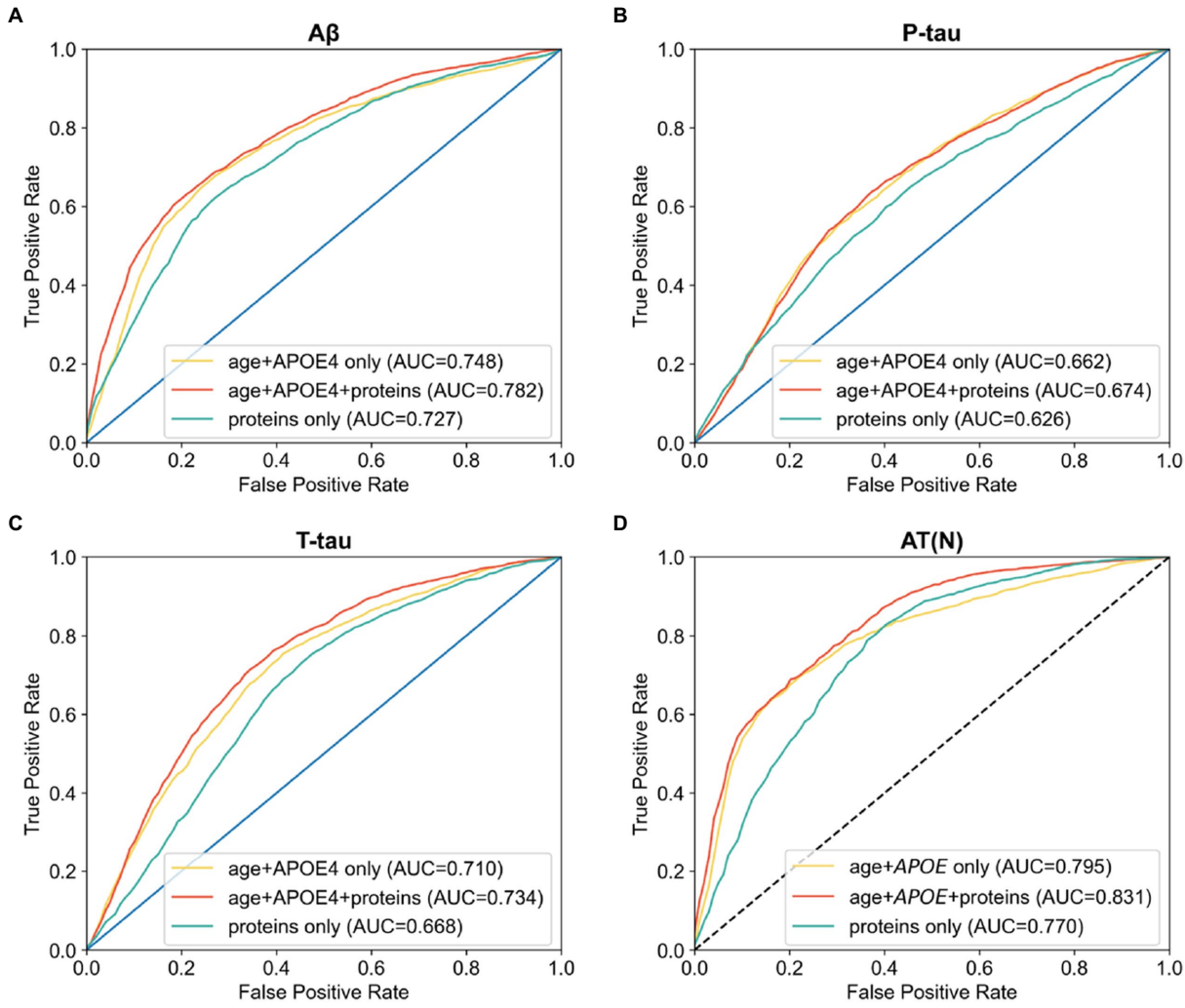

FIGURE 2
AUC ROCs of using age and *APOE* alone, age and *APOE* with proteins, and proteins alone to differentiate high vs. low **(A)** Aβ, **(B)** p-tau, **(C)** t-tau, and **(D)** combined AT(N) burden. For each target, the panel of proteins with the best performance were selected.

of all proteins reached statistical significance (uncorrected $p < 0.05$), and 1,038 of them reached the false discovery rate (corrected $p < 0.05$). Age and *APOE* ε4 together achieved an AUC of 0.710 (95% CI 0.708–0.713). With protein features alone, a panel of 33 proteins achieved the highest AUC of 0.668 (95% CI 0.660–0.675). Combining with age and *APOE* ε4, a panel of 29 proteins (see Supplementary Table 1) achieved the highest AUC of 0.734 (95% CI 0.729–0.738), significantly exceeding that of age and *APOE* alone ($p < 0.001$; Figure 2C).

Discrimination of A +T+N+ from A − T − N − using NNs

We further used proteins to differentiate subjects with extreme AT(N) profiles using NNs. High and low AT(N) levels (A + T + N+: $N = 298$; A − T − N−: $N = 229$) were defined using the cutoffs of binary Aβ, p-tau, and t-tau burden. In logistic regression analysis, 1,638 proteins reached statistical significance (uncorrected $p < 0.05$) in association with A + T + N+ and A − T − N−. 1,317 of them passed the false discovery rate (corrected $p < 0.05$). The correlations of protein p values between each pair of AD-related outcomes are listed in Supplementary Table 2.

In differentiating A + T + N+ and A − T − N−, age and *APOE* ε4 alone achieved an AUC of 0.795 (95% CI 0.793–0.798). Using the top 100 proteins as input features, we found that 86 proteins achieved the highest AUC of 0.770 (95% CI 0.765–0.774). The combination of age, *APOE* ε4, and proteins showed that a panel of 7 proteins (see Supplementary Table 1) reached the highest AUC of 0.831 (95% CI 0.827–0.835), which was significantly better than those obtained from age and *APOE* ε4 alone ($p < 0.05$; Figure 2D). All NN classification results are summarized in Table 2. NN performance scores of using from 1 to 100 top proteins with or without age and *APOE* status to classify each outcome are shown in Supplementary Figure 1.

TABLE 2 Summary of AUC scores (95% CI) of NN classification.

	Number of subjects (high/low)	Age + *APOE* only	Proteins only	Proteins + age + *APOE*
Aβ	503/378	0.748 (0.745–0.750)	0.727 (0.722–0.732)	0.782 (0.779–0.785)
P-tau	373/414	0.662 (0.658–0.666)	0.626 (0.615–0.636)	0.674 (0.669–0.678)
T-tau	415/376	0.710 (0.708–0.713)	0.668 (0.660–0.675)	0.734 (0.729–0.738)
AT(N)	298/229	0.795 (0.793–0.798)	0.770 (0.765–0.774)	0.831 (0.827–0.835)

AUC, area under the receiver operating characteristic curve; CI, confidence interval; NN, neural networks; APOE, apolipoprotein E; Aβ, amyloid-β; p-tau, phosphorylated-tau; t-tau, total tau; AT(N), amyloid/tau/neurodegeneration.

Enriched terms

Aggregately, 35 proteins were nominated for the pathway enrichment analysis. They were matched to 34 unique genes. The background list consisted of 3,306 unique proteins in UniProt identifiers, which were matched to 3,268 genes. A total of 11 pathways were identified (Table 3). They were grouped into five clusters based on their membership similarities. Each cluster was represented by its most significant pathway: human immunodeficiency virus 1 infection (uncorrected $p < 0.001$), p53 signaling pathway (uncorrected $p = 0.001$), phosphoinositide-3-kinase–protein kinase B/Akt (PI3K-Akt) signaling pathway (uncorrected $p = 0.009$), complement and coagulation cascades (uncorrected $p = 0.018$), and mitogen-activated protein kinase (MAPK) signaling pathway (uncorrected $p = 0.045$). The enriched pathways were not significant after correction for multiple comparisons (corrected $p > 0.05$). The protein–protein interaction analysis revealed three significant terms (Table 4): PI3K-Akt signaling pathway ($p < 0.001$), complement and coagulation cascades ($p < 0.001$), and proteoglycans in cancer ($p < 0.005$).

Discussion

In this study, we used regression analysis and NNs to obtain the optimal sets of protein features that discriminated high and low AT(N) burdens in AD. Age and *APOE* ε4 status alone achieved an AUC of 0.748 in predicting Aβ, an AUC of 0.662 in predicting p-tau, an AUC of 0.710 in predicting t-tau, and an AUC of 0.795 in predicting AT(N) abnormality. The addition of proteins significantly improved prediction of Aβ (AUC = 0.782), p-tau (AUC = 0.674), t-tau (AUC = 0.734) and AT(N) profiles (AUC = 0.831).

We selected the variables age and *APOE* genotype for comparison as advanced age and presence of the *APOE* ε4 allele are two of the strongest risk factors for AD (Riedel et al., 2016). In addition, our previous study confirmed that among age, sex, education, and *APOE* genotype, the combination of these two characteristics best predicts Aβ pathologies in the current cohort (Shi Y. et al., 2019). The previous study also classified amyloid burden using plasma proteomics and obtained similar results: the combination of age, *APOE* ε4 status, and proteins achieved the highest AUC score of 0.78, outperforming demographic variables alone. But as different protein ranking methods were employed, our panel of 11 proteins predicting Aβ has little overlap with the previously identified 44 proteins and provides novel candidates for validation. In the previous study, top proteins were selected through Lasso which uses a regularization technique to choose features that correlate with the outcome but not with each other, thus reducing redundant inputs. While this method can enhance prediction accuracy in an independent testing set, it may exclude proteins that have linearly redundant association with the outcome but nonlinear effects that can be detected by neural networks. As logistic regression does not penalize feature collinearity, the

TABLE 3 Pathway enrichment analysis revealed 11 significantly enriched pathways.

Term ID	Description	*P*-value (uncorrected)	*P*-value (corrected)
hsa05170	Human immunodeficiency virus 1 infection	< 0.001	0.203
hsa04218	Cellular senescence	0.009	0.641
hsa05145	Toxoplasmosis	0.015	0.754
hsa05014	Amyotrophic lateral sclerosis	0.036	1.000
hsa04115	p53 signaling pathway	0.001	0.209
hsa04114	Oocyte meiosis	0.005	0.524
hsa04151	PI3K-Akt signaling pathway	0.009	0.641
hsa05202	Transcriptional misregulation in cancer	0.013	0.747
hsa04610	Complement and coagulation cascades	0.018	0.770
hsa04936	Alcoholic liver disease	0.029	1.000
hsa04010	MAPK signaling pathway	0.045	1.000

They are grouped into five clusters based on membership similarities. PI3K-Akt, phosphoinositide-3-kinase–protein kinase B/Akt; MAPK, mitogen-activated protein kinase.

TABLE 4 Protein–protein interaction enrichment analysis revealed three significantly enriched terms.

Term ID	Description	*P*-value
hsa04151	PI3K-Akt signaling pathway	<0.001
hsa04610	Complement and coagulation cascades	<0.001
hsa05205	Proteoglycans in cancer	<0.005

PI3K-Akt, phosphoinositide-3-kinase–protein kinase B/Akt.

proteins selected using this method may retain meaningful information for neural network training. Their performance corroborates the utility of plasma proteomics in predicting Aβ pathology demonstrated in other recent studies (Ashton et al., 2019; Park et al., 2019; Westwood et al., 2020). Considering that AD is a complex disorder with mixed pathologies, we further evaluated the potential of plasma proteomics in predicting the other two components of the AT(N) framework. In accordance with previous findings (Shi et al., 2021), our results suggest that blood-based protein panels can reflect brain tau burden and neurodegeneration in addition to Aβ abnormality. Finally, a panel of proteins showed satisfactory performance in predicting combined AT(N) profiles, supporting the potential of plasma proteomics to act as comprehensive biomarkers for core AD pathologies. Interestingly, the statistical significance measures of the association between proteins and each AD-related outcomes have high correlations, suggesting that these pathological features are closely related, which is consistent with our previous finding showing that Aβ has a causal relationship with tau pathology (Shi L. et al., 2019).

We performed a pathway enrichment analysis on proteins in identified panels and found 5 clusters of pathways. One of them is the complement and coagulation cascades, which have been reported previously in a systematic review of blood-based protein biomarkers (Kiddle et al., 2014). Neuroinflammation is implicated as having substantial involvement in the pathogenesis of AD (Heneka et al., 2015). As part of the innate immune system, the complement system is activated by Aβ deposits and in turn damages the neurons *via* self-attack (McGeer and McGeer, 2002). Its activation is accompanied by an upregulation of coagulation factors (Amara et al., 2010) associated with the neurovascular damages observed in AD brain. A previous study supports the association between the peripheral activation of this pathway and AD-specific pathologies (Pillai et al., 2019). Notably, the complement protein C4 was nominated in multiple panels. A previous study has found that C4 could discriminate rapidly and slowly progressing AD (Thambisetty et al., 2010), suggesting that it might be indicative of AD severity and is a potentially promising biomarker for early stages of AD. Another significant pathway identified is the MAPK pathway, which has been recognized in the AlzPathway, a comprehensive map of pathways related to AD (Mizuno et al., 2012). In AD, activation of the serine/threonine MAPK in response to extracellular stimuli promotes neuronal apoptosis (Munoz and Ammit, 2010). C-Jun N-terminal kinases (JNK) and p38, two members of the MAPK family, are involved in the hyperphosphorylation of tau (Goedert et al., 1997; Reynolds et al., 2000). JNK is also thought to regulate the phosphorylation and degradation of amyloid precursor proteins (Muresan and Muresan, 2007; Colombo et al., 2009). Our results provide further evidence for the dysregulation of the MAPK cascade proteins in AD.

This study leveraged the advancement of ML. While traditional ML models have been predominant in previous investigation of AD biomarkers, deep NNs are expected to play a more significant role moving forward. They are capable of detecting complex nonlinear patterns in raw data and are highly sensitive to the relevance of information received (LeCun et al., 2015). Recent studies have demonstrated the superior performance of deep learning in detecting AD disease stage and predicting longitudinal progression of AD using multimodal information (Venugopalan et al., 2021; El-Sappagh et al., 2022). In agreement, our study indicates the great potential of deep learning approaches to capture the complexity of blood-based omics data and facilitate the discovery of candidate biomarkers. While the performance of NNs in this study did not exceed that of the support vector machine used in our previous study (Shi L. et al., 2019), this might result from scarcity of data as training of deep learning models typically benefits from extremely large sample sizes (Ellis and Morgan, 1999). A similar study found that the more conventional random forests outperformed deep learning models in differentiating AD from CN using plasma metabolomics and reached the same conclusion (Stamate et al., 2019). While NN behavior has been much less explored in bioinformatic data, extensive deep learning research in imaging, video, audio, and natural language processing has consistently shown that model performance increases with data size, a phenomenon now known as the scaling laws (Brown et al., 2020; Wei et al., 2022). In light of these observations, it is plausible that a similar effect would

become apparent in omics as data sizes grow orders of magnitude larger than thousands of samples still typically used in present-day studies. Model architecture should also be considered in the future development of AD biomarkers. More complex NNs can be adopted to take advantage of an increasing quantity of heterogeneous clinical and biological data. Recently, TabNet has been proposed as a NN architecture specializing in tabular data processing by applying sequential attention to select the best features at each decision step (Arık and Pfister, 2021). It would be interesting to see whether innovative models like TabNet could be applied to explore the predictive power of putative biomarkers and integrated into the biomarker development pipeline.

One limitation of the current study is that no data was withheld for validation of the effect of the nominated proteins. However, this helps minimize overfitting and optimize the generalizability of those proteins at the discovery stage. To assess their applicability in the larger population, future validation using independent cohorts is preferred. In addition, it is important to note that participants with AD were significantly older than MCI or CN participants in this study, so age and age-related changes in plasma profiles might contribute to most of the predictive accuracy. As development of AD is not always associated with age in the larger population, it is important to test the validity of candidate biomarkers among patients and controls of similar ages.

In conclusion, the opportunity of the clinical implementation of blood-based biomarkers for AD is exciting. The current study supports the use of proteomics measured by SOMAscan for the discovery blood-based biomarkers. In addition, NNs show great utility in predicting disease pathologies from proteomics which encourages the adoption of more advanced ML approaches in future investigation. Using these state-of-the-art technologies, we identified several proteins that are involved in AD-related pathways and can potentially serve as prescreening tools for the early detection of AD-specific pathologies when combined with demographic information.

Data availability statement

The data analyzed in this study is subject to the following licenses/restrictions: the dataset analyzed for this study is available upon request *via* the EMIF-AD Catalog (https://emif-catalogue.eu) after approval of the research question by all parent cohorts and the EMIF-AD team. Requests to access these datasets should be directed to EMIF-AD, https://emif-catalogue.eu.

Ethics statement

The studies involving human participants were reviewed and approved by Aristotle University of Thessaloniki Medical School Ethics Committee; Ethics Committee of the Medical Faculty Mannheim, University of Heidelberg; Ethic and Clinical Research Committee Donostia; Ethics Committee Inserm and Aix Marseille University; The Healthcare Ethics Committee of the Hospital Clínic; Central Clinical Research and Clinical Trials Unit (UICEC Sant Pau); INSERM Ethical Committee; Ethic Committee of the IRCCS San Giovanni di Dio FBF; Comitato Etico IRCCS Pascale - Napoli; Ethics Committee at Karolinska Institutet; Ethische commissie onderzoek UZ/KU Leuven; Research Ethics Committee Lausanne University Hospital; Medical Ethical Committee Maastricht University Medical Center; Committee on Health Research Ethics, Region of Denmark; Ethics Committee of Mediterranean University; University of Lille Ethics Committee; Ethical Committee at the Medical Faculty, Leipzig University; Ethical Committee at the Medical Faculty, University Hospital Essen; Ethics Committee University of Antwerp; Ethical Committee of University of Genoa; Ethics Committee, University of Gothenburg; Human Ethics Committee of the University of Perugia; and Medical Ethics Committee VU Medical Center. The patients/participants provided their written informed consent to participate in this study.

Author contributions

AN-H, LS, and YZ contributed to conception and design of the study. YZ analyzed the data, interpreted the results, and drafted and revised the manuscript. All authors contributed to the article and approved the submitted version.

Funding

This research was conducted as part of the EMIF-AD project which has received support from the Innovative Medicines Initiative Joint Undertaking under EMIF grant agreement no. 115372, resources of which are composed of financial contribution from the European Union's Seventh Framework Programme (FP7/2007–2013) and EFPIA companies' in-kind contribution. The authors declare that they have received funding from Astra Zeneca (SL) and Janssen (SL and ANH). The funders were not involved in the study design, collection, analysis, interpretation of data, the writing of this article, or the decision to submit it for publication. The DESCRIPA study was funded by the European Commission within the 5th framework program (QLRT-2001-2455). The EDAR study was funded by the European Commission within the 5th framework program (contract # 37670). The San Sebastian GAP study was partially funded by the Department of Health of the Basque Government (allocation 17.0.1.08.12.0000.2.454.01.41142.001.H). The research at VIB-CMN was funded in part by the University of Antwerp Research Fund. LS is funded by the Virtual Brain Cloud from European commission (grant no. H2020-SC1-DTH-2018-1). HZ is a Wallenberg Scholar supported by grants from the Swedish Research Council (#2018–02532), the European Research Council (#681712 and #101053962), Swedish State Support for Clinical Research (#ALFGBG-71320), the Alzheimer Drug Discovery Foundation (ADDF), United States (#201809–2016862), the AD Strategic Fund and the Alzheimer's Association (#ADSF-21-831376-C, #ADSF-21-831381-C, and #ADSF-21-831377-C), the Bluefield Project, the Olav Thon Foundation, the Erling-Persson

Family Foundation, Stiftelsen för Gamla Tjänarinnor, Hjärnfonden, Sweden (#FO2022-0270), the European Union's Horizon 2020 research and innovation programme under the Marie Skłodowska-Curie grant agreement no 860197 (MIRIADE), the European Union Joint Programme – Neurodegenerative Disease Research (JPND2021-00694), the UK Dementia Research Institute at UCL (UKDRI-1003), and the Lausanne cohort was supported by grants from the Swiss National Science Foundation (SNF 320030_141179), Synapsis Foundation – Dementia Research Switzerland (grant no. 2017-PI01). This work was supported by the Centre for Artificial Intelligence in Precision Medicines of the University of Oxford and King Abdulaziz University.

Conflict of interest

SL is named as an inventor on biomarker intellectual property protected by Proteome Sciences and Kings College London unrelated to the current study and within the past 5 years has advised for Optum labs, Merck, SomaLogic and been the recipient of funding from AstraZeneca and other companies *via* the IMI funding scheme. SL is employed by company Janssen. HZ has served at scientific advisory boards and/or as a consultant for Abbvie, Acumen, Alector, ALZPath, Annexon, Apellis, Artery Therapeutics, AZTherapies, CogRx, Denali, Eisai, Nervgen, Novo Nordisk, Passage Bio, Pinteon Therapeutics, Red Abbey Labs, reMYND, Roche, Samumed, Siemens Healthineers, Triplet Therapeutics, and Wave, has given lectures in symposia sponsored by Cellectricon, Fujirebio, Alzecure, Biogen, and Roche, and is a co-founder of Brain Biomarker Solutions in Gothenburg AB (BBS), which is a part of the GU Ventures Incubator Program, all unrelated to this study. AL has served at scientific advisory boards of Biogen, Fujirebio Europe, Eli Lilly, Grifols, Novartis, Nutricia, Roche, and Otsuka and is the inventor of a patent on synaptic markers in CSF, all unrelated to this study. JP has served at scientific advisory boards of Fujirebio Europe, Eli Lilly, and Nestlé Institute of Health Sciences, all unrelated to this study. SE has received unrestricted research grants from Janssen Pharmaceutica and ADx Neurosciences and has served at scientific advisory boards of Biogen, Eisai, Novartis, Nutricia/Danone, and Roche, all unrelated to this study.

The remaining authors declare that the research was conducted in the absence of any commercial or financial relationships that could be construed as a potential conflict of interest.

Publisher's note

All claims expressed in this article are solely those of the authors and do not necessarily represent those of their affiliated organizations, or those of the publisher, the editors and the reviewers. Any product that may be evaluated in this article, or claim that may be made by its manufacturer, is not guaranteed or endorsed by the publisher.

Supplementary material

The Supplementary material for this article can be found online at: https://www.frontiersin.org/articles/10.3389/fnagi.2022.1040001/full#supplementary-material

References

Amara, U., Flierl, M. A., Rittirsch, D., Klos, A., Chen, H., Acker, B., et al. (2010). Molecular intercommunication between the complement and coagulation systems. *J. Immunol.* 185, 5628–5636. doi: 10.4049/jimmunol.0903678

Apostolova, L. G. (2016). Alzheimer disease. *Continuum* 22, 419–434. doi: 10.1212/CON.0000000000000307

Arık, S. O., and Pfister, T. (2021). Tabnet: Attentive interpretable tabular learning. arXiv [Preprint]. 35, 6679–6687.

Ashton, N. J., Nevado-Holgado, A. J., Barber, I. S., Lynham, S., Gupta, V., Chatterjee, P., et al. (2019). A plasma protein classifier for predicting amyloid burden for preclinical Alzheimer's disease. Science. *Advances* 5:eaau7220. doi: 10.1126/sciadv.aau7220

Ashton, N. J., Pascoal, T. A., Karikari, T. K., Benedet, A. L., Lantero-Rodriguez, J., Brinkmalm, G., et al. (2021). Plasma p-tau231: a new biomarker for incipient Alzheimer's disease pathology. *Acta Neuropathol.* 141, 709–724. doi: 10.1007/s00401-021-02275-6

Beltrán, J. F., Wahba, B. M., Hose, N., Shasha, D., and Kline, R. P.For the Alzheimer's Disease Neuroimaging Initiative (2020). Inexpensive, non-invasive biomarkers predict Alzheimer transition using machine learning analysis of the Alzheimer's disease neuroimaging (ADNI) database. *PLoS One* 15:e0235663. doi: 10.1371/journal.pone.0235663

Bos, I., Vos, S., Vandenberghe, R., Scheltens, P., Engelborghs, S., Frisoni, G., et al. (2018). The EMIF-AD multimodal biomarker discovery study: design, methods and cohort characteristics. *Alzheimers Res. Ther.* 10:64. doi: 10.1186/s13195-018-0396-5

Brown, T., Mann, B., Ryder, N., Subbiah, M., Kaplan, J. D., Dhariwal, P., et al. (2020). Language models are few-shot learners. *Adv. Neural Inf. Proces. Syst.* 33, 1877–1901. doi: 10.48550/arXiv.2005.14165

Colombo, A., Bastone, A., Ploia, C., Sclip, A., Salmona, M., Forloni, G., et al. (2009). JNK regulates APP cleavage and degradation in a model of Alzheimer's disease. *Neurobiol. Dis.* 33, 518–525. doi: 10.1016/j.nbd.2008.12.014

Curtis, C., Gamez, J. E., Singh, U., Sadowsky, C. H., Villena, T., Sabbagh, M. N., et al. (2015). Phase 3 trial of flutemetamol labeled with radioactive fluorine 18 imaging and neuritic plaque density. *JAMA Neurol.* 72, 287–294. doi: 10.1001/jamaneurol.2014.4144

de Almeida, S. M., Shumaker, S. D., LeBlanc, S. K., Delaney, P., Marquie-Beck, J., Ueland, S., et al. (2011). Incidence of post-dural puncture headache in research volunteers. *Headache* 51, 1503–1510. doi: 10.1111/j.1526-4610.2011.01959.x

Dey, K. K., Wang, H., Niu, M., Bai, B., Wang, X., Li, Y., et al. (2019). Deep undepleted human serum proteome profiling toward biomarker discovery for Alzheimer's disease. *Clin. Proteomics* 16:16. doi: 10.1186/s12014-019-9237-1

Durstewitz, D., Koppe, G., and Meyer-Lindenberg, A. (2019). Deep neural networks in psychiatry. *Mol. Psychiatry* 24, 1583–1598. doi: 10.1038/s41380-019-0365-9

Ellis, D., and Morgan, N. (1999). Size matters: an empirical study of neural network training for large vocabulary continuous speech recognition. *IEEE*, 1013–1016. doi: 10.1109/ICASSP.1999.759875

El-Sappagh, S., Saleh, H., Ali, F., Amer, E., and Abuhmed, T. (2022). Two-stage deep learning model for Alzheimer's disease detection and prediction of the mild cognitive impairment time. *Neural Comput. Applic.* 34, 14487–14509. doi: 10.1007/s00521-022-07263-9

Goedert, M., Hasegawa, M., Jakes, R., Lawler, S., Cuenda, A., and Cohen, P. (1997). Phosphorylation of microtubule-associated protein tau by stress-activated protein kinases. *FEBS Lett.* 409, 57–62. doi: 10.1016/S0014-5793(97)00483-3

Gold, L., Ayers, D., Bertino, J., Bock, C., Bock, A., Brody, E., et al. (2010). Aptamer-based multiplexed proteomic technology for biomarker discovery. *Nat. Prec.* 5, e15004–e15004. doi: 10.1038/npre.2010.4538.1

Goudey, B., Fung, B. J., Schieber, C., Faux, N. G., Weiner, M. W., Aisen, P., et al. (2019). A blood-based signature of cerebrospinal fluid Aβ1–42 status. *Sci. Rep.* 9:4163. doi: 10.1038/s41598-018-37149-7

Heneka, M. T., Carson, M. J., Khoury, J. E., Landreth, G. E., Brosseron, F., Feinstein, D. L., et al. (2015). Neuroinflammation in Alzheimer's disease. *Lancet Neurol.* 14, 388–405. doi: 10.1016/S1474-4422(15)70016-5

Hye, A., Lynham, S., Thambisetty, M., Causevic, M., Campbell, J., Byers, H. L., et al. (2006). Proteome-based plasma biomarkers for Alzheimer's disease. *Brain* 129, 3042–3050. doi: 10.1093/brain/awl279

Jack, C. R., Knopman, D. S., Jagust, W. J., Petersen, R. C., Weiner, M. W., Aisen, P. S., et al. (2013). Tracking pathophysiological processes in Alzheimer's disease: an updated hypothetical model of dynamic biomarkers. *Lancet Neurol.* 12, 207–216. doi: 10.1016/S1474-4422(12)70291-0

Jiang, Y., Zhou, X., Ip, F. C., Chan, P., Chen, Y., Lai, N. C., et al. (2022). Large-scale plasma proteomic profiling identifies a high-performance biomarker panel for Alzheimer's disease screening and staging. *Alzheimers Dement.* 18, 88–102. doi: 10.1002/alz.12369

Karaglani, M., Gourlia, K., Tsamardinos, I., and Chatzaki, E. (2020). Accurate blood-based diagnostic biosignatures for Alzheimer's disease via automated machine learning. *J. Clin. Med.* 9:1036. doi: 10.3390/jcm9093016

Kiddle, S. J., Sattlecker, M., Proitsi, P., Simmons, A., Westman, E., Bazenet, C., et al. (2014). Candidate blood proteome markers of Alzheimer's disease onset and pogression: a systematic review and replication study. *J. Alzheimers Dis.* 38, 515–531. doi: 10.3233/JAD-130380

LeCun, Y., Bengio, Y., and Hinton, G. (2015). Deep learning. *Nature* 521, 436–444. doi: 10.1038/nature14539

Li, Z., Jiang, X., Wang, Y., and Kim, Y. (2021). Applied machine learning in Alzheimer's disease research: omics, imaging, and clinical data. *Emerg. Topics Life Sci.* 5, 765–777. doi: 10.1042/ETLS20210249

Lin, C.-H., Chiu, S.-I., Chen, T.-F., Jang, J.-S. R., and Chiu, M.-J. (2020). Classifications of neurodegenerative disorders using a multiplex blood biomarkers-based machine learning model. *Int. J. Mol. Sci.* 21:6914. doi: 10.3390/ijms21186914

Lopez, M. F., Mikulskis, A., Kuzdzal, S., Bennett, D. A., Kelly, J., Golenko, E., et al. (2005). High-resolution serum proteomic profiling of Alzheimer disease samples reveals disease-specific, carrier-protein–bound mass signatures. *Clin. Chem.* 51, 1946–1954. doi: 10.1373/clinchem.2005.053090

McGeer, P. L., and McGeer, E. G. (2002). The possible role of complement activation in Alzheimer disease. *Trends Mol. Med.* 8, 519–523. doi: 10.1016/S1471-4914(02)02422-X

Milà-Alomà, M., Ashton, N. J., Shekari, M., Salvadó, G., Ortiz-Romero, P., Montoliu-Gaya, L., et al. (2022). Plasma p-tau231 and p-tau217 as state markers of amyloid-β pathology in preclinical Alzheimer's disease. *Nat. Med.* 28, 1797–1801. doi: 10.1038/s41591-022-01925-w

Mizuno, S., Iijima, R., Ogishima, S., Kikuchi, M., Matsuoka, Y., Ghosh, S., et al. (2012). AlzPathway: a comprehensive map of signaling pathways of Alzheimer's disease. *BMC Syst. Biol.* 6:52. doi: 10.1186/1752-0509-6-52

Munoz, L., and Ammit, A. J. (2010). Targeting p38 MAPK pathway for the treatment of Alzheimer's disease. *Neuropharmacology* 58, 561–568. doi: 10.1016/j.neuropharm.2009.11.010

Muresan, Z., and Muresan, V. (2007). The amyloid-β precursor protein is phosphorylated via distinct pathways during differentiation, mitosis, stress, and degeneration. *Mol. Biol. Cell* 18, 3835–3844. doi: 10.1091/mbc.e06-07-0625

O'Bryant, S. E., Edwards, M., Johnson, L., Hall, J., Villarreal, A. E., Britton, G. B., et al. (2016). A blood screening test for Alzheimer's disease. *Alzheimers Dement.* 3, 83–90. doi: 10.1016/j.dadm.2016.06.004

Palmqvist, S., Zetterberg, H., Mattsson, N., Johansson, P., For the Alzheimer's Disease Neuroimaging InitiativeMinthon, L., et al. (2015). Detailed comparison of amyloid PET and CSF biomarkers for identifying early Alzheimer disease. *Neurology* 85, 1240–1249. doi: 10.1212/WNL.0000000000001991

Park, J.-C., Han, S.-H., Lee, H., Jeong, H., Byun, M. S., Bae, J., et al. (2019). Prognostic plasma protein panel for Aβ deposition in the brain in Alzheimer's disease. *Prog. Neurobiol.* 183:101690. doi: 10.1016/j.pneurobio.2019.101690

Pérez-Grijalba, V., Arbizu, J., Romero, J., Prieto, E., Pesini, P., Sarasa, L., et al. (2019). Plasma Aβ42/40 ratio alone or combined with FDG-PET can accurately predict amyloid-PET positivity: a cross-sectional analysis from the AB255 study. *Alzheimers Res. Ther.* 11:96. doi: 10.1186/s13195-019-0549-1

Pillai, J. A., Maxwell, S., Bena, J., Bekris, L. M., Rao, S. M., Chance, M., et al. (2019). Key inflammatory pathway activations in the MCI stage of Alzheimer's disease. *Ann. Clin. Transl. Neurol.* 6, 1248–1262. doi: 10.1002/acn3.50827

Ray, S., Britschgi, M., Herbert, C., Takeda-Uchimura, Y., Boxer, A., Blennow, K., et al. (2007). Classification and prediction of clinical Alzheimer's diagnosis based on plasma signaling proteins. *Nat. Med.* 13, 1359–1362. doi: 10.1038/nm1653

Reynolds, C. H., Betts, J. C., Blackstock, W. P., Nebreda, A. R., and Anderton, B. H. (2000). Phosphorylation sites on tau identified by nanoelectrospray mass spectrometry: differences in vitro between the mitogen-activated protein kinases ERK2, c-Jun N-terminal kinase and P38, and glycogen synthase kinase-3β. *J. Neurochem.* 74, 1587–1595. doi: 10.1046/j.1471-4159.2000.0741587.x

Riedel, B. C., Thompson, P. M., and Brinton, R. D. (2016). Age, APOE and sex: triad of risk of Alzheimer's disease. *J. Steroid Biochem. Mol. Biol.* 160, 134–147. doi: 10.1016/j.jsbmb.2016.03.012

Sattlecker, M., Kiddle, S. J., Newhouse, S., Proitsi, P., Nelson, S., Williams, S., et al. (2014). Alzheimer's disease biomarker discovery using SOMAscan multiplexed protein technology. *Alzheimers Dement.* 10, 724–734. doi: 10.1016/j.jalz.2013.09.016

Shi, Y., Lu, X., Zhang, L., Shu, H., Gu, L., Wang, Z., et al. (2019). Potential value of plasma amyloid-β, total tau, and neurofilament light for identification of early Alzheimer's disease. *ACS Chem. Neurosci.* 10, 3479–3485. doi: 10.1021/acschemneuro.9b00095

Shi, L., Westwood, S., Baird, A. L., Winchester, L., Dobricic, V., Kilpert, F., et al. (2019). Discovery and validation of plasma proteomic biomarkers relating to brain amyloid burden by SOMAscan assay. *Alzheimers Dement.* 15, 1478–1488. doi: 10.1016/j.jalz.2019.06.4951

Shi, L., Winchester, L. M., Westwood, S., Baird, A. L., Anand, S. N., Buckley, N. J., et al. (2021). Replication study of plasma proteins relating to Alzheimer's pathology. *Alzheimers Dement.* 17, 1452–1464. doi: 10.1002/alz.12322

Stamate, D., Kim, M., Proitsi, P., Westwood, S., Baird, A., Nevado-Holgado, A., et al. (2019). A metabolite-based machine learning approach to diagnose Alzheimer-type dementia in blood: results from the European medical information framework for Alzheimer disease biomarker discovery cohort. *Alzheimers Dement.* 5, 933–938. doi: 10.1016/j.trci.2019.11.001

Strozyk, D., Blennow, K., White, L. R., and Launer, L. J. (2003). CSF Aβ 42 levels correlate with amyloid-neuropathology in a population-based autopsy study. *Neurology* 60, 652–656. doi: 10.1212/01.WNL.0000046581.81650.D0

Thambisetty, M., Simmons, A., Velayudhan, L., Hye, A., Campbell, J., Zhang, Y., et al. (2010). Association of plasma clusterin concentration with severity, pathology, and progression in Alzheimer disease. *Arch. Gen. Psychiatry* 67, 739–748. doi: 10.1001/archgenpsychiatry.2010.78

Venugopalan, J., Tong, L., Hassanzadeh, H. R., and Wang, M. D. (2021). Multimodal deep learning models for early detection of Alzheimer's disease stage. *Sci. Rep.* 11:3254. doi: 10.1038/s41598-020-74399-w

Voyle, N., Baker, D., Burnham, S. C., Covin, A., Zhang, Z., Sangurdekar, D. P., et al. (2015). Blood protein markers of neocortical amyloid-β burden: a candidate study using SOMAscan technology. *J. Alzheimers Dis.* 46, 947–961. doi: 10.3233/JAD-150020

Wei, J., Tay, Y., Bommasani, R., Raffel, C., Zoph, B., Borgeaud, S., et al. (2022). Emergent abilities of large language models. arXiv: 2206.07682 [Preprint].

Westwood, S., Baird, A. L., Anand, S. N., Nevado-Holgado, A. J., Kormilitzin, A., Shi, L., et al. (2020). Validation of plasma proteomic biomarkers relating to brain amyloid burden in the EMIF-Alzheimer's disease multimodal biomarker discovery cohort. *J. Alzheimers Dis.* 74, 213–225. doi: 10.3233/JAD-190434

Whelan, C. D., Mattsson, N., Nagle, M. W., Vijayaraghavan, S., Hyde, C., Janelidze, S., et al. (2019). Multiplex proteomics identifies novel CSF and plasma biomarkers of early Alzheimer's disease. *Acta Neuropathol. Commun.* 7:169. doi: 10.1186/s40478-019-0795-2

Zhao, X., Kang, J., Svetnik, V., Warden, D., Wilcock, G., David Smith, A., et al. (2020). A machine learning approach to identify a circulating microRNA signature for Alzheimer disease. *J. Appl. Lab. Med.* 5, 15–28. doi: 10.1373/jalm.2019.029595

Zhou, Y., Zhou, B., Pache, L., Chang, M., Khodabakhshi, A. H., Tanaseichuk, O., et al. (2019). Metascape provides a biologist-oriented resource for the analysis of systems-level datasets. *Nat. Commun.* 10, 1–10. doi: 10.1038/s41467-019-09234-6

frontiers | Frontiers in Cellular Neuroscience

TYPE Original Research
PUBLISHED 01 December 2022
DOI 10.3389/fncel.2022.1069617

OPEN ACCESS

EDITED BY
Suman Dutta,
University of California, Los Angeles, United States

REVIEWED BY
Marion Hogg,
Nottingham Trent University, United Kingdom
Savina Apolloni,
University of Rome Tor Vergata, Italy

*CORRESPONDENCE
Yansu Guo
gys188@163.com

SPECIALTY SECTION
This article was submitted to Cellular Neuropathology, a section of the journal Frontiers in Cellular Neuroscience

RECEIVED 14 October 2022
ACCEPTED 15 November 2022
PUBLISHED 01 December 2022

CITATION
Zhang Y, Chen L, Li Z, Li D, Wu Y and Guo Y (2022) Endothelin-1, over-expressed in SOD1^{G93A} mice, aggravates injury of NSC34-hSOD1G93A cells through complicated molecular mechanism revealed by quantitative proteomics analysis.
Front. Cell. Neurosci. 16:1069617.
doi: 10.3389/fncel.2022.1069617

Endothelin-1, over-expressed in SOD1^{G93A} mice, aggravates injury of NSC34-hSOD1G93A cells through complicated molecular mechanism revealed by quantitative proteomics analysis

Yingzhen Zhang[1], Lin Chen[1], Zhongzhong Li[1], Dongxiao Li[1], Yue Wu[1] and Yansu Guo[1,2,3]*

[1]Department of Neurology, The Second Hospital of Hebei Medical University, Shijiazhuang, China, [2]Beijing Geriatric Healthcare Center, Xuanwu Hospital, Capital Medical University, Beijing, China, [3]Beijing Municipal Geriatric Medical Research Center, Beijing, China

Endothelin-1 (ET-1), a secreted signaling peptide, is suggested to be involved in multiple actions in various tissues including the brain, but its role in amyotrophic lateral sclerosis (ALS) remains unknown. In this study, we detected the expression changes as well as the cellular localization of ET-1, endothelin A (ET-A) and endothelin B (ET-B) receptors in spinal cord of transgenic SOD1-G93A (TgSOD1-G93A) mice, which showed that the two ET receptors (ET-Rs) expressed mainly on neurons and decreased as the disease progressed especially ET-B, while ET-1 expression was up-regulated and primarily localized on astrocytes. We then explored the possible mechanisms underlying the effect of ET-1 on cultured NSC34-hSOD1G93A cell model. ET-1 showed toxic effect on motor neurons (MNs), which can be rescued by the selective ET-A receptor antagonist BQ-123 or ET-B receptor antagonist BQ-788, suggesting that clinically used ET-Rs pan-antagonist could be a potential strategy for ALS. Using proteomic analysis, we revealed that 110 proteins were differentially expressed in NSC34-hSOD1G93A cells after ET-1 treatment, of which 54 were up-regulated and 56 were down-regulated. Bioinformatic analysis showed that the differentially expressed proteins (DEPs) were primarily enriched in hippo signaling pathway-multiple species, ABC transporters, ErbB signaling pathway and so on. These results provide further insights on the potential roles of ET-1 in ALS and present a new promising therapeutic target to protect MNs of ALS.

KEYWORDS

amyotrophic lateral sclerosis, TgSOD1-G93A, NSC34-hSOD1G93A cells, ET-1, ET-A, ET-B, proteomics, bioinfomatic analysis

Introduction

Amyotrophic lateral sclerosis (ALS) is a neurodegenerative disease featured with selective loss of motor neurons (MNs). The symptoms often manifest at first in distal muscles of a single limb and then spread throughout the body, which ultimately cause total paralysis (Maniatis et al., 2019; Masrori and Van, 2020). Although plenty of studies have been performed until now, the mechanisms through which it becomes pervasive, and the processes that initiate ALS pathology remain unclear. Transgenic mice overexpressing the G93A mutation in human SOD1 (hSOD1G93A) (Gurney et al., 1994) was widely used, which can recapitulate the typical phenotype of ALS patients (Beqollari et al., 2016). NSC34 cells transfected with hSOD1G93A (NSC34-hSOD1G93A cells) (Cashman et al., 1992) were also put to use for the reason that they can show decreased viability, lowered proliferation rate, mitochondrial dysfunction, and greater vulnerability to oxidation-induced cell death (Gomes et al., 2008). The above two models are classic for ALS studies.

Endothelin (ET) is a vasoactive peptide, consisting of three secreted ET peptide ligands (ET-1, ET-2 and ET-3). The three isoforms are 21-amino acid cyclic peptides which all contain an N-terminal that determines the affinity for their receptor and a C-terminal which mediates the receptor binding itself (Khimji and Rockey, 2010). Multiple functions of ET were postulated, especially the function of ET-1 in nervous system. For example, ET-1 plays roles in neurotransmission and induces excitation of neurons in the spinal cord and trigeminal system. In addition, ET-1 is implicated in many central nervous system (CNS) pathologies that involve reactive gliosis (Koyama, 2013; Jain et al., 2022). ET-1 can produce biological actions by acting on two types of receptors (ET-A and ET-B) (Arai et al., 1993; Haryono et al., 2022). In brain, high concentrations of ET-1 are generated by neurons, astrocytes and other glial cells and involved in neuronal proliferation, survival, and differentiation (Marola et al., 2022; Ranjan and Gulati, 2022). Meanwhile, both ET-A and ET-B receptors are implicated regulators of homeostatic conditions in the CNS, which adjust the sympathetic nervous system and cerebral blood flow (CBF) (Vidovic et al., 2008). Stimulation of different ET-1 receptors confers different pathogenetic functions, including the increase of free radical generation and subsequent mitochondrial dysfunction (Aliev, 2011), enhancing cerebral perfusion and behavioral results in rats suffered from traumatic brain insult (Kreipke et al., 2011) or resulting in activation of astrocytes proliferation, hypertrophy and cytoskeletal reorganization, eventually astrogliosis (Rogers et al., 2003).

ET-1 was involved in neurologic diseases including Alzheimer's disease (AD) and multiple sclerosis (MS). Tam et al. (2019) identified that overexpression of astrocytic ET-1 reinforced memory deficits in aged mice or in $APP^{K670/M671}$ mutant mice and induced cofilin rod formation thus producing toxic effects similar to Aβ on neurons. Meanwhile, ET-1-upregulated astrocytes exhibited amyloid secretion after hypoxic/ischemic injury through phosphoinositide 3-kinase (PI3K)/serine/threonine kinase (Akt)-dependent way, revealing the negative role of ET-1 (Hung et al., 2015). ET-1 released from such astrocytes may reach smooth muscle cells of the cerebral microvasculature and reduce cerebrospinal fluid (CBF). The presence of white matter lesions in AD was indeed associated with significantly reduced CBF compared to AD patients without these lesions. Compared to the age-match controls, increased ET-1 was detected in the frontal, temporal and occipital lobes of the post-mortem brain of AD patients with a more significant influence marked in the neurons, reactive astrocytes and cerebral vessel walls (Palmer et al., 2012). Similar to AD, the increasing ET-1 can explain why patients with MS have a reduced CBF in both white and gray matter. Treatment with the mixed ET receptor antagonist bosentan in MS patients restored CBF to levels found in controls. The possible source of this ET-1 production are reactive astrocytes in focal MS lesions that express high levels of ET-1, however, resting astrocytes in human brain visually do not exhibit ET-1 immunoreactivity (D'haeseleer et al., 2013). Besides, ET-1 signals indirectly inhibited oligodendrocyte progenitor cells (OPC) differentiation and remyelination through ET-B receptor in MS injury model (Hammond et al., 2014, 2015).

Recently, Ranno et al. (2014) found that expression of ET-1 was increased in the spinal cord reactive astrocytes of ALS mice and sporadic ALS patients, and its toxic effect was proved on cultured motor neurons through a series of *in vitro* experiments (Ranno et al., 2014). In addition, microarray analysis of fibroblasts from familial ALS patients with C9orf72p mutations identified ET-1 as one of the core genes in the protein-protein interaction network (Kotni et al., 2016). However, the exact mechanism of ET-1 is still unknown and there is a great interest in studying the physiological localization and pathological changes of ET-1 related signaling elements as well as its underlying molecular pathways in ALS.

In this study, we investigated the expression changes of ET-1/ET-Rs in the SOD1-G93A mouse model of ALS. Additionally, the effects of ET-1 on NSC34-hSOD1G93A cells were also assessed and potential molecular mechanism was explored using the strategy of integrated quantitative proteomics. Our findings help us better understand the detailed effect of ET-1 and give us more consideration to the possible neuroprotective strategies against ALS.

Materials and methods

Animals

Transgenic human SOD1-G93A mice and their non-transgenic (NTG) littermates were produced by breeding

female B6SJLF1 hybrids with male hemizygous carriers [B6SJL-Tg (SOD1-G93A) 1Gur/J], which were purchased from the Jackson Laboratory (Bar Harbor, ME, USA). The SOD1-G93A mouse genotyping was performed as described previously (Li et al., 2017). All animals were group-housed (4–5 mice/cage) under identical conditions (12 h light/dark cycle with free access to food and water). Since the clinical phenotype of SOD1-G93A mice, characterized by an adult onset of motor symptoms in the hind limbs, was first manifested around 12 weeks of age, and pathological changes in spinal cord begin to be observed around 60 days which progresses continuously to end stage at 17–20 weeks (Weydt et al., 2003; Ludolph et al., 2007), SOD1-G93A mice at three predefined stages were used in this study: (1) Pre-symptomatic: 40 days, postnatal, no signs of motor deficit; (2) Onset: 80 days, postnatal, initial signs of motor deficit; (3) End: animals can no longer right themselves 30 s after being placed on their backs or sides. The experiments were conducted in accordance with the regulations of laboratory animal management promulgated by the Ministry of Science and Technology of the People's Republic of China, and approved by the Ethics Committee of the Second Hospital of Hebei Medical University. All mice were narcotized under 1.0–3.0% (vol/vol) isoflurane (RWD, Shenzhen, China), and we made all efforts to minimize suffering.

Neuroblastoma/spinal cord hybrid cell line cells culture and endothelin-1 intervention

The mouse neuroblastoma/spinal cord hybrid cell line (NSC34) is a motoneuron-like cell line through the fusion of embryonic mouse spinal cord motor neurons and mouse neuroblastoma cells. NSC34 cells stably transfected with GFP-empty vector (E), GFP-human SOD1 wild type (hSOD1WT), or GFP-human SOD1G93A (hSOD1G93A) were established as previously described in our laboratory (Bai et al., 2021). The cell lines were incubated in Dulbecco's modified Eagle's medium (DMEM), including 10% heat-inactivated fetal bovine serum (FBS) and 1% penicillin streptomycin. To maintain the stable cell lines, 0.2 mg/mL Geneticin 418 sulfate (G418) was used. Cells were cultured at 37°C under a 5% CO_2 humidified atmosphere, refreshing the medium every 1–2 days. When 80–90% confluence was reached, cells were passaged using a 0.25% trypsin/EDTA solution for subsequent experiments. The cells were starved in serum-free DMEM for 24 h, and then incubated in medium containing ET-1 (1 nM, 10 nM, 100 nM, 1,000 nM) for 24 h or with a fixed 100 nM ET-1 concentration for different lengths of time (12 h, 24 h, 48 h). For rescue experiments, 100 nM ET-1 in combination with BQ123 or BQ788 was added to the cells and then incubated for 24 h.

Cell counting kit-8 assay

The measurement of cell viability was performed by a cell counting kit-8 (CCK-8) assay (BOSTER Biological Technology Co., Ltd., Wuhan, China) (Liu et al., 2014). In short, after a 24 h exposure to the respect treatment, we added 10 μL of CCK-8 solution to each well and incubated the cells at 37°C for 1 h in the dark. Then, a microplate reader was used to measure the absorbance at a wavelength of 450 nm (Tecan Spark 10 μM, Switzerland). All experiments were performed at least three times independently.

Immunohistochemistry

The SOD1-G93A mice and NTG mice at different disease stages were perfused with 0.1 M ice-cold phosphate buffered saline (PBS), followed by perfusion with 4% paraformaldehyde (PFA). The spinal cords were collected and lumbar segments (L3-5) were post-fixed in 4% PFA/PBS at 4°C for 24 h. The following day, the tissues were cryoprotected in 30% sucrose at 4°C overnight and then embedded in optimum cutting temperature (OCT) compound. The lumbar segments (L3-5) were sliced into coronal sections (25 μm thick) with a Leica cryostat (CM1850). Sections were treated with 3% hydrogen peroxide (H_2O_2) for 10 min and then washed in PBS with gentle agitation for 10 min. Afterward, the sections were permeabilized/blocked with 5% goat serum and 0.3% Triton X-100 in PBS and then co-immunostained for primary antibodies diluted in blocking solution at 4°C overnight. The primary antibodies include: rabbit anti-Endothelin-1(Abbiotec, 250633, 1:100), rabbit anti-ETA (Bioss, bs-1757R, 1:300) and rabbit anti-ETB (Abcam, ab117529, 1:500). After incubation, the tissues were washed in PBST (0.2% Tween 20 in PBS) three times, and then incubated with a corresponding biotin-conjugated secondary antibody (1:1,000). Next, after washing three times in PBS, incubating in Vectastain ABC Reagent (Vector Laboratories, Burlingame, CA, USA, PK-6100) for 40 min, color development was performed to the sections by the immPACT DAB Peroxidase Substrate Kit (Vector, SK-4105). At last, the slices were loaded onto slides and dried appropriately. The slides were soaked in anhydrous ethanol for 5 min, xylene for 10 min and finally sealed with Permount TM Mounting Medium (ZSGB-BIO, ZLI-9516). All images were photographed under an Olympus BX51 microscope equipped with a DP72 digital camera system (Olympus, Tokyo, Japan).

Immunofluorescence

For immunofluorescence, spinal cord sections (25 μm thick) were pretreated with 1% Triton X-100 in PBS for

30 min, and blocked with solution containing 5% donkey serum, 0.3% Triton X-100 and 0.2% dry milk in PBS for 30 min. The sections were then incubated with primary antibodies in blocking buffer overnight at 4°C. Primary antibodies include goat anti Iba-1 (Wako, 019-19741, 1:250), mouse anti-GFAP (Millipore, MAB360, 1:400), mouse anti-NeuN (Millipore, MAB377, 1:100), mouse anti-APC (Millipore, OP80, 1:400), rabbit anti-SOD1 (Immunoway, YT4364, 1:100), rabbit anti-cFOS (Abcam, ab222699, 1:100), rabbit anti-MAP1B (Proteintech, 21633-1-AP, 1:100), mouse anti-SMI32 (Biolegend, 801701, 1:100), rabbit anti-GFP (Life tech, G10362, 1:100), rabbit anti-Endothelin-1 (Abbiotec, 250633, 1:100), rabbit anti-ET-A (Bioss, bs-1757R, 1:300) and rabbit anti-ET-B (Abcam, ab117529, 1:500). Thereafter, the sections were washed for 30 min followed by incubation with the appropriate secondary antibody (Alexa Fluor 488, 594 or 647, Invitrogen) at room temperature for 2 h. After further rinsing in PBS for 30 min, sections were stained with mounting medium containing DAPI (VECTOR, VECTASHIELD H-1200) and sealed with nail polish.

Quantitative assessment of motor neuron labeling was performed as follows: Three representative images of the lumbar ventral horns from each tested animal were used for quantitative measurements of motor neurons. Motor neurons were defined according to the following criteria: (1) neurons were located in the anterior horn of the spinal cord and were $NeuN^+$ and (2) neurons with a diameter of 20 μm or larger had a distinct nucleolus (Manabe et al., 2003). The images from immunofluorescence staining were captured using an Olympus FV1000 confocal microscopy or Zeiss Vert. A1, German confocal microscopy. The numbers of motor neurons in the ventral horn area and quantification of fluorescence intensity were analyzed using ImageJ software (Java 8, National Institutes of Health, USA) (Jensen, 2013).

Western blotting

Total protein from frozen tissues was extracted using a protein extraction kit and phenylmethylsulfonyl fluoride protease inhibitors (Beijing Solarbio Science and Technology Co., Ltd., China). 30 μg of protein lysates from each sample were electrophoresed through a 10% or 12% SDS–PAGE and then transferred onto polyvinylidene fluoride (PVDF) membranes. The membranes were blocked with 5% non-fat milk, and, respectively incubated with primary antibodies overnight at 4°C, including rabbit anti-SOD1 (Immunoway, YT4364, 1:1,000), rabbit anti-GFP (Life tech, G10362, 1:1,000), rabbit anti-Endothelin-1 (Abbiotec, 250633, 1:300), rabbit anti-ET-A (Bioss, bs-1757R, 1:1,000), rabbit anti-ET-B (Abcam, ab117529, 1:4,000), and rabbit anti-GAPDH (Proteintech, 10494-1-AP, 1:5,000). After incubation, the membranes were washed three times (each for 10 min), and incubated with relevant fluorescence-conjugated secondary antibodies for 2 h at room temperature. Finally, the membranes were detected by an Odyssey Infrared Imaging System (LI-COR, Lincoln, NE, USA), and quantitatively analyzed by ImageJ (Java 8, National Institutes of Health,USA).

LC-MS/MS analysis

The detailed experimental methods for sample preparation before LC-MS/MS analysis can be found in **Supplementary Files**. For whole-cell proteome analysis, the tryptic peptides were loaded on an EASY-nLC1200 UPLC system (ThermoFisher Scientific). Tryptic peptides were dissolved in solvent A (0.1% formic acid, 2% acetonitrile/in water), separated with solvent B (0.1% formic acid in 90% acetonitrile) *via* a gradient from 8 to 23% (0–68 min), 23–32% (68–82 min) and climbing to 32–80% (82–86 min) then holding at 80% (86–90 min). Separation was analyzed in Orbitrap Exploris^{TM} 480 (Thermo Fisher Scientific) using a nano-electrospray ion source. The electrospray voltage applied was 2.3 kV and the full MS scan range was set from 400 to 1,200 m/z. Then, more than 25 most abundant precursors were selected for further MS/MS analyses by 20 s dynamic exclusion. The HCD fragmentation was operated at normalized collision energy (NCE) of 27%. The resolution for fragments were 15,000 in the Orbitrap and fixed first mass was set as 110 m/z. Automatic gain control (AGC) target was set at 100%, along with an intensity threshold of 2E4 and a maximum injection time of Auto.

Database search

The resulting MS/MS data were processed by Proteome Discoverer (v2.4.1.15) search engine (v.1.6.15.0). Tandem mass spectra were searched against the Mus musculus SwissProt database (20,387 entries) and concatenated with reverse decoy database. The detailed parameter settings are shown in **Supplementary Files**.

Bioinformatics analysis-protein function enrichment and cluster analysis

To further analyze hierarchical clustering based on functional classification of differentially expressed proteins (such as: GO, Domain, Pathway), all the categories obtained after enrichment along with their *P*-values were collated, and those categories that were at least enriched in one of the clusters

with $P < 0.05$ were filtered. We transformed the filtered P-value matrix by the function $\times = -\log10$ (P-value). At last, these $\times$ values were z-transformed for each functional category, and then clustered by one-way hierarchical clustering (Euclidean distance, average linkage clustering) in Genesis. A heat map with the "heatmap.2" function from the "gplots" R-package can visualize the cluster membership finally.

Parallel reaction monitoring analysis

Parallel reaction monitoring (PRM), a technique based on high-resolution and high-precision mass spectrometers (such as Q Exactive^{TM} Plus) can screen the remaining samples of LC-MS/MS proteome for further verification. The sample was slowly added to the final concentration of 20% v/v TCA to precipitate protein, then vortexed to mix and incubated for 2 h at 4°C. The precipitate was collected by centrifugation at 4,500 g for 5 min at 4°C. The precipitated protein was washed with pre-cooled acetone for 3 times and dried for 2 h. The protein sample was then redissolved in 200 mM TEAB and ultrasonically dispersed. Trypsin was added at 1:50 trypsin-to-protein mass ratio for the first digestion overnight. The sample was reduced with 5 mM dithiothreitol for 30 min at 56°C and alkylated with 11 mM iodoacetamide for 15 min at room temperature in darkness. The tryptic peptides were dissolved in 0.1% formic acid (solvent A), and were mounted to a home-made reversed-phase analytical column directly, with a gradient of 6–20% solvent B (0–40 min), then 23–35% (14 min), 20–30% (40–52 min), 30–80% (52–56 min) then 80% (56–60 min) on an EASY-nLC1000 UPLC system using the flow rate of 500 nL/min constantly. Later, risk assessment was performed in the proteins with fold change no less than 1.2 and $P < 0.05$, according to peptide hits, coverage, signal strength and number of second order maps. Risk was divided into high, medium and low risk of three gradients. After grading the peptide residues, they were ionized into the NSI ion source and then analyzed by Q ExactiveTM Plus mass spectrometry. The resulting MS data were processed using Skyline (v.21.1). Each protein in the experiment applied one, two or more unique peptides for quantitative analysis (Chai et al., 2020). Additional Methods showed the full details in **Supplementary Files**.

Statistical methods and analyses

Unpaired t-test was used to calculate significant differences between two groups and one-way ANOVA was used to assess significant differences within multiple groups. Data were analyzed by SPSS-23 software (IBM SPSS Statistics 23, USA) and GraphPad Prism software (5.0.0; GraphPad Software, USA) were applied to graphing. Statistical significance was defined as $P < 0.05$. Data were expressed as the mean ± SEM.

Results

Expression changes of endothelin-1 and ET-A/B receptors in the lumbar spinal cord of SOD1-G93A mice

To evaluate whether ET-1/ET-Rs signaling axis prompt neuron degeneration in ALS, we first observed the expression of ET-1, ET-A, and ET-B receptors in the spinal cords of SOD1-G93A mice at different disease stages using immunohistochemistry (**Figure 1**). An obvious increase of ET-1 positive cells, which were clearly glia-like cells (**Figure 1A**, arrows), was observed in the lumbar spinal cord of SOD1-G93A mice, especially at the end stage of disease. In NTG mice, ET-A receptor was observed mainly in nucleus, both neurons (**Figure 1A**, arrowheads) and glial cells (**Figure 1A**, arrows). With disease progression, ET-A-positive motor neurons reduced, while the total number of ET-A-positive nuclei increased. In addition, we found that ET-B receptor was mainly located in the cytoplasm of neurons (**Figure 1A**, arrowheads), and an obvious decrease of ET-B expression was observed with disease progression (**Figure 1A**). Consistent with morphological findings, western blotting results revealed an increase of ET-1 expression and decrease of two ET-Rs expression with disease progression (**Figure 1B**). Apparently, significant expression changes of ET-1 and ET-B receptor were observed at the end stage of SOD1-G93A mice (**Figures 1C,E**). For ET-A expression, although a decreasing trend was observed, statistically significant difference was not reached even at the end stage (**Figure 1D**). Together, above-mentioned results indicate that both glial cells and neurons play a vital role in ET-1/ET-Rs pathway thus contributing to ALS pathogenesis.

Cellular localization of endothelin-1, endothelin A and endothelin B receptors in the lumbar spinal cord of SOD1-G93A mice

To further test the cellular localization of ET-1 and ET-Rs, we then performed double immunofluorescence staining. ET-1 positive cells were mainly observed in proliferating GFAP-positive astrocytes in lumbar spinal cord of ALS mice (**Supplementary Figure 1**), which was in line with the previous opinions (D'haeseleer et al., 2013; Hostenbach et al., 2016). In normal spinal cord of NTG mice, ET-A expression was primarily located in the nucleus of neurons and glial cells, especially motor neurons. In the spinal cord of ALS mice at end stage, ET-A-positive motor neurons decreased obviously (**Figure 2A**, arrowheads). However, obvious expression of ET-A was identified in mature oligodendrocytes (APC-positive) (**Figure 2A**, arrows). Furthermore, just as reported

10.3389/fncel.2022.1069617

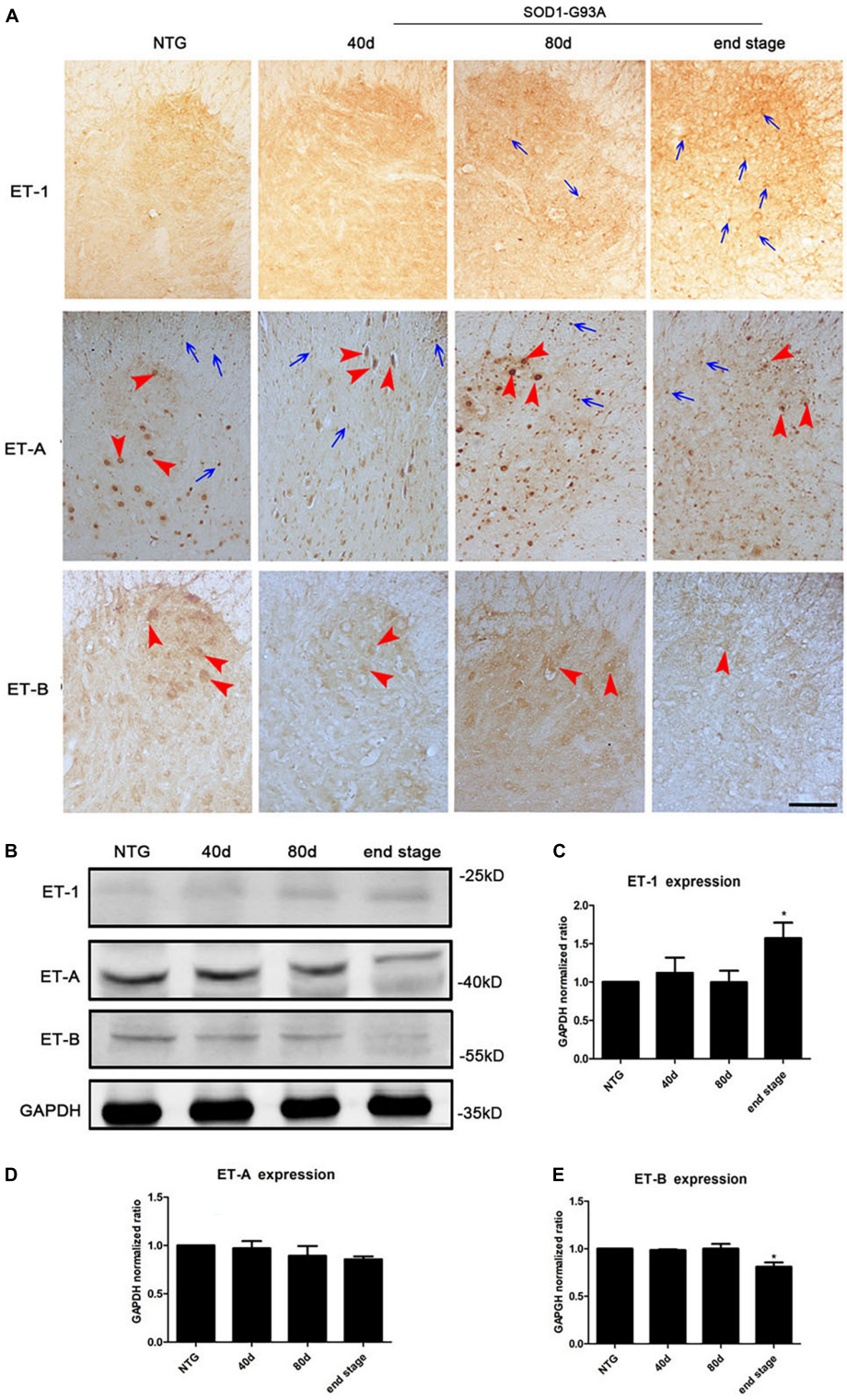

FIGURE 1
Expression changes of ET-1, ET-A, and ET-B receptors at the end stage of SOD1-G93A mice. **(A)** Immunohistochemical detection of ET-1, ET-A, and ET-B receptors in the lumbar spinal cord of non-transgenic (NTG) mice and SOD1-G93A transgenic mice at 40 days (d), 80 days (d) and end stage. **(B)** Western blot analysis of ET-1, ET-A, and ET-B receptor levels in the lumbar spinal cord of NTG mice and SOD1-G93A transgenic mice at 40d, 80d and end stage. **(C–E)** Quantitative analysis of B. Statistical significance was assessed by one-way ANOVA followed by LSD-*t* test. Data represent the mean ± SEM. *P* (ET-1, end stage vs. NTG) = 0.037; *P* (ET-A, end stage vs. NTG) = 0.159; *P* (ET-B, end stage vs. NTG) = 0.004. $n = 3$. $^*P < 0.05$. The arrows indicate glial cells, and the arrowheads indicate neurons. Bar = 100 μm.

(Ranno et al., 2014), increased ET-A expression was also notably observed on proliferating astrocytes in SOD1-G93A mice compared with NTG mice. In addition, certain ET-A positive microglia was also observed in the spinal cord of SOD1-G93A mice (**Figure 2A**, arrows).

Similarly, we detected the cellular localization of ET-B and found that ET-B was expressed primarily in the cytoplasm of motor neurons, which was in line with the previous study (Michinaga et al., 2013; **Figure 2B**, arrowheads). Sparse expression of ET-B in APC was also observed in the lumbar spinal cords of SOD1-G93A mice (**Figure 2B**, arrows). Interestingly, colocalization of ET-B with GFAP-positive astrocytes was occasionally seen in SOD1-G93A mice (**Figure 2B**, arrows) and no obvious colocalization of ET-B with Iba1-positive microglia was detected in our experiments either in SOD1-G93A mice or NTG mice (**Figure 2B**).

Since motor neurons are the main cells expressing both ET-A and ET-B receptors in the normal NTG spinal cord and they degenerate and loss with disease progression, we further ask whether the decrease in ET-A and ET-B expression reflects the general loss of motor neurons. Quantitative analysis showed that the loss of NeuN$^+$ motor neurons was parallel with the reduce of both ET-A and ET-B expressions in the spinal cord of SOD1-G93A mice at end stage (**Figures 2C–E**), which to a great extent explains that the reduce of ET-A and ET-B is largely due to the degeneration of motor neurons in SOD1-G93A mice. However, expression of ET-A and ET-B in proliferating glial cells may partly compensate this reduce.

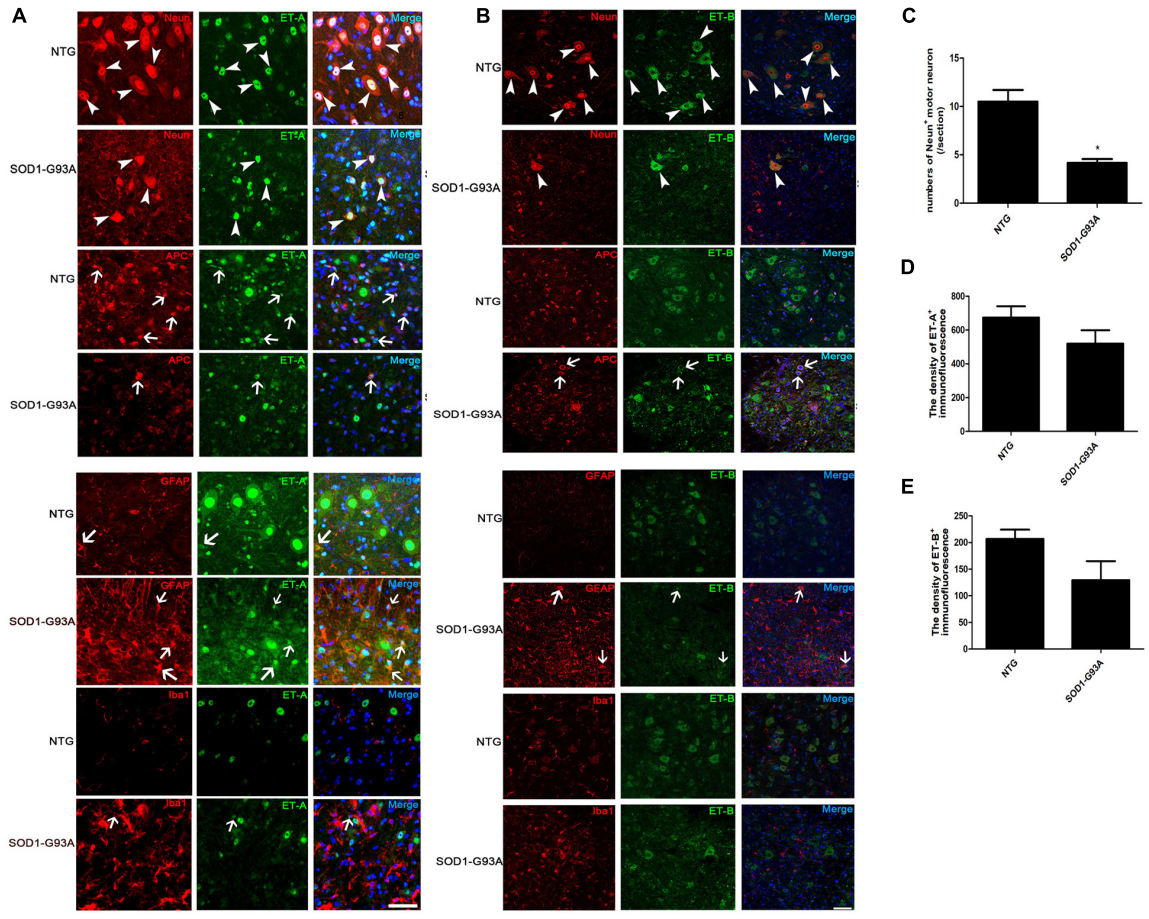

FIGURE 2
Cellular localization of ET-A and ET-B in the lumbar spinal cord of non-transgenic (NTG) mice and SOD1-G93A transgenic mice at end stage. **(A,B)** are photographed by Olympus FV1000 confocal microscopy, **(C,D)** are photographed by Zeiss Vert. A1, German confocal microscopy. **(A)** Colocalization of ET-A (green) with NeuN (red) in MNs and APC (red) in mature oligodendrocytes of NTG and SOD1-G93A mice; ET-A (green) colocalization with GFAP (red) in astrocytes and Iba1 (red) in microglia of NTG and SOD1-G93A mice. **(B)** Colocalization of ET-B (green) with NeuN (red) in MNs and APC (red) in mature oligodendrocytes of NTG and SOD1-G93A mice; ET-B (green) colocalization with GFAP (red) in astrocytes and Iba1 (red) in microglia, respectively, in the lumbar spinal cord of NTG and SOD1-G93A mice. **(C–E)** The statistical analysis of NeuN$^+$ motor neuron numbers, and the fluorescence intensity of ET-A, ET-B in the NeuN/ET-A or NeuN/ET-B co-labeled sections. Data represent the mean ± SEM, statistical significance was assessed by Unpaired *t*-test. $^*P < 0.05$. The arrows indicate glial cells, and the arrowheads indicate neurons. Bar = 50 μm.

Identification of the motor neuronal cell model of amyotrophic lateral sclerosis and its expression of ET receptors

Based on the above results, we proposed that astrocytic ET-1 might have an effect on motor neurons through ET-Rs. To assess the role of ET-1 on motor neurons, we used NSC34 cells stably expressing human SOD1, either wildtype (NSC34-hSOD1WT) or G93A mutated form (NSC34-hSOD1G93A), and NSC34 cells expressing only GFP (NSC34-E) was used as control and conducted a series of experiments (**Figure 3A**). In order to avoid interference of GFP fluorescence at channel 488, the appropriate secondary antibody (Alexa Fluor 647 or 594, Invitrogen) was used in the cell model.

First, reliability of the cell line model of ALS was confirmed. Western blotting showed that both NSC34-hSOD1 and NSC34-hSOD1G93A expressed GFP-human SOD1 (GFP-hSOD1) fusion proteins, while only GFP was observed in NSC34-E cells (**Supplementary Figure 2**). Successful transfection was further confirmed by tracing GFP-positive NSC34 cells through immunofluorescence staining for GFP and DAPI. The proportion of GFP-positive NSC34 cells is on average 61 ± 3% (NSC34-E), 66 ± 4% (NSC34-hSOD1WT), and 55 ± 9% (NSC34-hSOD1G93A) (**Supplementary Figure 2**). CCK-8 assay showed significantly lower cell viability in NSC34-hSOD1 cells, especially NSC34-hSOD1G93A cells compared with NSC34-E cells (**Figure 3B**). In addition, NSC34-hSOD1G93A cells displayed worse morphological differentiation characterized by less extending neurites which were clearly distinguishable after 24 h compared with NSC34-hSOD1WT or NSC34-E cells (**Figure 3C**).

Second, we examined the expression of MAP1B, which had been proved to influence the organization and dynamics of microtubules in growing and regenerating axons and growth cones (Vaz et al., 2015; Bora et al., 2021; Strohm et al., 2022), to evaluate the ability of differentiation of different cell lines. Even though the three cell groups extended neurites after 24 h, this characteristic was damaged in NSC34-hSODG93A cells. NSC34-E and NSC34-hSOD1WT cells revealed evident increase of neurites upon differentiation, while the neurites of NSC34-hSOD1G93A cells were not obvious (**Figure 4A**). By the concentric circle (Sholl's) analysis (Yang et al., 2016), we found that the neurite arborization of NSC34-E and NSC34-hSOD1WT cells had no significant changes while NSC34-hSODG93A cells were poorly differentiated (**Figure 4D**). The above results demonstrated that the constitutive expression of hSOD1G93A damaged the differentiate ability of NSC34 cells. Meanwhile, it was reported that cFOS can be activated after different stimuli in the CNS. For example, seizure induction caused expression changes of cFOS in the brain (Yang et al., 2019). Simultaneously, cFOS and c-jun take effect in the pathogenesis of AD, which might reflect the initiation of a cell death program in some neurons (Herrera and Robertson, 1996). Therefore, we wonder whether transfection of mutant SOD1 cause expression change of cFOS. Indeed, a remarkably high expression of cFOS was observed in NSC34-hSODG93A cells suggesting that mutant hSOD1G93A may be a kind of stimuli to cells (**Figures 4B,E**). We further investigated the expression of GFP-hSOD1 *via* immunofluorescence. Different from the uniform hSOD1 distribution in NSC34-hSOD1WT cells, dots indicating protein aggregates was observed in NSC34-hSOD1G93A cells (**Figures 4C,F**). In addition, consistent with that observed *in vivo*, double-labeling revealed that ET-A and ET-B receptors were both expressed in NSC34 cells (anti-SMI-32 labeled), but no significant expression difference of the two receptors was found among the three cell groups (**Figures 4G,H**).

Endothelin-1 is toxic for NSC34-hSOD1G93A cells in a time and concentration dependent manner and endothelin A as well as endothelin B receptors are both implicated in NSC34-hSOD1G93A cell injury

ET-1 in the brain is believed to be deeply involved in the central autonomous control and the subsequent cardiac respiratory homeostasis. It may play a role as a neuromodulator or hormone in the way of autocrine/paracrine locally, or be widely transmitted through cerebrospinal fluid (CSF). The concentration of ET-1 in CSF is higher than that in plasma. Through literature review, we have learned about the physiological, the pathological range of ET-1 in the brain, or the comparison of both (Tu et al., 2015). In a previous study, ET-1 exerted a toxic effect on the motor neuron cultures in a time- and concentration-dependent manner, with an exposure to 100–200 nM ET-1 for 48 h resulting in 40–50% cell death, which can indirectly illustrate the sensitive concentration range of neurons for ET-1 (Ranno et al., 2014). To further examine the effect of ET-1 on MNs survival in our experiment, cells were treated for different lengths of time and with different concentrations of the peptide. An exposure to 1, 10, 100, 1,000 nM ET-1 for 24 h revealed a concentration-dependent toxic effect on the three cell groups (**Figure 5A**). The CCK-8 results showed that the viability of NSC34-hSOD1G93A cells as well as NSC34-hSOD1WT cells decreased as the ET-1concentration increased, and the same ET-1 intervention caused a slight but no statistically significant decrease of cells viability in NSC34-E group. The relatively low concentrations (100 nM) which had been used frequently (Ranno et al., 2014) to study the toxic effects of ET-1 was also approximate near the median inhibitory concentration (IC50) in our experiment, therefore, 100 nM was chosen for further experiments. Furthermore, an exposure to 100 nM ET-1 for 12, 24, and 48 h revealed a time-dependent toxic effect to

10.3389/fncel.2022.1069617

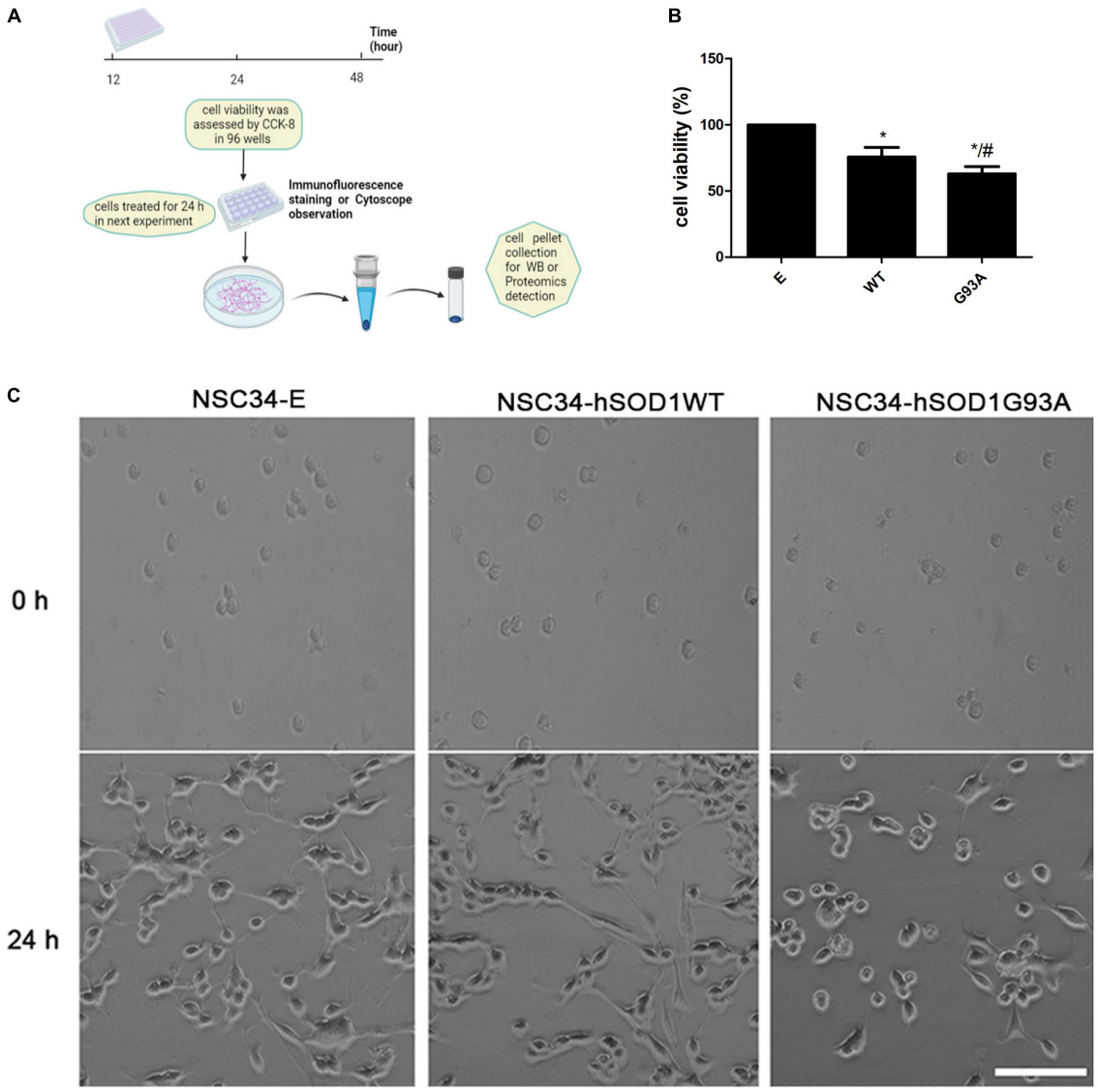

FIGURE 3
NSC34-hSODG93A cells as the *in vitro* model of ALS. **(A)** Schematic overview of cell experiments. **(B)** Cell viability of NSC34-E, NSC34-hSOD1WT and NSC34-hSOD1G93A cells. **(C)** Cells were seeded in culture dishes, differentiated for additional 24 h and photographed by phase contrast microscopy. Data represent the mean ± SEM, statistical significance was assessed by one-way ANOVA followed by LSD-*t* test. $^{*}P < 0.05$, *vs*. NSC34-E cells; $^{\#}P < 0.05$, NSC34-hSOD1WT cells *vs*. NSC34-hSOD1G93A cells. Bar = 100 μm.

MNs reaching a plateau at 24 h (Figure 5B). To validate the involvement of ET-A and ET-B in the process of MNs death, the ET-A competitive receptor antagonist BQ123 and ET-B competitive receptor antagonist BQ788 were used. A treatment of BQ123 or BQ788 together with ET-1 rescued the decrease of cell viability caused by ET-1 (Figure 5C) suggesting the involvement of ET-A and ET-B receptors. The ET-1 effect was obviously reversed by BQ123 (2 μM) and BQ788 (2 μM). Then, we asked whether ET-1 influenced the expression of ET-Rs on the cell model. Double-labeling revealed that ET-1 impaired ET-A and ET-B expression in NSC34-hSOD1G93A cells. When BQ123 or BQ788 was added, ET-Rs expression was greatly preserved (Figures 5D,E). For further quantification, western blot analysis was performed. No significant difference of ET-A or ET-B expression was observed among NSC34-E, NSC34-hSOD1WT and NSC34-hSOD1G93A cells. ET-1 treatment on NSC34-hSOD1G93A cells caused significant decrease of ET-B expression while no significant effect was reached on ET-A expression. In addition, BQ788 rescued the ET-B reduction caused by ET-1 treatment (Figures 5F–H).

The present results suggested that pathologically increased ET-1 might have a potential risk of inducing neuronal death and *via* using pharmacological approaches could potentially reverse the harmful effect. However, caution needs to be paid to further

10.3389/fncel.2022.1069617

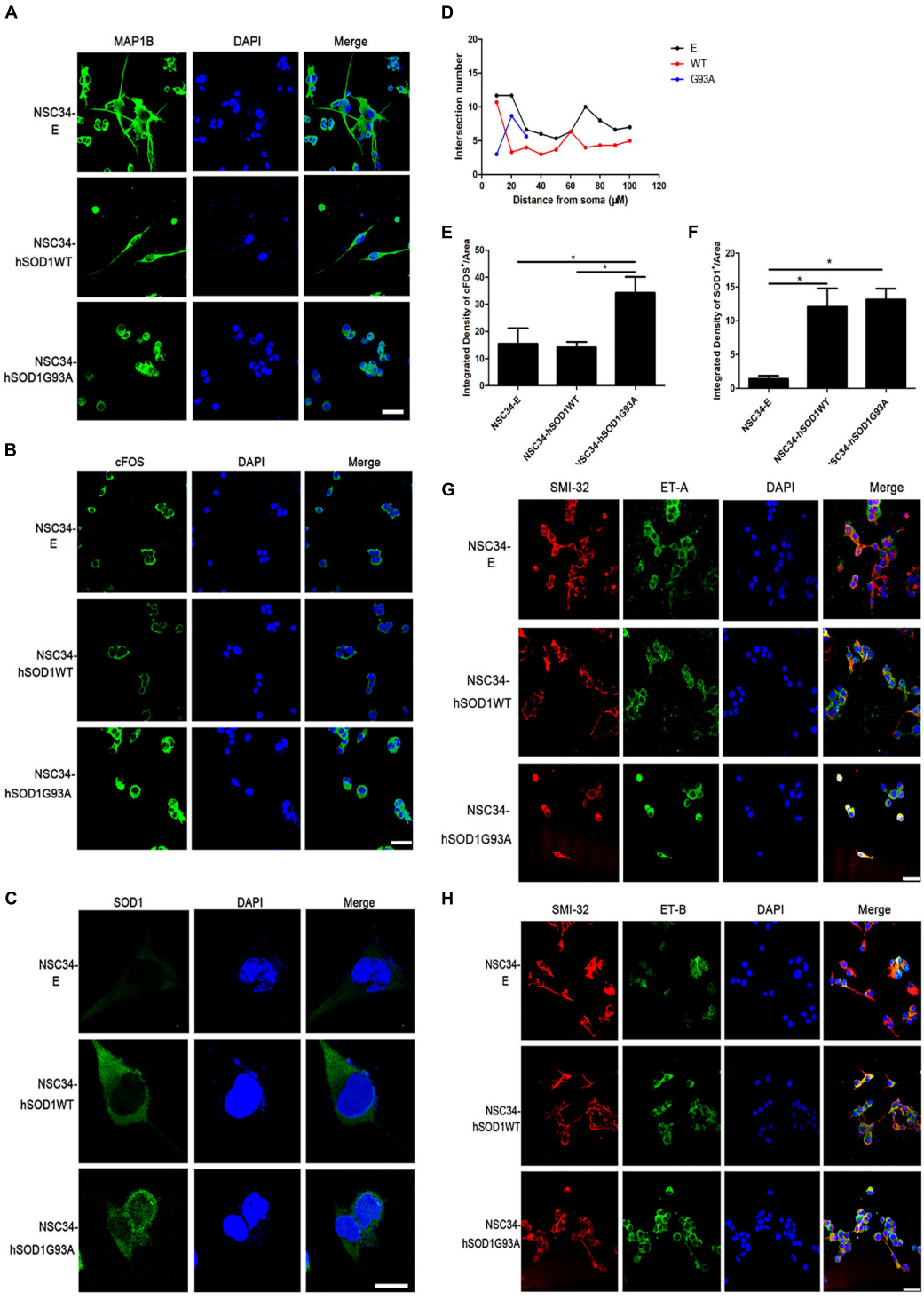

FIGURE 4
NSC34-hSOD1G93A cells display a series of injured features and ET-A and ET-B receptors are both expressed in the cell model. **(A)** Immunofluorescence labeling of MAP1B showing different neurites of the three cell groups (NSC34-E, NSC34-hSOD1WT and NSC34-hSOD1G93A). **(B)** Immunofluorescence staining indicates increased cFOS expression in NSC34-hSOD1G93A cells. **(C)** Immunofluorescence staining shows hSOD1-positive aggregates in NSC34-hSOD1G93A cells. **(D)** Quantification of neurite length from multiple fields of view was analyzed by the Sholl analysis. **(E,F)** Bar graphs showing quantification of cFOS and hSOD1 fluorescence intensities from multiple fields of view. *$P < 0.05$, a pairwise comparison marked by a horizontal line. Data represent the mean ± SEM, statistical significance was assessed by one-way ANOVA followed by LSD-*t* test. **(G,H)** Similar ET-A and ET-B expression are observed in the three cell groups. Bar = 50 μm in **(A,B,G,H)**. Bar = 20 μm in **(C)**.

10.3389/fncel.2022.1069617

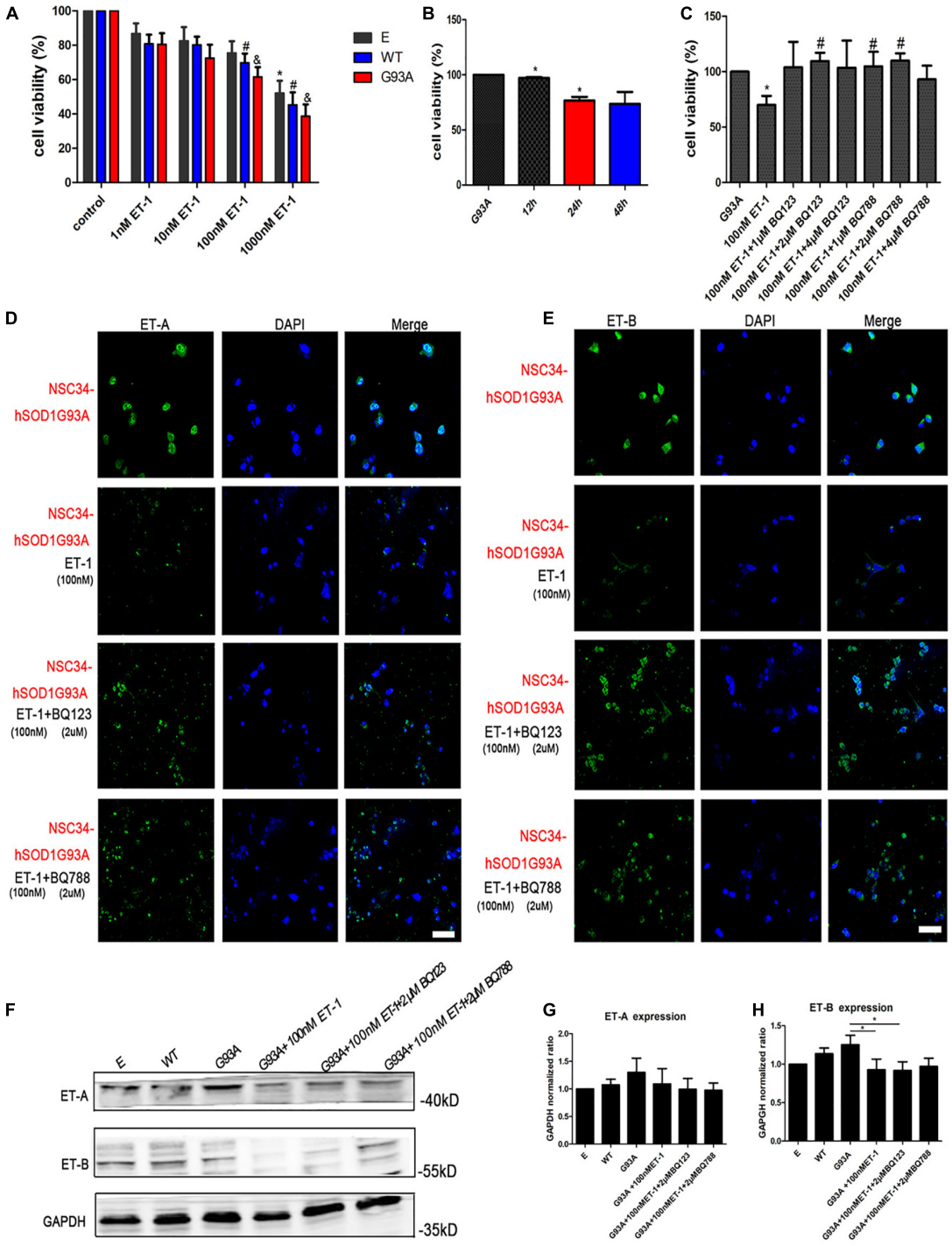

FIGURE 5
ET-1 decreased NSC34-hSOD1G93A cells viability and ET receptors were responsible for ET-1 toxicity. **(A)** Cell viability of NSC34-E, NSC34-hSOD1WT and NSC34-hSOD1G93A cells treated with ET-1 (1, 10, 100 or 1,000 nM) for 24 h. $^{*}P < 0.05$, *vs.* NSC34-E cells in control; $^{\#}P < 0.05$, *vs.* NSC34-hSOD1WT cells in control; $^{\&}P < 0.05$, *vs.* NSC34-hSOD1G93A cells in control. **(B)** Cell viability of NSC34-hSOD1G93A cells treated with 100 nM ET-1 for 12, 24, or 48 h. $^{*}P < 0.05$, *vs.* NSC34-hSOD1G93A cells. **(C)** Cell viability of NSC34-hSOD1G93A cells after 24 h treatment with ET-1 (100 nM) in the presence of BQ123 (1 μM, 2 μM, 4 μM) or BQ788 (1 μM, 2 μM, 4 μM). $^{*}P < 0.05$, *vs.* NSC34-hSOD1G93A cells; $^{\#}P < 0.05$, *vs.* NSC34-hSOD1G93A cells with 100 nM ET-1 treatment. **(D,E)** Confocal images of ET-A and ET-B expression after 24 h intervention of ET-1 (100 nM), ET-1 + BQ123 (2 μM), or ET-1 + BQ788 (2 μM). Bar = 50 μm. **(F–H)** Western blot analysis showing the expression of ET receptors in three cell groups and ET-1 effect on ET-A and ET-B expression. $^{*}P < 0.05$, a pairwise comparison marked by a horizontal line. Data represent the mean ± SEM of at least three independent experiments, statistical significance was assessed by one-way ANOVA followed by LSD-t test and Tamhane's T2 test.

investigate the changes of downstream signaling pathways and function-specificity behind ET-1/ET-Rs signaling axis.

Quantitative proteomic analysis among NSC34-hSOD1WT, NSC34-hSOD1G93A, and NSC34-hSOD1G93A cells treated with endothelin-1

To investigate the underlying pathogenesis of ET-1/ET-Rs signaling axis, we performed label-free LC-MS/MS proteomics analysis on NSC34-hSOD1WT (WT) cells, NSC34-hSOD1G93A (C) cells and NSC34-hSOD1G93A treated with 100 nM ET-1 (S) cells (**Figure 6A**). The above three groups were analyzed, and heatmap graphs of the hierarchical cluster were constructed to visualize the overall broad modulations of proteomes (**Figure 6B**). For confirmation of differentially expressed proteins (DEPs), the cutoffs for the fold change of abundance and *P*-value were set to 1.5 and 0.05, respectively. In this experiment, compared with WT cells, there were 322 up-regulated and 206 down-regulated DEPs in C cells (**Figure 6C**). 110 proteins (54 up-regulated proteins and 56 down-regulated proteins) were significantly modulated in S cells vs. C cells (**Figure 6D**). Interestingly, between the two comparable C/WT and S/C groups, 5 common up-regulated proteins (**Figure 6E**) and 2 common down-regulated proteins (**Figure 6F**) were identified. However, when the opposite tendency was analyzed, 11 common DEPs were found between the two comparable C/WT and S/C groups (**Figures 6G,H**). A total of 29 common proteins were identified in the C/WT and S/C groups and listed in the table (**Supplementary Table 1**). Subsequently, we found that some of the common proteins-ATP synthase protein 8 (Mtatp8) (**Supplementary Figure 3**), BCL2/adenovirus E1B 19 kDa protein-interacting protein 3-like (Bnip3l) (**Figure 7D**), ATP synthase-coupling factor 6, mitochondrial (Atp5pf) (**Figure 7D**), Valine-tRNA ligase, mitochondrial (Vars2) (**Supplementary Figure 3**) and Protein KIBRA (Wwc1) (**Figure 7D**) were strongly enriched in reactive oxygen species (**Figure 7D**), oxidative phosphorylation (**Supplementary Figure 3**), mitophagy-animal (**Figure 7D**), Alzheimer disease (**Figure 7D**), Parkinson disease (**Figure 7D**), Huntington disease (**Figure 7D**), Prion disease (**Figure 7D**), aminoacyl-tRNA biosynthesis (**Supplementary Figure 3**), ABC transporters (**Figure 7D**), Hippo signaling pathway (**Figure 7D**) and so on through Kyoto Encyclopedia of Genes and Genomes (KEGG) pathway analysis, which revealed that ET-1 treatment might play a role in these signaling pathways.

To investigate the associated functions of the identified DEPs in the cells model based on ALS disease, we obtained distinctive KEGG pathway and Gene Ontology (GO) terms analysis between the two comparable groups of C/WT and S/WT (**Supplementary Figure 3** and **Figure 7**). The KEGG pathway is used for analyzing the correlation among known molecular functions such as metabolic pathways, formation of complexes, and biochemical reactions (Wang et al., 2019). As it may be seen in **Supplementary Figure 3** of C/WT group, KEGG pathway analysis suggested that the up- and down-regulated DEPs were enriched in oxidative phosphorylation, reactive oxygen species, various neurodegenerative disease such as Parkinson disease and Alzheimer disease. For proteins that enriched in the S/C group, the KEGG analysis showed a strong interaction with a series of pathways related with neurodegenerative disease, such as Hippo signaling pathway-multiple species (Gogia et al., 2019), ABC transporters (Pahnke et al., 2021), oxidative phosphorylation, and ErbB signaling pathway (**Supplementary Figure 3**; Sun et al., 2020). In summary, these results suggest that ET-1 could induce a series of events in the cells model. In the part of GO enrichment analysis, C/WT group was highly enriched in extracellular region and synaptic cleft based on cellular component while S/C group was related to Gul4-RING E3 ubiquitin ligase complex and nuclear euchromatin (**Figure 7A**). In C/WT comparable group, significant changes occurred in some molecular functions like protein tyrosine kinase inhibitor activity, sphingomyelin phosphodiesterase activity while more DEPs were associated with xenobiotic transmembrane transporter activity, chromatin DNA binding and MAP kinase activity in the S/C group (**Figure 7B**). According to biological process enrichment, in C/WT group, mitochondrial membrane organization, mitochondrial transmembrane transport and organophosphate biosynthetic process were greatly enriched, while cellular response to laminar fluid shear stress, mitotic cell cycle phase transition and drug export were significantly involved in the S/C group (**Figure 7C**). KEGG pathway analysis showed that DEPs are located in important pathways such as allograft rejection and prion disease in C/WT group, however, in S/C group, DEPs were specifically enriched in Hippo signaling pathway-multiple species, ErbB signaling pathway and so on (**Figure 7D**).

Proteomic analysis revealed endothelin-1 affects neuron survival through the functions of differentially expressed proteins

The results of proteomic analysis exhibited that compared with C cells group (as positive control), there were 54 upregulated and 56 downregulated proteins after ET-1 intervention (**Figure 8A**). Gene ontology (GO) functional classification analysis showed that the DEPs in S/C comparable group mainly fell into cellular process, biological regulation, metabolic process, response to stimulus, multicellular organismal process, developmental process, localization

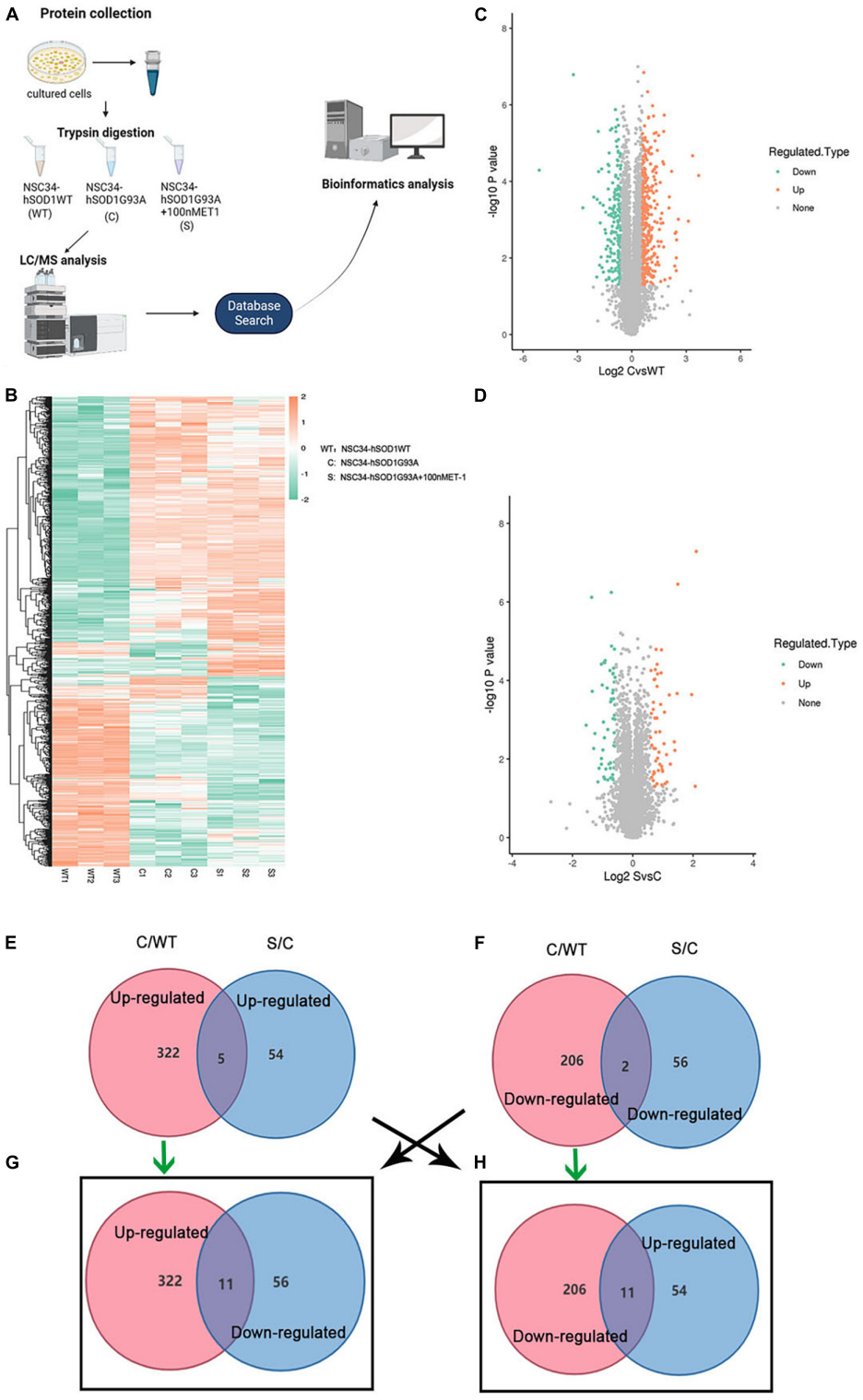

FIGURE 6
Differentially expressed proteins (DEPs) were evaluated by label-free proteomics. **(A)** Schematic diagram of experimental flow for quantitative proteomic analysis based on the ALS cells models. For each treatment, three biological replicates were prepared. **(B)** Heatmap showing DEPs in WT, C and S cells. **(C,D)** Volcano plots comparing protein abundance in WT, C and S cells. Each dot represents a single quantified protein. Proteins differentially expressed with fold change over 1.5 and $P < 0.05$ were marked in color ($n = 3$ independent biological samples). **(E–H)** Venn diagrams of enriched proteins identified in both C/WT and S/C groups. WT, NSC34-hSOD1WT cells. C, NSC34-hSOD1G93A cells. S, NSC34-hSOD1G93A cells treated with 100 nM ET-1. Pink represents the C/WT comparison group and blue represents the S/C comparison group.

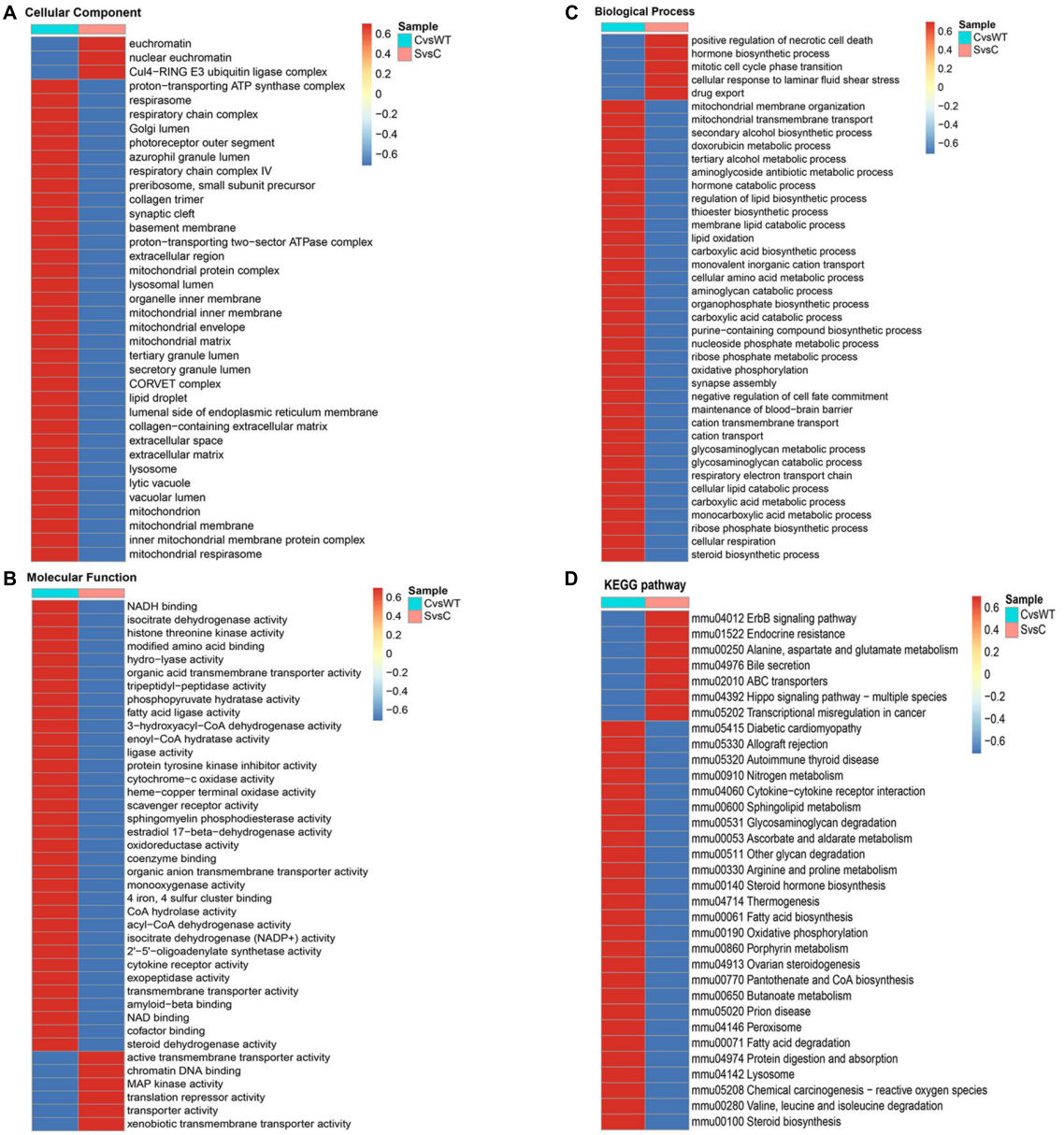

FIGURE 7
GO enrichment cluster analysis and KEGG pathways cluster analysis of differentially expressed proteins (DEPs) between C/WT and S/C group. **(A)** GO enrichment cluster analysis of DEPs based on cell component. **(B)** GO enrichment cluster analysis of DEPs based on molecular function. **(C)** GO enrichment cluster analysis of DEPs based on biological process. **(D)** KEGG pathway enrichment cluster of DEPs. WT, NSC34-hSOD1WT cells. C, NSC34-hSOD1G93A cells. S, NSC34-hSOD1G93A cells treated with 100 nM ET-1.

and other biological process (Supplementary Figure 4). The main results of the GO enrichment analysis are shown in Figures 8B–E. In particular, the DEPs based on cell components were enriched mainly in nuclear euchromatin and proton-transporting ATP synthase complex (Figure 8B). Molecular functions were enriched mainly in terms related to xenobiotic transmembrane transporter activity, MAP kinase activity, translation repressor activity and chromatin DNA binding (Figure 8C). Then, the DEPs were enriched in drug export, regulation of intestinal absorption, cellular response to laminar fluid shear stress, positive regulation of necrotic cell death, C2-steroid hormone metabolic process, hormone biosynthetic process, hippo signaling and other biological process (Figure 8D). Meanwhile, KEGG analysis showed that the DEPs were primarily enriched in Hippo signaling pathway-multiple species and ABC transporters (Figure 8E). By combining the results, we found that ET-1 significantly modulated protein metabolic process, signal transduction and

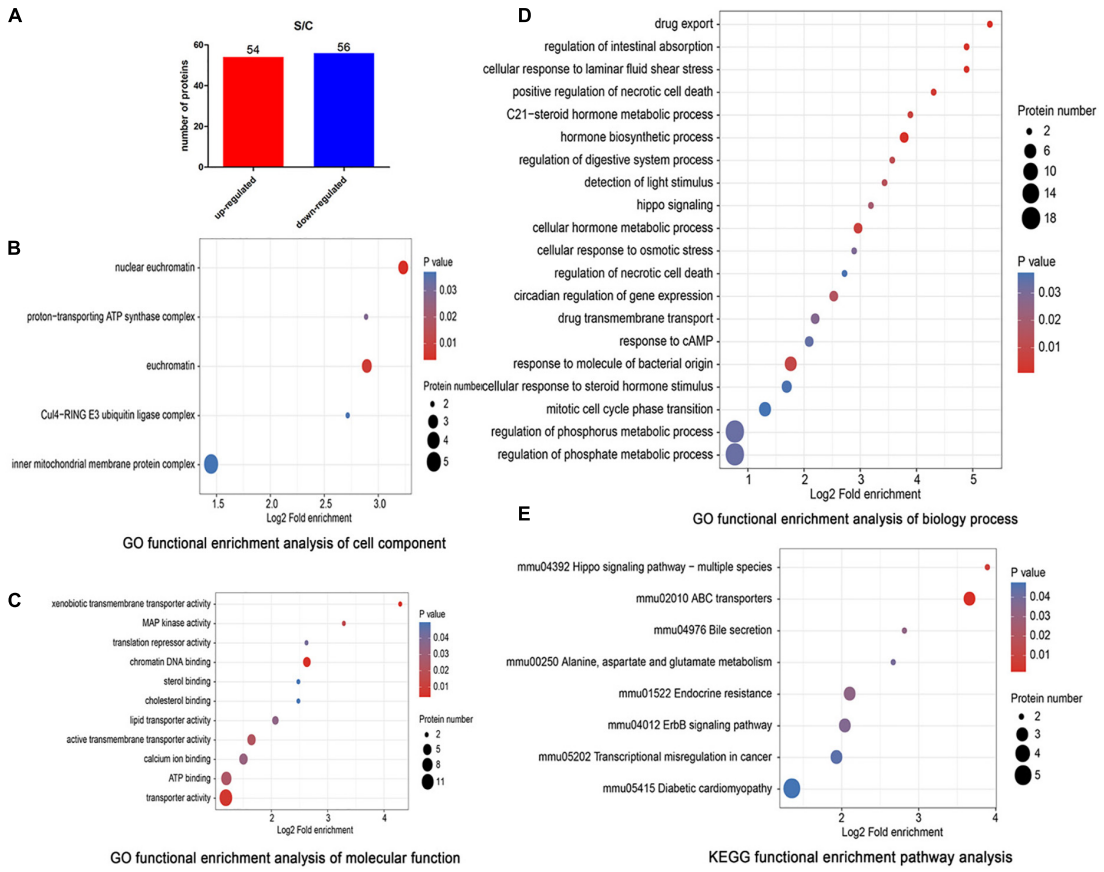

FIGURE 8
Proteomic analysis of the S/C comparable group. **(A)** In the S/C comparable group, we identified 110 DEPs, including 54 up-regulated and 56 down-regulated genes (using a 1.5-fold cutoff, $P < 0.05$). **(B)** The top 20 enriched GO terms of DEPs (fold change > 1.5) based on cellular component. **(C)** The top 20 enriched GO terms of DEPs (fold change > 1.5) based on molecular functions. **(D)** GO enrichment analysis of DEPs based on biological process (fold change > 1.5). **(E)** KEGG enrichment analysis following S/C group (fold change > 1.5). C, NSC34-hSOD1G93A cells. S, NSC34-hSOD1G93A cells treated with 100 nM ET-1.

response to stimulus. The subcellular localization analysis showed that most of the DEPs were distributed in the nucleus (27.46%, 30 proteins), cytoplasm (23.3%, 27 proteins), mitochondria (17.42%, 19 proteins), extracellular (12.88%, 14 proteins), and plasma membrane (10.98%, 12 proteins). The data revealed that except for the nucleus, the largest proportion of DEPs was located in cytoplasm, followed by mitochondria and extracellular (**Supplementary Figure 4**).

Mass spectrometry analysis of parallel reaction monitoring validation candidate peptides

To further confirm the cells proteome results related with ET-1 treatment, we performed PRM assay rather than the traditional western blot, which selected specific peptides or target peptides and then made the target protein quantified (Xu et al., 2018). According to risk assessment and limited to characteristics and abundances of 110 DEPs in the S/C comparable group, 16 target proteins were evaluated and then quantified in the experiment. At present, a total of 16 DEPs which had not previously been clearly reported to be relevant with ET-1 intervention on NSC34-hSOD1G93A cells was verified, including 9 up-regulated proteins and 7 down-regulated proteins identified in the basis of label-free quantitative analysis. The fragment ion peak of one peptide and corresponding proteins were displayed in **Supplementary Table 2**. 16 of identified proteins presented the same changing trend and the former 13 proteins that were identified significantly altered, demonstrating the consistency between PRM and LC-MS/MS proteome (**Supplementary Table 3**). These results suggested that the related effects of ET-1 on the NSC34-hSOD1G93A cells may closely connected with the functions of these proteins. Thus, ET-1 might influence kinds of signaling pathways to impose MNs damaging effects.

Among these verified differential proteins, we noticed that Cdkn1b (**Figures 9A,B**) and Eif4ebp1 (**Figure 9C**), significantly

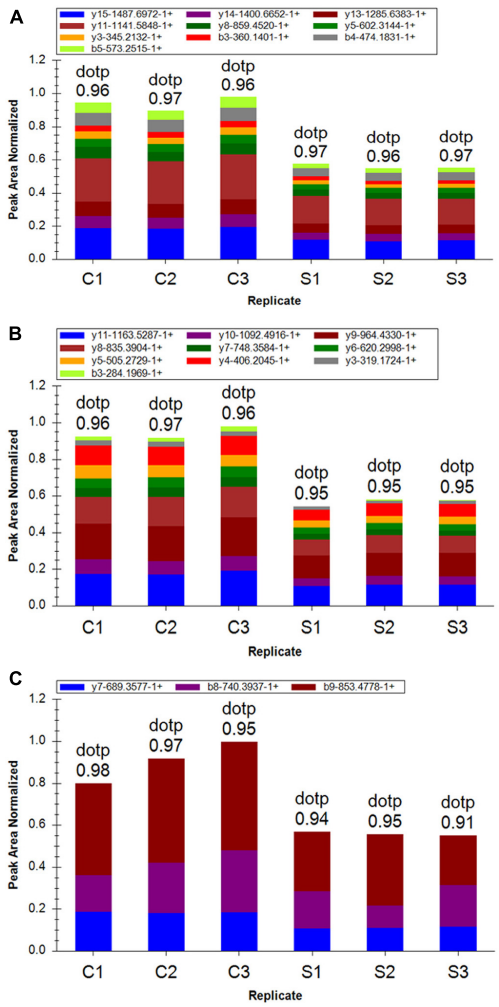

FIGURE 9
Differentially expressed proteins (DEPs) quantification by mass spectrometry-based targeted proteomics-parallel reaction monitoring (PRM). **(A)** Fragment ion peak area distribution of TEENVSDGSPNAGTVEQTPK peptide for Cdkn1b (P27). **(B)** Fragment ion peak area distribution of VLAQESQDVSGSR peptide for Cdkn1b (P27). **(C)** Verification of peptide VALGDGVQLPPGDYSTTPGGTLFSTTPGGTR targeting protein Eif4ebp1.

down-regulated when treated with ET-1, were particularly enriched in ErbB signaling pathway (pathway ID# mmu04012, **Supplementary Figure 5**). ErbB pathway dysregulation has been proposed to play a pathogenic role in ALS, especially ErbB4, a member of the epidermal growth factor (EGF) subfamily of receptor tyrosine kinases (RTKs) (Casanovas et al., 2017). These results suggest that the effects of ET-1 on NSC34-hSOD1G93A cells are closely concerned with the functions of mentioned proteins above and ET-1 can exert the related effects mainly through cell cycle and protein synthesis regulation. These proteins are anticipating targets for the study of ALS pathogenesis (**Figure 10**).

Discussion

The loss of upper and lower motor neurons in the structures such as cortex, brain stem and spinal cord, is a major contributor to the pathogenic mechanism of ALS, while neither highly effective treatments nor potent protective approaches have yet been identified (Yamanaka and Komine, 2018). In this study, we focused on exploring the location and expression of ET-1/ET-Rs on ALS mice then defining the effects of ET-1 intervention on NSC34-hSOD1G93A cells, and attempted to elucidate the mechanism of MNs injury through proteomics analysis. In general, our results showed ET-1 was mainly up-regulated in astrocytes, especially at the end stage of SOD1-G93A mice, which was in consistence with the previous study (Ranno et al., 2014). However, ET-A and ET-B receptors were mainly located in neurons and ET receptors-positive neurons were greatly reduced in end stage SOD1-G93A mice in spite of the expression of two receptors found in some kind of non-neuron cells occasionally. This provided a theoretical foundation for our following *in vitro* study on defining the effects of ET-1/ET-Rs on MNs and the expression profiles of critical proteins mediated by the exposure of ET-1.

Both ET-A and ET-B receptors were expressed on the motoneuron-like cells model, which is consistent with our *in vivo* cellular localization of ET-Rs on ALS mice model. ET-1 induced MNs death *in vitro* and the toxic effect could be partially blocked by specific antagonists BQ123 and BQ788, revealing an involvement of ET-A and ET-B receptors. Interestingly, we observed that ET-1 intervention decreased the expression of ET-A and ET-B receptors and reduced the cell viability of NSC34-hSOD1G93A cells. From these, we speculate that the increase of ET-1 expression in the spinal cords of SOD1-G93A mice may be *per se* toxic for MNs. Meanwhile, ET-1 could be an important indicator of changes in response to certain diseases and a potential candidate as a therapeutic target (Koyama et al., 2019). In this study, proteomics approach (Monti et al., 2019) was used to understand the possible molecular mechanism of ET-1 induced MNs damage in the *in vitro* ALS model. Proteins highly enriched in the S/C comparable group play a significant role in pathways such as Hippo signaling pathway-multiple species, ATP-binding cassette (ABC) transporters. According to previous studies, Hippo signaling pathways seem to be interesting therapeutic targets, which can alleviate the onset or progression of neurodegenerative diseases like ALS (Gogia et al., 2019). Hippo signaling dysregulation has also been identified in models of Alzheimer's disease and neuronal stem cells (Wu et al., 2003; Gogia et al., 2021; Xu et al., 2021). Thus, ET-1/ET-Rs/Hippo can be an interesting link in the neurodegenerative disorder like ALS. For another, one mechanism causing difficulties in remedying CNS diseases using pharmacotherapy (e.g., epilepsy and HIV-related neurological conditions) is the obstacle provided by the activity of ABC transporters in brain barrier

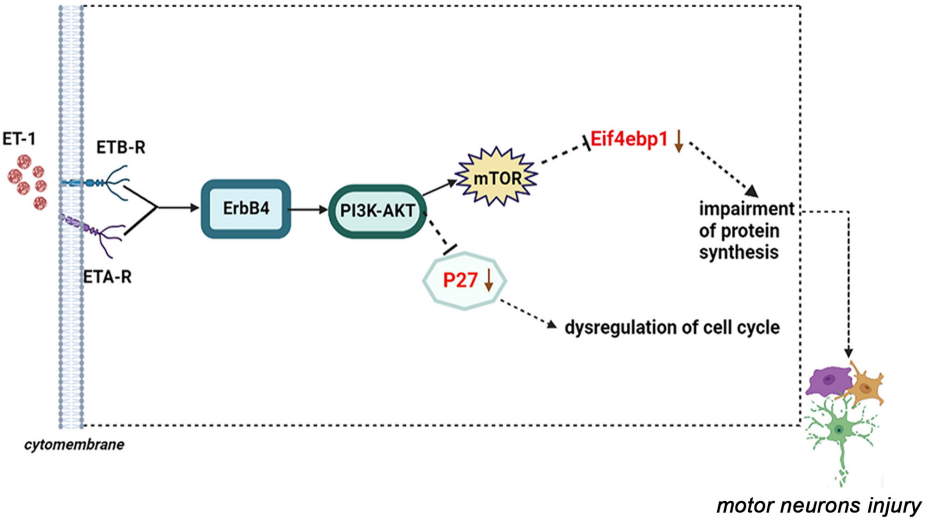

FIGURE 10
A proposed model of ET-1/ET-Rs axis interacts with the downstream molecular-P27 or Eif4ebp1 and the dysfunction of these genes may result in motor neurons injury (ErbB signaling pathway: pathway ID# mmu04012).

tissues (Eng et al., 2022). The transporters are ATP-driven efflux pumps with remarkably broad substrate specificity and are answerable for the high urine-to-plasma and bile-to-plasma concentration ratios seen for some xenobiotics (excretory function) and inhibit many xenobiotics to enter the CNS (barrier function) (Hagos et al., 2019). In light of the DEPs enriched in ABC transporters in the proteomic results of *in vitro* ALS model, understanding the alterations in ABC transporters induced by ET-1 intervention becomes increasingly relevant.

In order to validate the proteomic data, we selected several DEPs for more accurate quantitative evaluation by PRM. We found that 13 of these DEPs showed the significantly same expression tendency as that inferred through Label-free proteomics analysis. Strikingly, our results revealed that among these verified proteins, the protein expression of Eif4ebp1 and P27 was significantly down-regulated after ET-1 treatment on NSC34-hSOD1G93A cells and they were particularly enriched in ErbB signaling pathway through KEGG enrichment analysis (pathway ID# mmu04012). ErbB pathway dysregulation has been proposed to play a pathogenic role in ALS, especially one of the subtypes-ErbB4 (Sun et al., 2020). ErbB4 forms a homodimer or a heterodimer with ErbB2 or ErbB3 and is activated upon binding of neuregulins (NRGs) to the extracellular ligand-binding domain of ErbB4 (D'Antoni et al., 2017). ErbB4 could also mainly contribute to downstream signaling pathways phosphoinositide 3-kinase (PI3K)/Akt serine/threonine kinase (Akt) pathway activation (pathway ID# mmu04012), which had been tested for the possible involvement of its toxic action in ALS (Codeluppi et al., 2009). Studies suggested the existence of a causal relationship between PI3K/Akt pathway and mechanistic target of rapamycin kinase (mTOR) signaling in neurodegeneration and CNS injury. For instance, in a model of spinal cord injury, there was mTOR activation by Akt (Granatiero et al., 2021). Further, members of the PI3K family are lipid kinases participated in multiple cellular processes, such as proliferation, differentiation, migration, metabolism and survival (Li et al., 2022). Subsequently, PI3K will activate the downstream Akt to inner membranes and phosphorylates Akt on its serine/threonine kinase sites (Thr308 and Ser473). Recruited Akt participates in the downstream mTORC1 mediated response to biogenesis of protein and ribosome (Fan et al., 2018). Moreover, mTOR activation leads to the phosphorylation of Eif4ebp1/4EBP1 at Thr37/46 (Morita et al., 2015), a pivotal regulator of protein translation and cell growth (Fan et al., 2018), which simultaneously could be seen as its implication in transducing survival signals based on our proteomic results. Importantly, our results also showed PI3K/Akt signaling pathways activated cyclin-dependent kinase inhibitor $p27^{kip1}$ (Cdkn1b/P27) after ET-1 treatment on NSC34-hSOD1G93A cells, a critical determinant target for cell cycle progression, which was a vital regulation target of mitogenic signals (Muñoz et al., 2008). The alterations in P27 signaling molecules had been detectable in lymphoblasts from Alzheimer's disease (AD) patients, a kind of neurodegenerative disorders (Bartolomé et al., 2009).

From what has been discussed above, we clarify the importance of Cdkn1b (P27) and Eif4ebp1, as biomarkers for more comprehensively understanding and identifying the pathogenesis of ALS responding to ET-1 intervention. Thus, we drew a diagram of ET-1/ET-Rs axis inducing MNs damage through the ErbB4-PI3K/Akt-mTOR-Eif4ebp1 or ErbB4-PI3K/Akt-P27 pathway (**Figure 10**). By combining

our proteomic data with our preliminary observational data, the latter bioinformatics analysis provides us with a more comprehensive understanding of the mechanism of ET-1 intervention on ALS *in vitro* model, which no studies so far have addressed. In the future study, more attention should be paid to identify regulatory mechanisms of ErbB4-PI3K/Akt-mTOR-Eif4ebp1 or ErbB4-PI3K/Akt-P27 pathways and the potential role of ET-1 in the treatment of ALS.

There are several limitations of this study, requiring further examination and additional research. First, NSC34-hSOD1G93A cells model treated with ET-1 do not represent real *in vivo* ALS models. Further in-depth analysis of the ET-1 intervention effects *in vivo* models of ALS will be indispensable to prove preclinical efficacy by attenuating ET-1 induced neuronal toxicity. Second, the exact molecular pathways conducting the effect of ET-1/ET-Rs needs to be further verified.

Conclusion

ET-1/ET-Rs pathway plays a role in the pathogenesis of ALS. ET-1 induction of activated astrocytes may be toxic to ET-R-expressing motor neurons and multiple molecular mechanisms contribute to this damaging effect. Targeting ET-1 could be a potential therapeutic strategy for ALS.

Data availability statement

The datasets presented in this study can be found in online repositories. The names of the repository/repositories and accession number(s) can be found below: ProteomeXchange: PXD037555.

Ethics statement

The animal study was reviewed and approved by the Ethics Committee of the Second Hospital of Hebei Medical University.

Author contributions

YG designed the study. YZ performed the research, analyzed the data, and wrote the manuscript. LC, ZL, and YW assisted some of the experiments. DL analyzed the data and revised the manuscript. YG and YZ revised the manuscript. All authors have read and approved the final version of the manuscript.

Funding

This study was supported by funds from the National Natural Science Foundation of China, China (Grant No. 81971200) and the Beijing Municipal Natural Science Foundation, China (Grant No. 7222082).

Conflict of interest

The authors declare that the research was conducted in the absence of any commercial or financial relationships that could be construed as a potential conflict of interest.

Publisher's note

All claims expressed in this article are solely those of the authors and do not necessarily represent those of their affiliated organizations, or those of the publisher, the editors and the reviewers. Any product that may be evaluated in this article, or claim that may be made by its manufacturer, is not guaranteed or endorsed by the publisher.

Supplementary material

The Supplementary Material for this article can be found online at: https://www.frontiersin.org/articles/10.3389/fncel.2022.1069617/full#supplementary-material

References

Aliev, G. (2011). Oxidative stress induced-metabolic imbalance, mitochondrial failure, and cellular hypoperfusion as primary pathogenetic factors for the development of Alzheimer disease which can be used as an alternate and successful drug treatment strategy: Past, present and future. *CNS Neurol. Disord. Drug Targets* 10, 147–148. doi: 10.2174/187152711794480492

Arai, H., Hosoda, K., Shirakami, G., Yoshimasa, T., and Nakao, K. (1993). Nihon rinsho. *Jpn. J. Clin. Med.* 51, 1530–1539.

Bai, L., Wang, Y., Huo, J., Li, S., Wen, Y., Liu, Q., et al. (2021). Simvastatin accelerated motoneurons death in SOD1G93A mice through inhibiting Rab7-mediated maturation of late autophagic vacuoles. *Cell Death Dis.* 12:392. doi: 10.1038/s41419-021-03669-w

Bartolomé, F., Muñoz, U., Esteras, N., Esteban, J., Bermejo-Pareja, F., and Martín-Requero, A. (2009). Distinct regulation of cell cycle and survival in lymphocytes from patients with Alzheimer's disease and amyotrophic lateral sclerosis. *Int. J. Clin. Exp. Pathol.* 2, 390–398.

Beqollari, D., Romberg, C. F., Dobrowolny, G., Martini, M., Voss, A., Musarò, A., et al. (2016). Progressive impairment of CaV1.1 function in the skeletal muscle of mice expressing a mutant type 1 Cu/Zn superoxide dismutase (G93A) linked to amyotrophic lateral sclerosis. *Skelet. Muscle* 6:24. doi: 10.1186/s13395-016-0094-6

Bora, G., Hensel, N., Rademacher, S., Koyunoğlu, D., Sunguroğlu, M., Aksu-Mengeş, E., et al. (2021). Microtubule-associated protein 1B dysregulates

microtubule dynamics and neuronal mitochondrial transport in spinal muscular atrophy. *Hum. Mol. Genet.* 29, 3935–3944. doi: 10.1093/hmg/ddaa275

Casanovas, A., Salvany, S., Lahoz, V., Tarabal, O., Piedrafita, L., Sabater, R., et al. (2017). Neuregulin 1-ErbB module in C-bouton synapses on somatic motor neurons: Molecular compartmentation and response to peripheral nerve injury. *Sci. Rep.* 7:40155. doi: 10.1038/srep40155

Cashman, N. R., Durham, H. D., Blusztajn, J. K., Oda, K., Tabira, T., Shaw, I. T., et al. (1992). Neuroblastoma x spinal cord (NSC) hybrid cell lines resemble developing motor neurons. *Dev. Dyn.* 194, 209–221. doi: 10.1002/aja.10019 40306

Chai, Y. N., Qin, J., Li, Y. L., Tong, Y. L., Liu, G. H., Wang, X. R., et al. (2020). TMT proteomics analysis of intestinal tissue from patients of irritable bowel syndrome with diarrhea: Implications for multiple nutrient ingestion abnormality. *J. Proteomics* 231:103995. doi: 10.1016/j.jprot.2020.103995

Codeluppi, S., Svensson, C. I., Hefferan, M. P., Valencia, F., Silldorff, M. D., Oshiro, M., et al. (2009). The Rheb-mTOR pathway is upregulated in reactive astrocytes of the injured spinal cord. *J. Neurosci.* 29, 1093–1104. doi: 10.1523/JNEUROSCI.4103-08.2009

D'Antoni, S., Ranno, E., Spatuzza, M., Cavallaro, S., and Catania, M. V. (2017). Endothelin-1 induces degeneration of cultured motor neurons through a mechanism mediated by nitric oxide and PI3K/Akt pathway. *Neurotox. Res.* 32, 58–70. doi: 10.1007/s12640-017-9711-3

D'haeseleer, M., Beelen, R., Fierens, Y., Cambron, M., Vanbinst, A. M., Verborgh, C., et al. (2013). Cerebral hypoperfusion in multiple sclerosis is reversible and mediated by endothelin-1. *Proc. Natl. Acad. Sci. U.S.A.* 110, 5654–5658. doi: 10.1073/pnas.1222560110

Eng, M. E., Imperio, G. E., Bloise, E., and Matthews, S. G. (2022). ATP-binding cassette (ABC) drug transporters in the developing blood-brain barrier: Role in fetal brain protection. *Cell. Mol. Life Sci.* 79:415. doi: 10.1007/s00018-022-04432-w

Fan, Q. W., Nicolaides, T. P., and Weiss, W. A. (2018). Inhibiting 4EBP1 in glioblastoma. *Clin. Cancer Res.* 24, 14–21. doi: 10.1158/1078-0432.CCR-17-0042

Gogia, N., Chimata, A. V., Deshpande, P., Singh, A., and Singh, A. (2021). Hippo signaling: Bridging the gap between cancer and neurodegenerative disorders. *Neural Regen. Res.* 16, 643–652. doi: 10.4103/1673-5374.295273

Gogia, N., Sarkar, A., Mehta, A. S., Ramesh, N., Deshpande, P., Kango-Singh, M., et al. (2019). Inactivation of hippo and cJun-N-terminal Kinase (JNK) signaling mitigate FUS mediated neurodegeneration in vivo. *Neurobiol. Dis.* 140:104837. doi: 10.1016/j.nbd

Gomes, C., Palma, A. S., Almeida, R., Regalla, M., McCluskey, L. F., Trojanowski, J. Q., et al. (2008). Establishment of a cell model of ALS disease: Golgi apparatus disruption occurs independently from apoptosis. *Biotechnol. Lett.* 30, 603–610. doi: 10.1007/s10529-007-9595-z

Granatiero, V., Sayles, N. M., Savino, A. M., Konrad, C., Kharas, M. G., Kawamata, H., et al. (2021). Modulation of the IGF1R-MTOR pathway attenuates motor neuron toxicity of human ALS SOD1G93A astrocytes. *Autophagy* 17, 4029–4042. doi: 10.1080/15548627.2021.1899682

Gurney, M. E., Pu, H., Chiu, A. Y., Dal Canto, M. C., Polchow, C. Y., Alexander, D. D., et al. (1994). Motor neuron degeneration in mice that express a human Cu, Zn superoxide dismutase mutation. *Science* 264, 1772–1775. doi: 10.1126/science.8209258

Hagos, F. T., Adams, S. M., Poloyac, S. M., Kochanek, P. M., Horvat, C. M., Clark, R. S. B., et al. (2019). Membrane transporters in traumatic brain injury: Pathological, pharmacotherapeutic, and developmental implications. *Exp. Neurol.* 317, 10–21. doi: 10.1016/j.expneurol.2019.02.011

Hammond, T. R., Gadea, A., Dupree, J., Kerninon, C., Nait-Oumesmar, B., Aguirre, A., et al. (2014). Astrocyte-derived endothelin-1 inhibits remyelination through notch activation. *Neuron* 81:1442. doi: 10.1016/j.neuron.2013.11.015

Hammond, T. R., McEllin, B., Morton, P. D., Raymond, M., Dupree, J., and Gallo, V. (2015). Endothelin-B receptor activation in astrocytes regulates the rate of oligodendrocyte regeneration during remyelination. *Cell Rep.* 13, 2090–2097. doi: 10.1016/j.celrep.2015.11.002

Haryono, A., Ramadhiani, R., Ryanto, G., and Emoto, N. (2022). Endothelin and the cardiovascular system: The long journey and where we are going. *Biology* 11:759. doi: 10.3390/biology11050759

Herrera, D. G., and Robertson, H. A. (1996). Activation of c-fos in the brain. *Prog. Neurobiol.* 50, 83–107. doi: 10.1016/s0301-0082(96)00021-4

Hostenbach, S., D'haeseleer, M., Kooijman, R., and De Keyser, J. (2016). The pathophysiological role of astrocytic endothelin-1. *Prog. Neurobiol.* 144, 88–102. doi: 10.1016/j.pneurobio.2016.04.009

Hung, V. K., Yeung, P. K., Lai, A. K., Ho, M. C., Lo, A. C., Chan, K. C., et al. (2015). Selective astrocytic endothelin-1 overexpression contributes to dementia associated with ischemic stroke by exaggerating astrocyte-derived amyloid secretion. *J. Cereb. Blood Flow Metab.* 35, 1687–1696. doi: 10.1038/jcbfm.2015.109

Jain, A., Bozovicar, K., Mehrotra, V., Bratkovic, T., Johnson, M. H., and Jha, I. (2022). Investigating the specificity of endothelin-traps as a potential therapeutic tool for endothelin-1 related disorders. *World J. Diabetes* 13, 434–441. doi: 10.4239/wjd.v13.i6.434

Jensen, E. C. (2013). Quantitative analysis of histological staining and fluorescence using imageJ. *Anat. Rec.* 296, 378–381. doi: 10.1002/ar.22641

Khimji, A. K., and Rockey, D. C. (2010). Endothelin–biology and disease. *Cell. Signal.* 22, 1615–1625. doi: 10.1016/j.cellsig.2010.05.002

Kotni, M. K., Zhao, M., and Wei, D. Q. (2016). Gene expression profiles and protein-protein interaction networks in amyotrophic lateral sclerosis patients with C9orf72 mutation. *Orphanet J. Rare Dis.* 11:148. doi: 10.1186/s13023-016-0531-y

Koyama, Y. (2013). Endothelin systems in the brain: Involvement in pathophysiological responses of damaged nerve tissues. *Biomol. Concepts* 4, 335–347. doi: 10.1515/bmc-2013-0004

Koyama, Y., Sumie, S., Nakano, Y., Nagao, T., Tokumaru, S., and Michinaga, S. (2019). Endothelin-1 stimulates expression of cyclin D1 and S-phase kinase-associated protein 2 by activating the transcription factor STAT3 in cultured rat astrocytes. *J. Biol. Chem.* 294, 3920–3933. doi: 10.1074/jbc.RA118.005614

Kreipke, C. W., Rafols, J. A., Reynolds, C. A., Schafer, S., Marinica, A., Bedford, C., et al. (2011). Clazosentan, a novel endothelin A antagonist, improves cerebral blood flow and behavior after traumatic brain injury. *Neurol. Res.* 33, 208–213. doi: 10.1179/016164111X12881719352570

Li, D., Liu, C., Yang, C., Wang, D., Wu, D., Qi, Y., et al. (2017). Slow intrathecal injection of rAAVrh10 enhances its transduction of spinal cord and therapeutic efficacy in a mutant SOD1 model of ALS. *Neuroscience* 365, 192–205. doi: 10.1016/j.neuroscience.2017.10.001

Li, Z., Wang, J., Wu, J., Li, N., and Jiang, C. (2022). Long noncoding RNA LEMD1-AS1 increases LEMD1 expression and activates PI3K-AKT pathway to promote metastasis in oral squamous cell carcinoma. *Biomed. Res. Int.* 2022:3543948. doi: 10.1155/2022/3543948

Liu, Y., Duan, W., Guo, Y., Li, Z., Han, H., Zhang, S., et al. (2014). A new cellular model of pathological TDP-43: The neurotoxicity of stably expressed CTF25 of TDP-43 depends on the proteasome. *Neuroscience* 281, 88–98. doi: 10.1016/j.neuroscience.2014.09.043

Ludolph, A. C., Bendotti, C., Blaugrund, E., Hengerer, B., Löffler, J. P., Martin, J., et al. (2007). ENMC group for the establishment of guidelines for the conduct of preclinical and proof of concept studies in ALS/MND models. Guidelines for the preclinical in vivo evaluation of pharmacological active drugs for ALS/MND: Report on the 142nd ENMC international workshop. *Amyotroph. Lateral Scler.* 8, 217–223. doi: 10.1080/17482960701292837

Manabe, Y., Nagano, I., Gazi, M. S., Murakami, T., Shiote, M., Shoji, M., et al. (2003). Glial cell line-derived neurotrophic factor protein prevents motor neuron loss of transgenic model mice for amyotrophic lateral sclerosis. *Neurol. Res.* 25, 195–200. doi: 10.1179/016164103101201193

Maniatis, S., Äijö, T., Vickovic, S., Braine, C., Kang, K., Mollbrink, A., et al. (2019). Spatiotemporal dynamics of molecular pathology in amyotrophic lateral sclerosis. *Science* 364, 89–93. doi: 10.1126/science.aav9776

Marola, O. J., Howell, G. R., and Libby, R. T. (2022). Vascular derived endothelin receptor A controls endothelin-induced retinal ganglion cell death. *Cell Death Discov.* 8:207. doi: 10.1038/s41420-022-00985-8

Masrori, P., and Van, D. P. (2020). Amyotrophic lateral sclerosis: A clinical review. *Eur. J. Neurol.* 27, 1918–1929. doi: 10.1111/ene.14393

Michinaga, S., Ishida, A., Takeuchi, R., and Koyama, Y. (2013). Endothelin-1 stimulates cyclin D1 expression in rat cultured astrocytes via activation of Sp1. *Neurochem. Int.* 63, 25–34. doi: 10.1016/j.neuint.2013.04.004

Monti, C., Zilocchi, M., Colugnat, I., and Alberio, T. (2019). Proteomics turns functional. *J. Proteomics* 198, 36–44. doi: 10.1016/j.jprot.2018.12.012

Morita, M., Gravel, S. P., Hulea, L., Larsson, O., Pollak, M., St-Pierre, J., et al. (2015). mTOR coordinates protein synthesis, mitochondrial activity and proliferation. *Cell Cycle* 14, 473–480. doi: 10.4161/15384101.2014.991572

Muñoz, U., Bartolomé, F., Bermejo, F., and Martín-Requero, A. (2008). Enhanced proteasome-dependent degradation of the CDK inhibitor p27(kip1) in immortalized lymphocytes from Alzheimer's dementia patients. *Neurobiol. Aging* 29, 1474–1484. doi: 10.1016/j.neurobiolaging

Pahnke, J., Bascuñana, P., Brackhan, M., Stefan, K., Namasivayam, V., Koldamova, R., et al. (2021). Strategies to gain novel Alzheimer's disease diagnostics and therapeutics using modulators of ABCA transporters. *Free Neuropathol.* 2:33. doi: 10.17879/freeneuropathology-2021-3528

Palmer, J. C., Barker, R., Kehoe, P. G., and Love, S. (2012). Endothelin-1 is elevated in Alzheimer's disease and upregulated by amyloid-β. *J. Alzheimers Dis.* 29, 853–861. doi: 10.3233/JAD-2012-111760

Ranjan, A. K., and Gulati, A. (2022). Sovateltide mediated endothelin B receptors agonism and curbing neurological disorders. *Int. J. Mol. Sci.* 23:3146. doi: 10.3390/ijms23063146

Ranno, E., D'Antoni, S., Spatuzza, M., Berretta, A., Laureanti, F., Bonaccorso, C. M., et al. (2014). Endothelin-1 is over-expressed in amyotrophic lateral sclerosis and induces motor neuron cell death. *Neurobiol. Dis.* 65, 160–171. doi: 10.1016/j.nbd.2014.01.002

Rogers, S. D., Peters, C. M., Pomonis, J. D., Hagiwara, H., Ghilardi, J. R., and Mantyh, P. W. (2003). Endothelin B receptors are expressed by astrocytes and regulate astrocyte hypertrophy in the normal and injured CNS. *Glia* 41, 180–190. doi: 10.1002/glia.10173

Strohm, L., Hu, Z., Suk, Y., Rühmkorf, A., Sternburg, E., Gattringer, V., et al. (2022). Multi-omics profiling identifies a deregulated FUS-MAP1B axis in ALS/FTD-associated UBQLN2 mutants. *Life Sci. Alliance* 5:e202101327. doi: 10.26508/lsa.202101327

Sun, L., Cheng, B., Zhou, Y., Fan, Y., Li, W., Qiu, Q., et al. (2020). ErbB4 mutation that decreased NRG1-ErbB4 signaling involved in the pathogenesis of amyotrophic lateral sclerosis/frontotemporal dementia. *J. Alzheimers Dis.* 74, 535–544. doi: 10.3233/JAD-191230

Tam, S. W., Feng, R., Lau, W. K., Law, A. C., Yeung, P. K., and Chung, S. K. (2019). Endothelin type B receptor promotes cofilin rod formation and dendritic loss in neurons by inducing oxidative stress and cofilin activation. *J. Biol. Chem.* 294, 12495–12506. doi: 10.1074/jbc.RA118.005155

Tu, Y. F., Lin, C. H., Lee, H. T., Yan, J. J., Sze, C. I., Chou, Y., et al. (2015). Elevated cerebrospinal fluid endothelin 1 associated with neurogenic pulmonary edema in children with enterovirus 71 encephalitis. *Int. J. Infect. Dis.* 34, 105–111. doi: 10.1016/j.ijid.2015.03.017

Vaz, A. R., Cunha, C., Gomes, C., Schmucki, N., Barbosa, M., and Brites, D. (2015). Glycoursodeoxycholic acid reduces matrix metalloproteinase-9 and caspase-9 activation in a cellular model of superoxide dismutase-1 neurodegeneration. *Mol. Neurobiol.* 51, 864–877. doi: 10.1007/s12035-014-8731-8

Vidovic, M., Chen, M. M., Lu, Q. Y., Kalloniatis, K. F., Martin, B. M., Tan, A. H., et al. (2008). Deficiency in endothelin receptor B reduces proliferation of neuronal progenitors and increases apoptosis in postnatal rat cerebellum. *Cell. Mol. Neurobiol.* 28, 1129–1138. doi: 10.1007/s10571-008-9292-z

Wang, Z., Kim, U., Jiao, Y., Li, C., Guo, Y., Ma, X., et al. (2019). Quantitative proteomics combined with affinity MS revealed the molecular mechanism of ginsenoside antitumor effects. *J. Proteome Res.* 18, 2100–2108. doi: 10.1021/acs.jproteome.8b00972

Weydt, P., Hong, S. Y., Kliot, M., and Möller, T. (2003). Assessing disease onset and progression in the SOD1 mouse model of ALS. *Neuroreport* 14, 1051–1054. doi: 10.1097/01.wnr.0000073685.00308.89

Wu, S., Huang, J., Dong, J., and Pan, D. (2003). hippo encodes a Ste-20 family protein kinase that restricts cell proliferation and promotes apoptosis in conjunction with salvador and warts. *Cell* 114, 445–456. doi: 10.1016/s0092-8674(03)00549-x

Xu, X., Liu, T., Yang, J., Chen, L., Liu, B., Wang, L., et al. (2018). The first whole-cell proteome- and lysine-acetylome-based comparison between trichophyton rubrum conidial and mycelial stages. *J. Proteome Res.* 17, 1436–1451. doi: 10.1021/acs.jproteome.7b00793

Xu, X., Shen, X., Wang, J., Feng, W., Wang, M., Miao, X., et al. (2021). YAP prevents premature senescence of astrocytes and cognitive decline of Alzheimer's disease through regulating CDK6 signaling. *Aging Cell.* 20:e13465. doi: 10.1111/acel.13465

Yamanaka, K., and Komine, O. (2018). The multi-dimensional roles of astrocytes in ALS. *Neurosci. Res.* 126, 31–38. doi: 10.1016/j.neures.2017.09.011

Yang, H., Shan, W., Zhu, F., Yu, T., Fan, J., Guo, A., et al. (2019). C-Fos mapping and EEG characteristics of multiple mice brain regions in pentylenetetrazol-induced seizure mice model. *Neurol. Res.* 41, 749–761. doi: 10.1080/01616412.2019.1610839

Yang, Y., Wang, Z. H., Jin, S., Gao, D., Liu, N., Chen, S. P., et al. (2016). Opposite monosynaptic scaling of BLP-vCA1 inputs governs hopefulness-and helplessness-modulated spatial learning and memory. *Nat. Commun.* 7:11935. doi: 10.1038/ncomms11935

frontiers | Frontiers in Cellular Neuroscience

TYPE Systematic Review
PUBLISHED 24 January 2023
DOI 10.3389/fncel.2023.1044634

OPEN ACCESS

EDITED BY
Dirk M. Hermann,
University of Duisburg-Essen, Germany

REVIEWED BY
Sepideh Parsi,
Massachusetts General Hospital and Harvard Medical School, United States
Li Liu,
The First Affiliated Hospital of Xi'an Jiaotong University, China
Xiaoyong Li,
Shanghai Jiao Tong University, China

*CORRESPONDENCE
Mohammad Taheri
✉ mohammad.taheri@uni-jena.de
Soudeh Ghafouri-Fard
✉ s.ghafourifard@sbmu.ac.ir
Maryam Rezazadeh
✉ rezazadehma@tbzmed.ac.ir

SPECIALTY SECTION
This article was submitted to Cellular Neuropathology, a section of the journal Frontiers in Cellular Neuroscience

RECEIVED 14 September 2022
ACCEPTED 06 January 2023
PUBLISHED 24 January 2023

CITATION
Asadi MR, Abed S, Kouchakali G, Fattahi F, Sabaie H, Moslehian MS, Sharifi-Bonab M, Hussen BM, Taheri M, Ghafouri-Fard S and Rezazadeh M (2023) Competing endogenous RNA (ceRNA) networks in Parkinson's disease: A systematic review.
Front. Cell. Neurosci. 17:1044634.
doi: 10.3389/fncel.2023.1044634

Competing endogenous RNA (ceRNA) networks in Parkinson's disease: A systematic review

Mohammad Reza Asadi[1], Samin Abed[2], Ghazal Kouchakali[2], Fateme Fattahi[2], Hani Sabaie[1], Marziyeh Sadat Moslehian[2], Mirmohsen Sharifi-Bonab[1], Bashdar Mahmud Hussen[3,4], Mohammad Taheri[5,6]*, Soudeh Ghafouri-Fard[7]* and Maryam Rezazadeh[1,2]*

[1]Clinical Research Development Unit of Tabriz Valiasr Hospital, Tabriz University of Medical Sciences, Tabriz, Iran, [2]Department of Medical Genetics, Faculty of Medicine, Tabriz University of Medical Sciences, Tabriz, Iran, [3]Department of Biomedical Sciences, Cihan University-Erbil, Erbil, Iraq, [4]Department of Pharmacognosy, College of Pharmacy, Hawler Medical University, Erbil, Iraq, [5]Urology and Nephrology Research Center, Shahid Beheshti University of Medical Sciences, Tehran, Iran, [6]Institute of Human Genetics, Jena University Hospital, Jena, Germany, [7]Department of Medical Genetics, Shahid Beheshti University of Medical Sciences, Tehran, Iran

Parkinson's disease (PD) is a distinctive clinical syndrome with several causes and clinical manifestations. Aside from an infectious cause, PD is a rapidly developing neurological disorder with a global rise in frequency. Notably, improved knowledge of molecular pathways and the developing novel diagnostic methods may result in better therapy for PD patients. In this regard, the amount of research on ceRNA axes is rising, highlighting the importance of these axes in PD. CeRNAs are transcripts that cross-regulate one another *via* competition for shared microRNAs (miRNAs). These transcripts may be either coding RNAs (mRNAs) or non-coding RNAs (ncRNAs). This research used a systematic review to assess validated loops of ceRNA in PD. The Prisma guideline was used to conduct this systematic review, which entailed systematically examining the articles of seven databases. Out of 309 entries, forty articles met all criteria for inclusion and were summarized in the appropriate table. CeRNA axes have been described through one of the shared vital components of the axes, including lncRNAs such as NEAT1, SNHG family, HOTAIR, MALAT1, XIST, circRNAs, and lincRNAs. Understanding the multiple aspects of this regulatory structure may aid in elucidating the unknown causal causes of PD and providing innovative molecular therapeutic targets and medical fields.

KEYWORDS

Parkinson's disease, ceRNA, miRNA, lncRNA, circRNA, lincRNA, NEAT1, SNHG

1. Introduction

Parkinson's disease (PD) is a neurological disorder that affects over 6 million individuals worldwide and whose incidence is anticipated to double by 2040 (Dorsey et al., 2018a,b). It is distinguished by a core set of movement (motor) problems, including slowness of movement, muscular stiffness, and tremors, as well as a variety of non-motor symptoms, including constipation, anxiety, and dementia (Blochberger and Jones, 2011). A prodromal period of non-motor symptoms often precedes motor symptoms by several years (Sebastian et al., 2019). The main pathologic feature of PD is the presence of Lewy bodies, which are clumps of misfolded α-synuclein protein (encoded by the SNCA gene) that cause the loss of dopamine-producing neurons in the midbrain. However, the only diagnostic criteria for PD are clinical symptoms (Hughes et al., 1992; Tomlinson et al., 2010). As a result, Parkinsonism may be

regarded as a clinical condition with several aetiological paths that lead to the ultimate shared presentation of dopamine depletion and clinical Parkinsonism. There are currently no disease-modifying medications for PD and therapy is primarily focused on dopamine replacement to ameliorate symptoms. The most significant risk factor for PD development is age, and males are more vulnerable than women, with a prevalence ratio of around 3:2. Disease risk has a high hereditary component, with over 90 genetic risk loci already identified (Blauwendraat et al., 2020). Furthermore, PD often manifests sporadically; however, 15.7% of patients report an afflicted relative of the first degree (Bentley et al., 2018). Furthermore, some potentially modifiable environmental (e.g., pesticides, water pollutants) and behavioral variables (e.g., use of cigarettes, coffee, exercise, or head trauma) (Feigin and Collaborators, 2019) have been stated to have a role in the etiology of PD in various populations. While breakthroughs in etiology and epidemiology have been outstanding (Dickson et al., 2009; Poewe et al., 2017), the primary cause and fundamental mechanism of PD remain unknown, and no cure or preventative medication has yet been discovered. In this respect, focusing on the molecular mechanisms that have the potential to play a critical role in PD can be considered. The competing endogenous RNA (ceRNA) axis is one of the possible molecular mechanisms that attract much attention in PD.

CeRNAs are transcripts composed of messenger RNA (mRNAs) and non-coding RNAs (ncRNAs) that contest for shared microRNAs (miRNAs) to cross-regulate one another (Asadi et al., 2022). Franco-Zorrilla et al. reported a process known as "target mimicry," which occurs when a non-coding RNA in plants sequesters miR-399 and de-represses its target (Franco-Zorrilla et al., 2007). Ebert et al. identified a similar phenomenon in animal cells not long after. Ectopic production of a miRNA with a large number of binding sites [also known as miRNA response elements (MREs)] leads to barely visible miRNA sequestration but a 1.5–2.5-fold overexpression of the miRNA's targets in this study (Ebert et al., 2007). Consequently, the term "RNA sponge" was coined to describe the process of miRNAs being absorbed by overexpressed MRE-containing transcripts. Afterward, the RNA sponge process was discovered in various cancers (Selbach et al., 2008; Poliseno et al., 2010). In 2011, the word "ceRNA" was coined to describe this extra layer of post-transcriptional regulation, which includes mRNAs and ncRNAs (Salmena et al., 2011).

ncRNAs are classified into two types depending on their length: small ncRNAs (200 nucleotides) and long ncRNAs (>200 nucleotides) (Amin et al., 2019). MiRNAs, around 22 nucleotides long and regulating gene expression post-transcriptionally in a sequence-specific way, stand out among short ncRNAs (Singh and Storey, 2021). Approximately 70% of the known miRNAs are expressed in the brain (Cao et al., 2006), and they have been regarded as critical regulators of neuronal homeostasis, with their dysregulation linked to CNS pathology (Quinlan et al., 2017). Long ncRNAs (lncRNAs) are the most abundant ncRNAs in the mammalian genome, and they are further subdivided into linear RNAs and circular RNAs (Amin et al., 2019). Linear lncRNAs (referred to as lncRNAs) exhibit transcriptional and post-transcriptional activity comparable to protein-coding mRNA (Amin et al., 2019). However, lncRNAs have a distinct biological function from mRNAs. Furthermore, they have been linked to brain development, neuronal function, maintenance, and differentiation (Asadi et al., 2021). Circular RNAs (circRNAs) are a relatively new family of RNAs distinguished by a covalent connection that connects the 5′ and 3′ ends and offers more remarkable persistence (half-life of 48 vs. 10 h for mRNAs) (Jeck et al., 2013). CircRNAs are prevalent in the brain, are abundant in synaptoneurosomes, and are increased during neuronal development (Rybak-Wolf et al., 2015). Furthermore, despite being considered dormant gene sequences, a significant fraction of pseudogenes may be translated into ncRNAs (Pei et al., 2012; Guo et al., 2014). Indeed, there is accumulating evidence that pseudogenes might influence the expression of both parental and unrelated genes (Pei et al., 2012; Guo et al., 2014). As a result, altering pseudogene transcription might disrupt gene expression homeostasis, resulting in disease (Guo et al., 2014).

Surprisingly, all of the ncRNAs stated above can be integrated into the ceRNA axis, and these ncRNA components have been examined in the form of ceRNA networks in several studies. Because ceRNA interaction networks are multifactorial, they may help identify therapeutic targets for complex disorders like PD. By targeting only one of them, numerous disease-related RNA levels simultaneously alter (Moreno-García et al., 2020). In this work, we conducted a systematic review to investigate the possibility of verified ceRNA loops in PD. Our research focused on the ceRNA axis, which has been linked to PD pathogenesis and might be used as a therapeutic target.

2. Methods

2.1. Search strategy

The present systematic review was carried out in accordance with the PRISMA guideline (Moher et al., 2010). The following electronic databases were searched without constraints in order to find all published research up to August 26, 2022: PubMed, Embase, Scopus, Web of Science, and Cochrane, utilizing keywords, MeSH, or Emtree terms discovered in the original search. Google Scholar and ProQuest searched for unpublished research and gray literature. In a systematic PubMed search for PD, the crucial keywords were "idiopathic Parkinson's disease," "Parkinson*," "primary Parkinsonism," "Parkinsonian disorder," "Parkinsonian syndrome," "paralysis agitans," and "Lewy body."

2.2. Study selection and assessment of studies

Following the database search, all identified studies were imported into Endnote Version 20.2.1, and duplicates were eliminated. The remaining studies' titles and abstracts were reviewed, and all ceRNA axes in PD were included based on our inclusion criteria. The included publications satisfied the following criteria: they were (1) explicitly describing the ceRNA axis in PD, (2) published in English, and (3) original research. The following research was excluded: (1) non-PD or any neurodegenerative disease studies; (2) studies that did not include human specimens, cell lines, or animal models; and (3) studies that did not use a molecular method to validate the ceRNA loop components.

2.3. Data extraction

A self-conducted data extraction technique was used to obtain the necessary data from the research. It listed the authors, the year of publication, the origin, the type of study, human samples, cell lines, animal models, ceRNA(s), shared miRNA(s), major methods, and the major findings.

2.4. Bioinformatics analysis

Protein-protein interactions (PPI) were established based on target genes in the ceRNA axes in PD utilizing the Search Tool for the Retrieval of Interacting Genes (STRING) database (http://string-db.org/), which is a web-based tool for evaluating PPI data (Szklarczyk et al., 2021). Gene ontology (GO) enrichment analysis is a frequently used technique for assessing functional enrichment in high-throughput genomic or transcriptomic data. GO terminology is divided into biological process, molecular function, and cellular component. EnrichR, a web-based tool that gives various types of graphical representations of the collective functions of gene lists (Kuleshov et al., 2016), was utilized in this investigation to perform GO function enrichment analysis for ceRNA axis target genes.

3. Results

A total of 309 studies were discovered by searching the databases PubMed, Embase, Scopus, Web of Science, Google Scholar, ProQuest, and Cochrane, and 12 studies were identified by searching additional databases. After eliminating all duplicates, one hundred studies remained. The remaining articles' titles and abstracts were revised, and 16 studies were eliminated, leaving 86 studies. Each remaining article's full text was evaluated, and 46 studies were eliminated. Based on the given findings, the remaining 40 studies were all associated with our systematic review. The flowchart of the retrieval process utilized for the current study is shown in Figure 1.

Eligible studies were published between 2017 and 2022, which are included in Table 1. Based on the declared number, these studies included 264 samples of PD patients and 195 healthy controls. The patients' and controls' gender is rarely mentioned. Two animal models (mice and *C. elegans*) were used in 21 studies; in the majority, mice were the only animals involved. SH-SY5Y, HEK293, Hela, HepG2, BV2 cells, SK-N-SH, SK-N-AS, MN9D, and PC-12 are the cell lines utilized in these studies. Figure 2 illustrates the frequency of the genes targeted in the studies. In particular, most studies are restricted to China, Italy, India, and Iran, each of which has one study on the ceRNA axes in PD.

The analysis of the PPI network of the target genes of the ceRNA axes using STRING-DB identified a PPI network with 29 nodes and 37 edges, as demonstrated in Figure 3A. Furthermore, GO functional enrichment analysis indicated that shared genes were significantly enriched in numerous common biological processes, cellular compartments, and molecular functions of GO with $P < 0.05$ (Figures 3B–D). Among those significant pathways in biological processes, cellular response to metal ion, cellular response to oxidative stress, positive regulation of macromolecules metabolic process, canonical Wnt signaling pathway, and cellular response to catecholamine stimulus were among the processes with the highest number of genes. Cellular components were dedicated to lytic vacuole, lysosome, lytic vacuole membrane, and exocytic vesicle. Molecular functions were enriched in syntaxin-1 binding, syntaxin binding, signaling receptor complex adaptor activity, and copper ion binding. The expression levels of target genes in cell lines were provided in Supplementary Table 1 using the ProteomicsDB (Schmidt et al., 2018) based on the RNA-Seq method and transcripts per million (TPM) normalization method (Table 2).

4. Discussion

4.1. ncRNAs mechanism of actions

In particular, the ncRNAs that were involved in the ceRNA network in this study included miRNAs, lncRNAs, circRNAs, and pseudogenes, each of which exerts its effect through specific mechanisms; One of these mechanisms is sponging the target miRNA, which is involved in ceRNA axes (Moreno-García et al., 2020). Most research has shown that miRNA binds to specific regions of the 3′ UTR of its target mRNA, causing translation suppression, as well as decomposition of the mRNA adenylation and capping structure (Ipsaro and Joshua-Tor, 2015). Other mRNA regions containing miRNA binding sites have been discovered, including the 5′ UTR and the coding sequence, as well as inside the promoter areas (Xu et al., 2014). MiRNAs bound to the 5′ UTR and coding regions were found to suppress gene expression (Forman et al., 2008; Zhang J. et al., 2018), while miRNAs bound to gene promoters were found to stimulate transcription (Dharap et al., 2013). Furthermore, lncRNAs can exert their influence as guides, signals, decoys, and scaffolds in gene expression regulation (Wang and Chang, 2011). As a guide, lncRNAs can be incorporated into proteins such as chromatin-modifying enzymes, leading them to specific targets, thus mediating epigenetic change, and may modify the direction of gene expression in cis or trans through this advance. For example, ANRIL, XIST, HOTAIR, and KCNQ1OT1 lncRNAs can be used as chromatin modification enzymes that changes the epigenetic state (Bhat et al., 2016). LncRNA can also be used as a molecular signal, changing the structure of the chromatin, and recruiting transcription factors into the target gene, thereby increasing gene expression (Wang and Chang, 2011; Bhat et al., 2016). The functional versatility of lncRNA as a decoy mechanism allows it to behave as a "molecular sink" of RNA binding proteins (RBPs), which these groups of lncRNAs may be negative modulators, including transcription factors, regulatory factors, and chromatin modulators (Balas and Johnson, 2018). One of the advantages of LncRNAs is that they act as scaffolds to attach multiple efficient molecular partners with the capability of triggering or suppressing transcription and transfer them simultaneously to specific locations during transcription (Wang and Chang, 2011; Bhat et al., 2016).

In addition, it has been discovered that circRNAs have many possible biological activities depending on their properties. Nuclear persistent circRNAs have the ability to influence transcription and splicing (Prats et al., 2020). CircRNAs may perform their functions *via* associating with proteins, such as functioning as a protein sponge, protein scaffolding, and protein recruiting (Huang et al., 2020). In particular, circRNAs are capable of being translated, However, due to this ability, it is possible that circRNAs are not considered as ncRNAs, which requires potential studies (Miao et al., 2021). On

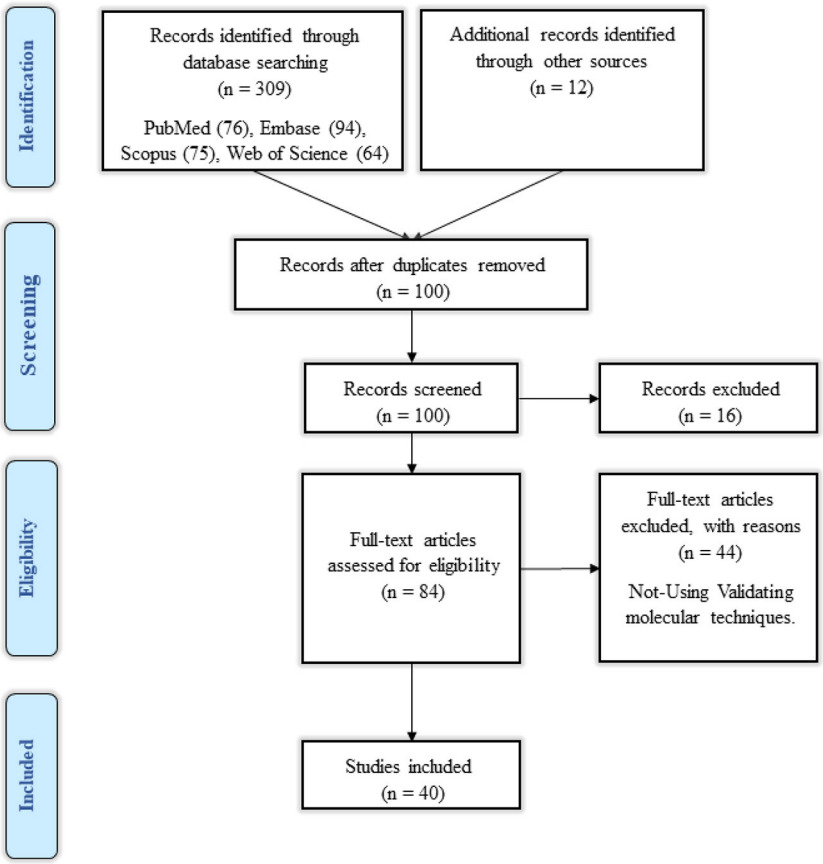

FIGURE 1
Flow chart of search strategy based on PRISMA flow diagram.

the other hand, pseudogenes can affect gene expression (not just the parent gene) at the transcription and post-transcription levels (Qi et al., 2015). A pseudogene may engage with a gene promoter at the transcriptional level. For example, pseudogene-generated antisense RNA interacts with mRNA with the same parent gene strand and blocks translation, and contributes to the creation of siRNA that can suppress the parent gene's expression (Hu et al., 2018).

4.2. ceRNAs axes potentials, from concepts to actual application

The ceRNA profile in PD may be different from the normal condition since the PD transcriptome differs significantly from the normal equivalents (Kurvits et al., 2021). Notably, ceRNA network regulation may be complicated. Predictions from the TargetScan database show that half of all miRNAs target 1–400 mRNAs and that a small percentage of miRNAs potentially target > 1,000 mRNAs. TargetScan also predicts that most ceRNAs include 1–10 MREs (Ala et al., 2013). As a result, multiple ceRNA-miRNA interactions result in very complex ceRNA networks (ceRNETs). It should be noted that studies in the field of ceRNA axes of PD are experiencing an upward trend, and since miRNAs are at the center of the ceRNA axes, it is fair to consider ceRNA related to PD as therapeutic targets, considering that miRNAs were introduced as a beneficial target in the measures of therapeutics of PD (Alieva et al., 2015; Nies et al., 2021). Feng et al. for example, used a synthetic sponge for miR-330 and suppressed miR-330, reducing chronic neuroinflammation in PD by decreasing inflammatory cytokines through the SHIP1/NF-B signaling pathway (Feng et al., 2021). In this regard, Titze-de-Almeida et al. thoroughly analyzed miRNAs as possible treatment targets for PD, analyzing their involvement in the disease's underlying processes, the approaches for suppressing aberrant expressions, and the existing technology for converting these small molecules from the laboratory to the clinic (Titze-de-Almeida et al., 2020).

In addition, the bioinformatic results of the current study, based on the enrichments of target genes involved in verified ceRNA axes, demonstrated that these genes are involved in critical pathways in PD. The cellular response to metal ion was the process in which most of the genes were enriched. It has been postulated that the toxicity of several peptides that aggregate may be connected to their capacity to attach ions of transition metals (Castellani et al., 2000). The involvement of metal ions in the pathogenesis of PD was reviewed in several studies (Castellani et al., 2000; Wei et al., 2021). Tosato and Di Marco also studied metal chelating treatment in PD, hypothesizing that around 250 metal-chelating characteristics toward Cu(II), Cu(I), Fe(III), Fe(II), Mn(II), and Zn(II) may be implicated in metal dyshomeostasis during PD (Tosato and Di Marco, 2019). Importantly, Deas et al. highlighted that α-synuclein

TABLE 1 CeRNAs axes studies in PD.

References	Origin	Type of study	Human samples	Cell line(s)	Animal model	CeRNA(s)	Shared miRNA(s)	Major methods	Major findings
Liu et al. (2017)	China	Animal study Cell culture	–	SH-SY5Y HEK293	Mice (C57BL/6)	MALAT1 ↑ miR-124 targets	miR-124 ↓	qRT-PCR, western blot, TUNEL assay, flow cytometry, caspase3 activity analysis, luciferase assay	In mouse and *in vitro* models, MALAT1 induces apoptosis by sponging miR-124, which can probably be applied to treating PD MALAT1 knockdown improved miR-124 expression in MPTP/MPP+ initiated models of PD
Wu et al. (2017)	China	Animal study Cell culture	–	SH-SY5Y	Rat	ABCA1 ↓ A20	miR-873 ↑	IHC, qRT-PCR, immunoblotting, dual-luciferase assay, transient transfection, and luciferase assays	Inhibiting A20 could aggravate the NF-κB signaling pathway by up-regulating miR-873 miR-873 sponge might be able to reduce PD symptoms by up-regulating ABCA1 and A20 Inhibition of miR-873 may play a dual protective role in PD as it induces intracellular cholesterol homeostasis and improves neuroinflammation
Straniero et al. (2017)	Italy	Case-control Cell culture	Post-mortem Brains (51 cases and 42 controls)	Hela HEK293 HepG2	–	GBAP1 ↓ GBA	miR-22-3p ↑	qRT-PCR, luciferase assay, western blot, GCase enzyme activity assays, analysis of the splicing pattern, and iPSC derivation	During dopaminergic differentiation, GBA will increase, while miR-22-3p will decrease GBPA1 (pseudogene) functioned as a GBA ceRNA and was identified as the first microRNA controlling GBA Confirmation of GBA/GBAP1/miR22-3p dysregulation in PD patients may lead to new treatment strategies by modulating the NMD pathway to increase GBAP1 levels or directing miRNA/pseudogene expression
Cao et al. (2018)	China	Animal study Cell culture	–	BV2 cells	Mice (C57BL/6)	SNHG1 ↑ NLRP3	miR-7 ↓	Luciferase assay, RNA IP, IHC, qRT-PCR, western blot, ELISA, caspase-3 activity assay	Neuroinflammation is promoted by SNHG1 through the miR-7/NLRP3 pathway SNHG1 downregulation increases miR-7 expression and suppresses dopaminergic neuron loss, microglial activation, and NLRP3 inflammasome expression in midbrain SNpc in MPTP-treated mice SHNG1 may be a potential therapeutic target for PD

(Continued)

10.3389/fncel.2023.1044634

TABLE 1 (Continued)

References	Origin	Type of study	Human samples	Cell line(s)	Animal model	CeRNA(s)	Shared miRNA(s)	Major methods	Major findings
Kumar et al. (2018)	India	Animal study	–	–	*C. elegans* (N2 and NL5901 strain)	circzip-2 ↓ zip-2	miR-60 ↑	qRT-PCR, sanger sequencing, imaging of α-synuclein protein aggregation, RNA-seq, quantification of ROS, acetylcholine and acetylcholinesterase estimation using amplex red, lifespan assay	Circzip-2 may have a protective role against PD Losing circzip-2 enhances miR-60 activity, decreasing protective genes, and when ZIP-2 is silenced, the protective activity is restored through the daf-16 pathway
Sang et al. (2018)	China	Cell culture	–	SH-SY5Y	–	CircSNCA ↓ SNCA	MiR-7 ↑	qRT-PCR, western blot, luciferase assay, immunofluorescence localization, MTT assay	CircSNCA knockdown resulted in downregulation of alpha-synuclein (SNCA), which proved circSNCA inhibition was effective in PD treatment CircSNCA up-regulates SNCA through miR-7 sponging, which decreased apoptosis and endorsed cell autophagy in PD
Xu et al. (2018)	China	Animal models Cell culture	–	SH-SY5Y	Mice (C57BL/6)	lincRNA-p21 ↑ miR-1277-5p target	miR-1277-5p ↓	qRT-PCR, cell nucleus, and cytoplasm fraction isolation, western blot, RIP assay, dual-luciferase activity assay, cell viability assay, cell apoptosis assay	In SH-SY5Y cells treated with MPP+, the lincRNA-p21/miR-1277-5p axis modulated cell viability and apoptosis by targeting α-synuclein LincRNA-p21 may be a valuable target in the treatment of PD
Ding et al. (2019)	China	Cell culture	–	SH-SY5Y	–	linc-p21 ↑ TRPM2	miR-625 ↓	qRT-PCR, TUNEL assay, MTT assay, LDH assay, caspase-3 assay, measurement of ROS generation, measurement of SOD activity, western blot, luciferase assay	TRPM2 expression is positively regulated by lnc-p21 that interacts with miR-625, and knockdown of TRPM2 reduces MPP+-induced neuroinflammation The Lnc-p21-miR-625-TRPM2 regulatory axis was identified as a potentiating axis in the pathogenesis of PD
Lin et al. (2019)	China	Animal models Cell culture	–	SH-SY5Y	Mice (C57BL/6)	HOTAIR ↑ RAB3IP	miR-126-5p ↓	Apoptosis assay, luciferase assay, RIP assay, qRT-PCR, western blot, CCK-8 assay, flow cytometry, morris water maze test, pole test, IHC, TUNEL assay	HOTAIR promotes PD by influencing cell proliferation and apoptosis by sponging miR-126-5p and regulating RAB3IP Knockdown of HOTAIR decreased the number of α-synuclein-positive cells while reducing the apoptosis rate among dopaminergic neurons

(Continued)

10.3389/fncel.2023.1044634

TABLE 1 (Continued)

References	Origin	Type of study	Human samples	Cell line(s)	Animal model	CeRNA(s)	Shared miRNA(s)	Major methods	Major findings
Liu et al. (2020)	China	Cell culture	–	SK-N-SH	–	NEAT1 ↑ RAB3IP	miR-212-5p ↓	qRT-PCR, western blot, CCK8 assay, RIP assay, cell apoptosis assay, flow cytometry, LDH release assay, ROS activity assay, SOD activity assay, dual-luciferase assay	In MPP+-treated SKN-SH cells, NEAT1, and RAB3IP were increased, whereas miR-212-5p was downregulated NEAT1 knockdown reduced MPP+-induced apoptosis, inflammation, and cytotoxicity in SK-N-SH cells *via* up-regulating miR-212-5p
Xu et al. (2020)	China	Animal study Cell culture	–	BV2 cells	Mice (C57BL/6)	GAS5 ↑ NLRP3	miR-223-3p ↓	qRT-PCR, cell viability test, apoptosis test, dual-luciferase assay, western blot, IHC,	GAS5 positively regulates NLRP3 by competitive sponging of miR-223-3p GAS5 knocked down enhances the expression of miR-223-3p, which reduces inflammatory factors GAS5 promotes PD development by targeting the miR-223-3p/NLRP3 axis
Zhang L. et al. (2020)	China	Animal study Cell culture	–	SH-SY5Y	Mice (C57BL/6)	AL049437 ↑ MAPK1	miR-205-5p ↓	qRT-PCR, CCK-8 assay, flow cytometry, ELISA, ROS species assay, luciferase assay, RNA pull-down assay, western blot	By adjusting miR-205-5p/MAPK1 in SH-SY5Y cells, lncRNA AL049437 alleviates MPP+-induced neuronal injury A high level of AL049437 reduces the expression of miR-205-5p in SH-SY5Y cells
Zhang X. et al. (2020)	China	Animal study	–	–	Mice (C57BL/6J)	LOC102633466 ↑ LOC102637865 ↑ LOC102638670 ↑ Col6a1 and Wnt6	miR-505-5p ↓ miR-188-3p ↓ miR-873a-5p ↓	qRT-PCR, RNA-seq, FastQC, HE staining, bioinformatic analysis	LOC102633466, LOC102637865, and LOC102638670 were significantly up-regulated in the aerobic exercise training group compared with the PD group Aerobic exercise may improve PD by acting on these three lncRNAs with a ceRNA mechanism
Meng et al. (2021)	China	Cell culture	–	SK-N-SH	–	Linc00943 ↑ RAB3IP	miR-15b-5p ↓	qRT-PCR, Cell transfection, western blot, MTT assay, flow cytometry, ELISA, dual-luciferase reporter analysis, and RIP	The MPP+-stimulated SK-N-SH cells led to an increase in LINC00943 abundance Silencing LINC00943 prevented MPP+-induced cell viability loss and increased apoptosis, inflammatory damage, and oxidative injury LINC00943 suppressed miR-15b-5p, and inhibiting miR-15b-5p reversed LINC00943-mediated mitigation of MPP+-induced neuronal injury. RAB3IP is targeted by miR-15b-5p, and LINC00943 might control RAB3IP *via* miR-15b-5p

(Continued)

10.3389/fncel.2023.1044634

TABLE 1 (Continued)

References	Origin	Type of study	Human samples	Cell line(s)	Animal model	CeRNA(s)	Shared miRNA(s)	Major methods	Major findings
Zhao J. et al. (2020)	China	Animal study Cell culture	–	SH-SY5Y	Mice (C57BL/6)	SNHG1 ↑ PTEN	miR-153-3p ↓	qRT-PCR, western blot, MTT assay, flow cytometry, luciferase assay, RNA pull-down analysis, apoptosis assay, RIP assay	SNHG1 expression was increased in both MPTP-induced PD mice and MPP+-treated SH-SY5Y cells SNHG1 knockdown inhibited MPP+-induced cytotoxicity in SH-SY5Y cells through the miR-153-3p/PTEN pathway
Zhao J. Y. et al. (2020)	China	Cell culture	–	SK-N-SH	–	HOTAIR ↑ ATG10	MIR-874-5P ↓	qRT-PCR, Cell viability assay, flow cytometry, western blot, ELISA, measurement of LDH activity, detection of ROS generation, determination of SOD activity, dual-luciferase assay, RIP assay	Silencing of HOTAIR decreases MPP+-triggered neuronal damage by regulating ATG10, which inhibits the effect of miR-874-5p on it
Zhou et al. (2020a)	China	Cell culture	–	SK-N-SH SK-N-AS	–	NORAD ↓ SLC5A3	miR-204-5p ↑	qRT-PCR, cell viability assay, cell apoptosis assay, western blot, detection of lactate dehydrogenase level, assessment of oxidative stress, enzyme-linked immunosorbent assay, dual-luciferase assay, RNA immunoprecipitation	NORAD was able to up-regulate SLC5A3 with interacting miR-204-5p and protected neuroblastoma cells from MPP+-induced damage As a result, NORAD is a PD inhibitor
Zhou et al. (2020b)	China	Cell culture Animal study	–	SK-N-SH	Mice (C57BL/6)	SNHG14 ↑ KLF4	miR-214-3p ↓	qRT-PCR, cell viability and apoptosis assays, ELISA, bioinformatics and dual-luciferase assay, RIP assay, western blot	SNHG14 acts as a miR-214-3p sponge and up-regulates miR-214-3p to reduce damage to MPPCS-stimulated SK-N-SH cells by downregulating KLF4 In PD models, SNHG14 was up-regulated, and miR-2143-p was down-regulated
Feng et al. (2021)	China	Cell culture Animal study	–	HEK293	Mice (C57BL/6)	MiR-330 synthetic sponge SHIP1, NF-κB	MiR-330 ↓	Dual-luciferase assay, inhibitor and agonist of SHIP1, western blot, qRT-PCR, AGO2-immunoprecipitation, ELISA, immunofluorescence, flow cytometry	Treatment of the cells with miR-330 sponge suppresses LPS-induced chronic neuroinflammation in PD by down-regulating the activity of microglia with reduced inflammatory cytokines *via* the SHIP1/NF-κB signaling pathway

(Continued)

10.3389/fncel.2023.1044634

TABLE 1 (Continued)

References	Origin	Type of study	Human samples	Cell line(s)	Animal model	CeRNA(s)	Shared miRNA(s)	Major methods	Major findings
Lian et al. (2021)	China	Cell culture	–	SK-N-SH	–	LINC00943 ↑ CXCL12	miR-7-5p ↓	qRT-PCR, cell viability assay, cell apoptosis assay, western blot, measurement of ROS generation and SOD activity, dual-luciferase assay, RIP assay	LINC00943 acted as a miR-7-5p sponge and regulated CXCL12 expression in MPP+-induced SK-N-SH cells LINC00943 knockdown may partially reduce neuronal damage caused by MPP + due to that LINC00943 was increased in MPP+-inducted PD models
Liu et al. (2021)	China	Cell culture Animal study	–	SK-N-SH HEK293T	Mice (C57BL/6)	NEAT1 ↑ AXIN1	miR-212-3p ↓	qRT-PCR, CCK-8 assay, flow cytometry, western blot analysis, ELISA, dual-luciferase reporter assay, RIP assay, statistical analysis	Silencing of NEAT1 may hinder PD progression due to its up-regulation in MPTP-treated PD mouse models and MPP+-stimulated PD cell models MiR-212-3p regulated the cell progression by targeting AXIN1, which sponge with NEAT1
Shen Y. et al. (2021)	China	Cell culture Animal study	–	SH-SY5Y	BALB/c mice	MIAT ↑ SYT1	miR-34-5p ↓	FISH, dual-luciferase assay, RIP assay, qRT-PCR, western blot, CCK-8 assays, annexin V-fluorescein isothiocyanate (FITC)/propidium iodide (PI) dual label staining, IHC, TUNEL assay, behavioral assays	MIAT sponge miR-34-5p and then regulate the SYT1 expression, as a result, exerts neuroprotective effects in PD and promotes the expression of Parkin in the SH-SY5Y cells MIAT expression is downregulated in various brain regions and protects the neural function of SH-SY5Y cells
Shen Y. E. et al. (2021)	China	Cell culture Animal study	–	SH-SY5Y	Mice (C57BL/6)	PART1 ↓ MCL1	miR-106b-5p ↑	Western blot, qRT-PCR, CCK8 assay, apoptosis detection, caspase 3 activity detection, ELISA, ROS detection, LDH detection, SOD detection, dual-luciferase assay, RIP assay, RNA pull-down assays	PART1 is a protecting factor for PD by sponging miR-106b-5p, and MCL1 is a direct target for miR-106b-5p Consequently, PART1 reduced MPP+-induced damage to SHSY5Y cells Reduced expression of PART1 is shown in PD
Sun et al. (2021)	China	Cell culture	-	SH-SY5Y	-	NEAT1 ↑ GJB1	miR-1301-3p ↓	qRT-PCR, western blot analysis, cell apoptosis analysis, IL-1β production analysis, dual-luciferase activity assay	Knockdown of NEAT1 inhibits MPP+-Induced neuronal apoptosis in PD *via* inhibition of α-Syn-Induced activation of the inflammatory form NLRP3 through upgrading the expression of miR-1301-3p and downregulation of GJB1 NEAT1 acted as a therapeutic factor in PD
Wang S. et al. (2021)	China	Cell culture	–	SK-N-SH SK-N-AS	–	NEAT1 ↑ SP1	miR-519a-3p ↓	qRT-PCR, MTT assay, flow cytometry analysis, western blot, dual-luciferase assay	NEAT1 expression is significantly up-regulated in MPP+-induced SK-N-SH and SK-N-AS cells in PD Silencing of NEAT1 applied protective effects in MPP+-induced neuroblastoma cell injury *via* regulating miR-519a-3p, which reduces SP1 expression

(Continued)

10.3389/fncel.2023.1044634

TABLE 1 (Continued)

References	Origin	Type of study	Human samples	Cell line(s)	Animal model	CeRNA(s)	Shared miRNA(s)	Major methods	Major findings
Xiao et al. (2021)	China	Cell culture Animal study	–	SK-N-SH MN9D	Mice (C57BL/6)	SNHG1 ↑ MAPK1	miR-125b-5p ↓	qRT-PCR, CCK-8 assay, apoptosis assay, caspase-3 and caspase-9 activity assay, LDH release, ROS and SOD activity assay, ELISA, dual-luciferase assay, western blot	MiR-125b-5p is sponged by SNHG1, and it suppresses MAPK1 Silencing of SNHG1 and overexpression of miR-125b-5p applied neuroprotective actions in MPP+-evoked neuronal injury in SK-N-SH and MN9D Cells and MPTP-Induced PD mice
Xie et al. (2021)	China	Cell culture	–	SH-SY5Y	–	SOX21-AS1 ↑ IRS2	miR-7-5p ↓	qRT-PCR, cell viability assay, lactate dehydrogenase assay, TUNEL assay, flow cytometry apoptosis analysis, western blot, measurement of ROS generation, measurement of SOD activity, nuclear-cytoplasmic separation assay, fluorescent *in situ* hybridization assay, luciferase gene assay	SOX21-AS1 seems to tie with miR-7-5p, whose overexpression diminished MPP+- initiated cell damage IRS2 served as the target quality of miR-7-5p, and its expression was positively modulated by SOX21-AS1
Xu et al. (2021)	China	Cell culture	–	SH-SY5Y	–	ID2-AS1 ↑ IFNAR1	miR-199a-5p ↓	Lactate dehydrogenase assay, flow cytometry, reactive oxygen species activity, western blot, subcellular fraction analysis, RNA immunoprecipitation assay, ELISA, dual-luciferase assay	ID2-AS1 down-regulation weakened MPP+ induced cytotoxicity in SH-SY5Y cells Down-regulation of ID2-AS1 alleviated the neuronal damage in PD by regulating the miR-199a-5p/IFNAR1/JAK2/STAT1 axis
Zhang et al. (2021)	China	Case-control Animal model Cell culture	PD patients (36 cases and 20 controls)	SH-SY5Y	Rats	SNHG7 ↑ TRAF5 NF-κB	miR-425-5p ↓	Immunofluorescence, IHC, qRT-PCR, western blot, MTT assay, measurement of MDA, SOD, and GSH-PX, ELISA, RIP assay, luciferase assay	SNHG7 works as a ceRNA by sponging miR-425-5p and promoting TRAF5 Low expression of SNHG7 or miR-425-5p overexpression attenuates neuronal apoptosis
Chen C. et al. (2022)	China	Case-control Cell culture	PD patients (99 cases and 93 controls)	SH-SY5Y	–	RMST ↑ miR-150-5p targets	miR-150-5p ↓	qRT-PCR, flow cytometry, CCK-8 assay, luciferase reporter assay	Serum RMST is a potential biomarker for PD diagnosis Downregulation of RMST may influence the onset and progression of PD by suppressing neuron cell death and the production of inflammatory cytokines through miR-150-5p
Zheng et al. (2021)	China	Cell culture	–	SK-N-SH	–	UCA1 ↑ KCTD20	miR-423-5p ↓	qRT-PCR, cell viability and apoptosis assays, western blot, ELISA, dual-luciferase assay, RIP assay	MPP+ causes PD-like symptoms, and the silencing of UCA1 protects SK-N-SH cells from MPP+-evoked cytotoxicity by targeting the miR-423-5p/KCTD20 axis

(Continued)

10.3389/fncel.2023.1044634

TABLE 1 (Continued)

References	Origin	Type of study	Human samples	Cell line(s)	Animal model	CeRNA(s)	Shared miRNA(s)	Major methods	Major findings
Zhou Q. et al. (2021)	China	Cell culture Animal model	–	SH-SY5Y PC-12	Mice (C57BL/6)	XIST ↑ Sp1	miR-199a-3p ↓	CCK-8 assay, flow cytometry, cell apoptosis analysis by annexin-V/PI staining, TUNEL assay, TUBB3, luciferase assay, RIP analysis, TH detection by IHC, H&E and TUNEL staining, western blot, qRT-PCR	XIST sponges miR-199a-3p to modulate Sp1 expression Behavioral indications of PD were successfully lightened upon shXIST or miR-199a-3p treatment
Zhou S. F. et al. (2021)	China	Cell culture	–	SK-N-SH SH-SY5Y	–	NEAT1 ↑ ARHGAP26	miR-1277-5p ↓	qRT-PCR, MTT assay, flow cytometry, western blot, ELISA, measurement of MDA, LDH, SOD, and GSH-Px, dual-luciferase assay	NEAT1 knockdown and miR-1277-5p overexpression can mitigate MPP+-induced neuron injury Upregulation of NEAT1 might contribute to MPP+-induced neuron injury through the NEAT1-miR-1277-5p-ARHGAP26 axis
Chen C. et al. (2022)	China	Cell culture Animal model	–	SH-SY5Y	Mice (C57BL/6)	CircTLK1 ↑ DAPK1	miR-26a-5p ↓	Histological analysis, assessment of motor function, cell culture and treatment, western blot, qRT-PCR, LDH cytotoxicity assay, cell viability and apoptosis, dual-luciferase gene assay	circTLK1 expression increased in PD models. The knockdown of circTLK1 alleviated the PD-induced neuron injury. Overexpression of DAPK1 and inhibition of miR-16a-5p rescinded the protective function of shcircTLK1 in neurons
Sun X. M. et al. (2022)	China	Cell culture Animal model	–	SK-N-SH	Mice (C57BL/6)	LINC00943 ↑ SP1	miR-338-3p ↓	MTT assay, EdU staining, flow cytometry, western blot, ELISA assay, qRT-PCR, subcellular localization assay, dual-luciferase assay, RIP assay	LINC00943 works as a ceRNA by sponging miR-338-3p and positively regulating SP1 Knockdown of LINC00943 could alleviate nerve cell injury
Cao et al. (2022)	China	Cell culture	–	SH-SY5Y	–	circ_0070441 ↑ IRS2	miR-626 ↓	qRT-PCR, Western blot, ELISA, CCK-8, flow cytometry, caspase-3 assay, RIP	In MPP+-treated SH-SY5Y cells, circ_0070441, and IRS2 levels increased while miR-626 expression decreased. Circ_0070441 depletion reduced MPP+-induced neuronal damage *via* controlling cell death and inflammation. IRS2 was a miR-626 target, and Circ 0070441 behaved as a sponge for it
Sun Z. M. et al. (2022)	China	Cell culture	–	SH-SY5Y	–	SNHG10 ↑ IRS2	miR-1277-5p ↓	qRT-PCR, western blot, ELISA, CCK-8, apoptosis detection by flow cytometry, luciferase assay, RNA pull-down	SNHG10 knockdown abates MPP+-induced damage in SH-SY5Y cells through the miR-1277-5p/IRS2 axis Overexpression of IRS2 or inhibition of miR-1277-5p reverses the effect of SNHG10 knockdown

(Continued)

10.3389/fncel.2023.1044634

TABLE 1 (Continued)

References	Origin	Type of study	Human samples	Cell line(s)	Animal model	CeRNA(s)	Shared miRNA(s)	Major methods	Major findings
Zhuang et al. (2022)	China	Cell culture	–	SK-N-SH	–	SNHG14 ↑ ATG10	miR-519a-3p ↓	qRT-PCR, western blot, MTS cell viability assay, flow cytometry, dual-luciferase reporter assay, RIP	SNHG14 and ATG10 were both ceRNAs for miR-519a-3p, and ATG10 expression may be favorably regulated by SNHG14 by sponging miR-519a-3p Targeting SNHG14 and reinstating miR-519a-3p might protect DAn against MPP+ toxicity through ATG10 regulation
Zhang et al. (2022)	China	Case-control Animal model Cell culture	PD patient's blood (40 cases and 20 controls)	SH-SY5Y Microglia BV2	Mice (C57BL/6)	MIR17HG ↑ SNCA	miR-153-3p ↓	APO-induced rotation test, rotarod test, passive avoidance test, tissue immunofluorescence, IHC, qRT-PCR, Western blot, ELISA, detection of oxidative stress	MIR17HG is overexpressed in PD tissues and cells, and reducing MIR17HG expression reduces neuronal apoptosis and inflammatory responses in microglia in PD models and regulates PD progression by modulating the miR-153-3p/SNCA axis
Yousefi et al. (2022)	Iran	Cell culture Case-control	PD patients PBMC (38 cases and 20 controls)	HEK293T	–	linc0938 ↑ LRRK2 linc001128 ↓ ATP13A2	miR-24-3p ↓ miR-30c-5p ↓	Plasmid construction, Dual-luciferase reporter assay, qRT-PCR	linc001128, has-miR-24-3p, and miR-30c-5p expression were downregulated in PD patients Expression of Linc00938, LRRK2, and ATP13A2 were up-regulated in PBMC of the PD patients Linc00938 directly sponged miR-30c-5p in PD patients.

The upward arrow indicates the increased expression. The downward arrow indicates the decreased expression.

10.3389/fncel.2023.1044634

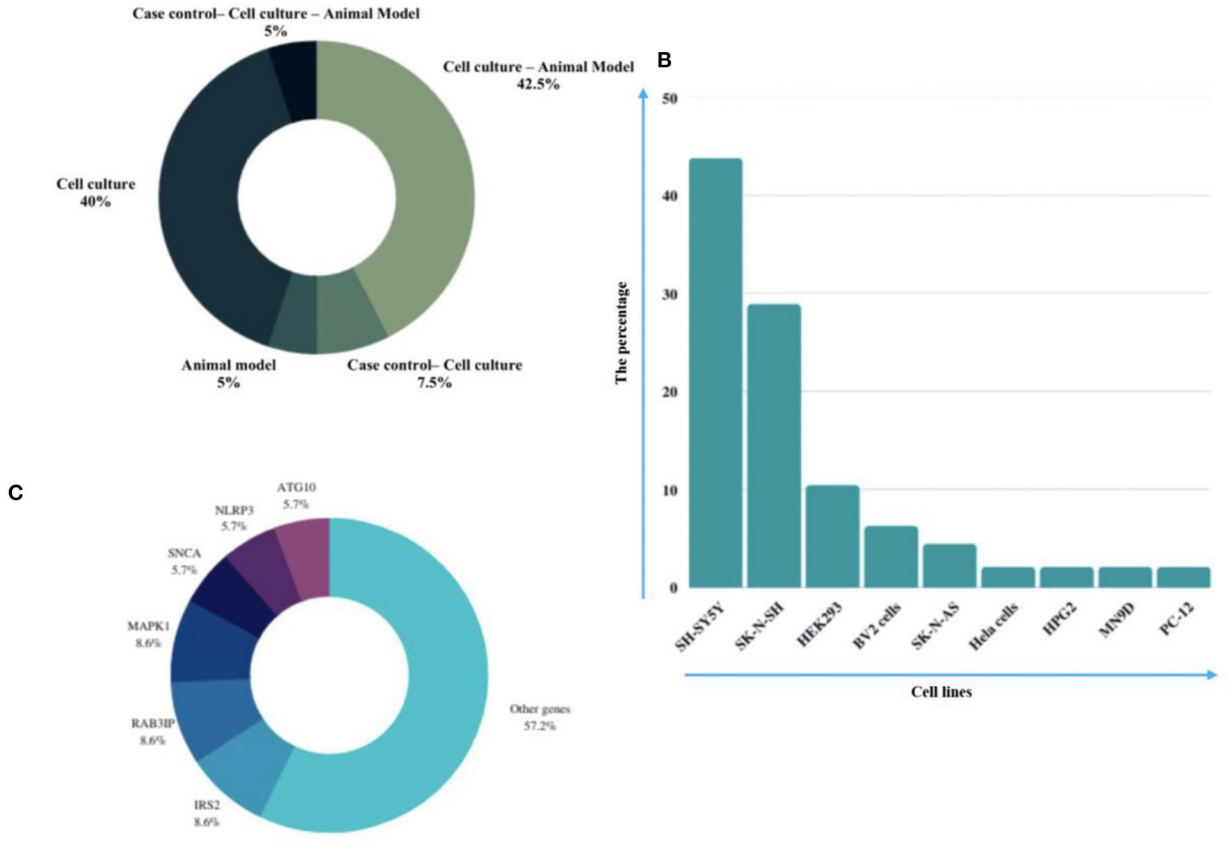

FIGURE 2
A summary of the qualified studies' details. **(A)** The design of studies. The majority of studies utilized cell culture and animal models (42.5%), and 40% of studies only utilized cell culture in their study design. **(B)** Percentage of cell lines utilized in the studies. SH-SY5Y (43.75%), SK-N-SH (22.88%), and HEK293 (10.48%) were the most used cell lines in the studies. **(C)** Percentage of targeted genes involved in ceRNA axes in PD. RAB3IP, SP1, and IRS2 were among the most targeted genes studied in PD's ceRNA axes. However, most of the axes involved novel genes, as provided by the other genes in the figure.

oligomers' interactions with metal ions might lead to oxidative stress in neurons produced from human iPSCs (Deas et al., 2016). Another notable process in the GO enrichment of the targeted genes implicated in the ceRNA axis in PD was the cellular response to oxidative stress. Evidence suggests that oxidative damage and mitochondrial malfunction contribute to the chain of events that lead to dopaminergic neurodegeneration (Beal, 2005; Jenner and Olanow, 2006; Parker et al., 2008; Winklhofer and Haass, 2010; Schapira and Jenner, 2011). It should be emphasized that dopaminergic neuron loss is a crucial factor in PD development (Mamelak, 2018). Remarkably, the results of the bioinformatics study with enrichment in the pathways that play a vital role in the development of PD emphasize the importance of these ceRNA axes in the pathogenesis of PD. On the contrary, the bioinformatics part of this study only focused on the enrichment of genes targeted in the ceRNA axes. And future bioinformatics research may explore this subject more thoroughly to highlight these axes' significance.

However, various challenges must first be overcome in order to bring the notion to fulfillment. At first, it is better to select axes that play a vital role, are known as hubs, and are connected to many post-transcriptional regulatory components that cannot be supplanted by the cell. One of the topics to consider in the following is the preceding one's emphasis; it seems almost impossible to impact an axis without altering ceRNET. Non-specific modification of the ceRNA network is dangerous because it has the ability to alter regular gene expression in unexpected ways. Finally, more studies are required to create therapeutic techniques and delivery systems for ceRNAs. However, vectors developed for gene therapy studies have the potential to be widely used in ceRNA-related research.

4.3. NEAT1-associated ceRNA axes in PD

NEAT1 (Nuclear Enriched Abundant Transcript 1) lncRNA was first described in 2007 and later altered to Nuclear Paraspeckle Assembly Transcript (Hirose et al., 2014). In humans, NEAT1 is transcribed from the multiple endocrine neoplasia type I (MEN 1) gene that is located on chromosome 11 (Yu et al., 2017). There are two isoforms for NEAT1 transcription; the shorter NEAT1 (NEAT1S) is 3,684 nucleotides, while the longer NEAT1 (NEAT1L) is 22,743 nucleotides (Boros et al., 2021). Studies in humans and other models have shown that NEAT1 may participate as a critical factor in neurodegenerative diseases, human tumors, and cancers. It has the potential as a biomarker and as a therapeutic target for PD (Asadi et al., 2021; Boros et al., 2021). In PD, NEAT1 sponging

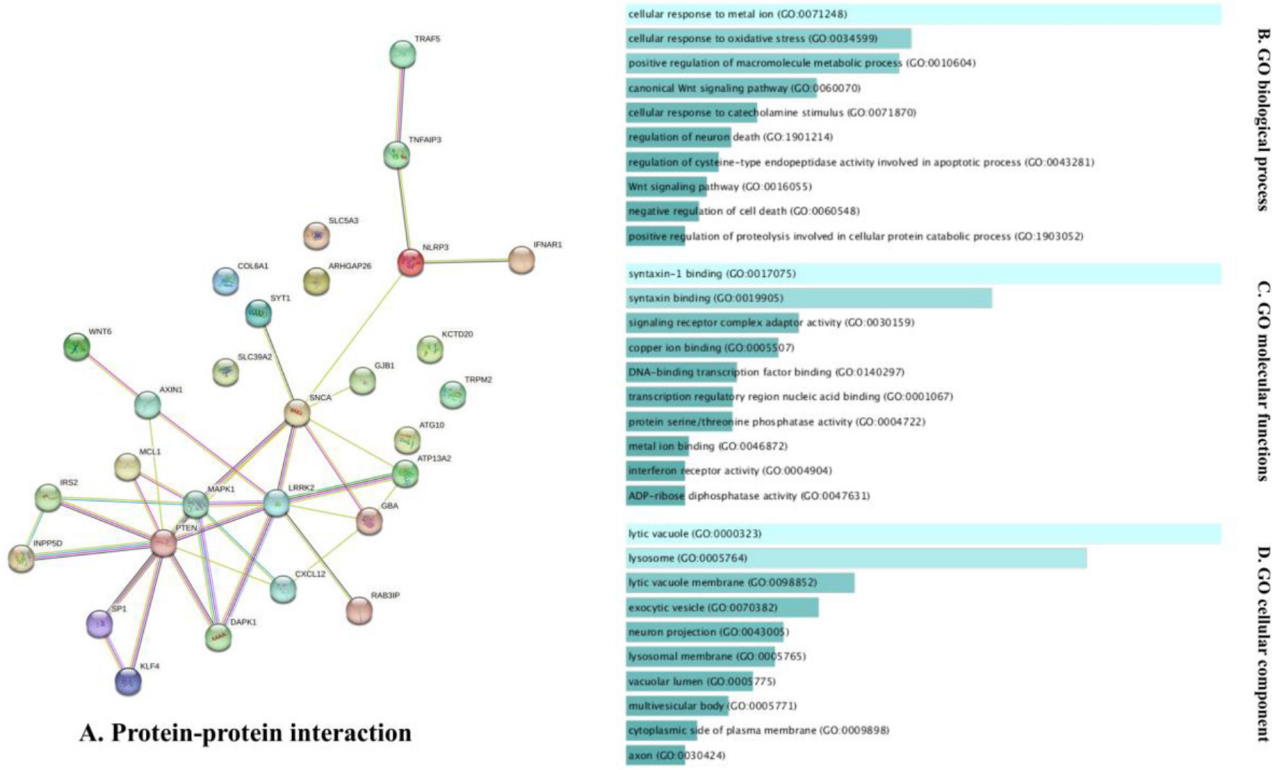

FIGURE 3
The PPI interaction and GO enrichment analysis of target genes involved in ceRNA axes in PD. **(A)** The PPI interaction was established using the STRING-DB and includes 29 nodes and 37 edges. **(B–D)** The GO enrichment of target genes on the verified ceRNA axes. The *P*-values are used to rank the importance of each group, with the length of each bar indicating the significance level. The order of the bars is based on the *p*-value. Note that the higher the association with a certain category, the less intense the color of the bars.

five different ceRNA axes, through NEAT1/miR-212-3p (Liu et al., 2020), NEAT1/miR-1301-3p (Sun et al., 2021), NEAT1/miR-519a-3p (Wang S. et al., 2021), NEAT1/miR-212-5p (Liu et al., 2021), NEAT1/miR-1277-5p (Zhou S. F. et al., 2021; Figure 4).

MiR-212-3p regulated the cell's progression by targeting AXIN1 (axis inhibition protein 1), which provides an interacting target for NEAT1. AXIN1 is a multifunctional scaffold protein whose functional role is related to the progression of many diseases (Li et al., 2013). Many current studies have shown that AXIN1 can act as a tumor suppressor to participate in the tumorigenesis (Saeed, 2018). Saeed identified that AXIN1 could serve as a new gene for PD through a GWAS meta-analysis (Saeed, 2018). Liu et al. found that NEAT1 was overexpressed in PD and that upregulation of AXIN1 resulted from the inhibition of miR-212-3p. As a result, the silencing of NEAT1 by affecting miR-212-3p/AXIN1 may hinder PD progression (Liu et al., 2021). Moreover, in the NEAT1/miR-1301-3p axis, GJB1 (Gap Junction Protein Beta 1), which encodes a member of the gap junction protein family, was regulated. Gap junction proteins are channels that facilitate the movement of ions and small molecules between cells (Zhang Z. et al., 2020). Recently, Reyes et al. have demonstrated that GJB1 is involved in the preferential uptake of α-syn oligomeric in neurons and that the upregulation of GJB1 is associated with α-syn accumulation in a PD model. This study indicated the potential and crucial role of GJB1 in the α-syn-induced neuronal apoptosis (Reyes et al., 2019). Sun et al. revealed that overexpression of NEAT1 was seen in PD while miR-1301-3p was down-regulated, and subsequent increased GJB1 and knockdown of NEAT1 may hinder PD progression (Sun et al., 2021). In addition, Wang et al. revealed that NEAT1 expression was significantly up-regulated in the NEAT1/miR-519a-3p axis in PD. In this axis, SP1 is overexpressed by down-regulation of miR-519a-3p (Wang S. et al., 2021). This gene produces a zinc-finger transcription factor that can activate or suppress transcription in response to stimuli. It binds to GC-rich motifs with high affinity and controls many gene expressions involved in various processes (Koutsodontis et al., 2002). Research revealed that SP1 might ameliorate PD-linked neuropathology by regulating leucine-rich repeat kinase 2 (LRRK2) transcription (Wang and Song, 2016). In addition, Chen et al. demonstrated that SP1 knockdown hindered the inhibitory impact of MPP+ exposure on endothelial protein C receptor (EPCR) in PD (Chen et al., 2015).

On the other axis, NEAT1/miR-212-5p, NEAT1 sponged miR-212-5p, and regulated RAB3A Interacting Protein (RAB3IP) expression (Liu et al., 2020). RAB3IP, a significant activator of Rab proteins, has been shown to affect neurite outgrowth and PD progression (Homma and Fukuda, 2016; Lin et al., 2019). Liu et al. reported that this lncRNA and RAB3IP were increased, whereas miR-212-5p was down-regulated in PD. Therefore, NEAT1 knockdown may play a protective role in PD (Liu et al., 2020). Likewise, NEAT1 regulated miR-1277-5p expression and targeted Rho GTPase Activating Protein 26 (ARHGAP26) (Zhou S. F. et al., 2021). Cell-extracellular matrix interactions initiate a signaling cascade that triggers integrin cell surface receptors and regulates

10.3389/fncel.2023.1044634

TABLE 2 The expression levels of RAB3IP, IRS2, and MAPK1 in different cell lines.

Gene symbol	Cell lines	Tissue synonym	Average TPM	Maximum TPM	Minimum TPM
RAB3IP	CACO-2 cell	Unknown	55.9	55.9	55.9
	T-47D cell	Breast	44.8	44.8	44.8
	A-431 cell	Skin	37.8	37.8	37.8
	MCF-7 cell	Breast	35.9	35.9	35.9
	HaCaT cell	Unknown	28.7	28.7	28.7
	RPMI-8226 cell	Circulatory_system	24.9	24.9	24.9
	PC-3 cell	Prostate	23.4	23.4	23.4
	HEK-293 cell	Kidney	22.4	22.4	22.4
	Hep-G2 cell	Liver	21.9	21.9	21.9
	MOLT-4 cell	Circulatory_system	21.9	21.9	21.9
	HL-60 cell	Circulatory system	21.9	21.9	21.9
	HEL cell	Circulatory_system	21.6	21.6	21.6
	A-549 cell	Lung	21	21	21
	SK-BR-3 cell	Unknown	20.1	20.1	20.1
	U2-OS cell	Bone	19.1	19.1	19.1
	U-251 MG cell	Brain	15.8	15.8	15.8
	U-937 cell	Unknown	14	14	14
	K-562 cell	Circulatory_system	10.5	10.5	10.5
	SH-SY5Y cell	Autonomic_nervous_system	10.2	10.2	10.2
	THP-1 cell	Circulatory_system	7.5	7.5	7.5
	HeLa cell	Cervix_uterine	5.9	5.9	5.9
MAPK1	K-562 cell	Circulatory_system	287.7	287.7	287.7
	HL-60 cell	Circulatory system	87.2	87.2	87.2
	U2-OS cell	Bone	82.9	82.9	82.9
	HEL cell	Circulatory_system	69.3	69.3	69.3
	A-431 cell	Skin	67.5	67.5	67.5
	HaCaT cell	Unknown	63.4	63.4	63.4
	HEK-293 cell	Kidney	61.5	61.5	61.5
	MOLT-4 cell	Circulatory_system	57.7	57.7	57.7
	U-251 MG cell	Brain	44.5	44.5	44.5
	PC-3 cell	Prostate	43.4	43.4	43.4
	A-549 cell	Lung	43.4	43.4	43.4
	U-937 cell	Unknown	41.2	41.2	41.2
	SK-BR-3 cell	Unknown	40.3	40.3	40.3
	T-47D cell	Breast	38.2	38.2	38.2
	CACO-2 cell	Unknown	31.8	31.8	31.8
	Hep-G2 cell	Liver	30.9	30.9	30.9
	HeLa cell	Cervix_uterine	30.1	30.1	30.1
	SH-SY5Y cell	Autonomic_nervous_system	29	29	29
	THP-1 cell	Circulatory_system	24.6	24.6	24.6
	MCF-7 cell	Breast	24.3	24.3	24.3
	RPMI-8226 cell	Circulatory_system	8	8	8
IRS2	SH-SY5Y cell	Autonomic_nervous_system	42.8	42.8	42.8

(Continued)

TABLE 2 (Continued)

Gene symbol	Cell lines	Tissue synonym	Average TPM	Maximum TPM	Minimum TPM
	THP-1 cell	Circulatory_system	42.3	42.3	42.3
	HEK-293 cell	Kidney	27.1	27.1	27.1
	HL-60 cell	Circulatory system	8.5	8.5	8.5
	U-937 cell	Unknown	8.1	8.1	8.1
	U-251 MG cell	Brain	7.1	7.1	7.1
	HeLa cell	Cervix_uterine	6.3	6.3	6.3
	A-549 cell	Lung	5.9	5.9	5.9
	A-431 cell	Skin	5.1	5.1	5.1
	HEL cell	Circulatory_system	2.6	2.6	2.6
	HaCaT cell	Unknown	2.3	2.3	2.3
	MCF-7 cell	Breast	2.3	2.3	2.3
	RPMI-8226 cell	Circulatory_system	1.9	1.9	1.9
	K-562 cell	Circulatory_system	1.7	1.7	1.7
	PC-3 cell	Prostate	1.3	1.3	1.3
	T-47D cell	Breast	0.8	0.8	0.8
	CACO-2 cell	Unknown	0.5	0.5	0.5
	MOLT-4 cell	Circulatory_system	0.1	0.1	0.1
	SK-BR-3 cell	Unknown	0.1	0.1	0.1

actin cytoskeleton organization. One of the proteins implicated in these cascades is focal adhesion kinase, a GTPase-activating protein encoded by this gene that binds to focal adhesion kinase and intervenes in the activity of the GTP-binding proteins RhoA and Cdc42 (Lopez-Ilasaca, 1998). In this respect, Zhou et al. discovered that the upregulation of NEAT1 might contribute to MPP+-induced neuron injury through the NEAT1-miR-1277-5p-ARHGAP26 axis in PD. Hence, NEAT1 knockdown and miR-1277-5p overexpression can mitigate neuron injury (Zhou S. F. et al., 2021). Studies analyzing NEAT1 have revealed the significance of this lncRNA in PD due to its potential role in ceRNA expression axes and have certainly made it a challenging target.

4.4. SNHG1, SNHG7, SNHG10, and SNHG14-associated ceRNA axes in PD

Small molecule RNA host gene 1 (SNHG1), also known as linc00057, is a lncRNA that was recently found and transcribed from UHG and is present on the 11q12.3 chromosome (Zhao J. et al., 2020). It was observed that SNHG1 was up-regulated in diverse types of cancer and that it served as a prognostic factor (Zhao et al., 2018). SNHG1 is also proven to elevate inflammation and autophagy of neurons in PD (Sabaie et al., 2021). The participation of SNHG1 in PD has been studied along several ceRNA axes, including SNHG1/miR-7/NLRP3, SNHG1/miR-125b-5p/MAPK1, SNHG1/miR-153-3p/PTEN. It should be noted that SNHG1 experiences up-regulation in all three axes (Cao et al., 2018; Zhao J. et al., 2020). Nod-like receptor protein 3 (NLRP3) activation results in the activation of caspase-1, cleaving interleukin (IL)-1β, and IL-18 into their active forms in response to infectious agents and cellular damage (Cao et al., 2018; Kelley et al., 2019). Cao et al. revealed that neuroinflammation is promoted by SNHG1 through the miR-7/NLRP3 pathway (Cao et al., 2018). MAPK1, a serine/threonine kinase member of the MAPK family, participates in several biological functions, including the cell cycle, cell death, and cell survival (Dzamko et al., 2014). Previous research has shown a link between MAPK1 and the progression of PD (Triplett et al., 2015). MAPK has been identified as a potent activator of neuronal apoptosis, and its overactivation results in neuronal death in PD (Mielke and Herdegen, 2000; Choi et al., 2014). Xiao et al. revealed that SNHG1 sponges miR-125b-5p and that it suppresses MAPK1 (Xiao et al., 2021). Phosphatase and tensin homolog (PTEN) is a kind of tumor suppressor gene that adjusts cell growth and cell death in cancers and neurodegenerative diseases (Ismail et al., 2012). A potential therapeutic target for the neurodegenerative disease could be PTEN, which could function as a moderator of Reactive Oxygen Species (ROS) generation in the neuronal death (Zhao J. et al., 2020). Zhao et al. revealed that the PTEN/AKT/mTOR signaling pathway would be activated in SH-SY5Y cells by targeting miR-153-3p (Zhao J. et al., 2020).

SNHG7 is an oncogenic lncRNA on chromosome 9q34.2 and is highly expressed in cancer cells and tumors (Bian et al., 2020). Tumor necrosis factor receptor-associated factor 5 (TRAF5) is a cytoplasmic adapter that can trigger the NF-κB signaling pathway *via* its receptors and can take part in modulating nerve cell death, inflammatory reactions, and other neurological processes (Zhang et al., 2021). Zhang et al. demonstrated that in PD, SNHG7 works as a ceRNA by sponging miR-425-5p and promoting TRAF5 (Zhang et al., 2021). In addition, SNHG10 is a lncRNA located on chromosome

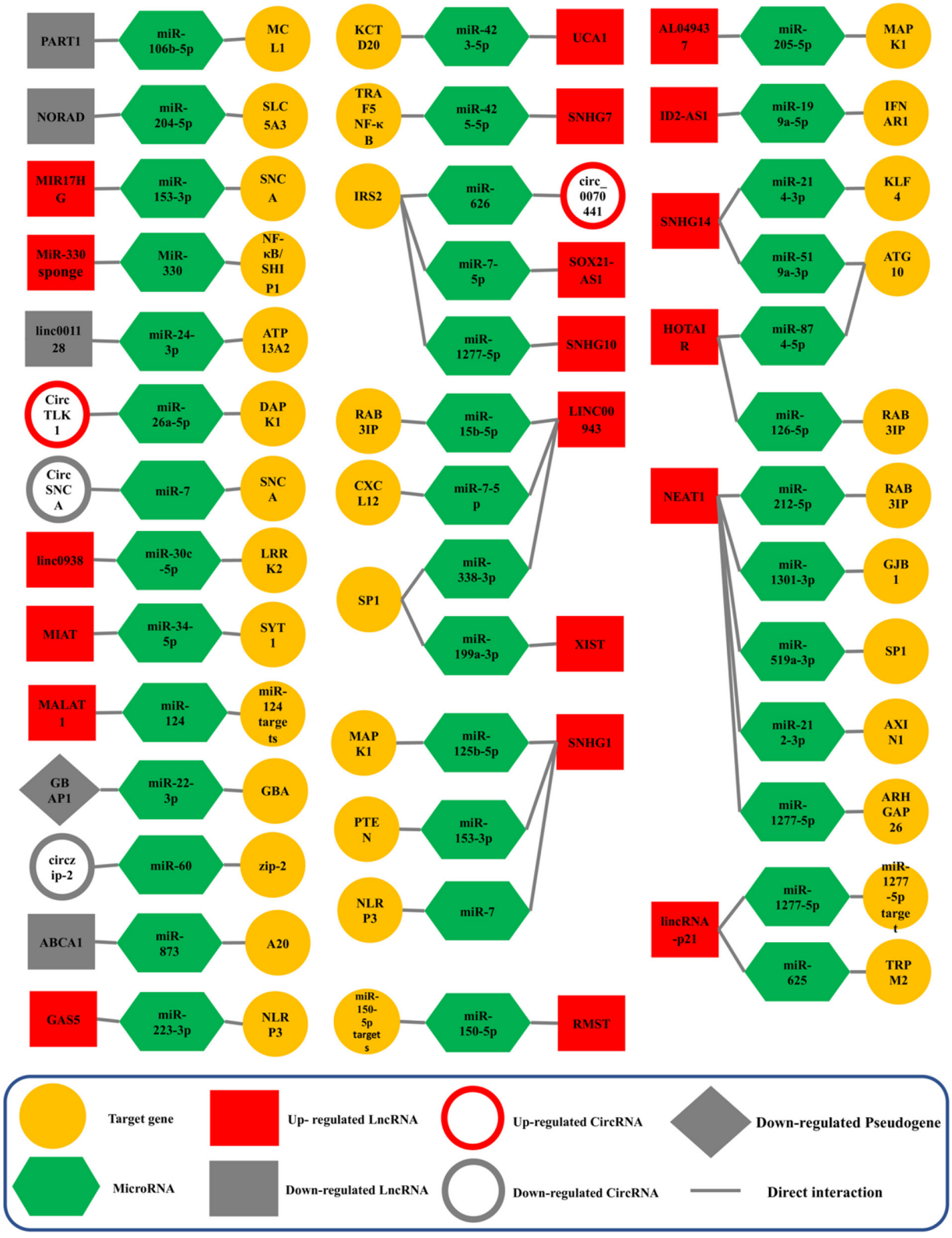

FIGURE 4
Validated ceRNA axes in PD. The red and gray colors of the squares indicate an increase and a decrease in the expression of lncRNAs, circRNAs, and pseudogenes, respectively. This schematic figure shows the importance of the constituent components of ceRNA axes. In addition, this figure shows that the studies around which of these components have been more extensive. NEAT1, the SNHG family, and LINC00943 were among the lncRNAs studied most on these axes. CircRNA, circular RNA; lncRNA, long non-coding RNA; miRNA, microRNA.

14q32.13 and is involved in advancing several types of cancer (Sun Z. M. et al., 2022). Insulin substrate receptor 2 (IRS2) is a cytoplasmic adaptor protein of the insulin signaling pathway and is a target of miR-1277-5p and shows a high expression level in the PD model. Sun et al. found that the knockdown of SNHG10 attenuates MPP+-induced damage in SH-SY5Y cells *via* the miR-1277-5p/IRS2 axis in PD (Sun Z. M. et al., 2022).

SNHG14 is detected on chromosome 15q11.2 and functions as an oncogene in cancers, kidney injury, and neurodegenerative diseases such as PD and AD, working as ceRNA (Qi et al., 2017; Wang et al., 2018; Zhuang et al., 2022). It was proved that SNHG14 is up-regulated in two ceRNA regulatory axes, including SNHG14/miR-519a-3p/ATG10 and SNHG14/miR-214-3p/KLF4 (Zhou et al., 2020b; Zhuang et al., 2022). Autophagy-related 10 (ATG10) is an E2-like enzyme involved in the autophagy (Zhang M.-Q. et al., 2018). Zhuang et al. revealed that the expression of ATG10 is positively regulated by SNHG14 through sponging miR-519a-3p (Zhuang et al., 2022). On the other hand, Krüppel-like factor 4 (KLF4) suppresses the cell cycle and is a kind of transcription factor, and it was shown that it could be pathogenic in AD and several human diseases (Zhou et al., 2020b). Zhou et al. disclosed that SNHG14, acting as a miR-214-3p sponge and up-regulating miR-214-3p, reduced damage to MPPCS-stimulated SK-N-SH cells by downregulating KLF4 (Zhou et al., 2020b). Altogether, studies have shown us that these members of the SNHG family can have a potential role as ceRNA in PD and can be promising in finding therapeutic approaches.

4.5. HOTAIR, MALAT1, and XIST associated ceRNA axes in PD

HOX antisense intergenic RNA (HOTAIR) is a 2.2 kb antisense transcript from the Homeobox C (HOXC) gene cluster located on 12q13.13 (Zhu and Zhu, 2022). HOTAIR has been shown to affect PD progression, although the exact function of this lncRNA remains unknown. In this respect, Lin et al. found that lncRNA HOTAIR is overexpressed in PD and influences the expression levels of RAB3IP by sponging miR-126-5p. The study shows that HOTAIR Knockdown has reduced the number of α-synuclein-positive cells (Lin et al., 2019). Similarly, Zhao et al. revealed that HOTAIR also experienced an up-regulation and regulated ATG10 expression by sponging miR-874-5p (Zhao J. Y. et al., 2020). The potential role of lncRNA HOTAIR makes it a challenging target for neurodegenerative diseases such as PD.

The metastasis-associated lung adenocarcinoma transcript 1 (MALAT1) lncRNA is located on human chromosome 11q13 (Zhang et al., 2017). Alternative splicing, transcriptional control, post-transcriptional control, and miRNA sponge interactions are just a few of the pathways in which lncRNA is implicated (Shi et al., 2015). MALAT1, which is abundantly expressed in brain tissues, is likely involved in forming synapses and other neurophysiological pathways (Abrishamdar et al., 2022). In this regard, Liu et al. reported that PD-related cell apoptosis is facilitated by MALAT1 through sponging miR-124. It is comprehended that MALAT1 is overexpressed in the PD model; however, additional research is necessary (Liu et al., 2017). X-inactive specific transcript (XIST) lncRNA is a crucial cell growth and development regulator. In addition to its original role in X-chromosome dosage adjustment, XIST acts as a ceRNA and contributes to the growth of tumors and other human disorders (Wang et al., 2021). Remarkably, Zhou et al. revealed that to regulate Sp1 expression, XIST sponges miR-199a-3p (Zhou Q. et al., 2021). Treatment with shXIST or miR-199a-3p successfully reduced behavioral signs of PD (Zhou Q. et al., 2021). Due to its crucial function in X-chromosome inactivation, XIST is a prominent lncRNA; nonetheless, more research is required to fully understand its function in PD.

4.6. linc-p21, LINC00943, LINC0938, and LINC001128 associated ceRNA axes in PD

Long intergenic non-coding RNAs (lincRNAs) are ncRNAs that are autonomously produced, have a length of more than 200 nucleotides, and do not overlap with identified coding genes. LincRNAs share characteristics with other members of the lncRNA family and account for more than half of all lncRNA transcripts in humans. LincRNAs were initially proposed by studies utilizing tiling arrays spanning genomic sequences, which discovered widespread transcription (Venter et al., 2001; Djebali et al., 2012) from areas with no identified coding genes (Kapranov et al., 2002; Rinn et al., 2003; Bertone et al., 2004; Maeda et al., 2006). The analysis of chromatin state signatures in murine cell types gave early evidence for the existence of functioning transcription units at the potential loci of these transcripts (Salditt-Georgieff and Darnell, 1982; Guttman et al., 2009). Because many lincRNAs overlap sequences with coding loci, they have been differentiated from the larger lncRNA class of transcripts. However, many publications fail to distinguish between these two types of transcripts and bundle them together as "lncRNAs." The rapid discovery and annotation of intergenic and genic lncRNAs have led to a growing understanding of the non-coding RNA's roles (Salditt-Georgieff and Darnell, 1982; Carninci et al., 2005).

The long intergenic non-coding RNA p21 (linc-p21) is localized on chromosome 6p21 (Amirinejad et al., 2020). It was initially discovered by stimulating the mouse's p53-dependent apoptosis (Ding et al., 2019). According to Ding et al. the linc-p21/miR-625/TRPM2 axis has a role in the etiology of PD. TRPM2 expression is increased by linc-p21, which interacts with miR-625, and TRPM2 knockdown lowers the MPP+-induced neuroinflammation (Ding et al., 2019). Similarly, Xu et al. discovered that linc-p21 sponges, miR-1277-5p, and the axis altered cell survival and apoptosis in MPP+-treated SH-SY5Y cells (Xu et al., 2018). linc-p21 is overexpressed in both the former and latter axes, and the probable involvement of linc-p21 in PD requires further investigation.

Long intergenic non-protein-coding RNA 943 (LINC00943) is a recently identified epigenetic transcript shown to be aberrantly produced in PD (Zhou et al., 2018). Furthermore, it was found that the downregulation of LINC00943 had a useful function in decreasing MPP+-induced neurotoxicity in SK-N-SH cells in an *in vitro* cellular model of PD (Meng et al., 2021). LINC00943 suppresses miR-15b-5p while increasing RAB3IP expression in PD (Meng et al., 2021). According to Lian et al. LINC00943 worked as a miR-7-5p sponge and controlled CXCL12 expression in MPP+-induced SK-N-SH cells, and LINC00943 knockdown may partly alleviate neuronal damage caused by MPP+, as LINC00943 was raised in MPP+-induced PD models (Lian et al., 2021). Similarly, Sun et al. demonstrated that knocking down LINC00943 might reduce nerve cell damage in a model of PD animal model. Linc00943 may favorably

regulate specificity protein 1 (SP1) by interacting with the ceRNA axis and inhibiting miR-338-3p (Sun X. M. et al., 2022). SP1 is a C2H2 zinc finger-structured DNA-binding protein that regulates gene transcription in some physiological and pathological processes (Chu, 2012). Monoamine oxidase B (MAO B) inhibitors, which block dopamine breakdown by inhibiting MAO B activity, are licensed and extensively used in the therapeutic treatment of PD (Yao et al., 2018). The promoter of the MAO B gene includes SP1 binding regions and its expression is directly regulated by SP1 (Shih et al., 2011).

Furthermore, Yousefi et al. investigated LINC0938 and LINC001128 involved in PD (Yousefi et al., 2022). Notably, LNC0938 was up-regulated, and on the other hand, LINC001128 was down-regulated. These two lincRNAs could be involved in ceRNA axes, including LINC0938/miR-24-3p/LRRK2, and LINC00112/miR-30c-5p/ATP13A2. Linc00938 could bind directly to hsa-miR-30c-5p, thus possibly regulating LRRK2 expression through the miR-30c-5p sponge (Yousefi et al., 2022). LRRK2 has a role in mitochondrial malfunction, intracellular ATP total, mitochondrial fission, mitochondrial transport, and oxidative stress (Sai et al., 2012; Park et al., 2018). Patients with the LRRK2 G2019S homozygous or R1441C heterozygous mutation have higher mitochondrial DNA (mtDNA) damage (Sanders et al., 2014). Another study found that LRRK2 is required to avoid ER stress and spontaneous neurodegeneration in *C. elegans* models missing the LRRK2 homolog (Sämann et al., 2009). On the other hand, on another axis, the increase in the ATP13A2 expression could be justified by two independent methods, one by binding hsa-miR-24-3p to ATP13A2 and the other by directly binding Linc01128 to ATP13A2. Therefore, the hsa-miR-24-3p and Linc01128 levels were decreased in PD; as a result, the ATP13A2 expression was increased in this disease (Yousefi et al., 2022). In this regard, the studies on the ceRNA axes involving lincRNAs must be continued in PD.

4.7. CircRNAs-associated ceRNA axes in PD

RNA sequencing is presently the only method that can provide a comprehensive landscape of circRNAs across the body and, in particular tissue locations (Philips et al., 2020). Specifically, ribo-minus RNA-Seq has enabled the identification of novel changes in circRNA expression as well as the investigation of these circRNAs' involvement in the condition of concern (Cooper et al., 2018). Circular RNAs are exceptionally stable regulatory molecules inside the cell because they are immune to exonuclease actions (Xie et al., 2017). CircRNAs have been characterized as protein decoys, scaffolds, and recruiters, as well as transcriptional regulators, miRNA sponges, and protein templates (Zhou W. Y. et al., 2020; Asadi et al., 2022). CircRNAs have an active role in muscular tissue formation (Legnini et al., 2017), synapse formation and activity field (Chen et al., 2019), neuronal gene expression regulation (van Rossum et al., 2016), and CNS differentiation and development (Mehta et al., 2020). CircRNAs are found in many different cell types but are especially abundant in neurons (Legnini et al., 2017; D'Ambra et al., 2019; Zhou W. Y. et al., 2020).

Notably, investigations into the involvement of circRNAs in PD are rising, and the roles of various circRNAs in the ceRNA axis have been established. In this regard, a circRNA derived from the SNCA gene (has_circ 0127305, commonly known as circSNCA) functions as a ceRNA of miR-7, up-regulating SNCA in PD. Moreover, pramipexol (PPX), a PD medication, suppresses circSNCA expression. Accordingly, Sang et al. demonstrated that inhibiting circSNCA and SNCA reduces apoptosis and promotes autophagy, reducing the development of PD (Sang et al., 2018). Furthermore, Chens et al. revealed increased circTLK1 expression in PD models (Chen W. et al., 2022). CircRNA circTLK1, encoded from TLK1 mRNA, was shown to be an oncogene in a renal cell cancer investigation. CircTLK1 acts as a molecular sponge for miR-136-5p, which increases CBX4 expression and promotes the development of renal cell carcinoma (Li et al., 2020). Afterward, Wu et al. discovered that circTLK1 had pro-ischemic stroke effects (Wu et al., 2019). Song et al. revealed the role of circTLK1 in myocardial ischemia/reperfusion damage (Song et al., 2020). The elimination of circTLK1 reduced PD-induced neuron damage. Overexpression of DAPK1 and suppression of miR-16a-5p abolished shcircTLK1's protective effect in neurons (Chen W. et al., 2022). Likewise, Cao et al. discovered that the expression of circ_0070441 increased in MPP+-treated SH-SY5Y cells (Cao et al., 2022). Furthermore, circ_0070441 suppresses miR-626 while increasing IRS2 expression levels through a ceRNA axis. Notably, circ_0070441 deficiency reduced MPP+-induced neuronal damage by regulating cell death and inflammation (Cao et al., 2022).

Unlike circSNCA, the circRNAs circzip-2 and circDLGAP4 have been identified to be changed in PD and to have a protective effect. On the one hand, Kumar et al. (2018) discovered circzip-2, a circRNA generated from the zip-2 gene, whose human homolog codes for CCAAT-enhancer-binding protein (C/EBP) which acted as bZIP transcription factor implicated in PD through regulating α-synuclein levels (Kumar et al., 2018; Valente et al., 2020). Cirzip-2 was predicted to sponge miR-60 using bioinformatic analysis. As a result, a reduction in circzip-2 may increase miR-60 activity, leading to downregulation of protective genes such as M60.4, ZK470.2, igeg-2, and idhg-1. On the other hand, Feng et al. (2020) reported in PD models (MPTP-induced animals and MPP+-induced cells) a reduction in the circDLGAP4 expression, which displayed neuroprotective effects *in vitro*. The authors expected that miR-134-5p might be a target for circDLGAP4 in both human and animal models, finding that this miRNA was elevated in both. Lastly, the same research established that the circDLGAP4/miR-134-5p axis influences CREB signaling and CREB downstream target gene transcription, including BDNF, Bcl-2, and PGC-1a, which are all neuroprotective proteins implicated in a variety of neurodegenerative diseases, including AD and PD (D'Orsi et al., 2017; Lv et al., 2018; Bawari et al., 2019).

4.8. Other ceRNAs axes

Under normal circumstances, the ceRNA axes within the cell are in equilibrium. Increasing or reducing the expression of each axis component might shift the direction in favor of abnormal circumstances (Sabaie et al., 2021). Remarkably, the majority of the remaining lncRNAs, which are the primary parts of the axes, are associated with increased expression. Xie et al. reported that SOX21-AS1 is overexpressed in MMP+-treated SH-SY5Y cells (Xie et al., 2021). In addition, SOX21-AS1 depletion weakened the

cell injury induced by MMP+. Moreover, SOX21-AS1 knockdown decreased ROS generation and levels of TNF-α, IL-1β, and IL-6 but increased SOD activity. However, SOX21-AS1 up-regulation led to the opposite results. Further, SOX21-AS1 could bind with miR-7-5p, whose overexpression relieved MMP+-induced cell injury. Additionally, insulin receptor substrate 2 (IRS2) served as the target gene of miR-7-5p, and its expression was positively modulated by SOX21-AS1. Similarly, IRS2 knockdown also had alleviative effects on cell injury stimulated by MMP+ treatment (Xie et al., 2021). In this regard, Xu et al. also reported increased expression levels of ID2-AS1 in SH-SY5Y cells. Furthermore, ID2-AS1 down-regulation weakened MPP+-induced cytotoxicity in SH-SY5Y cells and alleviated the neuronal damage in PD by regulating the miR-199a-5p/IFNAR1/JAK2/STAT1 axis (Xu et al., 2021). Similarly, Zheng et al. concluded that UCA1 experienced overexpression in MPP+-induced cytotoxicity in SH-SY5Y cells, and silencing of UCA1 protects SK-N-SH cells from MPP+-evoked cytotoxicity by targeting the miR-423-5p/KCTD20 axis. The overexpression of UCA1 causes KTCD20 expression levels to increase through inhibition of miR-423-5p (Zheng et al., 2021). KCTD20 can activate the Akt signaling pathway (Nawa and Matsuoka, 2013), which plays a crucial role in the pathogenesis of PD rats and the PD neurodegeneration (Huang et al., 2018; Furlong et al., 2019). It should be noted that AL049437 is one of the lncRNAs that is overexpressed in MPP+-treated SH-SY5Y cells. Zhang et al. reported that the high levels of AL049437 reduce the expression of miR-205-5p and increase the expression of MAPK1 in SH-SY5Y cells (Zhang L. et al., 2020). MAPK1 is also involved in another ceRNA axis in PD, such as SNHG1/miR-125b-5p/MAPK1 (Xiao et al., 2021). Conversely, Zhou et al. discovered that the expression levels of NORAD as a PD protector are decreased in PD, and it was concluded that NORAD was able to up-regulate SLC5A3 with interacting miR-204-5p and protect neuroblastoma cells from MPP+-induced damage (Zhou et al., 2020a). Similarly, PART1 is a protecting factor for PD by sponging miR-106b-5p, and MCL1 is a direct target for miR-106b-5p, and consequently, PART1 reduced MPP+-induced damage to SHSY5Y cells (Shen Y. E. et al., 2021).

In a creative procedure, Feng et al. used a synthetic miRNA sponge to assess miR-330/SHIP1/NF-κB ceRNA axes. Notably, the miR-330 synthetic sponge inhibits miR-330 and suppresses LPS-induced chronic neuroinflammation in PD by down-regulating the activity of microglia with reduced inflammatory cytokines *via* the SHIP1/NF-κB signaling pathway (Feng et al., 2021). Recent research indicates that neuroinflammation, defined by abnormal activation of microglia, may play a critical role in PD (Raza et al., 2019). Remarkably, Shen et al. revealed the protective effects of another lncRNA. MIAT causes neuroprotective effects in PD by inhibiting miR-34-5p and regulating SYT1 expression. As a crucial intercessor, SYT1 governs the release of the calcium-dependent neurotransmitter and is closely linked to physiological and cognitive development (Baker et al., 2018). Local amyloid peptide buildup is thought to cause neuronal degeneration, memory impairments, synapse loss, and malfunction (Mihaescu et al., 2022). SYT1 modulates synaptic amyloid; hence it might be used to treat nervous system problems (Kuzuya et al., 2016). It should be noted that the ABCA1/miR-873/A20 ceRNA axes can be used to target neuroinflammation. Inhibition of miR-873 through increased ABCA1 may play a dual protective role in PD as it induces intracellular cholesterol homeostasis and improves neuroinflammation (Wu et al., 2017).

Conversely, Xu et al. reported the non-protective role of GAS5 in PD. GAS5 positively regulates NLRP3 by competitive sponging of miR-223-3p. In addition, GAS5 knocking down causes an increase in the expression levels of miR-233-3p, which reduces inflammatory factors (Xu et al., 2020). Similarly, Zhang et al. revealed that decreasing the expression levels of MIR17HG reduces inflammatory responses in microglia in PD models. MIR17HG experiences an increase in PD inhibits miR-153-3p, and causes an increase in SNCA, directly affecting the PD development (Zhang et al., 2022).

5. Limitations

The present study had several limitations. On the one hand, this study attempted to serve as a road map for future research in this field and generate interest and excitement for future ceRNA investigations in PD, and these studies will undoubtedly assist in finishing this path. On the other hand, in the section on significant results, we attempted to provide all of the details relevant to all of these regulatory axes in Table 1. All precautions were made to avoid missing a study during the screening process, and three people collaborated on this part to ensure that this study included all of the studies completed in the area of PD. However, this is possible due to an individual mistake that may have left a study out.

6. Conclusion

In recent years, several ceRNA axes have been found and examined in various diseases. Because ceRNA interaction networks are multifactorial, they may provide an advantage in investigations of these complex neurodegenerative diseases such as PD, both at the level of biomarkers (combined RNA biomarkers panels) and targeted therapies (regulate the multiple disease-associated RNA levels at once by just targeting one). This study collected evidence that the ceRNA axis has a remarkable influence on PD development, each of which has the potential to be a distinguishing feature of this neurodegenerative disease. The multitude of studies in the field of ceRNA axes and the results of bioinformatic analysis of the enrichment of genes targeted in ceRNA axes, including cellular response to the metal ion, cellular response to oxidative stress, and positive regulation of macromolecule metabolic processes, indicate the importance of these axes in the development of PD. The strength of these studies appears to lie in how these axes provide the ability to narrow the border between diagnosis and treatment in PD. To conclude, the upward trend of studies around ceRNA axes will lead to the evolution of ceRNET and the evolution of our knowledge of this network as one of the superior molecular mechanisms that enable the transformation of studies in the field of treatment with a unique look at ceRNA axes.

Data availability statement

The original contributions presented in the study are included in the article/Supplementary material, further inquiries can be directed to the corresponding author.

Author contributions

MA, SG-F, and HS wrote the draft and revised it. MT and MR designed and supervised the study. BH, SA, GK, FF, MM, and MS-B collected the data and designed the figures and tables. All the authors read and approved the submitted version.

Acknowledgments

We would like to thank the Clinical Research Development Unit of Tabriz Valiasr Hospital, Tabriz University of Medical Sciences, Tabriz, Iran, for their assistance in this research.

Conflict of interest

The authors declare that the research was conducted in the absence of any commercial or financial relationships that could be construed as a potential conflict of interest.

Publisher's note

All claims expressed in this article are solely those of the authors and do not necessarily represent those of their affiliated organizations, or those of the publisher, the editors and the reviewers. Any product that may be evaluated in this article, or claim that may be made by its manufacturer, is not guaranteed or endorsed by the publisher.

Supplementary material

The Supplementary Material for this article can be found online at: https://www.frontiersin.org/articles/10.3389/fncel.2023.1044634/full#supplementary-material

References

Abrishamdar, M., Jalali, M. S., and Rashno, M. (2022). MALAT1 lncRNA and Parkinson's disease: the role in the pathophysiology and significance for diagnostic and therapeutic approaches. *Mol. Neurobiol.* 59, 5253–5262. doi: 10.1007/s12035-022-02899-z

Ala, U., Karreth, F. A., Bosia, C., Pagnani, A., Taulli, R., Léopold, V., et al. (2013). Integrated transcriptional and competitive endogenous RNA networks are cross-regulated in permissive molecular environments. *Proc. Nat. Acad. Sci. U.S.A.* 110, 7154–7159. doi: 10.1073/pnas.1222509110

Alieva, A. K., Filatova, E. V., Karabanov, A. V., Illarioshkin, S. N., Limborska, S. A., Shadrina, M. I., et al. (2015). miRNA expression is highly sensitive to a drug therapy in Parkinson's disease. *Parkinsonism Relat. Disord.* 21, 72–74. doi: 10.1016/j.parkreldis.2014.10.018

Amin, N., McGrath, A., and Chen, Y.-P. P. (2019). Evaluation of deep learning in non-coding RNA classification. *Nat. Mach. Intell.* 1, 246–256. doi: 10.1038/s42256-019-0051-2

Amirinejad, R., Rezaei, M., and Shirvani-Farsani, Z. (2020). An update on long intergenic noncoding RNA p21: a regulatory molecule with various significant functions in cancer. *Cell Biosci.* 10, 82. doi: 10.1186/s13578-020-00445-9

Asadi, M. R., Hassani, M., Kiani, S., Sabaie, H., Moslehian, M. S., Kazemi, M., et al. (2021). The perspective of dysregulated lncRNAs in Alzheimer's disease: a systematic scoping review. *Front. Aging Neurosci.* 13, 709568. doi: 10.3389/fnagi.2021.709568

Asadi, M. R., Moslehian, M. S., Sabaie, H., Sharifi-Bonab, M., Hakimi, P., Hussen, B. M., et al. (2022). CircRNA-associated CeRNAs regulatory axes in retinoblastoma: a systematic scoping review. *Front. Oncol.* 12, 910470. doi: 10.3389/fonc.2022.910470

Baker, K., Gordon, S. L., Melland, H., Bumbak, F., Scott, D. J., Jiang, T. J., et al. (2018). SYT1-associated neurodevelopmental disorder: a case series. *Brain* 141, 2576–2591. doi: 10.1093/brain/awy209

Balas, M., and Johnson, A. (2018). Exploring the mechanisms behind long noncoding RNAs and cancer. *Noncoding RNA Res.* 3, 108–117. doi: 10.1016/j.ncrna.2018.03.001

Bawari, S., Tewari, D., Argüelles, S., Sah, A. N., Nabavi, S. F., Xu, S., et al. (2019). Targeting BDNF signaling by natural products: novel synaptic repair therapeutics for neurodegeneration and behavior disorders. *Pharmacol. Res.* 148, 104458. doi: 10.1016/j.phrs.2019.104458

Beal, M. F. (2005). Mitochondria take center stage in aging and neurodegeneration. *Ann. Neurol.* 58, 495–505. doi: 10.1002/ana.20624

Bentley, S. R., Bortnick, S., Guella, I., Fowdar, J. Y., Silburn, P. A., Wood, S. A., et al. (2018). Pipeline to gene discovery-analysing familial Parkinsonism in the Queensland Parkinson's project. *Parkinsonism Relat. Disord.* 49, 34–41. doi: 10.1016/j.parkreldis.2017.12.033

Bertone, P., Stolc, V., Royce, T. E., Rozowsky, J. S., Urban, A. E., Zhu, X., et al. (2004). Global identification of human transcribed sequences with genome tiling arrays. *Science* 306, 2242–2246. doi: 10.1126/science.1103388

Bhat, S. A., Ahmad, S. M., Mumtaz, P. T., Malik, A. A., Dar, M. A., Urwat, U., et al. (2016). Long non-coding RNAs: Mechanism of action and functional utility. *Noncoding RNA Res.* 1, 43–50. doi: 10.1016/j.ncrna.2016.11.002

Bian, Z., Ji, W., Xu, B., Huang, W., Jiao, J., Shao, J., et al. (2020). The role of long noncoding RNA SNHG7 in human cancers (review). *Mol. Clin. Oncol.* 13, 45. doi: 10.3892/mco.2020.2115

Blauwendraat, C., Nalls, M. A., and Singleton, A. B. (2020). The genetic architecture of Parkinson's disease. *Lancet Neurol.* 19, 170–178. doi: 10.1016/S1474-4422(19)30287-X

Blochberger, A., and Jones, S. (2011). Clinical focus-parkinson's disease-clinical features and diagnosis. *Clin. Pharm.* 3, 361. doi: 10.1136/jnnp.2007.131045

Boros, F. A., Vécsei, L., and Klivényi, P. (2021). NEAT1 on the field of Parkinson's disease: offense, defense, or a player on the bench? *J. Parkinsons Dis.* 11, 123–138. doi: 10.3233/JPD-202374

Cao, B. Q., Wang, T., Qu, Q. M., Kang, T., and Yang, Q. (2018). Long noncoding RNA SNHG1 promotes neuroinflammation in parkinson's disease *via* regulating miR-7/NLRP3 pathway. *Neuroscience* 388, 118–127. doi: 10.1016/j.neuroscience.2018.07.019

Cao, X., Yeo, G., Muotri, A. R., Kuwabara, T., and Gage, F. H. (2006). Noncoding RNAs in the mammalian central nervous system. *Annu. Rev. Neurosci.* 29, 77–103. doi: 10.1146/annurev.neuro.29.051605.112839

Cao, X. Q., Guo, J. T., Mochizuki, H., Xu, D., Zhang, T., Han, H. P., et al. (2022). Circular RNA circ_0070441 regulates MPP+-triggered neurotoxic effect in SH-SY5Y cells *via* miR-626/IRS2 axis. *Metab. Brain Dis.* 37, 513–524. doi: 10.1007/s11011-021-00869-3

Carninci, P., Kasukawa, T., Katayama, S., Gough, J., Frith, M. C., Maeda, N., et al. (2005). The transcriptional landscape of the mammalian genome. *Science* 309, 1559–1563. doi: 10.1126/science.1112014

Castellani, R. J., Siedlak, S. L., Perry, G., and Smith, M. A. (2000). Sequestration of iron by Lewy bodies in Parkinson's disease. *Acta Neuropathol.* 100, 111–114. doi: 10.1007/s004010050001

Chen, B. J., Huang, S., and Janitz, M. (2019). Changes in circular RNA expression patterns during human foetal brain development. *Genomics* 111, 753–758. doi: 10.1016/j.ygeno.2018.04.015

Chen, C., Zhang, S., Wei, Y., and Sun, X. (2022). LncRNA RMST regulates neuronal apoptosis and inflammatory response *via* sponging miR-150-5p in Parkinson's disease. *Neuroimmunomodulation* 29, 55–62. doi: 10.1159/000518212

Chen, T., Hou, R., Li, C., Wu, C., and Xu, S. (2015). MPTP/MPP+ suppresses activation of protein C in Parkinson's disease. *J. Alzheimers Dis.* 43, 133–142. doi: 10.3233/JAD-140126

Chen, W., Hou, C., Wang, Y., Hong, L., Wang, F., and Zhang, J. (2022). Circular RNA circTLK1 regulates dopaminergic neuron injury during Parkinson's disease by targeting miR-26a-5p/DAPK1. *Neurosci. Lett.* 782, 136638. doi: 10.1016/j.neulet.2022.136638

Choi, B. S., Kim, H., Lee, H. J., Sapkota, K., Park, S. E., Kim, S., et al. (2014). Celastrol from 'Thunder God Vine' protects SH-SY5Y cells through the preservation of mitochondrial function and inhibition of p38 MAPK in a rotenone model of Parkinson's disease. *Neurochem. Res.* 39, 84–96. doi: 10.1007/s11064-013-1193-y

Chu, S. (2012). Transcriptional regulation by post-transcriptional modification-Role of phosphorylation in Sp1 transcriptional activity. *Gene* 508, 1–8. doi: 10.1016/j.gene.2012.07.022

Cooper, D. A., Cortés-López, M., and Miura, P. (2018). Genome-wide circRNA profiling from RNA-seq data. *Methods Mol. Biol.* 1724, 27–41. doi: 10.1007/978-1-4939-7562-4_3

D'Ambra, E., Capauto, D., and Morlando, M. (2019). Exploring the regulatory role of circular rnas in neurodegenerative disorders. *Int. J. Mol. Sci*. 20. doi: 10.3390/ijms20215477

Deas, E., Cremades, N., Angelova, P. R., Ludtmann, M. H., Yao, Z., Chen, S., et al. (2016). Alpha-synuclein oligomers interact with metal ions to induce oxidative stress and neuronal death in Parkinson's disease. *Antioxid. Redox Signal*. 24, 376–391. doi: 10.1089/ars.2015.6343

Dharap, A., Pokrzywa, C., Murali, S., Pandi, G., and Vemuganti, R. (2013). MicroRNA miR-324-3p induces promoter-mediated expression of RelA gene. *PLoS ONE* 8, e79467. doi: 10.1371/journal.pone.0079467

Dickson, D. W., Braak, H., Duda, J. E., Duyckaerts, C., Gasser, T., Halliday, G. M., et al. (2009). Neuropathological assessment of Parkinson's disease: refining the diagnostic criteria. *Lancet Neurol.* 8, 1150–1157. doi: 10.1016/S1474-4422(09)70238-8

Ding, X.-M., Zhao, L.-J., Qiao, H.-Y., Wu, S.-L., and Wang, X.-H. (2019). Long non-coding RNA-p21 regulates MPP+-induced neuronal injury by targeting miR-625 and derepressing TRPM2 in SH-SY5Y cells. *Chem. Biol. Interact*. 307, 73–81. doi: 10.1016/j.cbi.2019.04.017

Djebali, S., Davis, C. A., Merkel, A., Dobin, A., Lassmann, T., Mortazavi, A., et al. (2012). Landscape of transcription in human cells. *Nature* 489, 101–108. doi: 10.1038/nature11233

Dorsey, E., Elbaz, A., Nichols, E., Abd-Allah, F., Abdelalim, A., Adsuar, J., et al. (2018a). Global, regional, and national burden of Parkinson's disease, 1990–2016: a systematic analysis for the global burden of disease study 2016. *Lancet Neurol*. 17, 939–953. doi: 10.1016/S1474-4422(18)30295-3

Dorsey, E., Sherer, T., Okun, M. S., and Bloem, B. R. (2018b). The emerging evidence of the Parkinson pandemic. *J. Parkinsons Dis*. 8, S3–S8. doi: 10.3233/JPD-181474

D'Orsi, B., Mateyka, J., and Prehn, J. H. M. (2017). Control of mitochondrial physiology and cell death by the Bcl-2 family proteins Bax and Bok. *Neurochem. Int*. 109, 162–170. doi: 10.1016/j.neuint.2017.03.010

Dzamko, N., Zhou, J., Huang, Y., and Halliday, G. M. (2014). Parkinson's disease-implicated kinases in the brain; insights into disease pathogenesis. *Front. Mol. Neurosci*. 7, 57. doi: 10.3389/fnmol.2014.00057

Ebert, M. S., Neilson, J. R., and Sharp, P. A. (2007). MicroRNA sponges: competitive inhibitors of small RNAs in mammalian cells. *Nat. Methods* 4, 721–726. doi: 10.1038/nmeth1079

Feigin, V., and Collaborators, G. E. (2019). Global, regional, and national burden of epilepsy, 1990-2016: a systematic analysis for the global burden of disease study 2016. *Lancet Neurol*. 18, 357–375. doi: 10.1016/S1474-4422(18)30499-X

Feng, Y., Li, T., Xing, C., Wang, C., Duan, Y., Yuan, L., et al. (2021). Effective inhibition of miR-330/SHIP1/NF-κB signaling pathway *via* miR-330 sponge repolarizes microglia differentiation. *Cell Biol. Int*. 45, 785–794. doi: 10.1002/cbin.11523

Feng, Z., Zhang, L., Wang, S., and Hong, Q. (2020). Circular RNA circDLGAP4 exerts neuroprotective effects *via* modulating miR-134-5p/CREB pathway in Parkinson's disease. *Biochem. Biophys. Res. Commun*. 522, 388–394. doi: 10.1016/j.bbrc.2019.11.102

Forman, J. J., Legesse-Miller, A., and Coller, H. A. (2008). A search for conserved sequences in coding regions reveals that the let-7 microRNA targets Dicer within its coding sequence. *Proc. Natl. Acad. Sci. U.S.A*. 105, 14879–14884. doi: 10.1073/pnas.0803230105

Franco-Zorrilla, J. M., Valli, A., Todesco, M., Mateos, I., Puga, M. I., Rubio-Somoza, I., et al. (2007). Target mimicry provides a new mechanism for regulation of microRNA activity. *Nat. Genet*. 39, 1033–1037. doi: 10.1038/ng2079

Furlong, R. M., Lindsay, A., Anderson, K. E., Hawkins, P. T., Sullivan, A. M., and O'Neill, C. (2019). The Parkinson's disease gene PINK1 activates Akt *via* PINK1 kinase-dependent regulation of the phospholipid PI(3,4,5)P(3). *J. Cell Sci*. 132, jcs233221. doi: 10.1242/jcs.233221

Guo, X., Lin, M., Rockowitz, S., Lachman, H. M., and Zheng, D. (2014). Characterization of human pseudogene-derived non-coding RNAs for functional potential. *PLoS ONE* 9, e93972. doi: 10.1371/journal.pone.0093972

Guttman, M., Amit, I., Garber, M., French, C., Lin, M. F., Feldser, D., et al. (2009). Chromatin signature reveals over a thousand highly conserved large non-coding RNAs in mammals. *Nature* 458, 223–227. doi: 10.1038/nature07672

Hirose, T., Virnicchi, G., Tanigawa, A., Naganuma, T., Li, R., Kimura, H., et al. (2014). NEAT1 long noncoding RNA regulates transcription *via* protein sequestration within subnuclear bodies. *Mol. Biol. Cell* 25, 169–183. doi: 10.1091/mbc.e13-09-0558

Homma, Y., and Fukuda, M. (2016). Rabin8 regulates neurite outgrowth in both GEF activity-dependent and -independent manners. *Mol. Biol. Cell*. 27, 2107–2118. doi: 10.1091/mbc.E16-02-0091

Hu, X., Yang, L., and Mo, Y. Y. (2018). Role of pseudogenes in tumorigenesis. *Cancers* 10, 256. doi: 10.3390/cancers10080256

Huang, A., Zheng, H., Wu, Z., Chen, M., and Huang, Y. (2020). Circular RNA-protein interactions: functions, mechanisms, and identification. *Theranostics* 10, 3503–3517. doi: 10.7150/thno.42174

Huang, B., Liu, J., Meng, T., Li, Y., He, D., Ran, X., et al. (2018). Polydatin prevents lipopolysaccharide (LPS)-induced Parkinson's disease *via* regulation of the AKT/GSK3β-Nrf2/NF-κB signaling axis. *Front. Immunol*. 9, 2527. doi: 10.3389/fimmu.2018.02527

Hughes, A., Ben-Shlomo, Y., Daniel, S., and Lees, A. (1992). UK Parkinson's disease society brain bank clinical diagnostic criteria. *J. Neurol. Neurosurg. Psychiatry* 55, e4.

Ipsaro, J. J., and Joshua-Tor, L. (2015). From guide to target: molecular insights into eukaryotic RNA-interference machinery. *Nat. Struct. Mol. Biol*. 22, 20–28. doi: 10.1038/nsmb.2931

Ismail, A., Ning, K., Al-Hayani, A., Sharrack, B., and Azzouz, M. (2012). PTEN: A molecular target for neurodegeneratIve dIsorders. *Transl. Neurosci.* 3, 132–142. doi: 10.2478/s13380-012-0018-9

Jeck, W. R., Sorrentino, J. A., Wang, K., Slevin, M. K., Burd, C. E., Liu, J., et al. (2013). Circular RNAs are abundant, conserved, and associated with ALU repeats. *RNA* 19, 141–157. doi: 10.1261/rna.035667.112

Jenner, P., and Olanow, C. W. (2006). The pathogenesis of cell death in Parkinson's disease. *Neurology* 66 (10 Suppl. 4), S24–S36. doi: 10.1212/WNL.66.10_suppl_4.S24

Kapranov, P., Cawley, S. E., Drenkow, J., Bekiranov, S., Strausberg, R. L., Fodor, S. P., et al. (2002). Large-scale transcriptional activity in chromosomes 21 and 22. *Science* 296, 916–919. doi: 10.1126/science.1068597

Kelley, N., Jeltema, D., Duan, Y., and He, Y. (2019). The NLRP3 inflammasome: an overview of mechanisms of activation and regulation. *Int. J. Mol. Sci*. 20, 3328. doi: 10.3390/ijms20133328

Koutsodontis, G., Moustakas, A., and Kardassis, D. (2002). The role of Sp1 family members, the proximal GC-rich motifs, and the upstream enhancer region in the regulation of the human cell cycle inhibitor p21WAF-1/Cip1 gene promoter. *Biochemistry* 41, 12771–12784. doi: 10.1021/bi026141q

Kuleshov, M. V., Jones, M. R., Rouillard, A. D., Fernandez, N. F., Duan, Q., Wang, Z., et al. (2016). Enrichr: a comprehensive gene set enrichment analysis web server 2016 update. *Nucleic Acids Res*. 44, W90–W97. doi: 10.1093/nar/gkw377

Kumar, L., Shamsuzzama, J. P., Haque, R., Shukla, S., and Nazir, A. (2018). Functional Characterization of novel circular RNA Molecule, circzip-2 and its synthesizing gene zip-2 in C-elegans model of Parkinson's disease. *Mol. Neurobiol*. 55, 6914–6926. doi: 10.1007/s12035-018-0903-5

Kurvits, L., Lättekivi, F., Reimann, E., Kadastik-Eerme, L., Kasterpalu, K. M., Kõks, S., et al. (2021). Transcriptomic profiles in Parkinson's disease. *Exp. Biol. Med*. 246, 584–595. doi: 10.1177/1535370220967325

Kuzuya, A., Zoltowska, K. M., Post, K. L., Arimon, M., Li, X., Svirsky, S., et al. (2016). Identification of the novel activity-driven interaction between synaptotagmin 1 and presenilin 1 links calcium, synapse, and amyloid beta. *BMC Biol*. 14, 25. doi: 10.1186/s12915-016-0248-3

Legnini, I., Di Timoteo, G., Rossi, F., Morlando, M., Briganti, F., Sthandier, O., et al. (2017). Circ-ZNF609 is a circular RNA that can be translated and functions in myogenesis. *Mol. Cell*. 66, 22–37.e9. doi: 10.1016/j.molcel.2017.02.017

Li, J., Huang, C., Zou, Y., Ye, J., Yu, J., and Gui, Y. (2020). CircTLK1 promotes the proliferation and metastasis of renal cell carcinoma by sponging miR-136-5p. *Mol. Cancer* 19, 103. doi: 10.1186/s12943-020-01225-2

Li, J., Quan, H., Liu, Q., Si, Z., He, Z., and Qi, H. (2013). Alterations of axis inhibition protein 1 (AXIN1) in hepatitis B virus-related hepatocellular carcinoma and overexpression of AXIN1 induces apoptosis in hepatocellular cancer cells. *Oncol. Res. Feat. Preclin. Clin. Cancer Ther*. 20, 281–288. doi: 10.3727/096504013X13639794277608

Lian, H., Wang, B. H., Lu, Q., Chen, B., and Yang, H. (2021). LINC00943 knockdown exerts neuroprotective effects in Parkinson's disease through regulates CXCL12 expression by sponging miR-7-5p. *Genes Genom*. 43, 797–805. doi: 10.1007/s13258-021-01084-1

Lin, Q., Hou, S., Dai, Y., Jiang, N., and Lin, Y. (2019). LncRNA HOTAIR targets miR-126-5p to promote the progression of Parkinson's disease through RAB3IP. *Biol. Chem*. 400, 1217–1228. doi: 10.1515/hsz-2018-0431

Liu, R. G., Li, F. L., and Zhao, W. J. (2020). Long noncoding RNA NEAT1 knockdown inhibits MPP+-induced apoptosis, inflammation and cytotoxicity in SK-N-SH cells by regulating miR-212-5p/RAB3IP axis. *Neurosci. Lett*. 731, 135060. doi: 10.1016/j.neulet.2020.135060

Liu, T., Zhang, Y., Liu, W. H., and Zhao, J. S. (2021). LncRNA NEAT1 regulates the development of Parkinson's disease by targeting AXIN1 *via* sponging miR-212-3p. *Neurochem. Res*. 46, 230–240. doi: 10.1007/s11064-020-03157-1

Liu, W., Zhang, Q. S., Zhang, J. L., Pan, W. J., Zhao, J. Y., and Xu, Y. M. (2017). Long non-coding RNA MALAT1 contributes to cell apoptosis by sponging miR-124 in Parkinson disease. *Cell Biosci*. 7, 19. doi: 10.1186/s13578-017-0147-5

Lopez-Ilasaca, M. (1998). Signaling from G-protein-coupled receptors to mitogen-activated protein (MAP)-kinase cascades. *Biochem. Pharmacol*. 56, 269–277. doi: 10.1016/S0006-2952(98)00059-8

Lv, J., Jiang, S., Yang, Z., Hu, W., Wang, Z., Li, T., et al. (2018). PGC-1α sparks the fire of neuroprotection against neurodegenerative disorders. *Ageing Res. Rev*. 44, 8–21. doi: 10.1016/j.arr.2018.03.004

Maeda, N., Kasukawa, T., Oyama, R., Gough, J., Frith, M., Engström, P. G., et al. (2006). Transcript annotation in FANTOM3: mouse gene catalog based on physical cDNAs. *PLoS Genet*. 2, e62. doi: 10.1371/journal.pgen.0020062

Mamelak, M. (2018). Parkinson's disease, the dopaminergic neuron and gammahydroxybutyrate. *Neurol. Ther.* 7, 5–11. doi: 10.1007/s40120-018-0091-2

Mehta, S. L., Dempsey, R. J., and Vemuganti, R. (2020). Role of circular RNAs in brain development and CNS diseases. *Prog. Neurobiol.* 186, 101746. doi: 10.1016/j.pneurobio.2020.101746

Meng, C., Gao, J., Ma, Q., Sun, Q., and Qiao, T. (2021). LINC00943 knockdown attenuates MPP+-induced neuronal damage *via* miR-15b-5p/RAB3IP axis in SK-N-SH cells. *Neurol. Res.* 43, 181–190. doi: 10.1080/01616412.2020.1834290

Miao, Q., Ni, B., and Tang, J. (2021). Coding potential of circRNAs: new discoveries and challenges. *PeerJ* 9, e10718. doi: 10.7717/peerj.10718

Mielke, K., and Herdegen, T. (2000). JNK and p38 stresskinases–degenerative effectors of signal-transduction-cascades in the nervous system. *Prog. Neurobiol.* 61, 45–60. doi: 10.1016/S0301-0082(99)00042-8

Mihaescu, A. S., Valli, M., Uribe, C., Diez-Cirarda, M., Masellis, M., Graff-Guerrero, A., et al. (2022). Beta amyloid deposition and cognitive decline in Parkinson's disease: a study of the PPMI cohort. *Mol. Brain* 15, 79. doi: 10.1186/s13041-022-00964-1

Moher, D., Liberati, A., Tetzlaff, J., Altman, D. G., and Group, P. (2010). Preferred reporting items for systematic reviews and meta-analyses: the PRISMA statement. *Int. J. Surg.* 8, 336–341. doi: 10.1016/j.ijsu.2010.02.007

Moreno-García, L., López-Royo, T., Calvo, A. C., Toivonen, J. M., de la Torre, M., Moreno-Martínez, L., et al. (2020). Competing endogenous RNA networks as biomarkers in neurodegenerative diseases. *Int. J. Mol. Sci.* 21, 9582. doi: 10.3390/ijms21249582

Nawa, M., and Matsuoka, M. (2013). KCTD20, a relative of BTBD10, is a positive regulator of Akt. *BMC Biochem.* 14, 27. doi: 10.1186/1471-2091-14-27

Nies, Y. H., Mohamad Najib, N. H., Lim, W. L., Kamaruzzaman, M. A., Yahaya, M. F., and Teoh, S. L. (2021). MicroRNA dysregulation in Parkinson's disease: a narrative review. *Front. Neurosci.* 15, 660379. doi: 10.3389/fnins.2021.660379

Park, J. S., Davis, R. L., and Sue, C. M. (2018). Mitochondrial dysfunction in parkinson's disease: new mechanistic insights and therapeutic perspectives. *Curr. Neurol. Neurosci. Rep.* 18, 21. doi: 10.1007/s11910-018-0829-3

Parker, W. D. Jr., Parks, J. K., and Swerdlow, R. H. (2008). Complex I deficiency in Parkinson's disease frontal cortex. *Brain Res.* 1189, 215–218. doi: 10.1016/j.brainres.2007.10.061

Pei, B., Sisu, C., Frankish, A., Howald, C., Habegger, L., Mu, X. J., et al. (2012). The GENCODE pseudogene resource. *Genome Biol.* 13, 1–26. doi: 10.1186/gb-2012-13-9-r51

Philips, A., Nowis, K., Stelmaszczuk, M., Jackowiak, P., Podkowiński, J., Handschuh, L., et al. (2020). Expression Landscape of circRNAs in *Arabidopsis thaliana* seedlings and adult tissues. *Front. Plant Sci.* 11, 576581. doi: 10.3389/fpls.2020.576581

Poewe, W., Seppi, K., Tanner, C. M., Halliday, G. M., Brundin, P., Volkmann, J., et al. (2017). Parkinson disease. *Nat. Rev. Dis. Primers* 3, 17013. doi: 10.1038/nrdp.2017.13

Poliseno, L., Salmena, L., Zhang, J., Carver, B., Haveman, W. J., and Pandolfi, P. P. (2010). A coding-independent function of gene and pseudogene mRNAs regulates tumour biology. *Nature* 465, 1033–1038. doi: 10.1038/nature09144

Prats, A. C., David, F., Diallo, L. H., Roussel, E., Tatin, F., Garmy-Susini, B., et al. (2020). Circular RNA, the key for translation. *Int. J. Mol. Sci.* 21, 8591. doi: 10.3390/ijms21228591

Qi, X., Shao, M., Sun, H., Shen, Y., Meng, D., and Huo, W. (2017). Long non-coding RNA SNHG14 promotes microglia activation by regulating miR-145-5p/PLA2G4A in cerebral infarction. *Neuroscience* 348, 98–106. doi: 10.1016/j.neuroscience.2017.02.002

Qi, X., Zhang, D. H., Wu, N., Xiao, J. H., Wang, X., and Ma, W. (2015). ceRNA in cancer: possible functions and clinical implications. *J. Med. Genet.* 52, 710–718. doi: 10.1136/jmedgenet-2015-103334

Quinlan, S., Kenny, A., Medina, M., Engel, T., and Jimenez-Mateos, E. M. (2017). MicroRNAs in neurodegenerative diseases. *Int. Rev. Cell Mol. Biol.* 334, 309–343. doi: 10.1016/bs.ircmb.2017.04.002

Raza, C., Anjum, R., and Shakeel, N. U. A. (2019). Parkinson's disease: mechanisms, translational models and management strategies. *Life Sci.* 226, 77–90. doi: 10.1016/j.lfs.2019.03.057

Reyes, J. F., Sackmann, C., Hoffmann, A., Svenningsson, P., Winkler, J., Ingelsson, M., et al. (2019). Binding of α-synuclein oligomers to Cx32 facilitates protein uptake and transfer in neurons and oligodendrocytes. *Acta Neuropathol.* 138, 23–47. doi: 10.1007/s00401-019-02007-x

Rinn, J. L., Euskirchen, G., Bertone, P., Martone, R., Luscombe, N. M., Hartman, S., et al. (2003). The transcriptional activity of human chromosome 22. *Genes Dev.* 17, 529–540. doi: 10.1101/gad.1055203

Rybak-Wolf, A., Stottmeister, C., GlaŽar, P., Jens, M., Pino, N., Giusti, S., et al. (2015). Circular RNAs in the mammalian brain are highly abundant, conserved, and dynamically expressed. *Mol. Cell* 58, 870–885. doi: 10.1016/j.molcel.2015.03.027

Sabaie, H., Amirinejad, N., Asadi, M. R., Jalaiei, A., Daneshmandpour, Y., Rezaei, O., et al. (2021). Molecular insight into the therapeutic potential of long non-coding RNA-associated competing endogenous RNA axes in Alzheimer's disease: a systematic scoping review. *Front. Aging Neurosci.* 13, 742242. doi: 10.3389/fnagi.2021.742242

Saeed, M. (2018). Genomic convergence of locus-based GWAS meta-analysis identifies AXIN1 as a novel Parkinson's gene. *Immunogenetics.* 70, 563–570. doi: 10.1007/s00251-018-1068-0

Sai, Y., Zou, Z., Peng, K., and Dong, Z. (2012). The Parkinson's disease-related genes act in mitochondrial homeostasis. *Neurosci. Biobehav. Rev.* 36, 2034–2043. doi: 10.1016/j.neubiorev.2012.06.007

Salditt-Georgieff, M., and Darnell, J. E. Jr. (1982). Further evidence that the majority of primary nuclear RNA transcripts in mammalian cells do not contribute to mRNA. *Mol. Cell. Biol.* 2, 701–707. doi: 10.1128/mcb.2.6.701-707.1982

Salmena, L., Poliseno, L., Tay, Y., Kats, L., and Pandolfi, P. P. (2011). A ceRNA hypothesis: the rosetta stone of a hidden RNA language? *Cell* 146, 353–358. doi: 10.1016/j.cell.2011.07.014

Sämann, J., Hegermann, J., von Gromoff, E., Eimer, S., Baumeister, R., and Schmidt, E. (2009). Caenorhabditits elegans LRK-1 and PINK-1 act antagonistically in stress response and neurite outgrowth. *J. Biol. Chem.* 284, 16482–16491. doi: 10.1074/jbc.M808255200

Sanders, L. H., McCoy, J., Hu, X., Mastroberardino, P. G., Dickinson, B. C., Chang, C. J., et al. (2014). Mitochondrial DNA damage: molecular marker of vulnerable nigral neurons in Parkinson's disease. *Neurobiol. Dis.* 70, 214–223. doi: 10.1016/j.nbd.2014.06.014

Sang, Q. L., Liu, X. Y., Wang, L. B., Qi, L., Sun, W. P., Wang, W. Y., et al. (2018). CircSNCA downregulation by pramipexole treatment mediates cell apoptosis and autophagy in Parkinson's disease by targeting miR-7. *Aging* 10, 1281–1293. doi: 10.18632/aging.101466

Schapira, A. H., and Jenner, P. (2011). Etiology and pathogenesis of Parkinson's disease. *Mov. Disord.* 26, 1049–1055. doi: 10.1002/mds.23732

Schmidt, T., Samaras, P., Frejno, M., Gessulat, S., Barnert, M., Kienegger, H., et al. (2018). ProteomicsDB. *Nucleic Acids Res.* 46, D1271–D1281. doi: 10.1093/nar/gkx1029

Sebastian, H., Daniela, B., Thomas, G., Honglei, C., Chun, Y., Postuma Ronald, B., et al. (2019). Update of the MDS research criteria for prodromal Parkinson's disease. *Mov. Disord.* 34, 1464–1470. doi: 10.1002/mds.27802

Selbach, M., Schwanhäusser, B., Thierfelder, N., Fang, Z., Khanin, R., and Rajewsky, N. (2008). Widespread changes in protein synthesis induced by microRNAs. *Nature* 455, 58–63. doi: 10.1038/nature07228

Shen, Y., Cui, X. T., Hu, Y. H., Zhang, Z. Z., and Zhang, Z. Y. (2021). LncRNA-MIAT regulates the growth of SHSY5Y cells by regulating the miR-34-5p-SYT1 axis and exerts a neuroprotective effect in a mouse model of Parkinson's disease. *Am. J. Transl. Res.* 13, 9993–10013.

Shen, Y. E., Cui, X. T., Xu, N., Hu, Y. H., and Zhang, Z. Y. (2021). lncRNA PART1 mitigates MPP+-induced neuronal injury in SH-SY5Y cells *via* micRNA-106b-5p/MCL1 axis. *Am. J. Transl. Res.* 13, 8897–8908.

Shi, X., Sun, M., Wu, Y., Yao, Y., Liu, H., Wu, G., et al. (2015). Post-transcriptional regulation of long noncoding RNAs in cancer. *Tumour Biol.* 36, 503–513. doi: 10.1007/s13277-015-3106-y

Shih, J. C., Wu, J. B., and Chen, K. (2011). Transcriptional regulation and multiple functions of MAO genes. *J Neural Transm.* 118, 979–986. doi: 10.1007/s00702-010-0562-9

Singh, G., and Storey, K. B. (2021). MicroRNA cues from nature: a roadmap to decipher and combat challenges in human health and disease? *Cells* 10, 3374. doi: 10.3390/cells10123374

Song, Y. F., Zhao, L., Wang, B. C., Sun, J. J., Hu, J. L., Zhu, X. L., et al. (2020). The circular RNA TLK1 exacerbates myocardial ischemia/reperfusion injury *via* targeting miR-214/RIPK1 through TNF signaling pathway. *Free Radic. Biol. Med.* 155, 69–80. doi: 10.1016/j.freeradbiomed.2020.05.013

Straniero, L., Rimoldi, V., Samarani, M., Goldwurm, S., Di Fonzo, A., Krüger, R., et al. (2017). The GBAP1 pseudogene acts as a ceRNA for the glucocerebrosidase gene GBA by sponging miR-22-3p. *Sci. Rep.* 7, 12702. doi: 10.1038/s41598-017-12973-5

Sun, Q., Zhang, Y. L., Wang, S. L., Yang, F., Cai, H. X., Xing, Y., et al. (2021). NEAT1 decreasing suppresses Parkinson's disease progression *via* acting as miR-1301-3p sponge. *J. Mol. Neurosci.* 71, 369–378. doi: 10.1007/s12031-020-01660-2

Sun, X. M., Zhang, C. Y., Tao, H., Yao, S. Y., and Wu, X. L. (2022). LINC00943 acts as miR-338-3p sponge to promote MPP+-induced SKN-SH cell injury by directly targeting SP1 in Parkinson's disease. *Brain Res.* 1782, 147814. doi: 10.1016/j.brainres.2022.147814

Sun, Z. M., Song, L. X., and Li, J. Z. (2022). Knockdown of small nucleolar RNA host gene 10 (SNHG10) alleviates the injury of human neuroblastoma cells *via* the miR-1277-5p/insulin substrate receptor 2 axis. *Bioengineered* 13, 709–720. doi: 10.1080/21655979.2021.2012623

Szklarczyk, D., Gable, A. L., Nastou, K. C., Lyon, D., Kirsch, R., Pyysalo, S., et al. (2021). The STRING database in 2021: customizable protein–protein networks, and functional characterization of user-uploaded gene/measurement sets. *Nucleic Acids Res.* 49, D605–D612. doi: 10.1093/nar/gkab835

Titze-de-Almeida, S. S., Soto-Sánchez, C., Fernandez, E., Koprich, J. B., Brotchie, J. M., and Titze-de-Almeida, R. (2020). The promise and challenges of developing miRNA-based therapeutics for Parkinson's disease. *Cells* 9, 841. doi: 10.3390/cells9040841

Tomlinson, C. L., Stowe, R., Patel, S., Rick, C., Gray, R., and Clarke, C. E. (2010). Systematic review of levodopa dose equivalency reporting in Parkinson's disease. *Move. Disord.* 25, 2649–2653. doi: 10.1002/mds.23429

Tosato, M., and Di Marco, V. (2019). Metal chelation therapy and Parkinson's disease: a critical review on the thermodynamics of complex formation between relevant metal ions and promising or established drugs. *Biomolecules* 9, 269. doi: 10.3390/biom9070269

Triplett, J. C., Zhang, Z., Sultana, R., Cai, J., Klein, J. B., Büeler, H., et al. (2015). Quantitative expression proteomics and phosphoproteomics profile of brain from PINK1

knockout mice: insights into mechanisms of familial Parkinson's disease. *J. Neurochem*. 133, 750–765. doi: 10.1111/jnc.13039

Valente, T., Dentesano, G., Ezquerra, M., Fernandez-Santiago, R., Martinez-Martin, J., Gallastegui, E., et al. (2020). CCAAT/enhancer binding protein δ is a transcriptional repressor of α-synuclein. *Cell Death Differ*. 27, 509–524. doi: 10.1038/s41418-019-0368-8

van Rossum, D., Verheijen, B. M., and Pasterkamp, R. J. (2016). Circular RNAs: novel regulators of neuronal development. *Front. Mol. Neurosci*. 9, 74. doi: 10.3389/fnmol.2016.00074

Venter, J. C., Adams, M. D., Myers, E. W., Li, P. W., Mural, R. J., Sutton, G. G., et al. (2001). The sequence of the human genome. *Science* 291, 1304–1351. doi: 10.1126/science.1058040

Wang, J., and Song, W. (2016). Regulation of LRRK2 promoter activity and gene expression by Sp1. *Mol. Brain*. 9, 33. doi: 10.1186/s13041-016-0215-5

Wang, K. C., and Chang, H. Y. (2011). Molecular mechanisms of long noncoding RNAs. *Mol. Cell*. 43, 904–914. doi: 10.1016/j.molcel.2011.08.018

Wang, Q., Teng, Y., Wang, R., Deng, D., You, Y., Peng, Y., et al. (2018). The long non-coding RNA SNHG14 inhibits cell proliferation and invasion and promotes apoptosis by sponging miR-92a-3p in glioma. *Oncotarget* 9, 12112–12124. doi: 10.18632/oncotarget.23960

Wang, S., Wen, Q., Xiong, B., Zhang, L., Yu, X., and Ouyang, X. (2021). Long noncoding RNA NEAT1 knockdown ameliorates 1-methyl-4-phenylpyridine-induced cell injury through MicroRNA-519a-3p/SP1 axis in Parkinson disease. *World Neurosurg*. 156, e93–e103. doi: 10.1016/j.wneu.2021.08.147

Wang, W., Min, L., Qiu, X., Wu, X., Liu, C., Ma, J., et al. (2021). Biological function of long non-coding RNA (LncRNA) Xist. *Front. Cell Dev. Biol*. 9, 645647. doi: 10.3389/fcell.2021.645647

Wei, X., Cai, M., and Jin, L. (2021). The function of the metals in regulating epigenetics during Parkinson's disease. *Front. Genet*. 11, 616083. doi: 10.3389/fgene.2020.616083

Winklhofer, K. F., and Haass, C. (2010). Mitochondrial dysfunction in Parkinson's disease. *Biochim. Biophys. Acta*. 1802, 29–44. doi: 10.1016/j.bbadis.2009.08.013

Wu, F., Han, B., Wu, S., Yang, L., Leng, S., Li, M., et al. (2019). Circular RNA TLK1 aggravates neuronal injury and neurological deficits after ischemic stroke *via* miR-335-3p/TIPARP. *J. Neurosci*. 39, 7369–7393. doi: 10.1523/JNEUROSCI.0299-19.2019

Wu, J. H., Wu, J., Yu, X. M., Yang, Z. Q., Xie, X. F., and Yue, J. (2017). Inhibition of miR-873 provides therapeutic benefit in lipopolysaccharide-induced Parkinson disease animal model. *Chin. J. Pharmacol. Toxicol*. 31, 961–962. doi: 10.1155/2020/8735249

Xiao, X., Tan, Z., Jia, M., Zhou, X., Wu, K., Ding, Y., et al. (2021). Long noncoding RNA SNHG1 knockdown ameliorates apoptosis, oxidative stress and inflammation in models of Parkinson's disease by inhibiting the miR-125b-5p/MAPK1 axis. *Neuropsychiatr. Dis. Treat*. 17, 1153–1163. doi: 10.2147/NDT.S286778

Xie, L., Mao, M., Xiong, K., and Jiang, B. (2017). Circular RNAs: A novel player in development and disease of the central nervous system. *Front. Cell. Neurosci*. 11, 354. doi: 10.3389/fncel.2017.00354

Xie, Y., Zhang, S., Lv, Z., Long, T., Luo, Y., and Li, Z. (2021). SOX21-AS1 modulates neuronal injury of MMP+-treated SH-SY5Y cells *via* targeting miR-7-5p and inhibiting IRS2. *Neurosci. Lett*. 746, 135602. doi: 10.1016/j.neulet.2020.135602

Xu, F. R., Wang, H., Tian, J., and Xu, H. Y. (2021). Down-Regulation of ID2-AS1 alleviates the neuronal injury induced by 1-methy1-4-phenylpyridinium in human neuroblastoma cell line SH-SY5Y cells through regulating miR-199a-5p/IFNAR1/JAK2/STAT1 axis. *Neurochem. Res*. 46, 2192–2203. doi: 10.1007/s11064-021-03356-4

Xu, W., San Lucas, A., Wang, Z., and Liu, Y. (2014). Identifying microRNA targets in different gene regions. *BMC Bioinformatics* 15, S4. doi: 10.1186/1471-2105-15-S7-S4

Xu, W., Zhang, L., Geng, Y., Liu, Y., and Zhang, N. (2020). Long noncoding RNA GAS5 promotes microglial inflammatory response in Parkinson's disease by regulating NLRP3 pathway through sponging miR-223-3p. *Int. Immunopharmacol*. 85, 106614. doi: 10.1016/j.intimp.2020.106614

Xu, X. N., Zhuang, C. L., Wu, Z. M., Qiu, H. Y., Feng, H. X., and Wu, J. (2018). LincRNA-p21 inhibits cell viability and promotes cell apoptosis in Parkinson's disease through activating -synuclein expression. *Biomed. Res. Int*. 2018, 10. doi: 10.1155/2018/8181374

Yao, L., Dai, X., Sun, Y., Wang, Y., Yang, Q., Chen, X., et al. (2018). Inhibition of transcription factor SP1 produces neuroprotective effects through decreasing MAO B activity in MPTP/MPP(+) Parkinson's disease models. *J. Neurosci. Res*. 96, 1663–1676. doi: 10.1002/jnr.24266

Yousefi, M., Peymani, M., Ghaedi, K., Irani, S., and Etemadifar, M. (2022). Significant modulations of linc001128 and linc0938 with miR-24-3p and miR-30c-5p in Parkinson disease. *Sci. Rep*. 12, 2569. doi: 10.1038/s41598-022-06539-3

Yu, X., Li, Z., Zheng, H., Chan, M. T., and Wu, W. K. K. (2017). NEAT 1: a novel cancer-related long non-coding RNA. *Cell Prolif*. 50, e12329. doi: 10.1111/cpr.12329

Zhang, H., Wang, Z., Hu, K., and Liu, H. (2021). Downregulation of long noncoding RNA SNHG7 protects against inflammation and apoptosis in Parkinson's disease model by targeting the miR-425-5p/TRAF5/NF-κB axis. *J. Biochem. Mol. Toxicol*. 35, e22867. doi: 10.1002/jbt.22867

Zhang, J., Zhou, W., Liu, Y., Liu, T., Li, C., and Wang, L. (2018). Oncogenic role of microRNA-532-5p in human colorectal cancer *via* targeting of the 5'UTR of RUNX3. *Oncol. Lett*. 15, 7215–7220. doi: 10.3892/ol.2018.8217

Zhang, J. Z., Yang, Y., Zhou, C. Y., Zhu, R. L., Xiao, X., Zhou, B., et al. (2022). LncRNA miR-17-92a-1 cluster host gene (MIR17HG) promotes neuronal damage and microglial activation by targeting the microRNA-153-3p/alpha-synuclein axis in Parkinson's disease. *Bioengineered* 13, 4493–4516. doi: 10.1080/21655979.2022.2033409

Zhang, L., Wang, J., Liu, Q., Xiao, Z., and Dai, Q. (2020). Knockdown of long non-coding RNA AL049437 mitigates MPP+-induced neuronal injury in SH-SY5Y cells *via* the microRNA-205-5p/MAPK1 axis. *Neurotoxicology* 78, 29–35. doi: 10.1016/j.neuro.2020.02.004

Zhang, M.-Q., Li, J.-R., Peng, Z.-G., and Zhang, J.-P. (2018). Differential effects of autophagy-related 10 protein on HCV replication and autophagy flux are mediated by its cysteine44 and cysteine135. *Front. Immunol*. 9, 2176. doi: 10.3389/fimmu.2018.02176

Zhang, X., Hamblin, M. H., and Yin, K. J. (2017). The long noncoding RNA Malat1: its physiological and pathophysiological functions. *RNA Biol*. 14, 1705–1714. doi: 10.1080/15476286.2017.1358347

Zhang, X., Wang, Y. C., Zhao, Z. Q., Chen, X. X., Li, W., and Li, X. T. (2020). Transcriptome sequencing reveals aerobic exercise training-associated lncRNAs for improving Parkinson's disease. *3 Biotech* 10, 9. doi: 10.1007/s13205-020-02483-z

Zhang, Z., Yao, W., Yuan, D., Huang, F., Liu, Y., Luo, G., et al. (2020). Effects of connexin 32-mediated lung inflammation resolution during liver ischemia reperfusion. *Dig. Dis. Sci*. 65, 2914–2924. doi: 10.1007/s10620-019-06020-8

Zhao, J., Geng, L. J., Chen, Y., and Wu, C. F. (2020). SNHG1 promotes MPP+-induced cytotoxicity by regulating PTEN/AKT/mTOR signaling pathway in SH-SY5Y cells *via* sponging miR-153-3p. *Biol. Res*. 53, 11. doi: 10.1186/s40659-020-00278-3

Zhao, J. Y., Li, H. L., and Chang, N. (2020). lncRNA HOTAIR PROMOTES MPP plus -induced neuronal injury in parkinson's disease by regulating the MIR-874-5P/ATG10 AXIS. *EXCLI J*. 19, 1141–1153. doi: 10.17179/excli2020-2286

Zhao, S., Wang, Y., Luo, M., Cui, W., Zhou, X., and Miao, L. (2018). Long noncoding RNA small nucleolar RNA host gene 1 (SNHG1) promotes renal cell carcinoma progression and metastasis by negatively regulating miR-137. *Med. Sci. Monit*. 24, 3824–3831. doi: 10.12659/MSM.910866

Zheng, Y. H., Liu, J. P., Zhuang, J. J., Dong, X. Y., Yu, M., and Li, Z. H. (2021). Silencing of UCA1 protects against MPP+-induced cytotoxicity in SK-N-SH cells *via* modulating KCTD20 expression by sponging miR-423-5p. *Neurochem. Res*. 46, 878–887. doi: 10.1007/s11064-020-03214-9

Zhou, Q., Zhang, M. M., Liu, M., Tan, Z. G., Qin, Q. L., and Jiang, Y. G. (2021). LncRNA XIST soonges miR-199a-3p to modulate the Sp1/LRRK2 signal pathway to accelerate Parkinson's disease progression. *Aging* 13, 4115–4137. doi: 10.18632/aging.202378

Zhou, S. F., Zhang, D., Guo, J. N., Chen, Z. Z., Chen, Y., and Zhang, J. S. (2020a). Long non-codingRNANORAD functions as amicroRNA-204-5psponge to repress the progression of Parkinson's disease *in vitro* by increasing the solute carrier family 5 member 3 expression. *IUBMB Life* 72, 2045–2055. doi: 10.1002/iub.2344

Zhou, S. F., Zhang, D., Guo, J. N., Chen, Z. Z., Chen, Y., and Zhang, J. S. (2021). Deficiency of NEAT1 prevented MPP+-induced inflammatory response, oxidative stress and apoptosis in dopaminergic SK-N-SH neuroblastoma cells *via* miR-1277-5p/ARHGAP26 axis. *Brain Res*. 1750, 10. doi: 10.1016/j.brainres.2020.147156

Zhou, S. F., Zhang, D., Guo, J. N., Zhang, J. S., and Chen, Y. (2020b). Knockdown of SNHG14 alleviates MPP+-induced injury in the cell model of Parkinson's disease by targeting the miR-214-3p/KLF4 axis. *Front. Neurosci*. 14, 930. doi: 10.3389/fnins.2020.00930

Zhou, W. Y., Cai, Z. R., Liu, J., Wang, D. S., Ju, H. Q., and Xu, R. H. (2020). Circular RNA: metabolism, functions and interactions with proteins. *Mol. Cancer*. 19, 172. doi: 10.1186/s12943-020-01286-3

Zhou, Y., Gu, C., Li, J., Zhu, L., Huang, G., Dai, J., et al. (2018). Aberrantly expressed long noncoding RNAs and genes in Parkinson's disease. *Neuropsychiatr. Dis. Treat*. 14, 3219–3229. doi: 10.2147/NDT.S178435

Zhu, Y. S., and Zhu, J. (2022). Molecular and cellular functions of long non-coding RNAs in prostate and breast cancer. *Adv. Clin. Chem*. 106, 91–179. doi: 10.1016/bs.acc.2021.09.005

Zhuang, Z. J., Zhang, L. H., and Liu, C. C. (2022). snhg14 upregulation was a molecular mechanism underlying MPP+ neurotoxicity in dopaminergic SK-N-SH cells *via* SNHG14-miR-519a-3p-ATG10 ceRNA pathway. *Neurotox. Res*. 40, 553–563. doi: 10.1007/s12640-022-00488-5

Frontiers in
Aging Neuroscience

Explores the mechanisms of central nervous system aging and age-related neural disease

The third most-cited journal in the field of geriatrics and gerontology, with a focus on understanding the mechanistic processes associated with central nervous system aging.

Discover the latest Research Topics

See more →

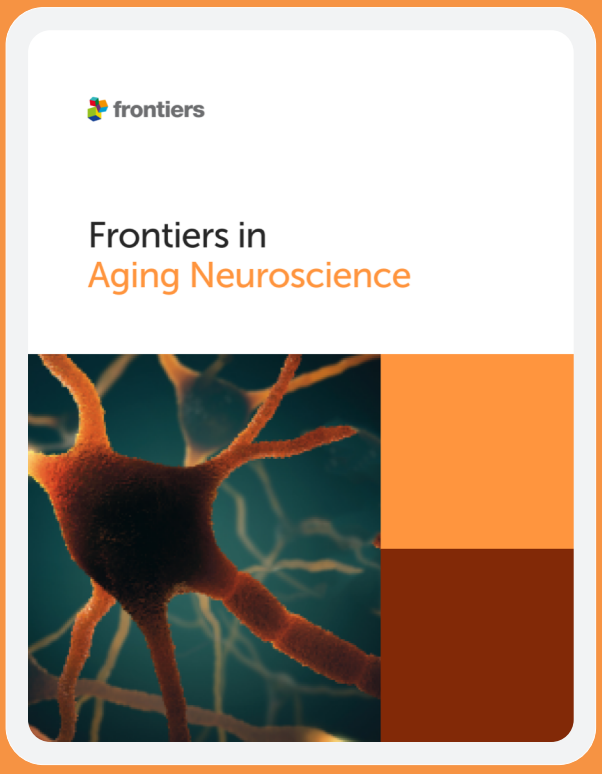

Frontiers

Avenue du Tribunal-Fédéral 34
1005 Lausanne, Switzerland
frontiersin.org

Contact us

+41 (0)21 510 17 00
frontiersin.org/about/contact